ASSESSING OPTIMAL INTERVENTION TARGETS FOR RESPIRATORY INFECTIONS IN STRUCTURED POPULATIONS

Natasha S. Wenzel

A dissertation
submitted in partial fulfillment of the
requirements for the degree of
Doctor of Philosophy

University of Washington
2019

Reading Committee:
M. Elizabeth Halloran, Chair
Katherine E. Atkins
Amanda Phipps

Program Authorized to Offer Degree:
Epidemiology

University of Washington

ABSTRACT

ASSESSING OPTIMAL INTERVENTION TARGETS FOR RESPIRATORY INFECTIONS IN STRUCTURED POPULATIONS

Natasha S. Wenzel

Chair of the Reading Committee:
Professor M. Elizabeth Halloran
Department of Biostatistics and Epidemiology

Background: Respiratory Viral Infections (RVI) are one of the most common health conditions globally, and are an enormous burden to health systems and society in terms of direct medical expenses and indirect productivity losses. Despite progress made in the 20th century with the introduction of antibiotics, vaccines, and antivirals there are no specific interventions for most respiratory infections of viral origin. There remains a need for new rationally designed therapeutics, and non-pharmaceutical interventions to prevent transmission. The objective of this project is improve current public health decision tools through an improved understanding of respiratory virus transmission from key 'driver' subgroups and

their interactions with other subgroups in a study population.

Methods: This research utilizes clinical epidemiology, infectious disease modeling, and extensive sensitivity analysis, to describe and evaluate current health decision-making processes related to two RVI. In the first chapter we infer exposure routes of Human parainfluenza virus-3 (HPIV-3) infection using a case-control study at a cancer-specific hospital. We examine locations and treatment exposures among patients that are associated with illness and make recommendations for the current intervention protocol based on the results. In the last two chapters we deal with previously quantified contact patterns. Using these contact patterns we evaluate the optimal vaccination intervention using cost-effectiveness analysis to compare the status quo influenza vaccination program to seven alternative strategies targeted at school age subgroups Preschool (2-4 years old), Primary school (5-11 years old), and Secondary school (12-16 years old). In the final chapter we deliberately incorporate social contact uncertainty into the same model as chapter 2 by using contact surveys from other countries and examine the variation in our cost-effectiveness results.

Results: In our case-control study, 50 case subjects with medical appointments during their exposure period were compared to 106 controls using matched conditional logistic regression. Although contact precautions were enforced for immunosuppressed patients, these patients were 9.59 times as likely to be infected. Contact with several healthcare workers, especially nonclinical staff (e.g. social workers) was also associated with increased infection odds. In chapter 2, the incremental analysis demonstrated vaccinating 5-11 year olds (Primary School) was the most cost-efficient strategy. Although all seven strategies had a 100% probability of being cost-effective at the current National Health Service (NHS) threshold of £20,000 per 1 QALY gained, vaccination of 5-11 year olds provided substantial indirect protection to other age groups. Additionally strategies which contained this age group were less sensitive to changes in total achieved coverage. The structural uncertainty analysis in chapter 3 revealed Bayesian model fits using the substituted prior information on contact patterns did not converge on the same posterior. Substitution of a counterfactual contact structure

in lieu of country-specific structure decreased the probability a strategy was cost-effective by propagating uncertainty through the model. We also determined that when a model's contact structure is substituted the relative importance of each age group to population-level disease transmission varies substantially rendering inconsistent cost-effectiveness results.

Conclusion: In this research we evaluated interventions aimed at reducing two respiratory viral infections: seasonal influenza and HPIV-3. In the latter our results suggest asymptomatic shedding among hospital staff, especially non-clinical staff (e.g. social workers), and viral persistence in environmental surfaces as possible exposure routes of patient HPIV-3 infection. In chapter 2, we determined improvement could be made to the current LAIV pediatric vaccination strategy of England and Wales by eliminating LAIV vaccination of 2-4 year olds and focusing on school-based delivery of LAIV to two key age groups, Primary and Secondary school-age children. However the conclusions of chapter 2, and all policy interventions based on simulating health outcomes and economic costs, are sensitive to the scientific judgements around social contact parameters. From chapter 3 we conclude there is added value in using country-specific contact data, and advocate that in the absence of country-specific contact patterns, structural uncertainty analysis should be undertaken when quantifying the effect of strategies that involve herd immunity.

Contents

Abbreviations

ANOVA Analysis of Variance.

BAL bronchoalveoloar lavage.

BE Belgium.

CEA Cost-Effectiveness Analysis.

CEAC Cost-Effectiveness Acceptability Curve.

CSF Cerebrospinal fluid.

DAG Directed Acyclic Graph.

DE Germany.

DFA Direct fluorescent antibody.

FI Finland.

FR France.

GB Great Britain.

GP General Practitioner.

HCW health care workers.

HPA Health Protection Agency.

HPIV-3 Human parainfluenza virus-3.

HSCT Hematopoietic stem cell transplantation.

ICER Incremental Cost-Effectiveness Ratio.

ILI Influenza-like-illness.

IT Italy.

LAIV Live-Attenuated Influenza Vaccine Nasal Spray.

LRTI Lower Respiratory Tract Infection.

LU Luxembourg.

MCMC Markov chain Monte Carlo.

NHB Net Health Benefits.

NHS National Health Service.

NICE National Institute for Health and Care Excellence of England and Wales.

NL Netherlands.

NPT nasopharyngeal-throat wash.

OR Odds Ratio.

ORCA Online Record of Clinical Activity.

PA Physician's Assistant.

PE Peru.

PHE Public Health England.

PL Poland.

QALY Quality-Adjusted-Life-Years.

QIV Quadrivalent Influenza Vaccine.

RCGP Royal College of General Practitioners Research and Surveillance Center.

RVI Respiratory Viral Infections.

SCCA Seattle Cancer Care Alliance.

SEIR Susceptible-Exposed-Infectious-Recovered Compartmental Model.

SQ Status Quo Strategy.

TIIV Trivalent Inactivated Influenza Vaccine.

UK United Kingdom.

URTI Upper Respiratory Tract Infection.

VE Vaccine Efficacy.

WTP Willingness-to-pay threshold.

ZI Zimbabwe.

List of Symbols

$\mathbf{C}_S$ predicted total of health care and vaccination costs associated with seasonal influenza as a result of an intervention strategy.

$\mathbf{C}_c$ predicted total of health care and vaccination costs associated with seasonal influenza as a result of the next non-dominated strategy.

$\mathbf{I}_{0,t}$ initial infectious seed for the epidemics per season t.

Ψ probability an influenza infection came from outside the population of interest.

α statistical significance level.

α_j Y-axis intercept term representing the odds of success when $x = 0$ varying for each of the j matched sets.

ϵ the probability a symptomatic case is ascertained by the health services.

ϵ_j Residual error term for the regression for each of the j matched sets.

λ decision-maker's willingness-to-pay per QALY gained.

σ_i susceptibility of age group i.

$\mathbf{c}_{ij}$ average number of contacts per day between an individual of age group i and an individual of age group j.

$\mathbf{q}_{strain}$ transmissibility of viral strain A/H1N1, A/H3N2, B.

$\mathbf{r}$ Quality-adjusted life years lost as a result of seasonal influenza under a strategy.

$\mathbf{r}$ Quality-adjusted life years lost as a result of seasonal influenza under the next non-dominated strategy.

$\mathbf{M}$ mathematical representation of the contact matrix.

Chapter 1

An outbreak of Human Parainfluenza Virus-3 at the Seattle Cancer Care Alliance Hospital

Abstract

Human parainfluenza virus-3 (HPIV-3) infections cause considerable morbidity and mortality among cancer patients receiving treatment. Between March 2015 and June 2015, 95 patients with HPIV-3 were recognized in the 900-bed Seattle Cancer Care Alliance (SCCA) hospital. To investigate hospital-related exposures associated with subsequent HPIV-3 infection a case-control study was carried out. Measuring this association was confounded by the underlying cancer diagnosis of a patient and the unobserved risk presented by the number of HPIV-3 infected persons at the hospital varying in time. Case subjects and controls were matched on medical procedure, appointment time (+/- 1 hour), and appointment date during their estimated exposure period. Data on potential treatment-related exposures (e.g. rooms, personnel) were retrieved by review of electronic medical records. After matching, 50 case subjects with appointments at the SCCA during their exposure period were compared to 106 controls using matched conditional logistic regression. Of the 50 cases the 44 (88%) immunosuppressed case-subjects had an adjusted odds ratio of infection by HPIV-3 of 9.59 (95% CI: 7.64, 12.04). The most common HPIV-3 symptoms among patients were cough, sputum production, and sinus congestion which affected 50% or more of patients both immunosuppressed and not. Of the hospital related exposures, contact with a procedure/recovery bed and several consultation rooms were associated with developing disease. In addition to locations, six clinical healthcare workers (e.g. Registered Nurse, Physician's Assistants), as well as hospital staff in the pharmacy and social work departments were associated with subsequent development of detectable HPIV-3 disease. Our results suggest asymptomatic shedding among hospital staff, including non-clinical staff, and viral persistence in environmental surfaces as possible exposure routes of patient infection.

1.1 Introduction

Respiratory viruses are the most common transmittable infections in patients receiving chemotherapy or a Hematopoietic stem cell transplantation (HSCT) for the treatment of cancer.[1, 2] Despite significant financial and personnel resources dedicated to Respiratory Viral Infections (RVI) control, incidence and related mortality remain high at the Seattle Cancer Care Alliance (SCCA).[3] A 2015 outbreak of Human parainfluenza virus-3 (HPIV-3) at the SCCA demonstrated the limitations of recommended HPIV-3 prevention strategies. Despite strict infection control procedures, respiratory isolation was required for approximately 70% of patients for an average of 13.6 days. Patients at SCCA that progress from RVI to lower respiratory tract involvement have mortality rates that reach close to 50% and cost an additional $250,000 in medical treatment per patient.[3] Costs of the 2015 outbreak are estimated conservatively to be over $2 million.

Parainfluenza viruses are usually transmitted by direct contact with infectious droplets or by airborne spread when an infected person breathes, coughs, or sneezes.[4] Infectious airborne droplets can remain viable on surfaces from 1-3 hours depending on environmental conditions.[5] HPIV-3 disease can present as uncomplicated upper respiratory tract infectionsUpper Respiratory Tract Infection (URTI), characterized by rhinorrhea symptoms to more severe Lower Respiratory Tract Infections (LRTI), which may lead to pneumonia, bronchiolitis, bronchitis, and respiratory failure.[6, 4] Risk factors for within-hospital exposure to HPIV-3 virus as well as patient characteristics that are associated with progression to HPIV-3 disease remain poorly defined.

We performed a case-control study to identify risk factors for HPIV-3 infection among patients at the SCCA during the 2015 outbreak. Specifically we sought to determine what in-hospital locations and staff as part of a patient's appointment were associated with subsequent HPIV-3 disease (e.g. Treatment Bay 1).

1.2 Methods

To determine locations at the SCCA where HPIV-3 exposure risk was elevated, we examined treatment areas such as a clinical room or the health care workers (HCW) who performed the procedure using a matched case-control study. Measuring this association was confounded by the underlying cancer diagnosis of a patient and the unobserved risk presented by the number of HPIV-3 infected persons at the hospital varying in time. As the same procedure can be performed on different patients simultaneously we conditioned on medical procedure, date, and appointment time, to retrospectively compare infection risk among locations where

case subjects and controls received treatment (e.g. Infusion Bay 1, Infusion Bay 2).

1.2.1 Infection-control measures

During the 2015 outbreak infection control procedures stated all patients with URTI symptoms undergo viral culture using samples from a nasopharyngeal-throat wash (NPT), nasal swab, nasal wash, sputum, or bronchoalveoloar lavage (BAL). Cases were defined as inpatients or outpatients who had a laboratory confirmed case of HPIV-3 by culture or evidence of parainfluenza antigen by Direct fluorescent antibody (DFA). All HCW, patients, and visitors were required to sign in stating that they did not have cough, sneezing, or uncontrolled rhinorrhea before gaining access to inpatient or outpatient wards. Staff members with these symptoms were restricted from patient care, and symptomatic visitors were prohibited access. In the outpatient examination and treatment rooms all surfaces and equipment were cleaned thoroughly between patients by using alcohol and quaternary ammonia–impregnated wipes.

Symptomatic inpatients, outpatients, and HCW underwent virology testing of nasopharyngeal wash specimens. Patients who were positive by NPT/BAL for HPIV-3 were placed in respiratory isolation to prevent transmission to HCW and other patients. Case-subjects underwent repeated testing via NPT at least monthly to determine clearance of the virus from nasopharyngeal secretions. Staff members who were positive by NPT/BAL for HPIV-3 or other respiratory viruses were sent home and underwent repeated testing via NPT until they received a negative laboratory result. This study was approved by the Institutional Review Board at the Fred Hutchinson Cancer Research Center.

1.2.2 Medical records data and preprocessing

The EpicCare system maintains a patient's health records over time. Clinical appointment records were extracted retrospectively from the SCCA's EpicCare database for the period March 15, 2015-June 30, 2015, and from the online record of clinical activity (ORCA) database for the same period. The unique patient identification number remained consistent if an individual had multiple appointments during the time period. For example a patient with alias 453 seen on March 25, 2015 would had the same alias if they returned for appointment on March 30, 2015. Once processed, the EpicCare database and Online Record of Clinical Activity (ORCA) database were merged on the variables 'patient alias', 'appointment date' and 'provider alias' to form the final analytic set used for matching cases and controls (Supplemental Figure 1.7.1).

EpicCare dataset

An average appointment record from the EpicCare data contained a patient's unique identification number, the procedure in progress, the unique identification number of the health care worker entering the electronic record, a room number or location, and the time when a patient checked in/out of the room or began/ended a procedure. We removed repeated records, records from other hospitals in the network, and rows missing procedure or appointment time data. Rows which had an identical appointment date, provider, procedure, location, and patient id with the exception of time, were first tested to determine if the time intervals overlapped or were consecutive. If time intervals overlapped or were consecutive these rows were collapsed by taking the earliest time point and the latest time point to represent the full length of the procedure. Further information on this process is described in Supplemental Section 1.7.

ORCA dataset

The clinical activity record of the appointment in the ORCA dataset contains patient responses to current health status questions (e.g. Musculoskeletal Symptoms, Patient Reported Urine Color), biometric data collected at the appointment (e.g. systolic blood pressure, temperature), as well as demographic data (e.g. age, marital status). Data were organized by appointment date meaning the set of questions asked by providers per appointment varied based on the purpose of the appointment and the procedure a patient was receiving that day. If a patient was missing data on characteristics which were independent of appointment date such as 'Age', 'marital status', or 'Tobacco Use', these values were carried forward from the other appointment records of the same patient. The variables studied to determine the risk-factors for HPIV-3 infection and for the descriptive study of the clinical characteristics of the infected patients, were as follows: age, education level, surgery within the last 30 days, presence and duration of procedures, tobacco use status, bone abnormalities, haematological abnormalities, and immune status.

1.2.3 Calculating exposure period

The earliest symptom start date among cases (e.g. cough, rhinorrhea) was obtained from records provided by the SCCA infection control department and from the ORCA patient records (Supplemental Section 1.7.1). HPIV-3 human-challenge studies concluded the incubation period–the time period from viral exposure to manifestation of respiratory symptoms–ranged from 3-6 days with a mean of four days in healthy adults (Figure 1.6.1).[7] Using the symptoms start date we backdated three days to obtain the latest date a case subject would

have been exposed, and subtracted an additional day to account for lags in reporting. Likewise we backdated seven days from the symptoms start date to obtain the earliest date a case subject would have been exposed (Supplemental Figure 1.6.3). We included one extra day over the maximum six day incubation range to accommodate lags in reporting symptoms from case subjects or medical providers. Appointment records for all case subjects were obtained for this period.

1.2.4 Identification of controls

For the first appointment during a case subject's exposure period, all procedures a patient received during their appointment were extracted and used to match controls. Controls were selected by identifying all individuals who did not have a laboratory record of being HPIV-3 positive and received the same procedure as the case subject, who received the procedure on the same date as the case subject, and had an appointment during the same time period as the case subject (within one hour of a case subject's appointment start or end time). Two control subjects were matched per case subject. For instance if a case subject had two procedures during their appointment such as 'Platelets' and 'O Team Lab Test', two controls who also had 'Platelets' as a procedure on the same date and time as the case subject were chosen, and two controls who also had 'O Team Lab Test' as a procedure on the same date and time as the case subject were chosen. In many situations more than two controls had the same procedure, same appointment date, and same appointment time as a case subject. In these situations we drew two random numbers from a uniform distribution with the minimum of one and a maximum of the number of records which matched the date and time criteria. The two random numbers were used as an index to select the two controls records from the subset of patients who met all the matching criteria. Control records who were previously matched could not be matched again. For example if a control with study id 2816 was previously matched with case subject 453 on the procedure 'Platelets' occurring on April 1st during the time period 1:30-3pm, the record for control subject 2816 could not be matched again with case subject 6479 for a 'Platelets' procedure on April 1st, 1:30-2:30pm. However control subject 2816 could be matched with case subject 6479 on a different procedure record (e.g. 'Gancyclovir', 'Blood 1 Unit') as long as the date and time records met the criteria. In addition to the date, time, and procedure criteria a control subject also had to have sufficient patient characteristics in the ORCA database for comparison with case subjects.

Determining immune status

Prior to the analysis it was determined a patient's immune status would be a confounder. We searched within the ORCA records using the 'grep' command in R, to determine which patients were described as immunocompromised or immunosuppressed in their chart by their provider. Search terms were not case-sensitive and included 'immuno*','immunos*', 'immunosupression', 'immunosuppressed' (where the asterisk represents a wildcard search). Any patient with a notation of immunosuppression in their file was considered immunosuppressed for the entire three month period. Provider notes on immunosuppression could only be entered in six categories in a patient record. The categories included 'BMT Symptom Management', "Nursing Intervention", "Allo Guideline Teach","Provider Dischg-Diet", "EDU Oncology Symptom Management Review", and "Issue discussed". To ensure a patient who did not have a note of immunosuppression was not an artifact of missing or incomplete data, only individuals who had one or more of these six categories but did not have an entry of 'immunnosuppression' were considered not immunosuppressed. The immunosuppresssion status for call case subjects was ascertained using this method. Potential controls who did not have information in either category were not considered during matching.

1.2.5 Statistical analysis

To increase study sensitivity, only the earliest appointment that occurred in a case subjects' estimated exposure period was used in the statistical analysis. For example if a case subject had two appointments during their exposure period, one on the April 5th and another on the April 8th, only the records for the appointment on the 5th would be used (Figure 1.6.3). Limiting our analysis to the first appointment equalized the disease exposure risk between cases and controls. Simply, only exposures among HPIV-3 naive cases and HPIV-3 naive controls were considered, rather than HPIV-3 naive controls and potentially incubating HPIV-3 cases.

Conditional logistic-regression models for matched sets were used to estimate odds ratios and for all adjusted analyses. The analysis was carried out in the R statistical language (version 3.6.1) [8], using R Studio (version 1.2.1335) using the R package 'survival'. Prior to the statistical analysis patient characteristics and exposure variables were mapped using a Directed Acyclic Graph (DAG)[9] for the causal pathway between in-hospital treatment factors (e.g. location, provider who performed procedure) and subsequent laboratory confirmed HPIV-3 infection (Supplemental Figure 1.7.3). Confounding variables 'appointment time', 'appointment date', and 'procedure' were controlled for during the matching process. The confounding variable 'Immune status' was adjusted for in the regression. Immune status

refers to a subject being listed as immunosuppressed or not in the ORCA database. A variable for 'Age' was also included as age-related immune decline may not have been captured under the label of 'immunosuppression'. Haematological abnormalities and bone abnormalities were also included in the regression as other immune status variables in anticipation of a subject's immune status being affected by treatments and medications not classified as immunosuppressed by providers.

In conjunction with the SCCA Infection Control department we hypothesized that duration of time in a waiting room, and duration of a procedure would be effect moderators on the causal pathway. We did not adjust for duration of time in a waiting room as it was an intermediate between treatment exposures and HPIV-3 exposure. Procedure duration was included both as a covariate and interaction effect. The two models in linear form are given below:

Model 1: $\text{logit}[p_j(x_{ij})] = \alpha_j + \beta_1 x_{1,ij} + \beta_2 x_{2,ij} + \beta_3 x_{3,ij} + \beta_4 x_{4,ij} + \beta_5 x_{5,ij} + \beta_6 x_{6,ij} + \beta_7 x_{7,ij} + \epsilon_j$

Model 2: $\text{logit}[p_j(x_{ij})] = \alpha_j + \beta_1 x_1 + \beta_2 x_{2,ij} + \beta_3 x_{3,ij} + \beta_4 x_{4,ij} + \beta_5 x_{5,ij} + \beta_6 x_{6,ij} + \beta_7 x_{7,ij} + \beta_{1*4} x_{1*4,ij} + \epsilon_j$

where x is the value of the explanatory variable for the ith individual in the jth matched set. Here the subscript '1' denotes treatment exposure variables, '2' denotes immunosuppression status, '3' denotes Age greater than 60, '4' denotes procedure duration, '5' denotes Haematological abnormalities, '6' denotes Bone abnormalities, '7' denotes surgery within the last 30 days, and '1*4' denotes an interaction term between duration and treatment exposure. The intercept term, α_j, is the odds of success when x = 0. The α_j will vary for each of the j matched sets. The different α_j for each matched set does not have an effect on the odds ratios because the α terms cancel out in the odds ratio calculations.The final conditional regression model was decided by an Analysis of Variance (ANOVA) and the likelihood ratio test.

1.2.6 Sensitivity analysis

Sensitivity analysis was performed by varying the duration of the exposure period, defining a pool of controls for that exposure period, and matching using the process above. We considered an exposure period with a minimum incubation period of 2-5 days and a maximum incubation period from 6-9 days. Each new set of case subjects and controls was analyzed using matched conditional regression with the same adjustment variables as the main model.

Fixed and random selection of controls

We considered two scenarios during the sensitivity analysis. One, where the starting seed for the random number generator used by the uniform distribution was fixed across all exposure period simulations. This results in the same controls being selected during every variation of the exposure period, as long as their matching case had an appointment in the exposure period. In the second scenario the starting seed for the random number generator was varied during every exposure period the regression was calculated for. This second scenario results in a new index number generated from the uniform distribution during every procedure record match and during every exposure period variation. The second scenario means that the same controls matched to each case would not be consistent between each exposure period scenario. In each instance we used only the first appointment during the calculated exposure period.

1.3 Results

Human Parainfluenza viruses were isolated from 95 (0.7%) of the 14,348 patients who attended medical appointments at the SCCA from March - June 2015. HPIV-3 was the most common HPIV strain among the laboratory samples collected during the study period (305 out of 309 samples). Other HPIV strain isolates from two case subjects included HPIV-2 and HPIV-4, but occurred outside the March - June 2015 period.

1.3.1 Case subject characteristics

The median age of a case was 54 years olds (95% Interquartile Range (IQR): 6, 76) (Supplementary Figure 1.7.2). The majority of cases were male (53%) by a small margin. The median age of a male case was 56 years old (95% IQR: 13, 76), while for women it was 53 (95% IQR 2, 74). Comparison of the age distribution among male and female did cases not reveal any significant differences. Of the 95 HPIV-3 case subjects, 65 (68%) had immunosuppression notation in their records during the 3.5 month period. Among case subjects, 65% of female cases were also immunosuppressed and 75% of male cases were also immunosuppressed; these differences were not significant under the Student's t-test ($p > 0.05$). Among case subjects the most common underlying cancer diagnosis was multiple myeloma and acute myeloid leukaemia.

1.3.2 Disease symptoms

The majority of case subjects (93%) experienced cough symptoms, and 63% experienced upper respiratory tract symptoms such as sputum production, sinus congestion, and rhinorrhea (Table 1.5.1). Post-nasal drip, shortness of breath, and wheezing occurred in less than 20% of case-patients. The median duration of cough symptoms for all cases was 16 days (95% CI: 4, 70 days). Cough duration and sore throat duration differed significantly between immunosuppressed and non-immunosuppressed persons (Table 1.5.2). Duration of other respiratory tract symptoms such as sputum production and rhinorrhea were not significantly different between immunosuppressed individuals and not.

Only one case subject received inhaled ribaviron a therapeutic treatment, with the majority receiving treatment with valacyclovir or Acyclovir, Micafungin, and Dapsone. While many also received Immunoglobulin G antibodies, it was unclear whether this was in response to infection or a patient's underlying malignancy. During the course of their HPIV-3 infection five patients were recorded as being co-infected with either Coronavirus, Influenza B, Viridans Streptococci, Respiratory Syncytial Virus, or Vancomycin-resistant enterococci. One patient was also recorded as having latent Tuberculosis.

1.3.3 Analysis of exposures to HPIV-3 related to medical treatment

The first HPIV-3 case at the SCCA was laboratory confirmed on January 20, 2015 and the second on January 22nd. However the majority of cases were identified by laboratory surveillance over the period March 23 to April 24 (Figure 1.6.4). The lag time between when a sample was taken to when the laboratory confirmed disease was estimated by the SCCA Infection Control Department at one day.[3] The lag time between first respiratory symptoms recorded for a patient and a positive cultured laboratory result was estimated at a mean 8.6 days, however the standard deviation spanned 47 days. Case subjects with such large lag times were usually cases identified in January or February but not tested until the end of March or April, after a HPIV-3 outbreak had been identified by the SCCA Infection Control Department.

Of the 95 cases, 87 were estimated to have had an exposure period between March 15-June 30. Of the 87, 68 case subjects (78%) had medical appointments at the SCCA during their estimated exposure period (Figure 1.6.2). Appointment records were initially obtained for each case subject using an exposure period of 2-7 days, with one day added to the maximum and minimum incubation time to account for lags in reporting. We found that there was no difference in the number of case subjects and the date of their first appointments when the exposure period was limited to 2-6 days or 2-5 days.

After matching on appointment date, medical procedure, and appointment time, 50 case subjects and 106 controls were identified and matched on procedure date and time into 116 unique sets. The demographic and clinical characteristics of the case subjects who contracted HPIV-3 during the study period and the 106 controls who did not develop HPIV-3 infection are shown in Table 1.5.3. Of the eight case subjects who did not have any record matches with any controls the major reason for exclusion was the appointment time restriction. Four of the eight unmatched case subjects were considered immunosuppressed.

We considered two conditional logistic regression models, one with procedure duration as a covariate, and one with an additional interaction term with between procedure duration and treatment exposure. Both an ANOVA and likelihood ratio test failed to reject the null hypothesis that the two models were significantly different ($p > 0.05$), therefore we used appointment duration as a covariate only, and did not model an interaction. In the main regression analysis the odds of HPIV-3 infection were 24% greater among patients below 60 years old. Likewise, procedure duration was significantly associated with subsequent infection; the adjusted odds of infection for a patient who spent an additional hour in a procedure was 2.1% higher than a patient who did not.

The SCCA hospital has six floors each of which have defined medical clinics. For example the fifth floor primarily provides infusions and apheresis. In addition to clinical areas the hospital includes multiple waiting room, a cafeteria, and pharmacy. The conditional logistic regression revealed eight significant treatment locations within the hospital associated with subsequent HPIV-3 infection (Table 1.5.4). The locations were in departments in the North-Northeast area of the hospital on Floors 2 and 6. These locations included the Preparation/Recovery beds and the HSCT consultation rooms (Supplementary Figure 1.7.4). The Preparation/Recovery beds consist of five beds located on Floor 2 which serve as supine position beds for patients prior to or after a procedure in the adjoining procedure rooms. The five beds are set up in a row on the East-West alignment of the hospital with curtains separating each bed from another. Of the six preparation/recovery beds, beds 2, 3, and 5 were used by both cases and controls during their exposure period. Patients who were placed in beds 3 and 5 were 0.31 (95% CI: 0.16, 0.57) times and 0.45 (95% CI: 0.23, 0.93) times as likely to be infected with HPIV-3 virus as those who were not placed in beds 3 or 5. Conversely, the odds of infection among patients who used Preparation/Recovery bed 2 were 1.91 (95% CI: 1.01, 3.61) times the odds of infection of those who did not. The preparation and recovery beds are mostly utilized for individual undergoing procedures in the adjoining procedure rooms 1, 2, and 3. However examination of the adjusted odds ratios for the procedure room did not demonstrate any significant differences ($p > 0.05$), suggesting that exposure to the procedure rooms was not associated with infection.

In addition to locations, treatment by nine health care workers seen by both cases and controls were associated with increased odds of HPIV-3 infection. Of these healthcare workers three were part of the 'G' treatment team which addresses pediatric malignancies, two were part of the 'R/O/T' team and one was part of the 'L' team, both of which address outpatients undergoing or who have undergone allogenic stem cell transplants. Of the team members all were either physician assistants or registered nurses. The remaining three health care workers were members of the Department of Physical and Occupational therapy, Pharmacy, and Social Work.

Sensitivity analysis

The sensitivity analysis varied the minimum incubation period between 2-4 days with the maximum incubation varied from 7-9 days (Supplemental Figure 1.7.5). In the scenario where the starting seed for the random number generator was fixed, the sensitivity analysis showed no variation when the exposure period was varied (Table 1.5.4). In the second scenario where the starting seed for the random number generator was varied during every range of exposure periods differences in the conditional regression results did occur. In the second scenario, exposures which remained significantly associated with HPIV-3 infection included Social Worker 1, 'R' Team Physician's Assistant (PA) 1, an immunosuppressed status, procedure duration, HSCT Consult Room F, 'BLY' Pharmacist 1, and the 'V' Team RN. The number of healthcare workers associated with infection decreased during the sensitivity analysis. Whereas nine hospital staff were associated with infection in the main analysis, in the sensitivity analysis exposure to the same social worker, same 'R' Team PA, and same pharmacist were all associated with increased odds of infection ($p < 0.05$). Likewise patients with exposure to the 6th floor triage nurse and preparation/recovery bed 3 had consistently lower odds of infection compared to those without these exposures. The covariates denoting a patient having had surgery within the last 30 days and the risk of infection associated with age were the most sensitive to changes in exposure period. In the main regression analysis the odds of HPIV-3 infection were 24% greater among patients below 60 years old. In the first sensitivity analysis scenario with the fixed starting seed, the odds of HPIV-3 infection reversed, meaning among patients below 60 years old the odds of infection were 21% reduced, OR=0.79 (95% CI: 0.66, 0.93). Similarly surgery in the last 30 days was protective in the main analysis with an odds ratio of 0.55 (95% CI: 0.42, 0.73), but in the sensitivity analysis again displayed a reversal. Patients who had had surgery within the last 30 days demonstrated an increased 22% and 48% odds of HPIV-3 infection in both the fixed starting seed and random starting seed scenarios.

1.4 Discussion

In this case–control study, subjects with increased odds of HPIV-3 infection shared exposure to HSCT consultation rooms, Preparation/Recovery Bed 2, as well as contact with HCW on the 'G', 'R', and 'L' transplant teams and three hospital staff who were associated with the social work, physical therapy, or pharmacy departments. Several potential confounding factors were considered. In particular we controlled for immune status which was captured with covariates relating to a notation of immunosuppressed status in a patient record (e.g. as a result of organ transplant), loss of immunocompetence with age greater then 60 years old, surgery in the last 30 days, and current history of a blood or bone abnormality which could affect lymphocyte or B-cell function. Without adjustment for these immune status confounders, many more HSCT treatment areas and HCW associated with HSCT were associated with HPIV-3 infection and many of the exposures identified in our main analysis were significant only at the α=0.10 level.

Cases identified in May or June were less likely to have had appointments during their estimated exposure period. This is likely the result of the SCCA Infection Control Department's increased surveillance and laboratory testing from the period of March onward, which would have identified community acquired cases that may not have otherwise been ascertained.

The symptoms of HPIV-3 that were experienced by the majority of patients included non-specific respiratory symptoms such as cough, sputum production, sinus congestion, and rhinorrhea. Differences in symptom presentation and symptom duration occurred between individuals identified as immunosuppressed and those who were not. Most notably, the duration of cough symptoms among immunosuppression persons was almost twice that of patients without immunosuppressed notation in their patient records. We recommend providers take notice of cough symptoms accompanied by sputum production lasting one to two and submit samples for testing as soon as symptoms are identified.

Examination of the epidemic curve and estimated exposure periods revealed that the earliest cases of HPIV-3 experienced a significant lag time between symptoms being observed in their patient record and laboratory confirmation of virus. As the laboratory processing time is estimated at one day, the majority of lag time between symptom recognition and a positive laboratory result is related to provider decisions around sampling. We recommend minimizing this lag time such that any patient with respiratory symptoms or suspected of having respiratory symptoms be sampled immediately.

As HPIV-3 consistently occurs in late spring and summer[10], we also recommend annual reminders reinforcing respiratory precautions among all hospital staff that come into contact

with patients. The consistent association between a pharmacist, social worker, and HPIV-3 infection across all the sensitivity analysis simulations may be indicative that individuals who are outside the sphere of clinical care, but have frequent contact with patients, may not have the same training and awareness in regard to respiratory viruses as clinical staff. Cross-referencing the hospital staff identified in our regression analysis with laboratory confirmed HPIV-3 positive hospital staff members revealed another social worker who tested positive for HPIV-3 in April, four HCW in the transplant units who tested positive in April and May, and one HCW who worked in the procedure suite. The direction of infection, whether patient to HCW or HCW to patient, cannot be determined due to the design of the case-control study. However the overlap in departments between the HCW in our analysis and those identified later in the outbreak may signify ongoing transmission among hospital staff. Additionally, our analysis was limited to the healthcare staff who were recorded as performing the procedure or entering the records, meaning other hospital staff (e.g. receptionists) and HCW who played an assisting role could have been omitted.

Differences in the odds between the case subjects and controls who were placed in Preparation/Recovery beds 2, 3, and 5 are likely attributed to different frequency of use among the beds. The doors of the procedure suites 1 and 2 are closets to to preparation/recovery beds 1 and 2 meaning bed 2 likely has a higher frequency of use than either 3 or 5. Even with sanitation, consecutive use of the preparation/recovery beds increases the possibility of fomites or droplets being passed from one consecutive patient to another. As the stability of HPIV-3 on a surface is impacted by time, temperature, and humidity we recommend the preparation/recovery beds use a rotating bed assignment scheme to ensure adequate time has passed before a bed is used again. Likewise the consistent association of the HSCT consultation rooms M, G, and F may indicate that these non-clinical rooms may need clinical level sanitation following a consultation.

1.4.1 Immunosuppression and HPIV-3

In immunocompetent persons HPIV-3 is considered primarily a respiratory virus that responds to respiratory contact precautions. However immunocompromised patients have been found to have HPIV infection in non-respiratory sites including Cerebrospinal fluid (CSF), pericardial fluid, white blood cells, and the liver.[11, 12] Respiratory precautions remain the front line in controlling HPIV-3, however in a cancer specific hospital it may be necessary to introduce blood and body fluid precautions during procedures which specifically involve CSF (e.g. Ommaya tap) or blood samples from immunosuppressed persons. Having immunosuppressed notation in a patient record increased the odds of a patient being positive

for HPIV-3 infection to OR=9.59 (95% CI: 7.64, 12.04), a result that was consistent across all the sensitivity analyses. Healthcare workers who are not aware of the potential for blood or body fluid-related HPIV-3 exposure may inadvertently infect themselves or others.

We examined age greater than or less than 60 years old as a potential immune status confounder with the idea it would capture age-related immune decline. In the main regression analysis the odds of HPIV-3 infection were 24% greater (OR=1.24 (95% CI: 1.06, 1.44) among individuals below 60 years old. It is possible case subjects greater than or equal to 60 years old may have received additional precautions during treatment due to perceptions of elderly health. However, the odds ratio for the age covariate was not consistent across different exposure periods in the sensitivity analysis. During some exposure periods older age was associated with increased odds of disease. This variation may mean the age covariate is time dependent or that HPIV-3 disease transmission may form clusters and move assortatively through different patient age groups.

1.4.2 Limitations

During the 2015 outbreak the SCCA screened patients with symptoms of upper or lower respiratory tract disease for the presence of any respiratory viruses.[3] This makes laboratory screening for virus dependent on a patient manifesting respiratory symptoms. Because of this it is unlikely a patient would be tested prior to respiratory symptoms being manifested. This dependence makes it unlikely a patient would be tested if they had an asymptomatic manifestation. It has been documented HPIV-3 infection can enter a carrier state persisting for 3-5 months among immunocompetent persons.[13] It is possible a patient could have manifested symptomatically without being observed then waned as they entered a carrier state. If this scenario occurred it would be unlikely to be identified by our analysis as it is essentially an asymptomatic phase without respiratory symptoms. We considered this situation unlikely among patients given their immune status, underlying conditions, and related treatment. Nevertheless, like other previous studies [1], we consider it very possible this situation occurred among hospital staff. To improve the ascertainment of asymptomatic HPIV-3 among staff we recommend a monthly respiratory virus testing scheme for clinical and non-clinical staff beginning in late January and continuing until the end of May.

Analysis of case exposures was limited to those contacts and treatment areas that cases visited during their first appointment in the exposure period. This approach was chosen to increase the sensitivity of the study with the trade off being a loss of specificity, this means that some of the exposures associated with HPIV-3 infection identified in our analysis may be false positive associations. To counter this issue we performed sensitivity analysis around

our selected exposure period in an effort to determine which treatment exposures associated with infection were sensitive to the date of their first appointment. In general, our results were consistent across the sensitivity analysis scenarios with the most differences occurring during the longest exposure period, 2-9 days. We did not consider importation of cases from other hospitals such as the University of Washington Medical Center as we lacked sufficient records for a similar analysis. Among case subjects six patients were co-infected with other viruses and bacteria, however we did not make adjustments for co-infections as interactions between HPIV-3 and other microbes have not been well described.

Our study was predicated on HPIV-3 transmission routes of droplet transfer or fomite transfer of virus during a patient appointment. Other potential transmission routes exist in-hospital that would not be recorded in electronic records (e.g. contact between patients and other patient visitors, hospital cafe food) and therefore could not be considered in our analysis. Likewise only clinical providers and hospital staff that were recorded as having appointments with case subjects or controls were considered in the analysis. While contact between patients and healthcare workers during their appointment was described by the ORCA and EpicCare database, notation of other medical support staff especially in instances when multiple providers were assisting patients at the same time were often missing.

This research provides several new insights about the epidemiological exposures associated with HPIV-3 infections among patients being treated for cancer. Previous examination of HPIV-3 outbreaks at the SCCA and elsewhere have focused on progression of HPIV-3 illness to lower respiratory tract infection, the illness's effect on transplant-related mortality, the effect of respiratory isolation, and the effectiveness of antiviral therapy.[1, 6, 14, 15] Several of these studies used molecular and epidemiological analysis in the post-outbreak period to determine common exposures among patients but were unable to discern any transmission chains.[1, 6] Our study is the first, to our knowledge, to use electronic medical records to examine hospital treatment-related exposures among patients and HPIV-3 infection. Given the 10-fold increase in HPIV-3 infection risk among immunosuppressed persons, more research into preventing respiratory virus transmission in a hospital environment should be a major priority in cancer and infectious disease research.

1.5 Tables

Symptoms	Not Immuno-suppressed Cases	(%)	Symptom Duration (Days)	Immuno-suppressed Cases	(%)	Symptom Duration (Days)
Description	**N=22**	**100%**	**Mean (SD)**	**N=37**	**100%**	**Mean (SD)**
Cough	22	100%	17 (13)	29	78%	33 (23)
Sputum Production	15	68%	14 (12)	23	62%	22 (22)
Sinus Congestion	11	50%	11 (12)	26	70%	17 (14)
Rhinorrhea	10	45%	17 (21)	27	73%	33 (33)
Sore Throat	7	32%	7 (16)	16	43%	7 (8)
Fever (>100.4 F)	8	36%	7 (5)	18	49%	4 (4)
'Post-Nasal Drip'	1	5%	6 (0)	9	24%	22 (21)
Shortness of Breath	5	23%	13 (9)	4	11%	11 (9)
Wheezing	1	5%	19 (0)	2	5%	15 (1)
Pneumonia	5	23%	62 (30)	10	27%	36 (30)
Hypoxia requiring supplemental oxygen	4	18%	21 (14)	10	27%	7 (6)
Hypoxia requiring intubation	2	9%	7 (6)	3	8%	16 (17)

Table 1.5.1: Recorded symptoms of HPIV-3 from both immunosuppressed and not-immunocompromised case subjects. Immunosuppressed status is defined as having notation to that effect in the ORCA clinical dataset. Detailed symptom reports provided by the SCCA infection control department were only available for 59 of 97 cases. Of the 59 cases 63% (N=22) had immunosuppression notation in their patient record for the period March 15, 2015-June 30, 2015.

Clinical Description	Immunosuppressed		Not Immunosuppressed		p-value
	N	**Median Duration (Days) (95% IQR)**	**N**	**Median Duration (Days) (95% IQR)**	
Cough	37	23 (6, 77)	22	14 (3, 44)	<0.000
Sinus Congestion	32	14 (2, 49)	11	8 (3, 42)	<0.03
Sore Throat	19	5 (1, 26)	7	10 (6, 45)	>0.05
Sputum Production	28	15 (5, 95)	13	8 (2, 38)	>0.05
Rhinorrhea	28	16 (5, 108)	7	13 (6, 66)	>0.05
Fever (>100.4 F)	29	3 (1, 15)	8	5 (1, 15)	>0.05
'Post-Nasal Drip'	10	16 (1, 53)	1	6 (6, 6)	–

Table 1.5.2: The average duration of HPIV-3 symptoms stratified by a case subject's immunosuppression status. P-values were calculated using a one-tailed Kolmogorov–Smirnov test where the null hypothesis is the CDF of symptom duration among the immunocompromised is greater than the CDF of symptoms among the non-immunocompromised (α=0.05). IQR= Interquartile range

Demographic and Clinical Characteristics of Subjects diagnosed with HPIV-3, and of their Controls			
Characteristic		**Case Subject**	**Controls**
		N=50 (%)	N=106 (%)
Age			
	<60 years old	19 (38)	38 (36)
	>= 60 years old	31 (62)	68 (64)
Marital Status			
	Single	13 (26)	25 (24)
	Significant Other	5 (10)	6 (7)
	Engaged	0 (0)	1 (0)
	Married	31 (62)	74 (70)
Education			
	Less than 12th Grade	1 (2)	4 (4)
	12th Grade	2 (4)	1 (1)
	Some College/ Technical Degree	3 (6)	6 (6)
	Bachelor's Degree	6 (12)	11 (10)
	Masters/Professional Degree	1 (2)	3 (3)
	Missing	38 (76)	81 (76)
Tobacco Use			
	Never smoked/used tobacco	48 (96)	97 (92)
	Former smoker/tobacco use	2 (4)	7 (6)
	Current smoker/tobacco use	0 (0)	2 (2)
Complication Risks			
Immunosuppression (%)		44 (88)	69 (65)
Surgery within 30 days of exposure period		5 (10)	9 (8)
Bone Abnormality (e.g. Multiple Myeloma, chronic STD)		7 (14)	12 (11)
Haematological abnormalities (e.g. platelets<50K, anticoagulation treatment)		5 (10)	6 (6)

Table 1.5.3: Demographic and clinical characteristics of subjects diagnosed with HPIV-3 and their matched controls

Odds of HPIV-3 Infection					
Varied Exposure Periods	Main Analysis 2-5 Days	Fixed Matching 3-6 Days, 4-6 Days, 5-9 Days, 3-7 Days, & 2-9 Days	Random Matching 2-7 Days, 3-7 Days, & 4-7 Days	4-8 Days, 3-8 Days,	2-9 Days
Treatment Area Exposures	**N=50 Cases**	**N=49 cases**	**N=49 cases**	**N=50 cases**	**N=50**
Autologus Nutrition Consult	1.79 (0.92, 3.47)*	1.08 (0.56, 2.09)	1.79 (0.92, 3.47)**	1.52 (0.77, 2.99)	2.17 (1.10, 4.26)*
HCW 7218	1.96 (0.23, 16.68)	0.43 (0.04, 4.80)	1.96 (0.23, 16.68)	13.34 (1.21, 147.48)**	3.32 (0.38, 28.73)
Blood Draw on 6th Floor	1.13 (0.37, 3.49)	0.98 (0.33, 2.97)	1.13 (0.37, 3.49)	1.88 (0.64, 5.52)	2.78 (0.90, 8.576)
'BLY' Team Nutrition Consult	1.45 (0.65, 3.2598)	1.26 (0.56, 2.82)	1.45 (0.65, 3.2598)	3.11 (0.97, 10.01)**	2.113 (0.67, 6.71)
HCW 2000	9.92 (2.842, 34.64)*	2.78 (0.81, 9.62)	9.92 (2.842, 34.64)**	7.96 (2.30, 27.51)**	8.84 (2.56, 30.52)**
Green CC RN	4.29 (1.24, 14.82)**	2.53 (0.74, 8.65)	4.29 (1.24, 14.82)**	3.51 (0.98, 12.53)*	2.42 (0.73, 8.07)
HSCT Consult Room C	2.03 (1.00, 4.10)*	1.06 (0.53, 2.14)	2.03 (1.00, 4.10)*	1.82 (0.86, 3.86)	2.58 (1.25, 5.33)**
HSCT Consult Room D	6.28 (1.11, 35.56)**	11.93 (2.18, 67.49)**	6.28 (1.11, 35.56)**	———-	———
HSCT Consult Room F	1.76 (0.96, 3.23)*	1.82 (0.99, 3.34)*	1.76 (0.96, 3.23)*	1.71 (0.93, 3.16)*	1.76 (0.96, 3.24)*
HSCT Consult Room G	3.84 (1.32, 11.14)**	2.95 (1.02, 8.59)**	3.84 (1.32, 11.14)**	3.07 (1.04, 9.07)**	2.07 (0.71, 6.03)
HSCT Consult room M	3.77 (1.41, 10.13)**	3.05 (1.14, 8.17)**	3.77 (1.41, 10.13)**	3.73 (1.37, 10.13)**	2.19 (0.82, 5.87)
HCW 9168	1.61 (0.82, 3.18)	0.98 (0.50, 1.92)	1.61 (0.82, 3.18)	1.38 (0.70, 2.76)	2.01 (1.00, 4.02)*
Preparation/Recovery Bed 2	1.92 (1.02, 3.63)*	1.36 (0.72, 2.57)	1.92 (1.02, 3.63)*	0.58 (0.24, 1.41)	0.95 (0.39, 2.31)**
Preparation/Recovery Bed 3	0.31 (0.17, 0.58)**	0.31 (0.17, 0.56)**	0.31 (0.17, 0.58)**	1.79 (0.86, 3.71)	2.31 (1.11, 4.78)**
Preparation/Recovery Bed 5	0.46 (0.23, 0.93)**	0.91 (0.43, 1.90)	0.46 (0.23, 0.93)**	1.39 (0.67, 2.87)	1.53 (0.74, 3.14)
Procedure Room 1	0.60 (0.28, 1.26)	0.62 (0.30, 1.30)	0.60 (0.28, 1.26)	2.90 (0.88, 9.54)	3.60 (1.09, 11.85)**
Radiology	0.77 (0.42, 1.3862)	0.56 (0.31, 1.02)	0.77 (0.42, 1.3862)	0.66 (0.35, 1.23)	1.06 (0.59, 1.91)*
'R' Team Unassigned PA	3.24 (1.52, 6.89)**	3.05 (1.42, 6.57)**	3.24 (1.52, 6.89)**	4.64 (2.14, 10.05)**	5.13 (2.39, 11.02)**
HCW 5480	9.38 (2.68, 32.81)**	2.64 (0.76, 9.14)	9.38 (2.68, 32.81)**	7.66 (2.21, 26.53)**	8.32 (2.41, 28.78)**
HCW 624	3.32 (1.12, 9.83)**	1.56 (0.53, 4.59)	3.32 (1.12, 9.83)**	1.66 (0.56, 4.88)	1.83 (0.62, 5.38)
'BLY' Pharmacist 1	2.08 (1.12, 3.88)**	2.04 (1.09, 3.81)**	2.08 (1.12, 3.88)**	1.91 (1.02, 3.58)*	1.86 (0.98, 3.47)*
Social Worker 1	6.28 (1.11, 35.56)**	11.93 (2.11, 67.49)**	6.28 (1.11, 35.56)**	——-	———
HCW 3031	0.03 (0.002, 0.32)**	2.38 (0.33, 17.12)	0.03 (0.002, 0.32)**	1.92 (0.29, 12.87)	3.38 (0.38, 30.41)
'V' Team RN	1.66 (0.94, 2.91)*	1.55 (0.88, 2.74)	1.66 (0.94, 2.91)*	1.61 (0.91, 2.87)*	1.68 (0.96, 2.95)*

Table 1.5.4 continued from previous page

Odds of HPIV-3 Infection					
Triage Nurse	0.36 (0.18, 0.71)**	0.42 (0.21, 0.82)**	0.36 (0.18, 0.71)**	1.46 (0.76, 2.81)	1.67 (0.88, 3.20)
Immunosuppressed	9.59 (7.64, 12.04)**	10.06 (7.92, 12.80)**	9.59 (7.64, 12.04)**	12.20 (9.07, 16.40)**	12.49 (9.56, 16.33)**
Age <60 years	1.24 (1.06, 1.442)**	0.79 (0.66, 0.93)**	1.24 (1.06, 1.442)**	1.78 (1.42, 2.23)**	1.77 (1.47, 2.13)*
Procedure Duration (Hours)	1.02 (1.01, 1.03)**	3.21 (1.52, 6.78) **	1.02 (1.01, 1.03)**	1.01 (1.00, 1.03)**	1.02 (1.01, 1.04)**
BloodAbnormality ('Yes')	4.69 (3.83, 5.75)*	3.17 (2.59, 3.86)**	4.69 (3.83, 5.75)**	2.91 (2.34, 3.62)**	0.90 (0.75, 1.08)
BoneAbnormality ('Yes')	2.40 (2.00, 2.88)**	6.79 (5.43, 8.49) **	2.40 (2.00, 2.88)*	16.22 (11.16, 23.58)**	2.17 (1.81, 2.61)**
InjurySurgery30days ('Yes')	0.554 (0.42, 0.73)**	1.22 (0.93, 1.58)	0.554 (0.42, 0.73)**	1.48 (1.11, 2.00)**	1.33 (1.04, 1.69)**
Concordance	0.825,(se = 0.011)	0.846,(se = 0.011)	0.825,(se = 0.011)	0.798,(se = 0.014)	0.756,(se = 0.016)

Table 1.5.4: Adjusted odds ratios for treatment exposures (e.g. rooms, personnel) associated with subsequent HPIV-3 infection among patients. The odds ratios were calculated using matched conditional regression. The results of the main analysis are shown in the first left-hand column, while the results of the two sensitivity analysis scenarios where the estimated exposure period has been varied are shown in the remaining columns. '*' notations represents a statistically significant exposure where $\alpha = 0.10$ and '**' $\alpha = 0.05$. HSCT= Haematopoietic stem cell transplant, HCW= Health Care Worker

1.6 Figures

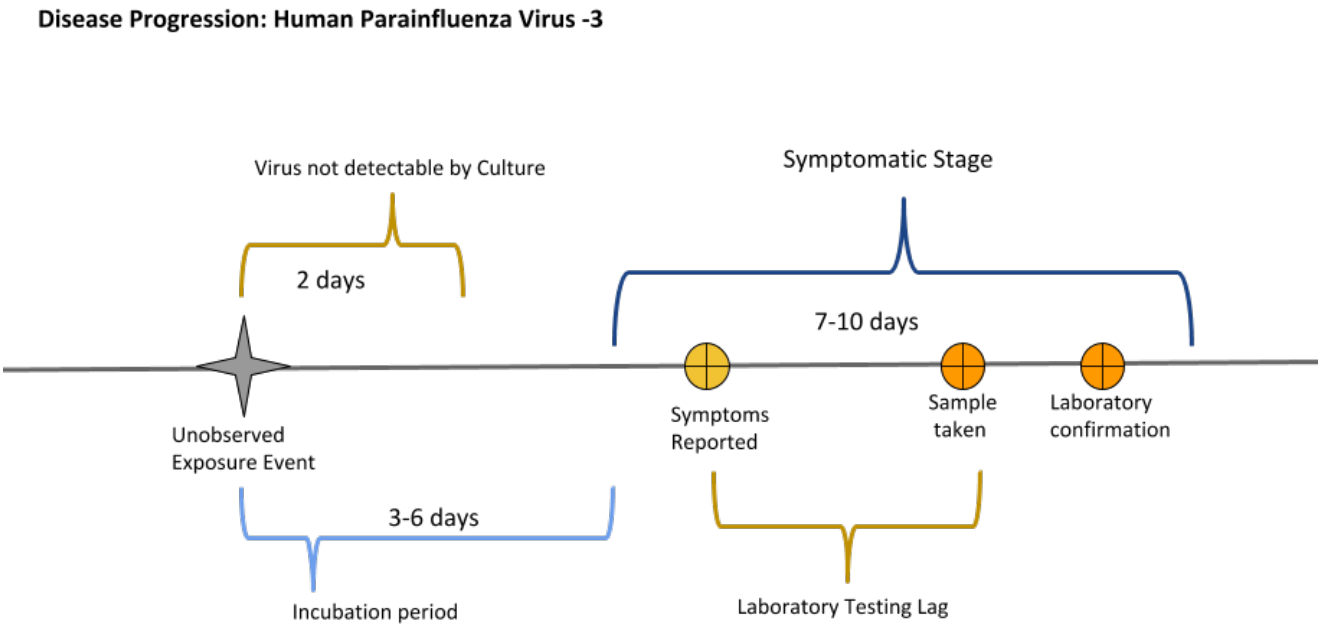

Figure 1.6.1: Disease progression of HPIV-3 demonstrating the incubation and symptomatic stages.

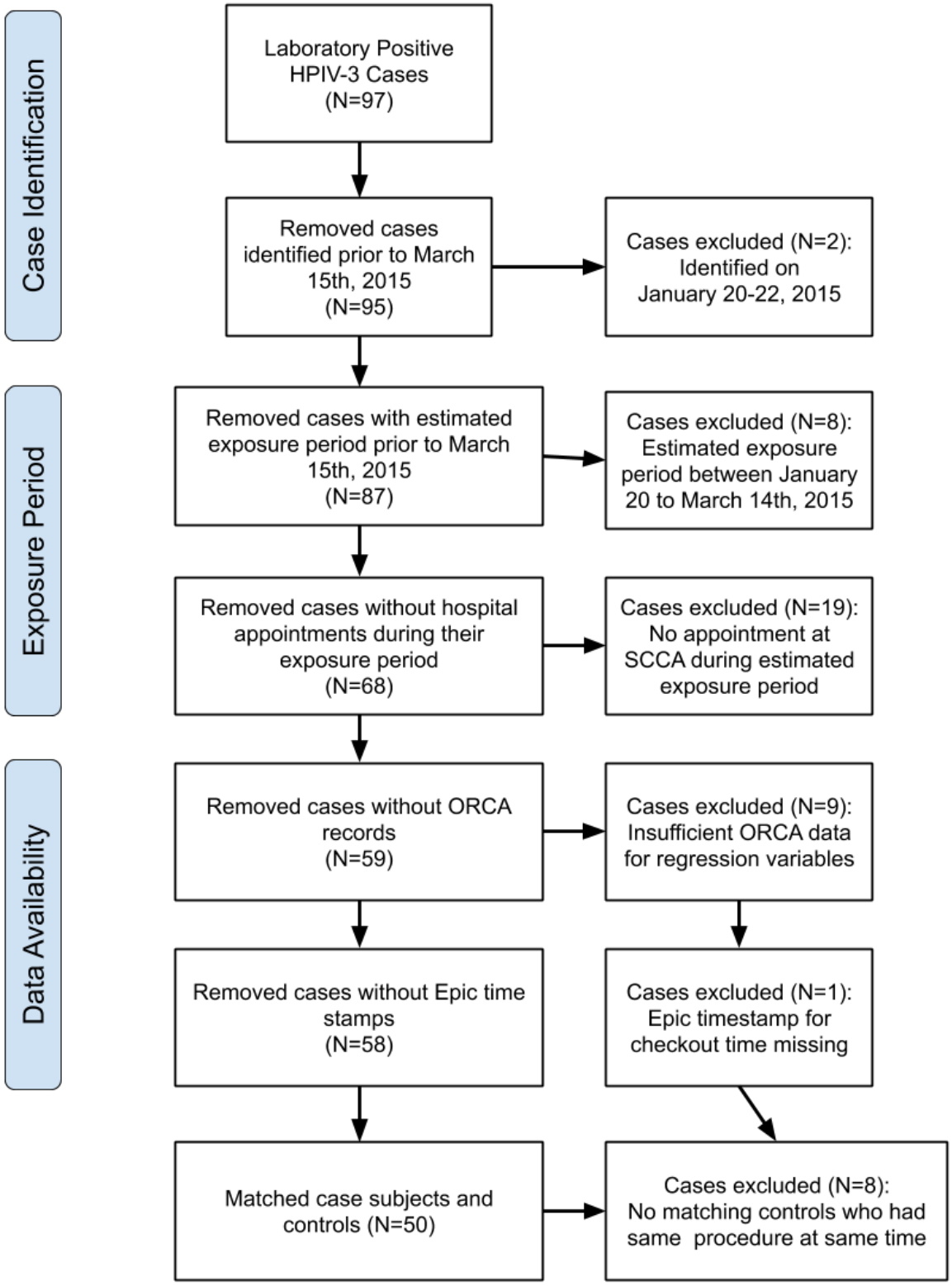

Figure 1.6.2: Flow chart of selection of cases for inclusion in the study and reasons for exclusion of some cases.

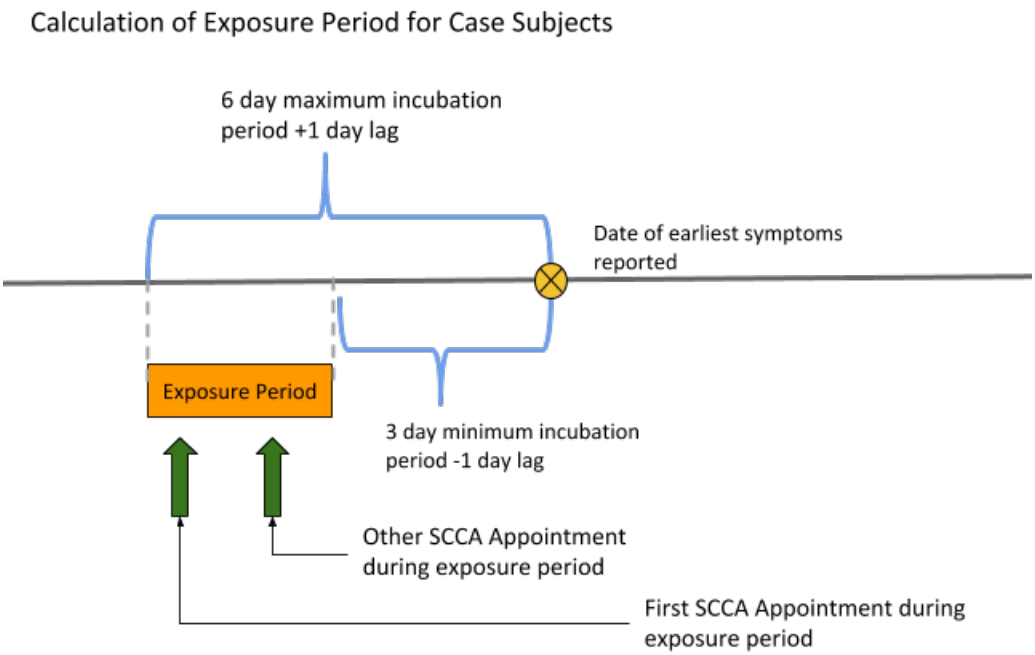

Figure 1.6.3: Diagram of the calculation used to estimated the exposure period based on the earliest reported symptoms, and the earliest appointment in the estimated exposure period.

Figure 1.6.4: Epidemiological curves of laboratory confirmed HPIV-3 cases (Red). The top graph shows all appointments attended by case subjects during their estimated exposure period. The bottom demonstrates the first appointment of the case subjects during their estimated exposure period–this latter set was used for the conditional regression analysis.

1.7 Supplementary Information

The following sections contain information on data cleaning and re-coding for the Online Record of Clinical Activity (ORCA) and EpicCare database, calculation of the estimated exposure period, and supporting information for the sensitivity analysis.

EpicCare data coding

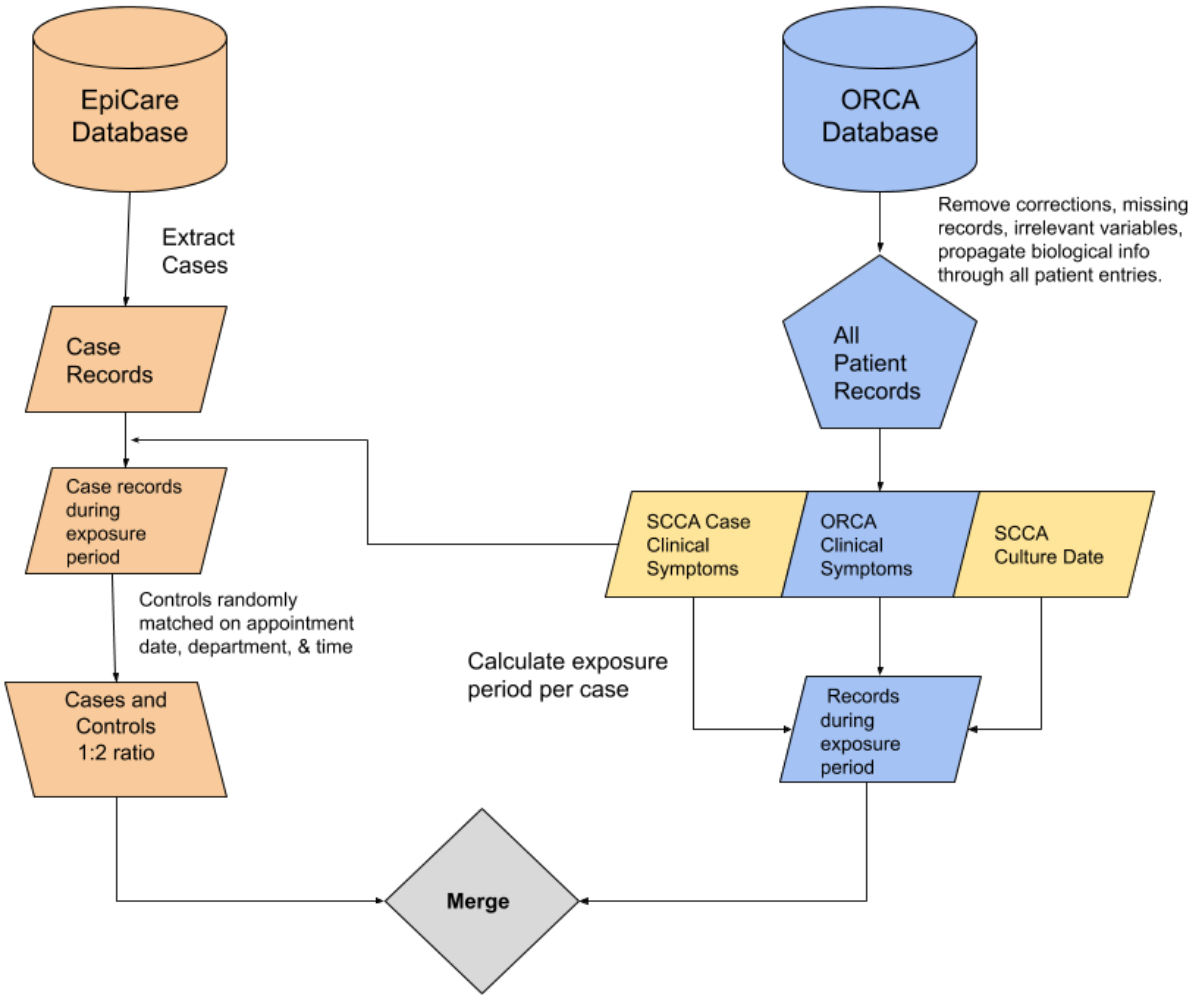

Figure 1.7.1: Diagram of the two data sources (EpicCare and ORCA) used to form the final analytic data set used in the conditional regression .

We collapsed procedures that were similar and would not affect the number of healthcare worker contacts or room allocation. For example an entry for 'CHEST XRAY' would be re-coded with the entry 'XRAY' as there would be no significant difference in location, room, or HCW contacts between the two. Several record entries had additional specific identifiers such as 'LH' or '1' to specify procedures performed by a specific provider. To have sufficient matches between case subjects and controls, and to include different locations (e.g. in the situation the same provider always uses the same location) these identifying initials were removed and the procedure name retained. In particular, procedures involving physical therapy had these identifying initials (e.g. PHY THERAPY NEW 60 LH, PHY THERAPY RET 60 HG) which we subsequently removed because there would not be enough control individuals who had the same specific physical therapy providers meaning most cases who received physical therapy would be eliminated from the analysis. Additionally the name of the physical therapy provider was usually coded into the treatment exposure category and it was not necessary to include it in the procedure category as well. Other procedure entries such as 'PLATELETS T' and 'PLATELETS' were not re-coded as the letter 'T' identified a similar procedure performed in a different location of the hospital. Entries separated by appointment duration (e.g. 'NUTRITION 1 30 MINUTES', 'RN ASSESSMENT-60') were collapsed into one term as duration of the procedure was accounted for by another covariate. A table displaying all procedure and department re-codes is displayed below:

Recodes for Procedures		
Entry 1	Entry 2	New Entry
HYDRATION 120 T	HYDRATION 180 T	HYDRATION 120-180 T
HYDRATION 150 T		
HYDRATION 240 T	HYDRATION 480 T	HYDRATION 240-480 T
HYDRATION 300 T		
HYDRATION 360 T		
BLOOD DRAW 6TH FLOOR	6TH FLOOR BLOOD DRAW	6TH FLOOR BLOOD DRAW
BLOOD DRAW 4TH FLOOR SCCA	4TH FLOOR BLOOD DRAW	4TH FLOOR BLOOD DRAW
PHY THERAPY NEW 60 CB		PHY THERAPY NEW 60
PHY THERAPY NEW 60 SF		
PHY THERAPY NEW 60 RD		
PHY THERAPY NEW 60 LH		
PHY THERAPY NEW 60 HG		
PHY THERAPY NEW 60 SI		
PHY THERAPY RET 60 CB		PHY THERAPY RET 60
PHY THERAPY RET 60 RD		
PHY THERAPY RET 60 SF		
PHY THERAPY RET 60 ET		
PHY THERAPY RET 60 LH		
PHY THERAPY RET 60 HG		
PHY THERAPY RET 60 SI		
RETURN 30		SCCA RETURN
RETURN 15		
RETURN 20		
NUTRITION - NWH		NUTRITION
NUTRITION 1		
NUTRITION 1 30 MINUTE		
NUTRITION 2		
NUTRITION 2-30 MINUTE		
NUTRITION 3		
NUTRITION 3-30 MINUTE		
XRAY	CHEST XRAY	XRAY
XRAY	SKELETAL XRAY	XRAY
REGISTER-*	REGISTER-T, REGISTER-WO, REGISTER-D etc	REGISTER
SCCA EKG-*	EKG-A, EKG-B, EKG-C, EKG-D etc.	SCCA EKG
RN ASSESSMENT*	RN ASSESSMENT-30, RN ASSESSMENT-60 etc.	RN ASSESSMENT
SCCA RECOVERY TIME*	SCCA RECOVERY, SCCA RECOVERY TIME-30, SCCA RECOVERY TIME-60 etc.	SCCA RECOVERY TIME
FINANCIAL COUNSELOR-1	FINANCIAL COUNSELOR-2	FINANCIAL COUNSELOR
INFUSION–NEW DRUG		INFUSION-NEW DRUG
BLOOD - 2 UNITS	BLOOD - 1 UNIT	BLOOD - 1 or 2 UNITS
BLOOD DRAW PICC	BLOOD DRAW PICC CLINIC	BLOOD DRAW PICC
CHEMO TEACH	CHEMO TEACHING	CHEMO TEACHING

where the asterisk * represents a wildcard string search

Recodes for Procedures		
Entry 1	Entry 2	New Entry
CHEST/ABD/PELVIS CT SCAN		
CHEST CT SCAN		
HEAD CT SCAN		
CT SCAN		
PELVIC CT SCAN		
SINUS CT SCAN		HEAD/CHEST/
PELVIC CT SCAN		ABD/PELVIS CT SCAN
NECK CT SCAN		
CT CHEST LOW DOSE SCREEN		
NECK/CHEST/ABD/PELVIS CT SCAN		
ABDOMEN & PELVIS CT SCAN		
ABDOMINAL CT SCAN		
Recodes for Departments		
SCCA SARCOMA CLINIC ML	SCCA SARCOMA CLINIC	SCCA SARCOMA CLINIC

where the asterisk * represents a wildcard string search

ORCA data coding

The ORCA database contained 1,756,791 records for the time period March 15, 2015- June 30, 2015. We extracted the 'Reason for Admission / Visit', 'Tobacco Use Status','Education Level', 'Marital Status - SW', 'Injury Risk - OFRIA', 'Age for Basal Energy Expenditure Calc', 'Age - OFRIA', and 'Present at the Visit'. Our variable for age was calculated using both 'Age for Basal Energy Expenditure Calc' and 'Age - OFRIA'. The variable 'Age for Basal Energy Expenditure Calc' listed the age of the patient in 2015, while 'Age - OFRIA' listed whether a patient was greater than or less than 60 years old. Combining both sets provided a new variables listing whether a patient was greater than or less than 60 years old. We created three new categories "Surgery w/in last 30 days", "Bone abnormality", and "Bleeding abnormality" from the Injury Risk data column. String searches of the Injury Risk column determined if a patient had a value of 'Yes' in any of the categories or a value of "None of the above = 0". For example if a patient had an entry for 'Injury Risk - OFRIA' of "Surgery w/in last 30 days = 1 , Bone abnormality" they would received a 'Yes' notation in the 'Surgery w/in last 30 days = 1' category and 'Bone abnormality' category, but an entry of 0 in the 'Blood Abnormality'.

Tobacco Use status and marital status were hypothesized to be confounders early on in the analysis, however we did not end up using them in the regression. For patient records who were missing entries for marital status, we used 'Present at visit'–a record of what family or friends accompanied a patient to an appointment–to fill in missing entries. We performed string searches for the terms 'husband', 'wife', and 'spouse' in the 'Present at visit' category. If a patient was visited by any of these individuals they were considered 'married'.

The subset of patients who were not considered married under the prior criteria had their records searched for the same terms 'husband', 'wife', 'spouse', 'widowed', 'widower', 'widow', 'divorced', 'engaged', 'fiancee' in an effort to ascertain their marital status. If these strings were not identified in any other aspect of a patient record we considered them single. The classification of 'significant other' was given to those who had this term explicitly added to their record under 'Marital Status - SW'.

1.7.1 Calculating exposure period

The SCCA Infection Control Department had recorded symptoms of HPIV-3 for 59 case subjects including the patient's estimated symptoms start date. The SCCA infection control department also recorded a case subject's earliest estimated symptom start date was used for calculation of their exposure period.

For the remaining case subjects who were not recorded by the infection control department we searched the ORCA records for the following word strings: 'rhino*' (short for rhinorrhea'), 'mucus', 'cold', 'recent', 'new', 'increasing', 'moist', 'secretions', 'runny', 'congestion', 'URI', and 'improving'. If a case-patient presented with respiratory symptoms but were later diagnosed with influenza or other respiratory viruses we did not make use of the dates associated with those symptoms. For example if an individual presented with rhinorrhea symptoms on March 6th, but on March 9th was diagnosed with influenza A/H1N1 we would not use the date of March 6th for our calculations. For the set of respiratory symptoms that were not associated with another respiratory illness, we took the earliest date of symptom identification and used it for calculating the estimated exposure period.

Although coughing was the most identified symptom among the SCCA infection control department recorded symptoms, the entries in the ORCA database which referred to coughing were not specific enough for HPIV-3 identification. ORCA entries often discussed 'dry' and 'unproductive coughs' or 'productive coughs', however the type of cough caused by HPIV-3 in immunosuppressed and non-immunosuppressed persons had not been well-defined. Additionally, trouble breathing is a common side-effect of chemotherapy and using 'cough' as a string search would not have been as specific as using 'rhinorrhea' or related symptoms as search strings.

1.7.2 Distribution of age among HPIV-3 cases

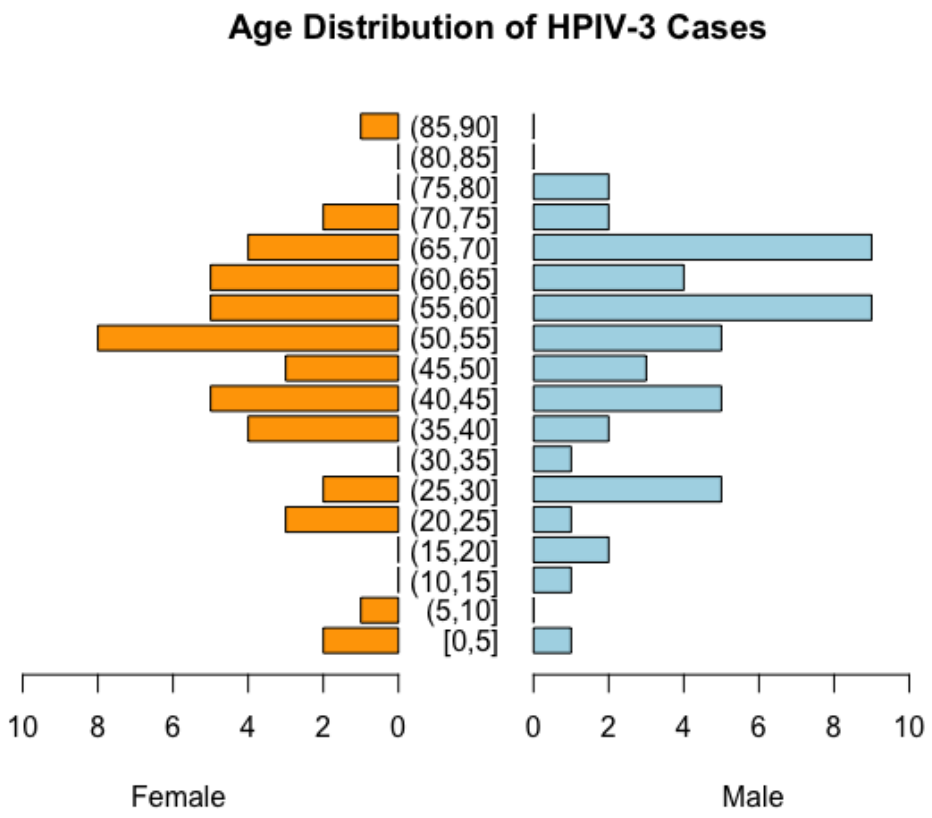

Figure 1.7.2: Distribution of age and sex among HPIV-3 cases. Comparison of the age distribution among males and females using the Student's t-test were not significant at the $p > 0.05$ level.

1.7.3 Directed acyclic graph

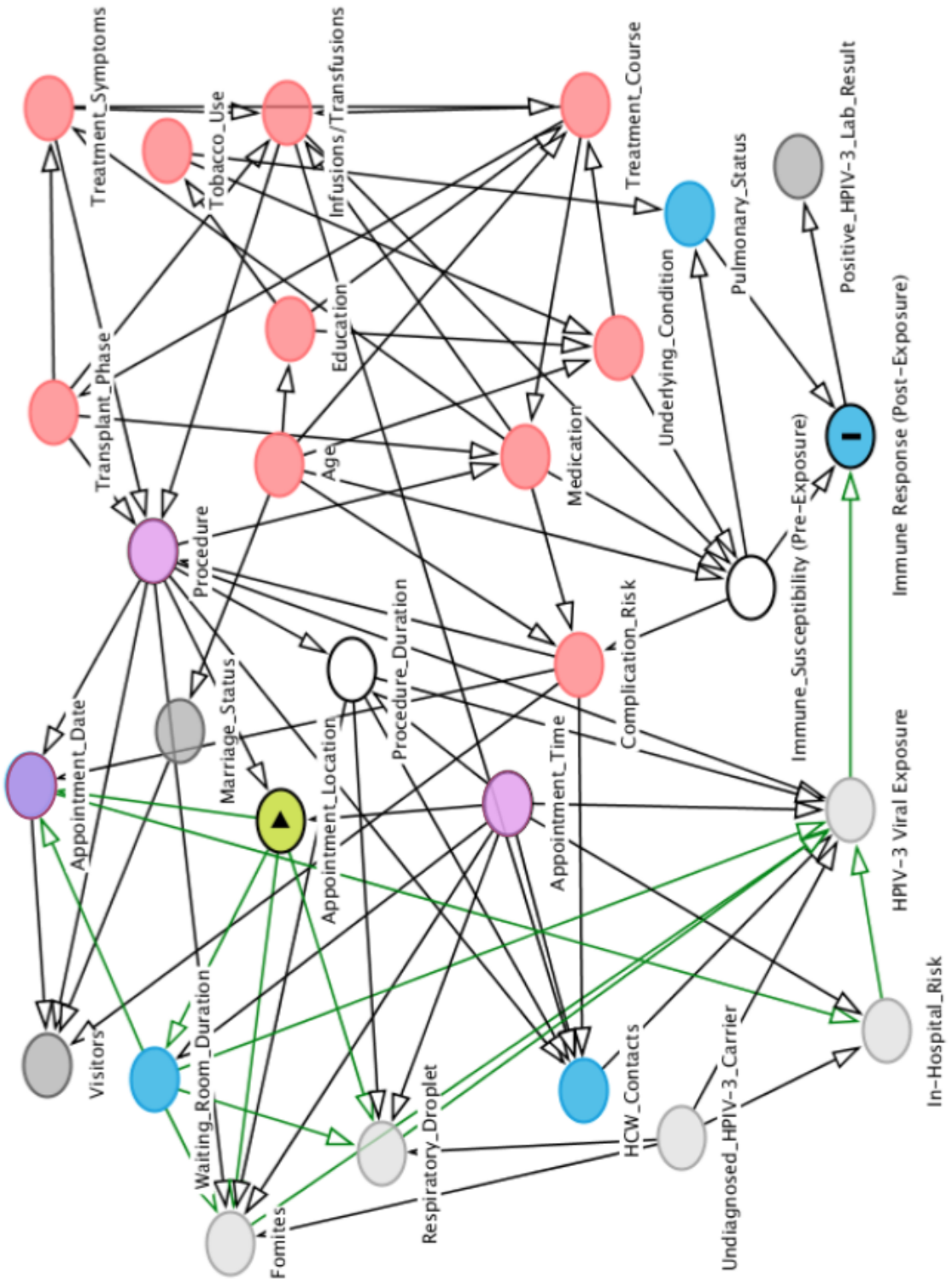

Figure 1.7.3: Directed Acyclic Graph (DAG)[9] made prior to the regression analysis to determine confounders on the causal pathway between exposure location and laboratory confirmed HPIV-3 diagnosis. Variables which have been adjusted for through regression are shown in white and variables used for matching are shown in purple. The variable labelled 'Complication Risk' stands in for Blood Abnormality, Bone Abnormality, and surgery within the last 30 days.

1.7.4 Diagram of the locations

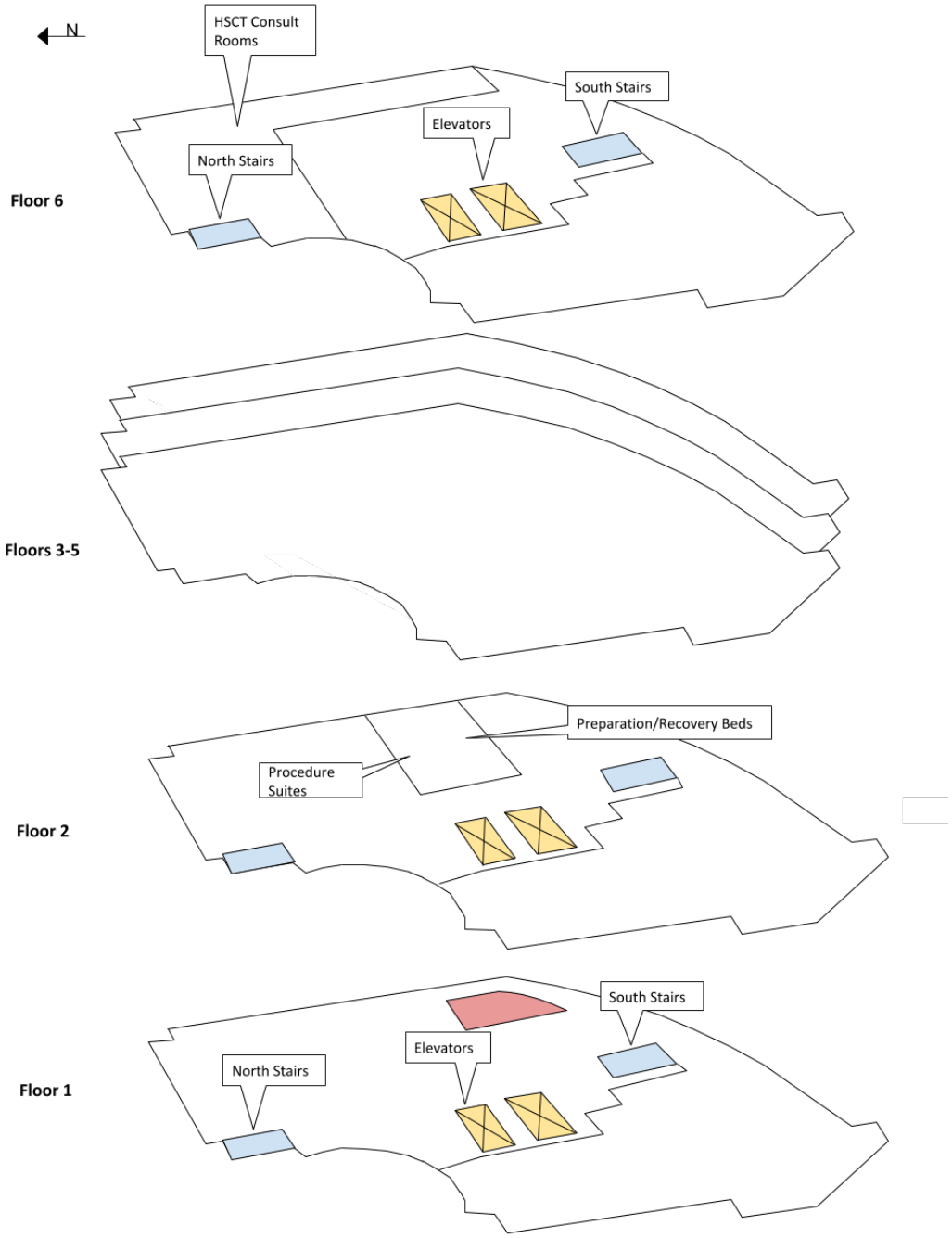

Figure 1.7.4: Floor-by-floor diagram of the hospital. Floors 2 and 6 contained locations that were associated with subsequent HPIV-3 infection. The two locations– Preparation/Recovery Beds and HSCT consultation rooms–are noted above.

1.7.5 Sensitivity analysis

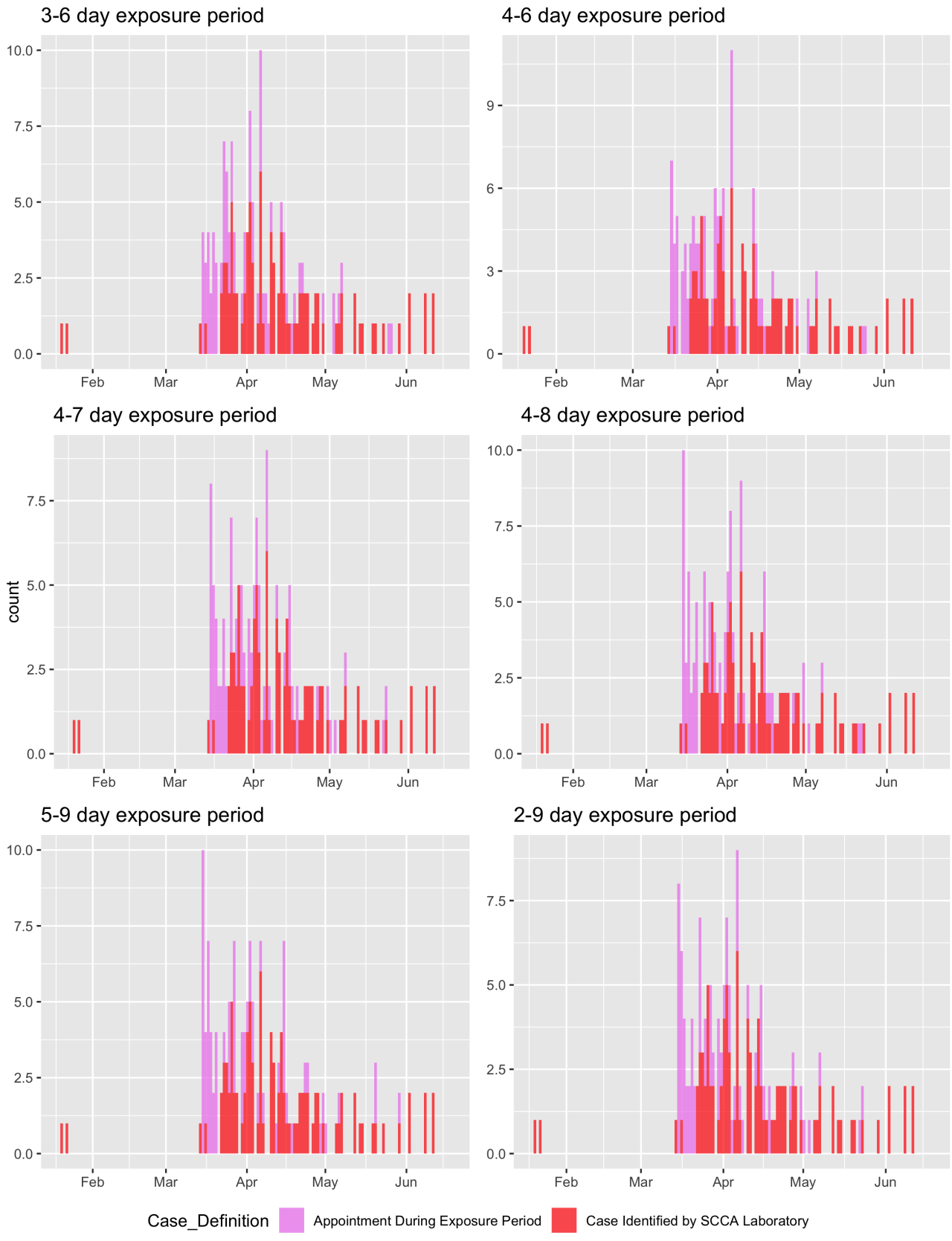

Figure 1.7.5: Comparison of the epidemiology curve for the first appointments for cases during their estimated exposure periods under varied maximum and minimum incubation periods used during the sensitivity analysis.

Chapter 2

Cost-Effectiveness of Live-Attenuated Influenza Vaccination Among School-Age Children

Abstract

Introduction: The current pediatric vaccination program in England and Wales administers Live-Attenuated Influenza Vaccine (LAIV) to all children ages 2-16 years old. Administering LAIV to all children in this age group annually is costly and poses substantial logistical issues. The present study aims to evaluate the cost-effectiveness of prioritizing influenza vaccination to different age groups within the 2-16 year old age range to mitigate the major operational and resource challenges posed by the current pediatric strategy.

Methods: We performed an economic evaluation comparing the historical influenza vaccination program from 1995-2013 to seven alternative strategies targeted at low-risk individuals along the school age divisions Preschool (2-4 years old), Primary school (5-11 years old), and Secondary school (12-16 years old). These extensions are evaluated incrementally on the status quo scenario (vaccination among subgroups at high risk of influenza-related complications and individual 65+ years old with empirical coverage levels). Impact of vaccination was assessed using a transmission model built and parameterized from a previously published study and updated with new virological, clinical, and epidemiological data. The study population is all individuals in England and Wales (52.6 million people) over 19 influenza seasons (1995–2013). Additionally, variation in vaccine coverage and its effect on the cost-effectiveness frontier and the rank order of interventions was evaluated.

Results: At all levels of coverage, all seven strategies had a 100% probability of being cost-effective at the current NHS threshold of £20,000 per 1 QALY gained. The incremental analysis demonstrated vaccinating 5-11 year olds (Primary School) was the most cost-efficient strategy compared incrementally against the others with an Incremental Cost-Effectiveness Ratio (ICER) of

£639 spent to gain 1 QALY (Net Benefit: 404 M£ [155, 795]). The probability a strategy was cost-effective was also less sensitive to changes in total achieved coverage when a strategy contained the 5-11year old age group. The optimal strategy–the strategy that maximizes the net health benefits– was the one, which distributed the most vaccine, vaccinating all individuals 2-16 year olds. Although school-age children were the target of vaccination the majority of QALY gains occurred in the 25-44 years old and 65+ age groups. Influenza strain A/H3N2 incurred the greatest health care costs and QALYs lost regardless of which intervention strategy was used.

Conclusions: Strategies that include vaccination of the 5-11 year old age group (Primary School) children are more likely to be very cost-effective (<£15,000 per QALY gained). In order, Primary school and secondary school children (12-16 year olds) are the priority vaccination subgroups. Improvement could be made to the current LAIV pediatric vaccination strategy by eliminating LAIV vaccination of 2-4 year olds and focusing on school-based delivery of LAIV to Primary and Secondary school-age children in tandem.

2.1 Introduction

In 2013, England and Wales began the phased extension of their seasonal influenza program, which recommended low risk children aged two to 16 be vaccinated with Live-Attenuated Influenza Vaccine Nasal Spray (LAIV) (Fluenz Tetra®) nasal spray.[16, 17] However, by 2025, when the pediatric program reaches full capacity, administering LAIV to all children will pose substantial economic and logistical issues. The 2019/2020 season will phase in school year six (11 year olds) to the existing program. To maintain herd immunity at 55% total coverage, the pediatric program will need to distribute an additional 375,000 LAIV doses to the 11 year old children between September and December. The increasing scale of this annual pediatric program, relying on trained nurses and a school-based delivery method, will be prohibitively demanding of National Health Service (NHS) resources. Prioritizing certain age groups within the 2-16 year old range will mitigate some of the implementation challenges of the strategy.

The basis for the pediatric program is a dynamic model by Baguelin et al.[18] It determined that the LAIV immunization of 2-16 year olds would indirectly decrease the force of infection in the general population; however, the previous analysis did not directly address school age subdivisions. That study included two pediatric interventions among other adult interventions and identified 5-16 year olds as the 'key drivers' of seasonal influenza epidemics.[19, 18] At the time, there was also insufficient data to examine seasons 2010-2014 and to integrate the vaccine uptake rates from 1995-2014. Therefore, there is a need for updated optimal vaccine strategy recommendations.

In this study we evaluate whether, in light of new age-specific data on influenza incidence, the current LAIV pediatric influenza program in England and Wales should be altered. Specifically, we examine whether targeting vaccination at the school-age subdivisions of preschool, primary school, and secondary school age groups has greater cost-utility than the programs in use from 1995/96-2013/14. Our expansion on the study by Baguelin et al.[18] includes updates to the surveillance and epidemiological data, additional age specific stratification, and vaccine uptake rates per month from 1995-2014.

2.2 Methods

2.2.1 Mathematical model

The direct and indirect vaccine effects of seasonal influenza immunization programs were evaluated using a previously described transmission model 'fluEvidenceSynthesis' calibrated to surveillance data from England and Wales.[20] The latest version of the 'fluEvidenceSynthe-

sis' package contains a modified Susceptible-Exposed-Infectious-Recovered Compartmental Model (SEIR) differential equation model which was used to simulate influenza infections, influenza-related complications, and resultant costs for each age strata and risk class.[20] Baguelin et al. used seven age groups which we have expanded to eleven age groups on the following intervals: 6 months-<1,1, 2-4, 5–11,12-14, 15–16, 17-24, 25–44, 45–64, 65-74, 75+ years old. Two risk strata for simulating high and low risk groups were included. In each age stratum the final SEIR model contains 22 separate age-risk strata. We considered the three influenza strains A/H1N1, A/H3N2, and B in our analysis.

2.2.2 Model calibration and data sources

The analysis was coded in R (version 3.5.0) [8], using R Studio (version 1.1.453) with the R package 'fluEvidenceSynthesis'.[21] The R package 'fluEvidenceSynthesis' model (version 1.0.0) has been revised from the developmental version previously used by Baguelin et al. and the previous package published on Github by van Leeuwen.[20, 21] Each of the 19 influenza seasons and three strains were fit independent of other seasons and strain. Each season used two chains for a total 38 Markov chain Monte Carlo (MCMC) calibrations per strain. Chain convergence was determined with the Gelman-Rubin diagnostic test using a potential scale reduction factor adjusted for sampling variability threshold of 1.2 or below for the nine parameters of interest. Any season that did not converge based on the Gelman-Rubin diagnostic was restarted with the last value of the previous Markov chain and the two chains were run for an additional 200,000 iterations. For most seasons approximately 1.4 million iterations were needed to achieve convergence.

Parameters of interest were the ascertainment probability (ϵ_i, i=0-14 years old, 15-64 years old, 65+ years old), virus transmissibility (q), the probability of becoming infected outside of the main epidemic (ϕ), age-group specific susceptibility (σ_i, i=0-14 years old, 15-64 years old, 65+ years old), and a coefficient for the initial number of infections each season (t) per strain ($I_{0,t}$). Prior distributions for epidemiological parameters are shown in (Supplemental Table 2.6.1). Further detail on the model construction and the R package have been described in earlier papers.[18, 20, 19]

The likelihood distribution for the MCMC summarized surveillance data from two sources: the number of weekly Influenza-like-illness (ILI) age-specific General Practitioner (GP) consultations, and the frequency of virologically-confirmed cases per week. For the period 2009/2010-2013/2014, we used a custom inference function in the R package to add the extra age classes from the data to the binomial and hypergeometric likelihood.

Respiratory Virus Royal College of General Practitioners Research and Surveillance Centre (RCGP)

During weeks of potential influenza activity, the Royal College of General Practitioners Research and Surveillance Center (RCGP) takes samples from patients with an ILI and records the weekly incidence of consultations among sentinel general practices across England.[22] We obtained the size of the monitored population in the sentinel network, and the total number of patients who consulted General Practitioners for an ILI. Additionally, we obtained the number of laboratory samples tested for suspected ILI cases, and the number of lab positives for influenza strains A/H1N1, A/H3N2, and B

Social mixing between groups

Social mixing parameters among the additional age groups were estimated using data from a pan-European survey of contact structure known as POLYMOD.[23] Survey data from the Great Britain (GB) cohort was sampled with replacement to generate multiple 11x11 contact rate matrices, where each cell describes the interaction frequency between age groups.[18] Further details are described in earlier papers.[20, 24]

Vaccine coverage updates

For the period 1995/1996-2003/2004 the total number of persons vaccinated was sourced from Joseph et al. and Health Protection Agency (HPA) reports[25, 26], however previous models did not include vaccine uptake rates. For this analysis, we included age-group stratified empirical data on Trivalent Inactivated Influenza Vaccine (TIIV), Quadrivalent Influenza Vaccine (QIV), and LAIV vaccine coverage for the remaining years 2004/2005-2013/2014, as well as the empirical rate per month or year that this coverage was achieved for the period 1995/1996-2013/2014. [27, 28, 29].

2.2.3 LAIV interventions

Using the posterior distributions of the calibrated model, we assessed the influenza incidence in England and Wales in the presence of seven vaccination programs targeted at school-age cohorts. The effectiveness of each alternative program was assessed by measuring the Quality-Adjusted-Life-Years (QALY) lost, number of febrile/symptomatic cases, and infection-related mortality prevented by one vaccine dose. In addition to a status quo strategy, we analyzed an additional 21 strategies. The 21 strategies were the seven basic strategies given below, and incremental extensions of them at 30%, 55%, and 70% final coverage levels,

representing the lower bound, average level, and upper bounds of empirical coverage. LAIV vaccination programs were simulated starting on September 1st, the usual start of the fall session, and ending on December 12, a week before the Christmas holiday.

1. SQ (Status Quo): Influenza vaccination program includes Low-Risk 65+ year olds, and high risk individuals in the age range 6 months to 65+ year olds vaccinated with TIIV or QIV at empirical coverage rates.

2. I1: Status Quo Strategy (SQ) + Low-risk Preschool aged children (2–4-y-olds) vaccinated with LAIV at 30%, 55%, 70% coverage.

3. I2: SQ + Low-risk Primary School aged children (5–11-y-olds) vaccinated with LAIV at 30%, 55%, 70% coverage.

4. I3: SQ + Low-risk Secondary School aged children (12–16-y-olds) vaccinated with LAIV at 30%, 55%, 70% coverage.

5. I4: I1+I2+SQ, i.e., combination of Status Quo, and scenarios 1 and 2.

6. I5: I1+I3+SQ, i.e., combination of Status Quo, and strategies I1 and I3.

7. I6: I2+I3+SQ, i.e., combination of strategies I2 and I3.

8. I7: I1+I2+I3+SQ, i.e., combination of strategies 1, I2, and I3.

LAIV efficacy

Vaccine Efficacy (VE) is dependent on two factors: (1) the degree of matching between vaccine strain and circulating strain that season, and (2) the quality of immune response generated in the host. High risk groups such as the immunocompromised and elderly subgroups are known to have increased susceptibility to disease and a poor immune response to the influenza vaccine resulting in low efficacy. Each age stratum was divided into individuals at low or high risk of complications associated with influenza (e.g. individuals with chronic conditions). We assumed the proportion of people in a risk group stratified by age is constant from 1995-2014 (Table 2.6.2). Following NHS 2018/2019 guidelines, our model assumed high risk individuals aged 6 months-2 years old and adults 18-64 years old received QIV.[30] Individuals aged 65+ years received TIIV.

We do not use empirical VE estimates, instead we use two average VE estimates from the Cochrane collaboration[31] to emulate strain matching between the vaccine and wild-type strain during poor and well-matched years. When the vaccine was well-matched with the

annual circulating strain VE was fixed at 70% in the general population and 42% in the clinical high risk and 65+ year old group. During poorly matched years we assigned 40% VE for the general population and 28% VE in the high risk and elderly group. We did not make specific allowances for differences in VE between the three vaccine types: LAIV, QIV, and TIIV. We assumed the 'all-or-nothing' mechanism of VE with a maximum protection period of one year. Likewise disease derived immunity lasted for one year maximum.

For the 1995-2009 period strain-matching information was taken from Public Health England (PHE), then HPA.[26] The degree of matching between the circulating and vaccine strains for the 2009/2010-2013/2014 seasons were obtained from PHE estimates (Table 2.6.4). We considered each influenza strain independently and calculated their cumulative clinical and economic effects as it is currently unknown how influenza strains interact within-host and within-population.

Health outcomes

This analysis was conducted from the perspective of the NHS/PHE using a one year time horizon recurring on September 1st. The discount rate, reflecting the fact that people prefer to receive benefits and save costs in the present relative to the future, were calculated annually at 3.5% as recommended by the National Institute for Health and Care Excellence of England and Wales (NICE).[32] Additionally we conducted a one-way sensitivity analysis at discount rate levels 0%, 1.5%. The estimated number of health outcomes and the commensurate QALY were calculated per influenza season and averaged across the 19 seasons during the subsequent cost-effectiveness analysis.

To account for uncertainty in the estimated number of different health outcomes attributable to influenza per year, we sampled the normal distributions from Cromer et al.'s regression analysis (Table 2.6.2).[33] Health outcomes examined included number of infections, number of symptomatic infections, influenza-related GP consultations, hospitalizations and mortality. We did not control for non–influenza-related complications or other confounding variables such as income, education, ethnicity, and number of co-morbidities.

The primary health-related quality of life measure for the analysis were QALY. Individuals with symptomatic influenza experienced an age-specific reduction in QALYs. Similarly, individuals infected with influenza who were hospitalized experienced a commensurate age and risk-specific quality of life loss. Fatal influenza infections were assumed to lose an age and risk-group specific discounted quality-adjusted life expectancy. Age-specific quality of life weights for respiratory illnesses were taken from Kind et al., using the EQ-5D rating scale (Table 2.6.3).[34] Average weights for children less than 18 years did not exist, therefore we estimated their average health-related quality of life weight as 0.9 based on estimates from

the 18–20 years old group.[19]

Health-related costs

Two elements of costs were included in the analysis. The first cost element was use of health services during the influenza season for the whole population of England and Wales. This was based on the calculated number of annual clinical cases, the number of general practitioner consultations, and the number of inpatient hospitalizations. The second element was the total cost per dose of vaccine acquisition, service, and provider reimbursement. We calculated the costs of influenza vaccine delivery through pharmacies, GP, and school-based programs from the NHS perspective. A summary of economic costs appear in Table 2.5.1 expressed in 2018 British Pounds Sterling. If costs were not available for the current year, costs from previous years were updated to 2018 British Pounds Sterling using the Consumer Price Index for Health Costs [35]. We assumed that services for waste disposal and sharps removal for all delivery methods–except school-based vaccination–were managed and paid for directly by the NHS with no additional cost. Productivity losses were not incorporated into the analysis.

Units of vaccine administration costs were obtained from previously published studies, and from PHE/NHS budget documents when available (Table 2.6.6). Differences in vaccine deployment costs were dependent on the age group targeted by the specific strategy and the coverage achieved. For example, in strategy S4 preschool (2-4 years old) and primary school aged children (5-11 years old) are targeted for vaccination. Low-risk preschool aged children would receive LAIV from their GP and incur the GP delivery cost, while low-risk primary school children receive school-based LAIV delivery and incur the school-delivery cost. Total Costs per vaccine dose administered were calculated as the sum of NHS vaccine service payment, the vaccine purchase payment, and dependent on the method of administration a delivery fee, Sonar reporting system fee, and disbursement fee. Further discussion on the vaccine cost derivation is in supplemental section 2.6.6.

Cost-effectiveness analysis

For each non-dominated strategy the Incremental Cost-Effectiveness Ratio (ICER) was calculated using the formula

$$ICER = (C_S - C_C)/(Q_C - Q_S)$$

where C_S is the predicted total of health care and vaccination costs and C_C the same total for its comparator. The predicted QALY losses for a strategy and its comparator are denoted as

Q_S and Q_C. The comparator of a strategy is the next non-dominated strategy with the next lower incremental cost. Using the average estimate of costs and QALY, strategies for which an alternative strategy would avert more QALYs at equal or lower cost were considered 'strongly dominated' and excluded. Strategies with a mean ICER that is higher than the ICER of a more costly strategy were deemed weakly dominated and excluded. ICER for the remaining strategies were then recalculated accordingly. We used the remaining strategies to define the cost-efficiency frontier of the cost-effectiveness plane.

Optimal strategy

The Cost-Effectiveness Acceptability Curve (CEAC) indicates the probability that an intervention is cost-effective compared with an alternative given the observed data for a range of willingness to pay values.[36] Costs and effectiveness for each strategy were derived from 2500 parameter sets drawn from the joint posterior distribution over Willingness-to-pay threshold (WTP) range of £1 to £30,000 per QALY.

To determine the optimal strategy, we conducted a probabilistic sensitivity analysis using a Net Health Benefits (NHB) approach. The NHB is calculated by first assuming a willingness to pay threshold, then converting monetary benefits 2018 British Pounds Sterling into the common metric of QALYs:

$$NHB = E - C/\lambda$$

where λ = decision-maker's willingness-to-pay per QALY gained; E = total annual QALYs lost to influenza; C = total annual healthcare costs. This process is repeated in 2,500 model simulations to estimate the probability a strategy is optimal. The optimal vaccination strategy was determined based on the proportion of parameter sets with the highest NHB across a willingness-to-pay range of £1 to £30,000 per QALY on increments of £250. The optimal strategy may vary from simulation to simulation as a consequence of parameter uncertainty.

2.3 Results

Our results suggest strategies which include primary school LAIV vaccination (5-11 years old) are more likely to be associated with cost-effectiveness. Potential replacement strategies to the current vaccination program are presented in the seven right hand columns of Table 2.5.2 ordered by net cost. We compared Strategies I1-I7 to the current NHS WTP threshold (£20,000 per QALY gained)–the amount the NHS is willing to pay for one QALY gained. This revealed all strategies had a 100% probability of being cost-effective at the

£20,000/QALY WTP threshold (Figure 2.5.1, Panel B). Strategies I2, I4, I6, and I7 were 100% likely to be cost-effective at £8,000/QALY, while Strategy I1 was the least likely to be cost-effective reaching 100% at at cost of £16,000/QALY. Next we used an incremental analysis to compare cost and health outcomes between all strategies. The incremental analysis demonstrated Strategy I2 was the most cost-efficient strategy compared incrementally against the others. The ICER for I2 was estimated at £639 spent to gain 1 QALY (Net Benefit: 404 M£ [155, 795]), well below the NHS threshold. (Table 2.5.3) The incremental analysis also demonstrated Strategy I5–vaccinating preschool and secondary school age children–was strongly dominated by Strategy I2 as I2 was both less expensive and more effective.(Figure 2.5.2) Although Strategy I2 was the the most cost-effective in the incremental analysis, Strategy I7 was determined to be the optimal strategy–the strategy which maximizes the net health benefits–in 44% of the simulations (Figure 2.5.1, Panel A). The next closest strategy was I6 which was optimal for 26% of simulations. Strategies I1-I3 were optimal for less than 10% of simulations suggesting these strategies are cost-effective but rarely optimal. No changes in the optimal order were observed for WTP>£20,000 per QALY. For less than £20,000 per QALY the status quo strategy was a contender for optimal strategy until WTP=£5250/QALY where it fell below 1% probability of being optimal (Figure 2.5.1, Panel A).

2.3.1 Cost outlay For vaccination programs

The total cost outlay – the sum of the vaccine purchase and the vaccine administration–of each strategy increased with the level of coverage and the size of the target vaccine population (Section 2.6.7). For example strategy I1 (2-4 year olds) is the least expensive intervention and I7 (2-17 year olds) is the most expensive. The cost-outlay for interventions which included school-based delivery among ages 5-11, or 12-16 were more expensive than those that included 2-4 year olds as school-based vaccine administration has the highest cost–£20.14 per LAIV dose. Aside from strategy I5, more expensive interventions that distributed more vaccine were more effective in reducing incidence and associated costs than the cheaper strategies. For example Strategy I7 (2-16 year olds) had the lowest annual GP and hospitalization costs, and I7 had the highest net-benefit among the interventions due to the large number of averted cases and deaths (Table 2.6.8). Although school-age children were the target of vaccination the majority of QALY gains compared to the status quo occurred in the 25-44 year old and 65+ age groups (Supplemental Section2.6.10).

2.3.2 Sensitivity analysis

We used a one-way sensitivity analysis to determine how robust each proposed strategy would be to changes in the discount rate and total achieved coverage. We compared intervention strategies side-by-side at 30%, 55%, and 70% total coverage, and at discount levels 0%, 1.5% and 3.5% (Table 2.5.3. Increasing the discount rate from 0% to 3.5% and fixing coverage at 55% resulted in increased cost per QALY gained and minor decreases to the overall net benefits (Table 2.5.2).

At all levels of coverage, strategies I1-I7 had a 100% probability of being cost-effective at the current NHS WTP and at the more conservative WTP of £15,000/QALYs gained (Figure 2.6.9). However uncertainty around cost-efficacy became more pronounced when coverage levels were varied. For example the acceptability curve for strategies I1 and I3 were insensitive to changes in total coverage, whereas increasing coverage for strategies I4, I7, and I6 increased the WTP level to achieve the same probability. Strategies which contained the 5-11 year old age group such as I2 (5-11 year olds) and I6 (5-16 year olds) achieved 100% probability of being cost-effective at WTP £7250/QALY at coverage levels of 55% and 70%. Likewise strategies I4 (2-11 year olds) and I7 (2-16 year olds) achieved 100% probability at WTP £7500/QALY gained. At 30% total coverage, where fewer vaccines were purchased and distributed, strategies had a higher probability of being cost-effectiveness at lower costs per QALY gained. Across seven strategies 70% coverage was determined to be the optimal strategy in 50% of simulations at WTP £20,000/QALY.

The probability a strategy was optimal, and its subsequent rank order in terms of the optimal strategy were generally insensitive to the change in discount rate. Under all coverage and discount levels the optimal strategy was consistently strategy I7 (Figure 2.6.11). Strategy I7 was very sensitive to increases in coverage gaining an additional 20-25% probability of being optimal with increases from 30% to 55% and 70% coverage. Conversely Strategy I6 (5-16 year olds) remained constant with 21-22% probability of being optimal when total coverage was increased from 30%-70%. The probability any remaining strategies I1-I5 were optimal decreased with as coverage increased.

Strain-specific differences

Under 55% achieved coverage each strain demonstrated a strain-specific cost-efficiency frontier (Figure 2.5.2. This indicates some strategies were more effective for some strains than others. The A/H3N2 cost-efficiency frontier most-resembled the frontier created from all three strains. Influenza strain A/H3N2 incurred the greatest health care costs and QALY losses regardless of which intervention strategy was used (Figure 2.6.8). Prevention of

A/H3N2-related health care and economic outcomes with interventions I1-I7 rendered all interventions cost-effective with a probability of 99% at £15000/QALY WTP at every discount and coverage level considered. Strains with lower severity like A/H1N1 rendered it the strain least likely to be associated with cost-effective estimates with an average 10% of simulations failing at £15000 willingness-to-pay threshold (Figure 2.6.9). Interestingly, among the three strains, strain B incurred the greatest number of GP consultation fees with an average £15.3 million spent annually at 55% coverage.

Fixing coverage at 70% and examining all three discount levels, revealed that for strain B and A/H1N1 less expensive strategies such as I1-I3 were associated with favorable cost-effectiveness outcomes. More expensive strategies such as Strategy I7 (2-16 year olds) were often weakly dominated by I2, I4, or I6. (Supplemental Section 2.6.16) Strategy I5 was strongly dominated in every sensitivity scenario except for strain A/H3N2 at 1.5% discount rate and 70% coverage.

2.4 Discussion

After examining seven school-age vaccine strategies, we conclude the most efficient way of reducing seasonal influenza-attributable morbidity and mortality in the United Kingdom (UK) is to use strategies that include the key school-age cohort: Primary School children (5-11 year olds). Vaccination of only the 5-11 year old age group is cost-effective at the NHS WTP, however strategies which were most cost-effective combined vaccination of this cohort with an age group directly above or below it. Depending on the resources available the NHS should consider priority groups for seasonal influenza vaccination as follows:

1. Adults aged 65 or older and persons aged 2-64 years with underlying chronic medical conditions (including pregnant women).

2. Children aged 5-11 years old via school-based vaccine delivery.

3. Children aged 12-16 years old via school-based vaccine delivery.

4. Children aged 2-4 years old via GP based vaccine delivery.

In the 2019/2020 influenza season school-based vaccine delivery will expand to include 11 year olds, remaining in the 5-11 year old age range. Our recommendations for the ongoing pediatric vaccination program is that the school-based vaccine delivery continue its phased introduction among 5-11 years old up to and including 12-16 year olds. Simultaneously LAIV vaccination of 2-4 year olds should be phased out.

Strategy I6–vaccinating children in primary school and secondary school–decreased QALYs lost from all sources to a level comparable to that of the 2-16 year old strategy (Figures 2.6.6, 2.6.7, 2.6.8). This strategy was also robust to variation in coverage rate remaining cost-effective at well below £15,000 per QALY gained for coverage as low and high as 30% and 70%. Strategy S6 has the advantage of reducing the implementation cost and complexity of a more expensive interventions like I7 (2-16 year olds) while delivering an equivalent amount of QALYs gained. The 2-4 year old age-group under interventions where 5-11 year olds were vaccinated with LAIV (strategy I2 and I6) had indirect protection equivalent to strategies where 2-4 year olds had direct protection as the vaccine target. The conclusions of our study are consistent with seasonal influenza studies from other countries[37, 38, 39] and previous research in the UK,[19, 40, 41, 42] which concluded that pediatric vaccination is effective at reducing morbidity and mortality in the wider population. School-age children have high rates of viral transmission due to little pre-existing immunity and increased exposure potential within their contact network.

School-based delivery of LAIV vaccine was calculated to have the highest cost per dose among the available delivery methods (Supplemental Section 2.6.6). Key contributors to the increased costs of the interventions were the increase in vaccine purchase price, the increased cost of hospitalization, and inclusion of waste disposal, administration, and travel costs associated with school-delivered LAIV sprays. Despite the initial increase in cost to implement the school program, we predict the total cost will slightly decrease over time as vaccine services (e.g. vaccine administration, waste disposal) are streamlined and integrated into the common practice of the NHS. Furthermore slow LAIV uptake wastes vaccine doses by inducing immunity in children too late to have any indirect effect on the wider population transmission.[43] Two to four year olds receive LAIV doses at GP offices which may result in slower vaccine uptake during the critical period between the start of the school season and the start of the influenza season. Administration of LAIV among 5-16 year olds would use the school-based delivery strategy allowing for greater oversight and a swift, regimented schedule of distribution in the available time window.

Finally, increasing research and therapeutic interventions for individuals diagnosed with influenza A/H3N2 may produce further cost-savings for the NHS in the long-term. Hospitalization costs from A/H3N2 were triple those of other strains (Figures 2.6.5). We also considered the cost-savings of changing the LAIV sprayer size because only 30% of the total sprayer holds vaccine (Section 2.6.7). However waste disposal is a minor fraction of the total cost per dose, and any expense reduction from sprayer size was already captured in the lower bound of the LAIV cost per dose distribution.

One limitation is that, although we have conducted extensive sensitivity analysis, sub-

stantial changes to influenza epidemiology may render the examined strategies suboptimal during future seasons. Our model is calibrated for seasonal influenza strains, meaning the final recommended strategy may not be robust to the high transmission intensity of pandemic strains (e.g. A/H5N1). Influenza viruses undergo antigenic changes and the benefits of vaccination are dependent on the seasonal components of VE. End-of-season results for 2017/2018 vaccine effectiveness against laboratory confirmed influenza estimated an all strain LAIV effectiveness among low-risk 2-17 year olds as 26.9%.[44] Vaccine effectiveness is generally lower than VE, meaning that our point estimate of 42% for poorly matched years may be an overestimate for some poorly matched years.

The sensitivity of cost-effectiveness recommendations to variation in social contact patterns has not been well-established. Given the small margins between the considered interventions, variation in contact rates, costs, or population age structure could render a strategy that was dominated in Great Britain cost-effective elsewhere. We caution against explicit mapping of the United Kingdom pediatric vaccination program to another setting without adjusting the cost and social contact parameters.

The LAIV pediatric program remains an innovative strategy for tackling seasonal influenza virus by exploiting its dependence on children as key spreaders and should continue deployment. In anticipation of the demands the LAIV pediatric program will put on the NHS at full capacity we have conducted a cost-effectiveness analysis to determine which school age groups should be prioritized in pediatric vaccine distribution. We recommend continuing the vaccination of high risk groups (e.g. chronic conditions) and 65+ year olds in tandem with any school-delivery strategy that includes Primary school (5-11 year olds) aged children. Our cost-effectiveness analysis for England and Wales concluded that an intervention targeted at 5-16 year olds would maximize QALYs gained for the lowest cost, allowing 2-4 year olds to be phased out. It remains to be seen if there are further age groups within the Primary school age cohort that should be prioritized during seasonal influenza vaccination in England and Wales.

2.5 Tables and Figures

2.5.1 Tables

Economic Parameter Table				
Item	**Estimate**	**Uncertainty**	**Inflation Adjustment**	**Source**
Cost of vaccination				
School-Delivery (per dose)	£20.14	Triangle(a=17, b=25, c=20.14)	None	Derived (Table 2.6.6)
Pharmacy Delivery (per dose)	£17.29	Triangle(a=14, b=22, c=17.29)	None	Derived (Table 2.6.6)
GP Delivery (per dose)	£19.66	Triangle(a=17, b=25, c=19.66)	None	Derived (Table 2.6.6)
Healthcare Costs				
Hospital cost (per episode)	£911	Lognormal (normal μ = 911, normal σ = 215)	1.085	[18]
GP cost (per consultation)	£39	Lognormal (normal μ = 39, normal σ =8.6)	1.046	[18]
Healthcare Provider Costs				
NHS Nurse Salary (per hour)	£36	–	None	[45]
NHS Band 1 Driver (per hour)	£9.88	–	None	[46]

Table 2.5.1: Economic parameters used to estimate intervention costs and costs to the National Health Service as a result of influenza infection. Here 'GP' denotes General Practitioner, 'NHS' National Health Service. Inflation adjustments for medical services sourced from King et al.[35]

Intervention Strategy	I1	I2	I3	I4	I5	I6	I7
Age Groups Vaccinated	**I1: Low-Risk 65+ , High risk 6 months-65+ 2-4 year olds**	**I2: Low-Risk 65+, High risk 6 months-65+ 5-11 year olds**	**I3: Low-Risk 65+, High risk 6 months-65+, 12-16 year olds**	**I4: Low-Risk 65+, High risk 6 months-65+, 2-11 year olds**	**I5: Low-Risk 65+, High risk 6 months-65+, 2-4 & 12-16 year olds**	**I6: Low-Risk 65+, High risk 6 months-65+, 5-16 year olds**	**I7: Low-Risk 65+, High risk 6 months-65+, 2-16 year olds**
Targeted School-Age Cohort	**Preschool**	**Primary School**	**Secondary School**	**Preschool, Primary School**	**Preschool, Secondary School**	**Primary School, Secondary School**	**Preschool, Primary School, Secondary School**
a) 3.5% Discount, 55% LAIV coverage (Reference Scenario)							
ICER	2419	1772	2699	2055	2576	2088	2267
Net-Benefit in Millions (£GBP)	120.1	404.4	203.7	500.4	326.3	599.0	693.5
NB Lower	42.0	154.8	71.7	189.2	112.5	218.3	260.5
NB Upper	241.3	795.3	406.1	984.6	676.8	1157.8	1387.6
b) 1.5% Discount, 55% LAIV coverage							
ICER	2308	1672	2535	1945	2402	2003	2169
Net-Benefit in Millions (£GBP)	125.1	424.1	214.9	528.1	349.1	622.2	723.4
NB Lower	43.8	169.4	81.7	201.6	127.6	237.0	269.5
NB Upper	254.0	827.6	416.4	1018.2	696.7	1240.4	1380.1
b) 0% Discount, 55% LAIV coverage							
ICER	2163	1578	2420	1846	2283	1884	2044
Net-Benefit in Millions (£GBP)	132.1	454.0	226.7	556.6	367.7	665.0	716.3
NB Lower	51.7	179.7	82.9	216.7	139.4	266.9	316.0
NB Upper	258.1	872.9	442.6	1122.8	720.3	1280.0	1433.2
d) 3.5% Discount, 70% LAIV coverage							
ICER	2367	1891	2778	2276	2508	2315	2607
Net-Benefit in Millions (£GBP)	154.1	487.2	250.0	589.5	417.0	698.2	783.2
NB Lower	57.4	181.4	87.8	202.2	149.4	255.8	277.3
NB Upper	312.7	936.5	515.3	1172.9	824.7	1433.9	1543.1
e) 3.5% Discount, 30% LAIV coverage							
ICER	2173	1456	2416	1630	2272	1668	1794
Net-Benefit in Millions (£GBP)	68.3	255.4	120.3	323.3	192.8	388.4	450.6
NB Lower	25.6	96.2	42.4	119.4	67.8	154.3	167.0
NB Upper	137.4	481.0	242.0	641.8	382.4	754.9	875.0

Table 2.5.2: Cost-effectiveness ratios (compared with the Status Quo intervention) and net benefits with associated 95% credibility range calculated under different discount rates for Quality-Adjusted Life Years (QALYs), and different total coverage for the LAIV strategy

Incremental Cost-Effectiveness Ratios							
Intervention Strategy	**Target Age-Group (Years)**	**Net Cost (£GBP Million)**		**Net QALY Difference**		**Incremental Comparison**	
		Mean	**95% Confidence Interval**	**Mean**	**95% Confidence Interval**	**Mean**	**95% Confidence Interval**
I1: Preschool School	Low-Risk 65+ , High risk 6 months - 65+	13.8	(10.1, 16.7)	6697	(2800, 12715)	2054	(825, 3282)
I3: Secondary School	Low-Risk 65+ , High risk 6 months - 65+, 12-16 years old	26.7	(23.1, 30.0)	11520	(4939, 21719)	2693	(2640, 2746)
I2: Primary School	Low-Risk 65+, High risk 6 months - 65+, 5-11 years old	33.4	(25.2, 40.3)	21890	(9480, 41089)	639	(-389, 1666)
I4: Preschool & Primary School	Low-Risk 65+ , High risk 6 months - 65+, 2-11 years old	48.7	(37.9, 56.8)	27456	(11972, 51960)	2761	(1723, 3799)
I6:Primary & Secondary School	Low-Risk 65+, High risk 6 months - 65+, 5-16 years old	59.5	(48.6, 69.2)	32925	(13961, 60995)	1972	(1468, 2476)
I7:Preschool & Primary & Secondary School	Low-Risk 65+, High risk 6 months - 65+, 2-16 years old	75.6	(62.2, 86.8)	38452	(16754, 73144)	2909	(1968, 3850)
Interventions ruled out by Dominance or Extended Dominance							
I5: Preschool & Secondary School	Low-Risk 65+, High risk 6 months - 65+, 2-4 years old, 12-16 years old	40.5	(33.9, 46.1)	18340	(7728, 35924)	**Dominated by: Primary School (5-11 year olds)**	

Table 2.5.3: Incremental Cost-Effectiveness Ratios (ICER) calculated with discount rate of 3.5% and final coverage uptake of 55% among the targeted age group. Of the proposed interventions all were associated with cost-effectiveness at the £20,000 Willingness-to-Pay, however Strategy I5 was strongly dominated meaning another strategy was less expensive and more effective.

2.5.2 Figures

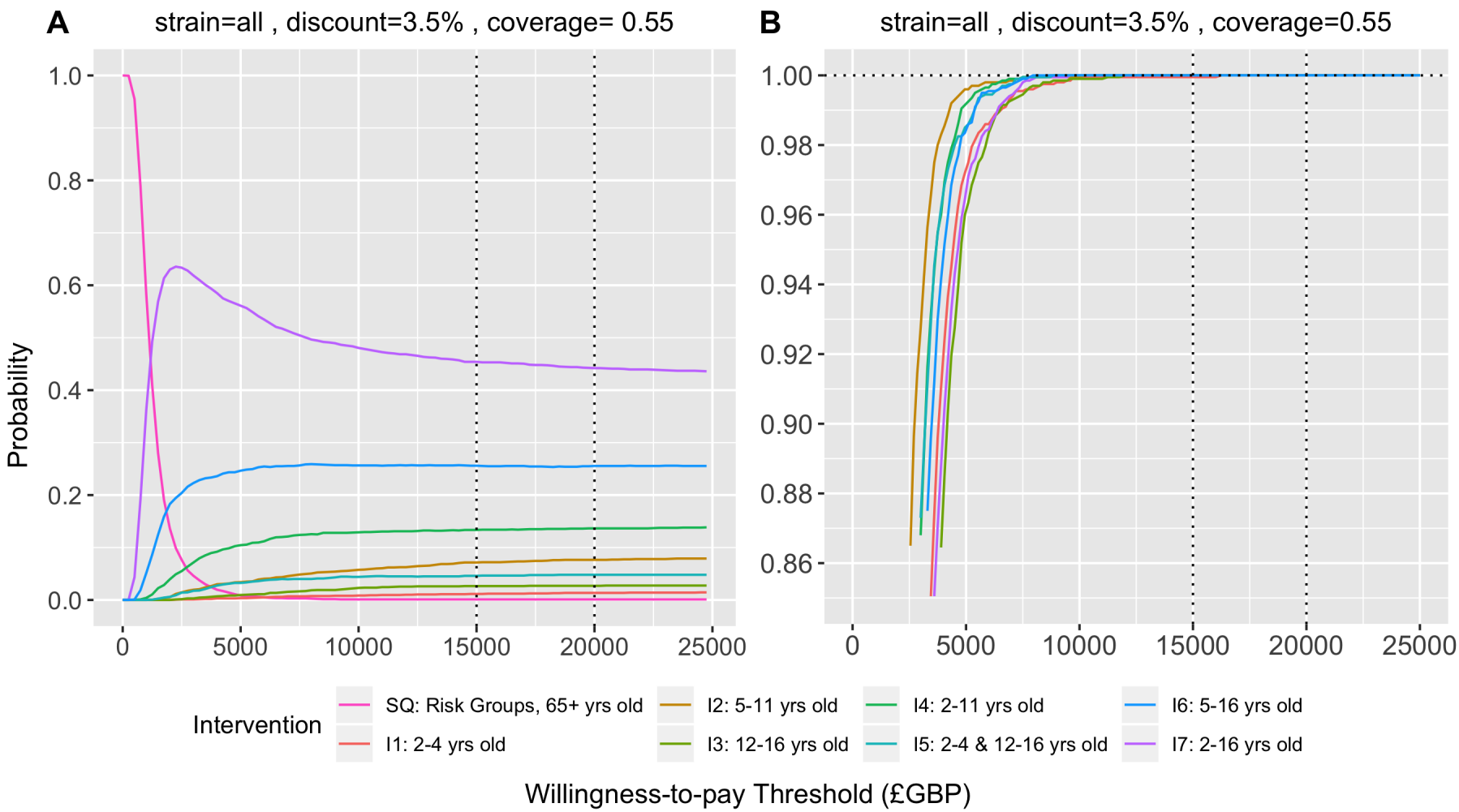

Figure 2.5.1: Acceptability curves delineating the probability that a strategy is optimal. Each curve depicts the probability that a strategy would confer the greatest net health benefit across a range of cost-effectiveness thresholds, estimated by the proportion of simulations in which that strategy was optimal at each threshold.

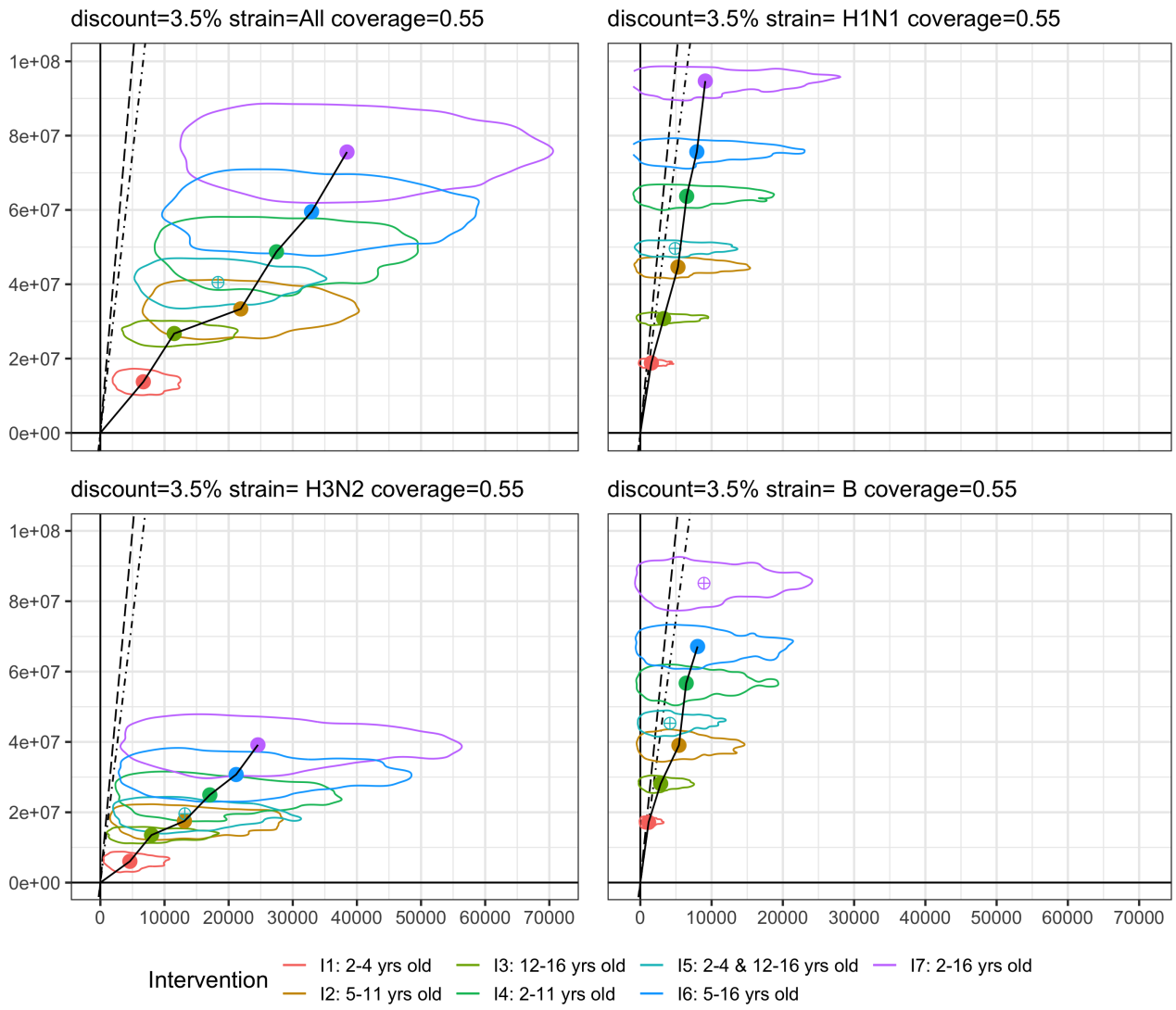

Figure 2.5.2: Incremental analysis with displaying average costs and quality-adjusted life years (QALYs) gained across all strains and stratified by strain. The graphs depict the estimated change in costs and QALYs gained over the reference strategy (Status Quo). Each contour line represents 90% of the Monte Carlo simulations with the coloured point inside being the mean outcome of the scenario. The two diagonal lines represent £15,000 (long-dash) and £20,000 (dash-dot) per QALY gained. Unfilled points indicate strategies that are dominated by others. The black line segments represent the cost efficiency frontier.

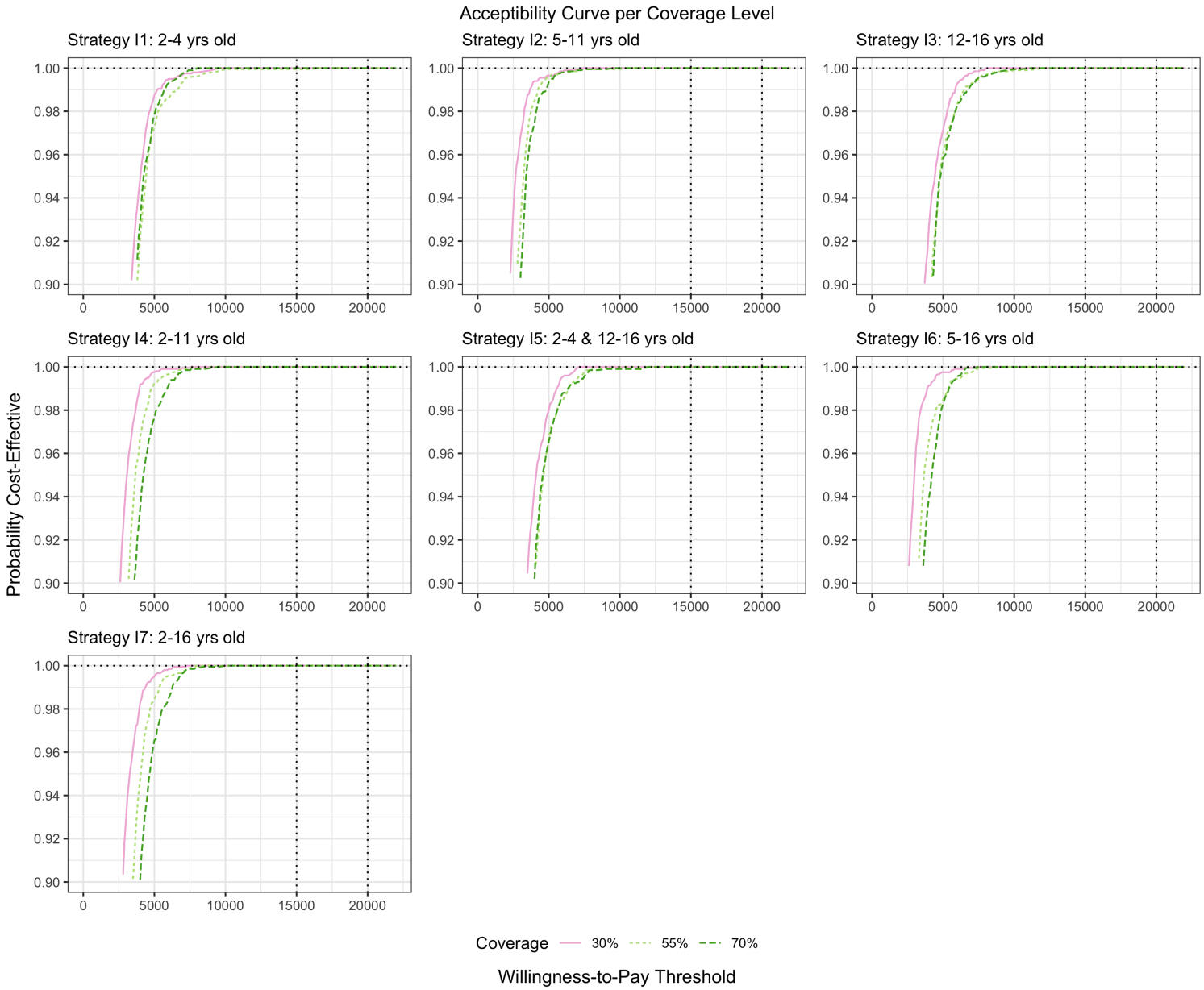

Figure 2.5.3: Acceptability curves delineating the probability that a strategy is cost-effective at a range of cost-effectiveness thresholds. The probability is estimated by the proportion of 2500 simulations that are less than or equal to the threshold (Y-Axis).

2.6 Supplementary Information

The following sections contain information on model parameters and model construction, derivation of vaccine costs, and age-structured health outcomes, and further sensitivity analysis.

2.6.1 Model calibration

R package

The analysis was coded in R (version 3.5.0) [8], using R Studio (version 1.1.453) with the R package 'fluEvidenceSynthesis'.[21, 20] The R package 'fluEvidenceSynthesis' model (version 1.0.0) has been revised from the developmental version previously used by Baguelin et al. and the previous package published on Github by van Leeuwan.[21] The package updates include new functionality features such as calculation of number of vaccine doses, credible interval functions, and inclusion of customized inference functions.

We utilized the functions 'adaptive.mcmc', and 'as.vaccine.calendar' along with the R package 'odin'[47] to write and fit a custom inference function that included additional age classes in the binomial and hypergeometric likelihood for the years 2009/2010-2013/2014. Likewise we re-derived the Royal College of General Practitioners Research and Surveillance Center (RCGP), POLYMOD, and Influenza-like-illness (ILI) datasets and several package functions to include the additional number of age classes.

Prior distributions for model parameters

Prior Distributions for Epidemiological Parameters			
Variable	Description	Prior Distribution or Base Case	Source
c_{ij}	contact rate between age group i and j	Bootstrapped POLYMOD data	[23]
ϵ_i	ascertainment probability of a symptomatic case	Fit, Priors Below	[48]
	0-14 years old	logNormal(-4.494, 0.286)	
	15-64 years old	logNormal(-4.117, 0.475)	
	65+ years old	logNormal(-2.978, 1.332)	
$\mathbf{v}$	immunization rate for age group i and risk group k		[25] [26]
σ	susceptibility of age group i	Fit, Priors below	[18]
	6 months old -14 years old	N(0.688, 0.083)	
	15 - 64 years old	N(0.529, 0.122)	
	65+	N(0.523, 0.175)	
q_{strain}	transmissibility of virus A/H3N2, A/H1N1, B	Fit, Prior: N(0.165, 0.028)	[48]
Ψ	outside infection probability	Fit, Prior: $Beta(z_{ij}^{outside}, z_{ij}^{inside})$, where z_{ij} is the incidence among the monitored population of age group i at week j of new cases arising from outside the main epidemic or inside	
γ_1	rate of loss of latency (γ_1=2.5/2)	1.8 days	[49]
γ_2	rate of loss of infectiousness(γ_2=1.1/2)	0.8 days	[49]
	delay from vaccination to immunity	2 weeks	Assumption in Baguelin et al. [50]
α_{ik_t}	all-or-nothing vaccine efficacy for age group i and risk group k per season	Well-matched: $0.7_{LowRisk}$, $0.4_{HighRiskand65+yrs}$ Poorly-matched: $0.42_{LowRisk}$, $0.28_{HighRisk}$	
I_t	initial infectious seed for the epidemics per season	Derived from σ, Fit	

Table 2.6.1: Prior distributions for each parameter used to fit the SEIR model via Markov chain Monte Carlo.

2.6.2 Age-risk stratification

Using this calibrated model, we assessed the influenza incidence in England and Wales in the presence of seven vaccination programs targeted at the following school age groups: (1) Preschool (2–4 years) (2) Primary School (5–11 years) (3) Secondary School (12–16 years) (4) Preschool and Primary school (2–11 years) (5) Primary School and Secondary School (5-16 years) (6) Preschool and Secondary School (2-4 years and 12-16 years) (7) Preschool, primary, and secondary school age (2–16 years). Eleven age groups were structured into the model on the following intervals: 6 months-<1,1, 2-4, 5–11,12-14, 15–16, 17-24, 25–44, 45–64, 65-74, 75+ years–over the seven groups previously used by Baguelin et al.[19] The SEIR model has 22 separate age-risk strata in total.

We considered three final coverage levels of 30%, 55%, and 70% representing the lower bound, average level, and upper bound coverage achieved by the current program.

Health-related Quality of Life Values					
Outcome	Age Group	Value or Distribution			Reference
QALY loss per non-fatal ILI case	All Ages	Bootstrap from data on H1N1 pdm			[52]
QALY loss per Hospitalization	All Ages	Normal(mu=0.018, sd=0.0018);			[53]
		Discount			
		0%	1.5%	3.5%	
	Low/High Risk 0-12 months old	60.93/69.96	37.06/40.77	22.61/24.07	
	Low/High Risk 1-4 years old	61.62/69.45	37.61/40.62	23.00/24.05	
	Low/High Risk 5-14 years old	54.96/61.64	35.19/37.84	22.32/23.18	
	Low/High Risk 15-44 years old	38.23/44.47	27.16/30.40	18.84/20.33	
	Low/High Risk 45-64 years old	19.75/24.14	16.09/19.10	12.71/14.62	
QALY loss per Death	Low/High Risk 65+	8.24/9.46	7.41/8.40	6.52/7.28	[34, 54, 19]

Table 2.6.3: Sources and values per age and risk group for health related quality of life lost (measured in qaly used to calculated number of qaly lost per influenza season. Outcomes for which qaly loss was calculated included Hospitalization, death/fatality.

2.6.3 Model fits

The 'fluEvidenceSynthesis' package independently estimates the incidence of influenza for strains A/H1N1, A/H3N2, and B per season. We achieved consistent results for the contact matrix and posterior parameters. For most seasons approximately 6-8 chains (1.2 million iterations) were needed for convergence. Any season that did not converge based on the Gelman-Rubin diagnostic was restarted with the last value of the Markov chain and the two chains were run for an additional 300,000 iterations. The Gelman–Rubin diagnostic evaluates Markov chain Monte Carlo (MCMC) convergence by comparing the variance between-chains and within-chain for each model parameter.[55] Large differences between the two variances

indicate non-convergence. Some influenza seasons where few cases were observed by the surveillance network (e.g. <6 cases per age group) had Gelman-Rubin diagnostics greater than 1.2. Given the low precision of the data for these seasons a higher Gelman -Rubin score for the model fit is not unexpected and does not change the results of our analysis.

The posterior distributions are sampled from 75% of the last chain. The posterior distributions for each season and year are shown in Appendix section A1.

2.6.4 Simulating LAIV vaccination

Modeling seasonal influenza vaccination

For this analysis, we included age-group stratified empirical data on annual Trivalent Inactivated Influenza Vaccine (TIIV), Quadrivalent Influenza Vaccine (QIV), and Live-Attenuated Influenza Vaccine Nasal Spray (LAIV) vaccine coverage for the remaining years 2004/2005-2013/2014, as well as the empirical rate per month or year that this coverage was achieved for the period 1995/1996-2013/2014. [27, 28, 29]. The rate of vaccination for high risk and low risk groups was assumed to be constant over a monthly or weekly period depending on the time period data available for the coverage rate.

Baguelin et al.	A/H1N1	A/H3N2	B
1995/96	M	U	U
1996/97	U	M	U
1997/98	M	U	U
1998/99	U	M	U
1999/00	U	M	U
2000/01	M	U	U
2001/02	M	M	U
2002/03	M	M	U
2003/04	M	U	U
2004/05	M	U	U
2005/06	M	M	U
2006/07	M	M	U
2007/08	M	M	U
2008/09	M	M	U

New Data	A/H1N1	A/H3N2	B
2009/10	U	U	U
2010/11	M	M	M
2011/12	M	U	M
2012/13	M	M	M
2013/14	M	M	M

Table 2.6.4: List of strain matching between circulating strain and vaccine strain used in the model for the years 1995/1996-2013/2014. U= Unmatched, M=Matched

When the vaccine is well-matched with the annual circulating strain Vaccine Efficacy (VE) was fixed at 70% in the general population and 42% in the clinical high risk and 65+ year old group. During poorly matched years we assigned 40% VE for the general population and 28% VE in the high risk and elderly group. We did not make specific allowances for differences in VE between the three vaccine types: LAIV, QIV, and TIIV.

2.6.5 Vaccine uptake rate for proposed interventions

Empirical coverage rates were available for the years 1995-2014 and were utilized in calibration of the model.

Status quo simulations

For simulation of the Status Quo program empirical coverage rates were used for 1995/1996-2011/2012. As the Pediatric program began its phased introduction in 2012/2013-2013/2014 we utilized empirical coverage rates for these two years for all ages and risk groups, except 2-16 year olds. In our Status Quo scenario 2-16 year olds who were at low risk for complications did not receive LAIV vaccination during 2012/2013-2013/2014 seasons meaning their total coverage was 0%.

Intervention simulations

The dates for the LAIV program simulation began on September 1 and ended on December 12. These dates were chosen as the standard beginning of the United Kingdom (UK) school year and approximately one week before the beginning of the Christmas school holiday. Logarithmic functions for coverage were fit using 6 data points and the R 'predict' function. (Table **??**) The first two points began with September 1st at 0% and December 12 as the total achieved coverage (eg. 55%, 70%). For the remaining three points we used empirical coverage rates from 2012/2013 for low risk 65+ and high risk age groups < 65 years old whose final coverage rates were closest to the strategic goal. As these are both the highest priority groups in the current vaccination scheme in the UK we assumed their vaccination rate would be roughly equivalent to that of the the school-based LAIV program.

Using the empirical coverage dataset we utilized the logarithmic function to predict the coverage level at each date for each season. For example the empirical coverage rates for Strategy I7 (2-16 year olds) for 1995 has data on the monthly intervals "1995-10-01" "1995-11-01" "1995-12-01" "1996-01-01" "1996-02-01". To calculate the coverage level at these dates for a program with 70% coverage we utilized the calculated logarithmic function and the R function 'predict' to estimate coverage for 2-16 year olds at these intervals. The results for this example would look like:

Empirical Dates	"1995-10-01"	"1995-11-01"	"1995-12-01"	"1996-01-01"	"1996-02-01"
Calculated Coverage	0.9%	15.0%	59.7%	70.7%	71.3%

If the function provided coverage levels prior to September 1 or after December 12 they were truncated to the minimum (0%) or the maximum achieved coverage for the simulation. For the 1995 example above the model simulation would use 70% in place of 70.7% and 71.3%.

2.6.6 Vaccine cost calculation

The cost per dose due for administering school-based vaccine delivery program was calculated using the same reimbursement cost as General Practitioner (GP) Nurses (£7.24) and the same vaccine acquisition cost as a GP office (£9.80).[56] Pilot areas of school-delivery estimated that a qualified nurse was able to immunize about 50 children per 2.5 hours– 20 LAIV doses per 1 hour.[28] After subtracting 2.5 hours for travel, set-up/break-down, and meals we estimated nurses would spend 5 hours actively vaccinating resulting in 100 doses dispersed per nurse per day. At an average hourly rate of £36 per hour,[45] the service cost for school-based delivery attributed to administration was £2.70 per dose. In some pilot areas drivers were used to deliver bulk vaccine to the school beforehand allowing immunization teams to concentrate on administration sessions. We estimated a large delivery to be the average number of pupils in a primary school–approximately 260 doses. For every 260 doses we added a service cost based on an estimated band 1 National Health Service (NHS) driver hourly wage (£9.88/hour)—this added an additional £0.10 per dose.[46] Therefore the total service cost of the school based program was £2.80 per dose. Added to the reimbursement cost and acquisition cost we calculated a triangular cost distribution for school delivery that was very similar to previous cost distributions for GP, and pharmacy vaccine delivery.

The average hourly wage for nurses were derived from UK nation-wide estimates [45]. The vaccine purchase payment estimates for the pharmacy delivered vaccines were taken from a survey conducted in the London-area.[57]

2.6.7 Costs for vaccine refrigeration and waste disposal

We assumed that services for waste disposal and sharps removal already exist at pharmacies and GP locations and are paid for directly by the NHS. For school-delivery, immunization teams would concentrate on the vaccination session therefore we assumed nurses did not return empty sprayers to their office for disposal. Waste disposal for school-based delivery was calculated as the cost of disposing clinical waste and a delivery fee to the waste disposal

unit which we estimated at £0.148 per 100 sprayers). For delivery of clinical waste the same service cost as vaccine delivery based for a band 1 NHS driver hourly wage per 260 doses was used, and assumed delivery was completed in 1 hour.

Additional costs for refrigeration were not considered as the vaccine is kept in secure cool bags during school delivery and LAIV can be kept at room temperature for up to 12 hours.[28] Vaccine wastage was not considered a problem as pilot studies found few vaccines were wasted due to children moving away at the last moment or dropped applicators.[28]

Utility of changing sprayer weight

The recommended LAIV dose of 0.2mL (0.1mL per nostril) is contained in a 1 mL capacity sprayer. We estimated the change in efficacy if the 1mL sprayer was reduced to a 0.5mL dispenser holding the same amount of vaccine. Halving the sprayer weight means the cost of clinical waste disposal is £0.074 per 100 sprayers (£0.148/2 per 100 sprayers). We assumed the driver would still pick up and dispose of the sprayers based on scheduling not weight, therefore the cost of delivery remains the same. If waste disposal of the 1 mL sprayer cost a total of £3.95 per 100 sprayers, for a 0.5 mL sprayer as £3.87, a savings of £0.07 per 100 doses.

2.6.8 Calculated vaccine outlay cost

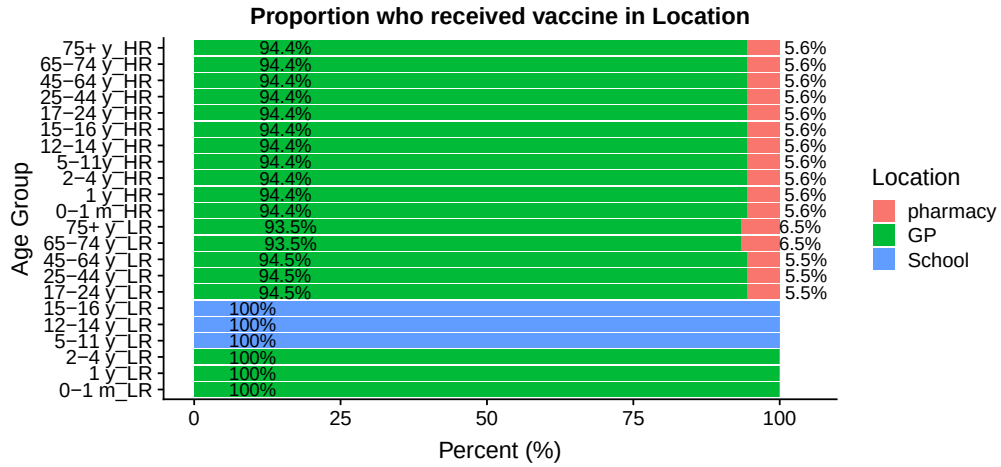

Figure 2.6.1: Proportion Vaccinated in each Age Group at each Location

Outcome Risks					
Parameter Description	**Strain**	**Age Group**	**Value Used in Base Case**	**Distribution used in Sensitivity Analysis**	**Reference**
Proportion of Symptomatic Influenza Cases	All Strains	All Ages	0.407	Triangular(a=0.309, b=0.513, c=0.396)	[51]
Risk of Hospitalization	A/H1N1	Low/High Risk 0 - 6 months ;	0.002/0.000	Sampled from Regression Normal Distributions	[33]
		Low/High Risk 6 months - 4 years;	0.002/0.002		
		Low/High Risk 5-14 years old	0.000/0.000		
		Low/High Risk 15-44 years old	0.000/0.000		
		Low/High Risk 45-64 years old	0.000/0.001		
		Low/High Risk 65+ years old	0.000/0.010		
	A/H3N2	Low/High Risk 0 - 6 months ;	0.012/0.000	Sampled from Regression Normal Distributions	[33]
		Low/High Risk 6 months - 4 years;	0.008/0.009		
		Low/High Risk 5-14 years old;	0.000/0.001		
		Low/High Risk 15-44 years old	0.000/0.001		
		Low/High Risk 45-64 years old	0.000/0.002		
		Low/High Risk 65+ years old	0.008/0.015		
	B	Low/High Risk 0 - 6 months ;	0.015/0.011	Sampled from Regression Normal Distributions	[33]
		Low/High Risk 6 months - 4 years;	0.004/0.000		
		Low/High Risk 5-14 years old;	0.000/0.000		
		Low/High Risk 15-44 years old	0.000/0.000		
		Low/High Risk 45-64 years old	0.001/0.000		
		Low/High Risk 65+ years old	0.000/0.001		
Risk of Mortality During Hospitalization	A/H1N1	Low/High Risk 0 - 6 months ;	0.000/0.000	Sampled from Regression Normal Distributions	[33]
		Low/High Risk 6 months - 4 years;	0.000/0.000		
		Low/High Risk 5-14 years old;	0.000/0.000		
		Low/High Risk 15-44 years old	0.000/0.000		
		Low/High Risk 45-64 years old	0.000/0.000		
		Low/High Risk 65+ years old	0.001/0.004		
	A/H3N2	Low/High Risk 0 - 6 months ;	0.000/0.000	Sampled from Regression Normal Distributions	[33]
		Low/High Risk 6 months - 4 years;	0.000/0.000		
		Low/High Risk 5-14 years old;	0.000/0.000		
		Low/High Risk 15-44 years old	0.000/0.000		
		Low/High Risk 45-64 years old	0.000/0.000		
		Low/High Risk 65+ years old	0.002/0.007		
	B	Low/High Risk 0 - 6 months ;	0.000/0.000	Sampled from Regression Normal Distributions	[33]
		Low/High Risk 6 months - 4 years;	0.000/0.000		
		Low/High Risk 5-14 years old;	0.000/0.000		
		Low/High Risk 15-44 years old	0.000/0.000		
		Low/High Risk 45-64 years old	0.000/0.000		
		Low/High Risk 65+ years old	0.000/0.001		
Risk of GP Consult	A/H1N1	Low/High Risk 0 - 6 months ;	0.042/0.063	Sampled from Regression Normal Distributions	[33]
		Low/High Risk 6 months - 4 years;	0.034/0.052		
		Low/High Risk 5-14 years old;	0.018/0.027		
		Low/High Risk 15-44 years old	0.002/0.002		
		Low/High Risk 45-64 years old	0.006/0.010		
		Low/High Risk 65+ years old	0.051/0.077		
	A/H3N2	Low/High Risk 0 - 6 months ;	0.281/0.424	Sampled from Regression Normal Distributions	[33]
		Low/High Risk 6 months - 4 years;	0.208/0.314		
		Low/High Risk 5-14 years old;	0.042/0.064		
		Low/High Risk 15-44 years old	0.015/0.023		
		Low/High Risk 45-64 years old	0.029/0.043		
		Low/High Risk 65+ years old	0.082/0.124		
	B	Low/High Risk 0 - 6 months ;	0.279/0.423	Sampled from Regression Normal Distributions	[33]
		Low/High Risk 6 months - 4 years;	0.288/0.438		
		Low/High Risk 5-14 years old;	0.088/0.134		
		Low/High Risk 15-44 years old	0.071/0.108		
		Low/High Risk 45-64 years old	0.079/0.120		
		Low/High Risk 65+ years old	0.000/0.000		

Table 2.6.2: Age and risk group (Low/High Risk) probabilities of each Hospitalization, Mortality, and gp Consult per influenza strain.

Simulated Coverage Uptake						
Points for Logarithmic Fit						
Dates	"2012-09-01"	"2012-09-24"	"2012-10-01"	"2012-10-22"	"2012-11-19"	"2012-12-12"
70%	0.000	0.065	0.170	0.489	0.679	0.7
30%	0.000	0.016	0.046	0.176	0.294	0.3
Dates	"2012-09-01"	"2012-09-24"	"2012-10-08"	"2012-10-22"	"2012-11-19"	"2012-12-12"
55%	0.000	0.1010	0.1760	0.2980	0.4720	0.55

Logarithmic Model	**Intercept 1 (b)**	**Intercept 2 (d)**	**Intercept 3 (e)**
70%	-9.839e-02	7.133e-01	1.563e+04
55%	-6.2773e-02	5.6676e-01	1.5635e+04
30%	-1.3002e-01	3.0030e-01	1.5632e+04

Table 2.6.5: Logarithmic Functions for calculating coverage at any date. The functions use manipulated objects of classes "POSIXlt" and "POSIXct" to represent calendar dates and times. As functions were fit to data from 2012/2013 any predicted outcomes for years other than 2012 must recenter around the POSIXct date '15584' or September 1, 2012.

Cost of Vaccination					
Parameter	**Original Value**	**Year**	**Inflation Adjustment**	**2018 Value**	**Source**
GP Delivery Cost Per Dose					
NHS vaccine service payment	£9.80	2018	–	£9.80	[56]
Vaccine Purchase Payment	£7.24	2014/2015	1.041	£7.54	[57]
Dispensing Fee	£2.25	2014/2015	1.045	£2.32	[57]
GP Cost Total per Dose				**£19.66**	
Pharmacy Delivery Cost Per Dose					
NHS vaccine service payment	£9.80	2018	–	£9.80	[56]
Vaccine Purchase Payment	£7.08	2014/2015	1.041	£7.37	[57]
Sonar Service Fee	£0.12	2018	–	£0.12	[57]
Pharmacy Total Cost per Dose				**£17.29**	
School-Delivery Cost Per Dose					
NHS Vaccine Service Payment	£9.80	2018	–	£9.80	[56]
Vaccine Purchase Payment	£7.24	2014/2015	1.041	£7.54	[57]
Dispensing Fee	£2.70	2016/2017	1.088	£2.72	[45]
Delivery Fee	£9.88 per hour per 260 doses	2018	–	£0.038 per/1 dose	[46, 58]
Waste Disposal Fee	£0.148 per 100 empty dispensers	2018	–	£0.148 per 100 empty dispensers	[59]
School Delivery Total Cost per Dose				**£20.14**	

Table 2.6.6: Itemized costs used to calculated the total cost per vaccine dose for each method of delivery. Inflation adjustments for medical services and medical equipment sourced from King et al.[35]

Mean Annual Vaccination Outlay Cost (95% Confidence Interval)								
	SQ: Status Quo	**S1: Preschool School**	**S2: Primary School**	**S3: Secondary School**	**S4: Preschool & Primary & School**	**S5: Preschool & Secondary & School**	**S6:Primary & Secondary & School**	**S7:Preschool & Primary & Secondary & School**
	Low-Risk 65+ , High risk 6 months - 65+	Low-Risk 65+ , High risk 6 months - 65+, 2-4 years old	Low-Risk 65+, High risk 6 months - 65+, 5-11 years old	Low-Risk 65+ , High risk 6 months - 65+, 12-16 years old	Low-Risk 65+ , High risk 6 months - 65+, 2-11 years old	Low-Risk 65+, High risk 6 months - 65+, 2-4 years old, 12-16 years old	Low-Risk 65+, High risk 6 months - 65+, 5-16 years old	Low-Risk 65+, High risk 6 months - 65+, 2-16 years old
LAIV Sprayers (Millions)	6.9	7.9	9.2	8.5	10.1	9.4	10.7	11.6
GP Delivery Cost (£ GBP Millions)	134.0 (129.1, 138.8)	153.3 (148.4, 158.4)	133.9 (129.0, 138.8)	133.9 (129.1, 140.0)	153.4 (148.5, 158.8)	153.4 (148.4, 158.8)	133.9 (129.9, 138.8)	153.4 (148.5, 158.8)
Pharmacy Delivery Cost (£ GBP Millions)	7.3 (7.0, 7.6)	7.3 (7.0, 7.6)	7.3 (7.0, 7.6)	7.3 (7.0, 7.6)	7.3 (7.0, 7.6)	7.3(7.0, 7.6)	7.3 (7.0, 7.6)	7.3 (7.0, 7.6)
School Delivery Cost (£ GBP Millions)	0	0	46.2 (44.6, 47.9)	31.6 (30.9, 32.6)	46.2 (44.6, 47.9)	31.7 (30.8, 32.4)	77.9 (76.2, 79.7)	77.9 (76.1, 79.7)
Total Cost (£GBP Millions)	141.2 (139.2, 143.2)	160.7 (158.6, 162.8)	187.5 (184.9, 190.3)	172.9 (170.8, 175.1)	207.0 (204.3, 209.7)	192.4 (190.0, 195.6)	219.3 (216.4, 221.9)	238.7 (235.8, 241.6)

Table 2.6.7: Average Annual vaccine outlay cost for each strategy

2.6.9 Average annual health outcomes

All Strains: Discount 3.5%, LAIV Coverage 55%									
Scenario		**Reference Strategy**	**S1**	**S3**	**S2**	**S5**	**S4**	**S6**	**S7**
Targeted School-Age Cohort		**None**	**Preschool**	**Secondary School**	**Primary School**	**Preschool & Secondary School**	**Preschool & Primary School**	**Primary & Secondary School**	**Preschool, Primary & Secondary School**
Total Influenza Infections (Millions)		15.539	13.913	12.690	10.037	11.003	8.692	7.322	6.218
	Upper Bound	16.605	14.921	13.711	11.278	11.988	9.839	8.479	7.397
	Lower Bound	14.486	12.956	11.698	8.970	10.032	7.648	6.276	5.233
Symptomatic Cases (Mean)		6,310,972	5,640,608	5,145,081	4,071,142	4,476,315	3,536,324	2,980,143	2,518,605
	Upper Bound	7177641	6,503,387	5,924,057	4,772,753	5,217,594	4203447	3670783	3,111,087
	Lower Bound	5,470,976	5,640,608	4,376,314	3,423,717	3,833,674	2,921,130	2,406,679	1,977,710
GP Consults (Mean)		770,477	658,563	636,236	493,392	523,513	406,681	350,546	280,601
	Upper Bound	976,303	823,526	803,812	634,630	665,921	517,410	460,722	382,776
	Lower Bound	620,106	528,312	500,535	375,396	408,117	308,817	255,241	195,235
Hospitalizations		13,791	11,112	11,582	8871	9009	6,920	6674	5112
	Upper Bound	20,699	16,945	16,888	12,796	13,184	10,340	9776	7481
	Lower Bound	9,896	7,782	8,154	6406	6303	4,893	4,706	3,557
Deaths (Mean)		1749	1569	1453	1177	1263	1030	913	791
	Upper Bound	664	3421	3136	2502	2717	2202	1932	1742
	Lower Bound	3996	623	572	457	495	420	371	329
Death-Associated QALY Loss		14,226	12,803	11,852	9731	10,323	8,557	7,612	6,586
	Upper Bound	28,958	26,388	24,717	18,738	20,120	17,814	14,928	12,748
	Lower Bound	6,576	5,648	5,267	4,566	4,733	4,172	3,601	3,054
Total QALYs Lost		61,224	54,959	50,718	40,495	44,092	35,694	30,065	25,683
	Upper bound	115,644	108,379	97,703	77,168	85,719	70,334	61,222	49,463
	Lower Bound	27,496	22,273	21,248	17,837	17,505	15,434	11,775	10,330
Vaccination Program Cost (£ Million)		141.195	167.587	184.172	203.788	210.407	230.107	246.653	272.942
	Upper Bound	143.248	169.834	186.625	206.850	212.820	233.378	249.934	276.551
	Lower Bound	139.253	165.242	181.713	200.716	208.030	227.106	243.418	269.549
GP Consultation Costs (£ Million)		30.33	25.88	25.12	19.17	20.566	15.76	13.756	11.02
	Upper Bound	46.77	39.01	37.91	28.98	31.833	24.79	21.750	17.27
	Lower Bound	16.83	14.25	14.08	10.70	11.233	8.34	6.952	5.73
Hospitalization Costs (£ Million)		12.67	10.23	10.76	7.95	8.226	6.26	6.132	4.66
	Upper Bound	22.42	17.46	18.56	28.98	13.692	11.06	10.01	8.15
	Lower Bound	5.88	4.74	5.51	10.07	3.817	3.14	3.16	2.10
Total Costs (£ Millions)		183.887	197.384	209.936	216.245	222.265	231.846	241.857	258.019
	Upper Bound	201.886	213.172	225.329	229.226	236.937	241.258	251.387	266.362
	Lower Bound	167.655	183.697	196.591	205.558	211.662	223.449	234.031	251.218

Table 2.6.8: The average annual number of influenza-like illness (febrile) cases, GP consultations, etc. are shown along with measures of their distribution for each of the strategies (columns) GP, General practitioner; QALY, Quality-adjusted life year

2.6.10 Age-Stratified health-related outcomes

Discount rate=3.5%, total coverage=55%

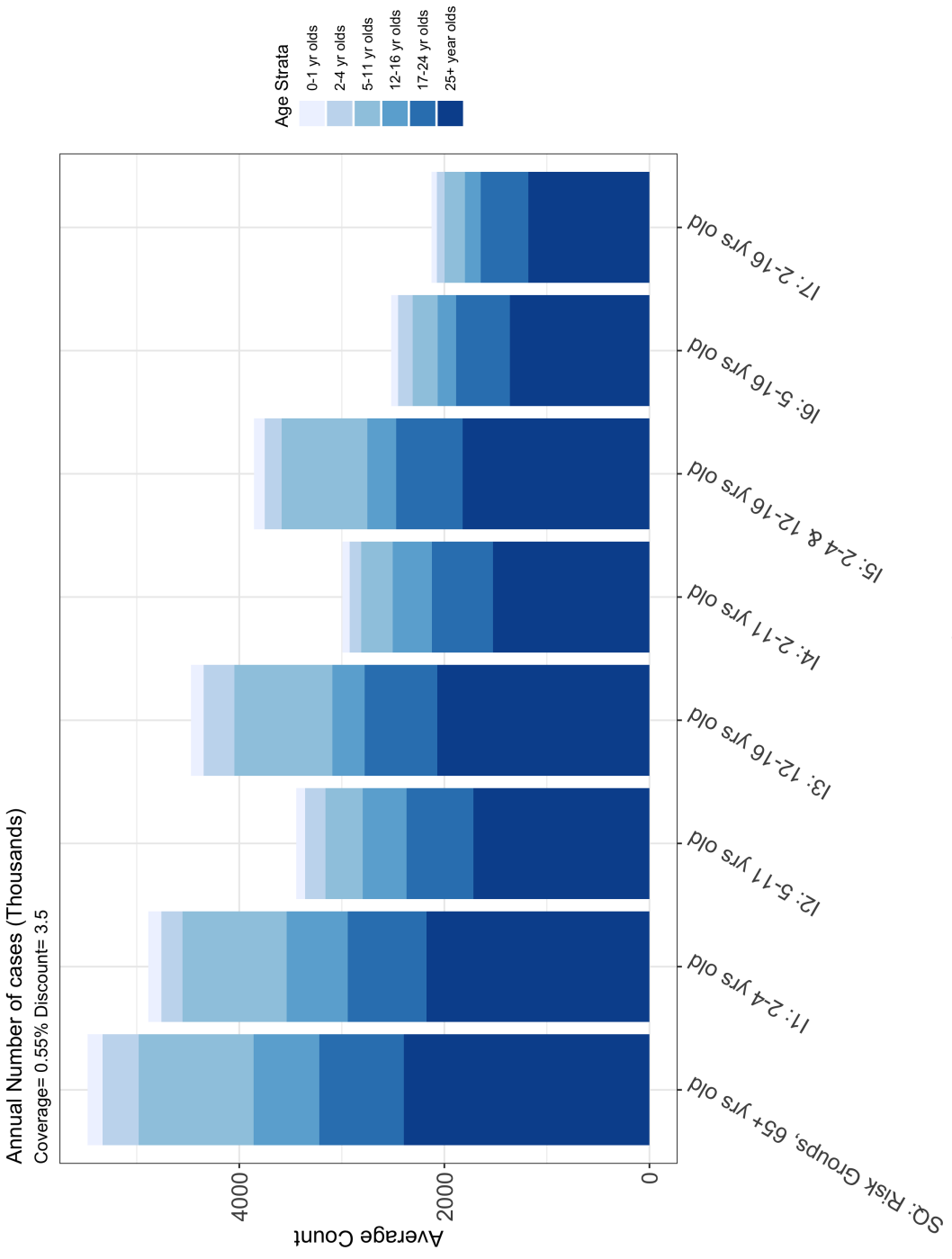

Figure 2.6.2: Average annual symptomatic cases under each intervention (Influenza A/H1N1, A/H3N2, B) stratified by age.

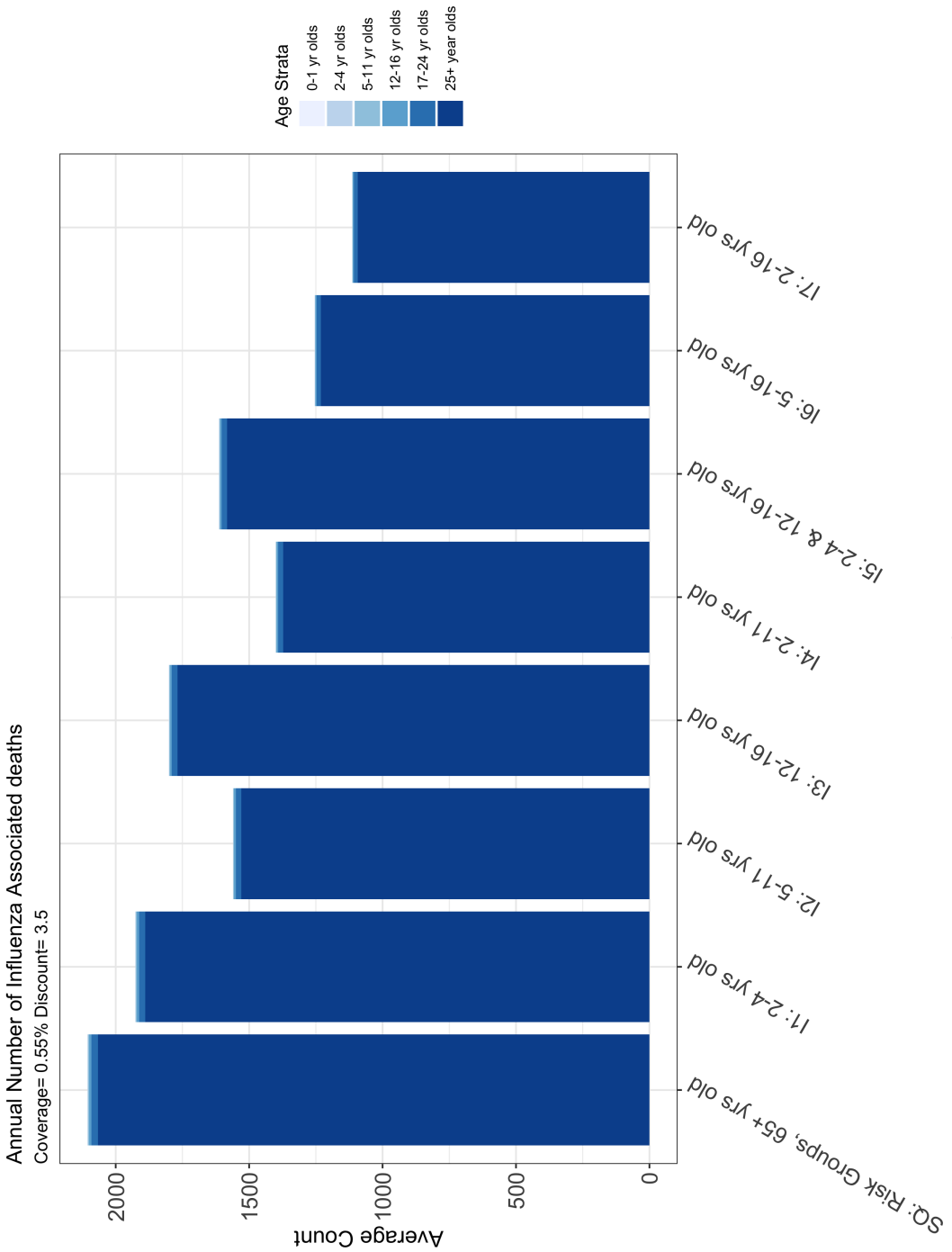

Figure 2.6.3: Influenza associated mortality under each intervention (Influenza A/H1N1, A/H3N2, B) stratified by age

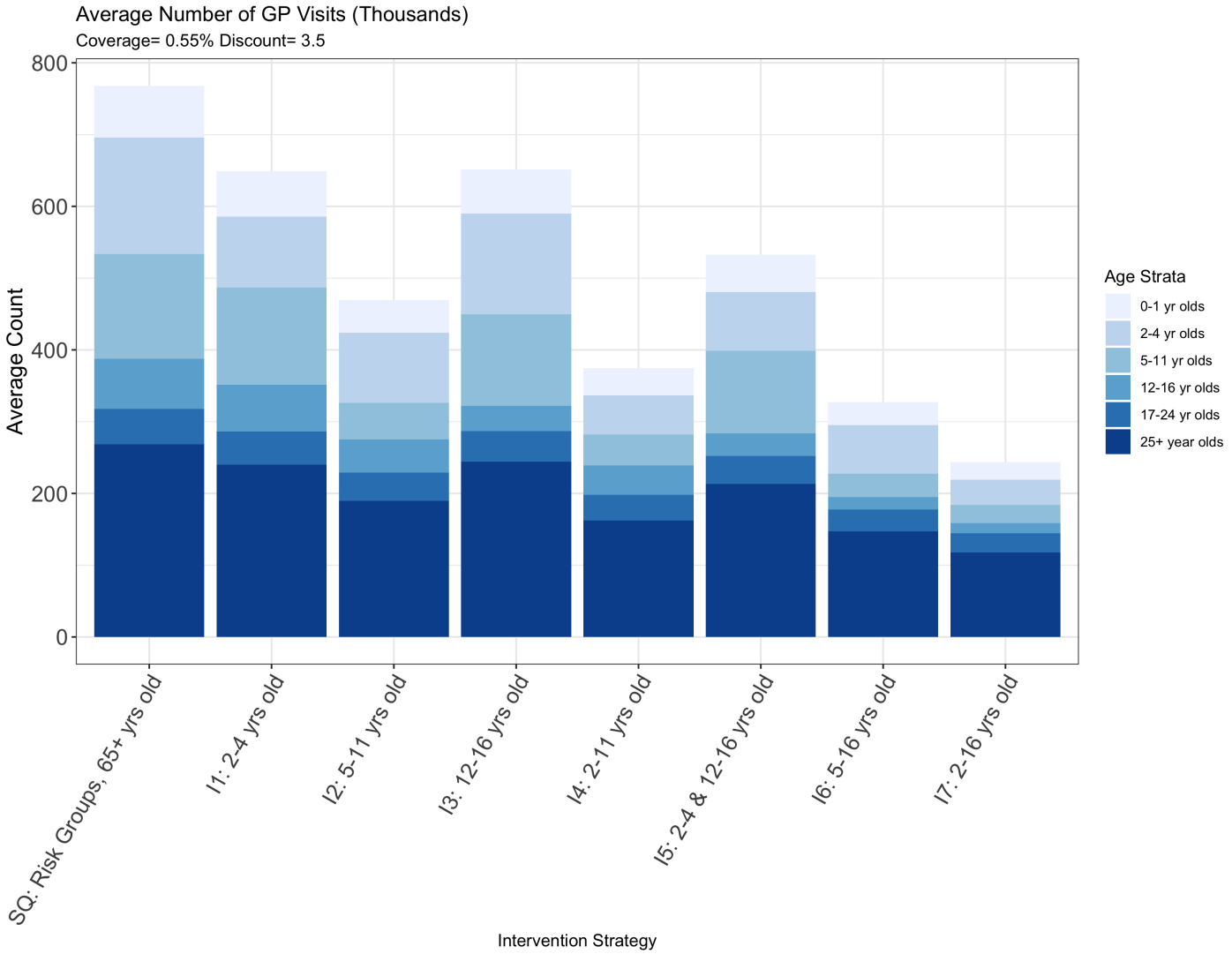

Figure 2.6.4: Average annual general practitioner consultations under each intervention (Influenza A/H1N1, A/H3N2, B) stratified by age.

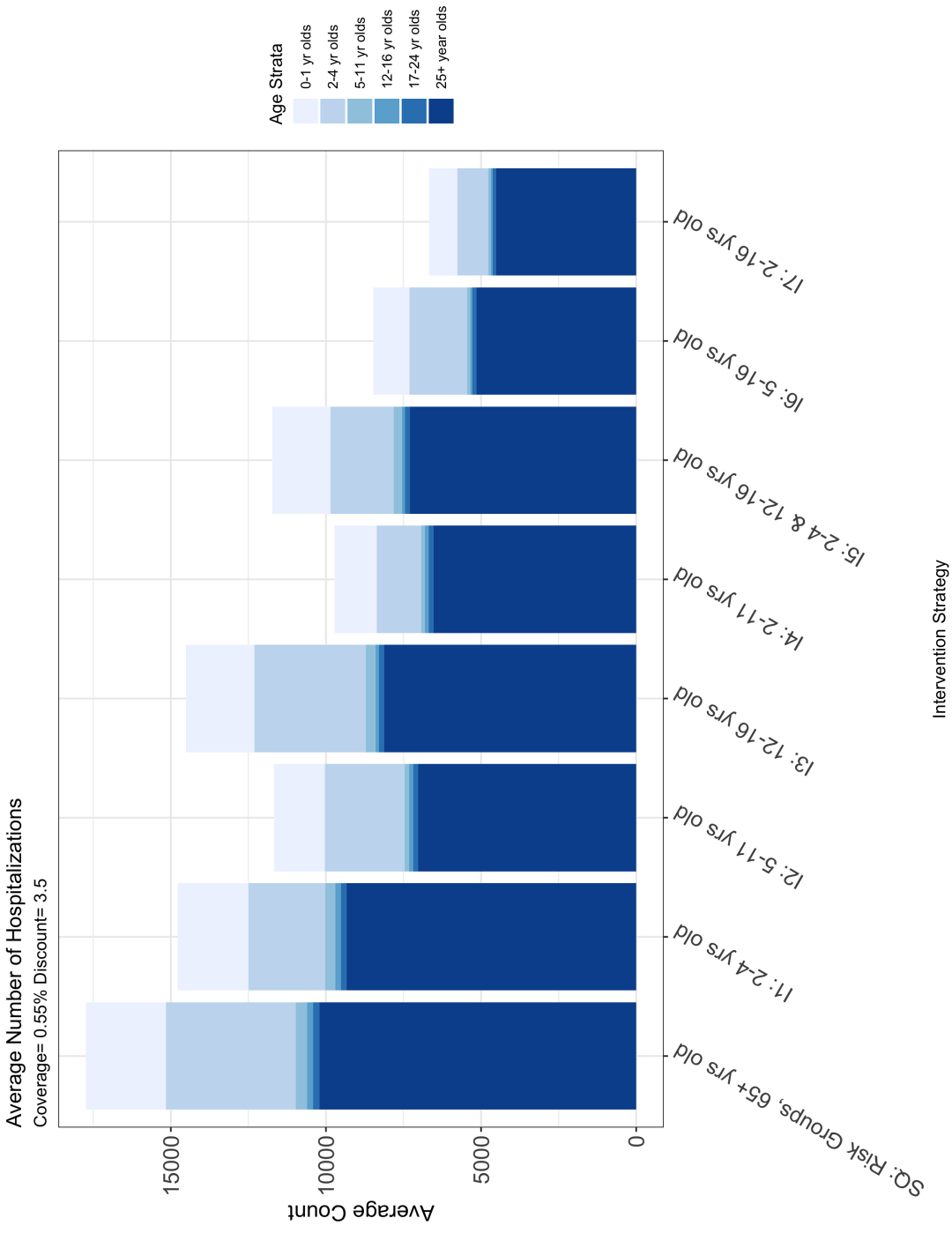

Figure 2.6.5: Annual number of Influenza associated hospitalizations under each intervention (Influenza A/H1N1, A/H3N2, B) stratified by age.

QALY gains stratified by age

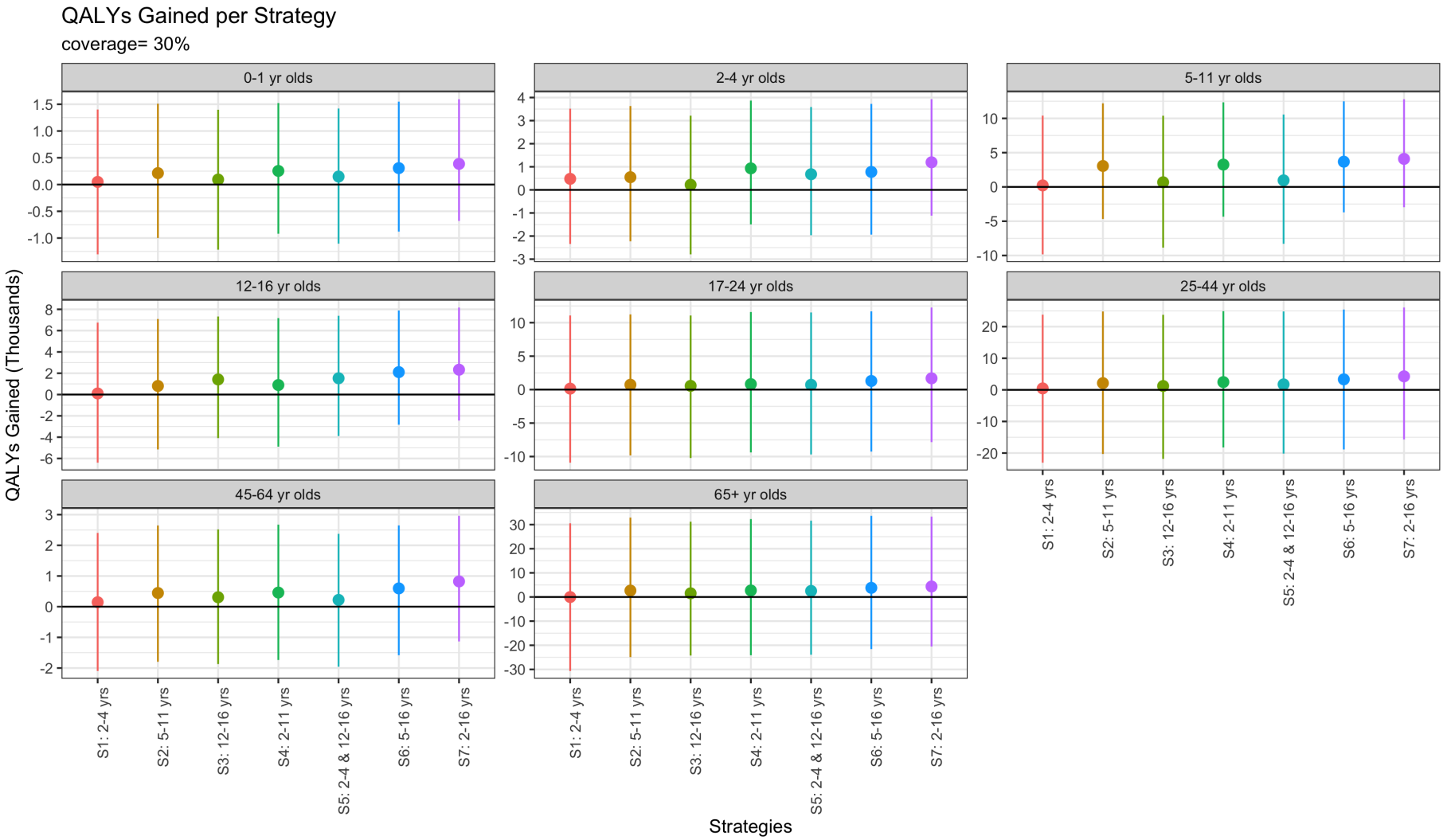

Figure 2.6.6: Average annual QALY gained per strategy stratified by age with total coverage was 30%.

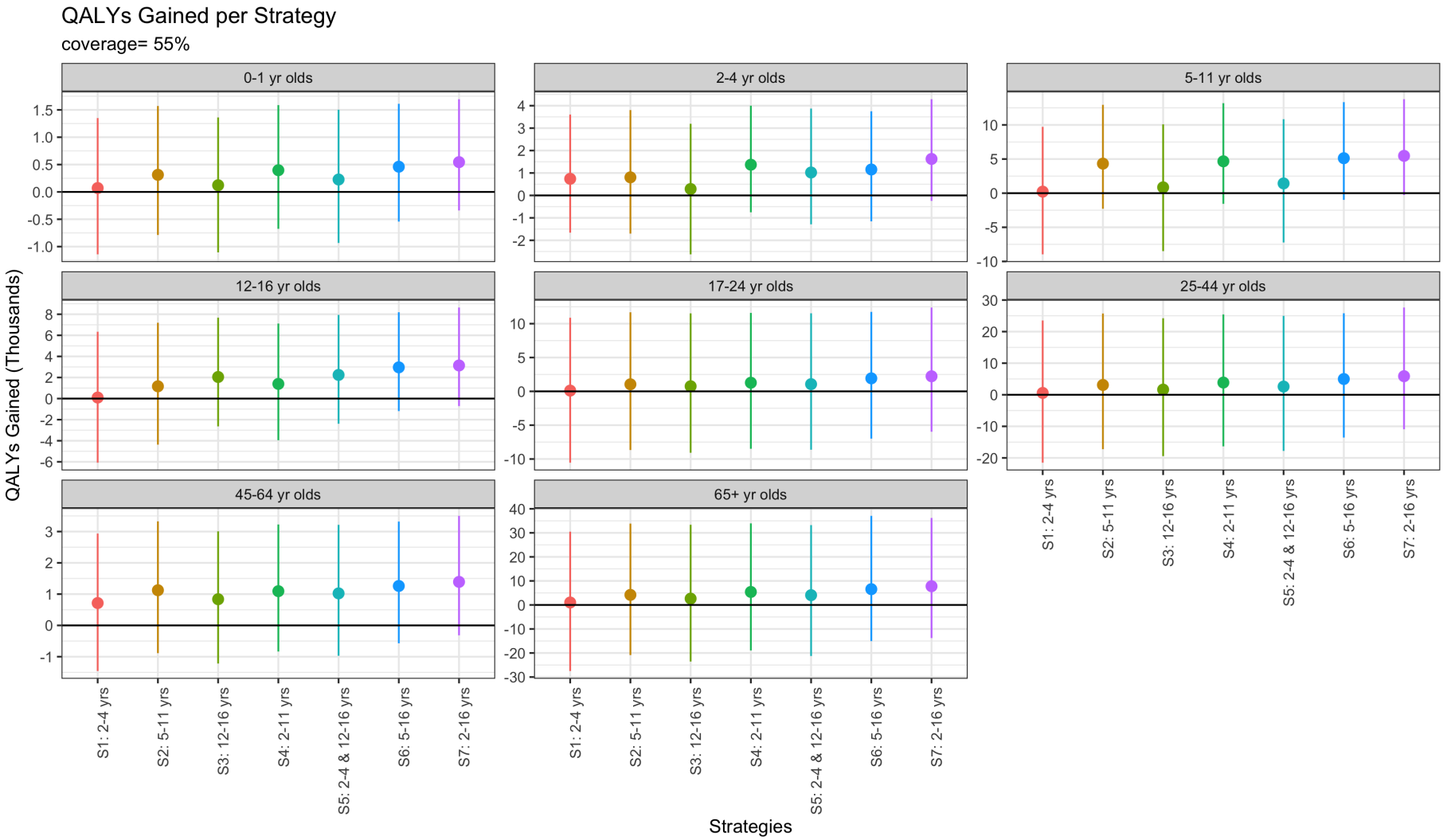

Figure 2.6.7: Average annual QALY gained per strategy stratified by age with total coverage was 55%

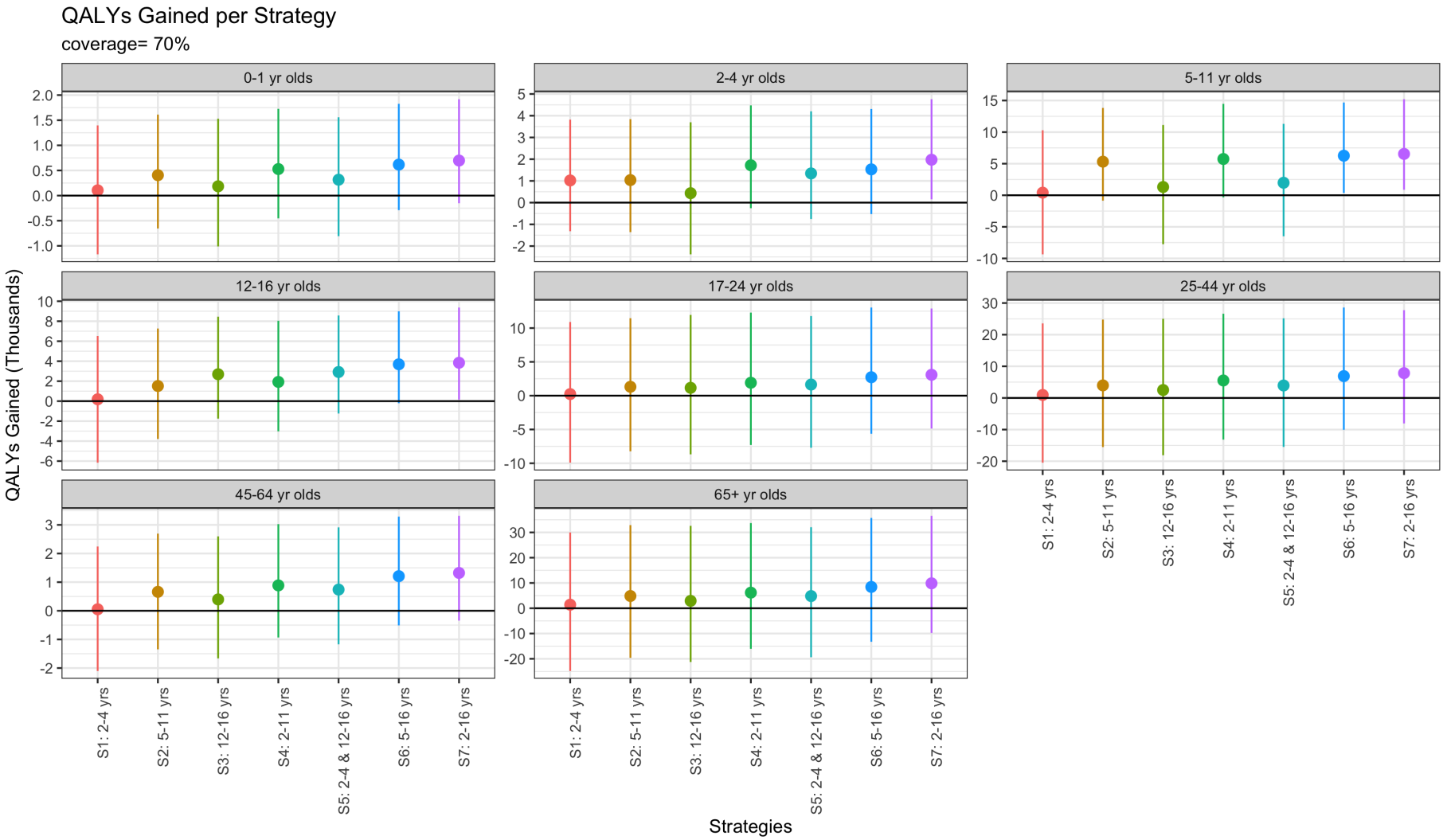

Figure 2.6.8: Average annual QALY gained per strategy stratified by age with total coverage was 70%

2.6.11 Sensitivity analysis

2.6.12 Acceptability curve all strains

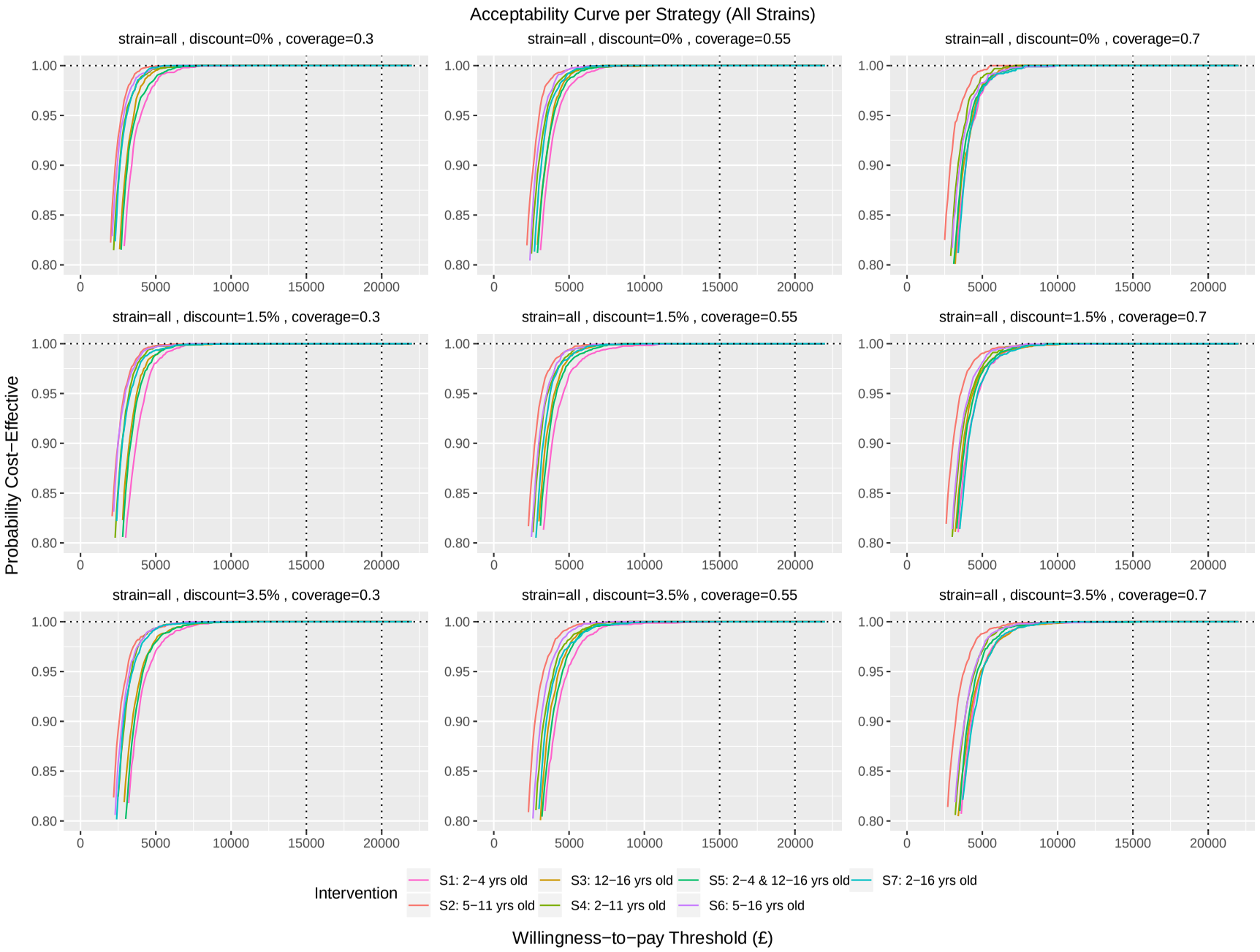

Figure 2.6.9: Acceptability Curve for strategies I1-I7 demonstrating the probability a strategy is cost-effective at different WTP under varied coverage and discount.

2.6.13 Cost-effectiveness plane under varied total coverage

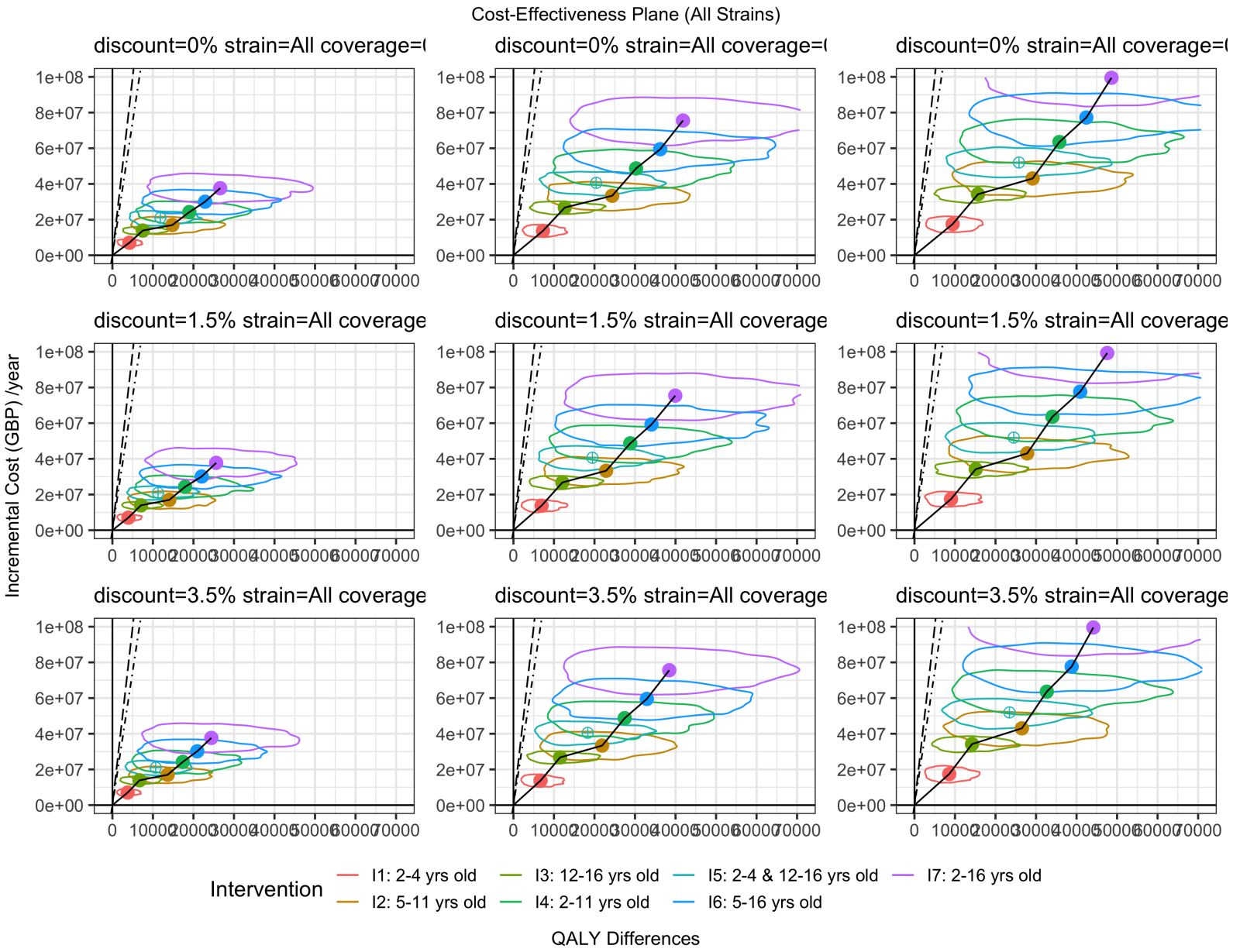

Figure 2.6.10: Cost-Efficiency frontier for all strains under 30%, 50%, and 70% achieved total coverage, evaluated at a WTP=£20,000.

2.6.14 Probability a strategy is optimal under varied total coverage and discount rates

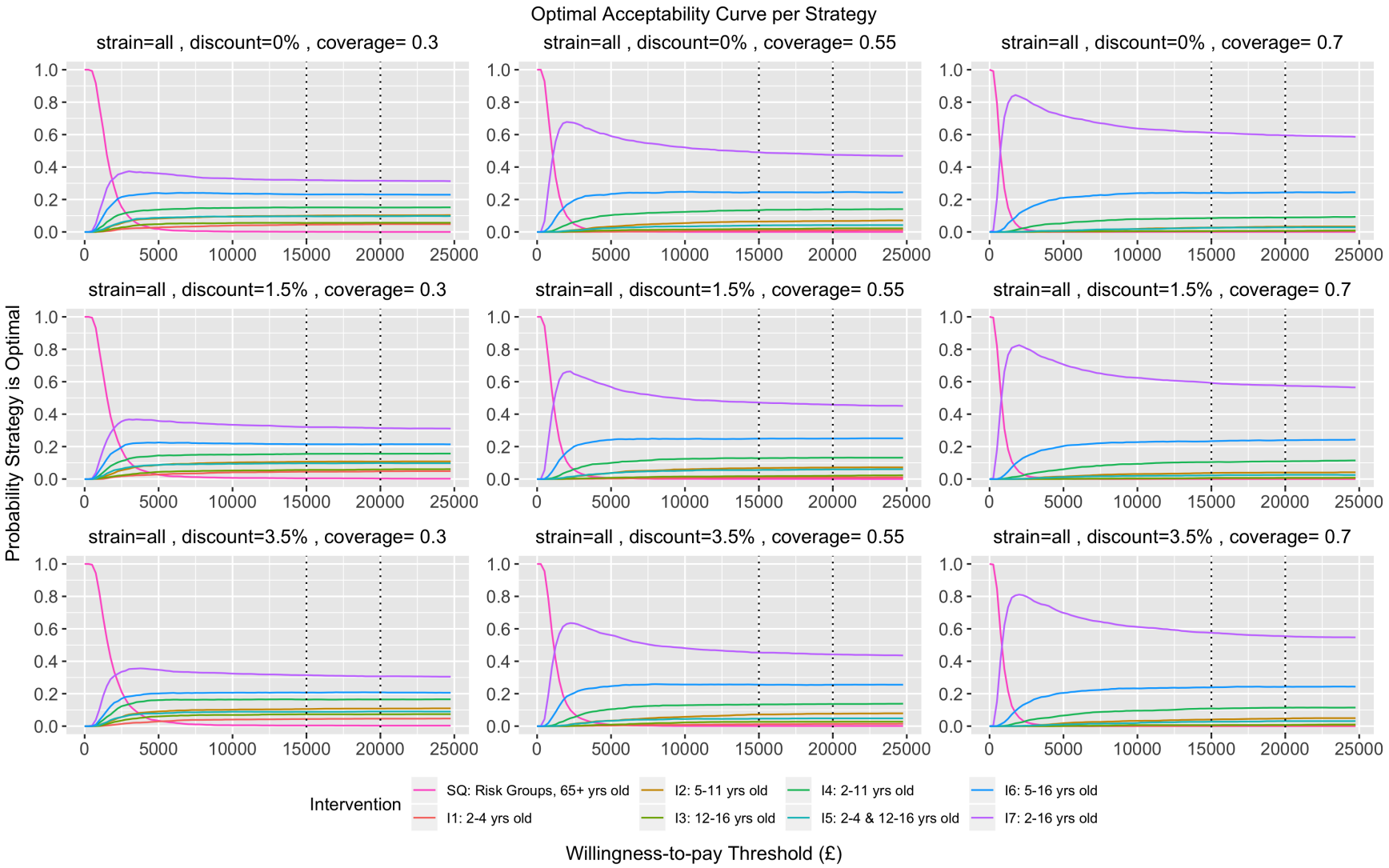

Figure 2.6.11: Probability a strategy is optimal at each coverage and discount level. The cumulative outcomes of all strains are considered.

2.6.15 Fixed discount, varied total achieved coverage

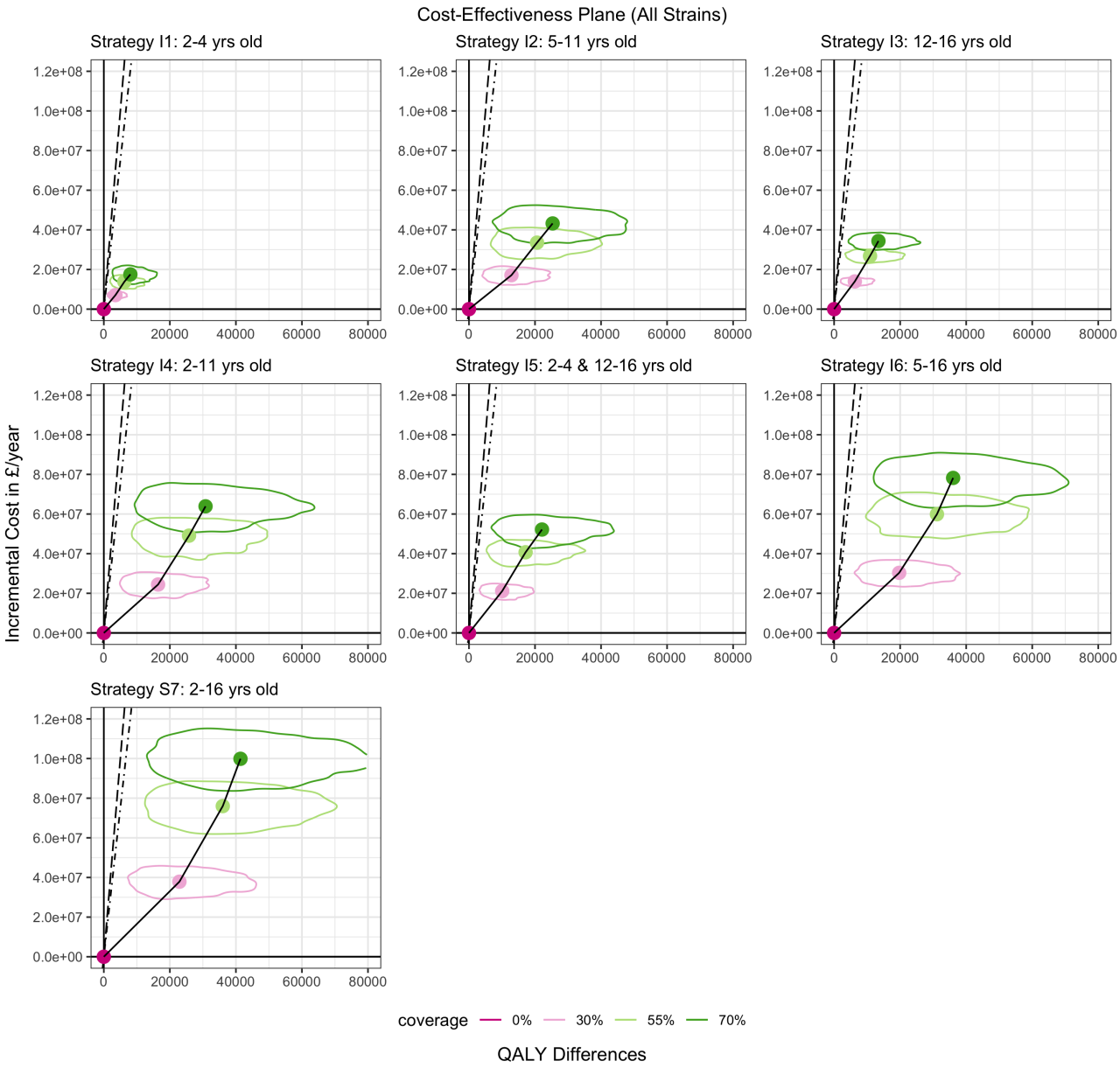

Figure 2.6.12: Cost-effectiveness plane for increasing coverage on the increments 30%, 55%, and 70% and where the discount is fixed at 3.5%. All strategies are examining in individual panels.

2.6.16 Strain-specific differences in cost-effectiveness plane under varied total coverage and discount

Cost-effectiveness plane stratified by influenza strain comparing all strategies where achieved coverage has been increased on the increments 30%, 55%, and 70% (Horizontal), and discounts have been increased on the increments 0%, 1.5%, and 3.5% (Vertical).

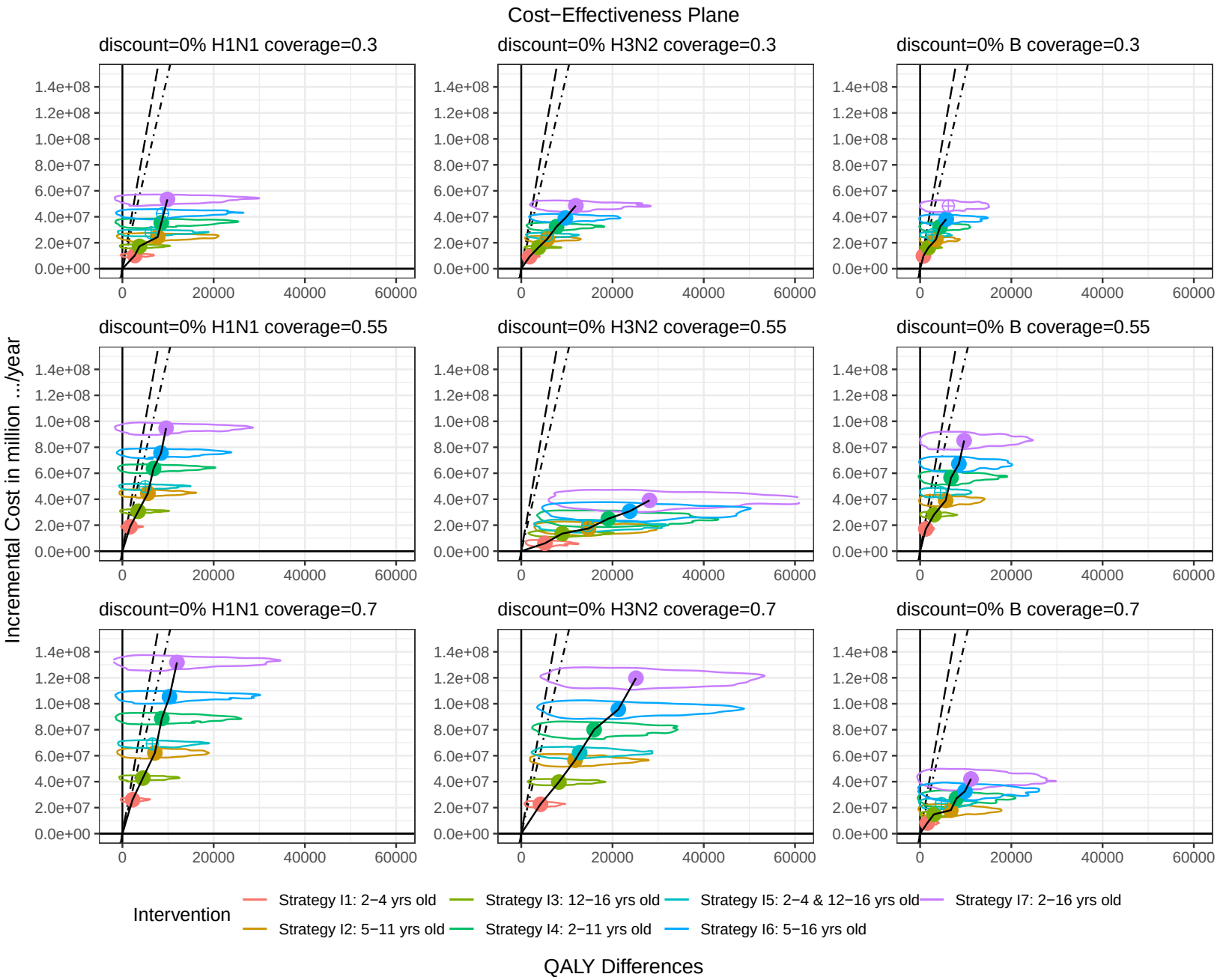
Cost−Effectiveness Plane
discount=0% H1N1 coverage=0.3
discount=0% H3N2 coverage=0.3
discount=0% B coverage=0.3
discount=0% H1N1 coverage=0.55
discount=0% H3N2 coverage=0.55
discount=0% B coverage=0.55
discount=0% H1N1 coverage=0.7
discount=0% H3N2 coverage=0.7
discount=0% B coverage=0.7
Incremental Cost in million .../year
0.0e+00
2.0e+07
4.0e+07
6.0e+07
8.0e+07
1.0e+08
1.2e+08
1.4e+08
0
20000
40000
60000
Intervention
Strategy I1: 2−4 yrs old
Strategy I2: 5−11 yrs old
Strategy I3: 12−16 yrs old
Strategy I4: 2−11 yrs old
Strategy I5: 2−4 & 12−16 yrs old
Strategy I6: 5−16 yrs old
Strategy I7: 2−16 yrs old
QALY Differences

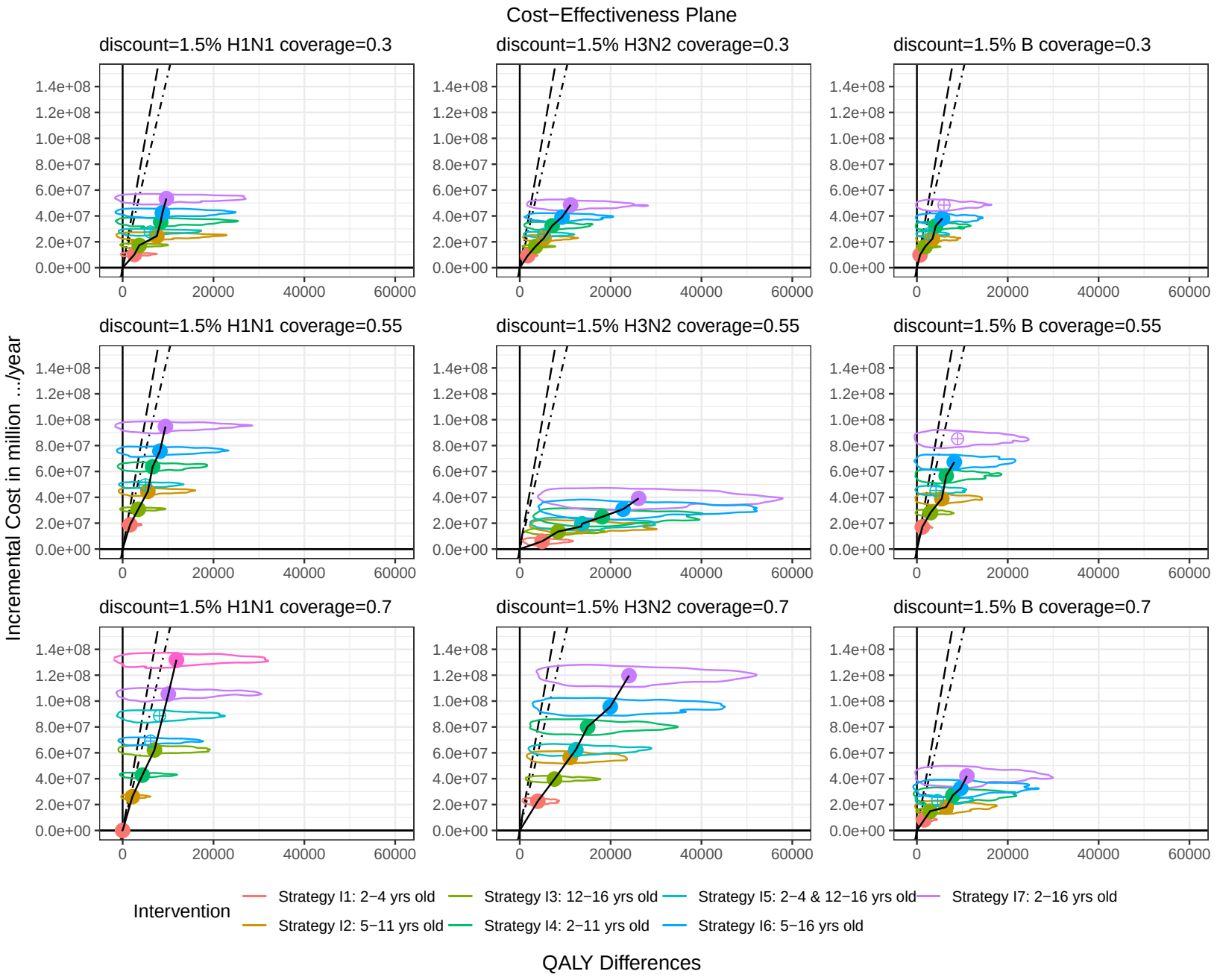
Cost−Effectiveness Plane
discount=1.5% H1N1 coverage=0.3
discount=1.5% H3N2 coverage=0.3
discount=1.5% B coverage=0.3
discount=1.5% H1N1 coverage=0.55
discount=1.5% H3N2 coverage=0.55
discount=1.5% B coverage=0.55
discount=1.5% H1N1 coverage=0.7
discount=1.5% H3N2 coverage=0.7
discount=1.5% B coverage=0.7
Incremental Cost in million .../year
0.0e+00
2.0e+07
4.0e+07
6.0e+07
8.0e+07
1.0e+08
1.2e+08
1.4e+08
0
20000
40000
60000
Intervention
Strategy I1: 2−4 yrs old
Strategy I2: 5−11 yrs old
Strategy I3: 12−16 yrs old
Strategy I4: 2−11 yrs old
Strategy I5: 2−4 & 12−16 yrs old
Strategy I6: 5−16 yrs old
Strategy I7: 2−16 yrs old
QALY Differences

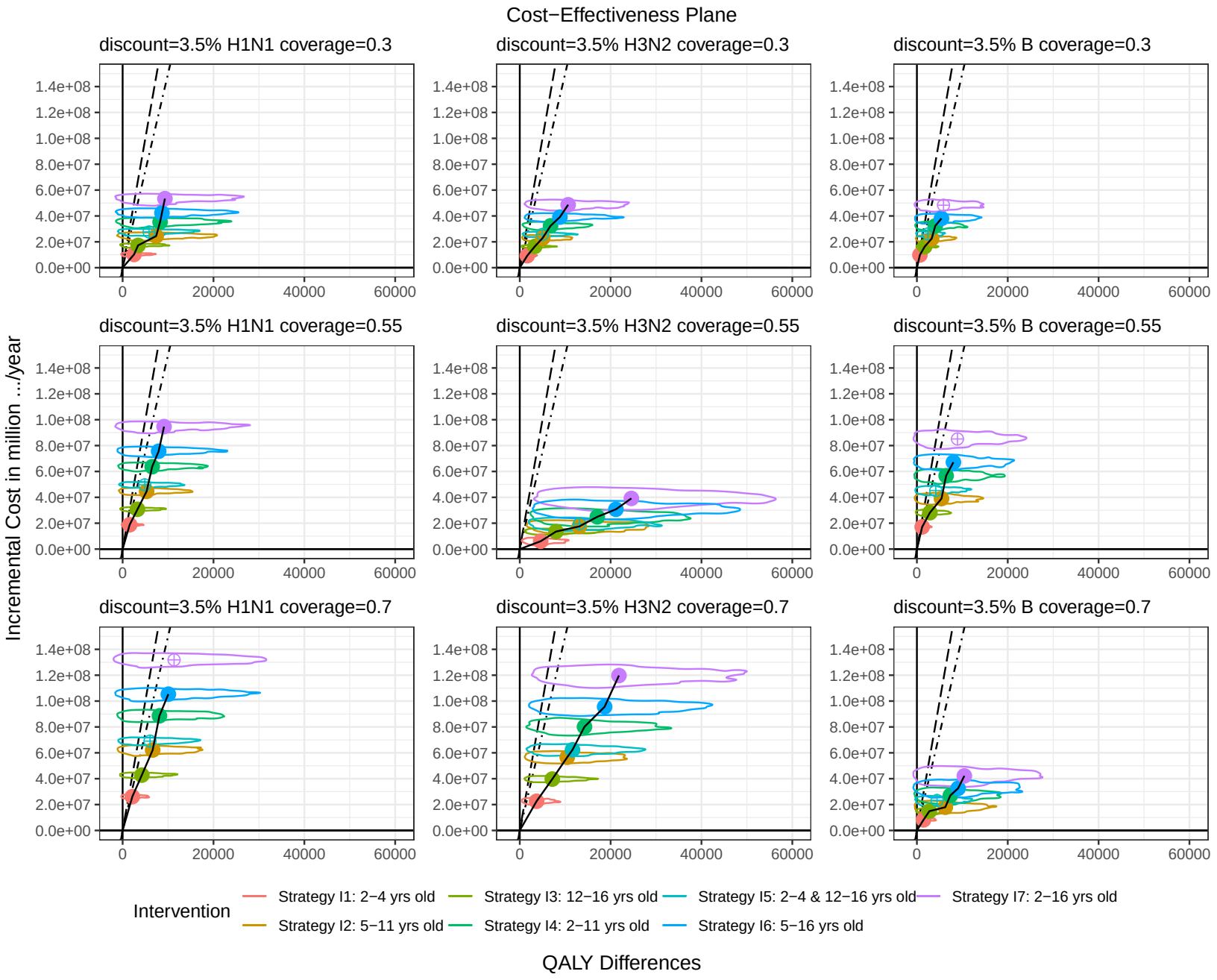
Cost−Effectiveness Plane
discount=3.5% H1N1 coverage=0.3
discount=3.5% H3N2 coverage=0.3
discount=3.5% B coverage=0.3
discount=3.5% H1N1 coverage=0.55
discount=3.5% H3N2 coverage=0.55
discount=3.5% B coverage=0.55
discount=3.5% H1N1 coverage=0.7
discount=3.5% H3N2 coverage=0.7
discount=3.5% B coverage=0.7
Incremental Cost in million .../year
1.4e+08
1.2e+08
1.0e+08
8.0e+07
6.0e+07
4.0e+07
2.0e+07
0.0e+00
0
20000
40000
60000
Intervention
Strategy I1: 2−4 yrs old
Strategy I2: 5−11 yrs old
Strategy I3: 12−16 yrs old
Strategy I4: 2−11 yrs old
Strategy I5: 2−4 & 12−16 yrs old
Strategy I6: 5−16 yrs old
Strategy I7: 2−16 yrs old
QALY Differences

Strain-specific differences in acceptability curves

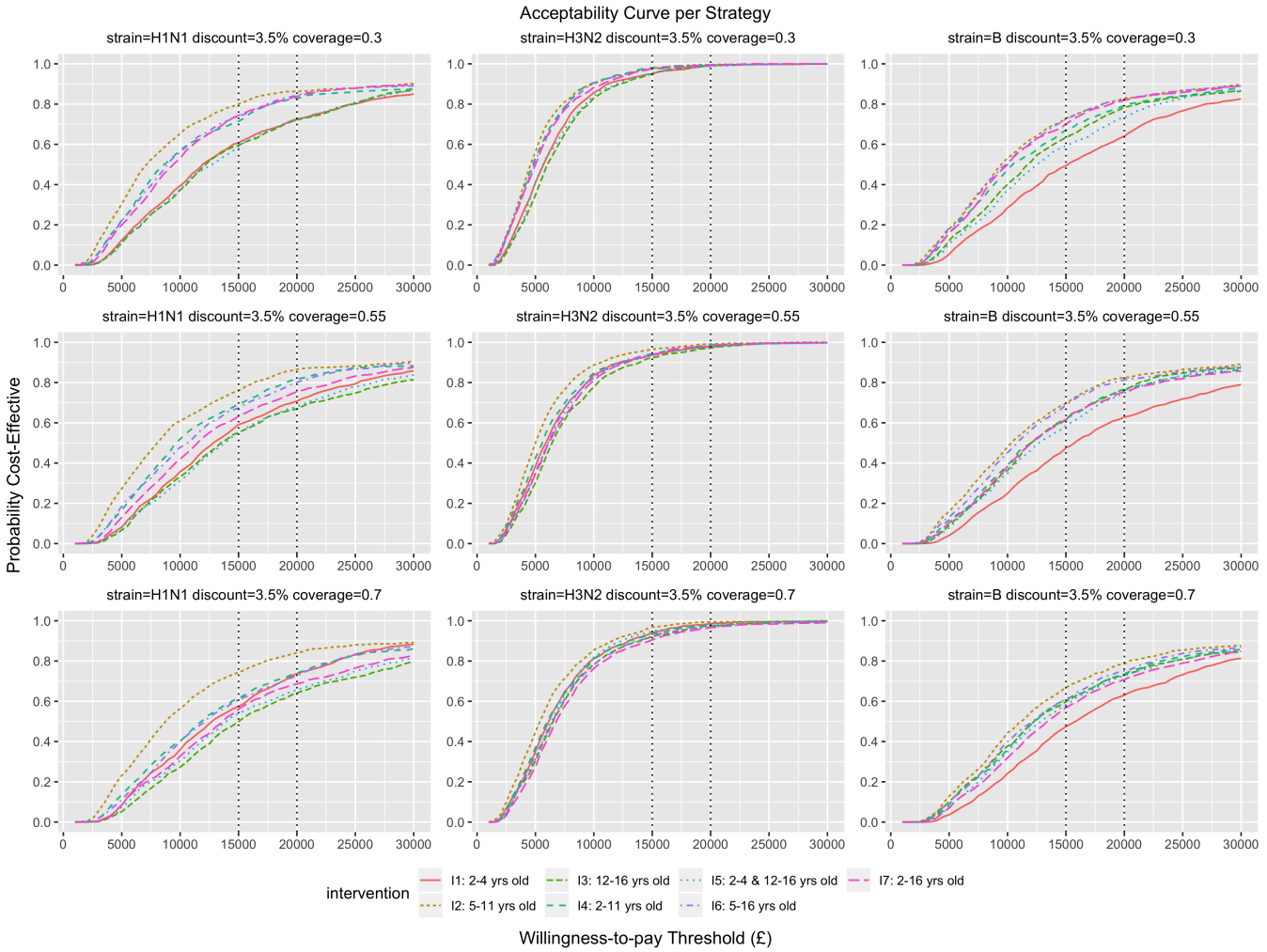

Figure 2.6.13: CEAC indicates the probability that an intervention is cost-effective compared with an alternative given the observed data for a range of willingness to pay values. Here the CEAC is shown for each strategy under influenza strains A/H1N1, A/H3N2, and B (Horizontal) and under total coverage varied a 30%, 55%, and 70%.

Chapter 3

Sensitivity of optimal choice of vaccination strategy to changes in social contact patterns

Abstract

Background The Bayesian framework allows one to use prior information when calibrating transmission models of vaccination policy. Previous transmission models have not assessed the value of prior information of the contact patterns. However, many vaccine policy decisions are based on quantifying the value of indirect effects from vaccination, such as Live-Attenuated Influenza Vaccine Nasal Spray (LAIV). Many countries do not have empirical studies describing their contact patterns, and often those of geographical neighbours are used.

Methods We fit and parameterized a transmission model of influenza in Great Britain using survey data from 10 other countries to construct counterfactual contact patterns. Using the counterfactual contact patterns we conducted cost-effectiveness analysis of three pediatric vaccination policies and compared the results to those derived using the country-specific Great Britain contact structure.

Results Country-specific contact patterns add value in calibrating transmission models. Specifically, the prior information on contact patterns do not converge on the same posterior, such that one's posterior belief about the relative importance of each age group in transmission changes based on the prior information We show the relative impact of age groups on transmission that come from the choice of contact patterns used as priors decrease the probability a strategy is considered cost-effective by propagating uncertainty through the model.

Conclusion Even using substitute patterns as prior information can alter vaccine decision-making. Therefore, we would advocate that in the absence of country-specific contact patterns, structural uncertainty analysis should be undertaken when quantifying the effect of strategies that involve herd immunity

3.1 Introduction

The increasing profile of decision analysis in public health planning and emergency responses (e.g. 2014 Ebola crises, Disease X) highlights a commensurate need for increased accuracy in health policy recommendations. Although statistical models are calibrated with empirical evidence, models which use a Bayesian framework first express uncertain quantities using a probability distribution that is informed by the researcher's beliefs. In particular, disease transmission models are sensitive to potential bias derived from the choice of social contact data used to emulate viral transmission. Vaccination policy decisions are based on quantifying the potential health-economic value of indirect vaccine effects in the population. With vaccination, indirect effects are produced by an increase in herd immunity–the collective immunological status of the population. Consequently, an individual or subgroup may have many different potential disease outcomes depending on the vaccination status of their potential contacts. In this situation researcher beliefs about the underlying social structure of a population introduce bias into the estimation of a vaccination strategy's effectiveness and any subsequent cost-effectiveness calculations based on these results.

Social contact data often stratify individuals by age, risk group, or sex and calculate the number of interactions between these subgroups. The resulting interactions are summarized in contact matrices whose entries represent the average number of contacts per unit time between individuals of group i with individuals of group j.[60] This approach relies on assumptions of homogeneous mixing within each subgroup and on the social contact data being representative of the average mixing behavior between classes.[61] The data to build these matrices are derived from large, often expensive, prospective cohort surveys meant to represents the population of interest.[62] The difficulties of collecting data have led to a scarcity of population-specific contact data,[63] and this scarcity has led to researchers make an equivalence assumption expressing their belief about the type of social contact occurring. For example, if the contact matrix of Sweden has not been determined a contact matrix from Finland might be substituted assuming equivalence between the two population social contact networks.[64] In many situations this equivalence assumption is the most parsimonious course of action. However, previous studies of disease transmission models have not assessed the value of country-specific information for social contact patterns.

It is critical the structural uncertainty derived from researcher choice of contact structure be quantified. An accurate description of human contacts reduces bias in vaccine intervention predictions and provides a more discriminating choice between overlapping or closely related strategies. To resolve questions about the effect parameterization of social contacts have on decision model outcomes, we deliberately incorporated structural uncertainties into a model

of influenza incidence in England and Wales. As the first step in resolving this problem we perform sensitivity analysis on an existing model of influenza incidence contained in the R package 'fluEvidenceSynthesis'. We achieve this by varying the choice of contact matrix among the empirical social contact patterns of ten countries.

3.2 Methods

3.2.1 Contact survey

Survey data on social contacts were obtained from multiple prospective studies conducted to measure and compare the structure of contacts. Survey participants were asked to complete diaries recording with whom they had contacts during a day. Diaries also recorded contact characteristics such as the age of the contact, the nature of the contact (conversational or physical contact), and the nature of the day (weekday, weekend, or holiday). The majority of our social contact data came from the POLYMOD study, a European Commission project which recorded interaction data for individuals in the Great Britain (GB), Belgium (BE), Germany (DE), the Netherlands (NL), Poland (PL), Finland (FI), Luxembourg (LU), and Italy (IT).[62] We also obtained survey data from similar published studies examining Peru (PE)[65], France (FR)[66], and Zimbabwe (ZI)[67] which utilized the POLYMOD questionnaire format. We considered only conversational contacts for this study as physical contact is not necessary to spread respiratory viruses like influenza.

3.2.2 Estimating the contact matrix

It has previously been demonstrated that a contact matrix directly inferred from the POLYMOD sample means was unable to explain disease dynamics in the population of Great Britain.[68] We assumed there exists among each country-specific survey a set of resampled participants that represents an appropriate structure of contacts in terms of disease transmission. Therefore population mixing was described by randomly sampling the empirical country-specific survey data with replacement. This process was performed on the data from all 10 countries to represent multiple iterations of the participant survey—as if the survey had been performed multiple times. After weighting by weekends vs weekdays following the method described in Baguelin et al.[69] each bootstrapped result was used to generate an 11-by-11 contact matrix containing a total 121 measures of the average contact rate between each age group. Each cell of the contact matrix contains the effective contact rate between each of the 11 age groups. For example, the average number of contacts per day between the 5-11 year old group and the 12-14 year old group would be the effective contact rate for an

individual aged 7 years old with an individual aged 13 years old. In this study, we consider an average contact matrix over the epidemic season and do not consider holiday periods or weekends.

3.2.3 Mathematical model

The original 'fluEvidenceSynthesis' model estimated the historical influenza-related morbidity and mortality that would have occurred from 1995-2009 under various seasonal influenza vaccination policies for influenza strains A/H1N1, A/H3N2, and B.[18] The compartmental model divides individuals into susceptible (S), latent (E), infected (I), recovered (R) states with different epidemiological compartments determined by vaccine history and age classes. We structured eleven age groups into the model on the intervals: 0-<1,1, 2-4, 5–11,12-14, 15–16, 17-24, 25–44, 45–64, 65-74, 75+ years. In addition to age stratification, two risk strata for simulating individuals at low and high risk of complications from influenza infection were included (e.g. immunosuppressed persons). The final Susceptible-Exposed-Infectious-Recovered Compartmental Model (SEIR) model contains a total 22 separate age-risk strata.

Parameters of interest were the ascertainment probability (ϵ_i, i=0-14 years old, 15-64 years old, 65+ years old), virus transmissibility (q), the probability of becoming infected outside of the main epidemic (ϕ), age-group specific susceptibility (σ_i, i=0-14 years old, 15-64 years old, 65+ years old), and a coefficient for the initial number of infections each season per strain (I_0). Prior distributions for epidemiological parameters are shown in (Supplemental Table 3.6.3). Further detail on the model construction and the R package have been described in earlier papers.[18, 20, 19]

3.2.4 Model calibration

Using the empirical contact matrix for GB each influenza season during the years 1995/1996-2008/2009 was fit independently using an adaptive Markov chain Monte Carlo (MCMC) algorithm. The MCMC was performed using the function 'adaptive.mcmc' contained in the R package 'fluEvidenceSynthesis'. Ten additional MCMCs were also performed, again using the influenza model of Great Britain, except the GB survey data that is resampled during the MCMC fitting process is replaced with one of the ten survey datasets derived from other countries (e.g. FR, DE). Each seasonal MCMC averaged 1.4 million iterations before convergence. Chain convergence was determined with the Gelman-Rubin diagnostic test using a potential scale reduction factor adjusted for sampling variability threshold of 1.2 or below.[70, 55]

The MCMC algorithm compares the likelihood of the $(k-1)th$ and kth model iterations

using a proposed set of parameters. At each kth iteration in the Markov chain the matrix is updated by randomly sampling with replacement from the empirical country-specific contact data. Thus the contact matrix is inferred within the MCMC algorithm via a novel random-walk type of proposal on the matrix space. The contact matrix is combined with the age-structured demographic data and scaled by q–the transmissibility of the virus–resulting in the transmission matrix of the virus. To simulate the seasonal influenza epidemics the SEIR model utilizes this transmission matrix to determine the probability of transmitting influenza virus when an individual in age group i makes respiratory contact with an individual in age group j. After convergence examination of the set of accepted transmission matrices form a posterior distribution that approximates the appropriate disease transmission contact structure per influenza season and strain. To conserve memory during the MCMC, we store a vector of participant id numbers per iteration instead of the proposed transmission matrix itself. The unique ids are used to reconstruct the proposed contact matrix from the survey data, which–after re-normalization and adjustments for symmetry–are used for intervention simulations.

3.2.5 Alternative scenario simulations

For each season we drew 3000 samples from the joint posterior parameter distribution estimated by the MCMC for the specific season and strain. For every set of parameters we simulated influenza incidence under each of the following vaccine interventions:

- **Strategy SQ:** Influenza vaccination program includes Low-Risk 65+ year olds, and high risk individuals in the age range 6 months to 65+ year olds vaccinated with Trivalent Inactivated Influenza Vaccine (TIIV) at empirical coverage levels.
- **Strategy I1:** In addition to the reference strategy, low-risk Preschool aged children (2–4-y-olds) are vaccinated to 55% achieved coverage.
- **Strategy I2:** In addition to the reference strategy, low-risk Primary School aged children (5–11-y-olds) are vaccinated to 55% achieved coverage.
- **Strategy I3:** In addition to the reference strategy, low-risk Secondary School aged children (12–16-y-olds) are vaccinated to 55% achieved coverage.

This process was repeated for each alternative contact matrix scenario under influenza strains A/H1N1 and A/H3N2. The status quo in addition to the three alternative vaccine strategies for the 11 contact matrices constitute 44 unique model simulations per strain. Live-Attenuated Influenza Vaccine Nasal Spray (LAIV) vaccination programs were simulated

starting on September 1st, the usual start of the fall session, and ending on December 12, a week before the Christmas holiday (Supplemental Section 3.6.8).

Vaccine efficacy

Influenza Vaccine Efficacy (VE) is dependent on two factors: (1) the degree of matching between vaccine strain and circulating strain that season, and (2) the quality of immune response generated in the host. High risk groups such as the immunocompromised and elderly subgroups are known to have increased susceptibility to disease and a poor immune response to the influenza vaccine resulting in low efficacy. Each age stratum was divided into individuals at low or high risk of complications associated with influenza (e.g. individuals with chronic conditions). We assumed the proportion of people in a risk group stratified by age is constant over the period 1995-2009 (Supplemental Table 3.6.1). Following National Health Service (NHS) 2018/2019 guidelines, our model assumed high risk individuals aged 6 months-2 years old and adults 18-64 years old received Quadrivalent Influenza Vaccine (QIV) and individuals aged 65+ years received TIIV.[30]

We do not use empirical VE estimates, instead we use two average VE estimates from the Cochrane collaboration[31] to emulate strain matching between the vaccine and wild-type strain during poor and well-matched years. When the vaccine was well-matched with the annual circulating strain VE was fixed at 70% in the general population and 42% in the clinical high risk and 65+ year old group. During poorly matched years we assigned 40% VE for the general population and 28% VE in the high risk and elderly group. We did not make specific allowances for differences in vaccine efficacy between the three vaccine types: LAIV, QIV, and TIIV. We assumed the 'all-or-nothing' mechanism of vaccine efficacy with a maximum protection period of one year. Likewise disease derived immunity lasted for one year maximum. For the 1995-2009 period strain-matching information was taken from Public Health England (PHE), then Health Protection Agency (HPA).[26]

3.2.6 Health-economic outcomes

The estimated number of health outcomes and the commensurate Quality-Adjusted-Life-Years (QALY) were calculated per influenza season and averaged across the 14 seasons. We considered health services use and the associated costs during the influenza season for the whole population of England and Wales. This was based on the calculated number of annual clinical cases, the number of general practitioner consultations, and the number of inpatient hospitalizations. Intervention costs included the per dose cost of vaccine acquisition, vaccine service, and provider reimbursement. Units of vaccine administration costs were

obtained from previously published studies, and from PHE/NHS budget documents when available. We calculated the costs of influenza vaccine delivery through pharmacies, General Practitioner (GP) consultations, and school-based programs as slight differences in cost exist between methods (Supplemental Table 3.6.5).

All costs are expressed in 2018 Great Britain Pounds Sterling. If costs were not available for the current years, costs from previous years were updated to 2018 Great Britain Pounds Sterling using the Consumer Price Index for Health Costs [35]. We assumed that services for waste disposal and sharps removal for all delivery methods–except school-based vaccination–were managed and paid for directly by the NHS with no additional cost.

Annual health outcomes estimated included cumulative infections, cumulative symptomatic infections, cumulative influenza-related GP consultations, hospitalizations, and cumulative influenza-mortality. To account for uncertainty in the estimated number of different health outcomes attributable to influenza per year, we sampled the normal distributions from Cromer et al.'s regression analysis (Supplemental Table 3.6.1) rather than using the reported mean estimates.[33] Individuals with symptomatic influenza experience an age/risk-specific reduction in QALY. Similarly, individuals infected with influenza who were hospitalized experienced a commensurate age and risk-specific quality of life lost, and fatal influenza infections were assumed to lose the average age and risk-group specific discounted quality-adjusted life expectancy. Age-specific quality of life weights for respiratory illnesses were taken from Kind et al., using the EQ-5D rating scale.[34, 71] We did not control for non–influenza-related complications or other confounding variables such as income, education, ethnicity, and number of co-morbidities.

3.2.7 Cost-effectiveness analysis

The cost-effectiveness analysis was conducted from the perspective of the NHS/PHE using a 14-year time horizon recurring on September 1st. Discount rates were calculated annually at 3.5% as recommended by the National Institute for Health and Care Excellence of England and Wales (NICE).[32]

We considered intervention strategies for which an alternative strategy would avert more QALYs at equal or lower cost were 'strongly dominated' and excluded them from the cost-effectiveness analysis. For each non-dominated strategy the Incremental Cost-Effectiveness Ratio (ICER) was calculated using the formula

$$ICER = (C_S - C_C)/(Q_C - Q_S)$$

where C_S is the predicted total of health care and vaccination costs and C_C the same total for

its comparator. The predicted QALY losses for a strategy and its comparator are designated as Q_S and Q_C, respectively. The comparator of a strategy is the next non-dominated strategy with the next lower incremental cost. Strategies with an ICER that is higher than the ICER of a more costly strategy were considered weakly dominated and excluded. ICERs for the remaining strategies were then recalculated accordingly. We used the remaining strategies to define the cost-efficiency frontier of the cost-effectiveness plane. In accordance with the NICE guidelines we classified an intervention strategy as 'cost-effective' if its ICER was less than £20,000 per QALY gained,[32] and also included a 'very cost-effective' definition if the ICER was less than £15,000 per QALY gained.

Calculating the optimal strategy

To incorporate parameter uncertainty into our analysis, we conducted a probabilistic sensitivity analysis using a Net Health Benefits (NHB) approach. The net-health benefits approach uses the cost-effectiveness threshold to convert the additional cost of a strategy and the health benefits conferred into a single metric. For each of the 3000 parameter sets drawn from the joint posterior distribution, we calculated the NHB and identified the intervention strategy that conferred the greatest net health benefits at a given cost-effectiveness threshold. We conducted this analysis across a range of Willingness-to-pay threshold (WTP) thresholds from £0-£40,000 on increments of £500. The strategy with the largest probability of conferring the greatest net health benefit across a range of cost-effectiveness thresholds was considered "optimal".

Comparison of the posteriors and prior distributions

For each substituted contact matrix scenario we compared the fitted posterior parameters to those from GB using the Two-sample Kolmogorov-Smirnov (KS test) test at a significance level $\alpha = 0.05$. The KS test is a non-parametric goodness-of-fit test where the null hypothesis is the two samples come from the same distribution, with the alternative hypothesis being the two samples do not follow the same distribution.[72]. The KS test was used to compare posterior parameters from each substituted scenario per season against the parameters of the GB scenario of the same season.

3.2.8 Calculating assortativity

Assortativity of a network has long been implicated in enabling disease transmission. For example individuals who are unvaccinated are more likely to associate with other unvaccinated persons.[73] We calculated the assortativity coefficient (r) for each influenza season's

set of posterior contact matrix using the formula:

$$r = \frac{diag(M) - \sum M^2}{1 - \sum M^2}$$

where M represents the contact matrix.[74] Positive values of r indicate a correlation between groups of similar ages, while negative values indicate relationships between groups of different ages.

3.3 Results

The MCMC using the ZI contact matrix failed to converge after 500,000 iterations therefore we excluded it from the subsequent analysis. We have chosen to display and discuss structural uncertainty results for simulations with influenza strain A/H1N1 as the cost and health margins between competing intervention strategies for this strain were narrower. The severity of influenza strain A/H3N2 infections resulted in all three strategies being cost-effective in all substituted scenarios (Supplemental section 3.6.14).

3.3.1 Posterior parameters

Statistically significant differences were observed between posterior parameter distributions derived by the MCMC in scenarios where contact survey data from other countries were substituted for that of GB survey. Comparison between the substituted parameter sets and GB parameter sets per season demonstrated that the parameter for the susceptibility of an individual in age group 6m-14 years old to influenza A/H1N1 ($\sigma_{6m-14yrs}$) rejected the null hypothesis across all substituted contact matrices except in the BE scenario ($p<0.01$). Despite the statistical differences, the order of the three age specific values of susceptibility parameters (σ) remained the same across substituted simulations.(Figure 3.5.1) For example, the probability an individual aged 65+ was susceptible was consistently higher than the susceptibility of children six months to 14 years old. Parameter fits for the FR substitution were most likely to reject the null hypothesis. For the FR simulation only the parameters for case ascertainment among 65+ year olds ($\epsilon_{65+yearsold}$) and the probability of outside infection (ϕ) failed to reject the null hypothesis during the majority of seasons ($p<0.05$).

Posterior contact matrices

Given different contact structure information, posterior contact matrices did not converge on the same posterior distribution of average daily contacts (Supplemental Section 3.6.5).

When contact matrices generated from bootstrapping the empirical surveys were compared with posterior contact matrices from the MCMC, the results showed the bootstrapped survey distribution underestimated the overall number of contacts, especially among young children and older adults. The posterior contact matrices from the MCMC has highly assortative mixing, meaning individuals were more likely to associate with others individuals from the same age group as themselves. Compared to their naive bootstrap, the posterior contact matrices showed increases in the average number of contacts per day among ages 2-24 years old. For example comparison of the contact matrices generated by the bootstrap and the matrices from the posterior in the substitute IT simulation (Figure 3.6.6) showed an increase in the average contact rate between 5-11 year old survey participants and 5-11 year old contacts ($c_{5-11,5-11}$) from 3-5 contacts to 5-7 contacts per day.

To understand the shift in relative importance of age groups caused by the substitution of a country-nonspecific contact matrix, we compared the assortativity coefficient (r) for each posterior contact matrix to its average reproductive number (R_0) over the 14 seasons (Supplemental Figure 3.6.18). Most simulations spanned a range of assortativity coefficients, but all followed a similar trend: that increased assortativity was associated with increases in R_0. Assortativity coefficients between 0.9 and 0.92 were associated with crossing the the epidemic threshold ($R_0 > 1$), for simulations BE, PL, IT, LU, and GB. Simulations for FR and Peru (PE) had the highest estimated assortativity and the highest mean R_0, but also had the same linear relationship between the assortativity coefficient and R_0.

3.3.2 Vaccination strategy effectiveness sensitivity

Examination of the age-stratified infections averted per 1000 vaccine doses revealed indirect effects vary between simulations because of different contact rates between age groups. For simulations of strategies I2 or I3, the contact matrix of FI consistently produced the fewest number of averted infections per 1000 vaccine doses, 23 (95% CI 20, 25) and 34 (95% 28,41) for I2 and I3 (Supplemental Figure 3.6.15). Under strategy I2 the infections averted per 1000 doses produced similar results when the contact data for FI and LU was substituted. However, under strategy I3 the simulation for LU increased the number of infections averted from 27 to 62, while the simulation for FI remained equivalent to its values under strategy I2. Comparisons of the contact matrices of FI and LU revealed a daily contact rate between 17-24 year olds and 15-16 year olds of 1.6 to 2.1 in the LU simulations. The contact rate between the same age groups in the FI simulations was lower at 0.7 to 0.8 contacts per day. Likewise simulations under the PE contact matrix increased from 62 infections averted under I2 to 198 infection under strategy I3. Examination of the PE contact matrices again revealed

a similar pattern to that of LU, where the average number of daily contacts between 17-24 year olds and 15-16 year olds was 6.9.

Shifts in the relative importance of each age group in population-level disease transmission meant each substituted scenario responded differently to the intervention strategies despite simulations using fixed costs, fixed coverage rates, and a fixed population. Stratifying by age revealed where these differential responses to the vaccination strategy occurred. For example simulations using data from the NL or PE had a large reduction in influenza incidence among teenagers under Strategy I3 because of the direct effects of vaccination. However in scenarios with NL and PE, Strategy I3 indirectly decreased in the number of symptomatic cases among unvaccinated 17-24 years old. Under the Peru scenario symptomatic cases among 17-24 year olds were reduced 73% compared to the status quo strategy with the same contact matrix. These indirect effects were consistently high in the PE scenario also decreasing symptomatic infections among 0-1 year olds, 5-11 year olds, and individuals aged 25 or older (Supplemental Figure 3.6.11). These indirect effects were not replicated or replicated to a much lower degree in simulations with other contact matrices.

Cost-effectiveness sensitivity

Among scenarios where the contact matrix had been substituted with that of another country, Strategy I3–LAIV vaccination of 12-16 year olds–resulted in the lowest influenza incidence and had the highest probability of being cost-effective (Figure 3.5.2). Strategy I3 produced the fewest symptomatic cases although the degree of illness reduction and the level of vaccine effectiveness varied substantially between substituted simulations (Supplemental Table 3.6.6). Strategy I2, vaccination of primary school children aged 5-11 years old, was strongly dominated by Strategy I3 in the GB scenario and all substituted scenarios, meaning no other strategy could avert more QALYs at a lower cost per QALY. Substituting the GB matrix for that of FR, DE, or NL lead to both Strategy I3 and I1 associated with cost-effectiveness. In the FI simulation none of the proposed strategies I1-I3 were considered cost-effective.

Uncertainty around the probability a strategy is cost-effective under varied Willingness-to-pay (WTP) levels was examined using an acceptability curve for each substituted simulation (Figure 3.5.3). Substituted simulations all had increased uncertainty around a strategy's cost-effectiveness. For instance the probability Strategy I3 was cost-effective at the £20,000/QALY WTP was 40%. Under substituted scenarios at WTP £20,000 and the probability Strategy I3 was cost-effective ranged from 20%-38% with a minimum under the FI scenario and maximum under the NL scenario. Under the GB scenario the probability strategy I1 and I2 are cost-effective are comparable for the WTP range £0-40,000. In the substituted simulations using BE, IT, FI, DE, and PL Strategy I2 and I1 do not have equiv-

alent probabilities. In scenarios with BE, IT, and PL strategy I2 has a greater probability that I1 of being cost effective, while in DE and FI the Strategy I1 has a greater probability. Comparison of the acceptability curves between scenarios also revealed differences in the marginal increases in probability per incremental increase in WTP. For example the gradient of the acceptability curve of GB, NL, FR, and PE follows a logistic growth curve, while that of BE, FI, and DE have lower marginal gradients and follow a linear distribution.

Optimal strategy sensitivity

The probability a strategy was optimal, and its subsequent rank order in terms of the optimal strategy were sensitive to the changes in the choice of contact survey.(Figure 3.5.4). Each curve depicts the probability that I1, I2, I3 or the Status Quo Strategy (SQ) strategy would confer the greatest net health benefit across a range of WTP thresholds. The rank order of optimal strategies in the GB scenario varied from that of the substituted scenarios. Despite the fact strategy I2 was strongly dominated in the GB cost-effectiveness analysis strategy I2 was the optimal strategy for WTP levels of £8000 per QALY gained and greater, including at the NICE WTP of £20000 per QALY gained. This means, under the GB contact matrix, strategy I2 produces the largest net health benefit of all strategies, but does not achieve these benefits in a cost-effective manner. For simulations using the FR, NL, PE, and LU contact matrix Strategy I3 had a greater probability of being optimal than Strategy I2 at the £20,000 WTP threshold. In the FI scenario the status quo strategy was optimal up until the £22,000 WTP threshold, consistent with a strategy not being cost-effective. The WTP threshold at which strategy I1 intersects the status quo also varied substantially between all substituted scenarios. In scenarios with large incidence such as FR the intersection occurred at WTP £6000/QALY, while for other scenarios such as FI, NL, and PE the intersection between I1 and the SQ strategy did not occur on the WTP range £0-£40,000.

The variation caused by contact matrix choice was most evident in a side-by-side comparison of the cost-effectiveness acceptability frontier–the frontier that would be chosen under rules maximizing net health benefit (Figure 3.5.5).[75] The Cost-Effectiveness Acceptability Curve (CEAC) in substituted scenarios was similar to the general trend of the 'true' GB CEAC, but was most likely to shift right meaning inflection points between competing strategies occurred at higher WTP. In no scenario was Strategy I1 an optimal strategy, meaning it is cost-effective under some scenarios but never optimal. With the exception of the PE scenario, all scenarios demonstrated a CEAC curve where either SQ, I2, or I3 had a 35%-40% of being optimal at the £20,000 WTP threshold. The PE scenario was the only scenario with a 57% probability of strategy I3 being optimal.

3.4 Discussion

Cost-effectiveness estimates and the model simulations these estimates are based on are significantly reliant on the scientific judgments surrounding the choice of contact matrix. Substitution of contact data (e.g. data for France in-lieu of data for GB) in a well-converged model does not produce the same quantitative conclusions as the results from country-specific contact data. Examination of the acceptability curve demonstrated the probability a substituted strategy was cost-effective was consistently lower in substituted scenarios than when a country-specific contact matrix was used. Comparisons between epidemic simulations under the GB contact matrix and simulations with substituted contact matrices demonstrate researcher choice regarding contact matrices provide information beyond that of surveillance data and increase the predictive accuracy of stratified models.

Although all substituted models were able to identify strategy I3 as cost-effective and Strategy I2 as dominated, 60% of the substituted simulations ruled out Strategy I1 through strong dominance. The differential cost-effectiveness conclusions regarding Strategy I1 can be interpreted in two ways. The first is a cautionary tale, where cost-effectiveness simulations of multiple vaccine policies with small margins may make it possible for viable strategies to be ruled out due to the uncertainty propagated through model simulations by country-nonspecific contact data. On the other hand use of substituted contact matrices as a structural uncertainty analysis tool may weed out vaccination strategies that are not robust to variation in key age groups or to certain populations. As in the simulation of FI, we discovered that no pediatric LAIV vaccination scheme was cost-effective in a population with low contact rates between vaccinated 15-16 year olds and naive 17-24 year olds ($c_{17-24,15-16}$). Conversely when this rate was high–as in the LU scenario–vaccination strategies like I3 drastically increased the number of infections averted through indirect effects. More influenza infections were averted per dose when an adjacent or 'bridge' age group connected a vaccinated age group with other large age groups. Depending on the level of uncertainty decision makers are willing to accept, the use of substitute contact matrices may add nuance to adopting strategies in areas where social contact structure may be rapidly changing (e.g. refugee camps) to ensure viability or the at-risk population age structure does not allow for sufficient driver age groups or 'bridge' groups to have a cost-effective impact (e.g. prisons, schools). However it is important to note the contact structure of the population is largely immutable in terms of direct policy interference, meaning vaccine policy must suit the social contact structure and not the other way around.

For our cost-effectiveness analysis we considered a health care provider perspective meaning we did not consider demographic characteristics such as gender, income, or spatial char-

acteristics. A major model assumption is that talking with another person as conversational contact constitutes the main at-risk events for transmitting infectious diseases. In reality, there exist other at-risk events that are not captured in our analysis (e.g. surface fomites).

A linear trend exists between R_0 and the assortativity coefficient of the contact matrix, but this trend had no bearing on determining if a strategy would be cost-effective. For example the two substituted scenarios with the highest R_0–PE and FR–converged on Strategy S3 as the most cost-effective but had completely divergent outcomes in terms of average influenza incidence, total healthcare costs, and QALY lost. We did not identify any other linear correlations between the contact matrix and a simulation subsequently being cost-effective.

The contact surveys for FR[76] and PE[77] were not part of the Mossong et al.[23] 2008 study but were conducted separately using the same questionnaire and study guidelines. During our assessment of assortativity FR and PE had the highest R_0 and assortativity coefficients which could be the result of differences between the original Mossong et al. survey and subsequent surveys. However we think survey-related differences are unlikely given that the high assortativity of both FR and PE is easily explained by the high number of average contacts in both surveys. Furthermore both surveys in PE and FR were conducted separately and were still able to converge on a similar trajectory when plotted against R_0.

Our methodology followed the approach of a one-way sensitivity analysis where one or more parameters are perturbed and the corresponding effects on an outcomes are examined .[78, 79] Instead of perturbation we used 10 empirical contact matrices to represent counterfactual socialization scenarios for GB. Varying each matrix cell incrementally or between probability distribution extremes would produce an unfeasible amount of contact scenarios of which many would be non-viable. Using empirical matrices also sidestepped the issue of preserving higher order dependencies between contact matrix subgroups. In a population each subgroup i needs a feasible number of contacts j that constrains the remaining matrix rows. Any sensitivity analysis perturbations to the contact rate between two subgroups would have to simultaneously produce a change in the interactions of both parties and with all remaining subgroups. Eigen-based decomposition methods used in the literature can reproduce these higher order dependencies, but these methods sacrifice real-world epidemiological interpretability through re-scaling. As interpretation of contact rates and interactions was an important aspect of our research into the variations of cost-effectiveness, use of empirical contact matrices were again the obvious choice. Research on simulating contact matrices using demographic data[80] or serology [81] has been published, but we were unable to include simulated matrices in our analysis. The fitting process used by the MCMC to estimate the contact matrix is reliant on bootstrapping the original survey data with the expectation an appropriate disease transmission contact structure exists among the possible

sets of re-sampled participants.[18] Without original survey data the to resample during the MCMC the posterior contact matrix cannot cannot be calculated using this method.

Although we only had 10 matrices available, ours is the first study to our knowledge, that identifies the structural uncertainties between assumptions regarding contact patterns and cost-effectiveness analysis. Going forward there is no expectation that researchers wait for perfectly accurate social contact data before conducting a cost-effectiveness analysis for vaccine policy. We advocate that in the absence of country-specific contact patterns, structural uncertainty analysis should be undertaken when quantifying the health and cost effects of vaccine strategies that involve herd immunity.

3.5 Figures

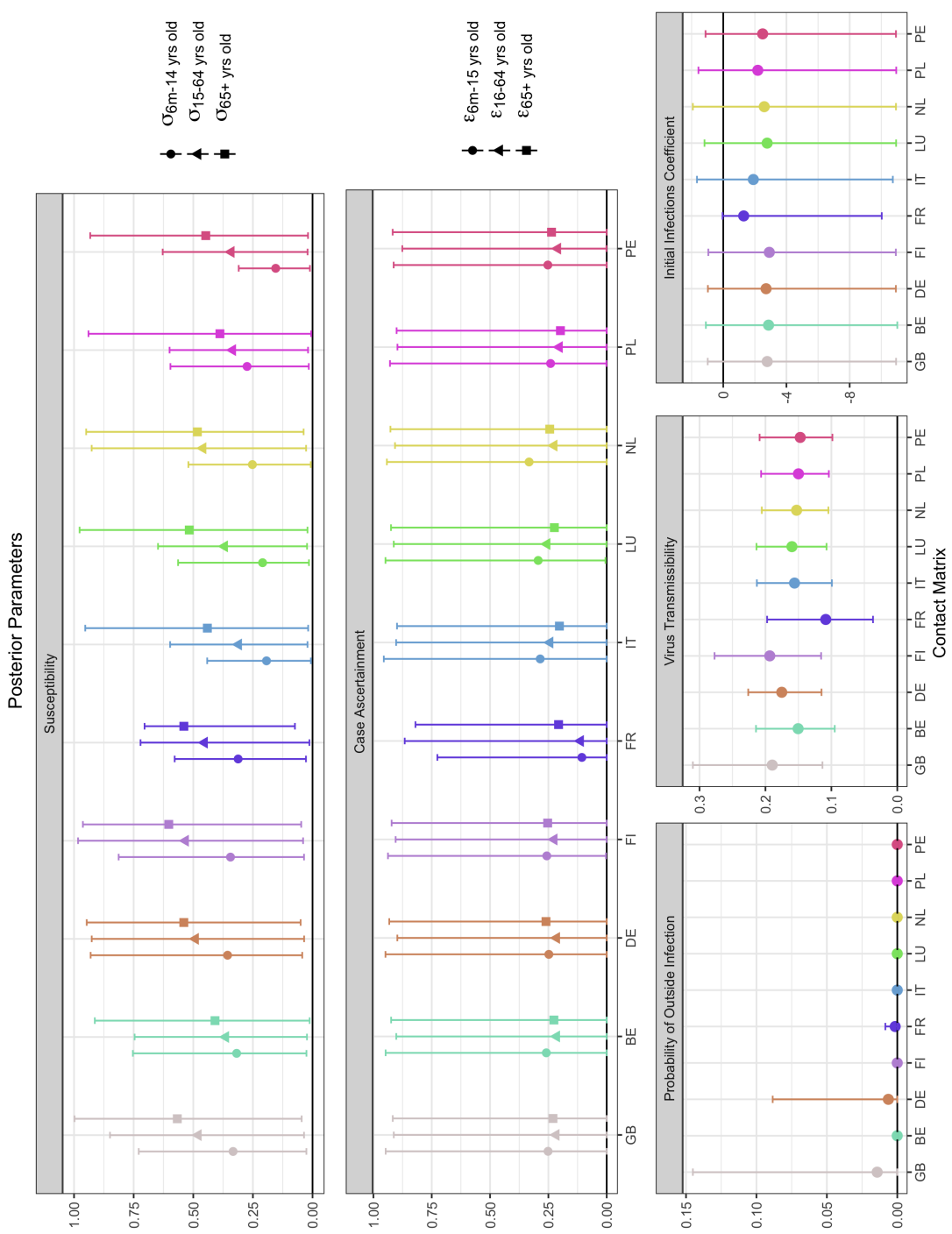

Figure 3.5.1: Posterior distributions of fitted parameters for each contact matrix.

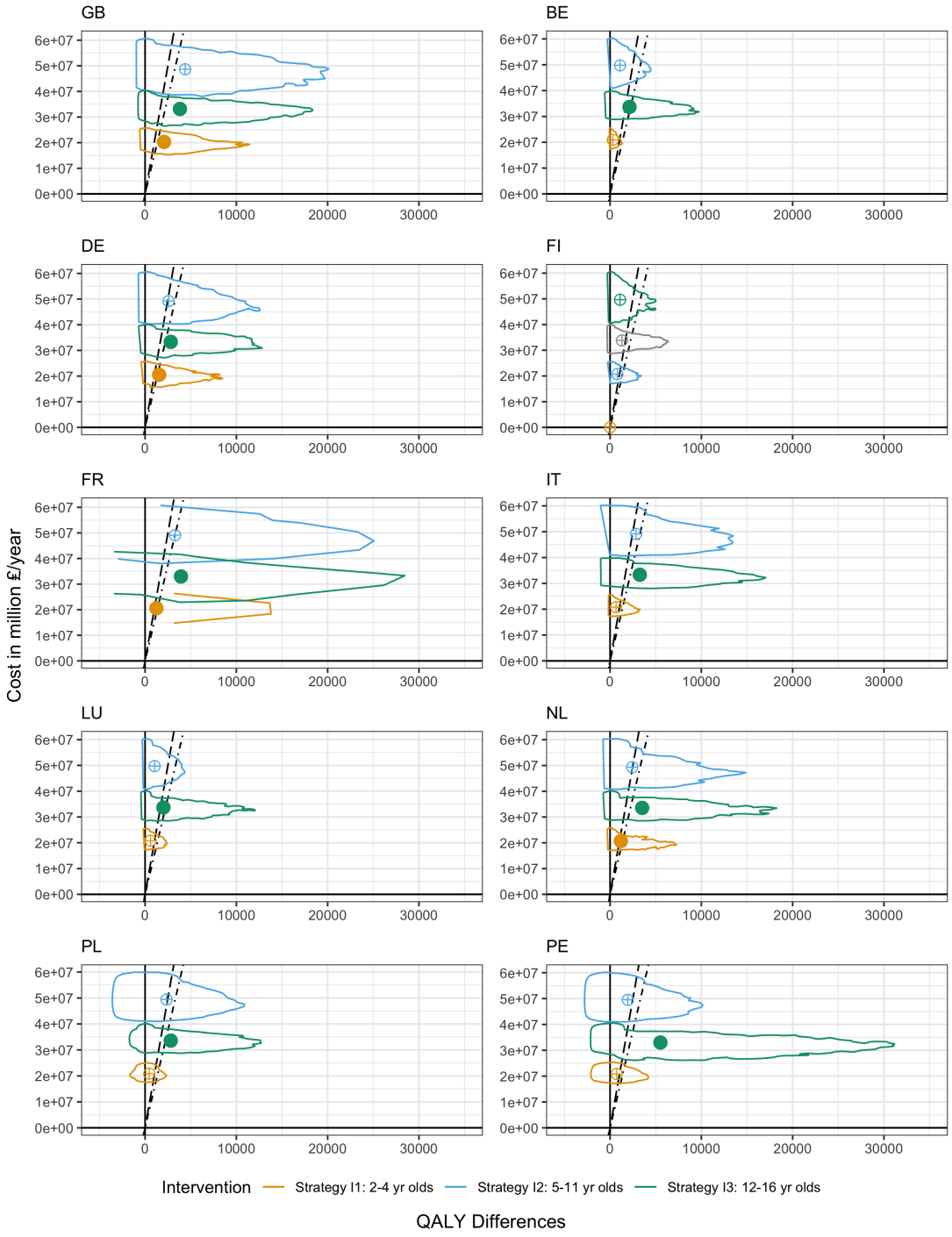

Figure 3.5.2: Cost-effectiveness frontier for strategies I1, I2, and I3 in Great Britain and Wales under different contact matrix assumptions. Filled circles represent the mean value is cost-effective at the £20,000 per QALY willingness-to-pay threshold (dashed-dot line). The £15,000 per QALY willingness-to-pay threshold (dashed line) line is also shown for reference. Quartered circles represent the intervention has been dominated. The cloud of incremental cost-effectiveness estimates is represented by the colored outline containing 90% of the estimates.

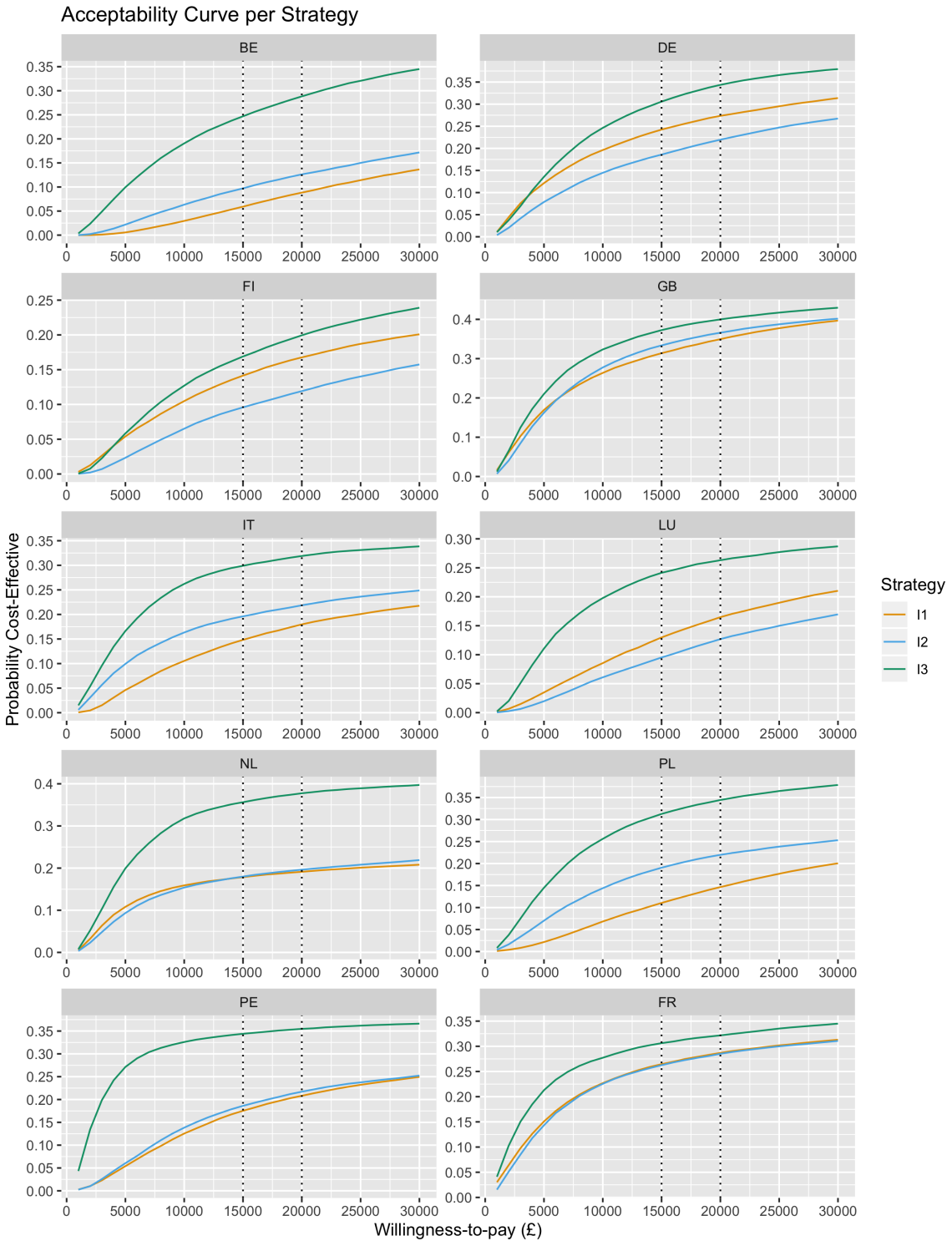

Figure 3.5.3: Statistical uncertainty around the probability a strategy is cost-effective at varied Willingness-to-pay thresholds for the NHS (£0-£30,000 per 1 QALY gained) for strategies I1, I2, and I3 under varied contact matrix assumptions. The NICE recommended willingness-to-pay thresholds are shown by the black vertical lines at £20,000 and £15,000.

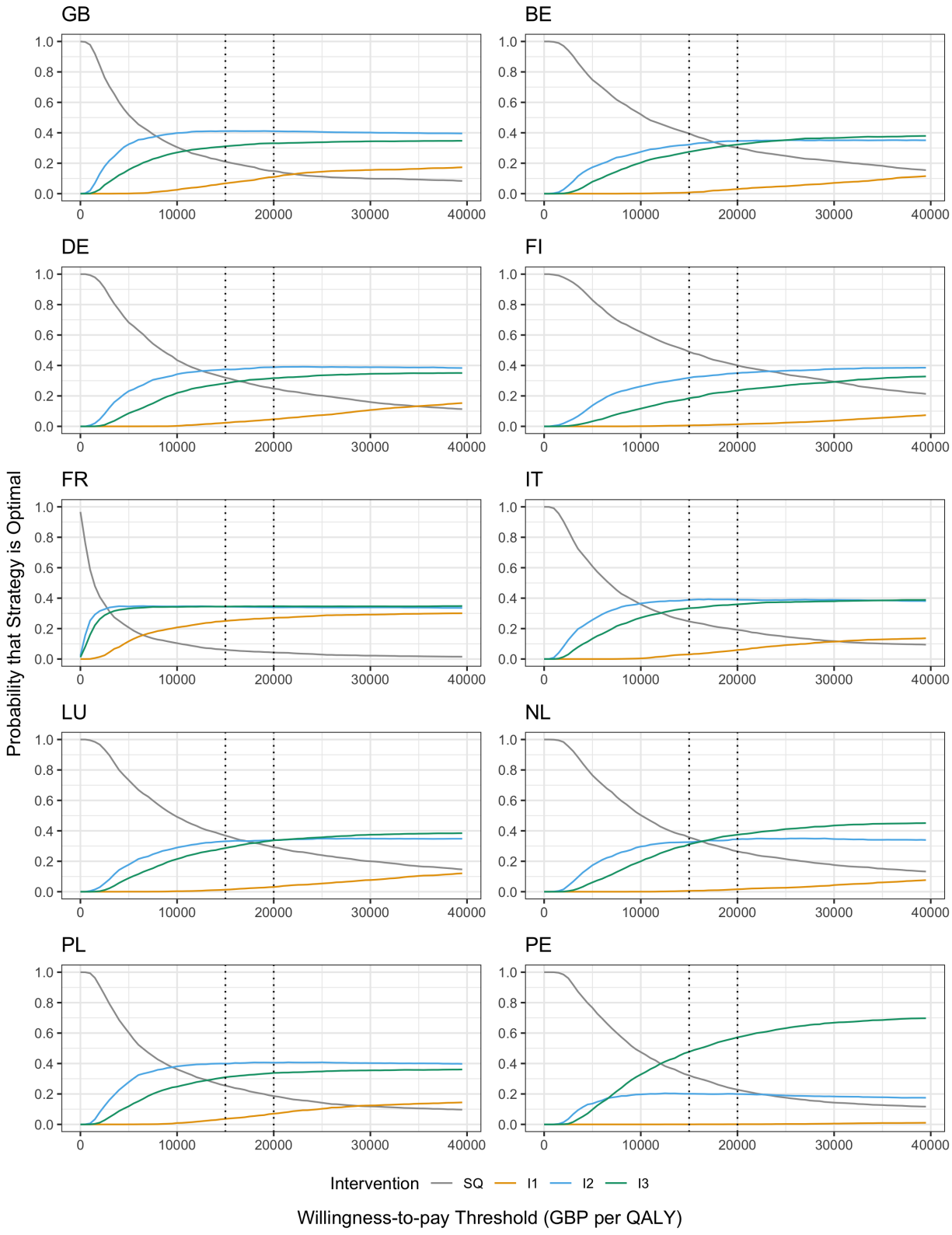

Figure 3.5.4: Uncertainty around the optimal NHB among strategies SQ, I1, I2, and I3 for each substituted simulation. Note the rank order of Strategy I1 and I2 varies across simulations. The NICE recommended willingness-to-pay thresholds are shown by the black vertical lines at £20,000 and £15,000 per QALY gained.

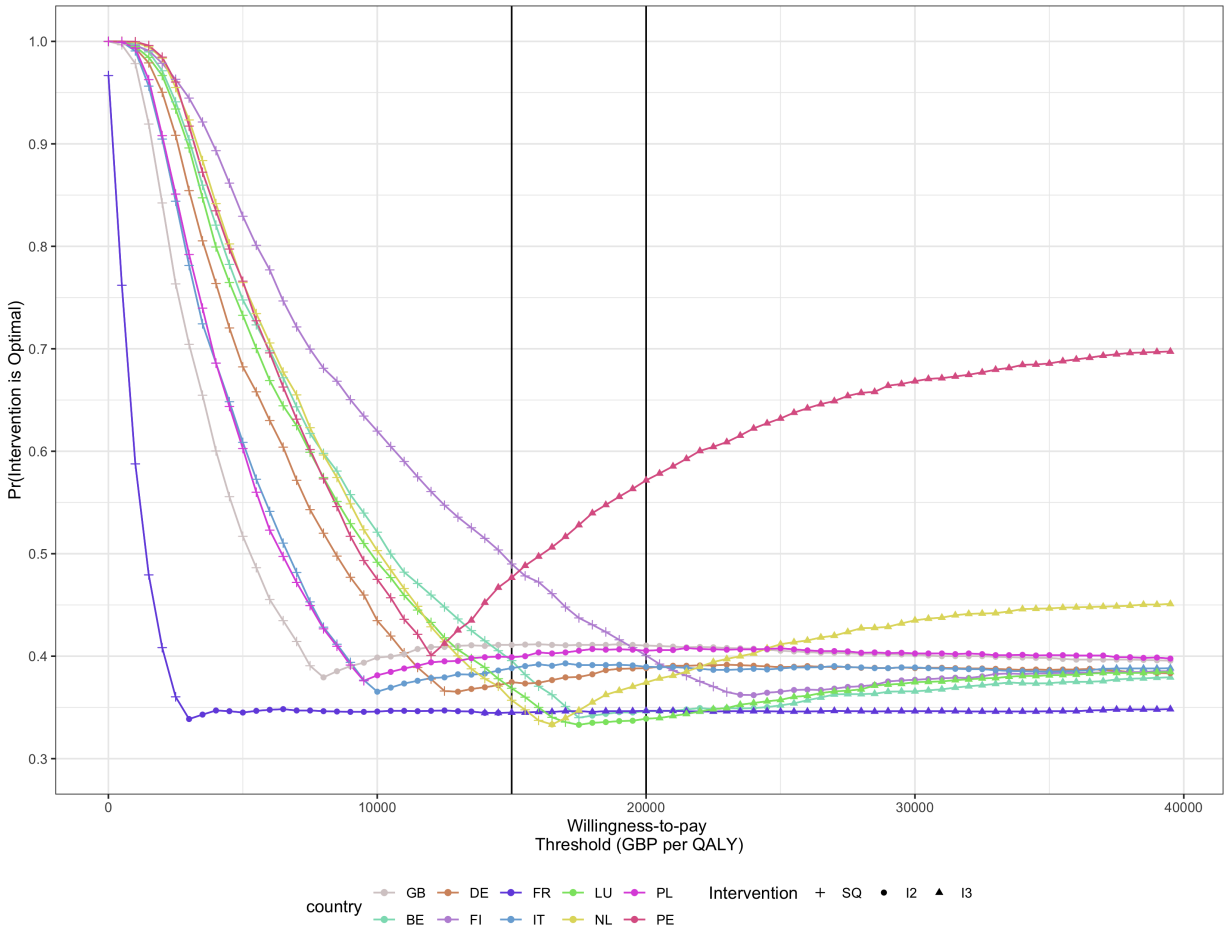

Figure 3.5.5: Side-by-side comparison of the CEAC: the frontier that maximizes NHB among competing vaccination strategies (SQ, I1, I2, and I3). The NICE recommended willingness-to-pay thresholds are shown by the black vertical lines at £20,000 and £15,000 per QALY gained.

3.6 Supplementary Information

The following sections contain information on model parameters and model construction, derivation of vaccine costs, age-structured health outcomes, the re-sampled survey and posterior distributions of each contact matrix, and further sensitivity analysis.

3.6.1 Model Calibration

R package

The analysis was coded in R (version 3.5.0) [82], using R Studio (version 1.1.453) with the R package 'fluEvidenceSynthesis'.[21, 20] The R package 'fluEvidenceSynthesis' model (version 1.0.0) has been revised from the developmental version previously used by Baguelin et al. and the previous package published on Github by van Leeuwan.[21] We utilized the functions 'adaptive.mcmc', and 'as.vaccine.calendar' along with the R package 'odin'[47] to write and fit a custom inference function that included additional age classes in the binomial and hypergeometric likelihood for the years 2009/2010-2013/2014. Likewise we re-derived the Royal College of General Practitioners Research and Surveillance Center (RCGP), POLYMOD, and influenza-like-illness datasets and several package functions to include the additional number of age classes.

3.6.2 Age-risk stratification

Using this calibrated model, we assessed the influenza incidence in England and Wales in the presence of seven vaccination programs targeted at the following school age groups: (1) Preschool (2–4 years) (2) Primary School (5–11 years) (3) Secondary School (12–16 years) (4) Preschool and Primary school (2–11 years) (5) Primary School and Secondary School (5-16 years) (6) Preschool and Secondary School (2-4 years and 12-16 years) (7) Preschool, primary, and secondary school age (2–16 years). Eleven age groups were structured into the model on the following intervals: 6 months-<1,1, 2-4, 5–11,12-14, 15–16, 17-24, 25–44, 45–64, 65-74, 75+ years. Baguelin et al.[19] previous used seven age groups, which we have expanded to encompass school age divisions (e.g. Primary school, Preschool). The Susceptible-Exposed-Infectious-Recovered Compartmental Model (SEIR) model has 22 separate age-risk strata in total.

Outcome Risks					
Parameter Description	**Strain**	**Age Group**	**Value Used in Base Case**	**Distribution used in Sensitivity Analysis**	**Reference**
Proportion of Symptomatic Influenza Cases	All Strains	All Ages	0.407	Triangular(a=0.309, b=0.513, c=0.396)	[51]
Risk of Hospitalization	A/H1N1	Low/High Risk 0 - 6 months ;	0.002/0.000	Sampled from Regression Normal Distributions	[33]
		Low/High Risk 6 months - 4 years;	0.002/0.002		
		Low/High Risk 5-14 years old	0.000/0.000		
		Low/High Risk 15-44 years old	0.000/0.000		
		Low/High Risk 45-64 years old	0.000/0.001		
		Low/High Risk 65+ years old	0.000/0.010		
	A/H3N2	Low/High Risk 0 - 6 months ;	0.012/0.000	Sampled from Regression Normal Distributions	[33]
		Low/High Risk 6 months - 4 years;	0.008/0.009		
		Low/High Risk 5-14 years old;	0.000/0.001		
		Low/High Risk 15-44 years old	0.000/0.001		
		Low/High Risk 45-64 years old	0.000/0.002		
		Low/High Risk 65+ years old	0.008/0.015		
	B	Low/High Risk 0 - 6 months ;	0.015/0.011	Sampled from Regression Normal Distributions	[33]
		Low/High Risk 6 months - 4 years;	0.004/0.000		
		Low/High Risk 5-14 years old;	0.000/0.000		
		Low/High Risk 15-44 years old	0.000/0.000		
		Low/High Risk 45-64 years old	0.001/0.000		
		Low/High Risk 65+ years old	0.000/0.001		
Risk of Mortality During Hospitalization	A/H1N1	Low/High Risk 0 - 6 months ;	0.000/0.000	Sampled from Regression Normal Distributions	[33]
		Low/High Risk 6 months - 4 years;	0.000/0.000		
		Low/High Risk 5-14 years old;	0.000/0.000		
		Low/High Risk 15-44 years old	0.000/0.000		
		Low/High Risk 45-64 years old	0.000/0.000		
		Low/High Risk 65+ years old	0.001/0.004		
	A/H3N2	Low/High Risk 0 - 6 months ;	0.000/0.000	Sampled from Regression Normal Distributions	[33]
		Low/High Risk 6 months - 4 years;	0.000/0.000		
		Low/High Risk 5-14 years old;	0.000/0.000		
		Low/High Risk 15-44 years old	0.000/0.000		
		Low/High Risk 45-64 years old	0.000/0.000		
		Low/High Risk 65+ years old	0.002/0.007		
	B	Low/High Risk 0 - 6 months ;	0.000/0.000	Sampled from Regression Normal Distributions	[33]
		Low/High Risk 6 months - 4 years;	0.000/0.000		
		Low/High Risk 5-14 years old;	0.000/0.000		
		Low/High Risk 15-44 years old	0.000/0.000		
		Low/High Risk 45-64 years old	0.000/0.000		
		Low/High Risk 65+ years old	0.000/0.001		
Risk of GP Consult	A/H1N1	Low/High Risk 0 - 6 months ;	0.042/0.063	Sampled from Regression Normal Distributions	[33]
		Low/High Risk 6 months - 4 years;	0.034/0.052		
		Low/High Risk 5-14 years old;	0.018/0.027		
		Low/High Risk 15-44 years old	0.002/0.002		
		Low/High Risk 45-64 years old	0.006/0.010		
		Low/High Risk 65+ years old	0.051/0.077		
	A/H3N2	Low/High Risk 0 - 6 months ;	0.281/0.424	Sampled from Regression Normal Distributions	[33]
		Low/High Risk 6 months - 4 years;	0.208/0.314		
		Low/High Risk 5-14 years old;	0.042/0.064		
		Low/High Risk 15-44 years old	0.015/0.023		
		Low/High Risk 45-64 years old	0.029/0.043		
		Low/High Risk 65+ years old	0.082/0.124		
	B	Low/High Risk 0 - 6 months ;	0.279/0.423	Sampled from Regression Normal Distributions	[33]
		Low/High Risk 6 months - 4 years;	0.288/0.438		
		Low/High Risk 5-14 years old;	0.088/0.134		
		Low/High Risk 15-44 years old	0.071/0.108		
		Low/High Risk 45-64 years old	0.079/0.120		
		Low/High Risk 65+ years old	0.000/0.000		

Table 3.6.1: Age and risk group (Low/High Risk) probabilities of each Hospitalization, Mortality, and GP Consult per influenza strain.

Health-Related Quality of Life Values					
Outcome	Age Group	Value or Distribution			Reference
QALY loss per non-fatal ILI case	All Ages	Bootstrap from data on H1N1 pdm			[52]
QALY loss per Hospitalization	All Ages	Normal(mu=0.018, sd=0.0018);			[53]
		Discount			
		0%	1.5%	3.5%	
	Low/High Risk 0-12 months old	60.93/69.96	37.06/40.77	22.61/24.07	
	Low/High Risk 1-4 years old	61.62/69.45	37.61/40.62	23.00/24.05	
	Low/High Risk 5-14 years old	54.96/61.64	35.19/37.84	22.32/23.18	
	Low/High Risk 15-44 years old	38.23/44.47	27.16/30.40	18.84/20.33	
	Low/High Risk 45-64 years old	19.75/24.14	16.09/19.10	12.71/14.62	
QALY loss per Death	Low/High Risk 65+	8.24/9.46	7.41/8.40	6.52/7.28	[34, 54, 19]

Table 3.6.2: Sources and values per age and risk group for health related quality of life lost used to calculate the number of QALYS lost per influenza season. Outcomes for which QALY loss was calculated included Hospitalization, death/fatality.

Weights for children less than 18 years old was not available, therefore it was assumed that their average quality-of-life weight was 0.9.

3.6.3 Model fits

The 'fluEvidenceSynthesis' package independently estimates the incidence of influenza for strains A/H1N1 and A/H3N2 per season. We achieved consistent results for the contact matrix and posterior parameters. For most seasons approximately 6-8 chains (1.6 million iterations) were needed for convergence. Any season that did not converge based on the Gelman-Rubin diagnostic was restarted with the last value of the Markov chain and the two chains were run for an additional 300,000 iterations. The Gelman–Rubin diagnostic evaluates Markov chain Monte Carlo (MCMC) convergence by comparing the variance between-chains and within-chain for each model parameter.[55] Large differences between the two variances indicate non-convergence. Some influenza seasons where few cases were observed by the surveillance network (e.g. < 10 cases per age group) had Gelman-Rubin diagnostics greater than 1.2. Given the low precision of the data for these seasons a higher Gelman-Rubin score for the model fit is not unexpected and does not change the results of our analysis. The posterior distributions are sampled from 75% of the last chain.

3.6.4 Prior distributions for model parameters

The prior distributions for the model parameters and their descriptions are listed below.

Prior Distributions for Epidemiological Parameters			
Variable	Description	Prior Distribution or Base Case	Source
c_{ij}	contact rate between age group i and j	Bootstrapped POLYMOD data	[23]
ϵ_i	ascertainment probability of a symptomatic case	Fit, Priors Below	[48]
	0-14 years old	logNormal(-4.494, 0.286)	
	15-64 years old	logNormal(-4.117, 0.475)	
	65+ years old	logNormal(-2.978, 1.332)	
$\mathbf{v}$	immunization rate for age group i and risk group k		[25] [26]
σ	susceptibility of age group i	Fit, Priors below	[18]
	6 months old -14 years old	N(0.688, 0.083)	
	15 - 64 years old	N(0.529, 0.122)	
	65+	N(0.523, 0.175)	
q_{strain}	transmissibility of virus A/H3N2, A/H1N1, B	Fit, Prior: N(0.165, 0.028)	[48]
Ψ	outside infection probability	Fit, Prior: $Beta(z_{ij}^{outside}, z_{ij}^{inside})$, where z_{ij} is the incidence among the monitored population of age group i at week j of new cases arising from outside the main epidemic or inside	
γ_1	rate of loss of latency (γ_1=2.5/2)	1.8 days	[49]
γ_2	rate of loss of infectiousness(γ_2=1.1/2)	0.8 days	[49]
	delay from vaccination to immunity	2 weeks	Assumption in Baguelin et al. [50]
α_{ik_t}	all-or-nothing vaccine efficacy for age group i and risk group k per season	Well-matched: $0.7_{LowRisk}$, $0.4_{HighRiskand65+yrs}$ Poorly-matched: $0.42_{LowRisk}$, $0.28_{HighRisk}$	
I_t	initial infectious seed for the epidemics per season	Derived from σ, Fit	

Table 3.6.3: Prior distributions for each parameter used to fit the SEIR model via Markov chain Monte Carlo.

For parameters σ_i, susceptibility to infection, data for prior distributions included age groups 6m-14 year old, 15-64 years old and 65+ years old. We assumed data for the 6m-1 year old age group mapped onto the model age group of 0-1 year old.

3.6.5 Calculating the naive bootstrap 'Prior'

Uncertainty surrounding contact rates are usually not included in standard uses of contact matrices. However we estimated the naive bootstrap distribution for the contact matrix for each substituted country and have visually compared the naive bootstrap to the posteriors estimated from the model (3.6.5). Returning to the observed POLYMOD survey data we drew a random number, n, from the total number of observations then made n random draws from the POLYMOD row ids. The content of the drawn row ids were replaced with the content of an equivalent number of draws from the same data set. This re-sampling process was repeated 10000 times to create 10000 contact matrices from the observed data. The new contact matrices were used to estimate the naive bootstrap distribution of the observed contact matrix. The standard deviation of each transmission rate was evaluated as

$$\sqrt{1/N \sum_{n=2}^{N-1} (x_{n+1} - x_1)^2}$$

where we assume the initial contact rate from the original data represents the mean of the naive bootstrap. Among the empirical survey data there were few individuals aged 75+ years old included, therefore for the naive bootstrap we considered individuals 65-74 and individuals 75+ to have the same contact rate.

Distributions for substitute contact matrices

We assumed contact making between individuals of each age group is symmetric: the number of contacts in the population resulting from people from age group i meeting with people from age group j is the same as the number of contacts made by people from age group j meeting with people from age group i. The probability two randomly selected individuals in group i and j get in contact can be expressed as $c_{ij} = c_{ji}$ under symmetry. However when survey data is used to calculate the average number of contacts per day, symmetry between averages will not usually be achieved because of reporting or participation biases. To achieve symmetry of the contact matrix c_{ij}, we followed the same method as described by Baguelin et al.[18] which averages the two symmetric cells $c^*_{ij} = \frac{c_{ij}+c_{ji}}{2}$. In the SEIR simulations for model fitting and during SEIR modeling simulating interventions the number of contacts

between distinct age groups is re-normalised following this method. The naive bootstrap and posterior contact matrices for Great Britain (GB) and each substituted scenario are shown below with adjustments for symmetry.

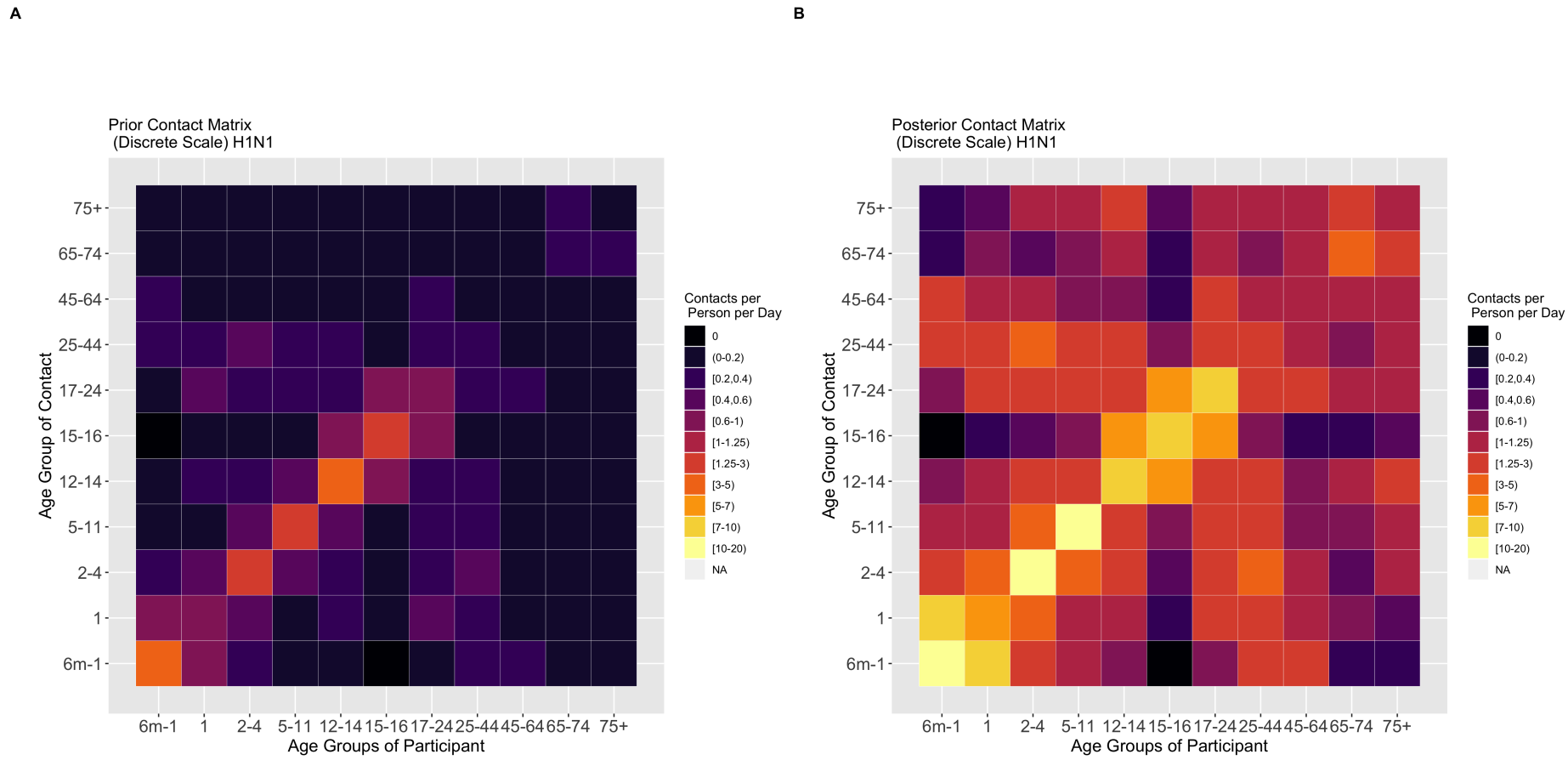

Figure 3.6.1: **Great Britain**: The re-sampled survey contact matrix used to fit the MCMC is shown in panel A. The posterior contact matrix used for model simulations is shown in panel B. Both matrices describe the average number of contacts per day between the age groups on the X and Y-Axis.

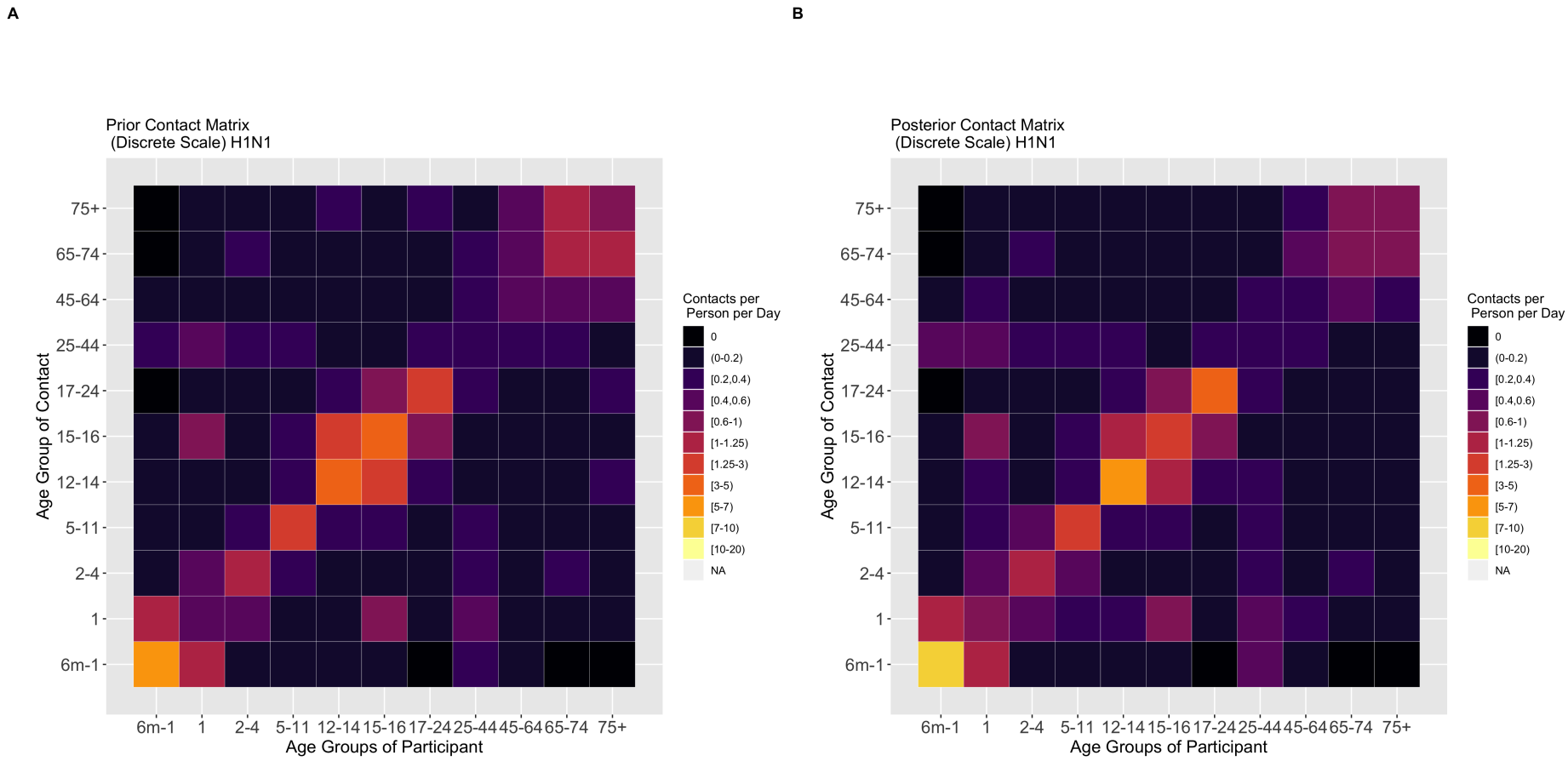

Figure 3.6.2: **Belgium**: The re-sampled survey contact matrix used to fit the MCMC is shown in panel A. The posterior contact matrix used for model simulations is shown in panel B. Both matrices describe the average number of contacts per day between the age groups on the X and Y-Axis.

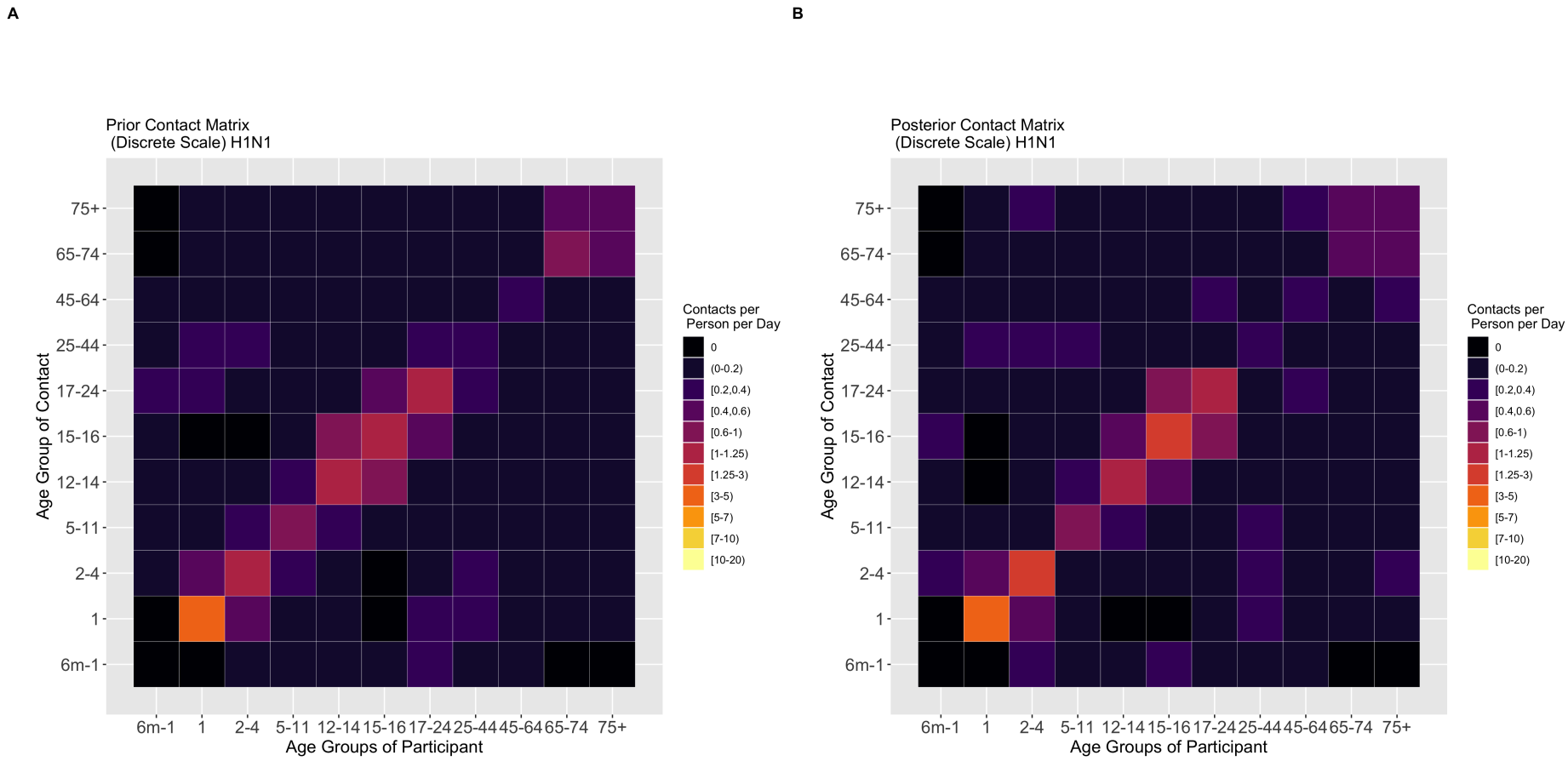

Figure 3.6.3: **Germany**: The re-sampled survey contact matrix used to fit the MCMC is shown in panel A. The posterior contact matrix used for model simulations is shown in panel B. Both matrices describe the average number of contacts per day between the age groups on the X and Y-Axis.

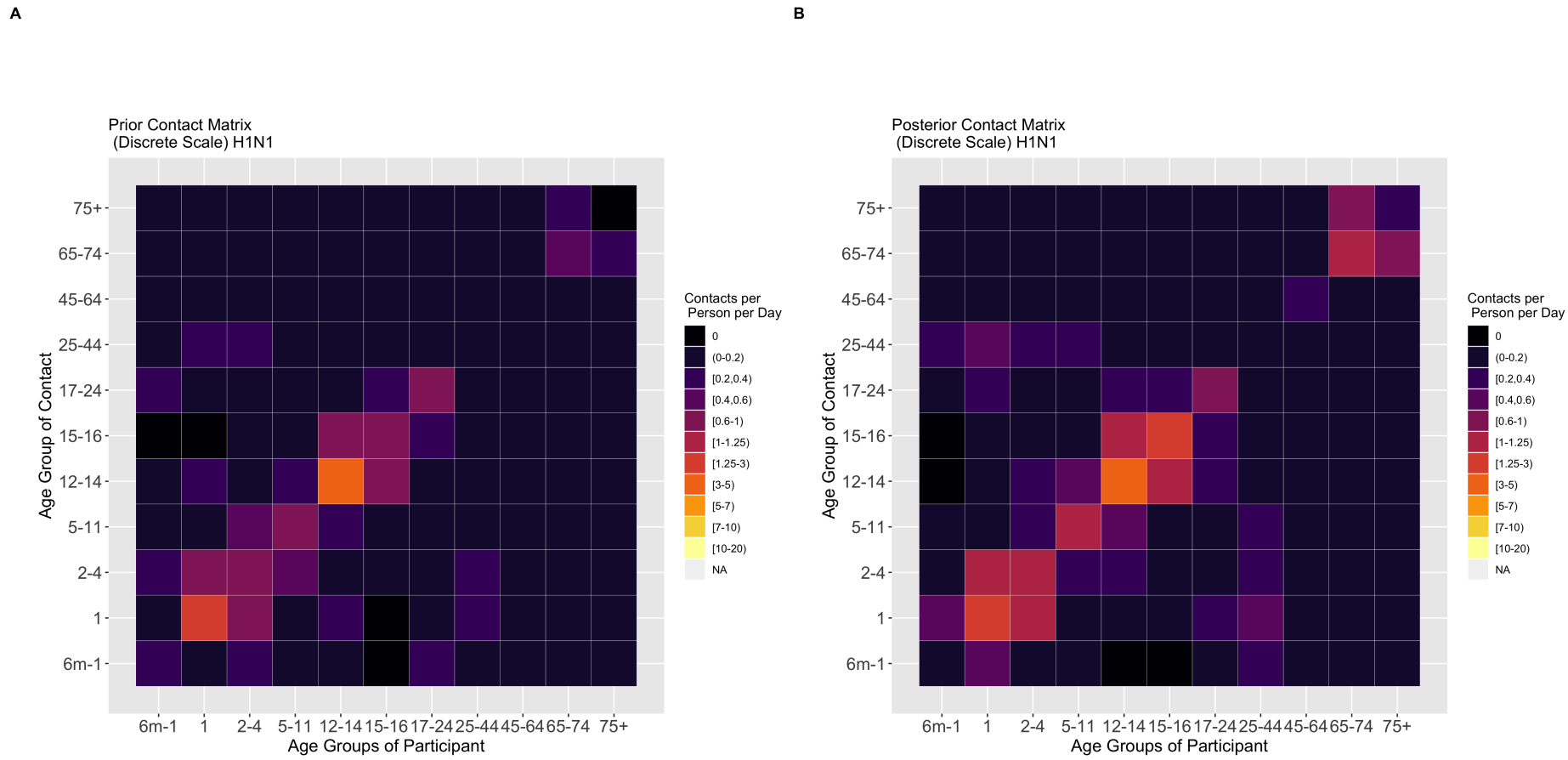

Figure 3.6.4: **Finland**: The re-sampled survey contact matrix used to fit the MCMC is shown in panel A. The posterior contact matrix used for model simulations is shown in panel B. Both matrices describe the average number of contacts per day between the age groups on the X and Y-Axis.

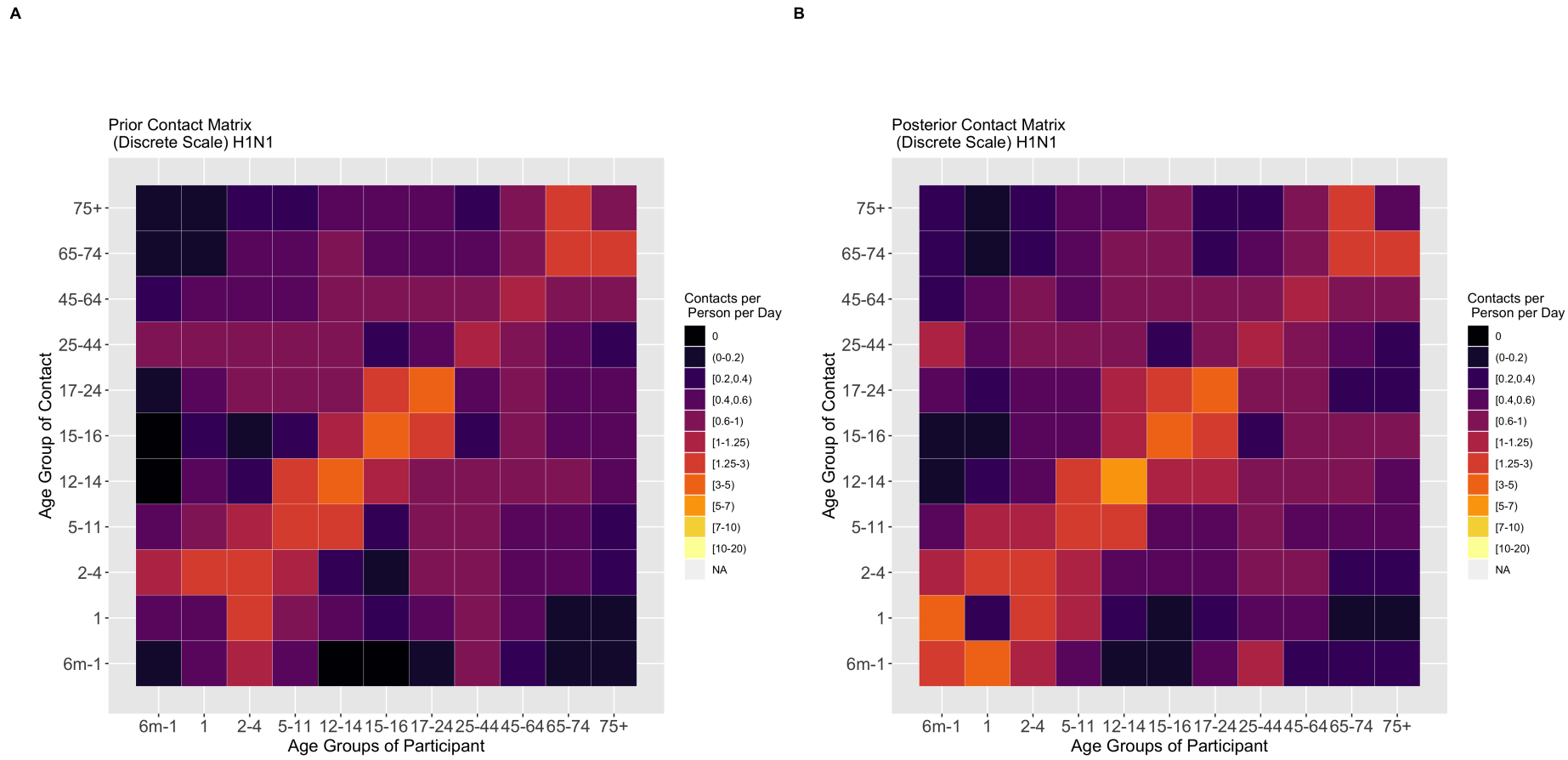

Figure 3.6.5: **France**: The re-sampled survey contact matrix used to fit the MCMC is shown in panel A. The posterior contact matrix used for model simulations is shown in panel B. Both matrices describe the average number of contacts per day between the age groups on the X and Y-Axis.

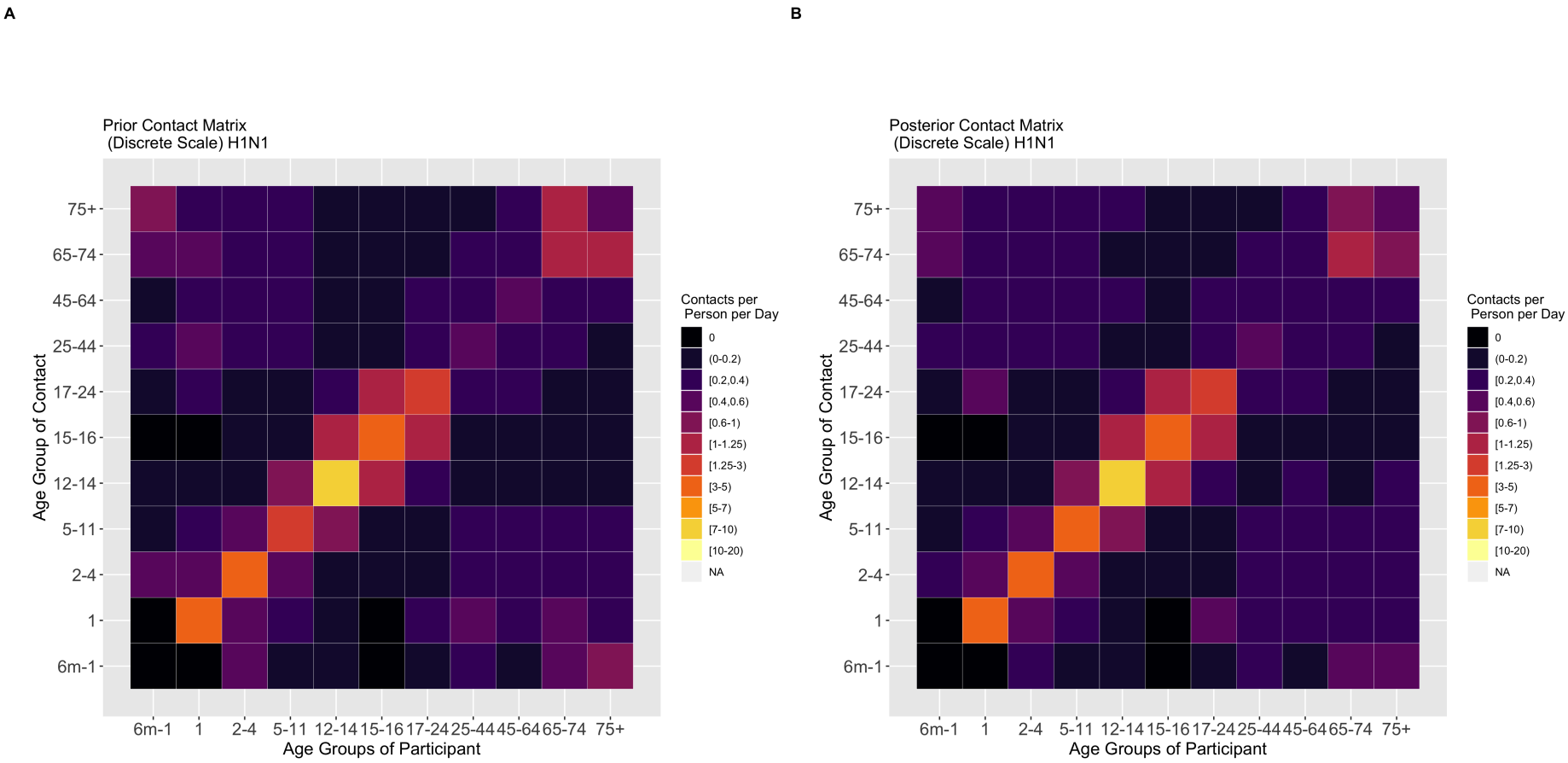

Figure 3.6.6: **Italy**: The re-sampled survey contact matrix used to fit the MCMC is shown in panel A. The posterior contact matrix used for model simulations is shown in panel B. Both matrices describe the average number of contacts per day between the age groups on the X and Y-Axis.

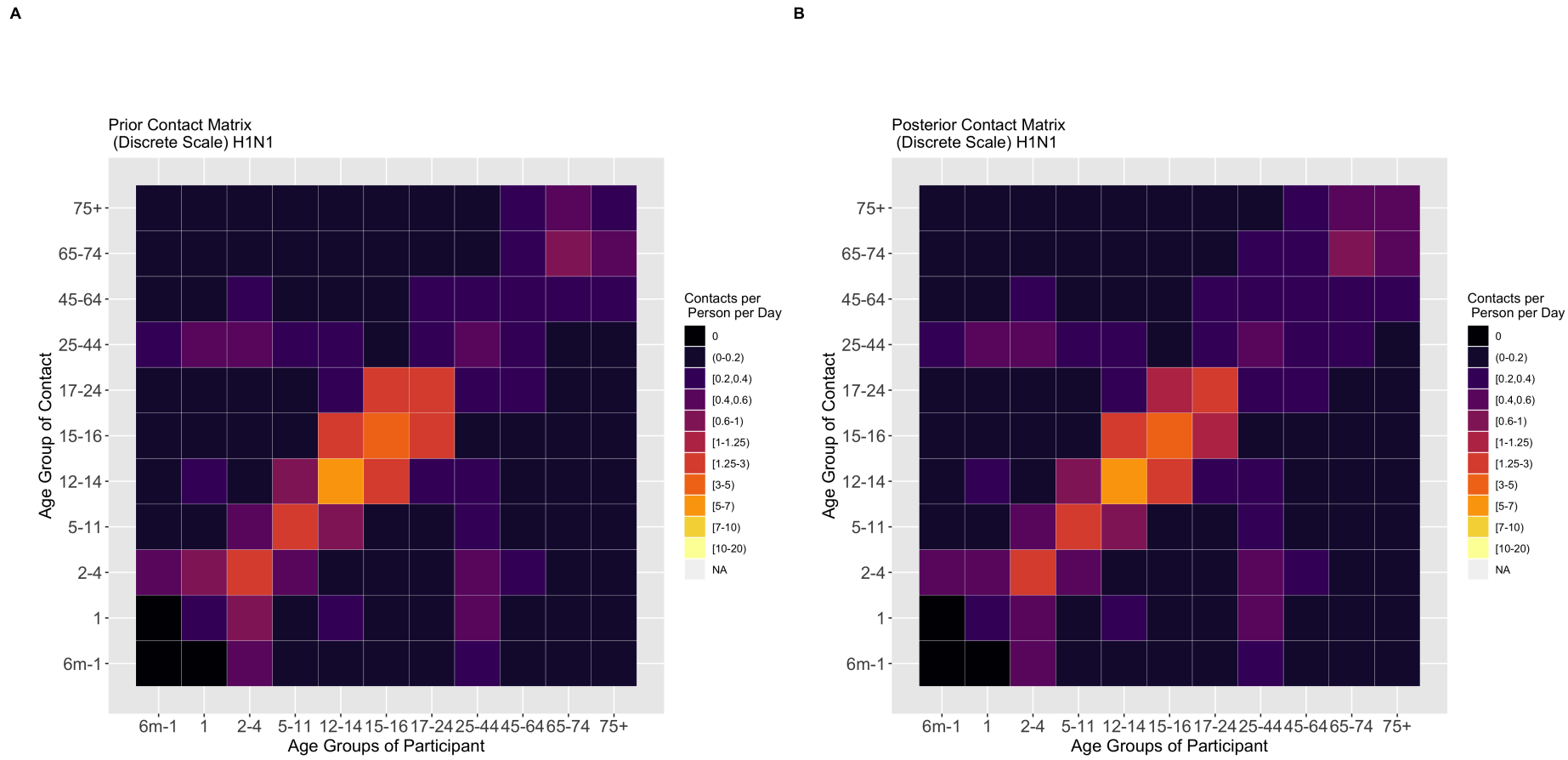

Figure 3.6.7: **Luxembourg**: The re-sampled survey contact matrix used to fit the MCMC is shown in panel A. The posterior contact matrix used for model simulations is shown in panel B. Both matrices describe the average number of contacts per day between the age groups on the X and Y-Axis.

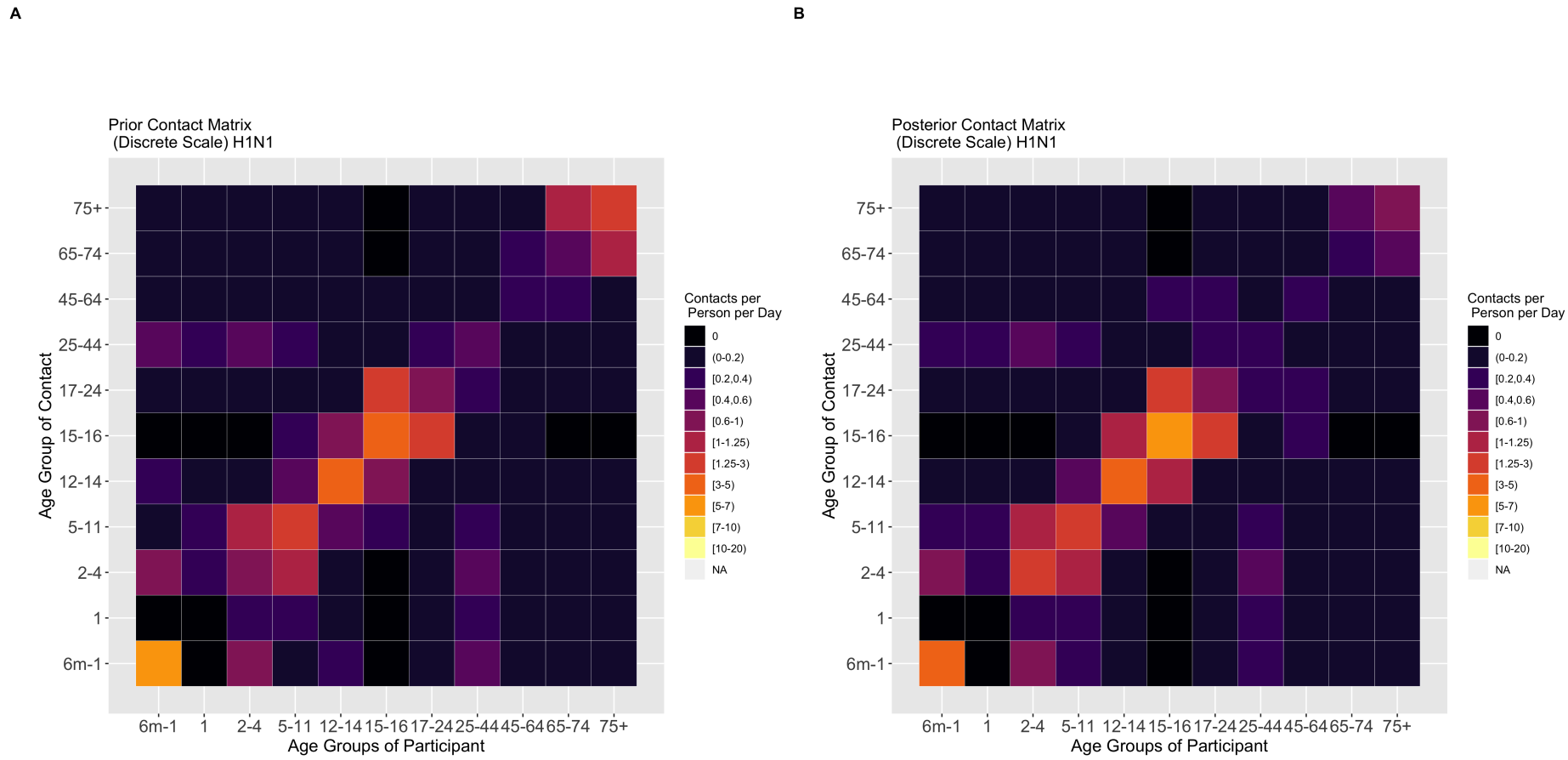

Figure 3.6.8: **Netherlands**: The re-sampled survey contact matrix used to fit the MCMC is shown in panel A. The posterior contact matrix used for model simulations is shown in panel B. Both matrices describe the average number of contacts per day between the age groups on the X and Y-Axis.

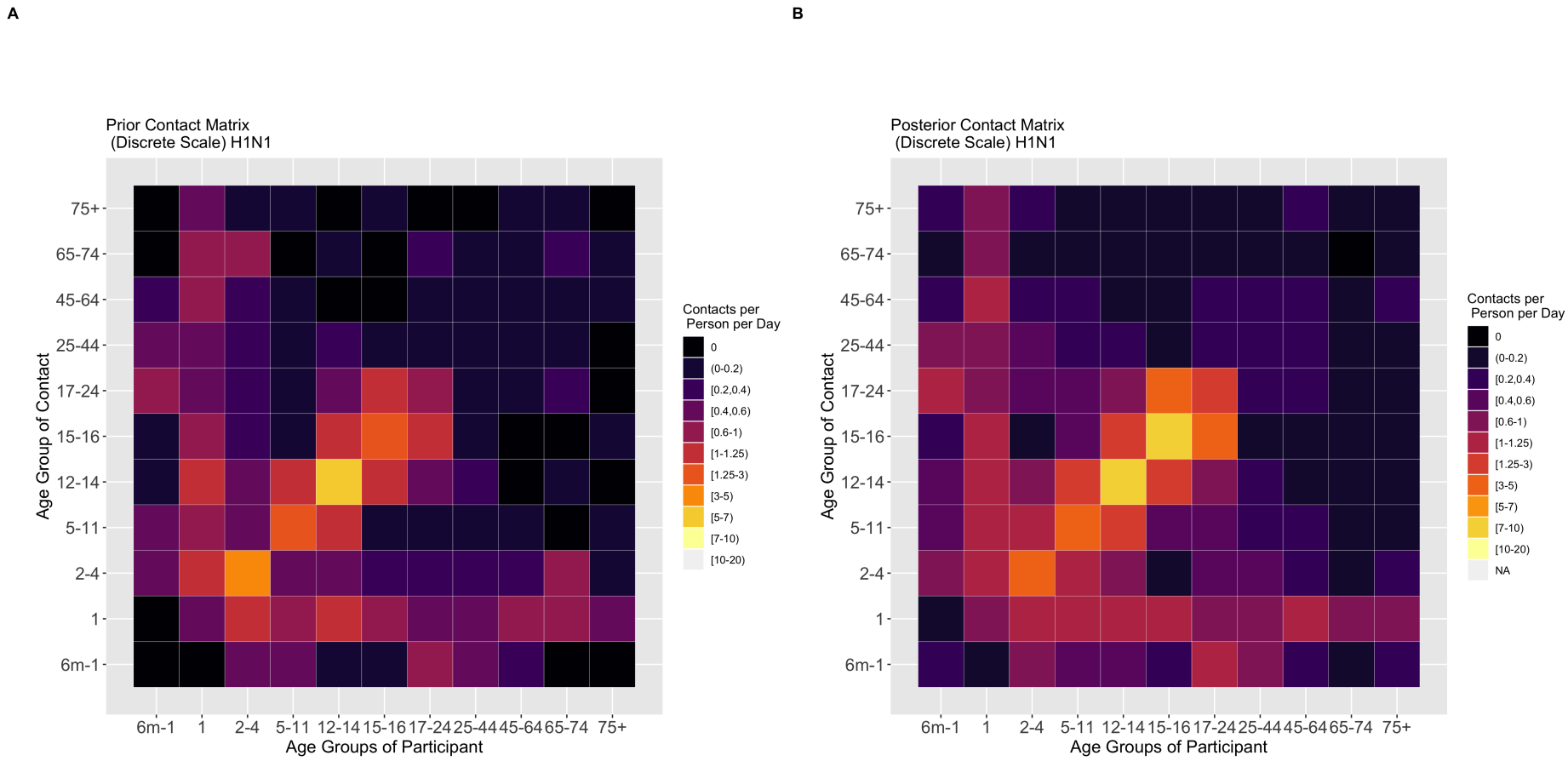

Figure 3.6.9: **Peru**: The re-sampled survey contact matrix used to fit the MCMC is shown in panel A. The posterior contact matrix used for model simulations is shown in panel B. Both matrices describe the average number of contacts per day between the age groups on the X and Y-Axis.

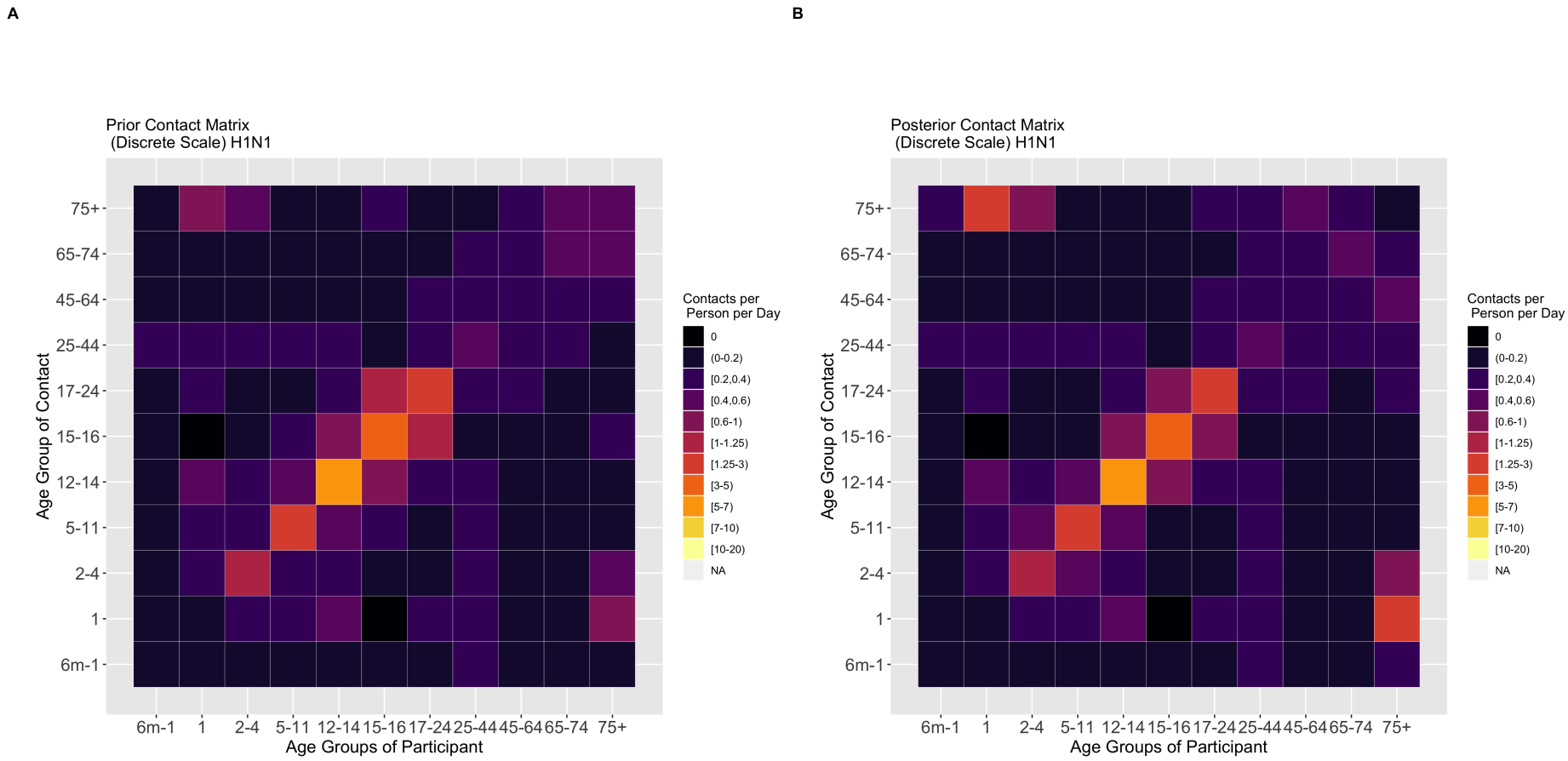

Figure 3.6.10: **Poland**: The re-sampled survey contact matrix used to fit the MCMC is shown in panel A. The posterior contact matrix used for model simulations is shown in panel B. Both matrices describe the average number of contacts per day between the age groups on the X and Y-Axis.

3.6.6 Mean number of contacts and mean relative number of contacts

For easy access the mean number of contacts per day per age group and the mean number of relative contacts per day are shown next to each other. The mean number of contacts and associated variance, as well as the the relative number of contacts and associated variance for each country across all seasons used to generate the below graph are available in Appendix Section A2.

Average Number of Contacts per day BE

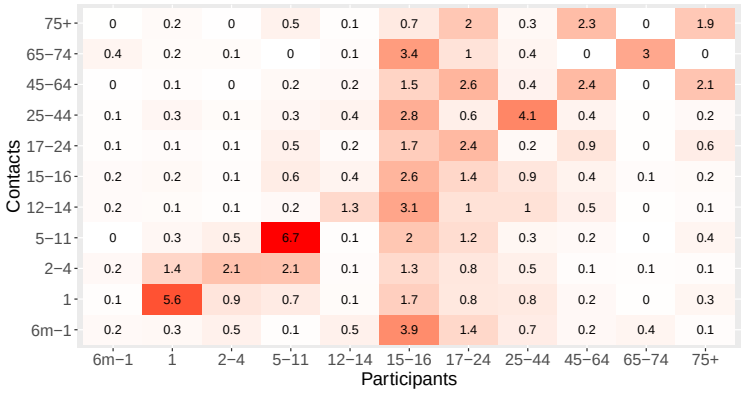

Proportion of Contacts per Age group BE

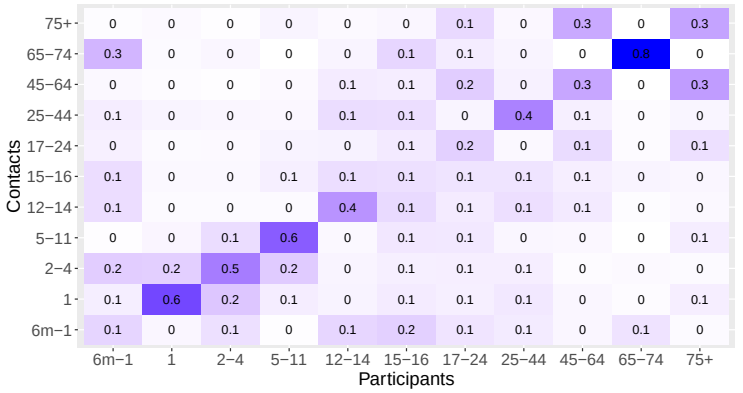

Average Number of Contacts per day DE

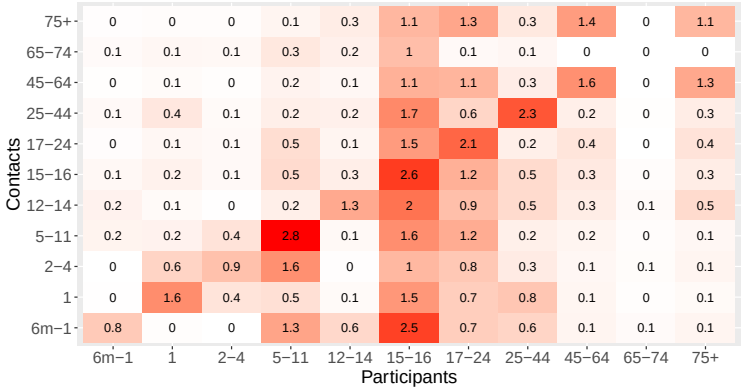

Proportion of Contacts per Age group DE

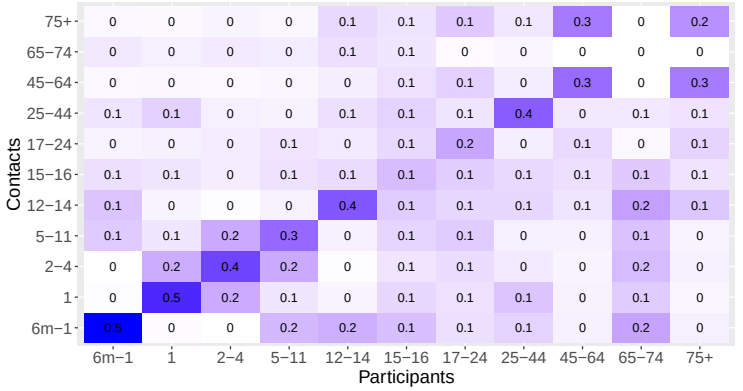

Average Number
of Contacts per day FI

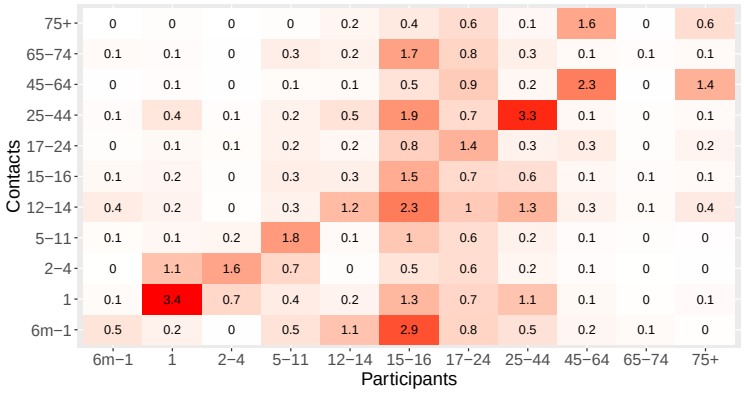

Proportion of Contacts
per Age group FI

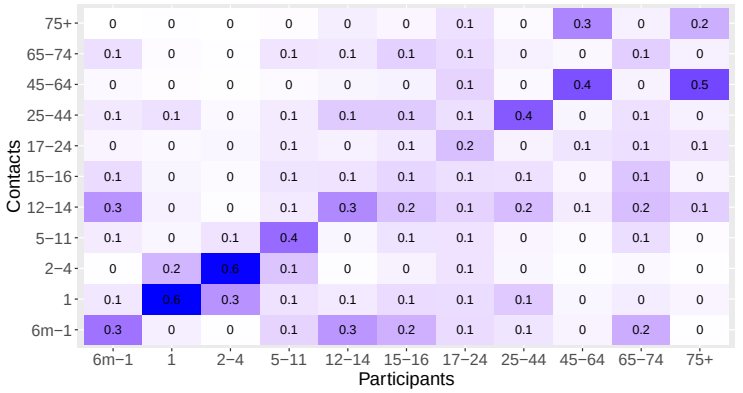

Average Number
of Contacts per day GB

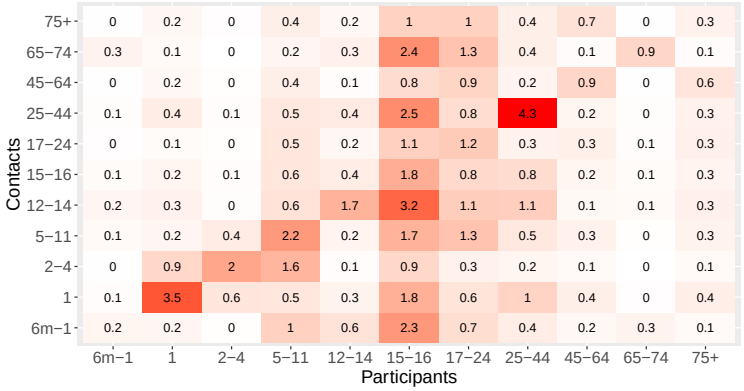

Proportion of Contacts
per Age group GB

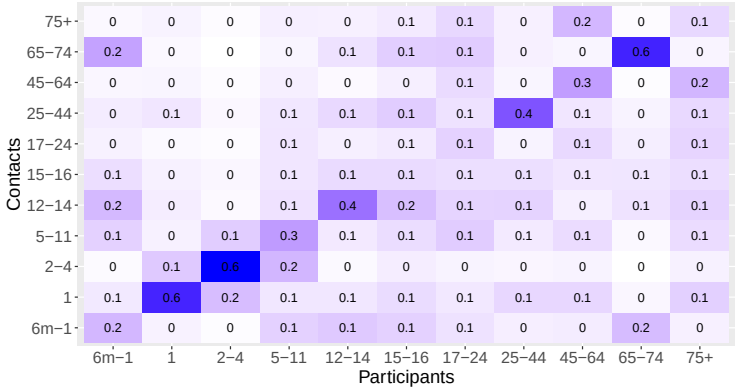

Average Number
of Contacts per day IT

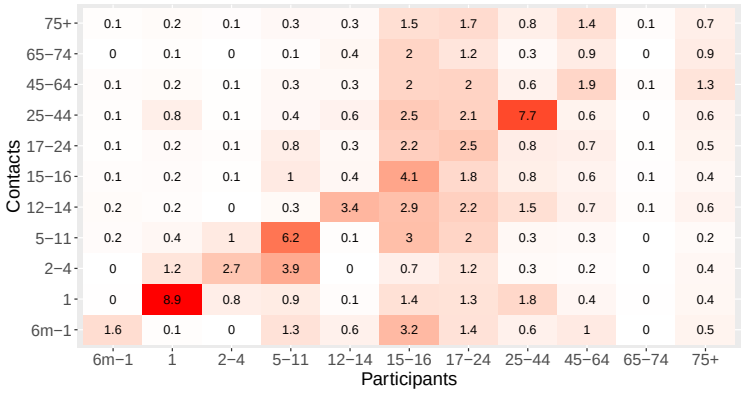

Proportion of Contacts
per Age group IT

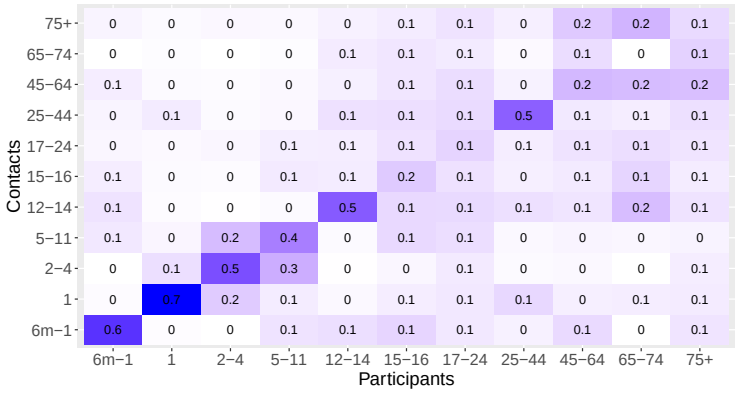

Average Number
of Contacts per day LU

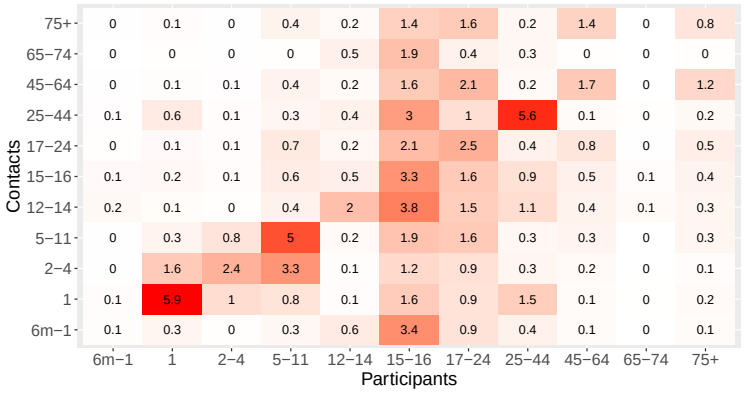

Proportion of Contacts
per Age group LU

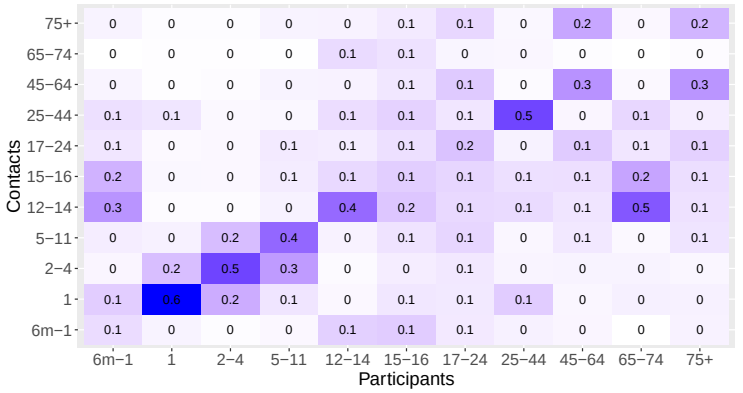

Average Number
of Contacts per day NL

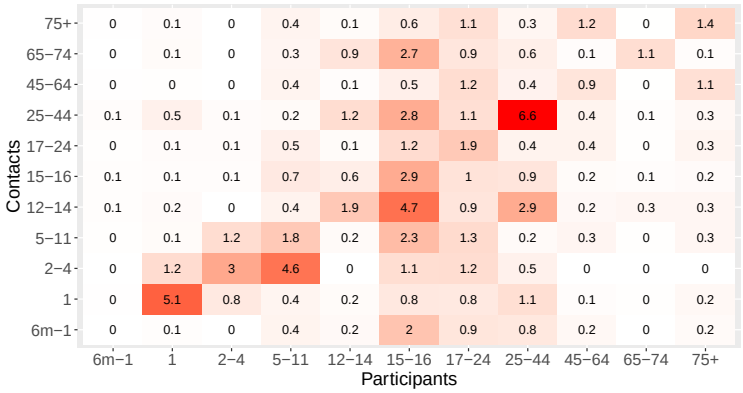

Proportion of Contacts
per Age group NL

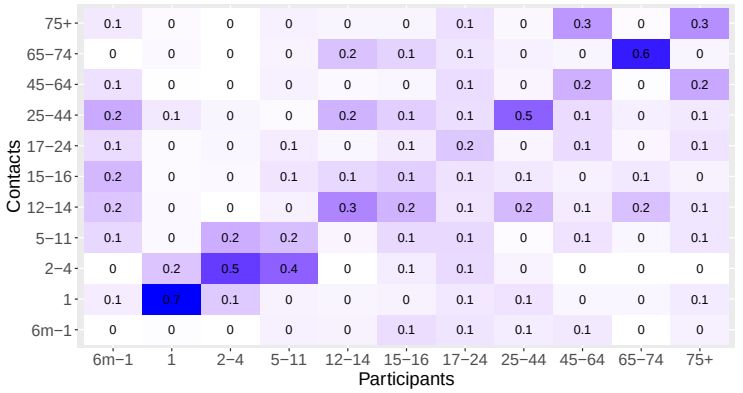

Average Number
of Contacts per day PL

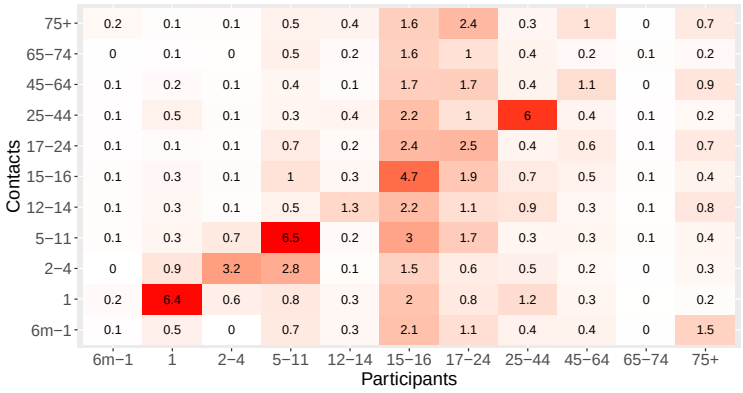

Proportion of Contacts
per Age group PL

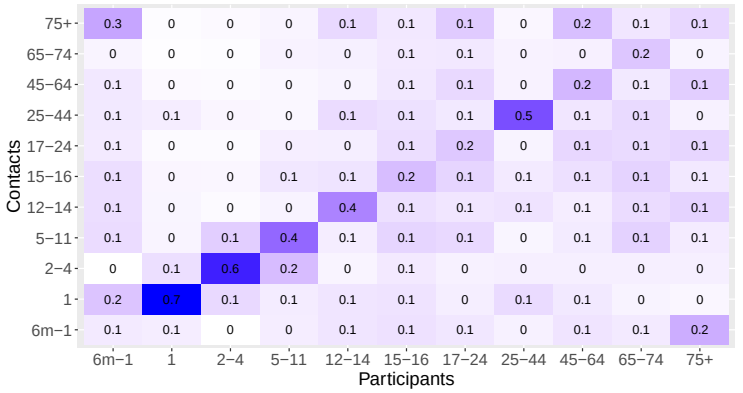

Average Number of Contacts per day PE

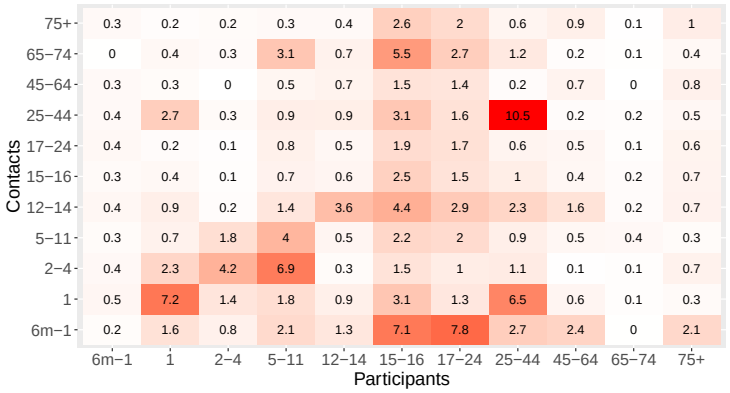

Proportion of Contacts per Age group PE

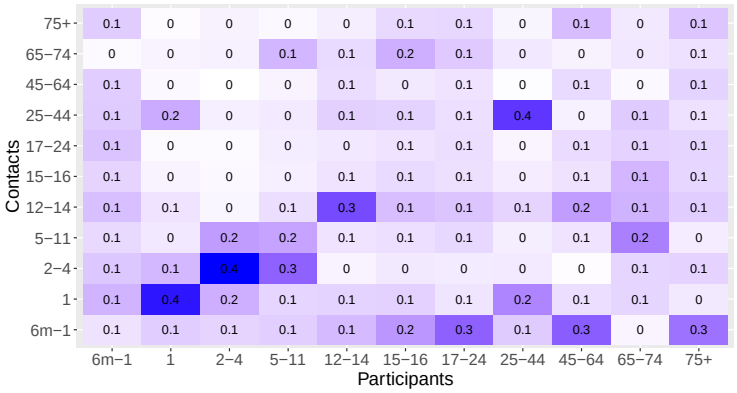

Average Number of Contacts per day FR

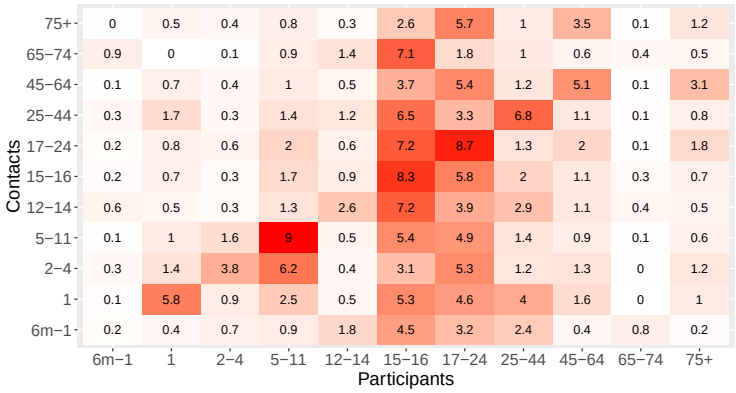

Proportion of Contacts per Age group FR

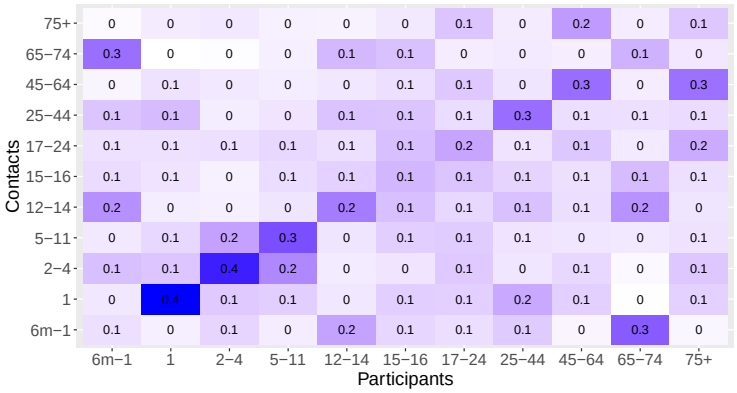

Simulated Coverage Uptake						
Points for Logarithmic Fit						
Dates	"2012-09-01"	"2012-09-24"	"2012-10-01"	"2012-10-22"	"2012-11-19"	"2012-12-12"
70%	0.000	0.065	0.170	0.489	0.679	0.7
30%	0.000	0.016	0.046	0.176	0.294	0.3
Dates	"2012-09-01"	"2012-09-24"	"2012-10-08"	"2012-10-22"	"2012-11-19"	"2012-12-12"
55%	0.000	0.1010	0.1760	0.2980	0.4720	0.55

Logarithmic Model	**Intercept 1 (b)**	**Intercept 2 (d)**	**Intercept 3 (e)**
70%	-9.839e-02	7.133e-01	1.563e+04
55%	-6.2773e-02	5.6676e-01	1.5635e+04
30%	-1.3002e-01	3.0030e-01	1.5632e+04

Table 3.6.4: Logarithmic Functions for calculating coverage at any date. The functions use manipulated objects of classes "POSIXlt" and "POSIXct" to represent calendar dates and times. As functions were fit to data from 2012/2013 any predicted outcomes for years other than 2012 must recenter around the POSIXct date '15584' or September 1, 2012.

3.6.7 Vaccine uptake rate for proposed interventions

3.6.8 Empirical coverage data

Empirical coverage rates were available for the years 1995-2009 and were utilized in calibration of the model.

Status quo simulations

For simulation of the Status Quo program empirical coverage rates were used for 1995/1996-2008/2009.

Intervention simulations

The dates for the Live-Attenuated Influenza Vaccine Nasal Spray (LAIV) program simulation began on September 1 and ended on December 12. These dates were chosen as the standard beginning of the United Kingdom (UK) school year and approximately one week before the beginning of the Christmas school holiday. Logarithmic functions for coverage were fit using 6 data points and the R 'predict' function. (Table 3.6.4) The first two points began with September 1st at 0% and December 12 as the total achieved coverage (eg. 55%, 70%). For the remaining three points we used empirical coverage rates from 2012/2013 for low risk 65+ and high risk age groups < 65 years old whose final coverage rates were closest to the strategic goal. As these are both the highest priority groups in the current vaccination scheme in the UK we assumed their vaccination rate would be roughly equivalent to that of the the school-based LAIV program.

Using the empirical coverage dataset we utilized the logarithmic function to predict the

coverage level at each date for each season. For example the empirical coverage rates for Strategy I7 (2-16 year olds) for 1995 has data on the monthly intervals "1995-10-01" "1995-11-01" "1995-12-01" "1996-01-01" "1996-02-01". To calculate the coverage level at these dates for a program with 70% coverage we utilized the calculated logarithmic function and the R function 'predict' to estimate coverage for 2-16 year olds at these intervals. This results for this example would look like:

Empirical Dates	"1995-10-01"	"1995-11-01"	"1995-12-01"	"1996-01-01"	"1996-02-01"
Calculated Coverage	0.9%	15.0%	59.7%	70.7%	71.3%

If the function provided coverage levels prior to September 1 or after December 12 they were truncated to the minimum (0%) or the maximum achieved coverage for the simulation. For the 1995 example above the model simulation would use 70% in place of 70.7% and 71.3%.

3.6.9 Vaccine cost calculation

The cost per dose due for administering school-based vaccine delivery program was calculated using the same reimbursement cost as General Practitioner (GP) Nurses (£7.24) and the same vaccine acquisition cost as a GP office (£9.80).[56] Pilot areas of school-delivery estimated that a qualified nurse was able to immunize about 50 children per 2.5 hours– 20 LAIV doses per 1 hour.[28] After subtracting 2.5 hours for travel, set-up/break-down, and meals we estimated nurses would spend 5 hours actively vaccinating resulting in 100 doses dispersed per nurse per day. At an average hourly rate of £36 per hour,[45] the service cost for school-based delivery attributed to administration was £2.70 per dose. In some pilot areas drivers were used to deliver bulk vaccine to the school beforehand allowing immunization teams to concentrate on administration sessions. We estimated a large delivery to be the average number of pupils in a primary school–approximately 260 doses. For every 260 doses we added a service cost based on an estimated band 1 National Health Service (NHS) driver hourly wage (£9.88/hour)—this added an additional £0.10 per dose.[46] Therefore the total service cost of the school based program was £2.80 per dose. Added to the reimbursement cost and acquisition cost we calculated a triangular cost distribution for school delivery that was very similar to previous cost distributions for GP, and pharmacy vaccine delivery.

The average hourly wage for nurses were derived from UK nation-wide estimates [45]. The vaccine purchase payment estimates for Pharmacy delivered vaccines were taken from a survey conducted in the London-area.[57]

Cost of Vaccination					
Parameter	**Original Value**	**Year**	**Inflation Adjustment**	**2017/2018 Value**	**Source**
GP Delivery Cost Per Dose					
NHS vaccine service payment	£9.80	2018	–	£9.80	[56]
Vaccine Purchase Payment	£7.24	2014/2015	1.041	£7.54	[57]
Dispensing Fee	£2.25	2014/2015	1.045	£2.32	[57]
GP Cost Total per Dose				**£19.66**	
Pharmacy Delivery Cost Per Dose					
NHS vaccine service payment	£9.80	2018	–	£9.80	[56]
Vaccine Purchase Payment	£7.08	2014/2015	1.041	£7.37	[57]
Sonar Service Fee	£0.12	2018	–	£0.12	[57]
Pharmacy Total Cost per Dose				**£17.29**	
School-Delivery Cost Per Dose					
NHS Vaccine Service Payment	£9.80	2018	–	£9.80	[56]
Vaccine Purchase Payment	£7.24	2014/2015	1.041	£7.54	[57]
Dispensing Fee	£2.70	2016/2017	1.088	£2.72	[45]
Delivery Fee	£9.88 per hour per 260 doses	2018	–	£0.038 per/1 dose	[46, 58]
Waste Disposal Fee	£0.148 per 100 empty dispensers	2018	–	£0.148 per 100 empty dispensers	[59]
School Delivery Total Cost per Dose				**£20.14**	

Table 3.6.5: Inflation adjustments for medical services and medical equipment from King et al.[35]

3.6.10 Costs for vaccine refrigeration and waste disposal

We assumed that services for waste disposal and sharps removal already exist at pharmacies and GP locations and are paid for directly by the NHS. For school-delivery, immunization teams would concentrate on the vaccination session therefore we assumed nurses did not return empty sprayers to their office for disposal. Waste disposal for school-based delivery was calculated as the cost of disposing clinical waste and a delivery fee to the waste disposal unit which we estimated at £0.148 per 100 sprayers). For delivery of clinical waste the same service cost as vaccine delivery based for a band 1 NHS driver hourly wage per 260 doses was used, and assumed delivery was completed in 1 hour.

Additional costs for refrigeration were not considered as the vaccine is kept in secure cool bags during school delivery and LAIV can be kept at room temperature for up to 12 hours.[28] Vaccine wastage was not considered a problem as pilot studies found few vaccines were wasted due to children moving away at the last moment or dropped applicators.[28]

3.6.11 Health outcomes

Interventions	SQ (95% Confidence Interval)	I1 (95% Confidence Interval)	I2 (95% Confidence Interval)	I3 (95% Confidence Interval)
Costs of Vaccines Annually (£ Millions)	129.63 (127.34, 131.90)	149.86 (147.43, 152.33)	177.66 (174.72, 180.56)	162.51 (160.03, 165.04)
Great Britain				
Annual Influenza A/H1N1 Incidence (Millions)	3.43 (3.14, 3.75)	2.99 (2.68, 3.33)	2.42 (2.05, 2.80)	2.51 (2.15, 2.87)
Cost of Hospitalization Annually (£ Thousands)	2592 (26, 14043)	2115 (23, 11454)	1782 (13, 9722)	1977 (20, 10464)
Cost of GP Consults Annually (£ Thousands)	1766 (60, 6289)	1465 (54, 5334)	1146 (30, 4321)	1311 (45, 4599)
Total Costs (£ Million)	134.0 (129.07, 145.95)	154.30 (149.79, 164.55)	182.67 (178.0, 191.12)	167.15 (162.82 176.0)
QALYs Lost - Deaths	4269 (3, 18074)	3543 (0, 23138)	2951 (0, 19710)	3193 (0, 20729)
QALYs Lost - Total	14,744 (4602, 31137)	12668 (996, 37651)	10296 (793, 30702)	10850 (776, 33070)
Belgium				
Annual Influenza A/H1N1 Incidence (Millions)	1.84 (1.57, 2.16)	1.76 (1.50, 2.06)	1.54 (1.31, 1.80)	1.26 (1.06, 1.52)
Cost of Hospitalization Annually (£ Thousands)	1285 (11, 6753)	1223 (10, 6461)	1157 (6, 6568)	1042 (3, 5473)
Cost of GP Consults Annually (£ Thousands)	838 (27, 3379)	780 (24, 3174)	663 (16, 2833)	549 (8, 2410)
Total Costs (£ Million)	131.77 (128.40, 138.18)	152.7 (149.23, 158.80)	181.53 (177.45, 187.85)	165.46 (162.14, 170.88)
QALYs Lost - Deaths	2255 (1, 9924)	2206 (0, 14668)	2084 (0, 13944)	1884 (0, 12357)
QALYs Lost - Total	7874 (2517, 16971)	7434 (570, 23994)	6766 (506, 20135)	5876 (446, 19047)
Germany				
Annual Influenza A/H1N1 Incidence (Millions)	2.09 (2.013, 2.18)	1.81 (1.74, 1.89)	1.62 (1.54, 1.69)	1.53 (1.44, 1.63)

Table 3.6.6 continued from previous page

Interventions	SQ (95% Confidence Interval)	S1 (95% Confidence Interval)	S2 (95% Confidence Interval)	S3 (95% Confidence Interval)
Cost of Hospitalization Annually (£ Thousands)	1654 (4, 8981)	1266 (3, 6986)	1070 (2, 5848)	1067 (2, 5877)
Cost of GP Consults Annually (£ Thousands)	883 (12, 3975)	694 (10, 3229)	585 (5, 2719)	581 (6, 2640)
Total Costs (£ Million)	132.16 (128.32, 140.48)	152.65 (149.05, 159.44)	181.38 (177.46, 187.12)	165.52 (162.16, 171.11)
QALYs Lost - Deaths	2962 (0, 12297)	2276 (0, 14686)	1883 (0, 12198)	1903 (0, 12549)
QALYs Lost - Total	9314 (2810, 20179)	7738 (576, 23072)	6869 (556, 20071)	6499 (495, 18726)
Finland				
Annual Influenza A/H1N1 Incidence (Millions)	1.10 (1.0, 1.19)	0.97 (0.87, 1.05)	0.90 (0.80, 0.99)	0.82 (0.70, 0.92)
Cost of Hospitalization Annually (£ Thousands)	1366 (4, 7683)	1145 (3, 6465)	1091 (2, 5970)	1110 (2, 6204)
Cost of GP Consults Annually (£ Thousands)	652 (9, 3010)	546 (8, 2545)	515 (6, 2347)	511 (6, 2498)
Total Costs (£ Millions)	131.64 (128.11, 138.13)	152.37 (148.97, 158.0)	181.29 (177.35, 187.03)	165.5 (162.07, 171.20)
QALYs Lost - Deaths	2522 (0, 11352)	2130 (0, 13859)	2051 (0, 13508)	2070 (0, 13374)
QALYs Lost - Total	5887 (1536, 14396)	5148 (326, 18205)	4775 (295, 17680)	4570 (292, 17311)
France				
Annual Influenza A/H1N1 Incidence (Millions)	14.17 (13.72, 14.65)	13.86 (13.43, 14.38)	13.40 (12.96, 13.99)	13.28 (12.86, 13.79)
Cost of Hospitalization Annually (£ Thousands)	17397 (66, 93887)	17111 (65, 92571)	16656 (68, 90153)	16617 (66, 93086)
Cost of GP Consults Annually (£ Thousands)	8922 (187, 39296)	8747 (184, 38430)	8500 (162, 36980)	8461 (162, 37610)
Total Costs (£ Million)	156.20 (130.33, 239.22)	176.82 (151.38, 259.79)	205.01 (180.41, 286.04)	189.06 (164.64, 263.98)

Table 3.6.6 continued from previous page

Interventions	SQ (95% Confidence Interval)	S1 (95% Confidence Interval)	S2 (95% Confidence Interval)	S3 (95% Confidence Interval)
QALYs Lost - Deaths	31347 (7, 132997)	30927 (0, 194353)	30259 (0, 192631)	29951 (0, 190539)
QALYs Lost - Total	74361 (20469, 183287)	73149 (4696, 263642)	71389 (4313, 251525)	69952 (4545, 257677)
Italy				
Annual Influenza A/H1N1 Incidence (Millions)	2.78 (2.37, 3.21)	2.63 (2.23, 3.03)	2.11 (1.68, 2.57)	2.0 (1.58, 2.46)
Cost of Hospitalization Annually (£ Thousands)	1874 (16, 9926)	1726 (14, 9332)	1360 (8.396225, 7396)	1364 (8, 7240)
Cost of GP Consults Annually (£ Thousands)	1261 (40, 4765)	1153 (37, 4450)	853 (22, 3507)	861 (22, 3369)
Total Costs (£ Million)	132.73 (128.57, 141.78)	153.54 (149.41, 162.26)	181.89 (177.51, 188.85)	166.05 (162.34, 172.90)
QALYs Lost - Deaths	3166 (1, 13866)	2994 (0 18903)	2303 (0, 15326)	2288 (0, 15081)
QALYs Lost - Total	11714 (3675, 26039)	11150 (911, 33940)	8764 (681, 25096)	8417 (665, 25345)
Luxemborgh				
Annual Influenza A/H1N1 Incidence (Millions)	1.85 (1.59, 2.10)	1.73 (1.48, 1.96)	1.63 (1.40, 1.86)	1.39 (1.13, 1.65)
Cost of Hospitalization Annually (£ Thousands)	1444 (4, 8298)	1294 (4, 7570)	1232 (3, 7076)	1085 (3, 6112)
Cost of GP Consults Annually (£ Thousands)	776 (10, 3619)	698 (9, 3341)	656 (7, 3004)	576 (7, 2796)
Total Costs (£ Million)	131.87 (128.29, 139.63)	152.70 (149.11, 159.83)	181.57 (177.44, 187.98)	165.54 (162.14, 171.59)
QALYs Lost - Deaths	2602 (0, 11781)	2331 (0, 15839)	2211 (0, 15298)	1970 (0, 13727)
QALYs Lost - Total	8224 (2505, 18762)	7625 (581, 23403)	7189 (555, 22983)	6185 (425, 19564)
Netherlands				

Table 3.6.6 continued from previous page

Interventions	SQ (95% Confidence Interval)	S1 (95% Confidence Interval)	S2 (95% Confidence Interval)	S3 (95% Confidence Interval)
Annual Influenza A/H1N1 Incidence (Millions)	1.80 (1.38, 2.13)	1.49 (1.12, 1.82)	1.18 (0.85, 1.52)	0.83 (0.29, 1.25)
Cost of Hospitalization Annually (£ Thousands)	979 (12, 5096)	782 (8, 4272)	622 (4, 3325)	597 (4, 31268)
Cost of GP Consults Annually (£ Thousands)	732 (28, 2807)	568 (19, 2326)	405 (10, 1752)	398 (11, 1525)
Total Costs (£ Million)	131.35 (128.27, 136.41)	152.07 (149.06, 156.46)	180.73 (177.20, 184.72)	164.88 (161.88, 168.60)
QALYs Lost - Deaths	1577 (1, 7133)	1308 (0, 9013)	1029 (0, 6636)	1013 (0, 7277)
QALYs Lost - Total	7071 (2251, 15208)	5857 (478, 17366)	4625 (376, 13604)	3567 (251, 12225)
Poland				
Annual Influenza A/H1N1 Incidence (Millions)	3.0 (2.52, 3.55)	2.89 (2.43, 3.41)	2.40 (1.84, 2.96)	2.25 (1.73, 2.81)
Cost of Hospitalization Annually (£ Thousands)	1475 (18, 8328)	1378 (16, 7870)	1153 (7, 6478)	1118 (8, 6131)
Cost of GP Consults Annually (£ Thousands)	1118 (41, 4109)	1041 (37, 3873)	780 (19, 3357)	783 (20, 3341)
Total Costs (£ Million)	132.21 (128.35, 139.99)	153.10 (149.25, 160.20)	181.58 (177.59, 187.69)	165.77 (162.37, 171.42)
QALYs Lost - Deaths	2372 (2, 10945)	2251 (0, 15135)	1884 (0, 12490)	1874 (0, 12899)
QALYs Lost - Total	11588 (35889, 24140)	11255 (969, 32236)	9082 (828, 27028)	8828 (736, 25444)
Peru				
Annual Influenza A/H1N1 Incidence (Millions)	1.87 (1.61, 2.22)	1.70 (1.47, 1.98)	1.37 (1.13, 1.57)	0.40 (0.24, 0.68)
Cost of Hospitalization Annually (£ Thousands)	918 (1, 4598)	784 (10, 3949)	640 (7, 3075)	225 (2, 1190)

Table 3.6.6 continued from previous page

Interventions	SQ (95% Confidence Interval)	S1 (95% Confidence Interval)	S2 (95% Confidence Interval)	S3 (95% Confidence Interval)
Cost of GP Consults Annually (£ Thousands)	746 (30, 2583)	645 (27, 2297)	495 (15, 1848)	174 (6, 705)
Total Costs (£ Million)	131.30 (128.36, 136.16)	152.11 (149.16, 156.38)	180.83 (177.35, 185.03)	164.25 (161.6354 166.86)
QALYs Lost - Deaths	1335 (1, 6165)	1176 (0, 8071)	933 (0, 5862)	338 (0, 2502)
QALYs Lost - Total	7045 (2363, 14617)	6367 (539, 18300)	5141 (442, 15067)	1551 (114, 5269)

Table 3.6.6: Average annual outcomes for each substituted simulation over the period 1995/1996-2008/2009 for influenza A/H1N1 incidence, cost of influenza-related hospitalization, cost of influenza-related GP appointments, total cost of seasonal influenza vaccination and healthcare, the number of QALYs lost from influenza-related death, and the number of QALYs lost from all sources (Death, Symptomatic Illness, Hospitalization, and GP visits). The 95% confidence interval for each value is shown in parenthesis.

Age-stratified outcomes

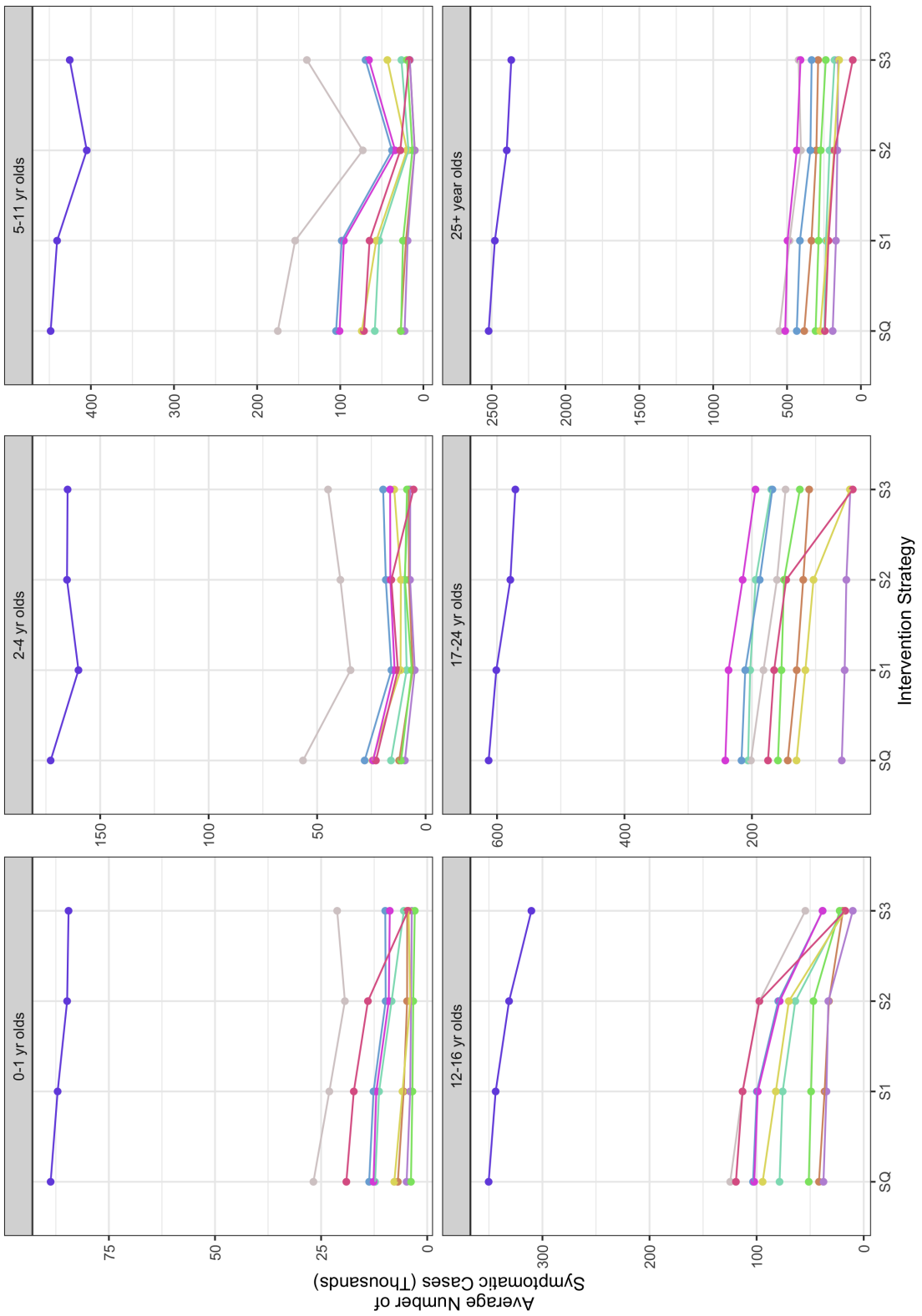

Figure 3.6.11: The average annual influenza A/H1N1 symptomatic cases per season under each substituted simulation and that of Great Britain. The outcomes have been stratified by age to demonstrate age-structured differences in sumulations under each strategy (SQ-I3).

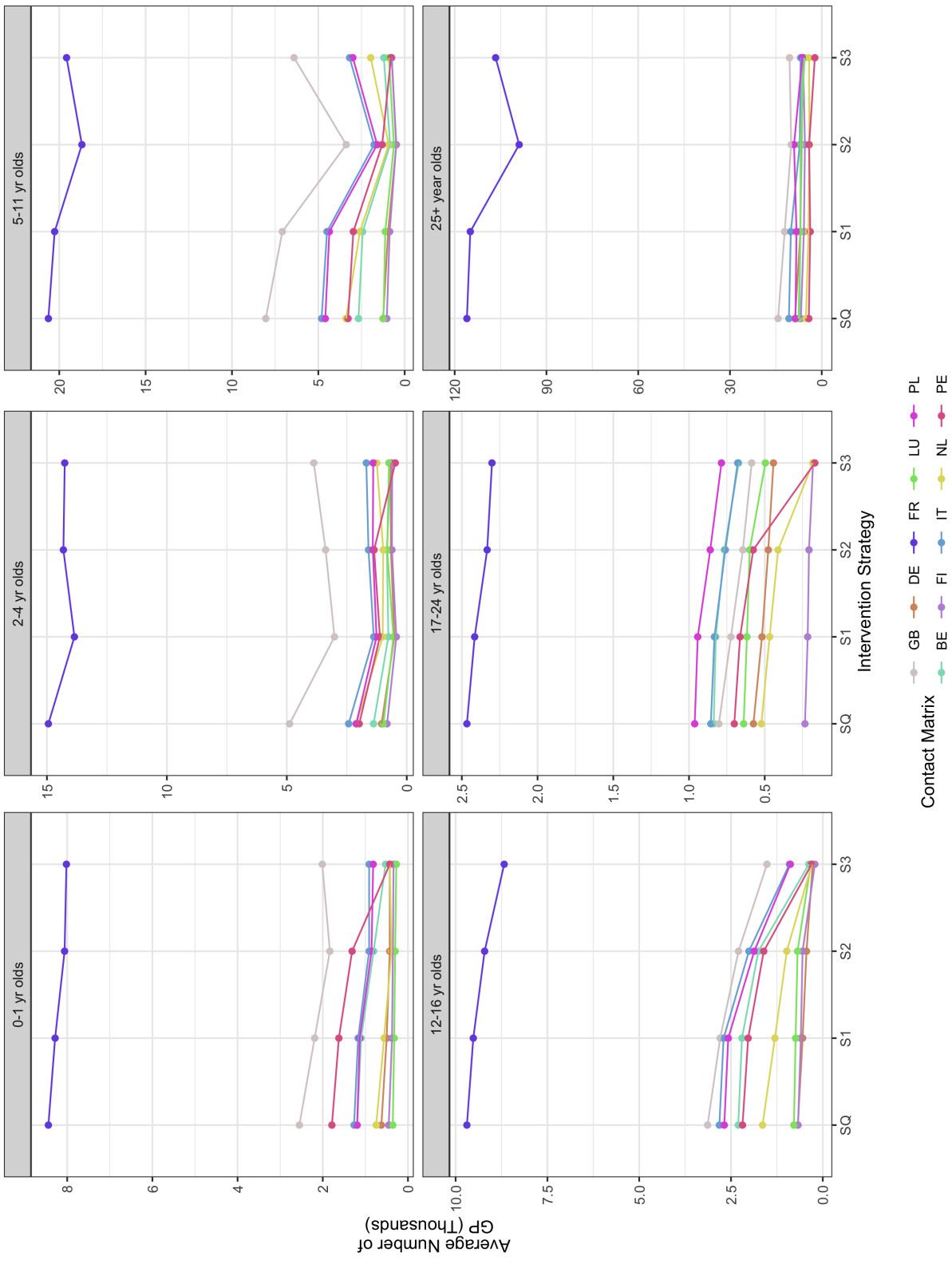

Figure 3.6.12: The average annual influenza A/H1N1 general practitioner consultations per season under each substituted simulation and that of Great Britain. The outcomes have been stratified by age to demonstrate age-structured differences in simulations under each strategy (SQ-I3).

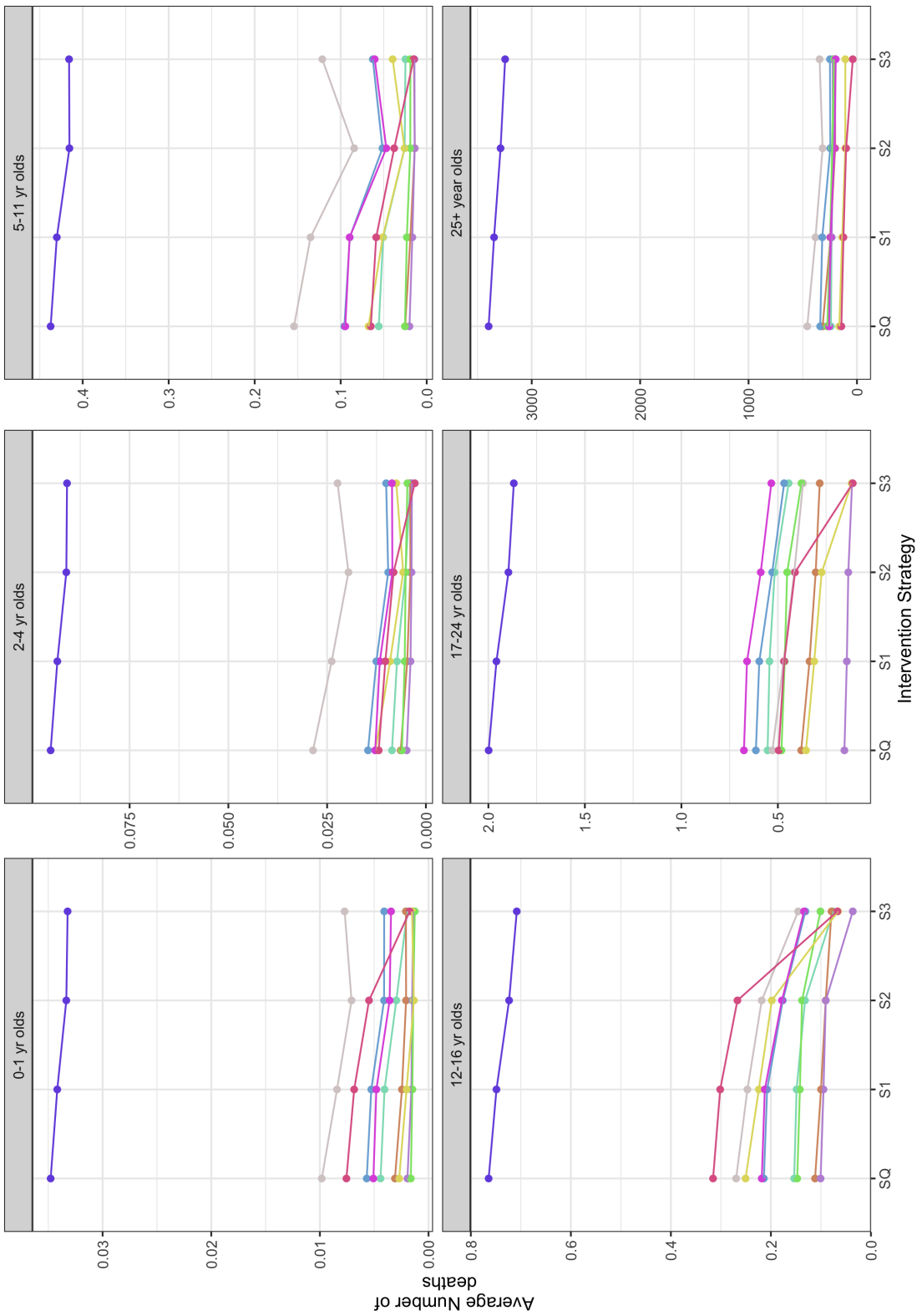

Figure 3.6.13: The average annual influenza A/H1N1 associated mortality under each substituted simulation and that of Great Britain. The outcomes have been stratified by age to demonstrate age-structured differences in simulations under each strategy (SQ-I3).

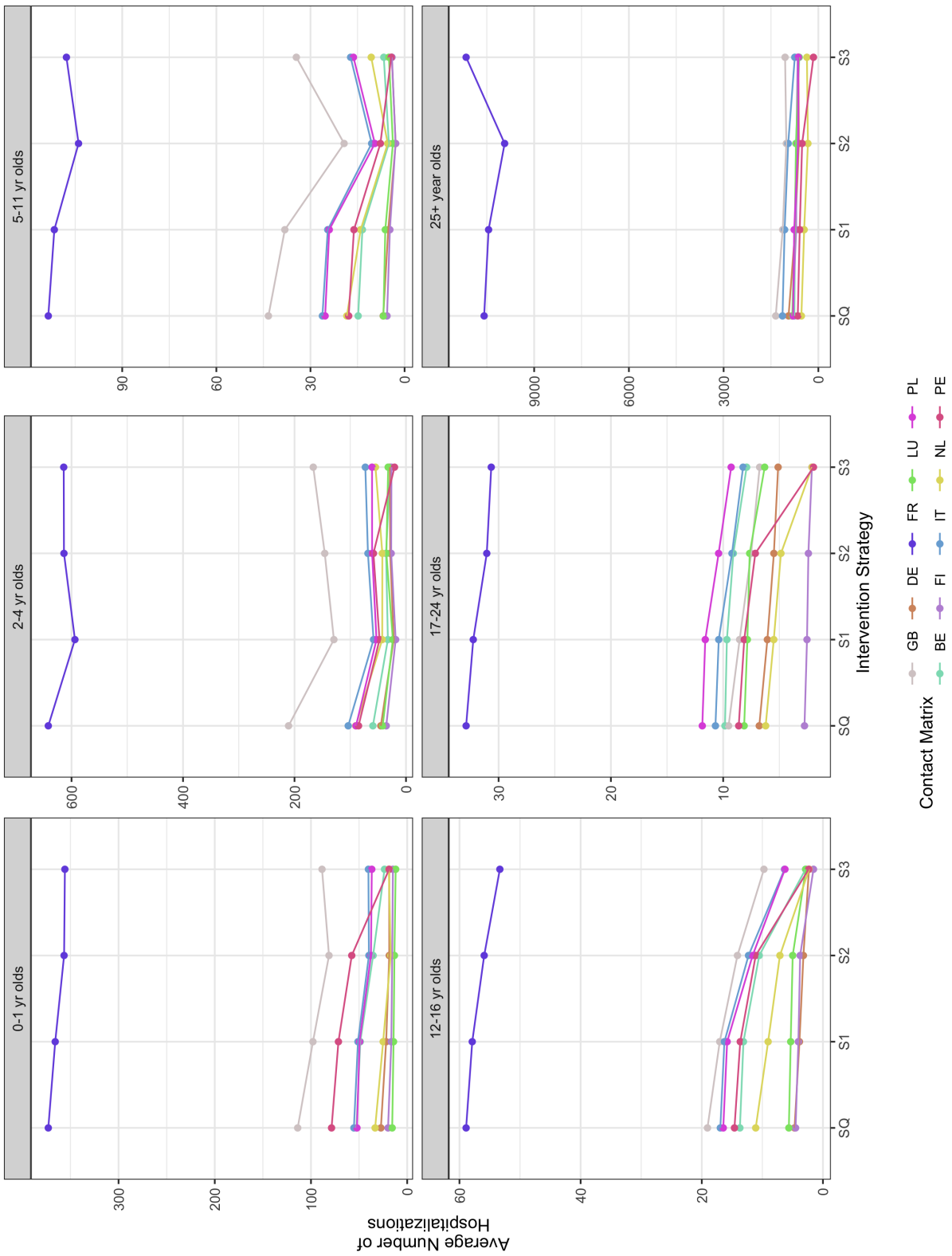

Figure 3.6.14: The average annual influenza A/H1N1 associated hospitalizations per season under each substituted simulation and that of Great Britain. The outcomes have been stratified by age to demonstrate age-structured differences in simulations under each strategy (SQ-I3).

3.6.12 Infections averted per vaccine dose

Total infections averted per 1000 vaccine doses

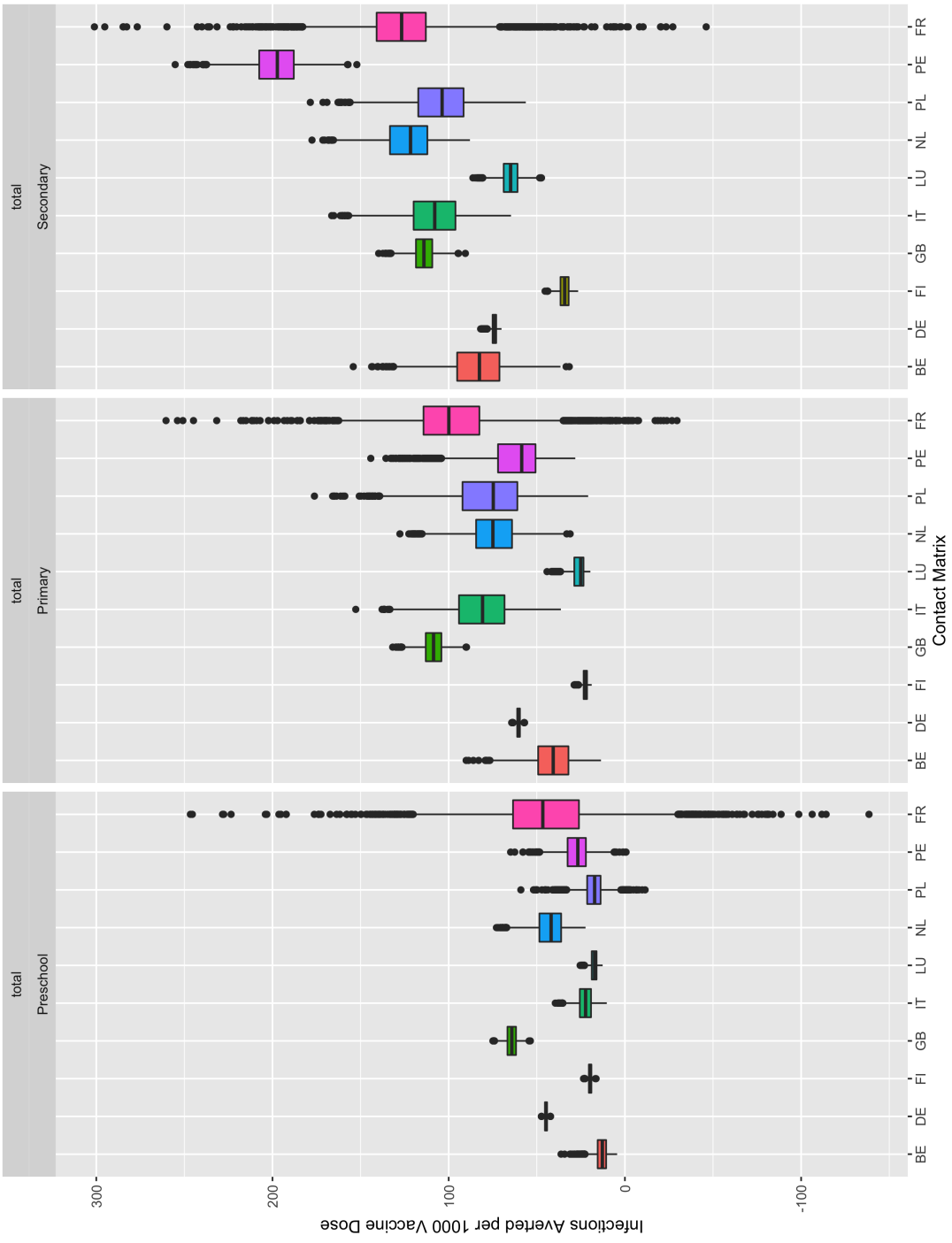

Figure 3.6.15: Boxplots of the average number of influenza A/H1N1 infections averted per 1000 vaccine doses for each substituted scenario under each intervention strategy I1, I2, and I3.

Infections averted per 1000 vaccine doses stratified by age

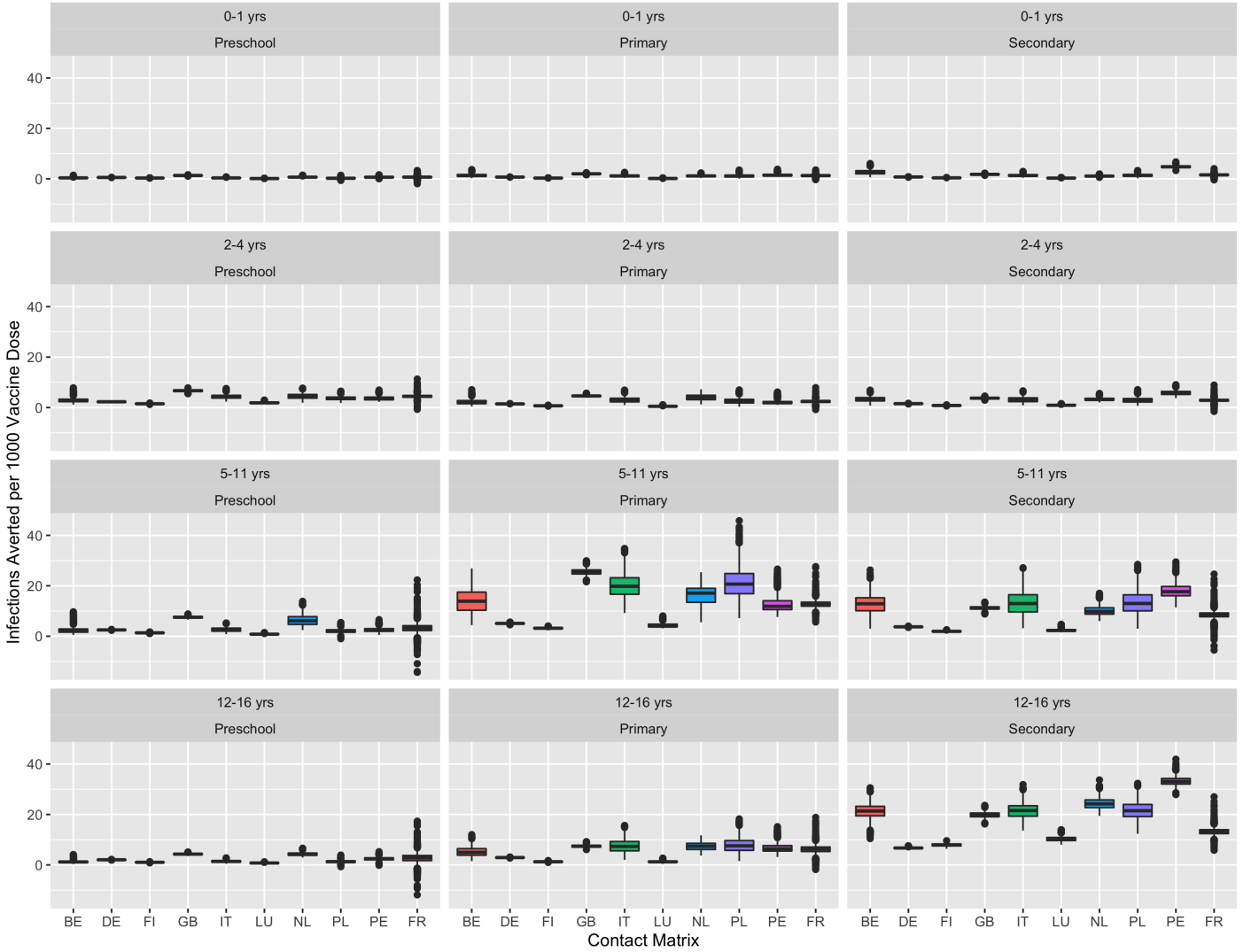

Figure 3.6.16: Boxplots of the average number of influenza A/H1N1 infections averted per age group per 1000 vaccine doses distributed to the entire population. Age groups 6 months - 16 year olds are shown above with the intervention strategy being simulated listed in the header. Each color box plot represents a substituted simulation.

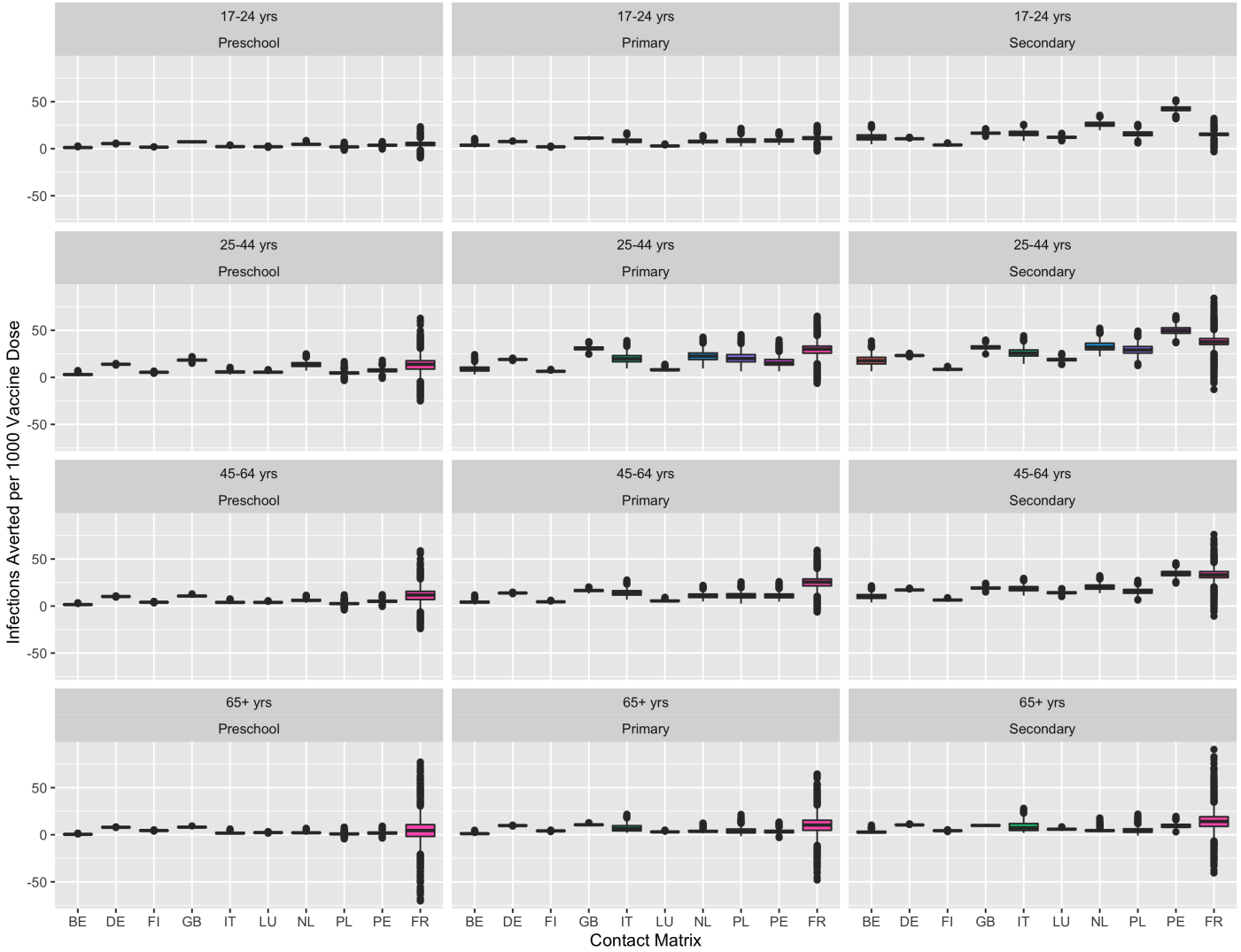

Figure 3.6.17: Boxplots of the average number of influenza A/H1N1 infections averted per age group per 1000 vaccine doses distributed to the entire population. Age groups 17 - 75+ year olds are shown above with the intervention strategy being simulated listed in the header. Each color box plot represents a substituted simulation.

3.6.13 Basic reproductive number

Calculation of the basic reproductive number was carried out according to the Next-Generation method described by Diekman et al. [83].

Reproductive numbers for influenza seasons 1995/1996-2008/2009

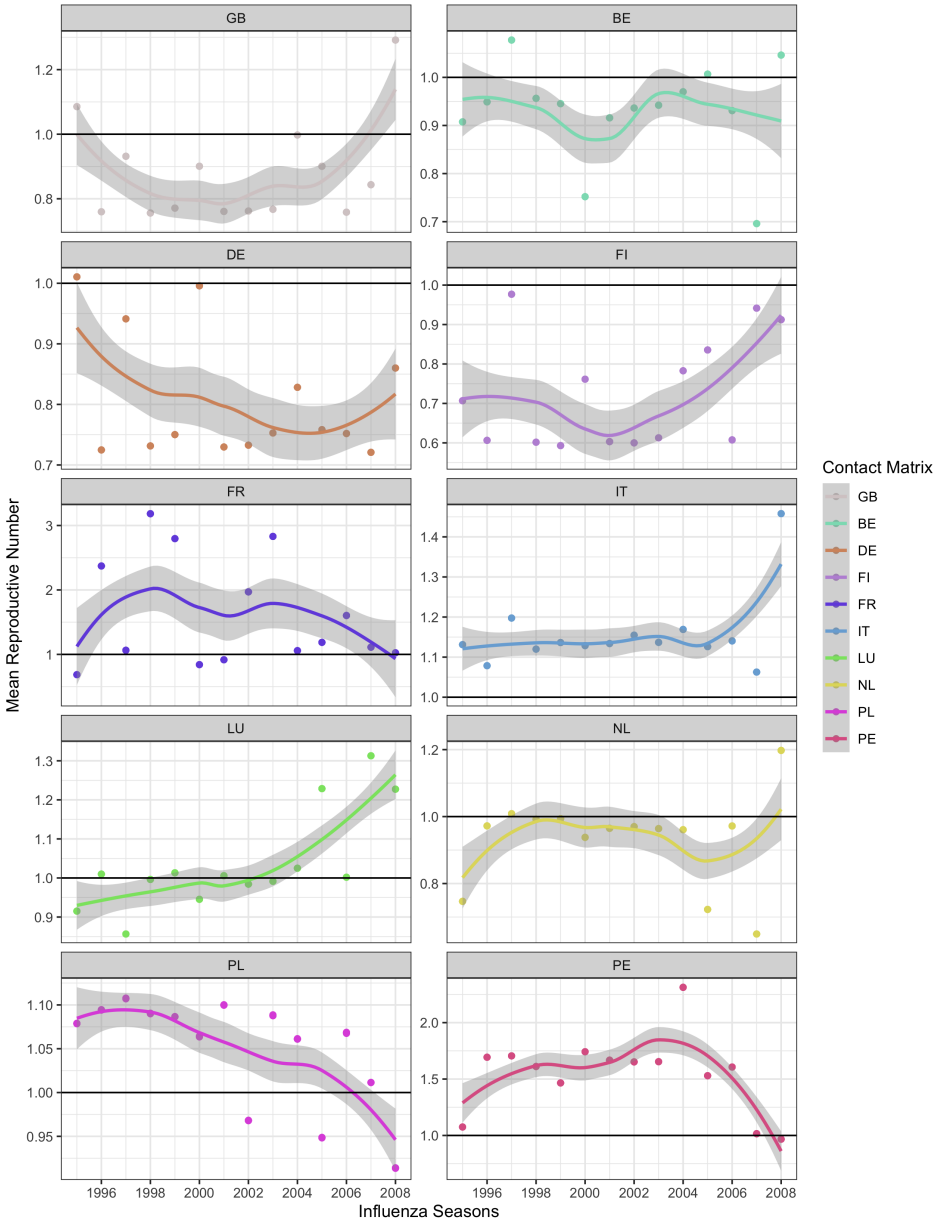

Figure 3.6.18: The average basic reproductive number over the period 1995/1996-2008/2009 per substituted contact matrix scenario. The 95% confidence intervals are shown in gray Lines are fitted and smoothed using locally estimated scatterplot smoothing ('LOESS').

Reproductive numbers for influenza seasons 1995/1996-2008/2009

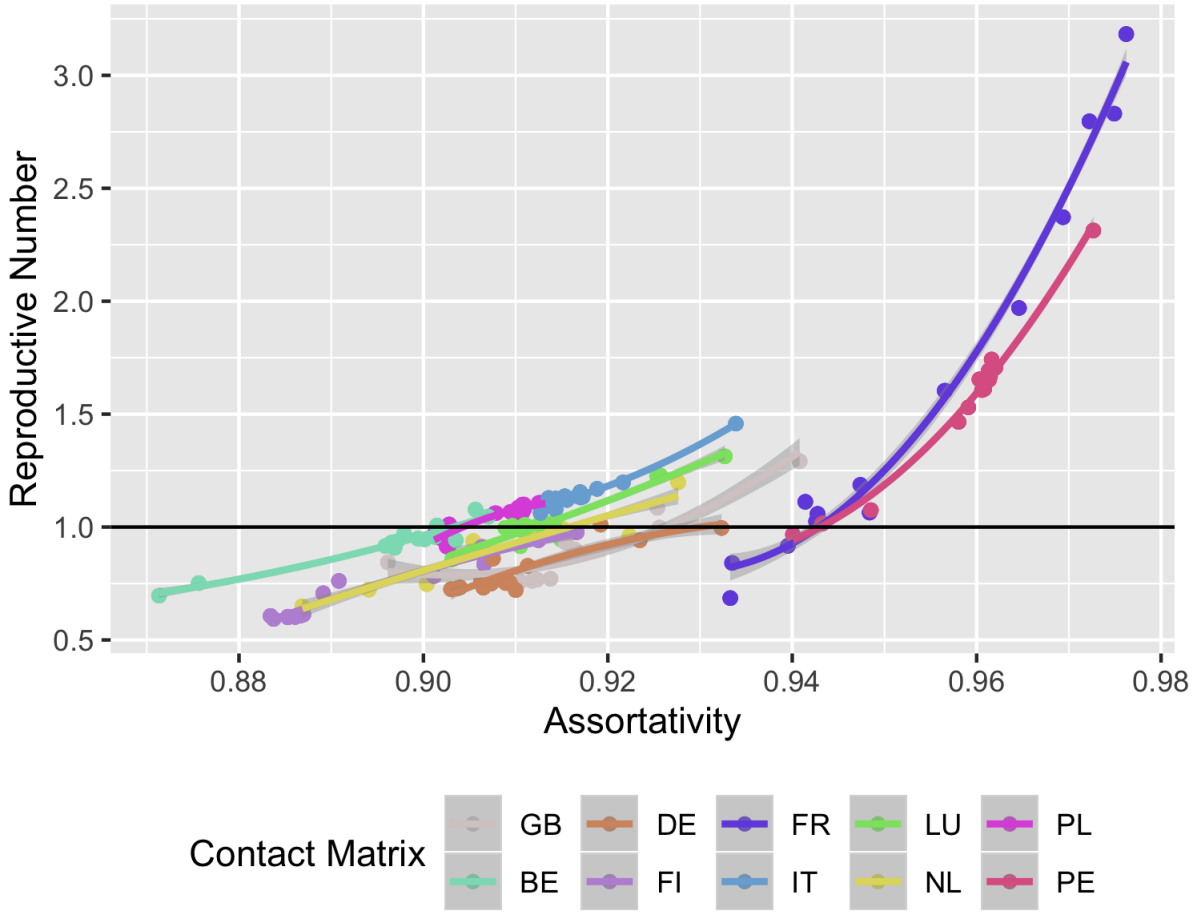

Figure 3.6.19: The mean basic reproductive number over the period 1995/1996-2008/2009 per substituted contact matrix scenario (y-axis) graphed against the assortativity quotient of each substituted contact matrix (x-axis) demonstrating increased basic reproductive numbers (R_0) values are associated with increases in the assortativity quotient. The 95% confidence intervals are shown in gray Lines are fitted and smoothed using locally estimated scatterplot smoothing ('LOESS').

3.6.14 Uncertainty in cost-effectiveness analysis of influenza A/H3N2

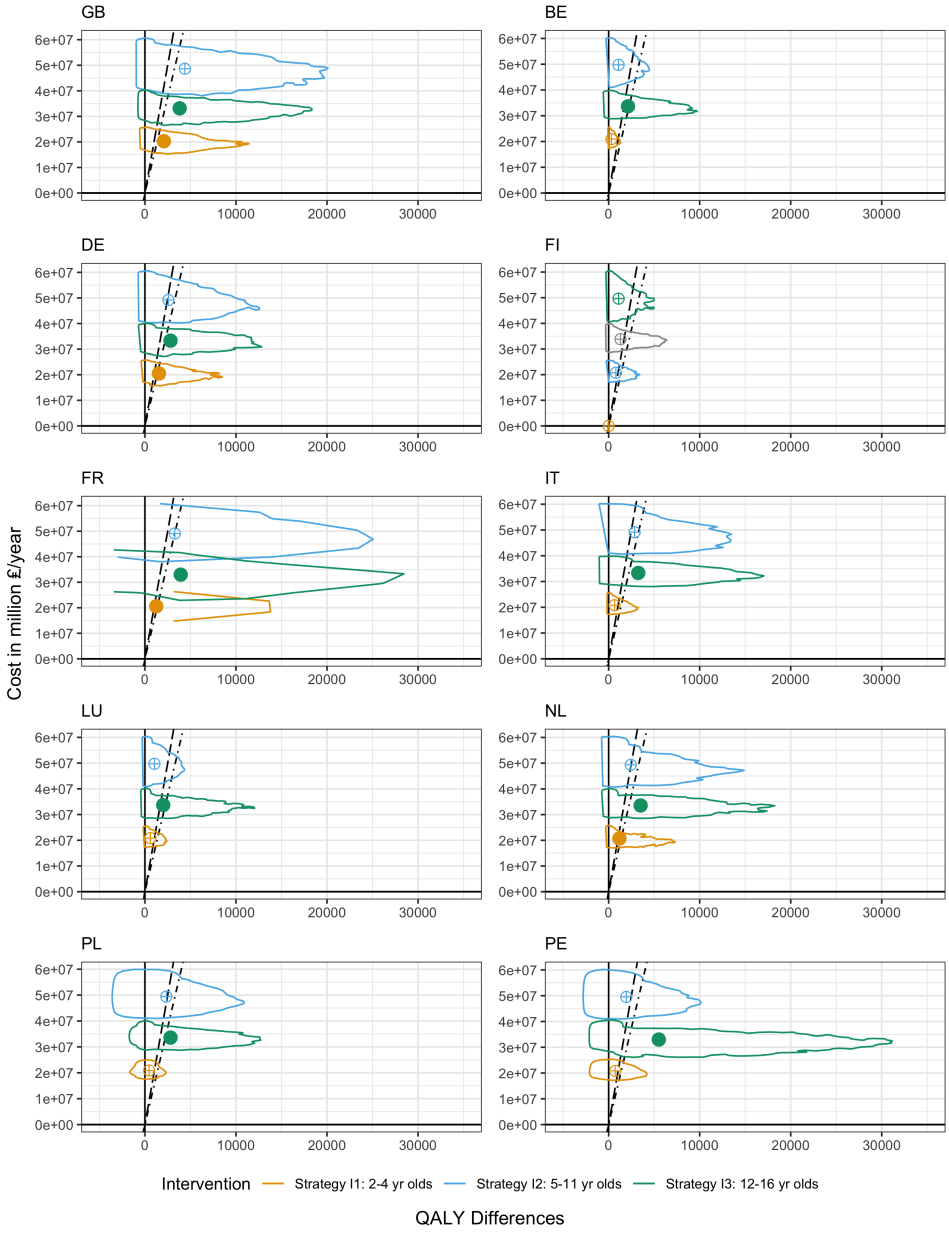

Figure 3.6.20: Cost-effectiveness frontier for strategies I1, I2, and I3 in Great Britain and Wales under different contact matrix assumptions. Filled circles represent the mean value is cost-effective at the £20,000 per QALY willingness-to-pay threshold (dashed-dot line). The £15,000 per QALY willingness-to-pay threshold (dashed line) line is also shown for reference. Quartered circles represent the intervention has been dominated. The cloud of incremental cost-effectiveness estimates is represented by the colored outline containing 90% of the estimates.

Influenza A/H3N2 epidemiological outcomes

Age-stratified outcomes

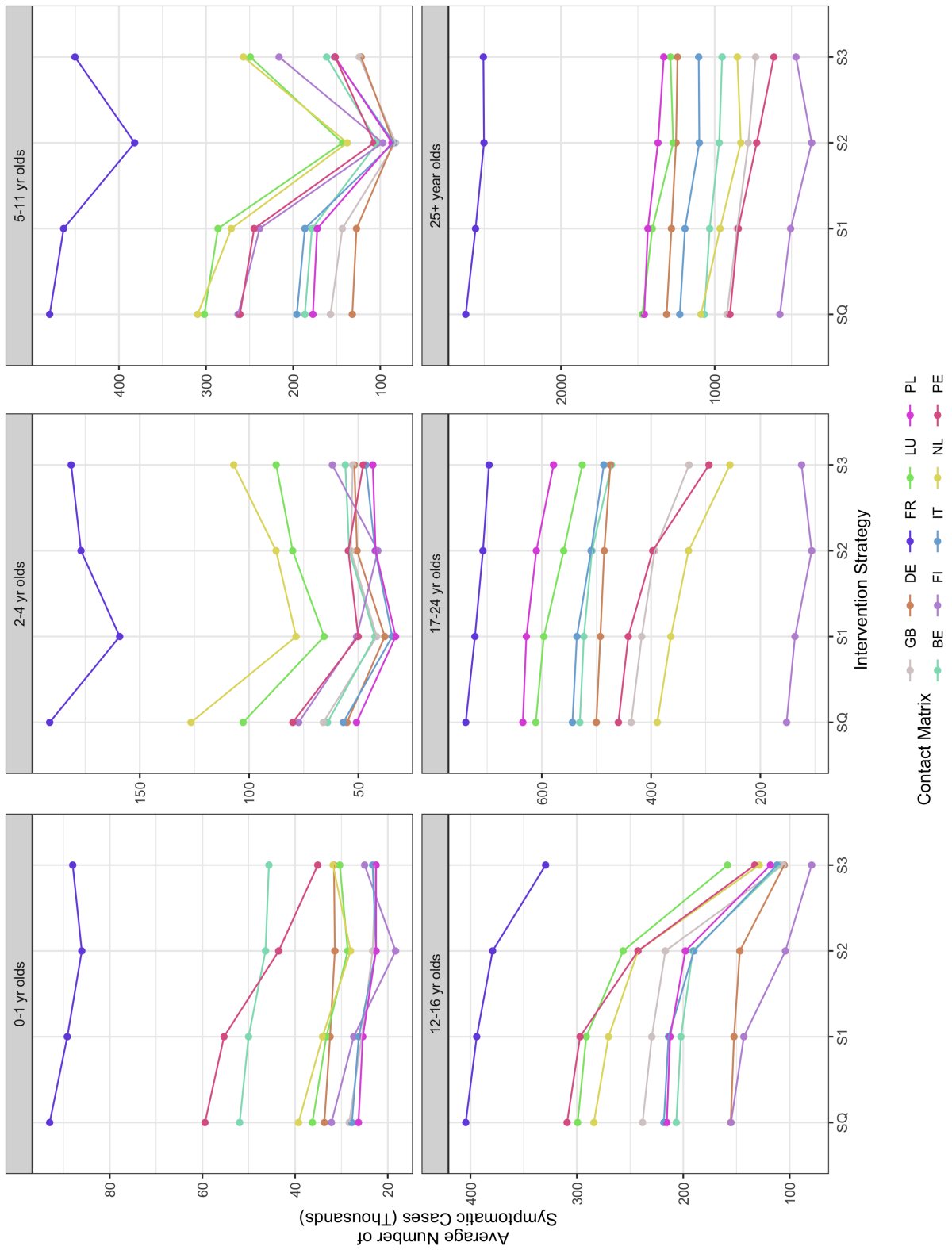

Figure 3.6.21: The average annual influenza A/H3N2 symptomatic cases per season under each substituted simulation and that of Great Britain. The outcomes have been stratified by age to demonstrate age-structured differences in simulations under each strategy (SQ-I3).

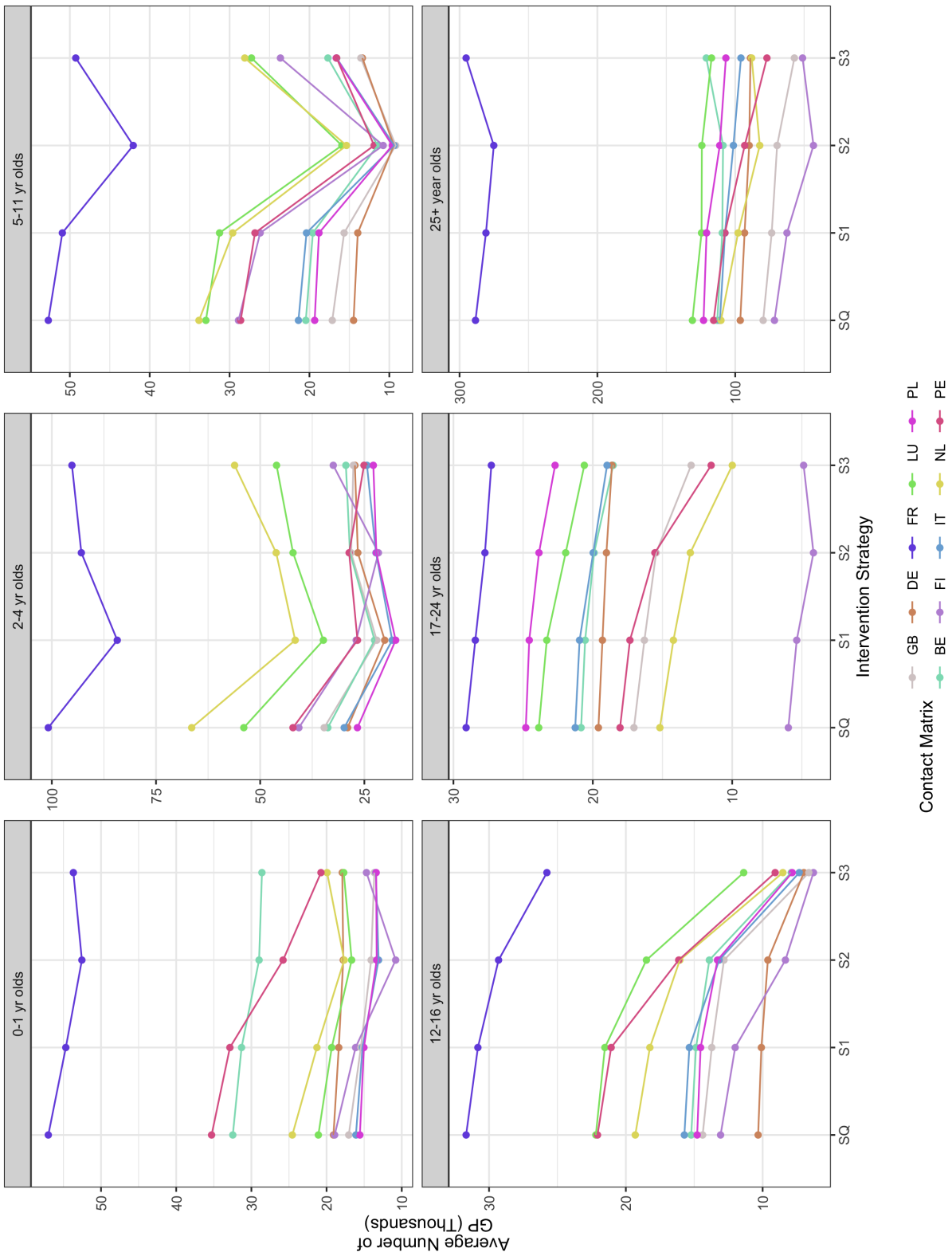

Figure 3.6.22: The average annual influenza A/H3N2 general practitioner consultations per season under each substituted simulation and that of Great Britain. The outcomes have been stratified by age to demonstrate age-structured differences in simulations under each strategy (SQ-I3).

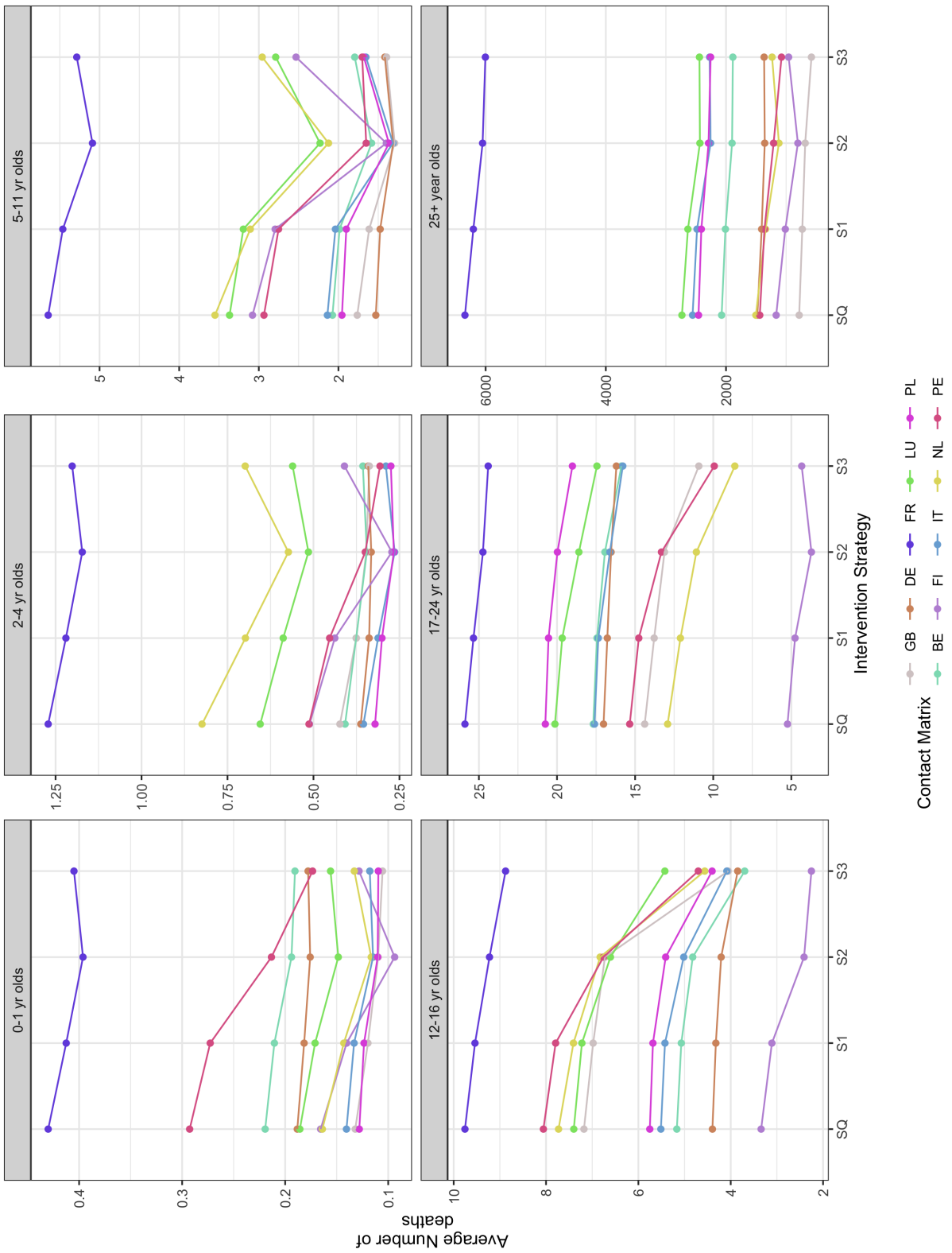

Figure 3.6.23: The average annual influenza A/H3N2 associated mortality under each substituted simulation and that of Great Britain. The outcomes have been stratified by age to demonstrate age-structured differences in simulations under each strategy (SQ-I3).

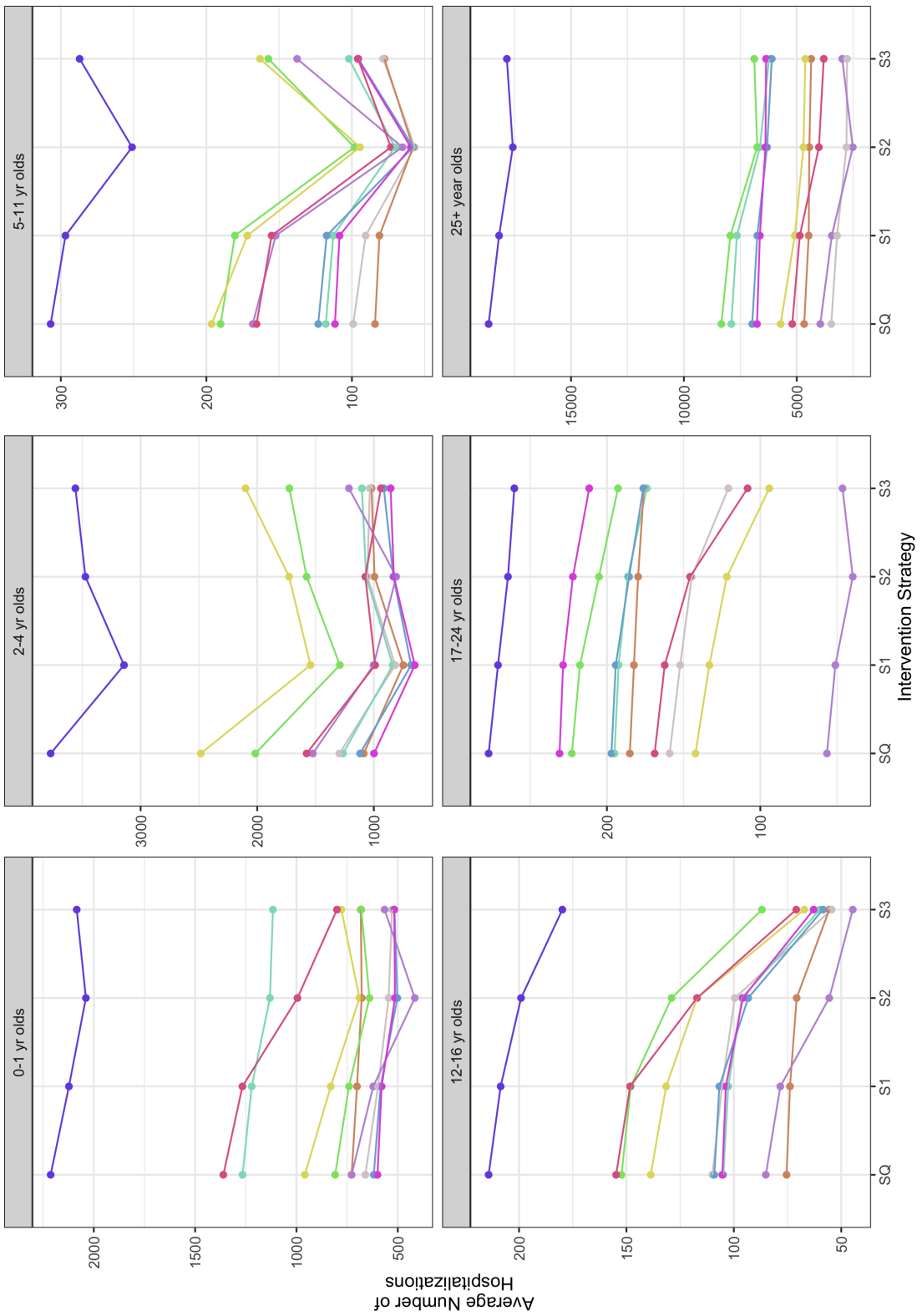

Figure 3.6.24: The average annual influenza A/H3N2 associated hospitalizations per season under each substituted simulation and that of Great Britain. The outcomes have been stratified by age to demonstrate age-structured differences in simulations under each strategy (SQ-I3).

Influenza A/H3N2 total infections averted per 1000 vaccine doses

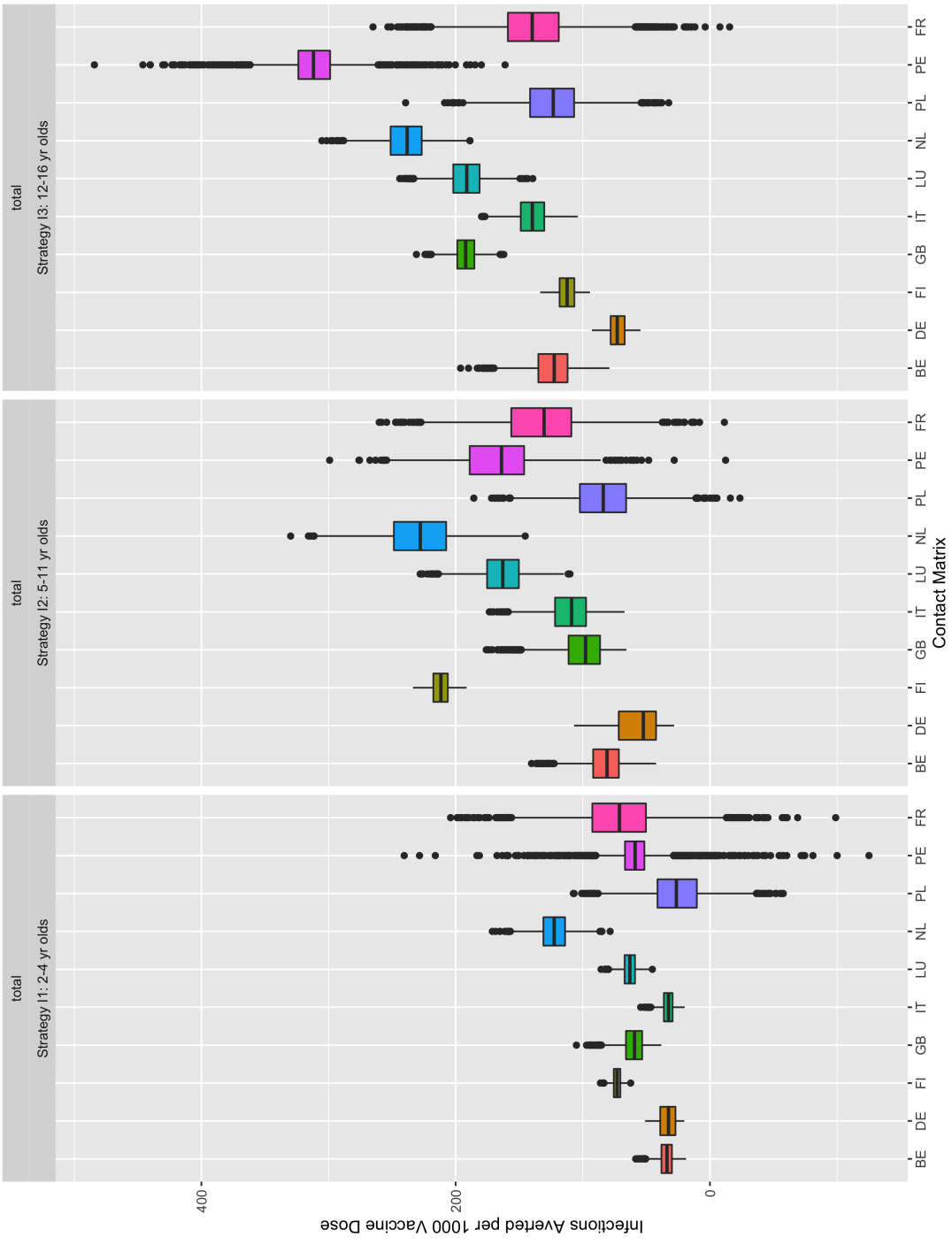

Figure 3.6.25: Boxplots of the average number of influenza A/H3N2 infections averted per 1000 vaccine doses for each substituted scenario under each intervention strategy I1, I2, and I3.

Infections averted per 1000 vaccine doses stratified by age

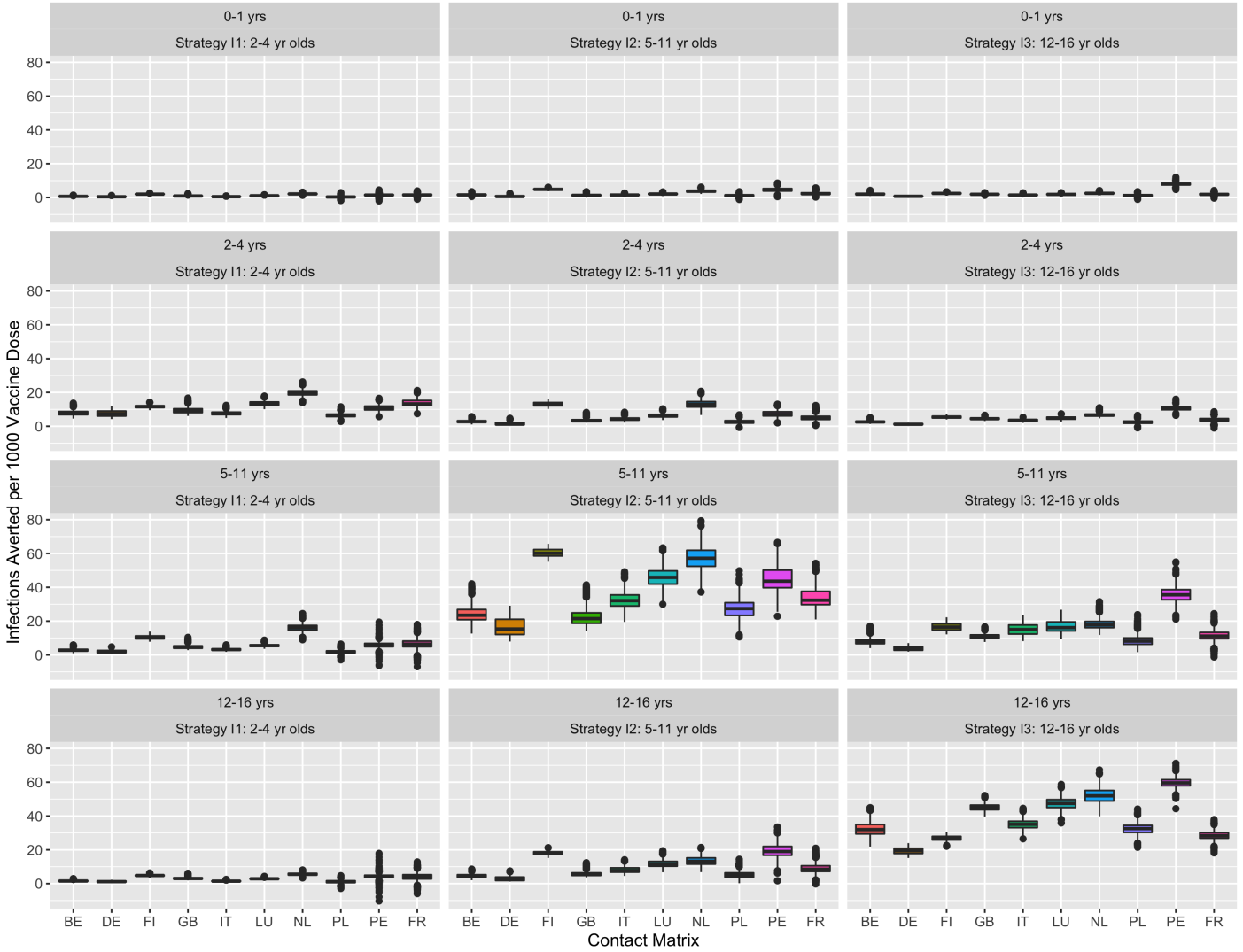

Figure 3.6.26: Boxplots of the average number of influenza A/H3N2 infections averted per age group per 1000 vaccine doses distributed to the entire population. Age groups 6 months - 16 year olds are shown above with the intervention strategy being simulated listed in the header. Each color box plot represents a substituted simulation.

Infections averted per 1000 vaccine doses stratified by age

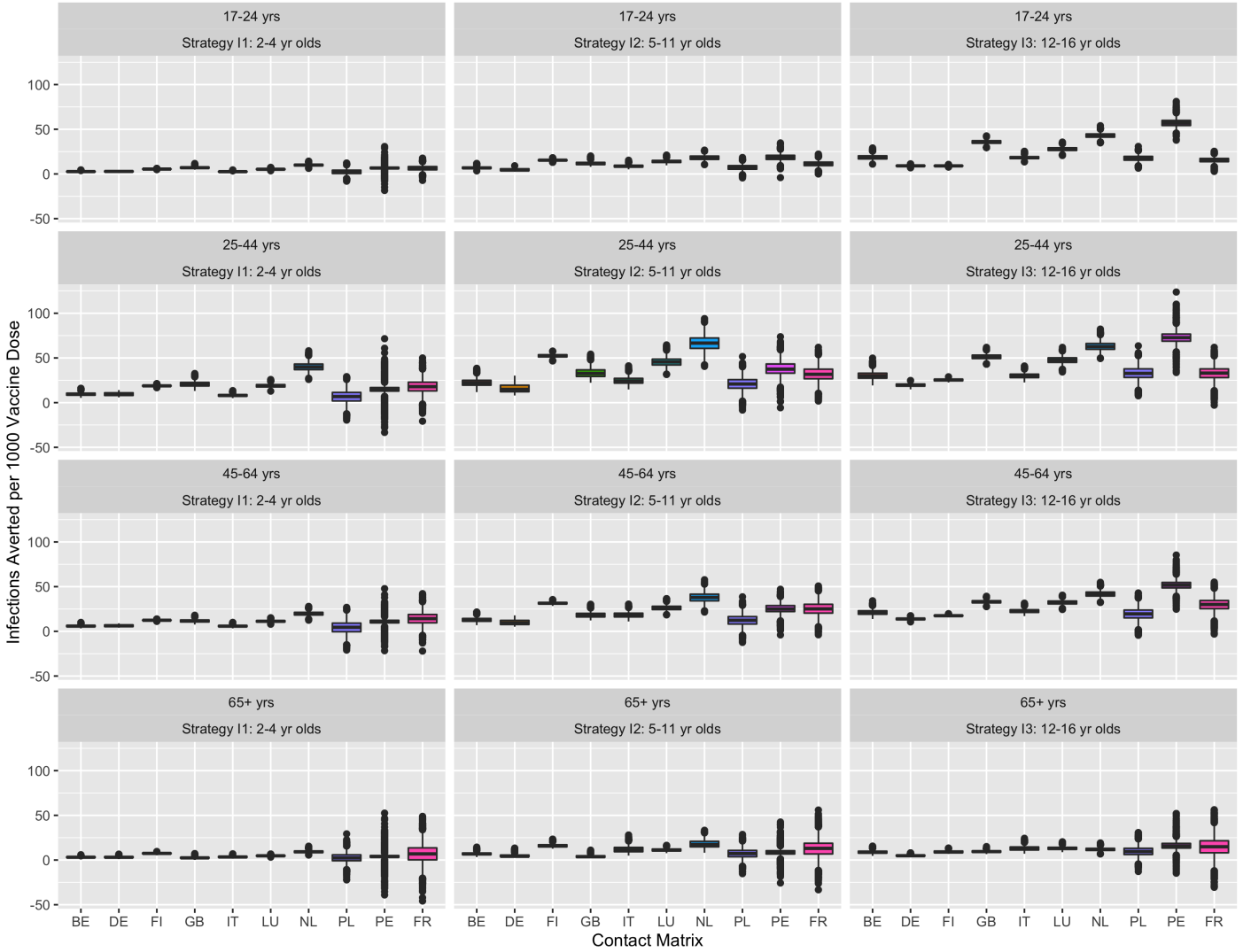

Figure 3.6.27: Boxplots of the average number of influenza A/H3N2 infections averted per age group per 1000 vaccine doses distributed to the entire population. Age groups 17-75+ year olds are shown above with the intervention strategy being simulated listed in the header. Each color box plot represents a substituted simulation.

Chapter 4

Appendices

A1 Inference for 19 seasons and 3 strains for Chapter 1

Inference results for H1N1 during the 1995-2013 season. A: Comparison of the fit of the model to the age-specific time-series of positive ILI cases estimated from the data. For the model, the mean ILI estimates (red line) are based on the binomial process $m_+ \, Binom(Z_\theta, \epsilon)$. For the data, since the unbiased estimator for m_{ij} is $n_{ij} * m_{ij}/n_{ij}$ (black dots) and its 95% CI can be computed using a hyper-geometric distribution (gray error bars).

A1.1 Model Fits for Influenza Strain A/H1N1

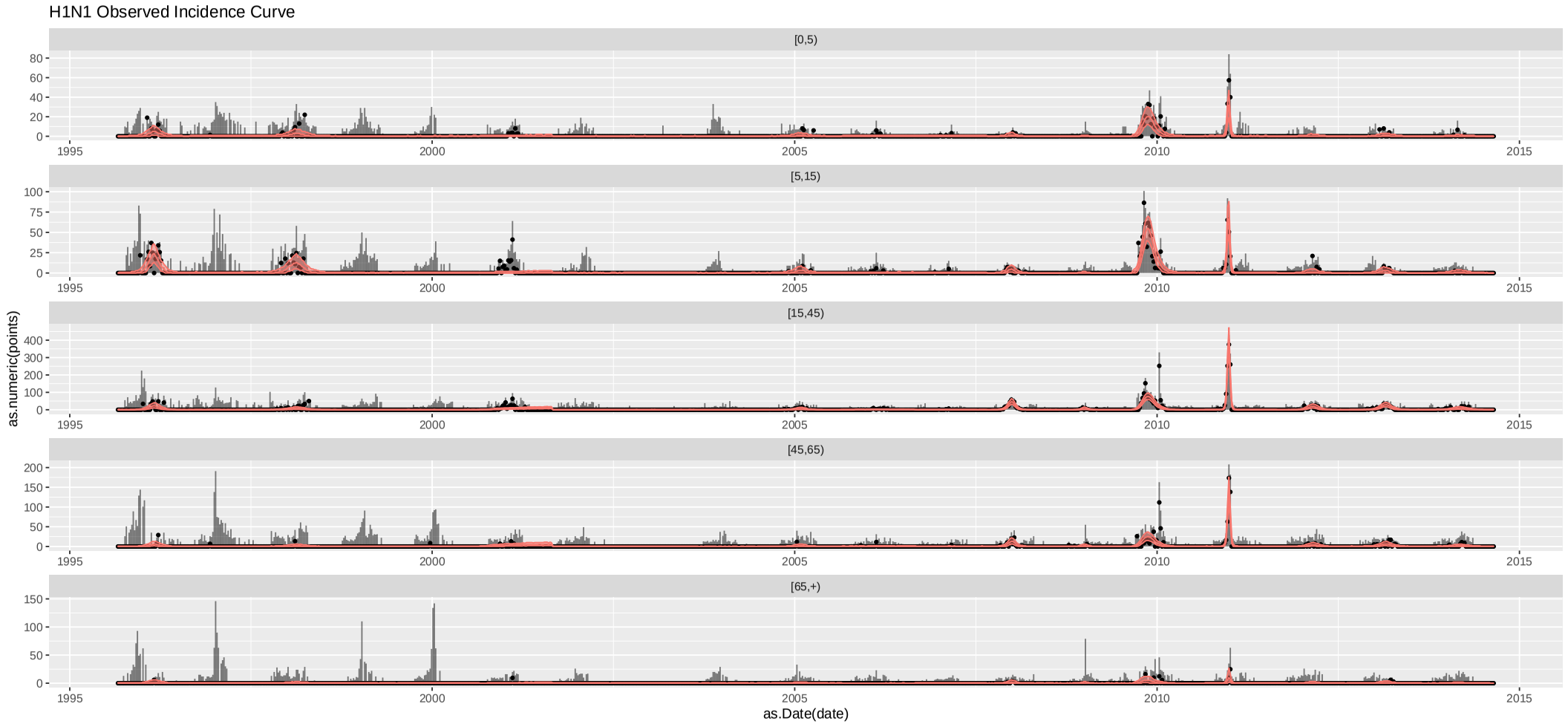
H1N1 Observed Incidence Curve
[0,5)
[5,15)
[15,45)
[45,65)
[65,+)
as.numeric(points)
as.Date(date)
1995
2000
2005
2010
2015

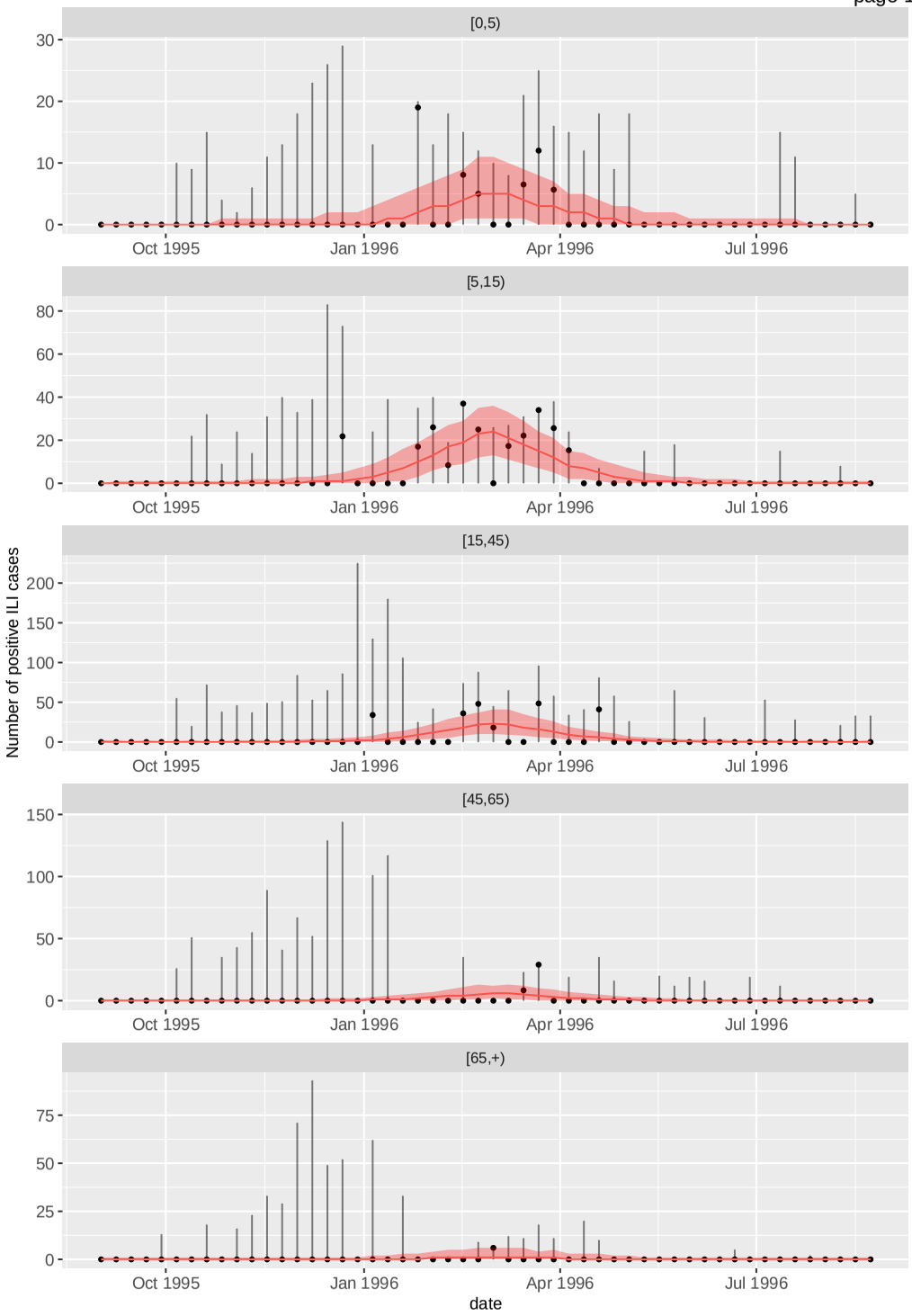
[0,5)
[5,15)
[15,45)
[45,65)
[65,+)
Number of positive ILI cases
Oct 1995
Jan 1996
Apr 1996
Jul 1996
date

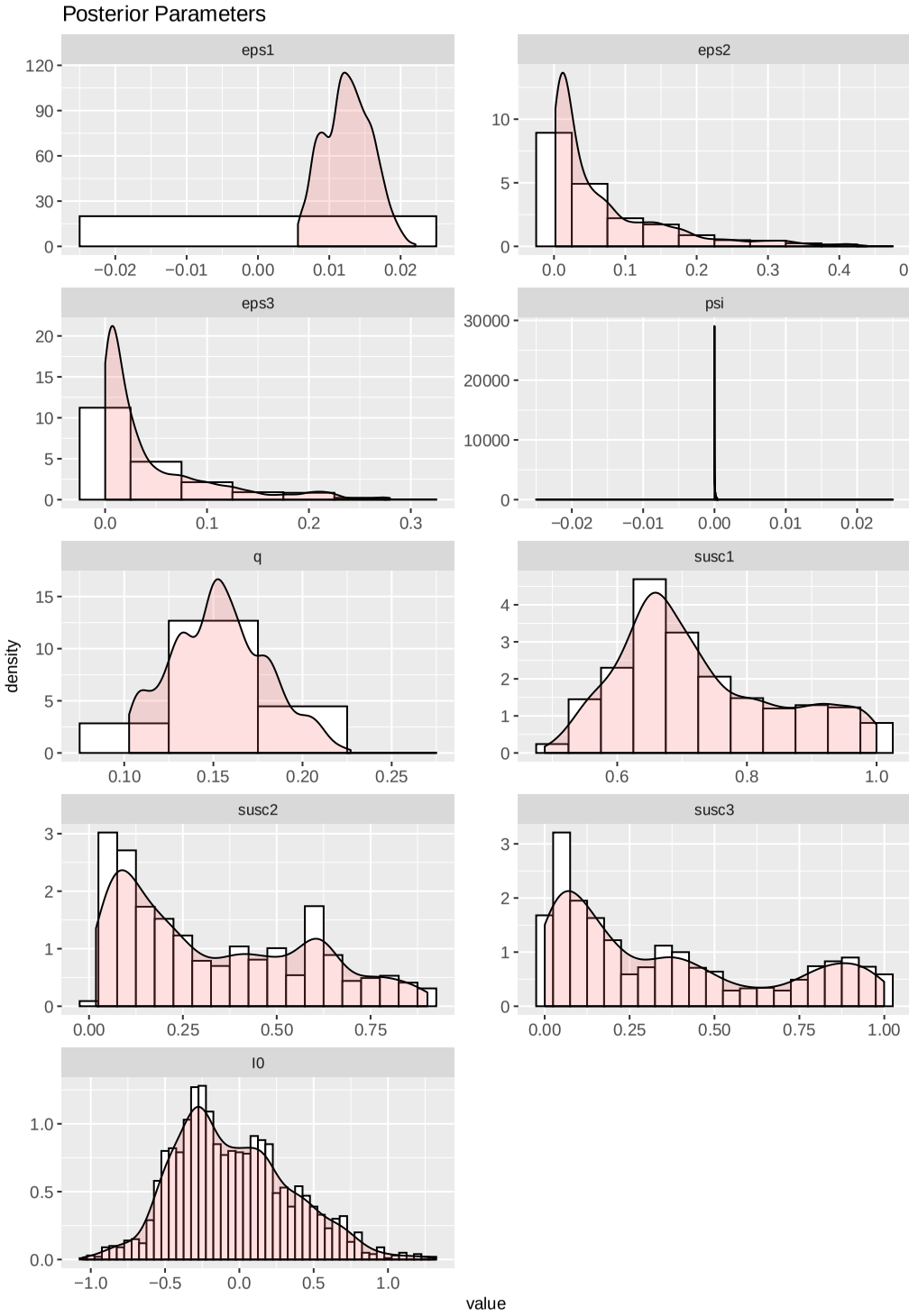
Posterior Parameters
eps1
eps2
eps3
psi
q
susc1
susc2
susc3
I0
density
value

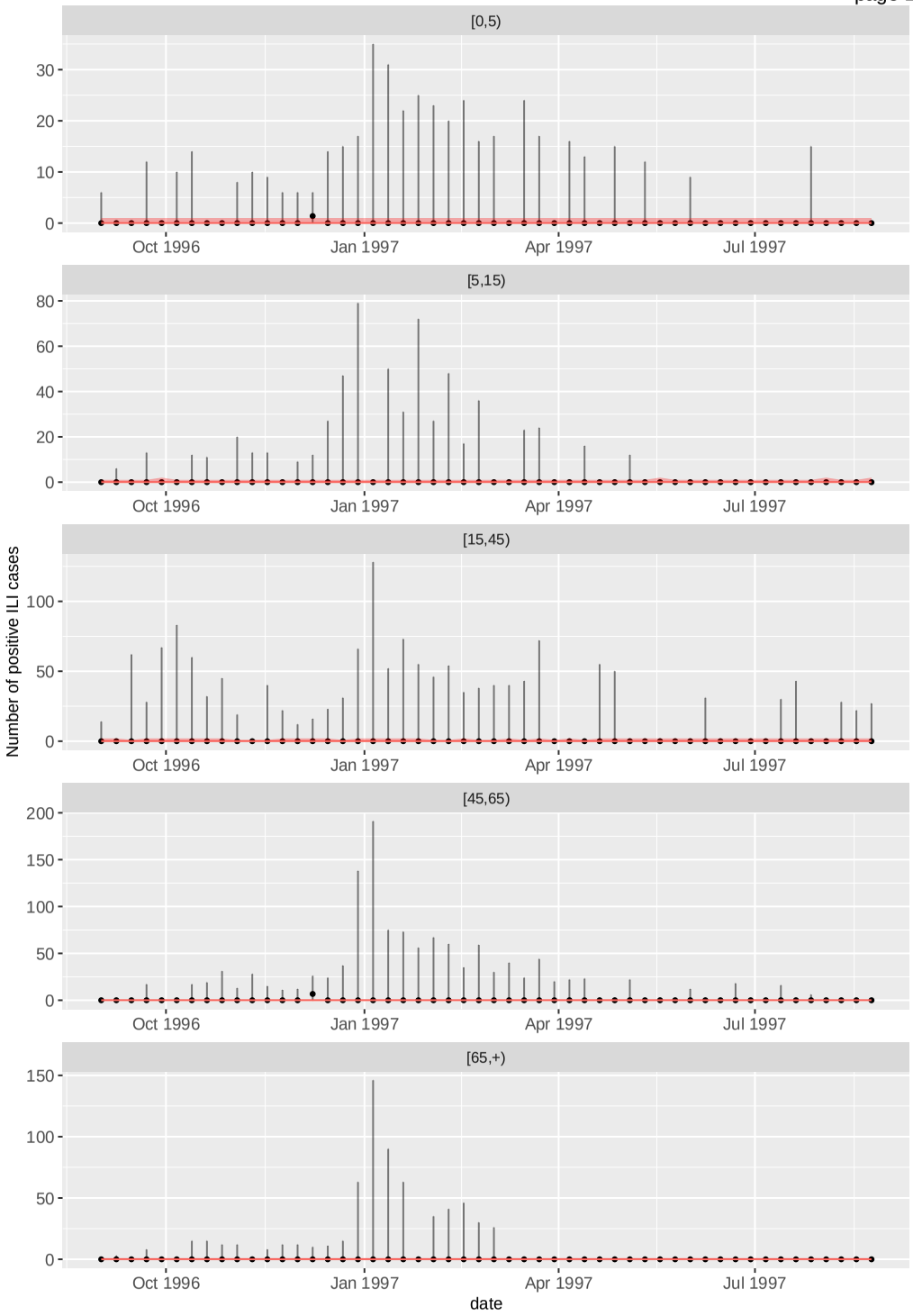
[0,5)
[5,15)
[15,45)
[45,65)
[65,+)
Number of positive ILI cases
Oct 1996
Jan 1997
Apr 1997
Jul 1997
date

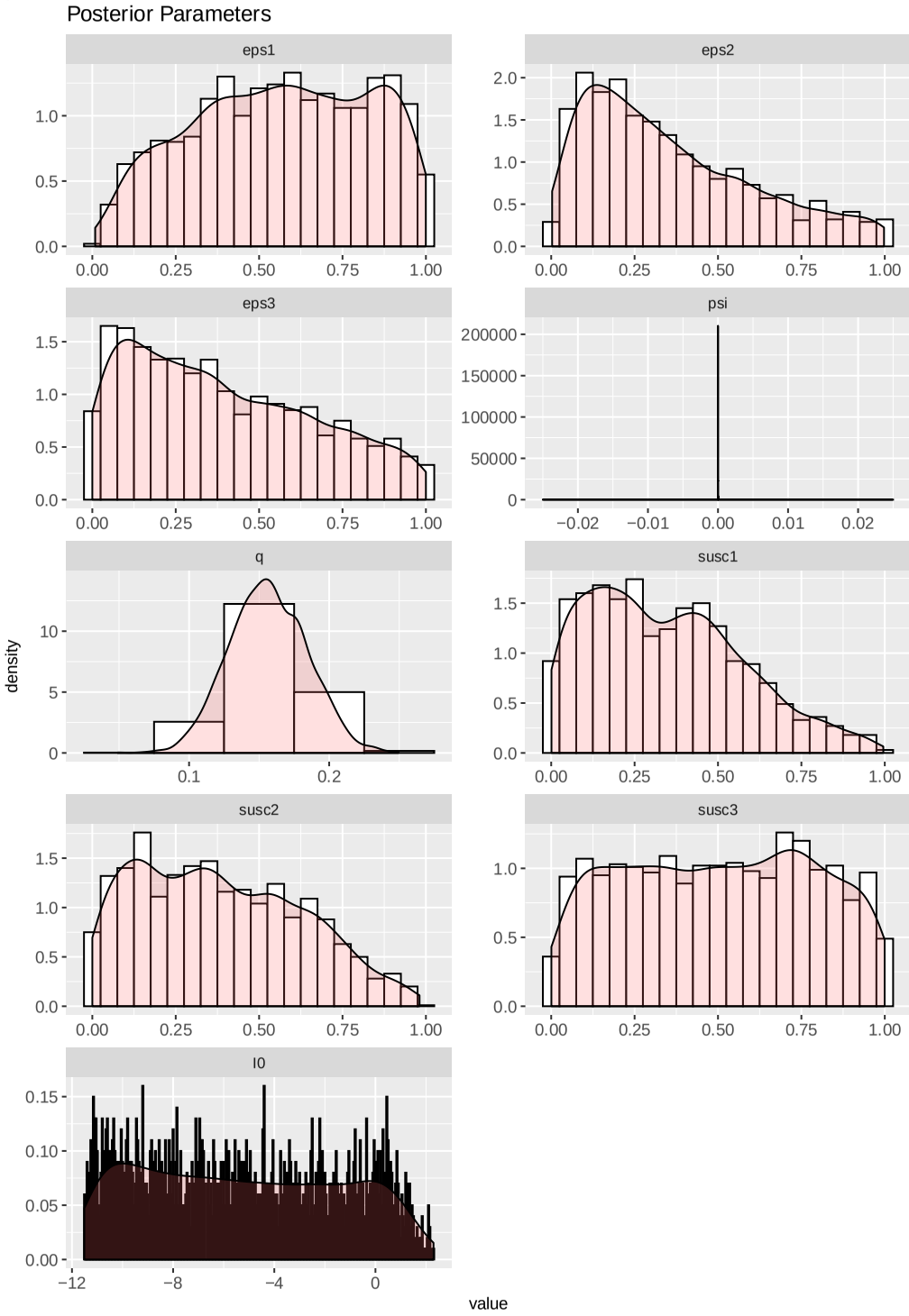
Posterior Parameters
eps1
eps2
eps3
psi
q
susc1
susc2
susc3
I0
density
value

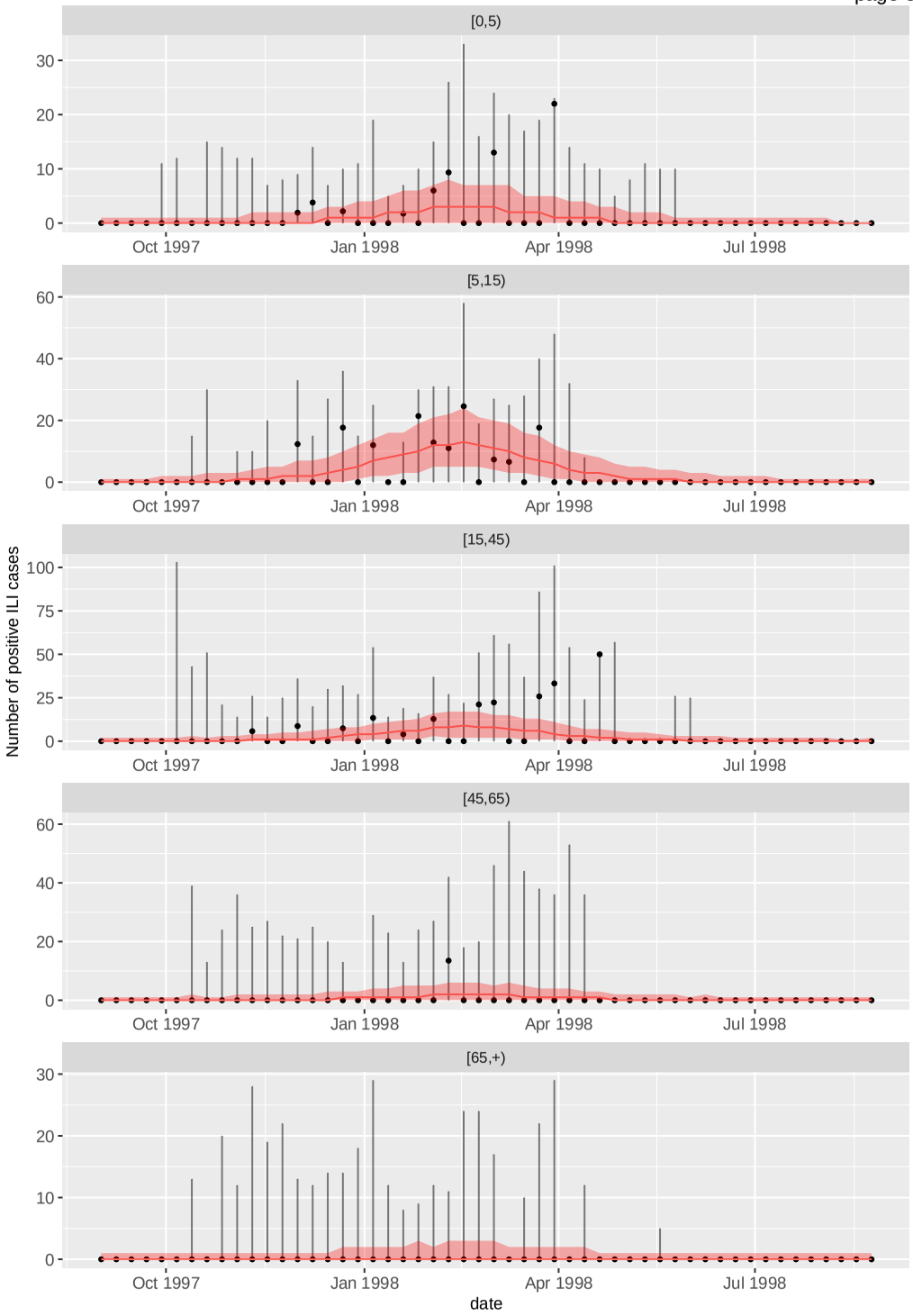
[0,5)
[5,15)
[15,45)
[45,65)
[65,+)
Number of positive ILI cases
Oct 1997
Jan 1998
Apr 1998
Jul 1998
date

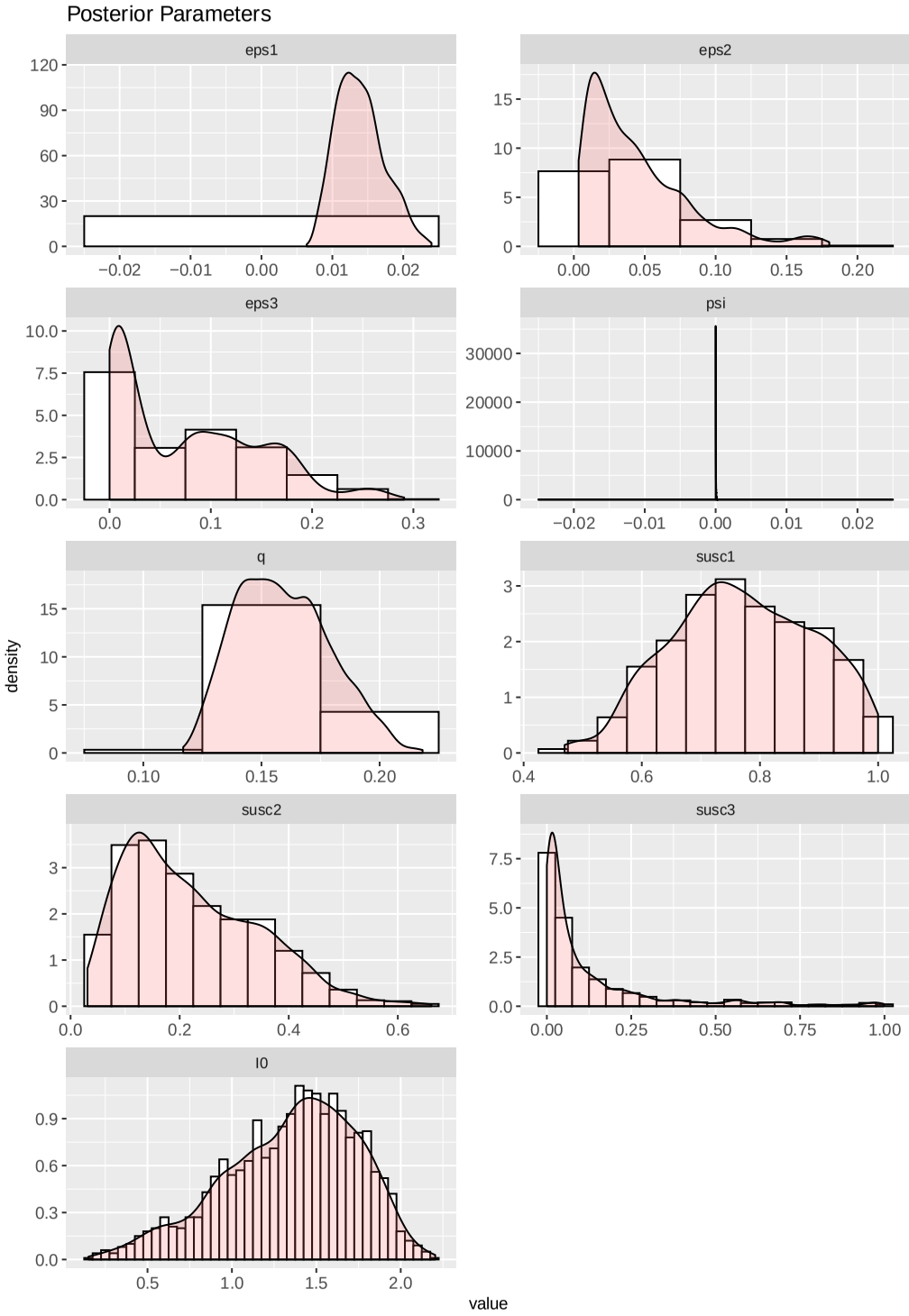
Posterior Parameters
eps1
eps2
eps3
psi
q
susc1
susc2
susc3
I0
density
value

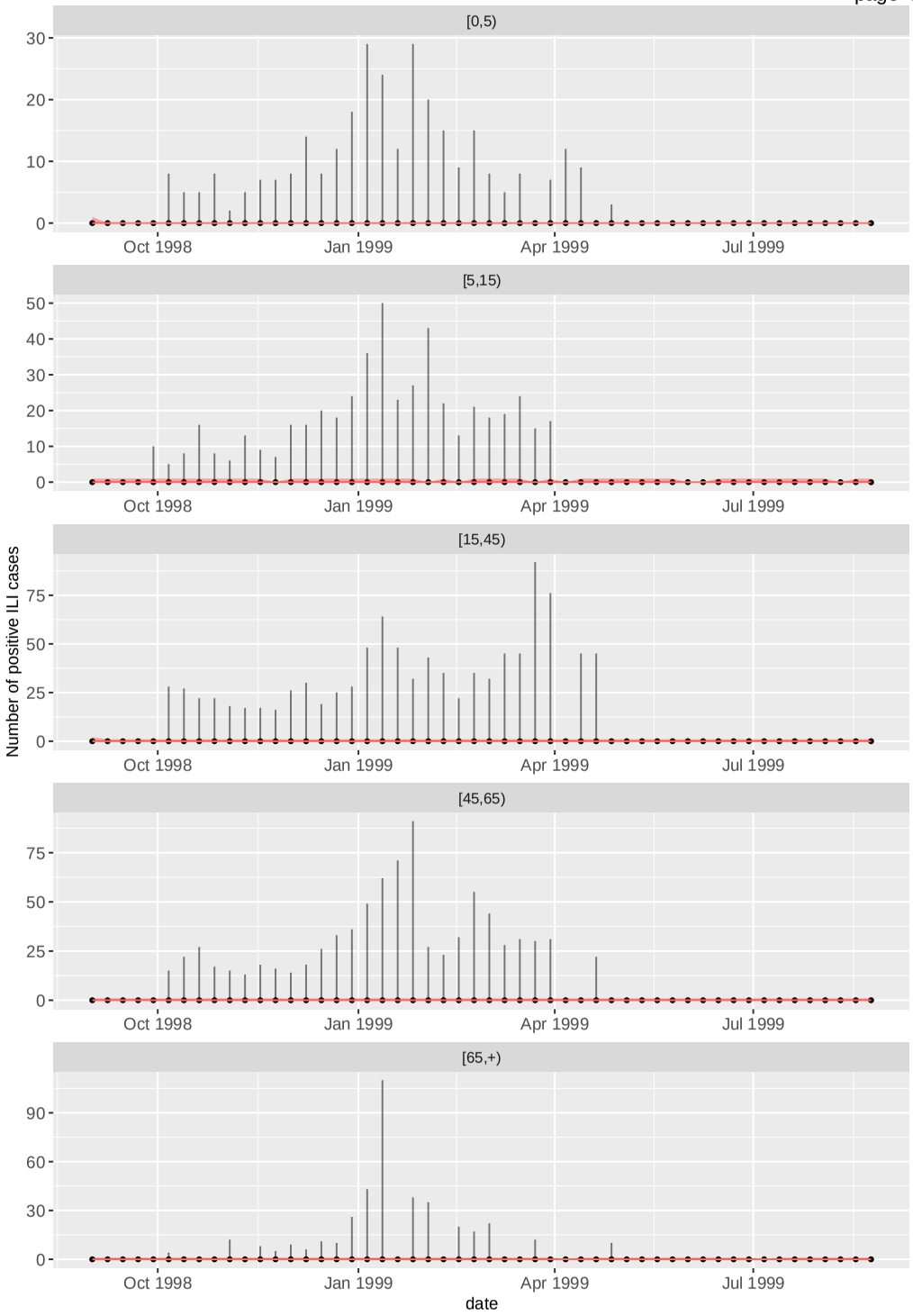
[0,5)
[5,15)
[15,45)
[45,65)
[65,+)
Oct 1998
Jan 1999
Apr 1999
Jul 1999
Number of positive ILI cases
date

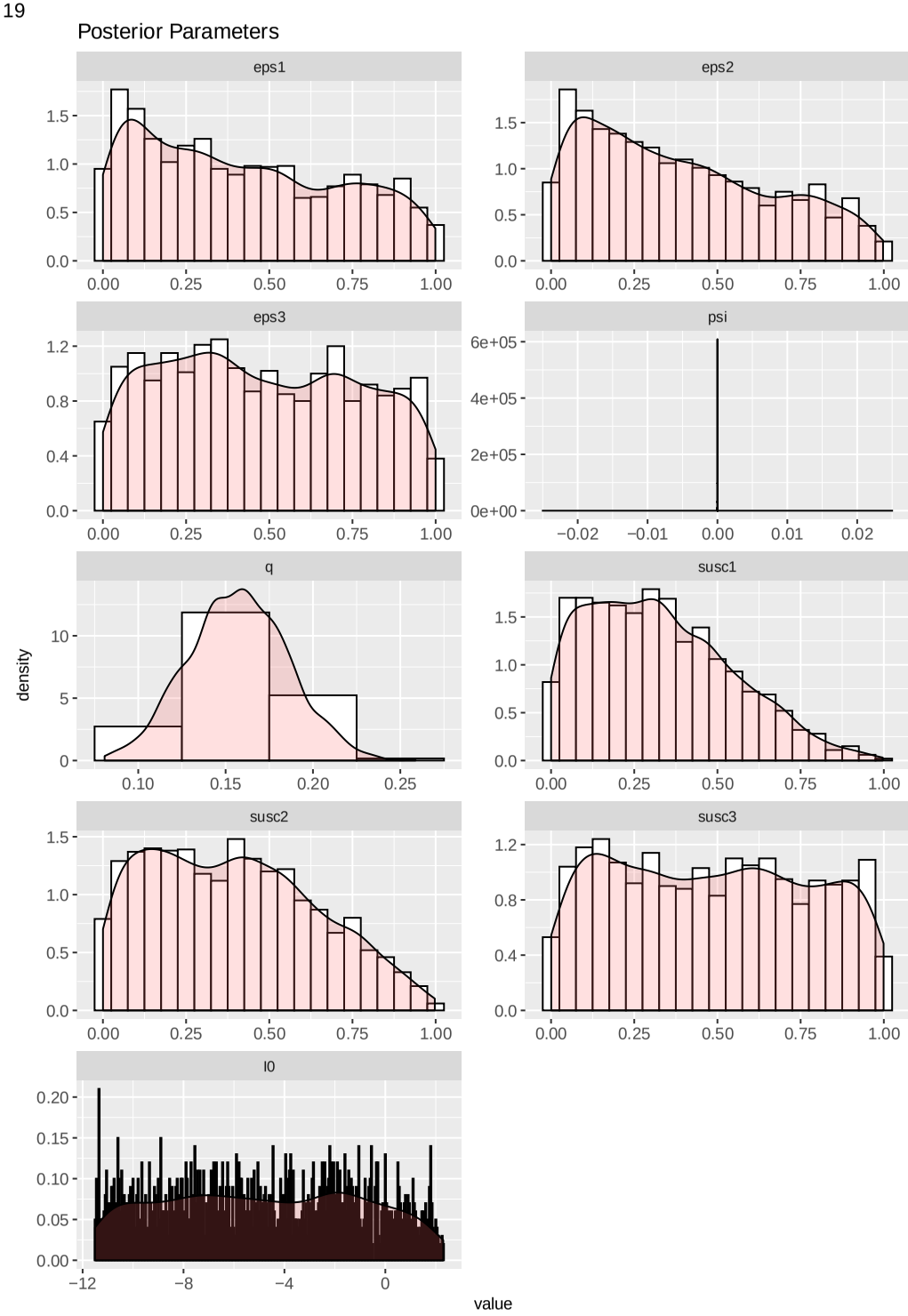
Posterior Parameters
eps1
eps2
eps3
psi
q
susc1
susc2
susc3
I0
density
value

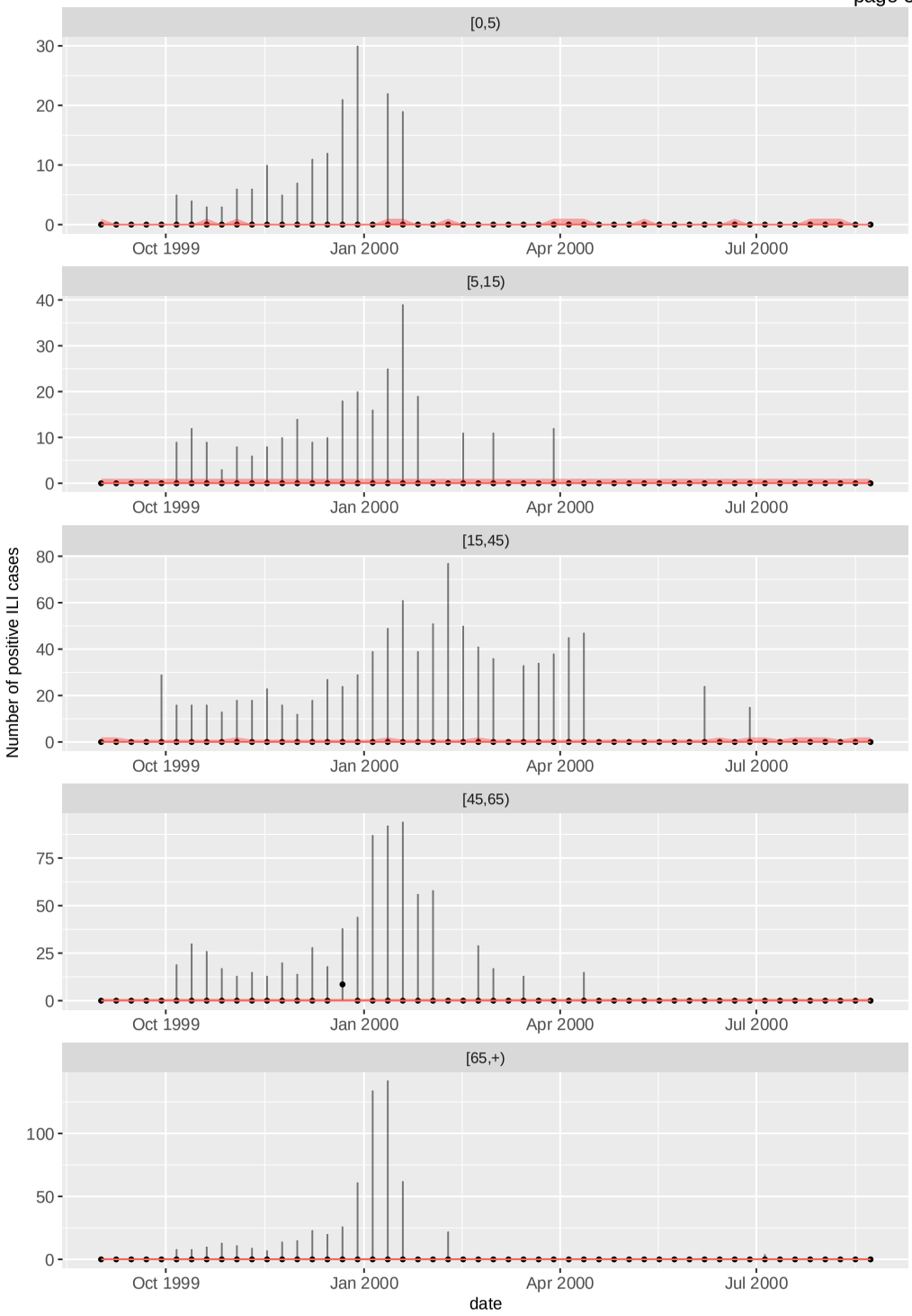
[0,5)
[5,15)
[15,45)
[45,65)
[65,+)
Number of positive ILI cases
Oct 1999
Jan 2000
Apr 2000
Jul 2000
date

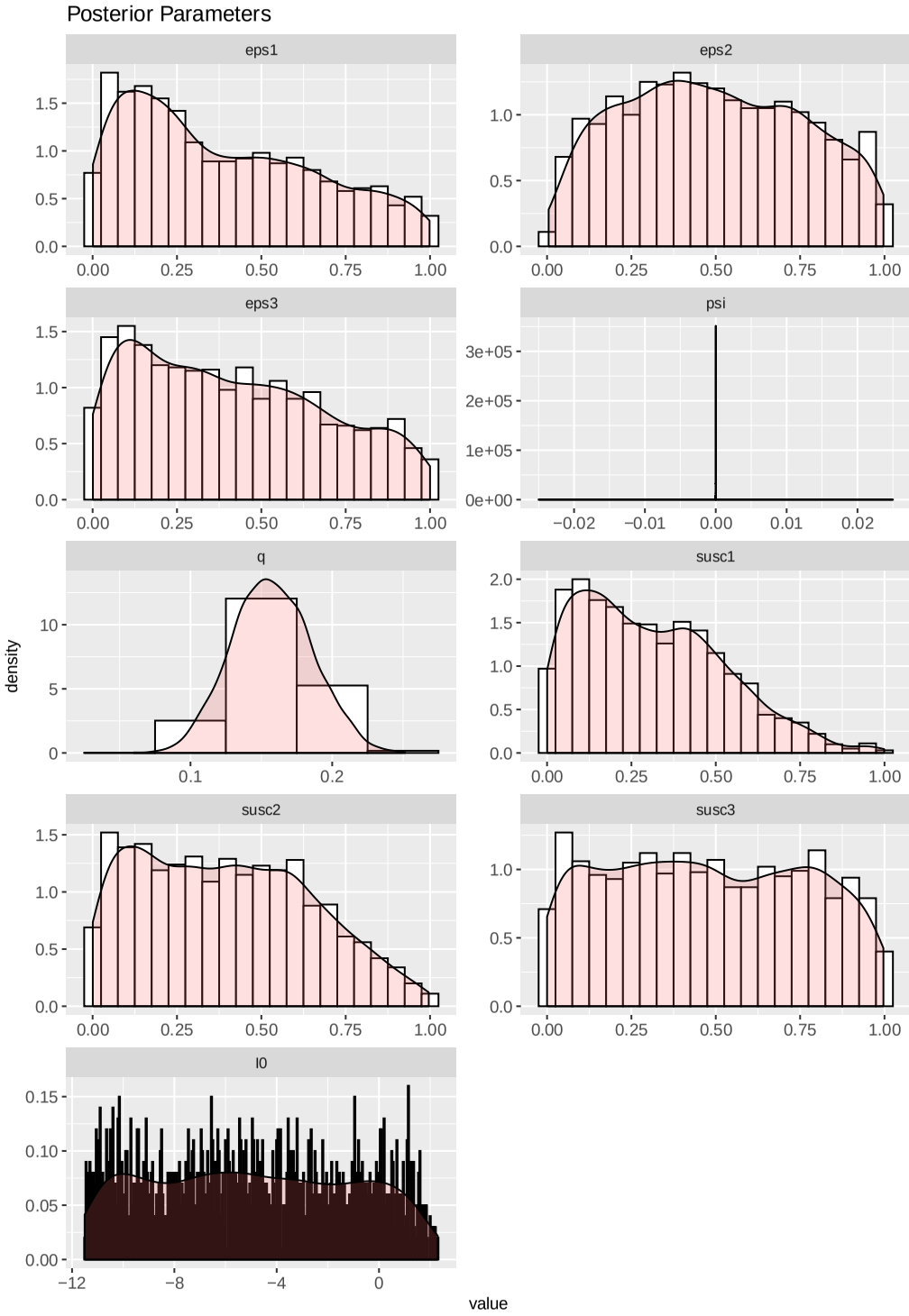
Posterior Parameters
eps1
eps2
eps3
psi
q
susc1
susc2
susc3
I0
density
value

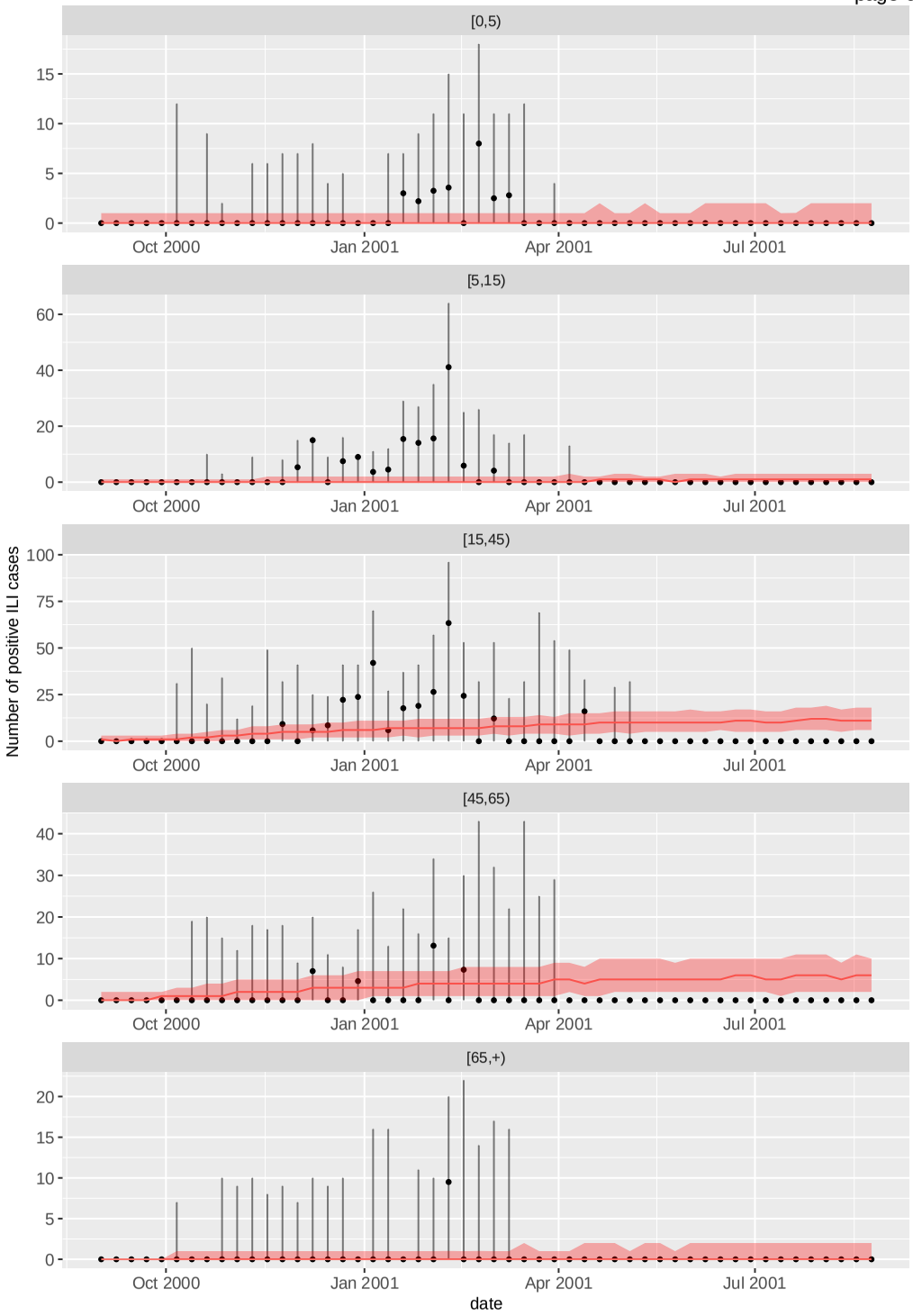
[0,5)
[5,15)
[15,45)
[45,65)
[65,+)
Number of positive ILI cases
Oct 2000
Jan 2001
Apr 2001
Jul 2001
date

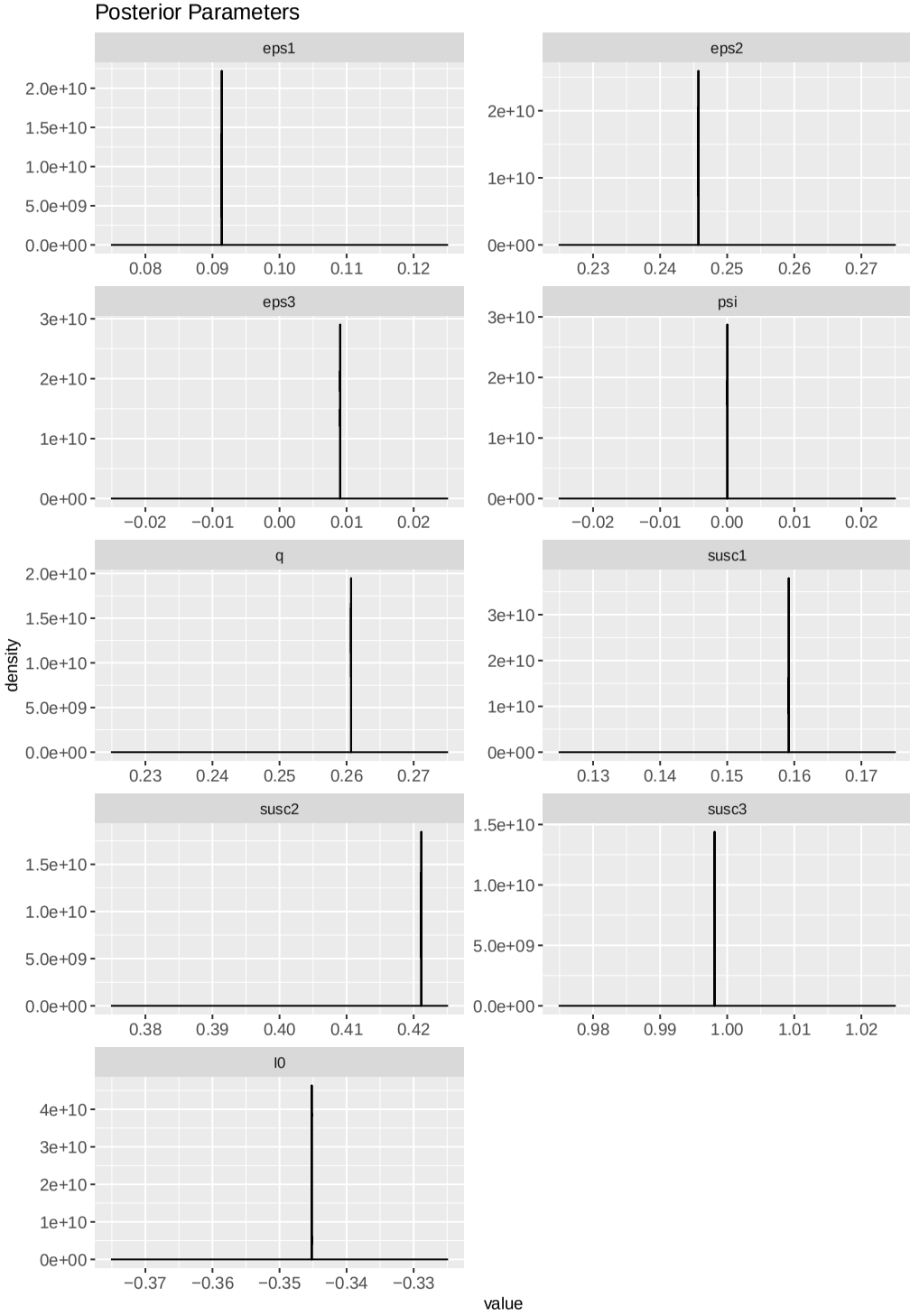
Posterior Parameters
eps1
eps2
eps3
psi
q
susc1
susc2
susc3
I0
density
value

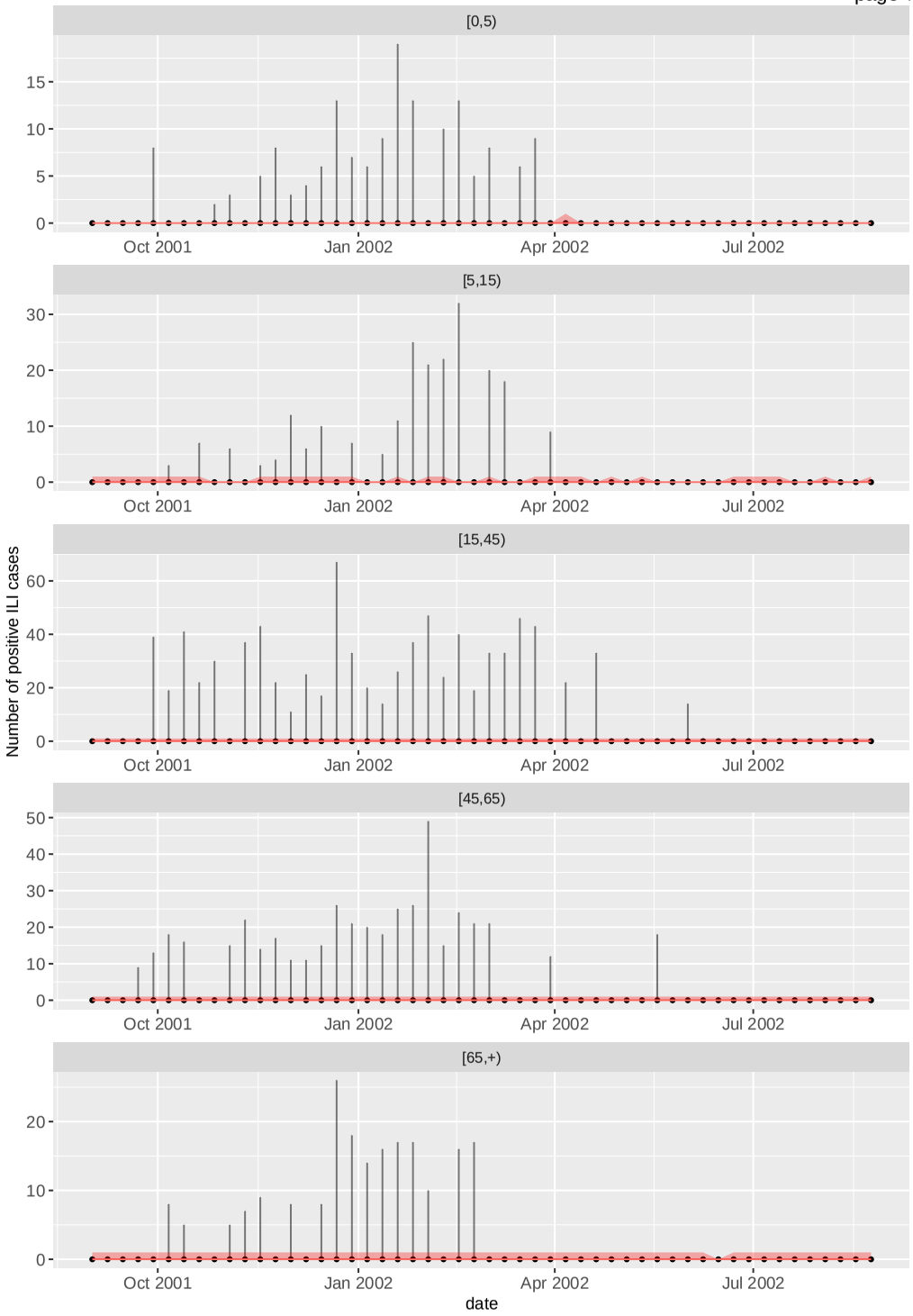
[0,5)
[5,15)
[15,45)
[45,65)
[65,+)
Oct 2001
Jan 2002
Apr 2002
Jul 2002
Number of positive ILI cases
date

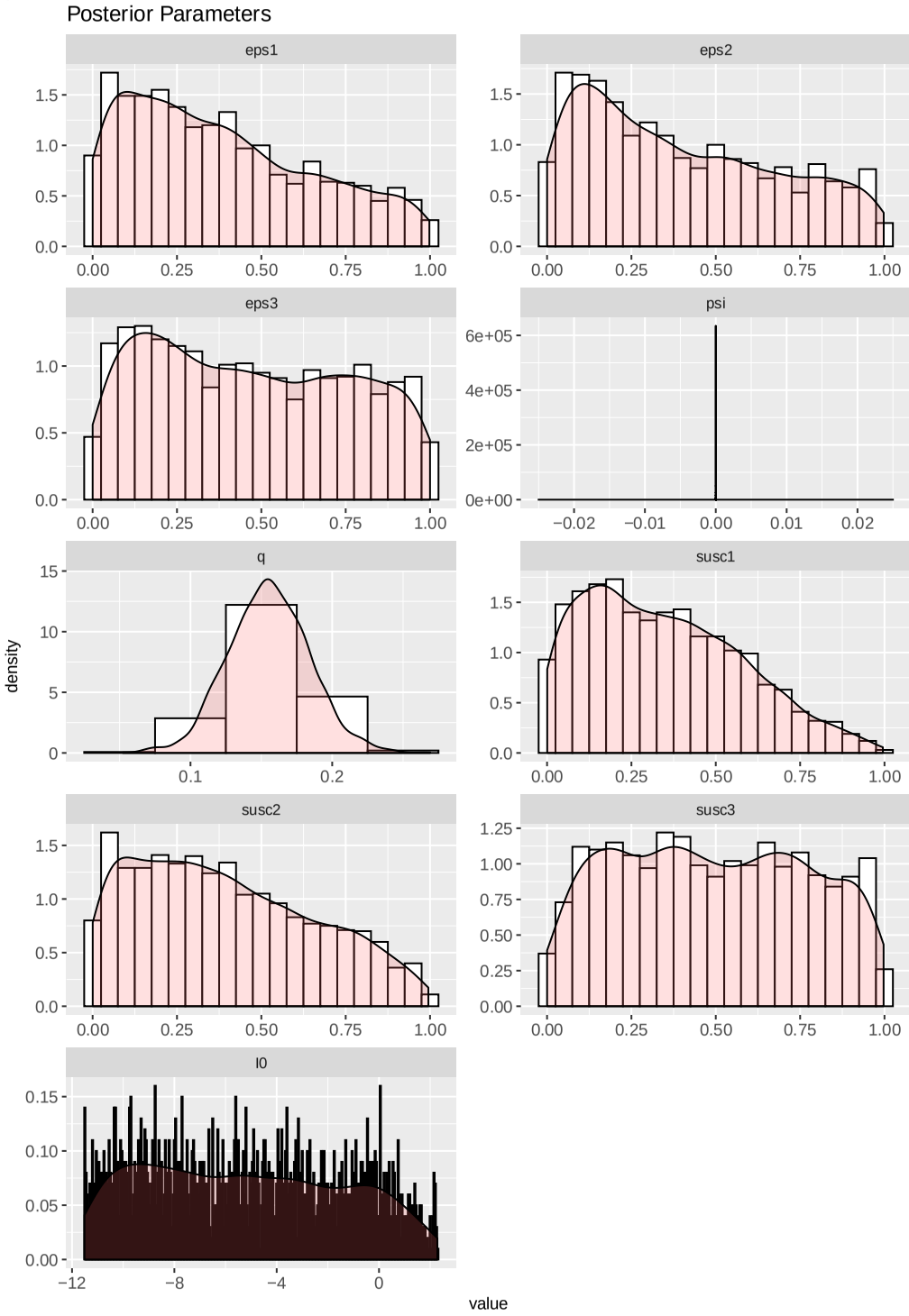
Posterior Parameters
eps1
eps2
eps3
psi
q
susc1
susc2
susc3
I0
density
value

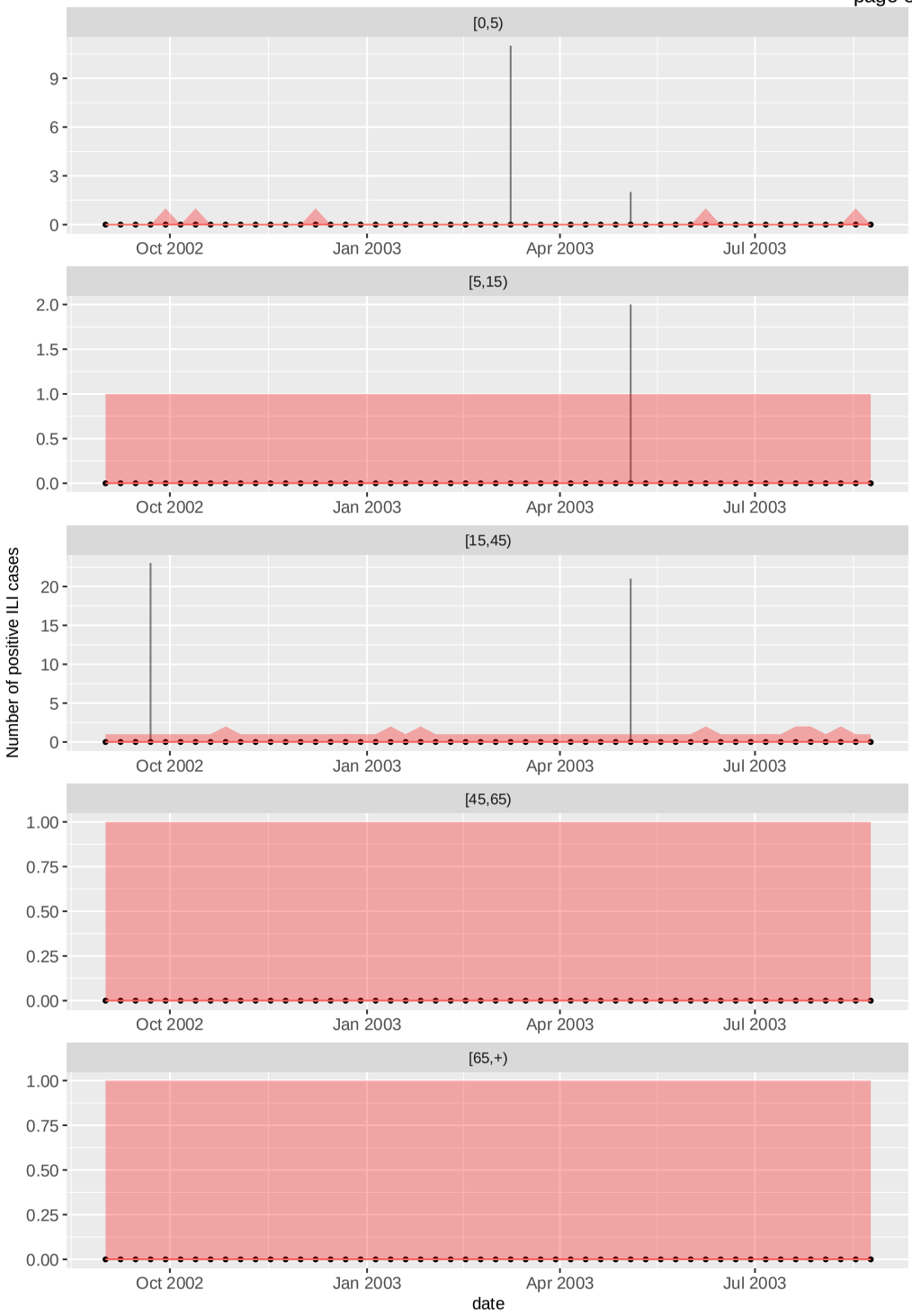
[0,5)
[5,15)
[15,45)
[45,65)
[65,+)
Oct 2002
Jan 2003
Apr 2003
Jul 2003
Number of positive ILI cases
date

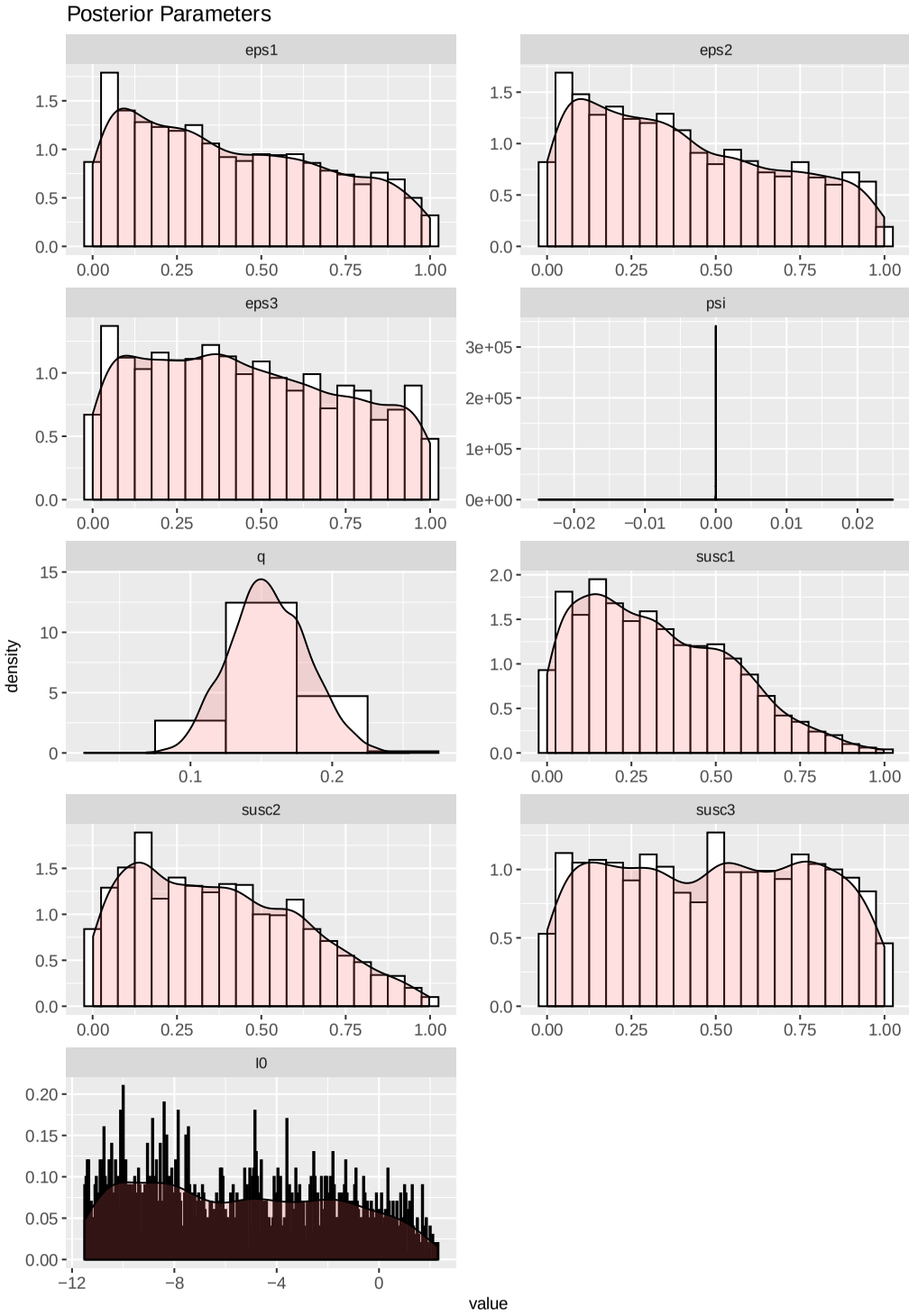
Posterior Parameters
eps1
eps2
eps3
psi
q
susc1
susc2
susc3
I0
density
value

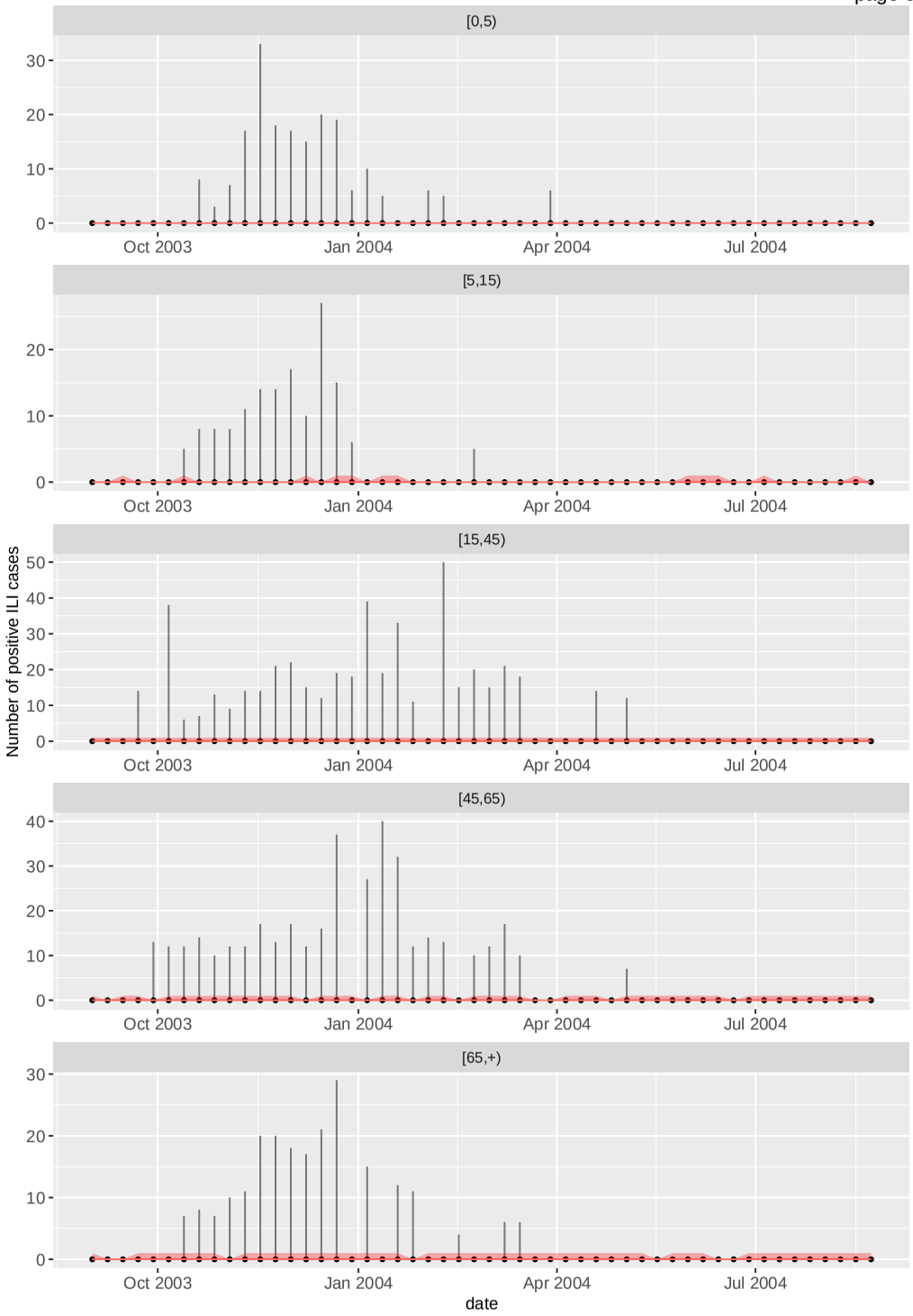
[0,5)
[5,15)
[15,45)
[45,65)
[65,+)
Oct 2003
Jan 2004
Apr 2004
Jul 2004
Number of positive ILI cases
date

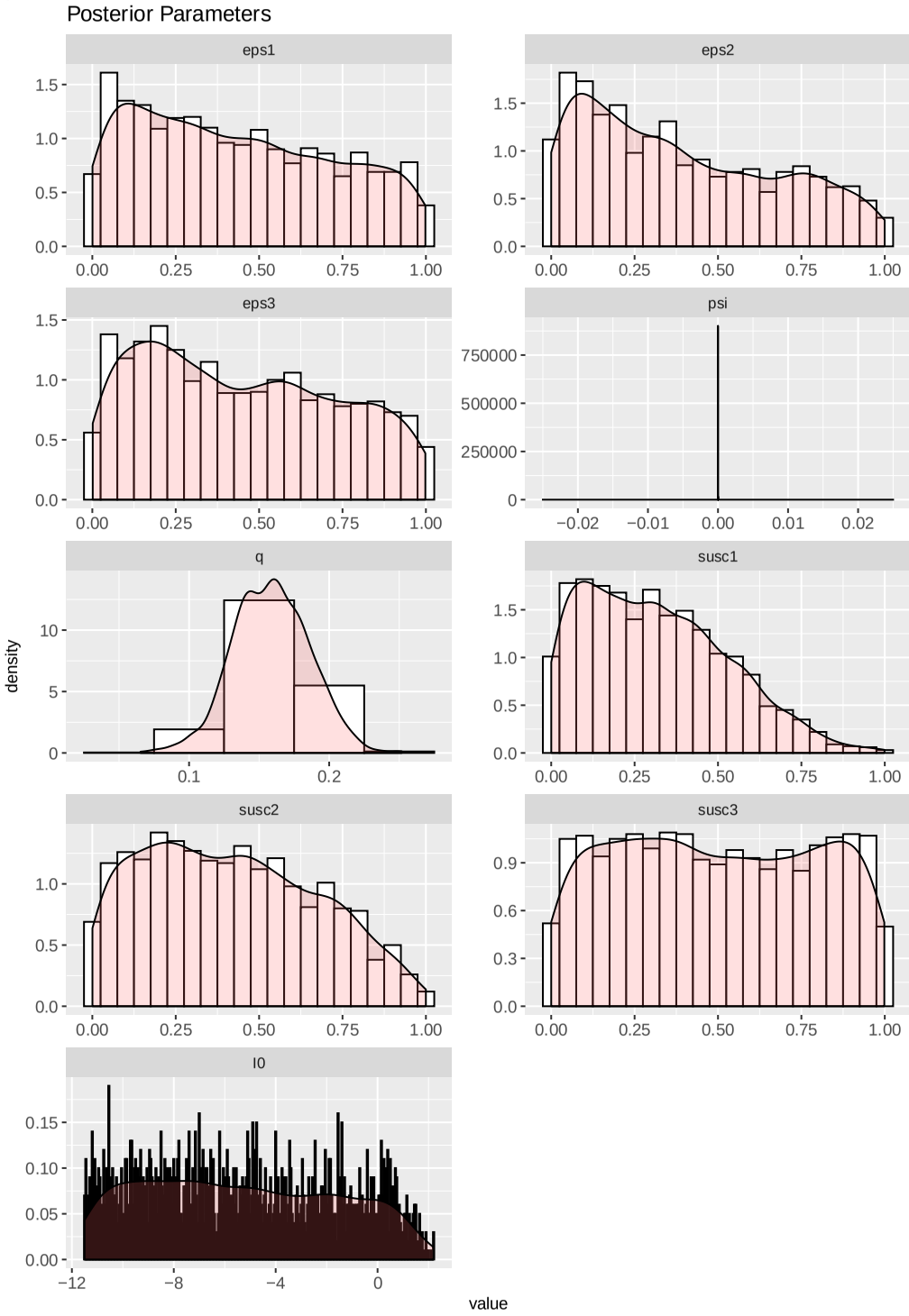
Posterior Parameters
eps1
eps2
eps3
psi
q
susc1
susc2
susc3
I0
density
value

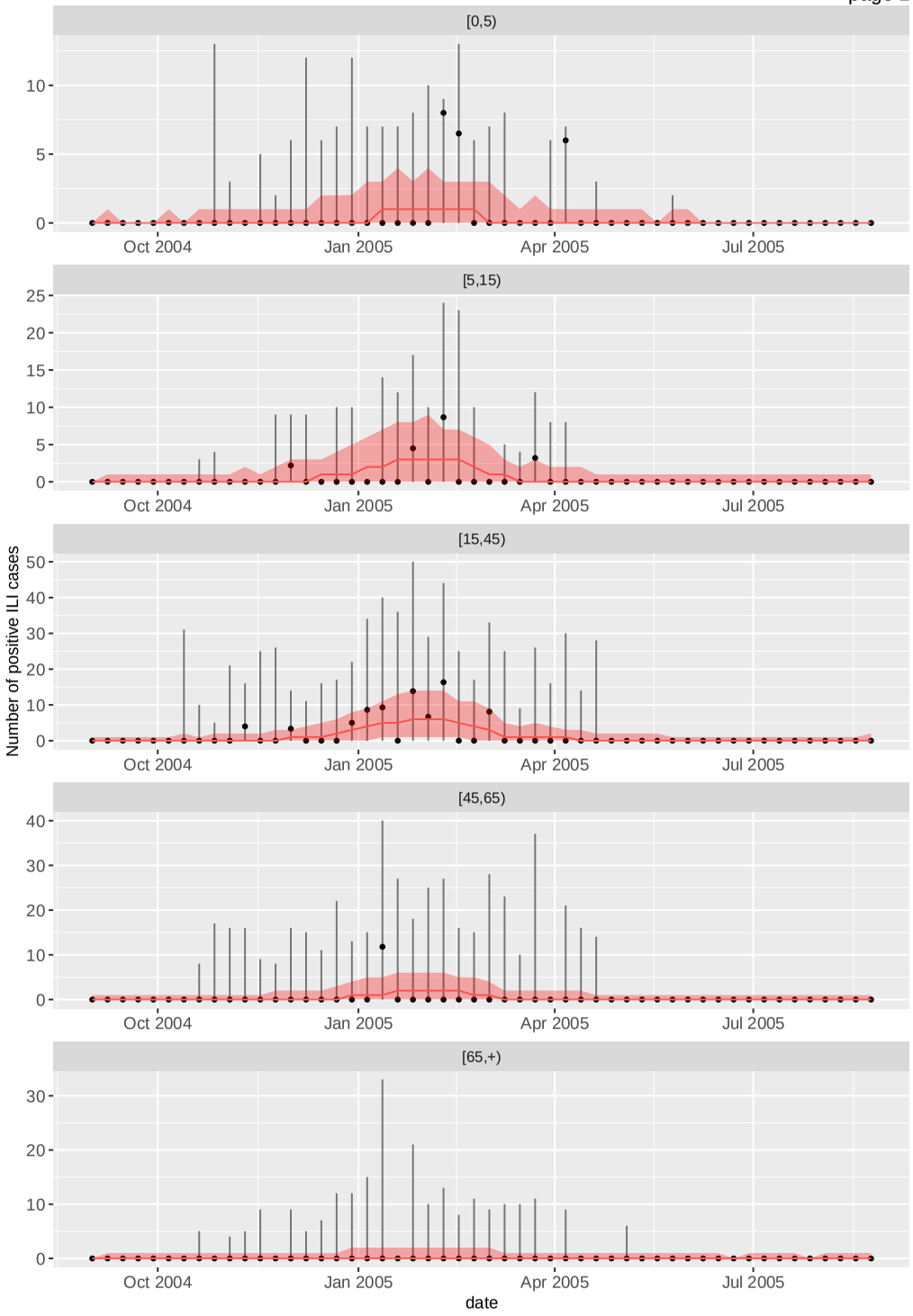
[0,5)
[5,15)
[15,45)
[45,65)
[65,+)
Number of positive ILI cases
Oct 2004
Jan 2005
Apr 2005
Jul 2005
date

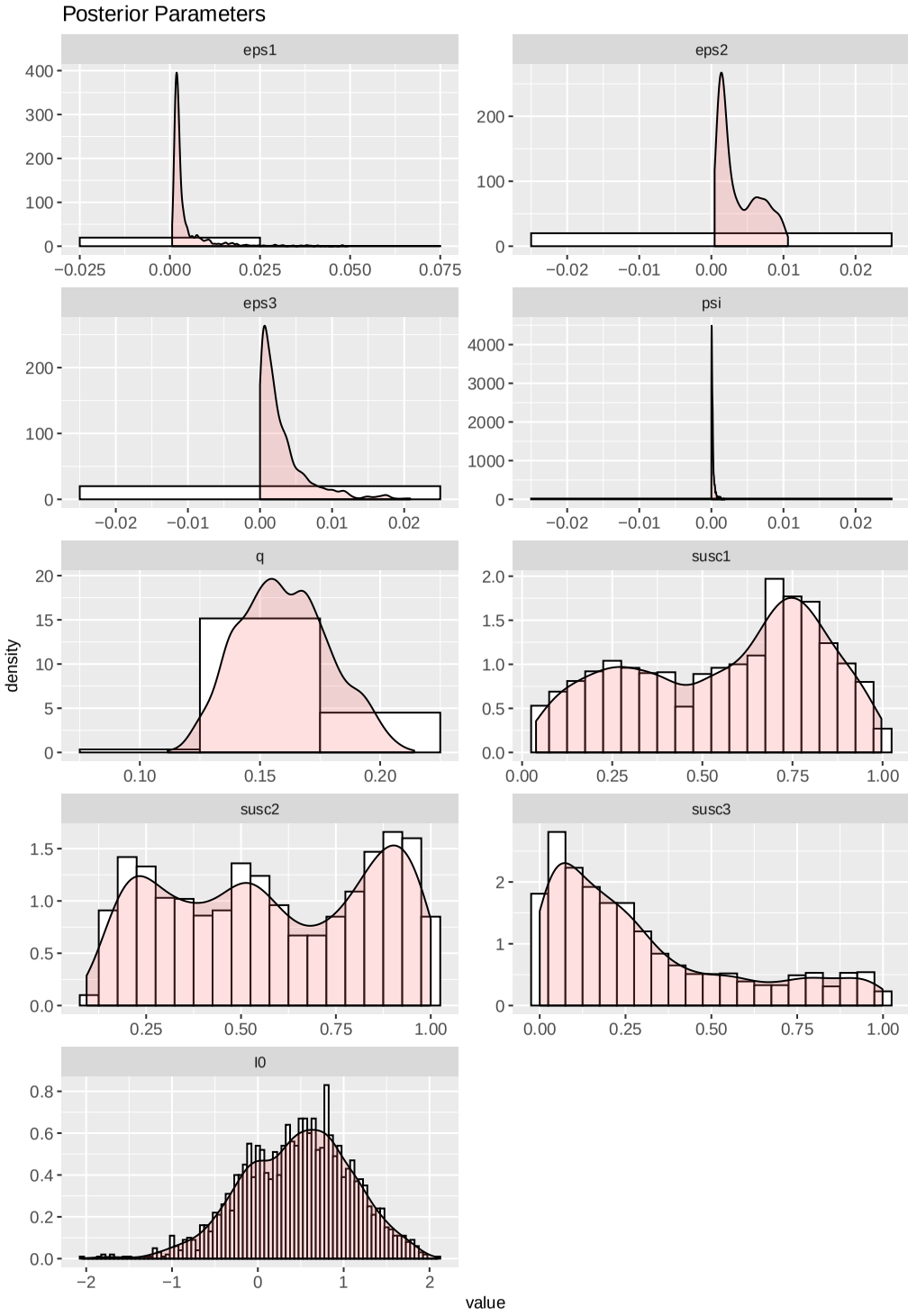
Posterior Parameters
eps1
eps2
eps3
psi
q
susc1
susc2
susc3
I0
density
value

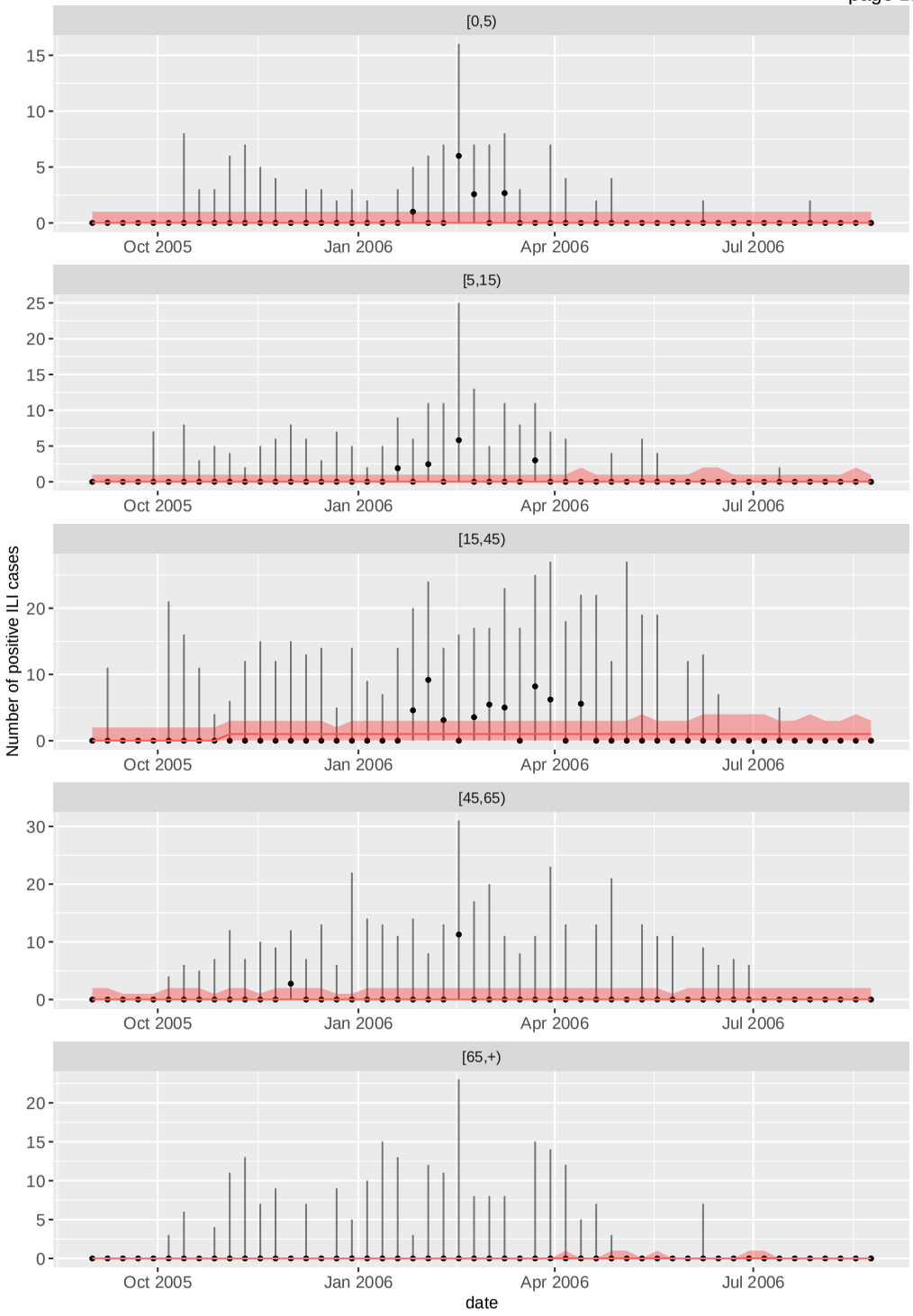
[0,5)
[5,15)
[15,45)
[45,65)
[65,+)
Number of positive ILI cases
Oct 2005
Jan 2006
Apr 2006
Jul 2006
date

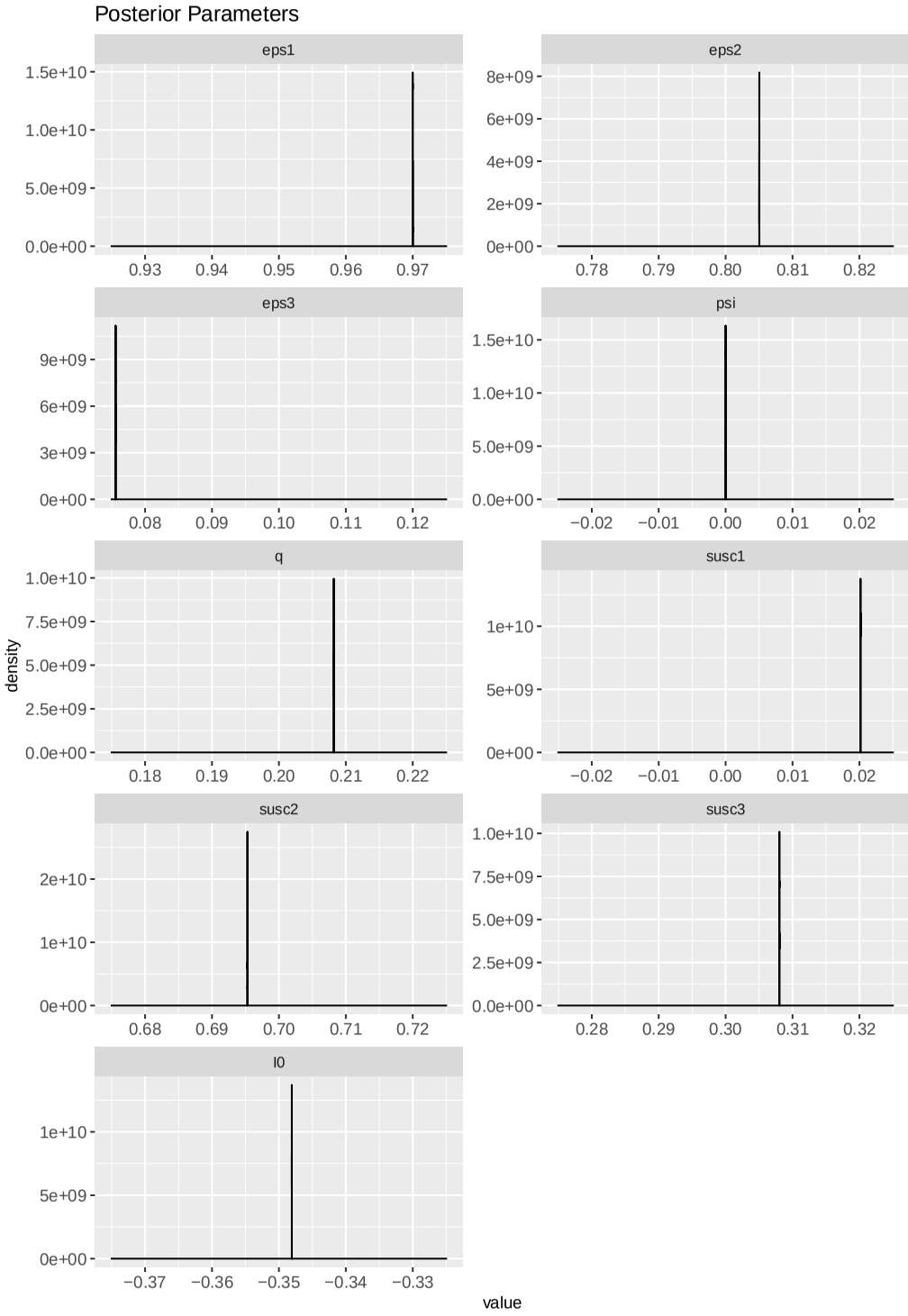
Posterior Parameters
eps1
eps2
eps3
psi
q
susc1
susc2
susc3
I0
density
value

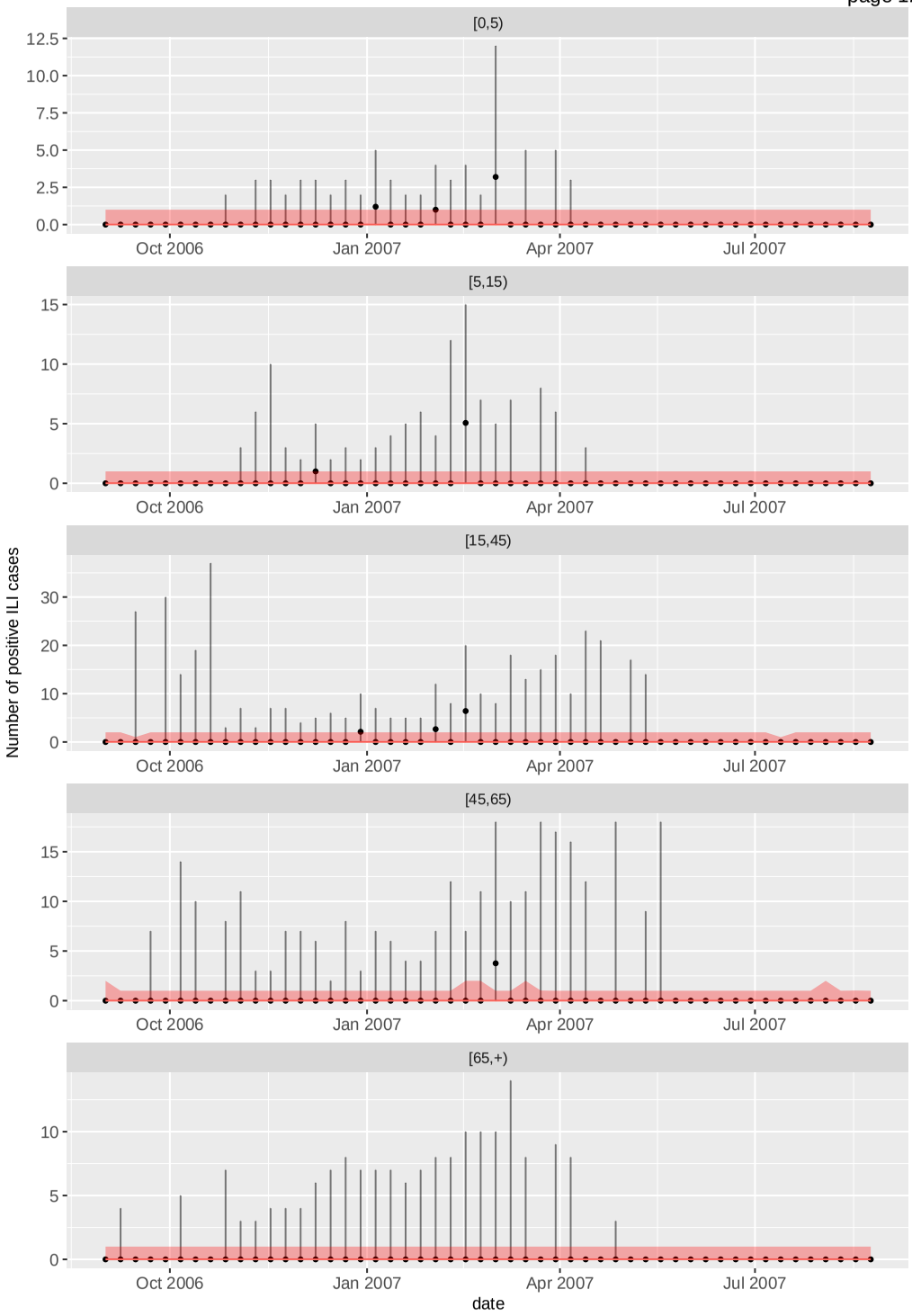
[0,5)
[5,15)
[15,45)
[45,65)
[65,+)
Oct 2006
Jan 2007
Apr 2007
Jul 2007
Number of positive ILI cases
date

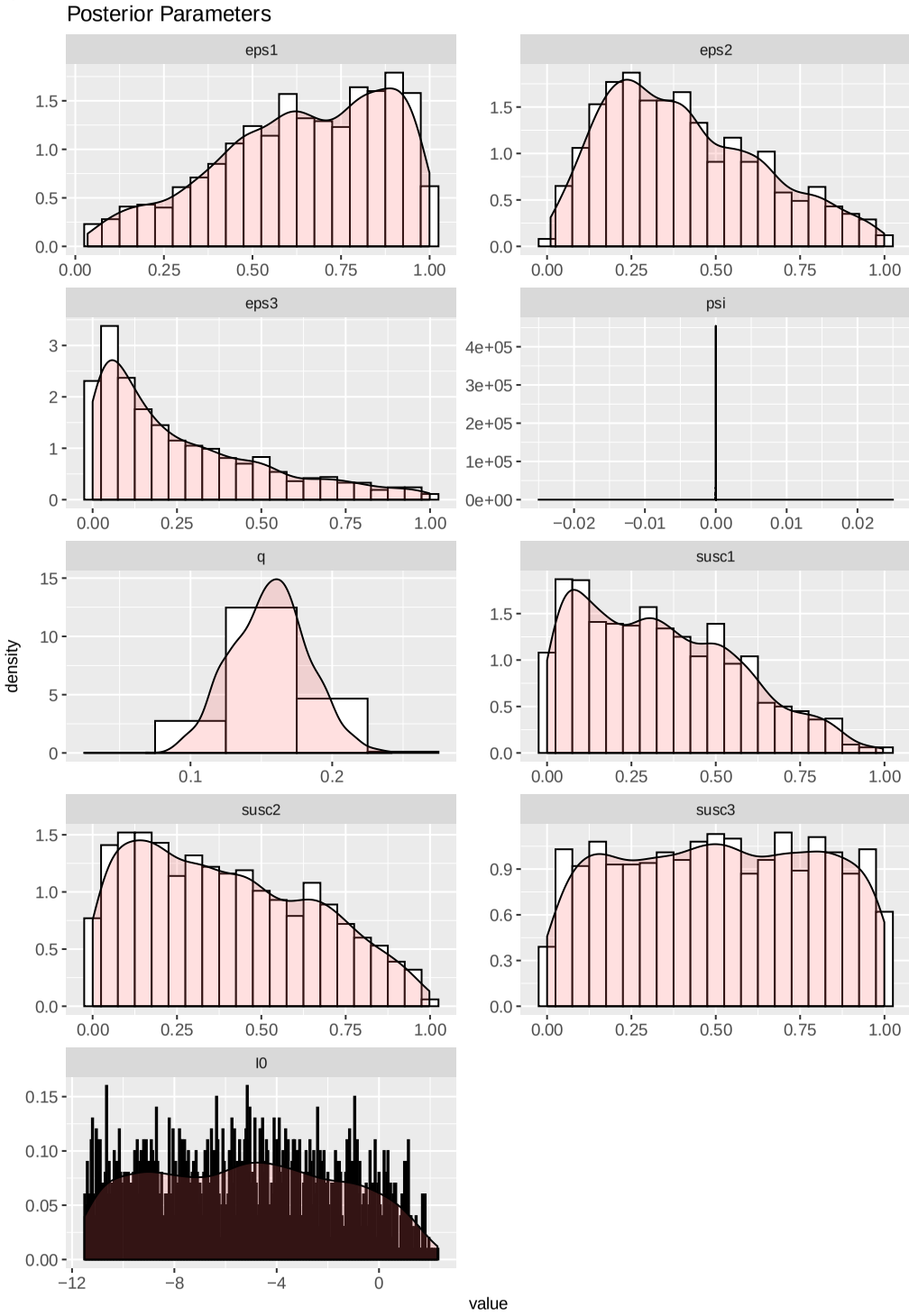
Posterior Parameters
eps1
eps2
eps3
psi
q
susc1
susc2
susc3
I0
density
value

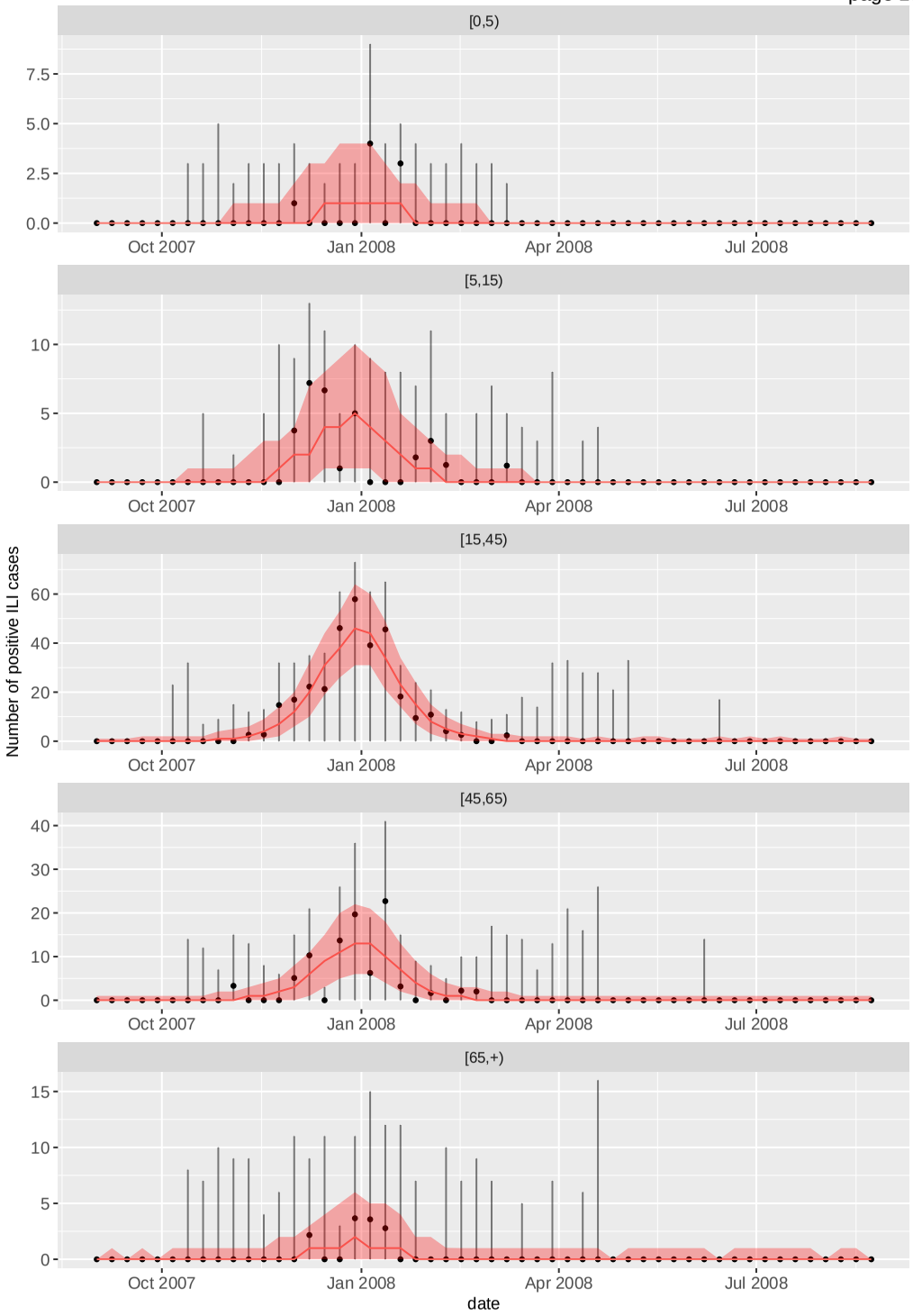
[0,5)
[5,15)
[15,45)
[45,65)
[65,+)
Oct 2007
Jan 2008
Apr 2008
Jul 2008
Number of positive ILI cases
date

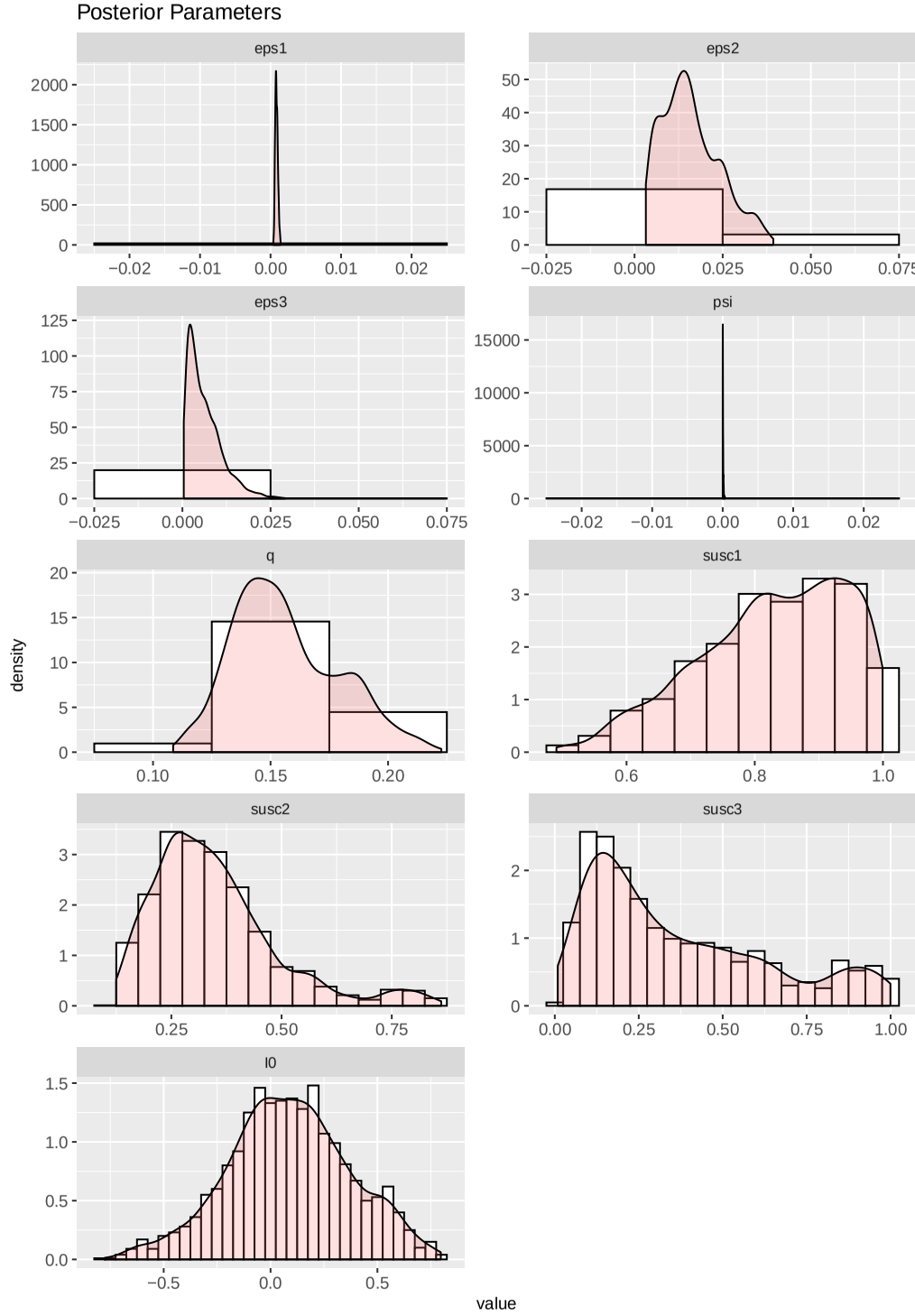
Posterior Parameters
eps1
eps2
eps3
psi
q
susc1
susc2
susc3
I0
density
value

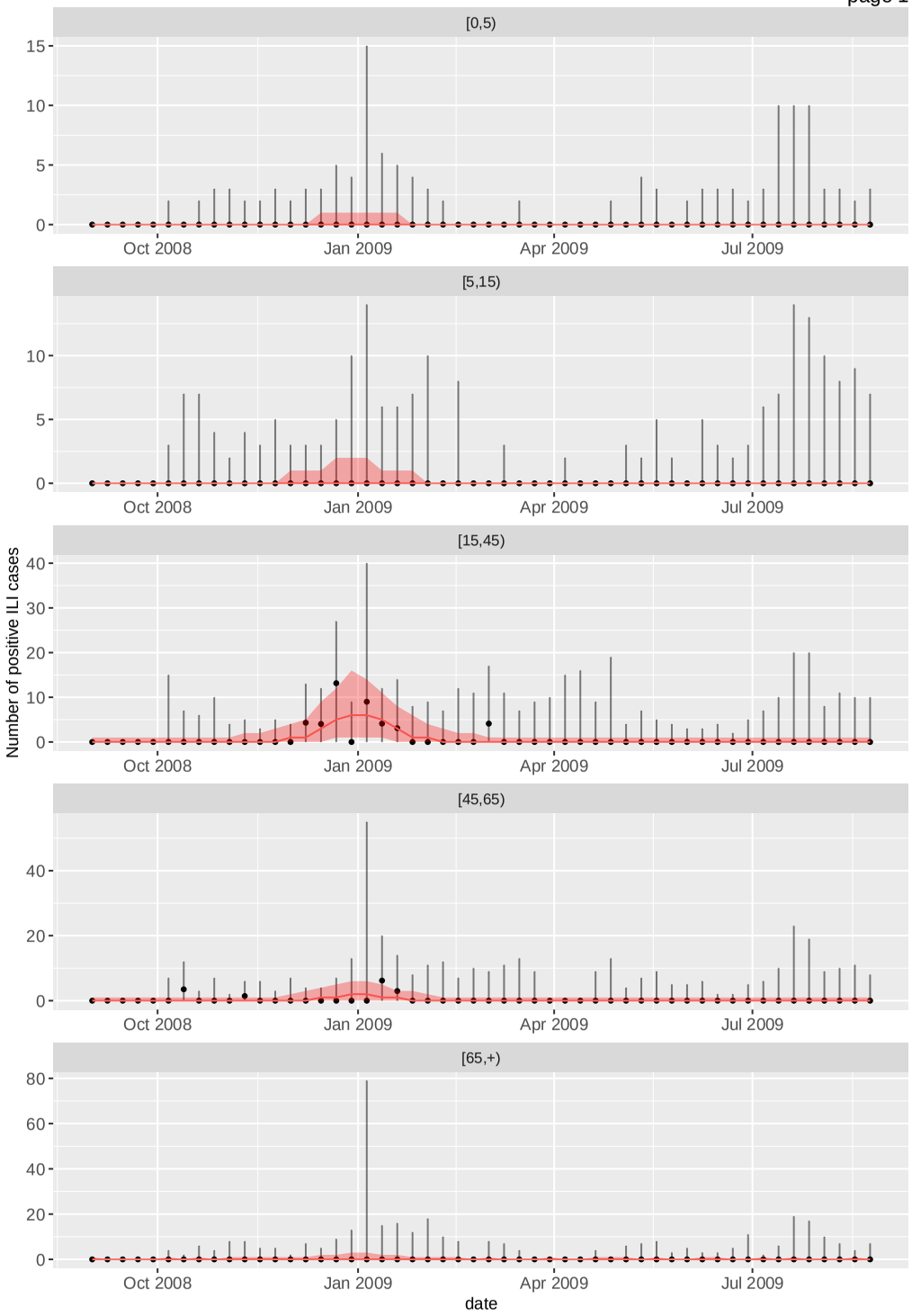
[0,5)
[5,15)
[15,45)
[45,65)
[65,+)
Number of positive ILI cases
Oct 2008
Jan 2009
Apr 2009
Jul 2009
date

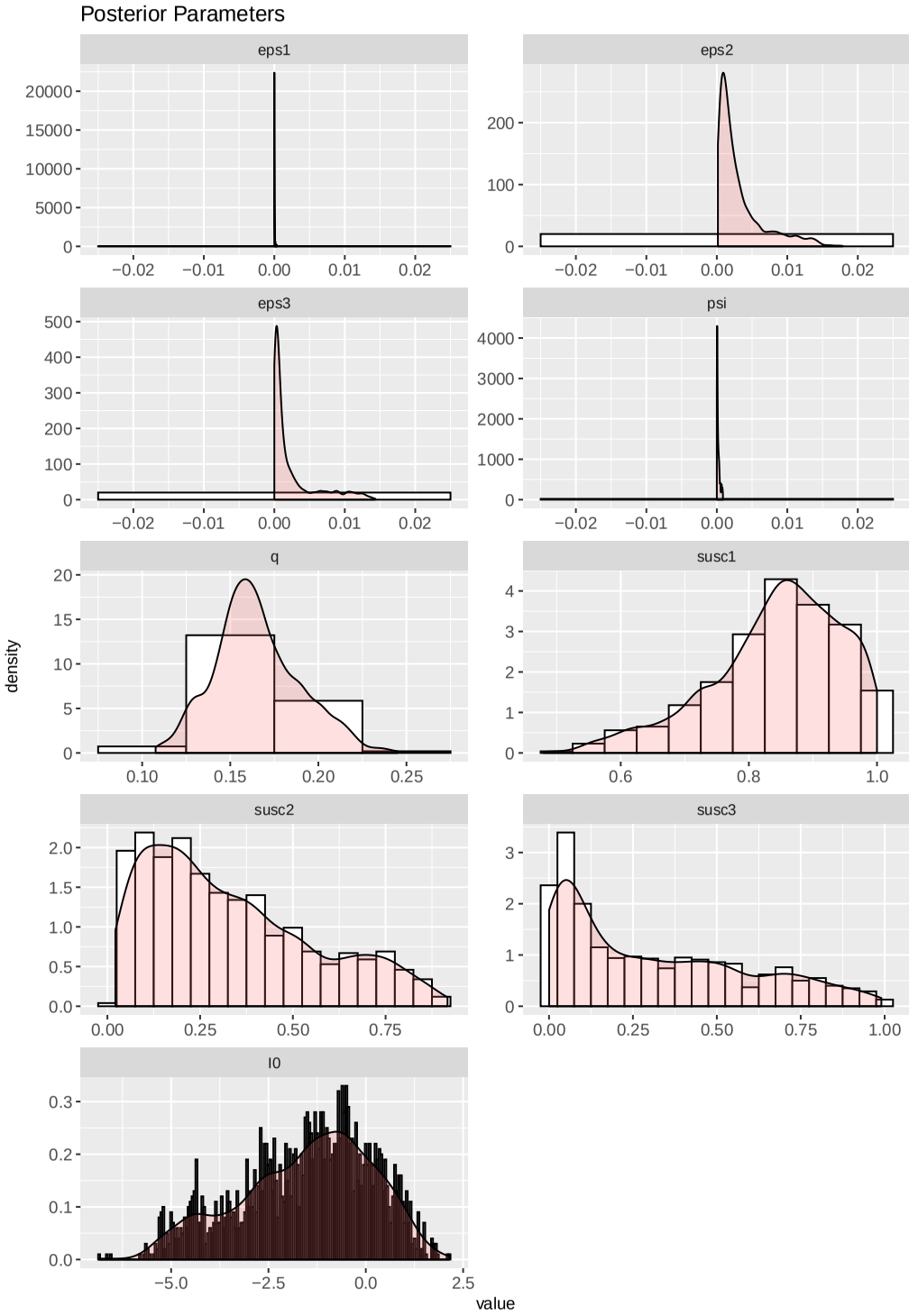
Posterior Parameters
eps1
eps2
eps3
psi
q
susc1
susc2
susc3
I0
density
value

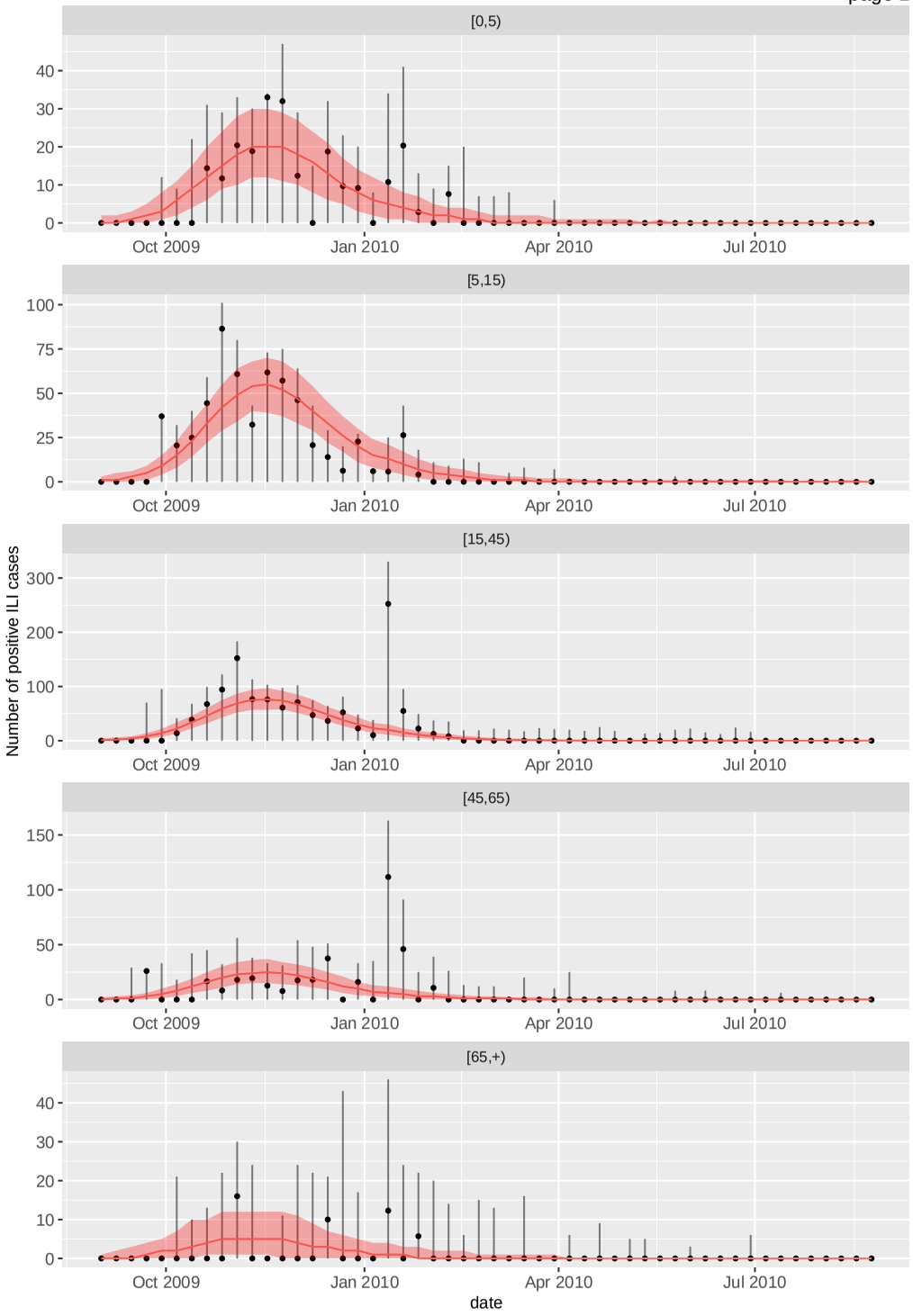
[0,5)
[5,15)
[15,45)
[45,65)
[65,+)
Number of positive ILI cases
Oct 2009
Jan 2010
Apr 2010
Jul 2010
date

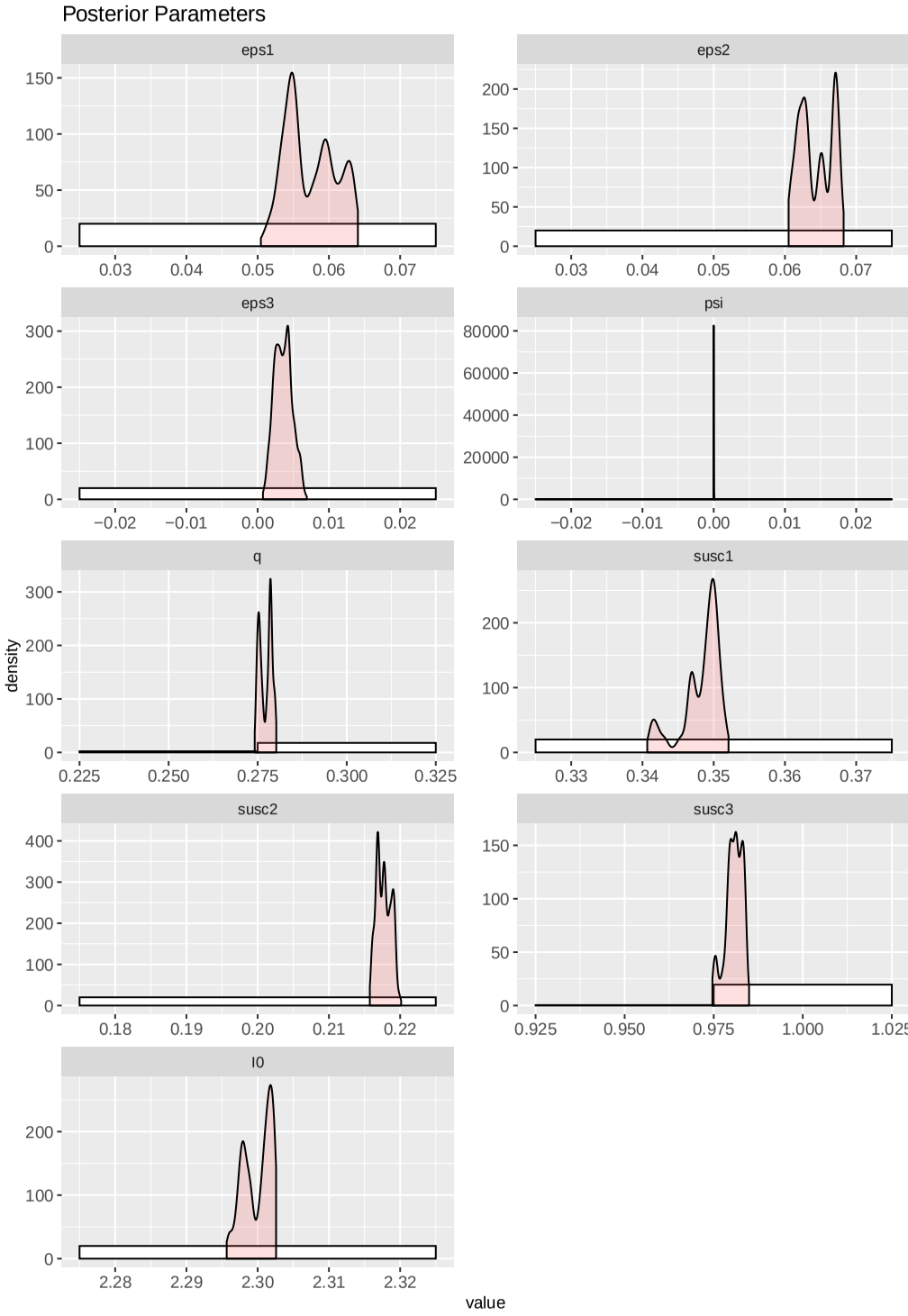
Posterior Parameters
eps1
eps2
eps3
psi
q
susc1
susc2
susc3
I0
density
value

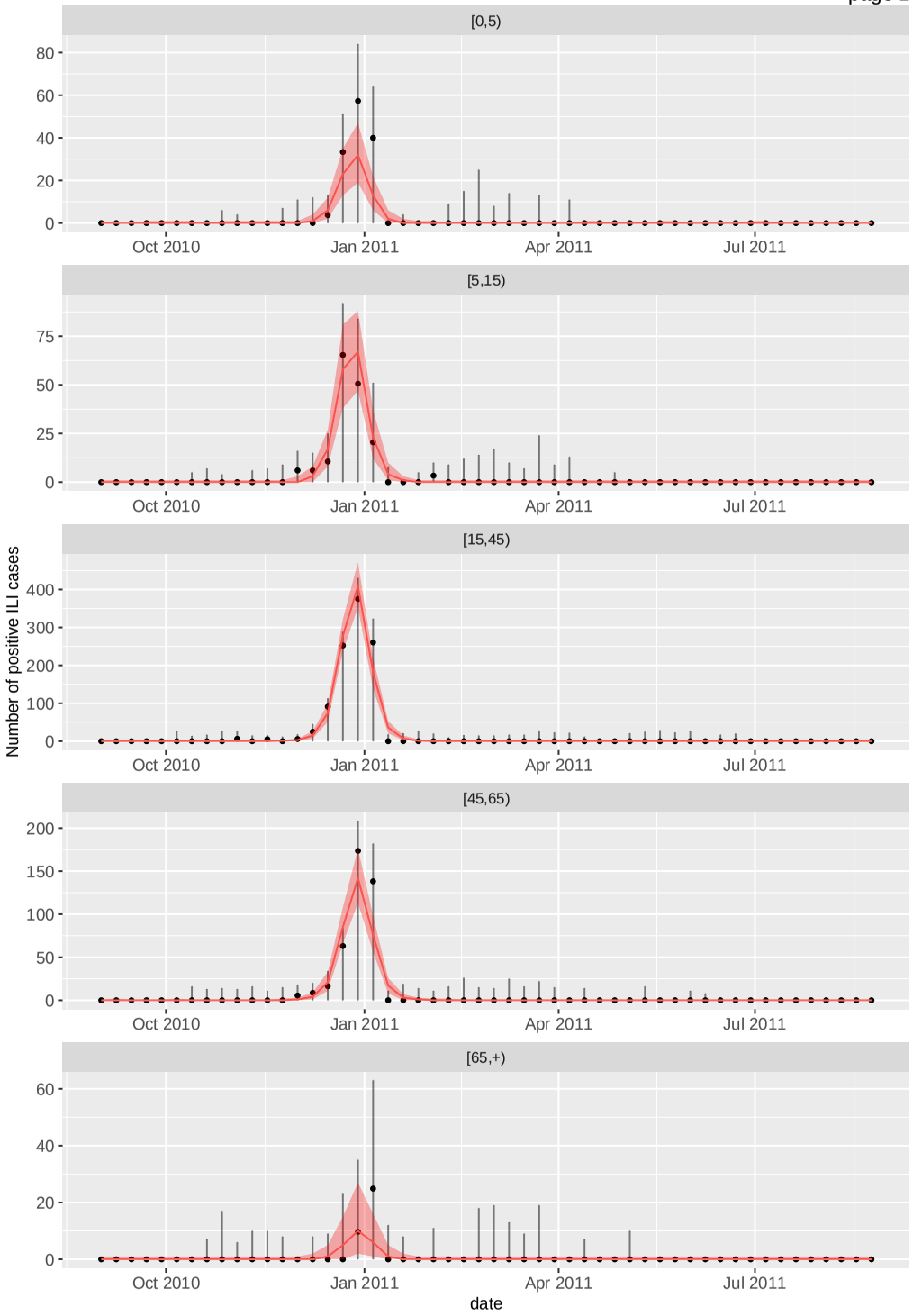
[0,5)
[5,15)
[15,45)
[45,65)
[65,+)
Number of positive ILI cases
Oct 2010
Jan 2011
Apr 2011
Jul 2011
date

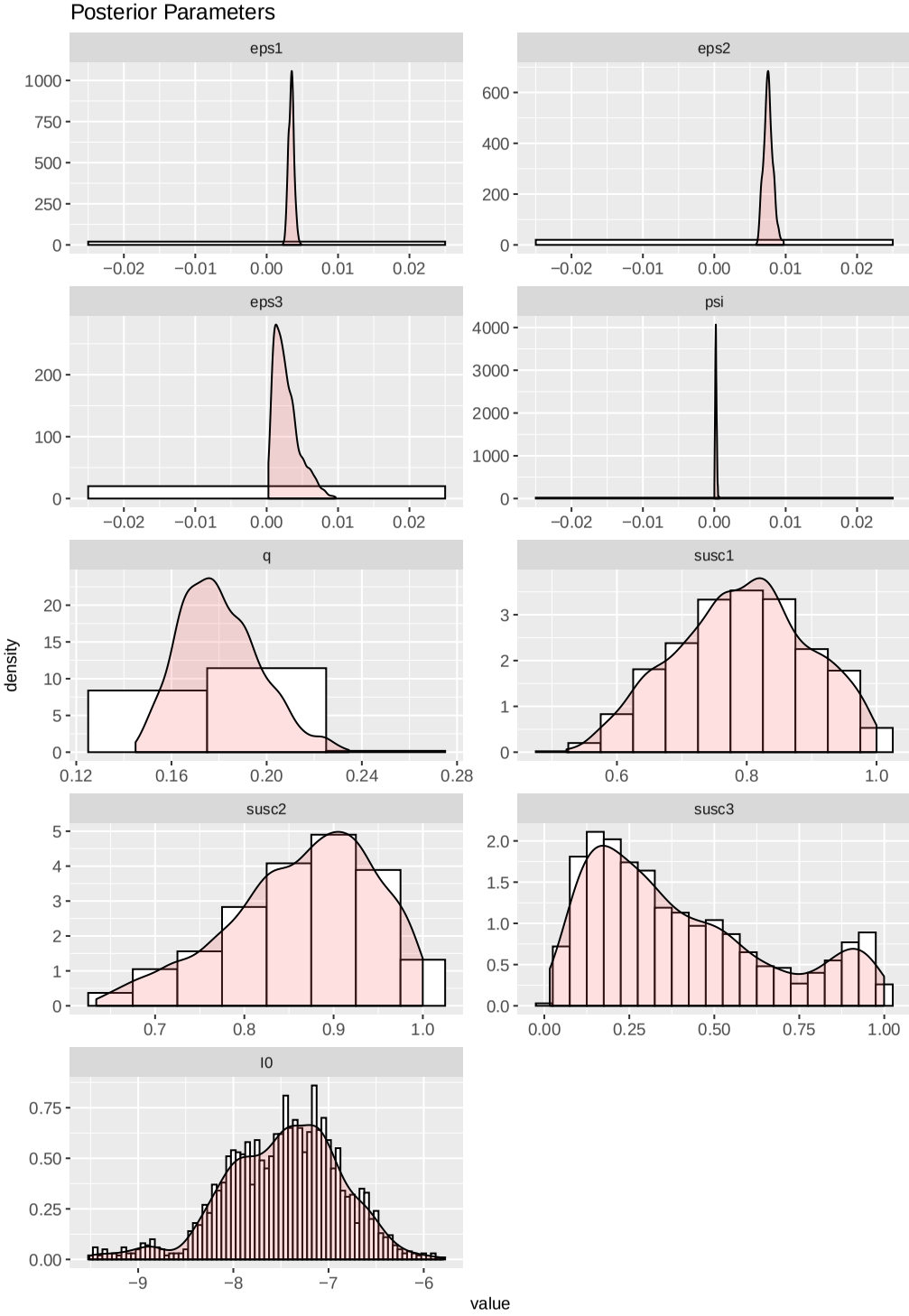
Posterior Parameters
eps1
eps2
eps3
psi
q
susc1
susc2
susc3
I0
density
value

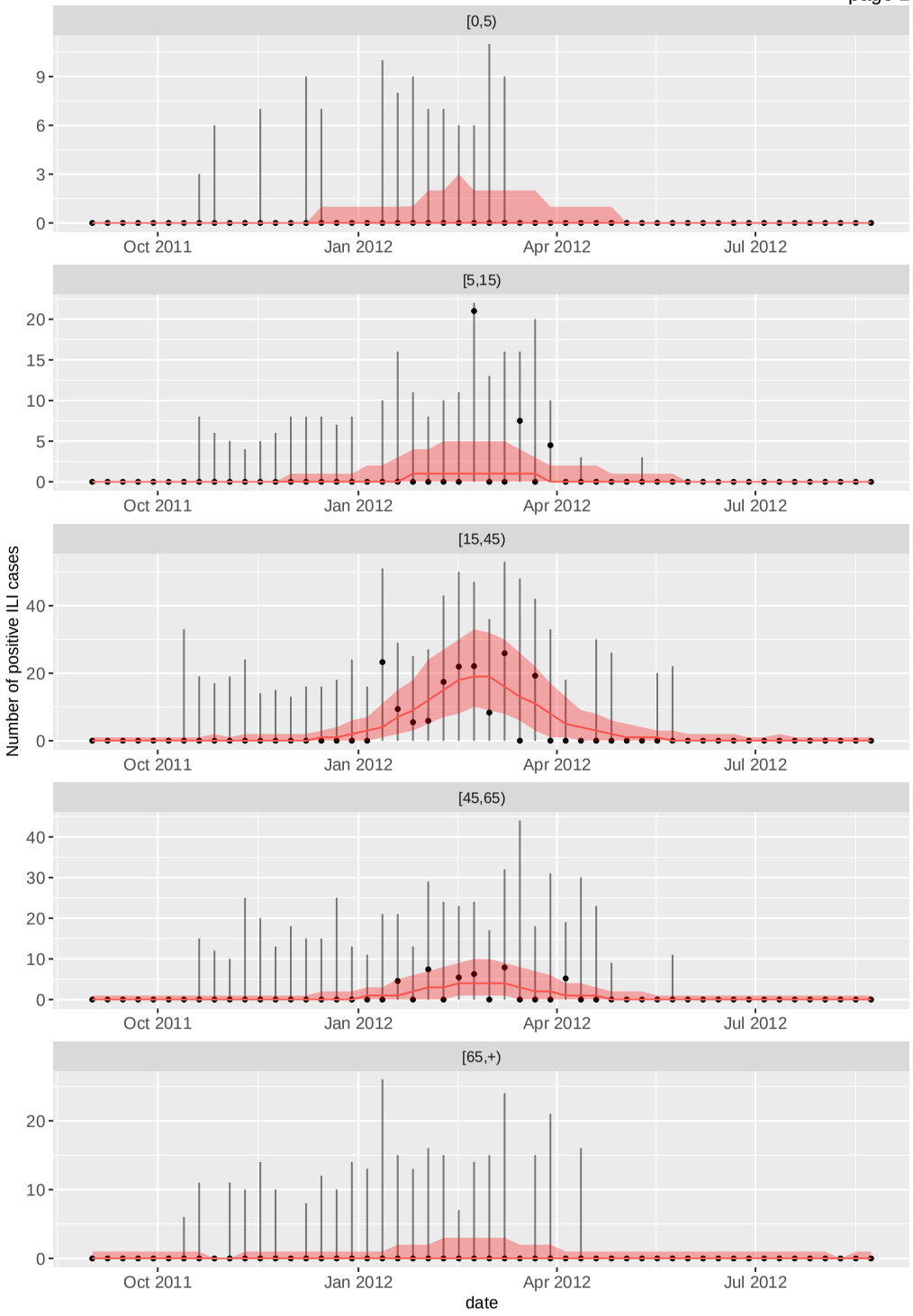
[0,5)
[5,15)
[15,45)
[45,65)
[65,+)
Oct 2011
Jan 2012
Apr 2012
Jul 2012
Number of positive ILI cases
date

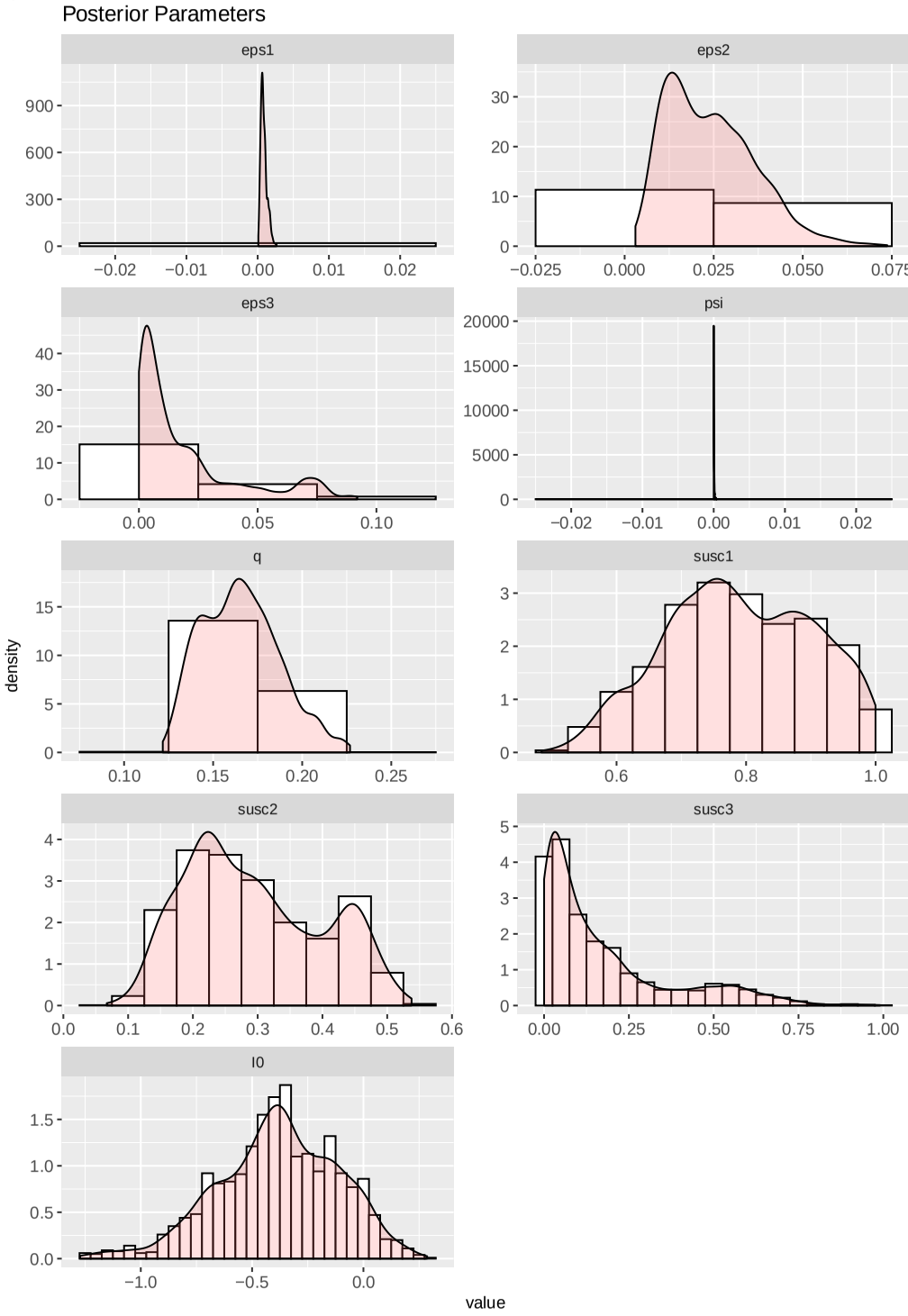
Posterior Parameters
eps1
eps2
eps3
psi
q
susc1
susc2
susc3
I0
density
value

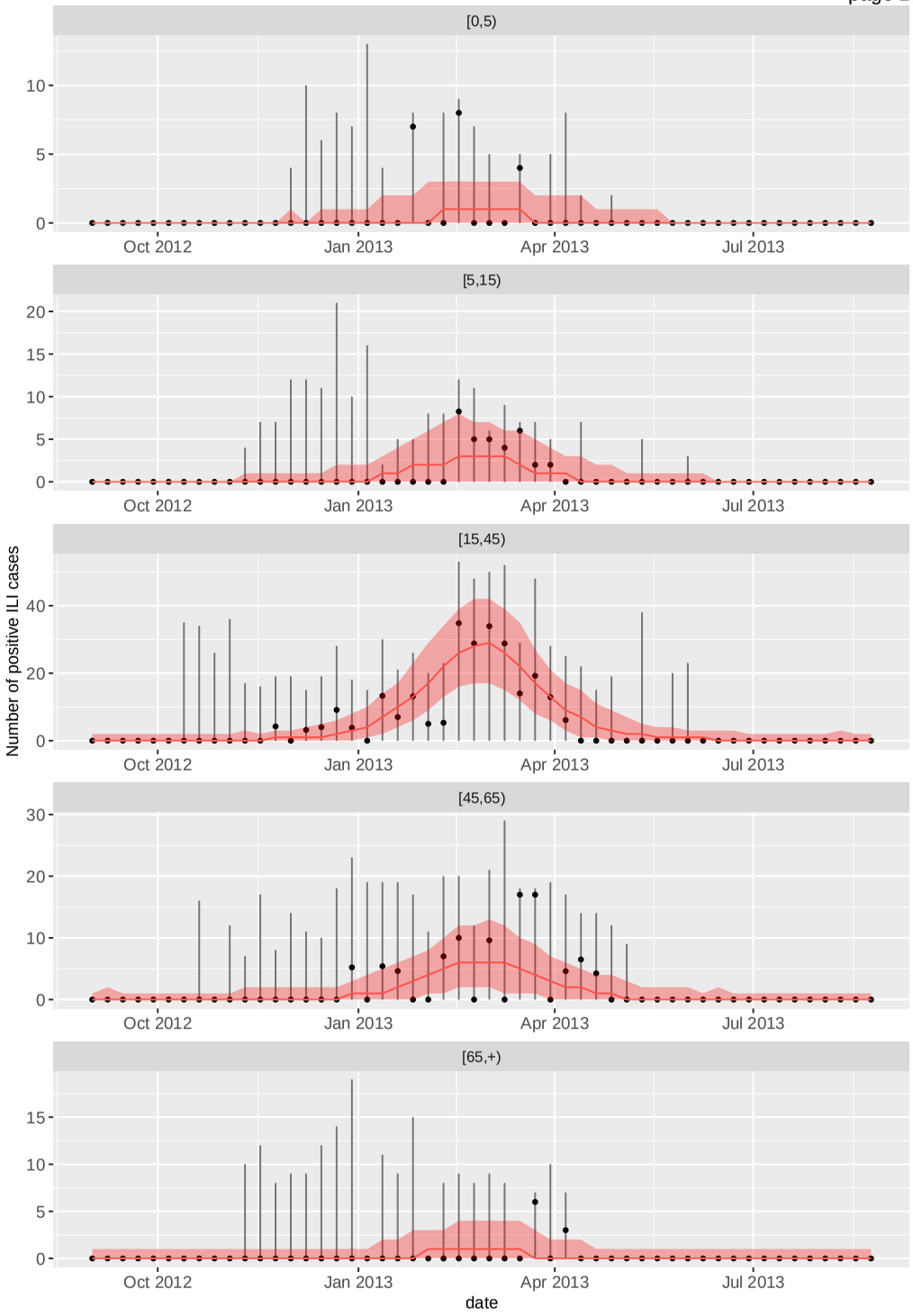
[0,5)
[5,15)
[15,45)
[45,65)
[65,+)
Oct 2012
Jan 2013
Apr 2013
Jul 2013
Number of positive ILI cases
date

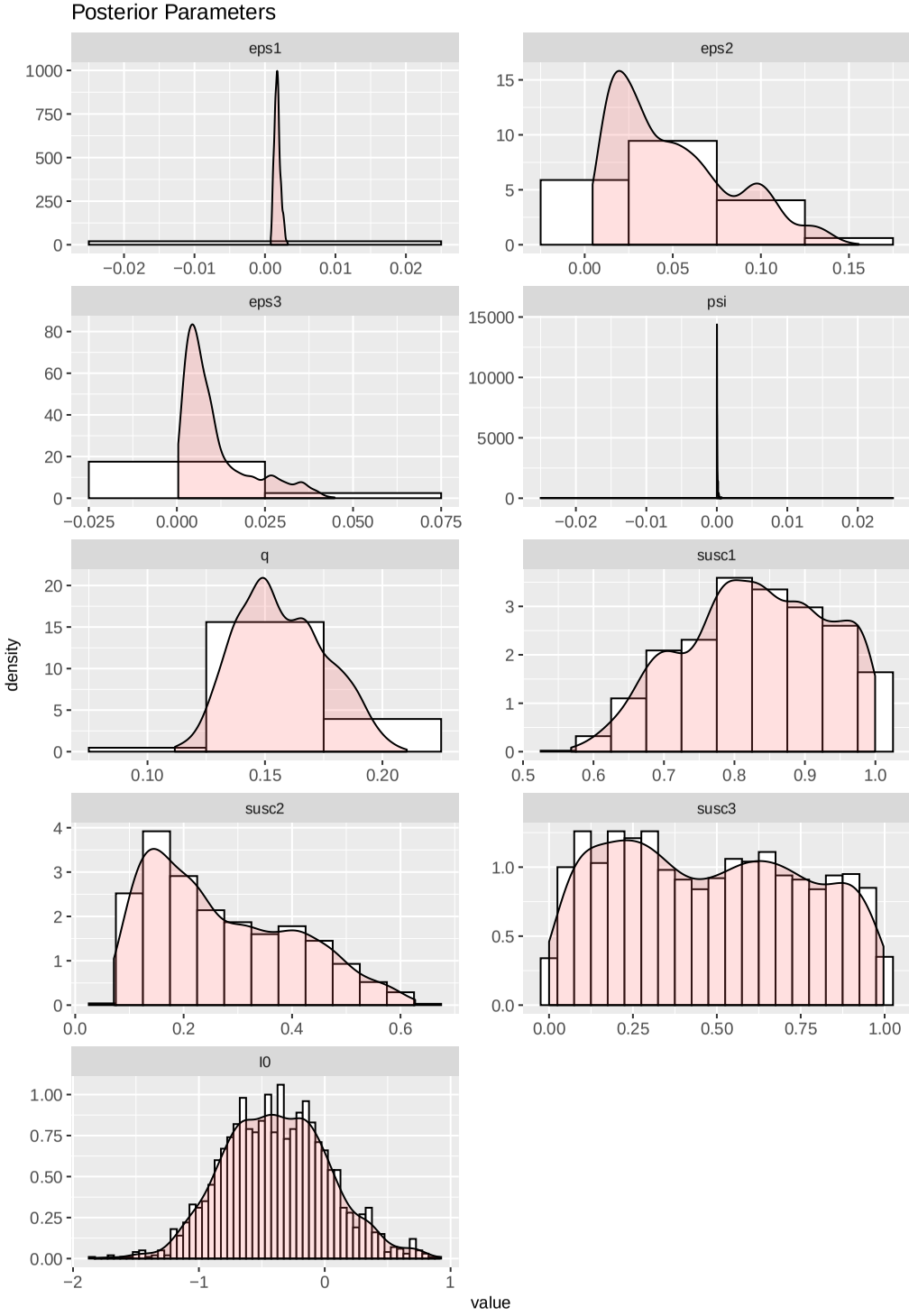
Posterior Parameters
eps1
eps2
eps3
psi
q
susc1
susc2
susc3
I0
density
value

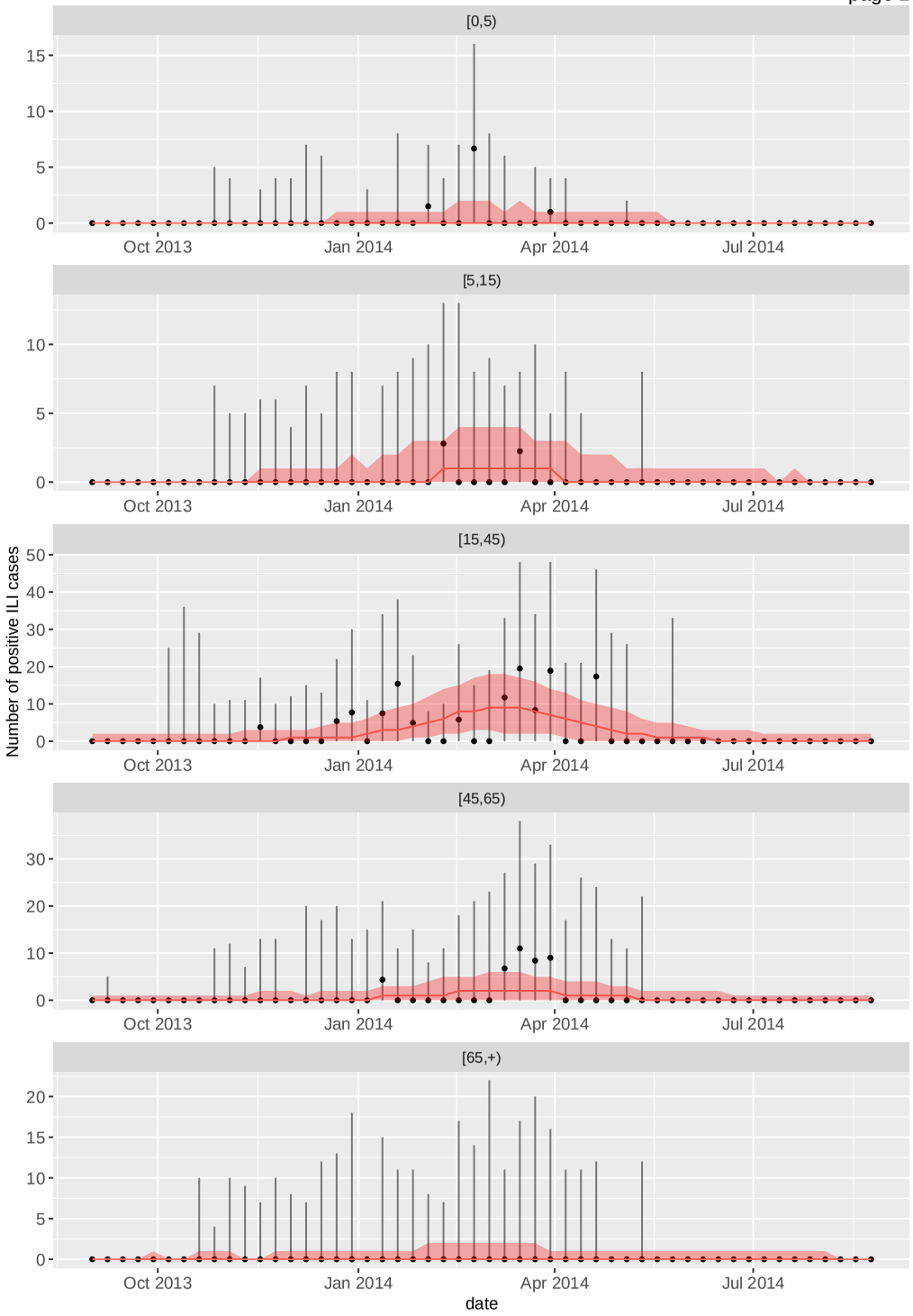
[0,5)
[5,15)
[15,45)
[45,65)
[65,+)
Number of positive ILI cases
Oct 2013
Jan 2014
Apr 2014
Jul 2014
date

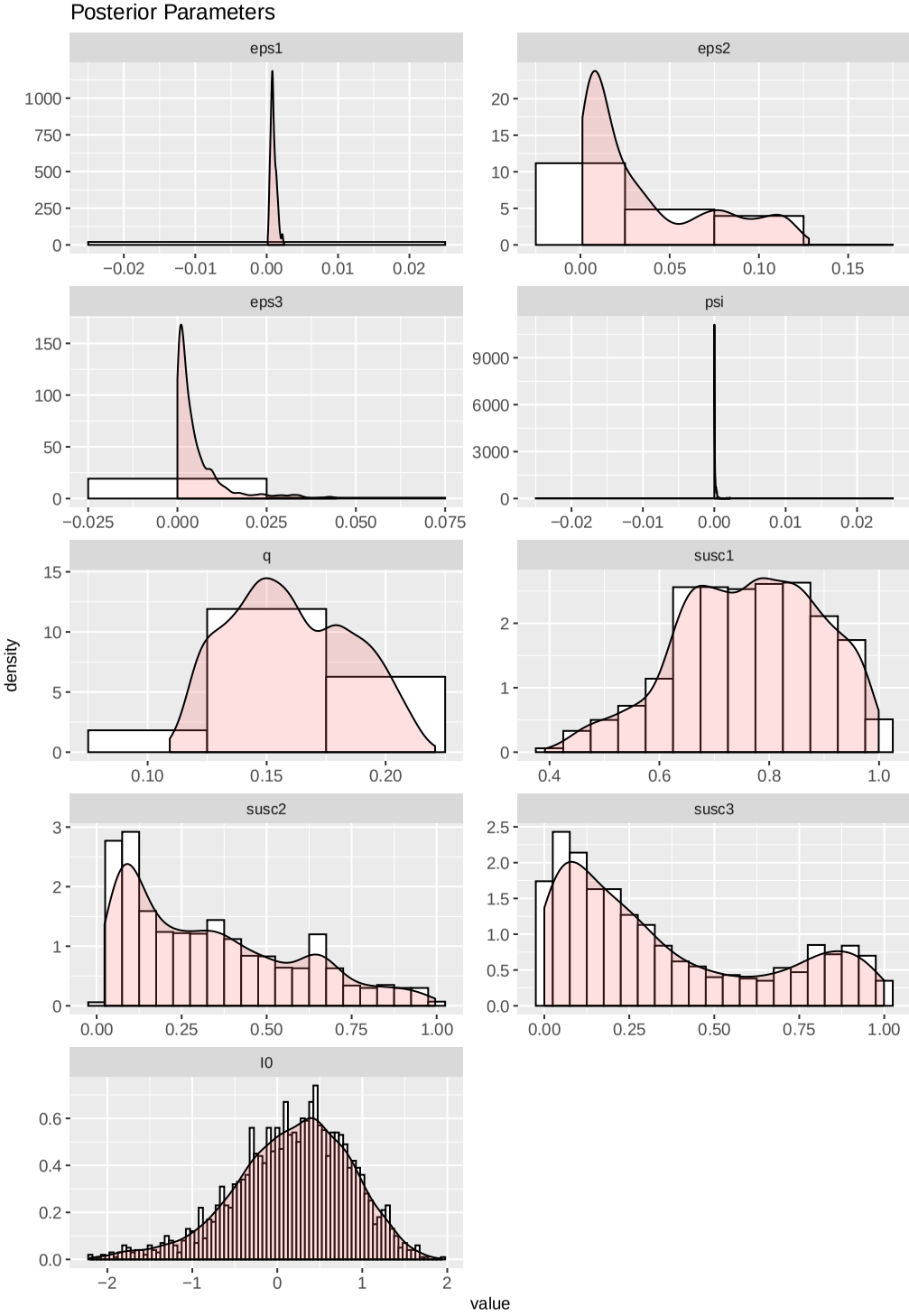
Posterior Parameters
eps1
eps2
eps3
psi
q
susc1
susc2
susc3
I0
density
value

A1.2 Model Fits for Influenza Strain A/H3N2

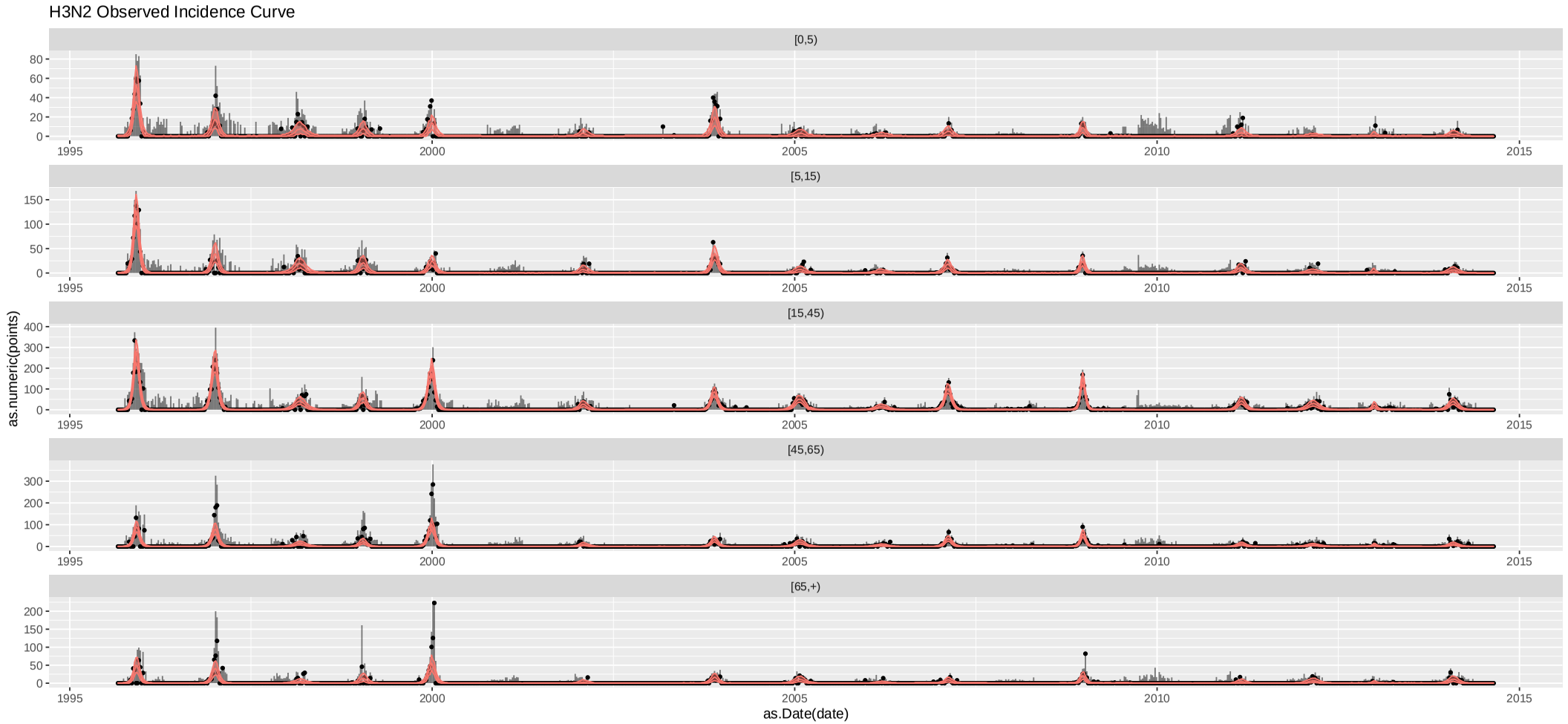
H3N2 Observed Incidence Curve
[0,5)
[5,15)
[15,45)
[45,65)
[65,+)
as.numeric(points)
as.Date(date)
1995
2000
2005
2010
2015

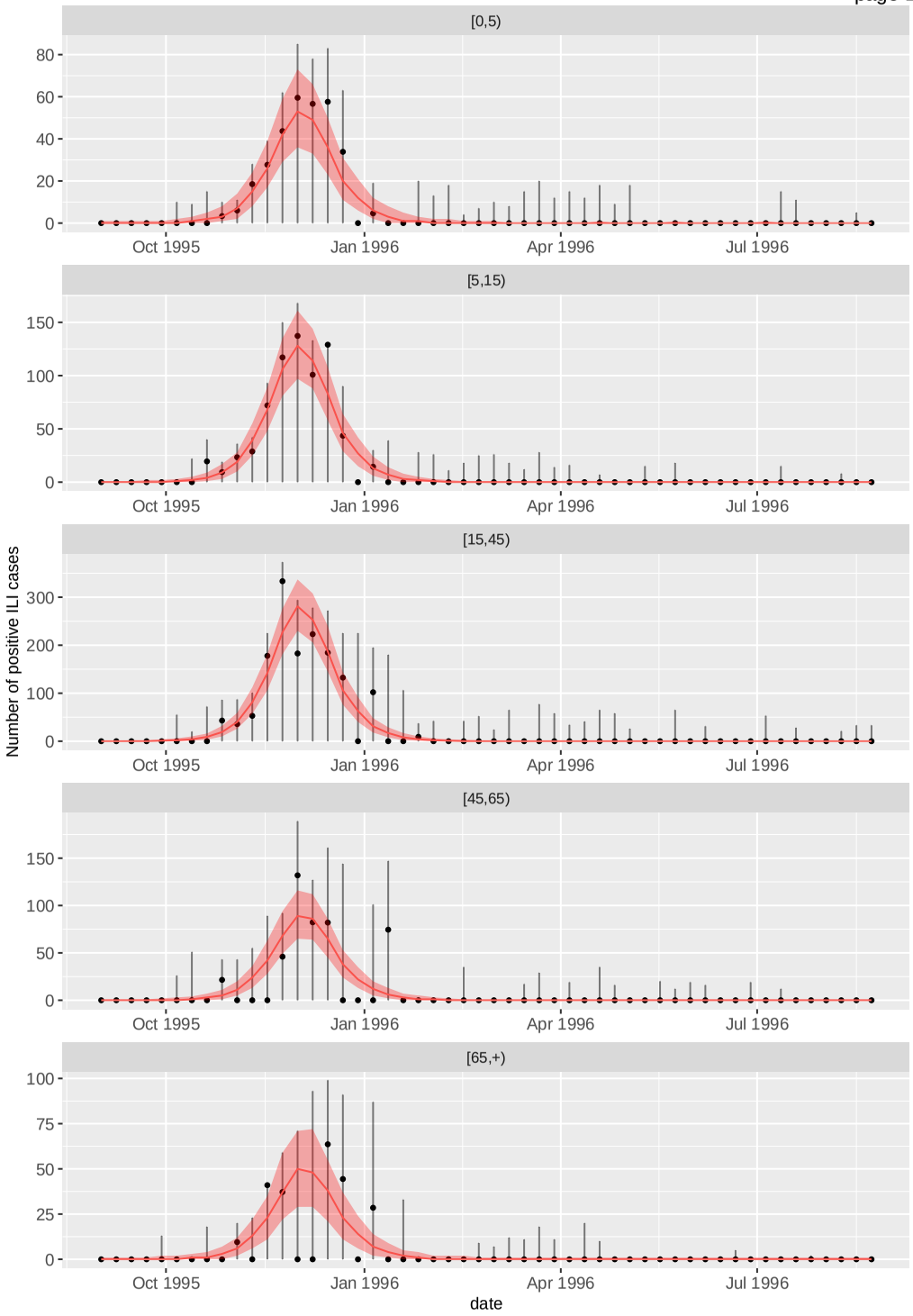
[0,5)
[5,15)
[15,45)
[45,65)
[65,+)
Oct 1995
Jan 1996
Apr 1996
Jul 1996
Number of positive ILI cases
date

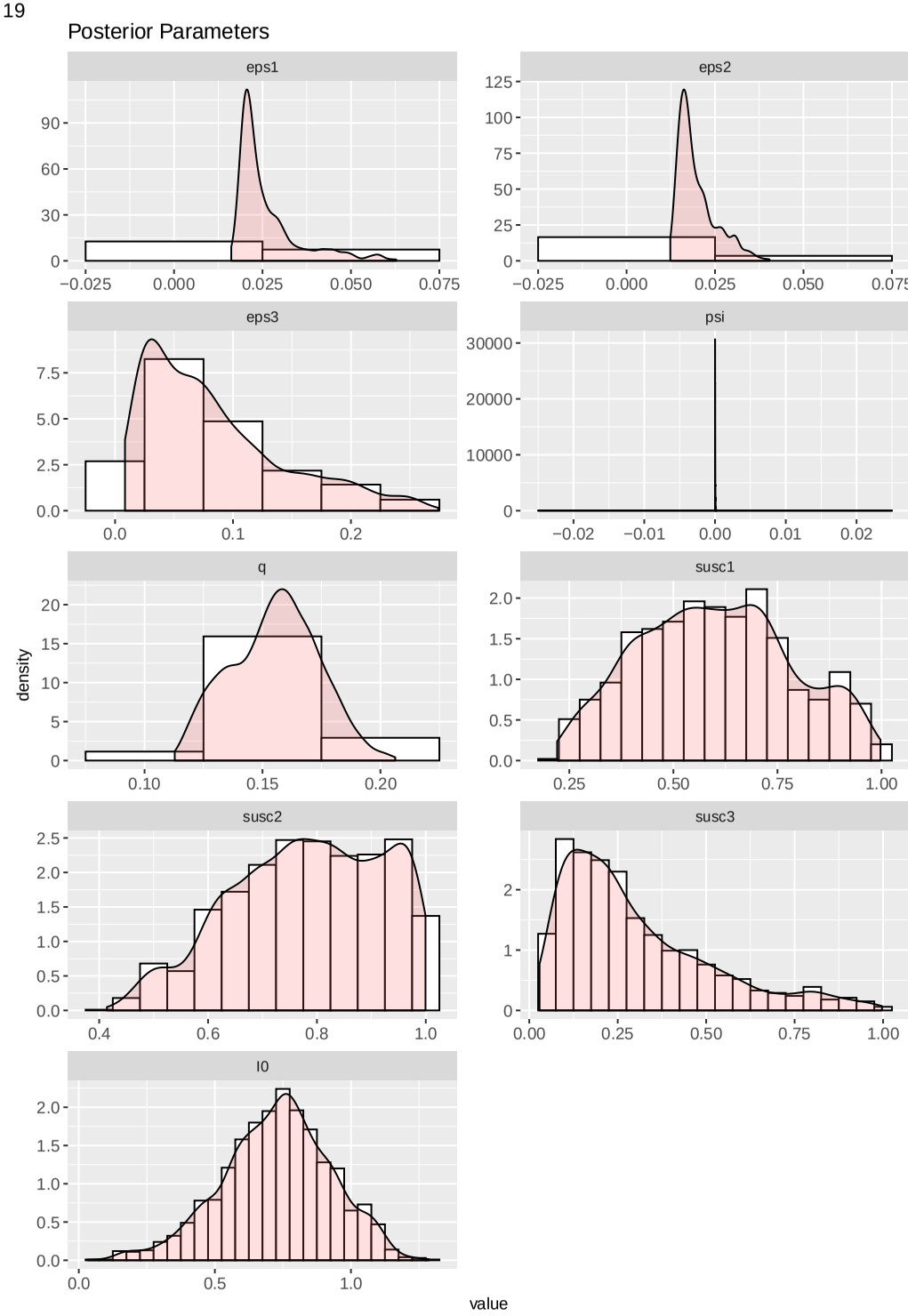
Posterior Parameters
eps1
eps2
eps3
psi
q
susc1
susc2
susc3
I0
density
value

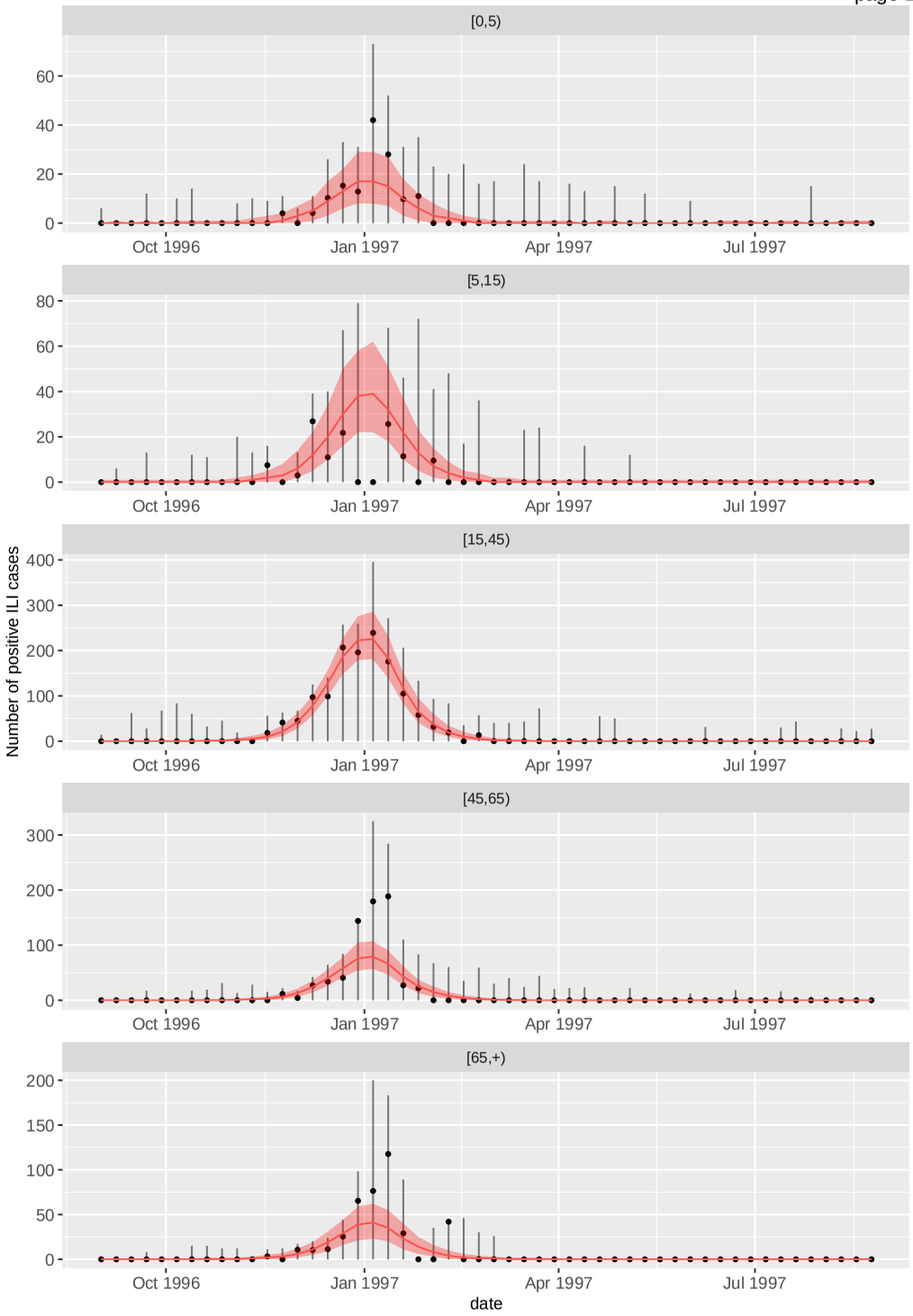
[0,5)
[5,15)
[15,45)
[45,65)
[65,+)
Number of positive ILI cases
Oct 1996
Jan 1997
Apr 1997
Jul 1997
date

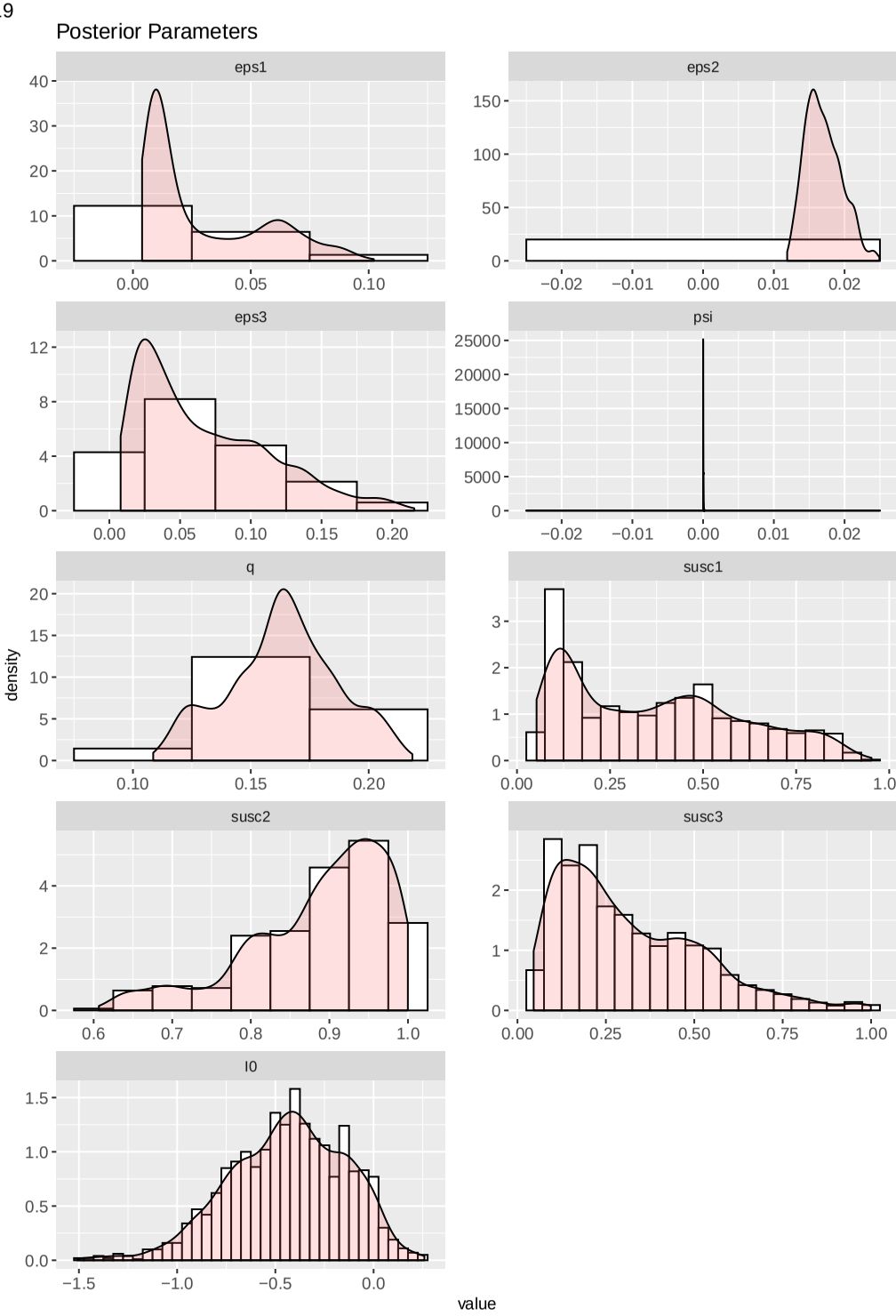
Posterior Parameters
eps1
eps2
eps3
psi
q
susc1
susc2
susc3
I0
density
value

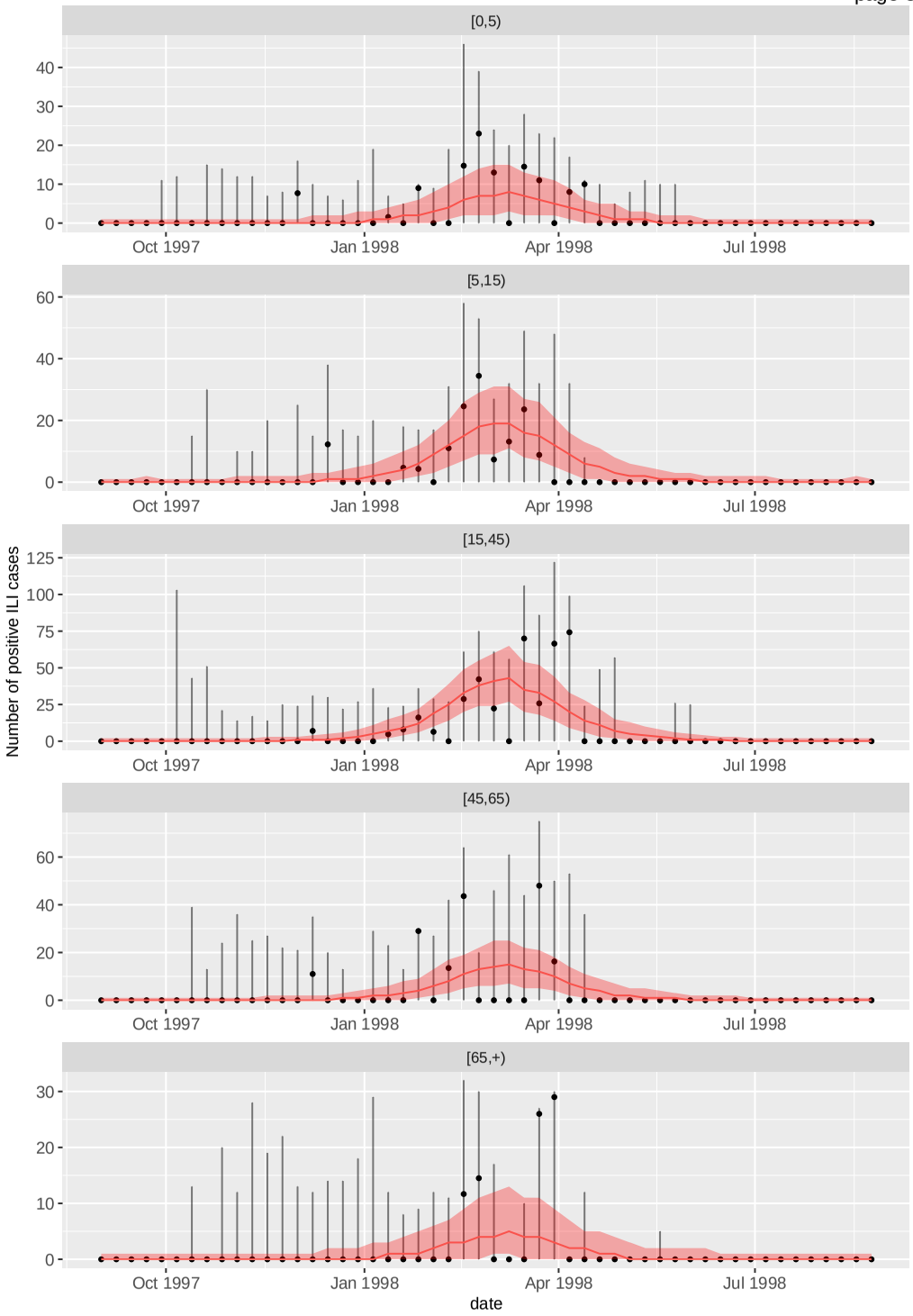
[0,5)
[5,15)
[15,45)
[45,65)
[65,+)
Number of positive ILI cases
Oct 1997
Jan 1998
Apr 1998
Jul 1998
date

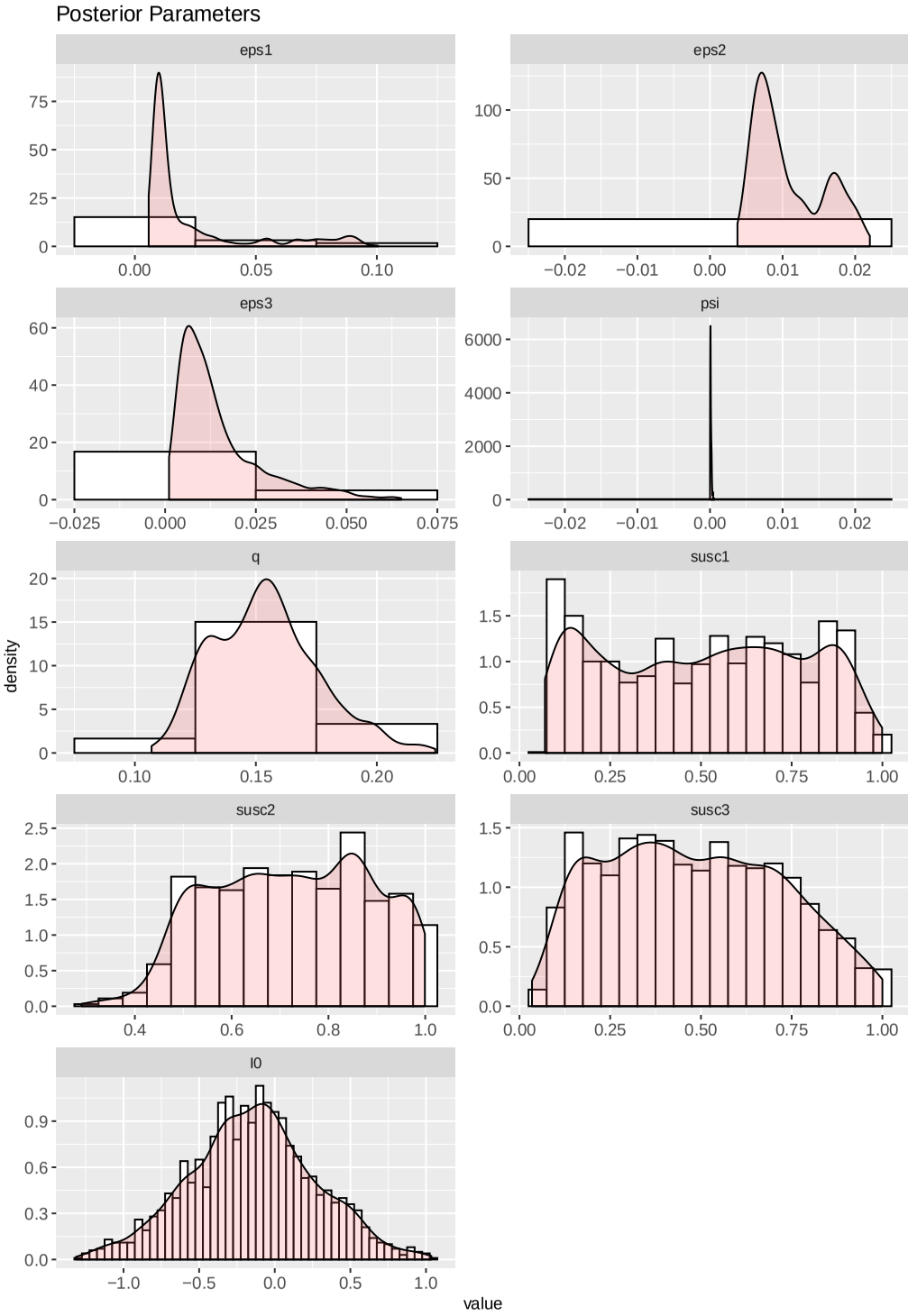
Posterior Parameters
eps1
eps2
eps3
psi
q
susc1
susc2
susc3
I0
density
value

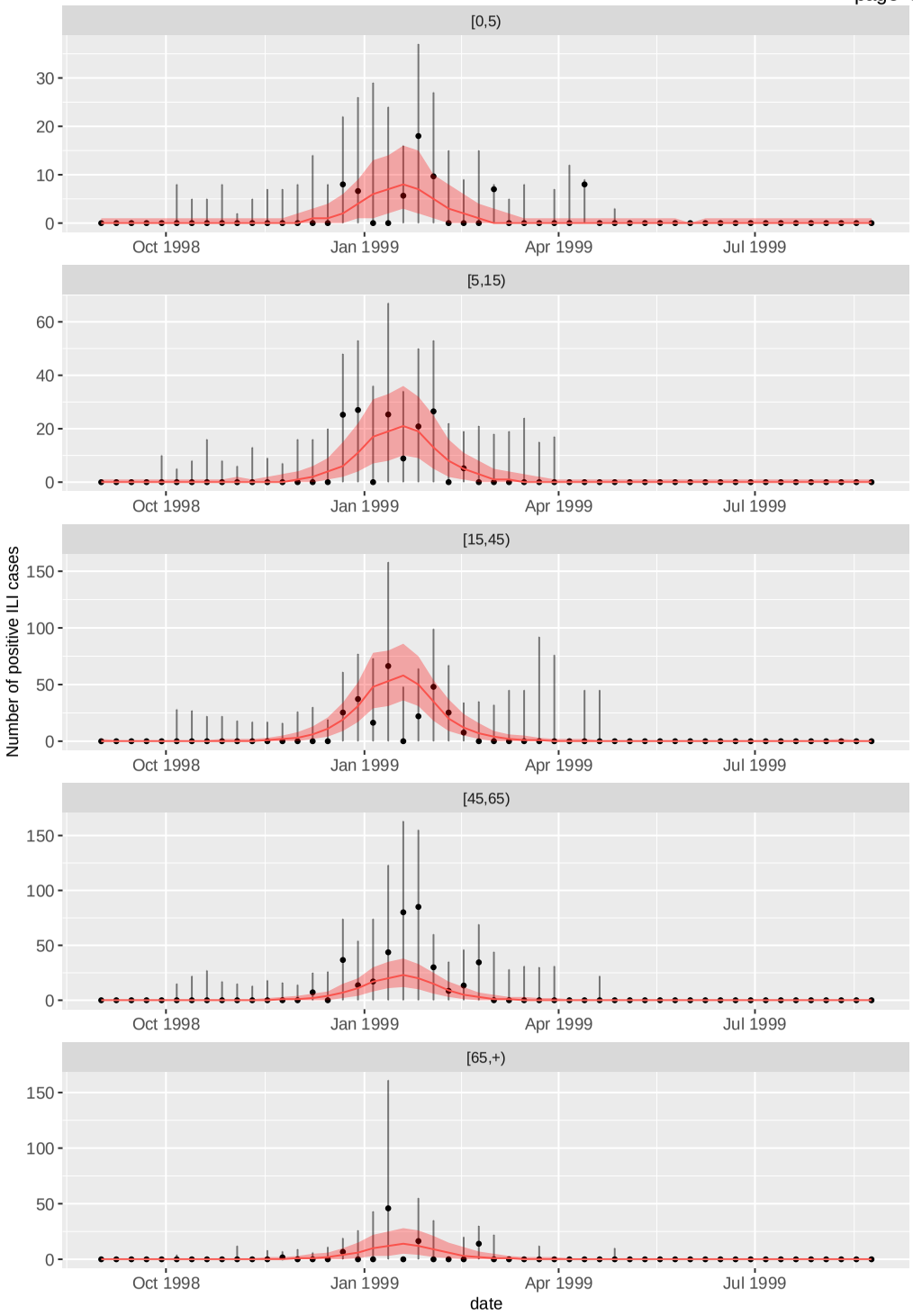
[0,5)
[5,15)
[15,45)
[45,65)
[65,+)
Number of positive ILI cases
Oct 1998
Jan 1999
Apr 1999
Jul 1999
date

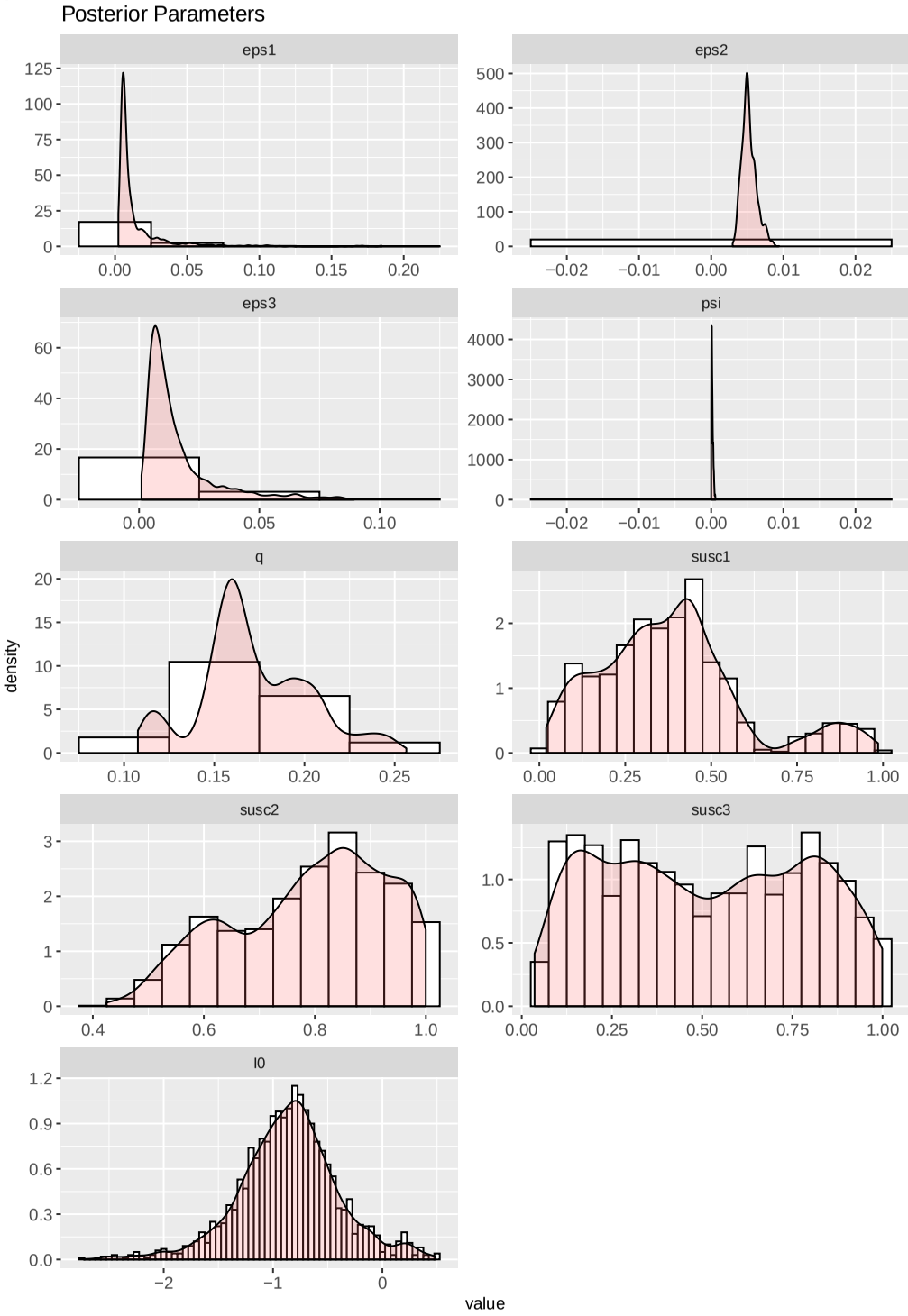
Posterior Parameters
eps1
eps2
eps3
psi
q
susc1
susc2
susc3
I0
density
value

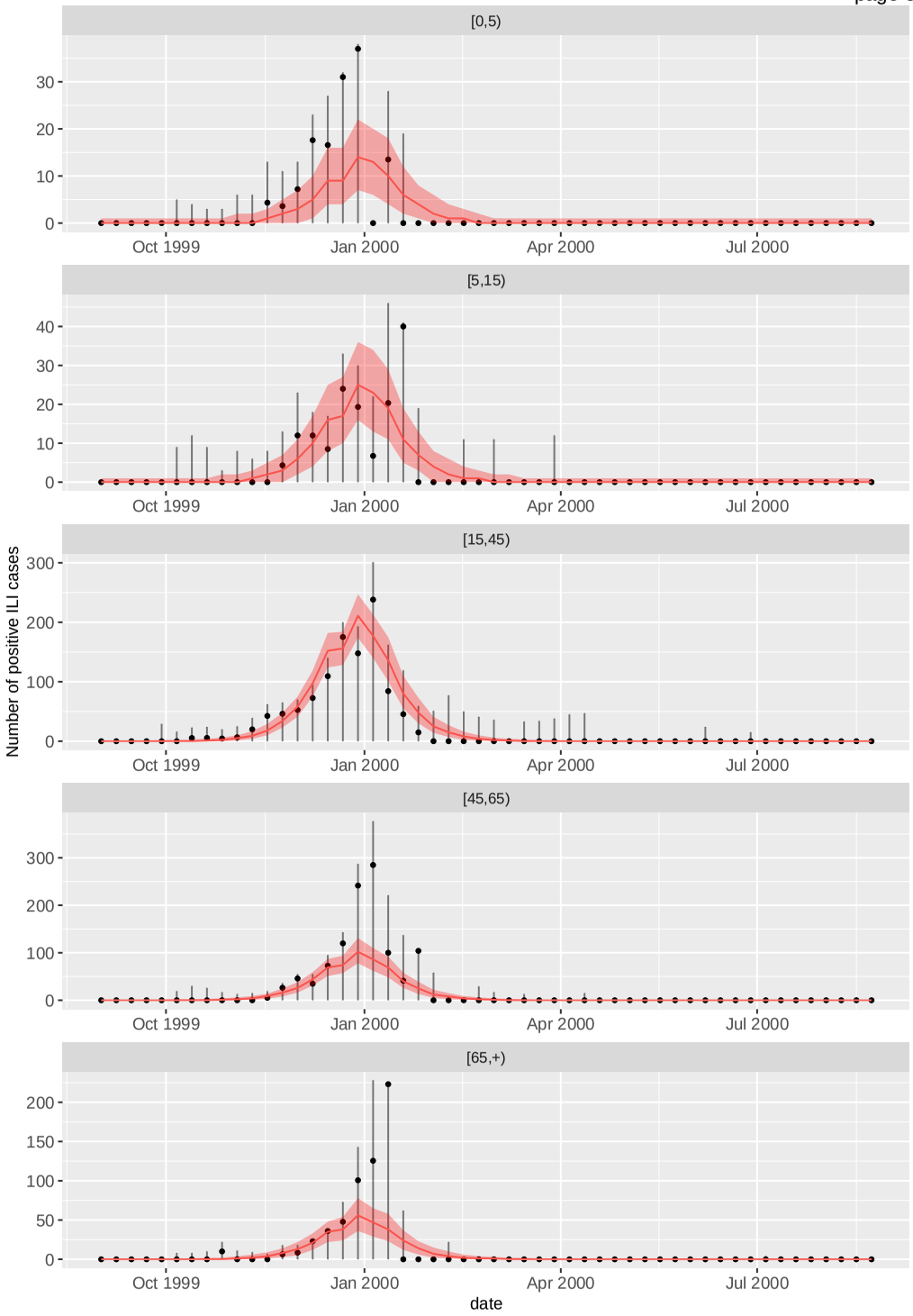
[0,5)
[5,15)
[15,45)
[45,65)
[65,+)
Number of positive ILI cases
Oct 1999
Jan 2000
Apr 2000
Jul 2000
date

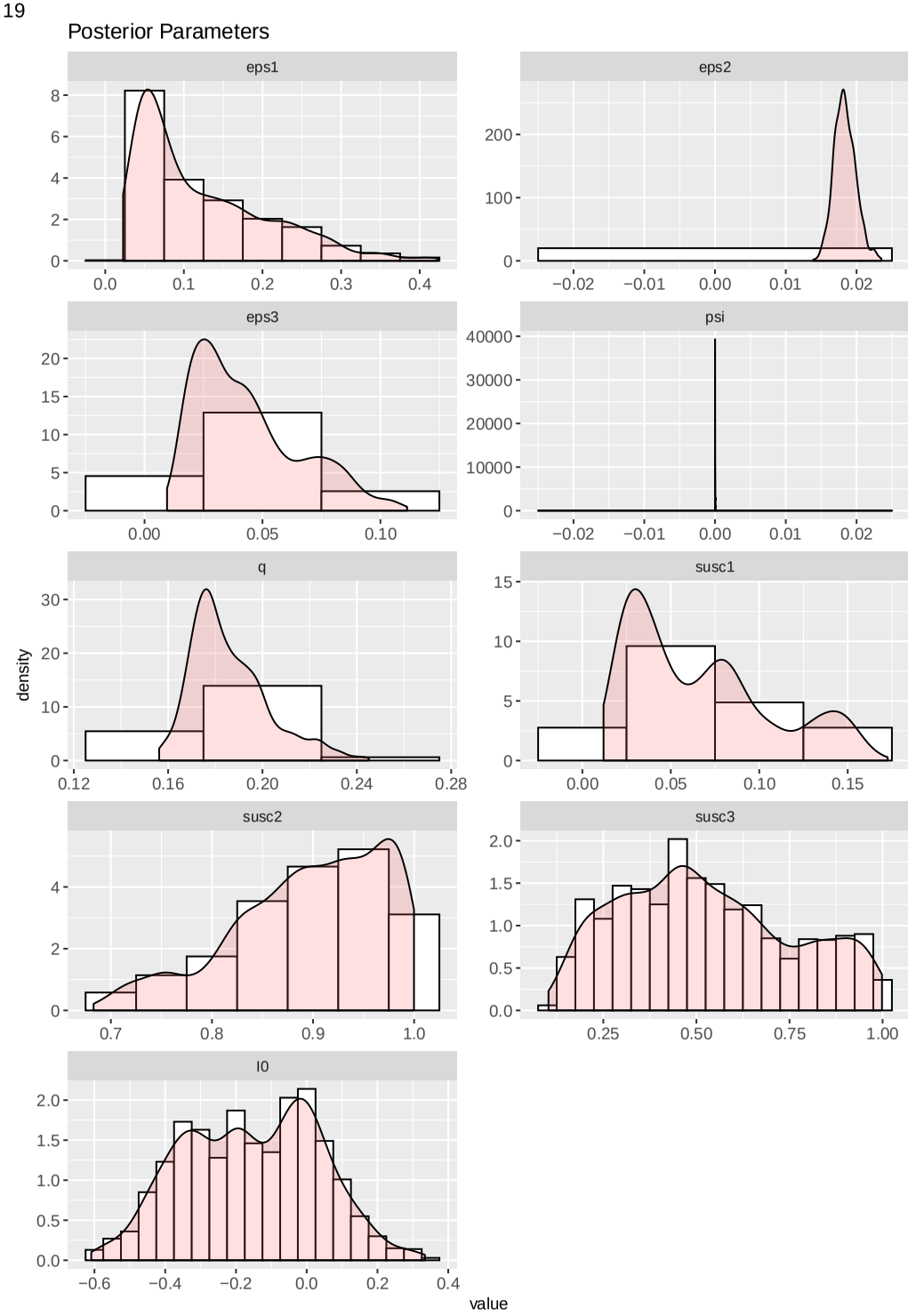
Posterior Parameters
eps1
eps2
eps3
psi
q
susc1
susc2
susc3
I0
density
value

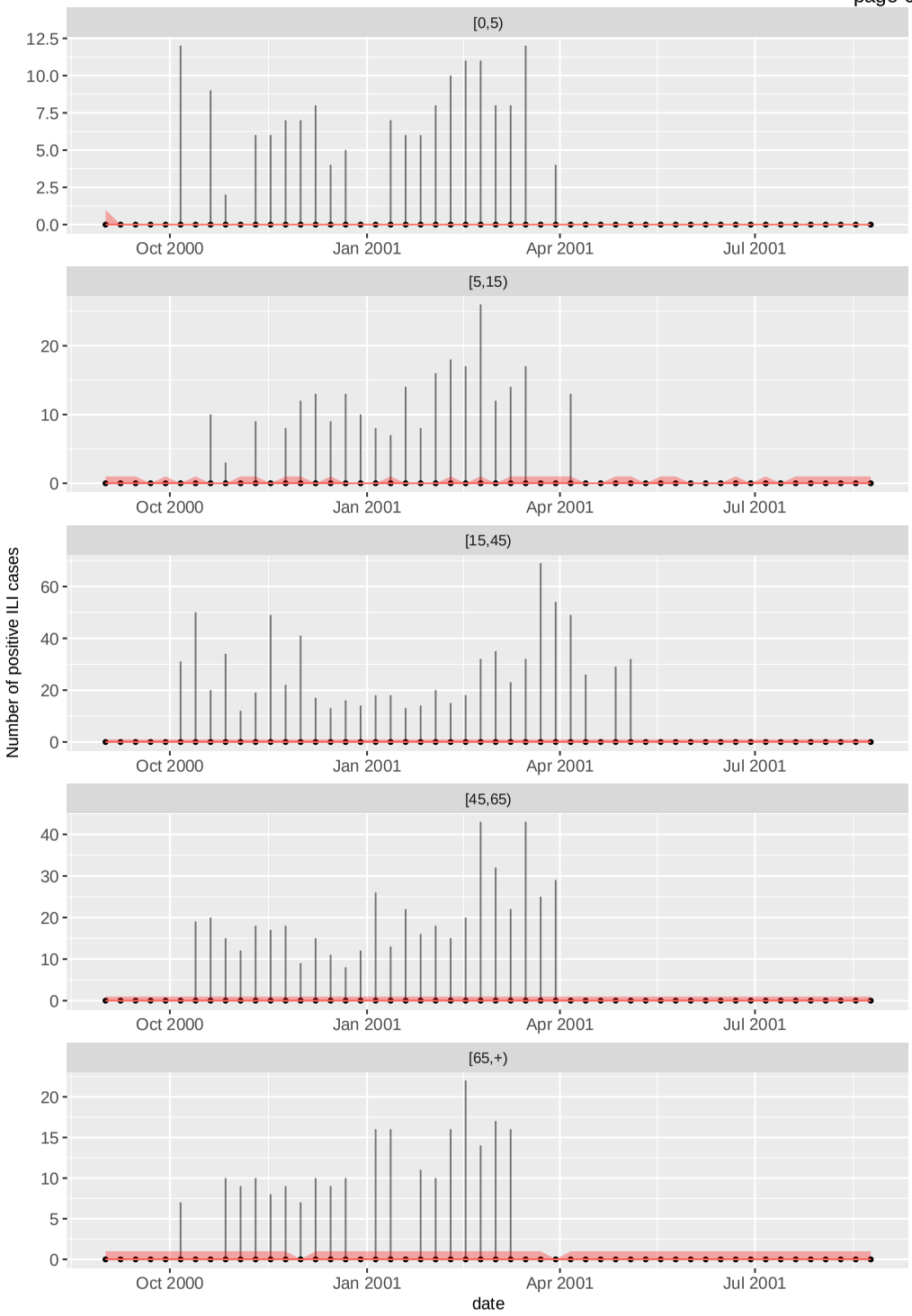
[0,5)
[5,15)
[15,45)
[45,65)
[65,+)
Oct 2000
Jan 2001
Apr 2001
Jul 2001
Number of positive ILI cases
date

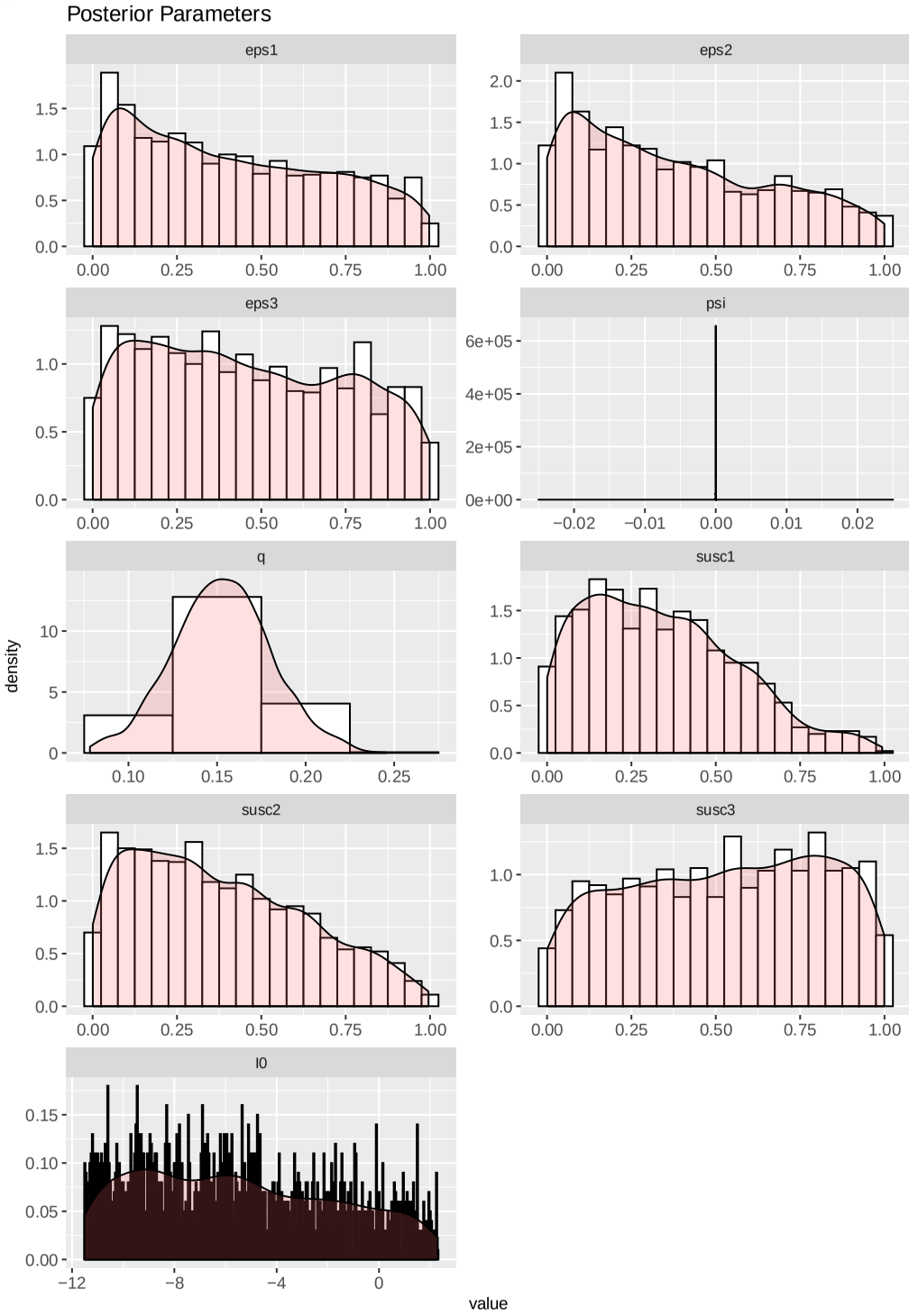
Posterior Parameters
eps1
eps2
eps3
psi
q
susc1
susc2
susc3
I0
density
value

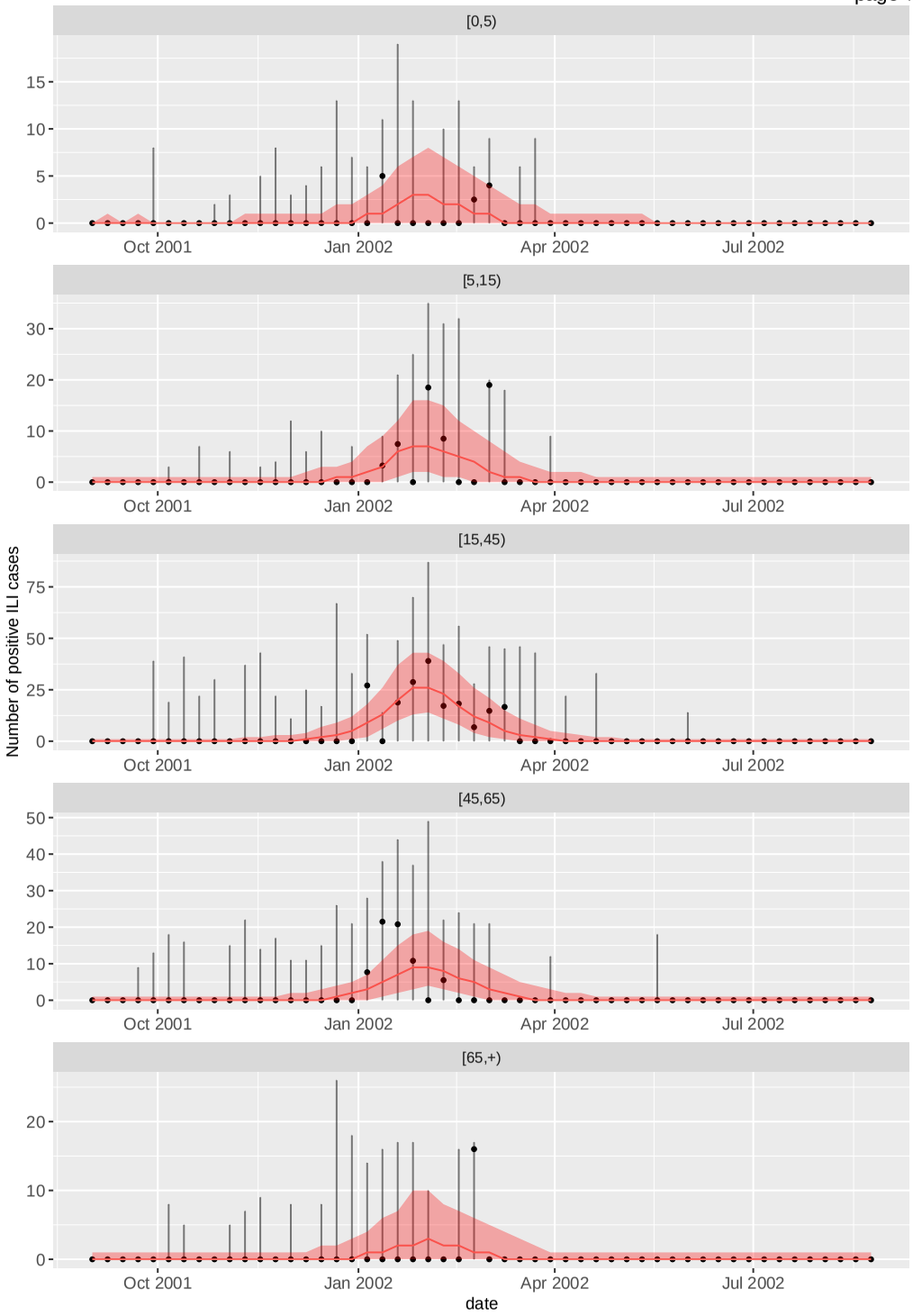

Posterior Parameters

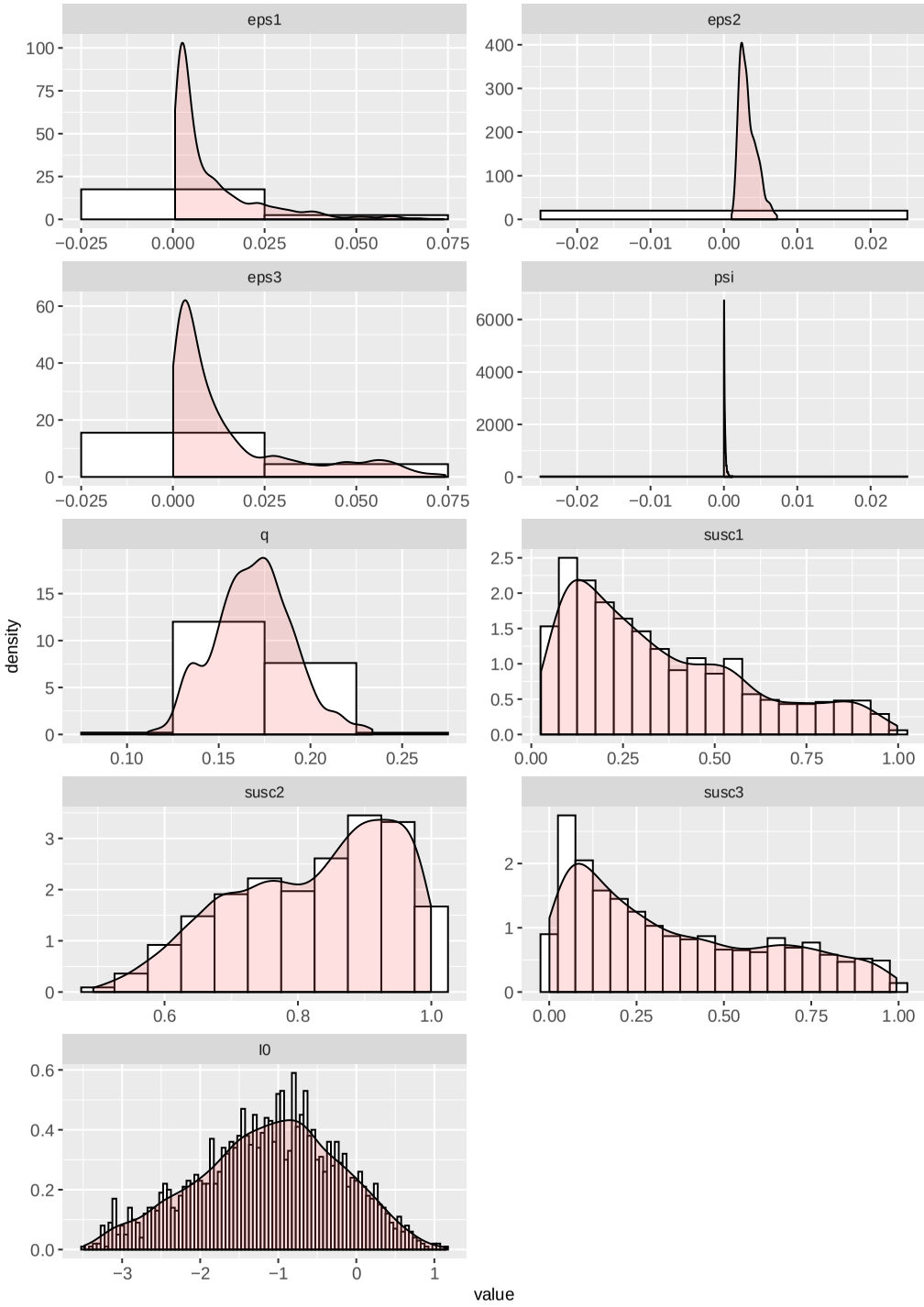

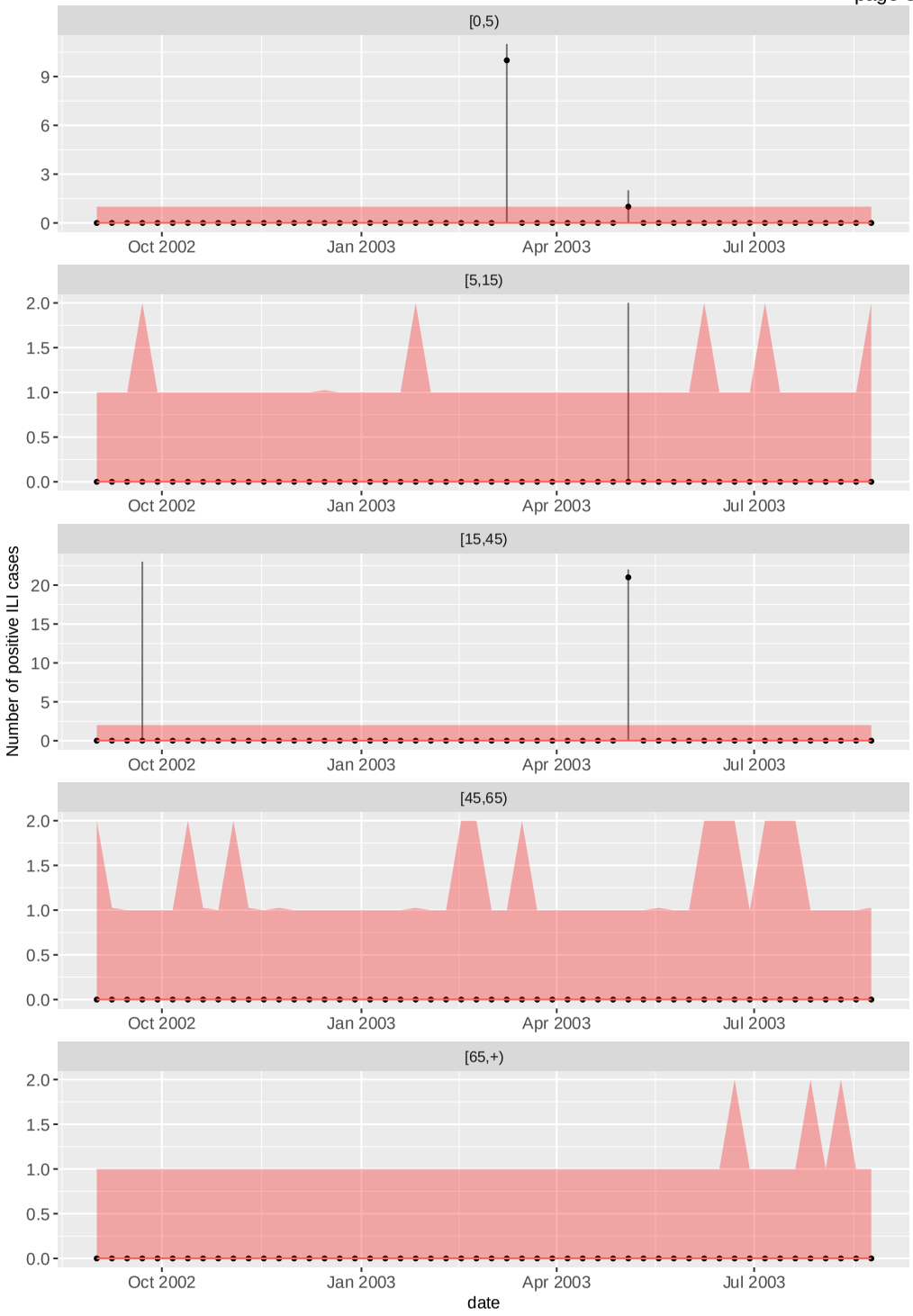
[0,5)
[5,15)
[15,45)
[45,65)
[65,+)
Number of positive ILI cases
Oct 2002
Jan 2003
Apr 2003
Jul 2003
date

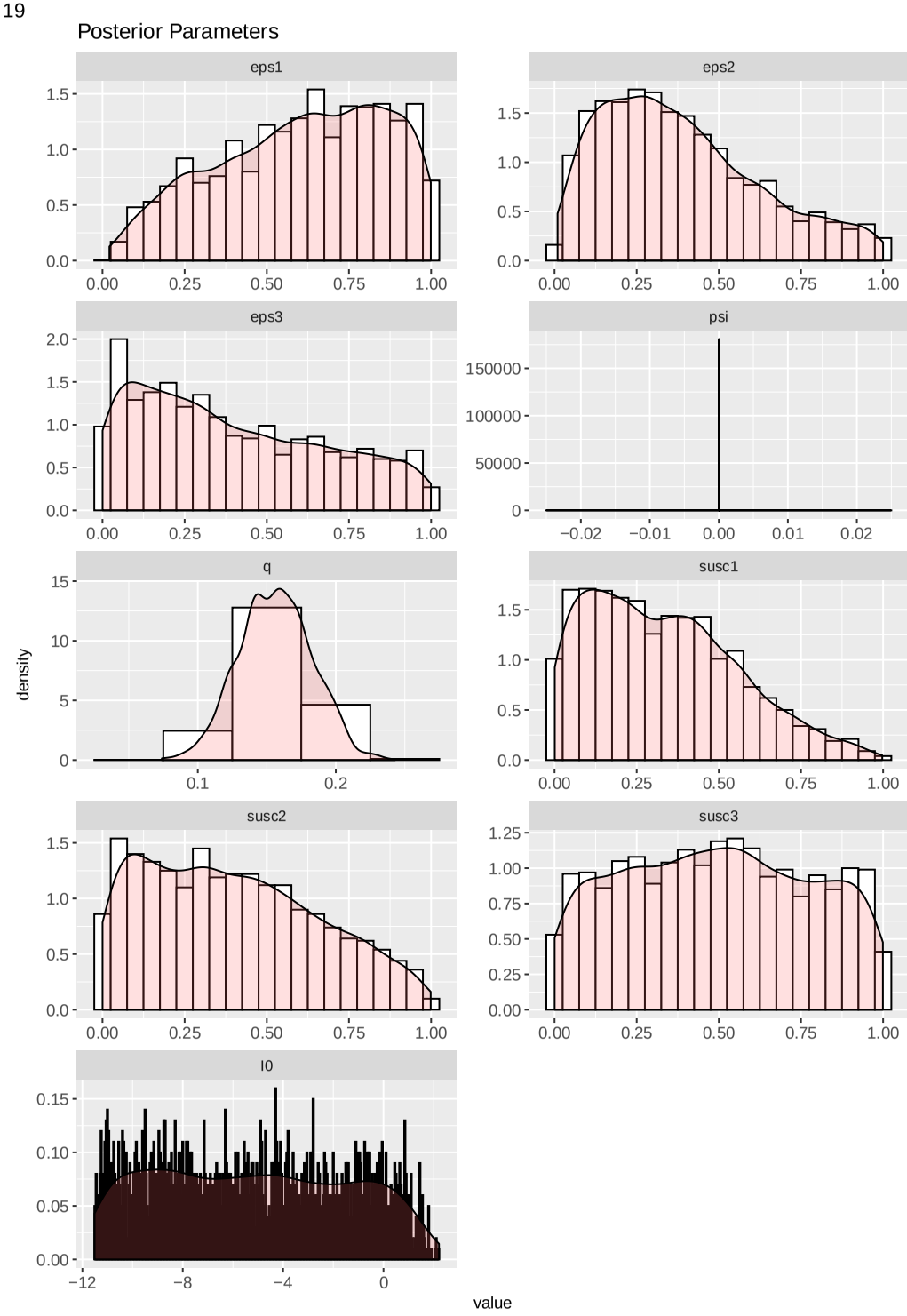
Posterior Parameters
eps1
eps2
eps3
psi
q
susc1
susc2
susc3
I0
density
value

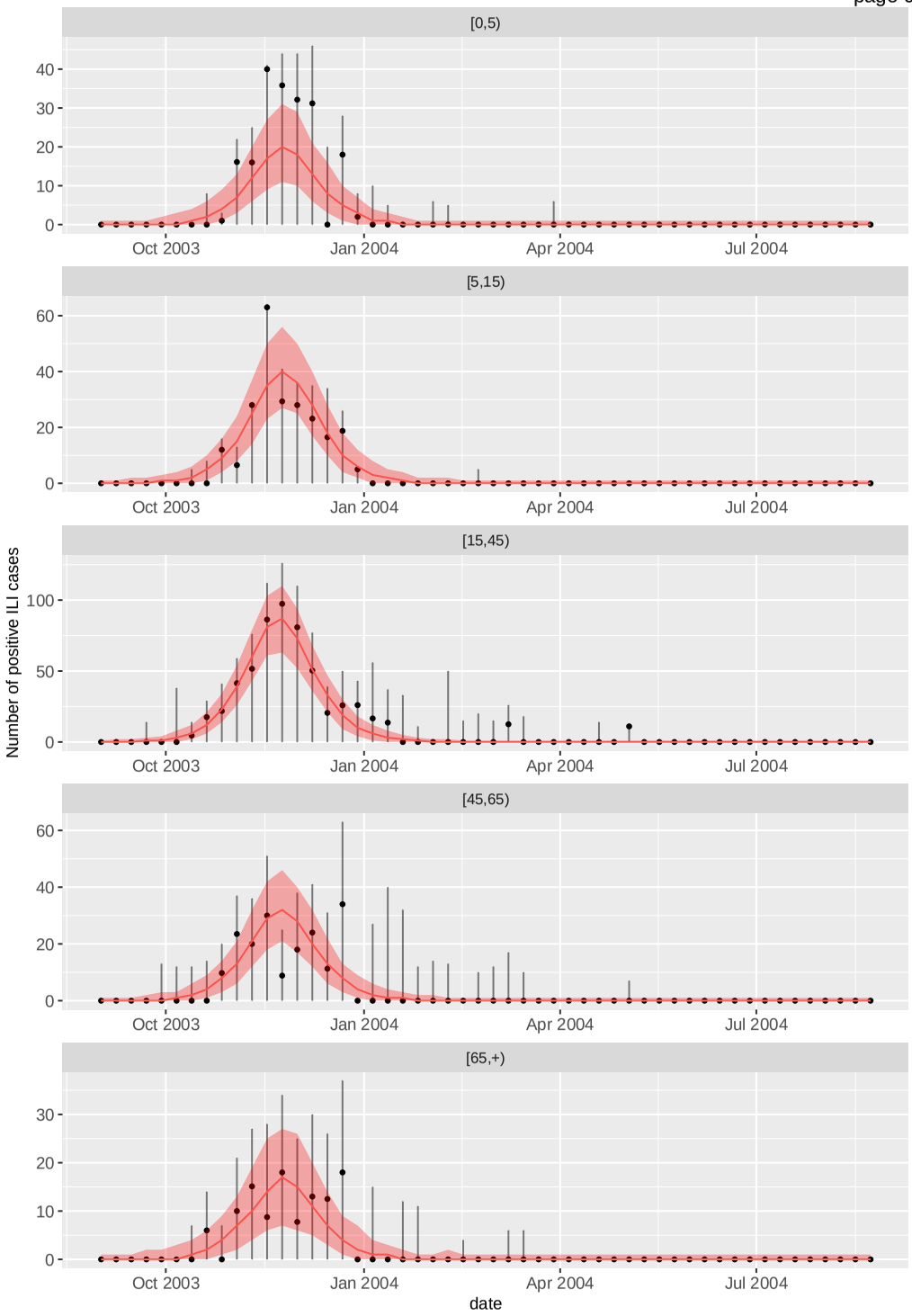
[0,5)
[5,15)
[15,45)
[45,65)
[65,+)
Oct 2003
Jan 2004
Apr 2004
Jul 2004
Number of positive ILI cases
date

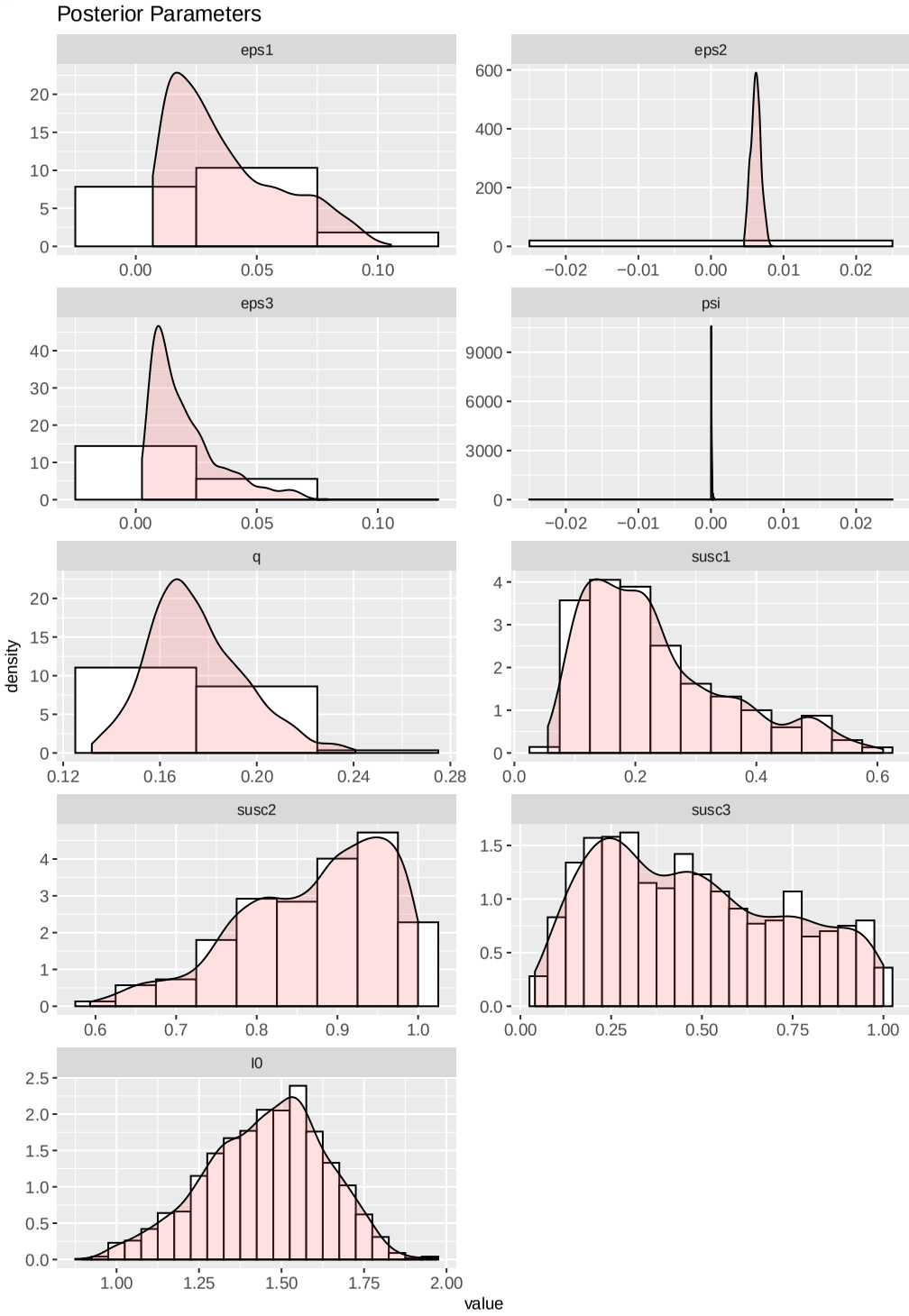
Posterior Parameters
eps1
eps2
eps3
psi
q
susc1
susc2
susc3
I0
density
value

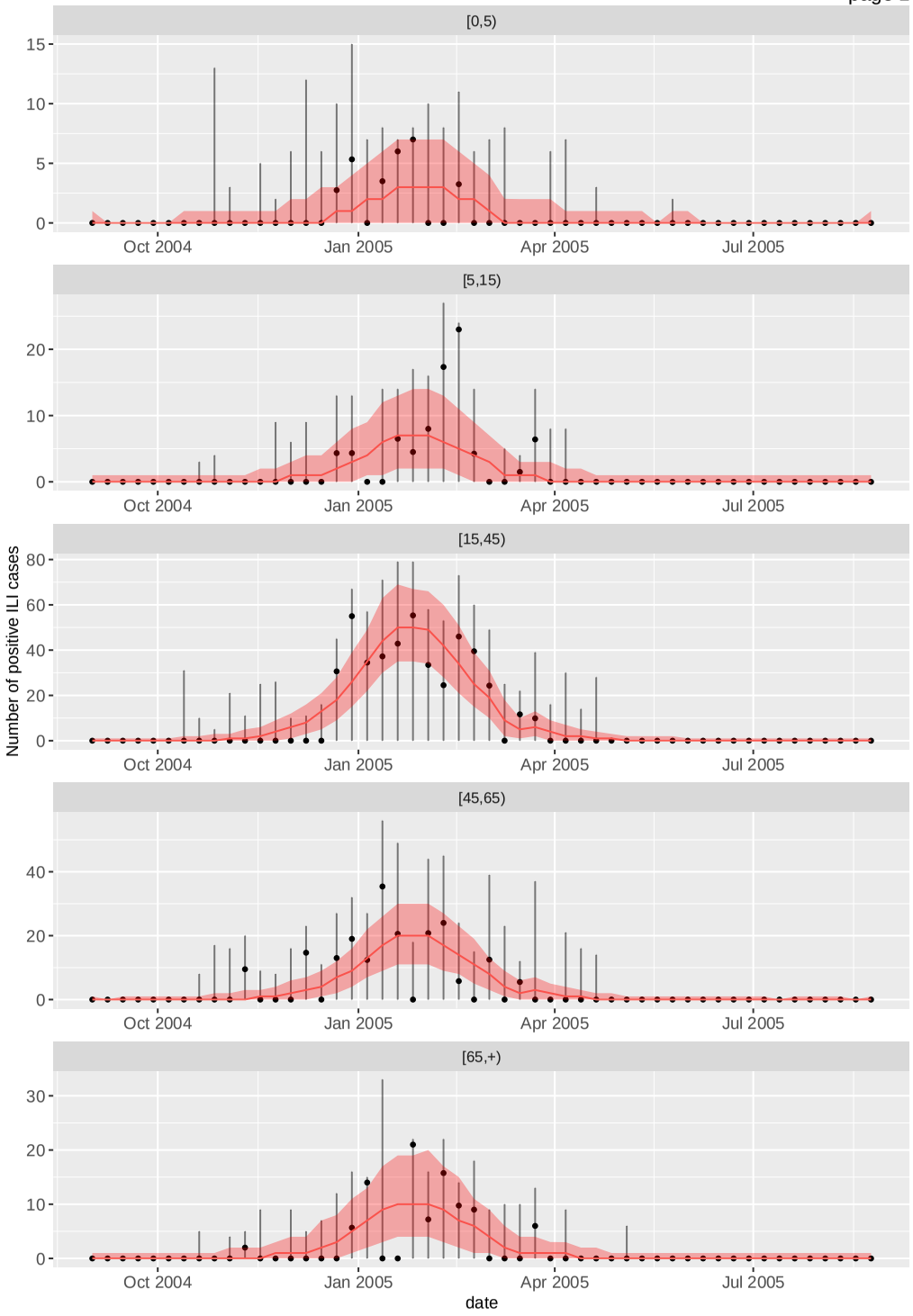
[0,5)
[5,15)
[15,45)
[45,65)
[65,+)
Number of positive ILI cases
Oct 2004
Jan 2005
Apr 2005
Jul 2005
date

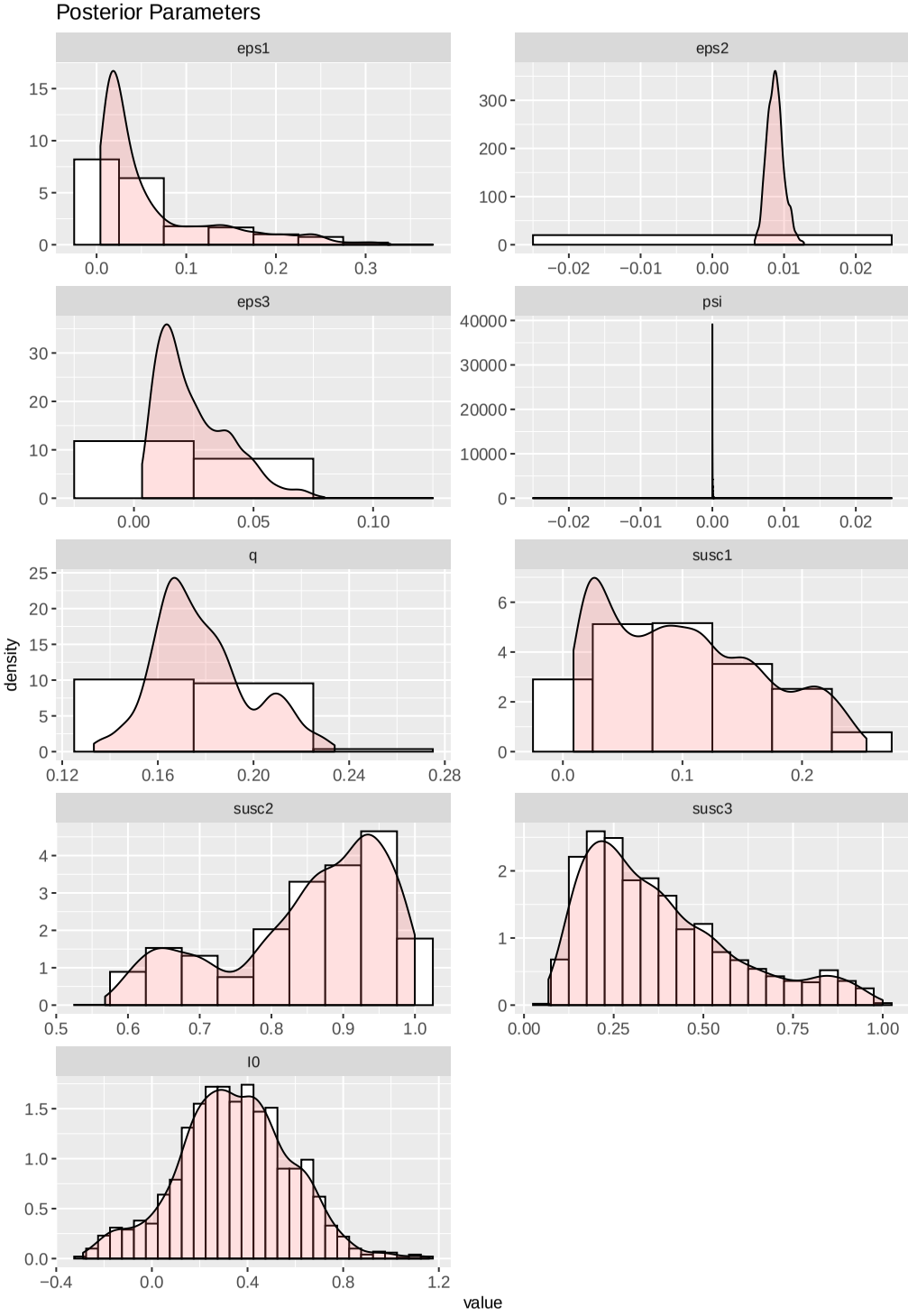
Posterior Parameters
eps1
eps2
eps3
psi
q
susc1
susc2
susc3
I0
density
value

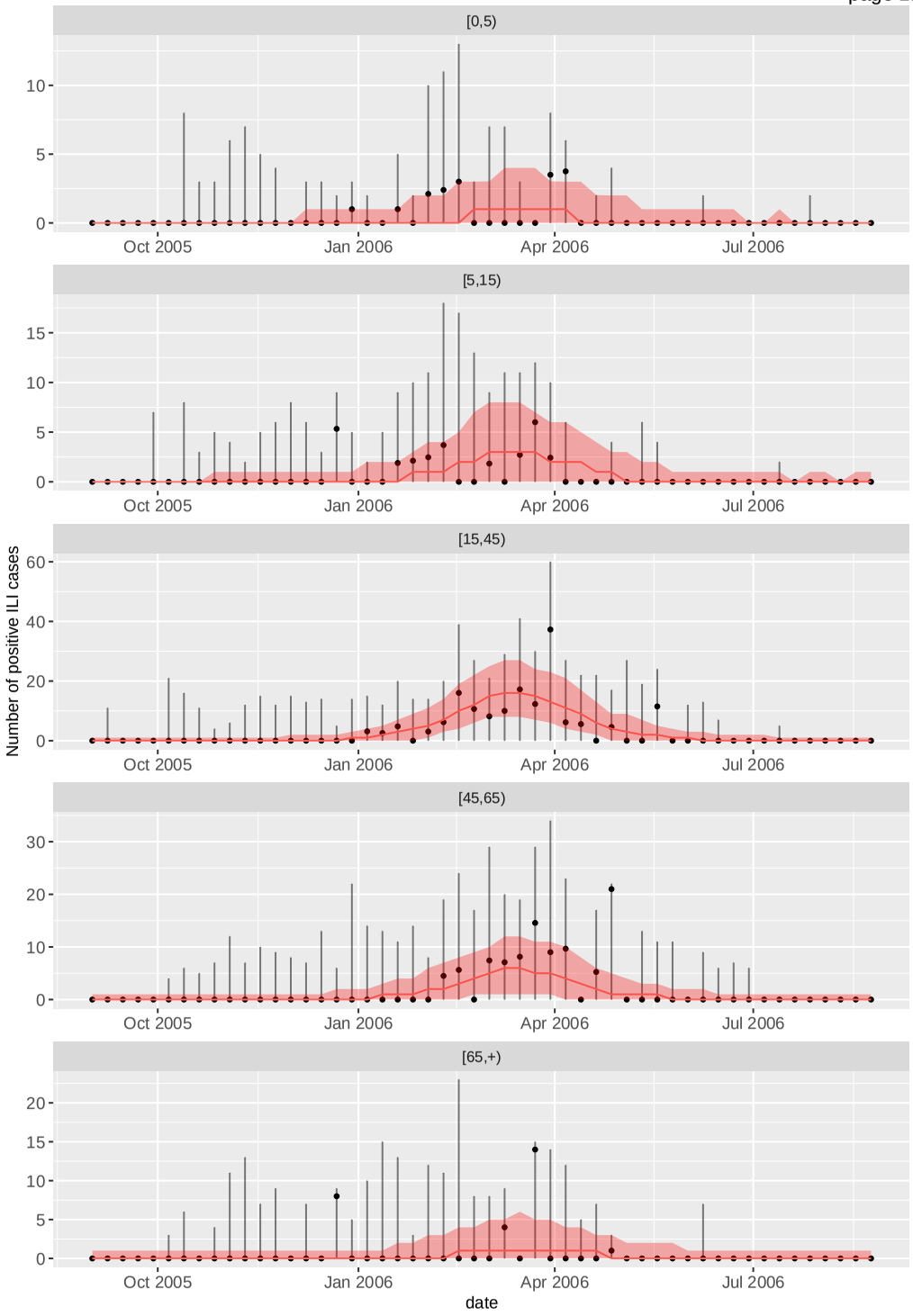
[0,5)
[5,15)
[15,45)
[45,65)
[65,+)
Number of positive ILI cases
Oct 2005
Jan 2006
Apr 2006
Jul 2006
date

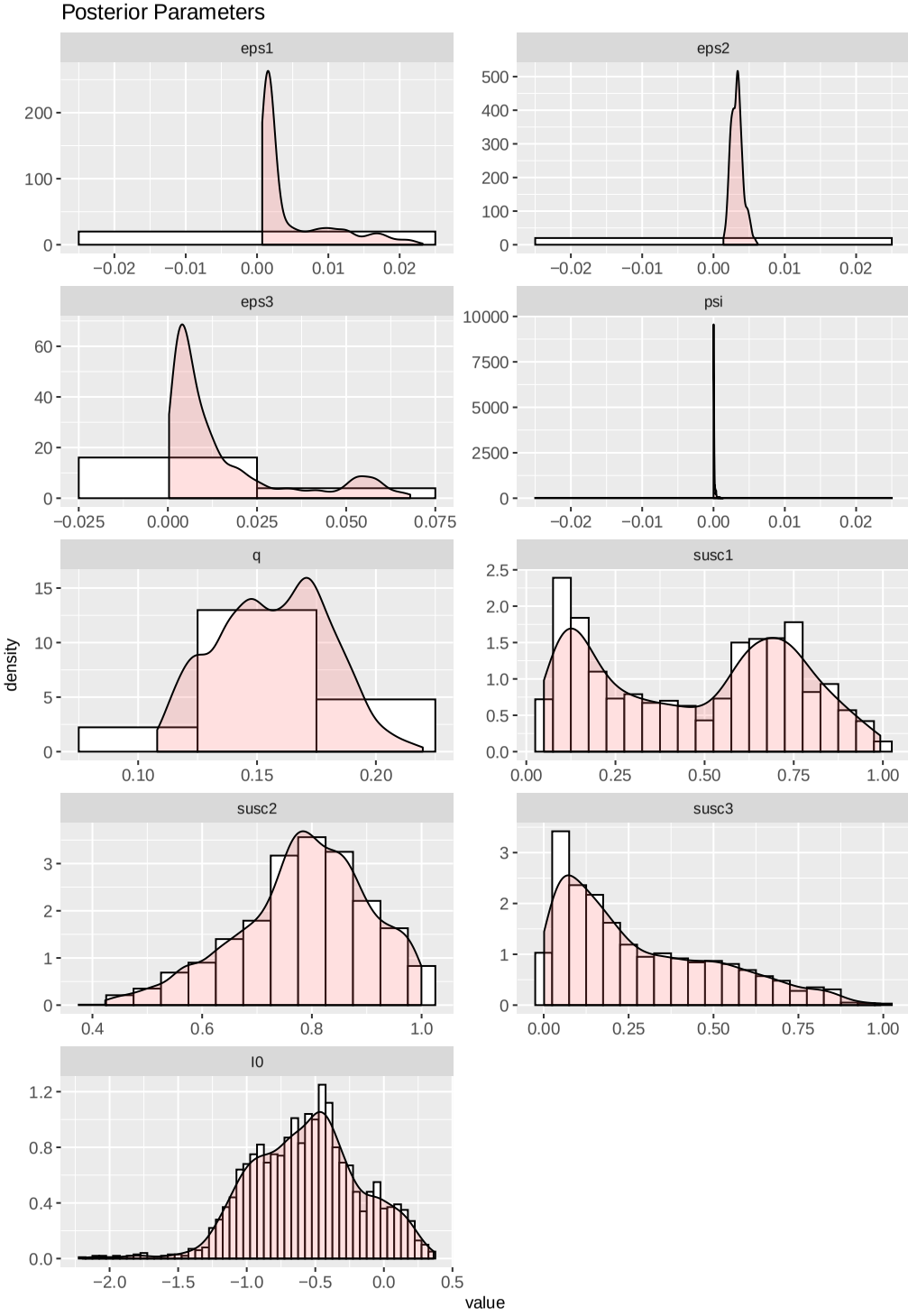
Posterior Parameters
eps1
eps2
eps3
psi
q
susc1
susc2
susc3
I0
density
value

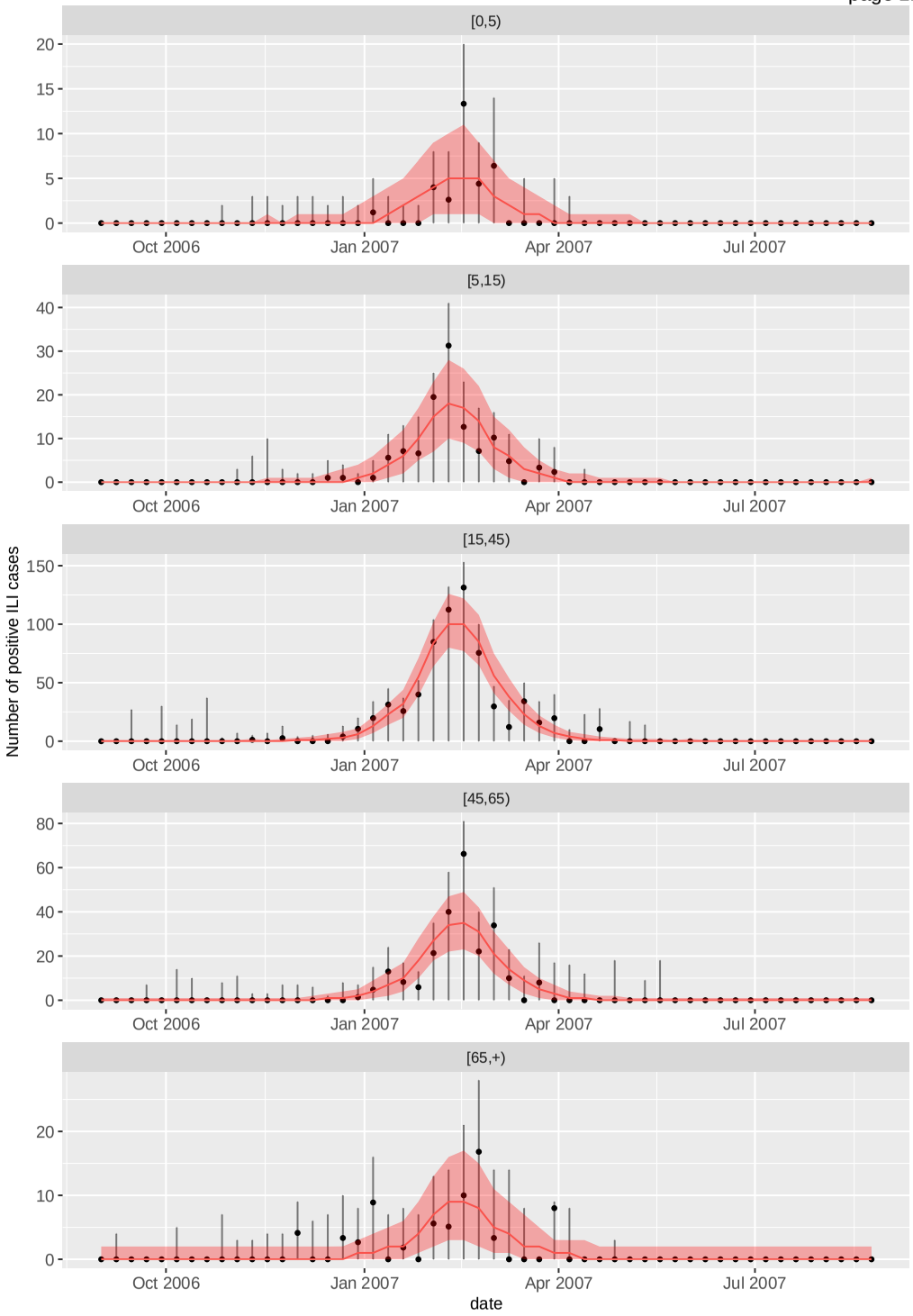
[0,5)
[5,15)
[15,45)
[45,65)
[65,+)
Oct 2006
Jan 2007
Apr 2007
Jul 2007
Number of positive ILI cases
date

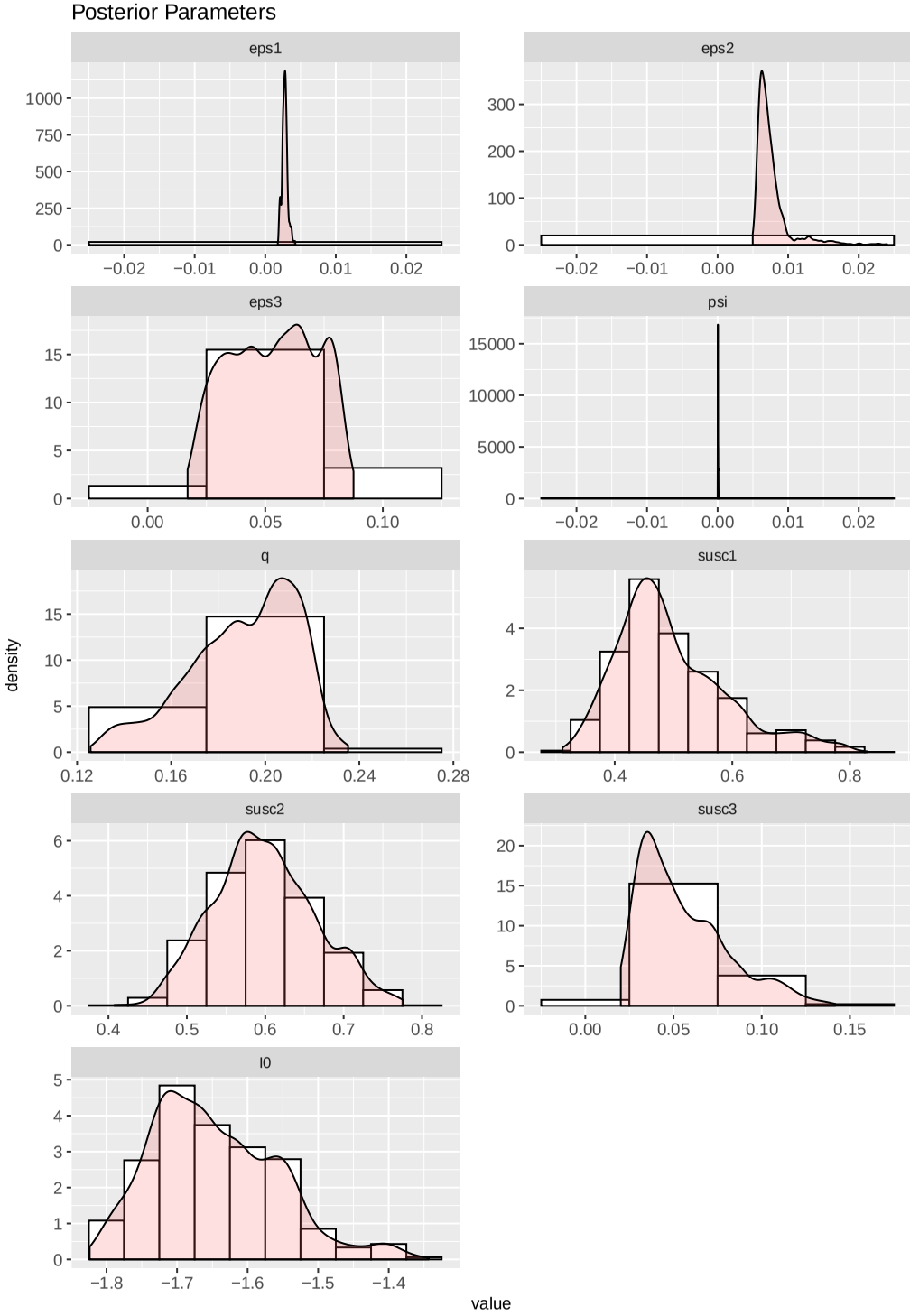
Posterior Parameters
eps1
eps2
eps3
psi
q
susc1
susc2
susc3
l0
density
value

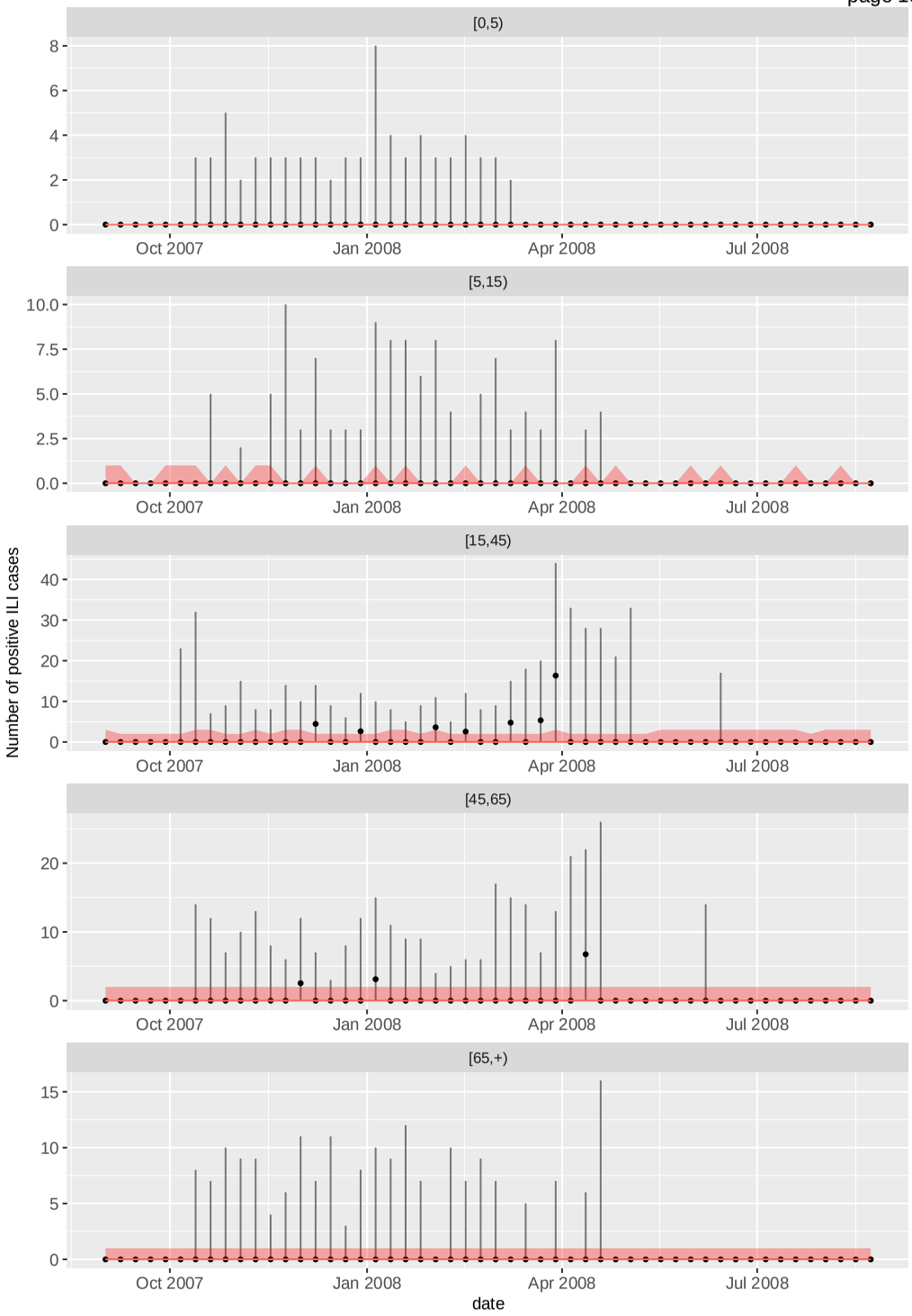
[0,5)
[5,15)
[15,45)
[45,65)
[65,+)
Oct 2007
Jan 2008
Apr 2008
Jul 2008
Number of positive ILI cases
date

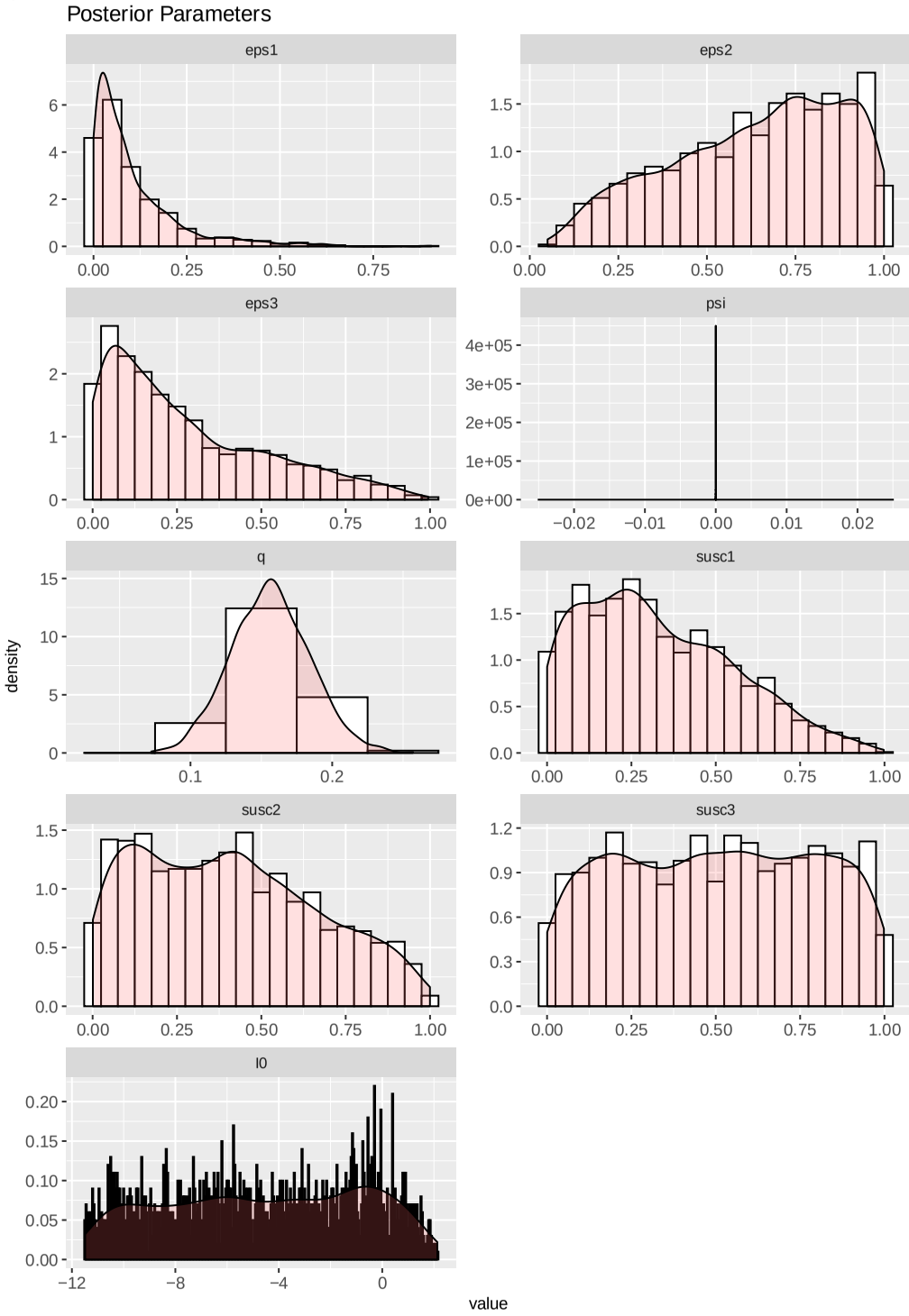
Posterior Parameters
eps1
eps2
eps3
psi
q
susc1
susc2
susc3
I0
density
value

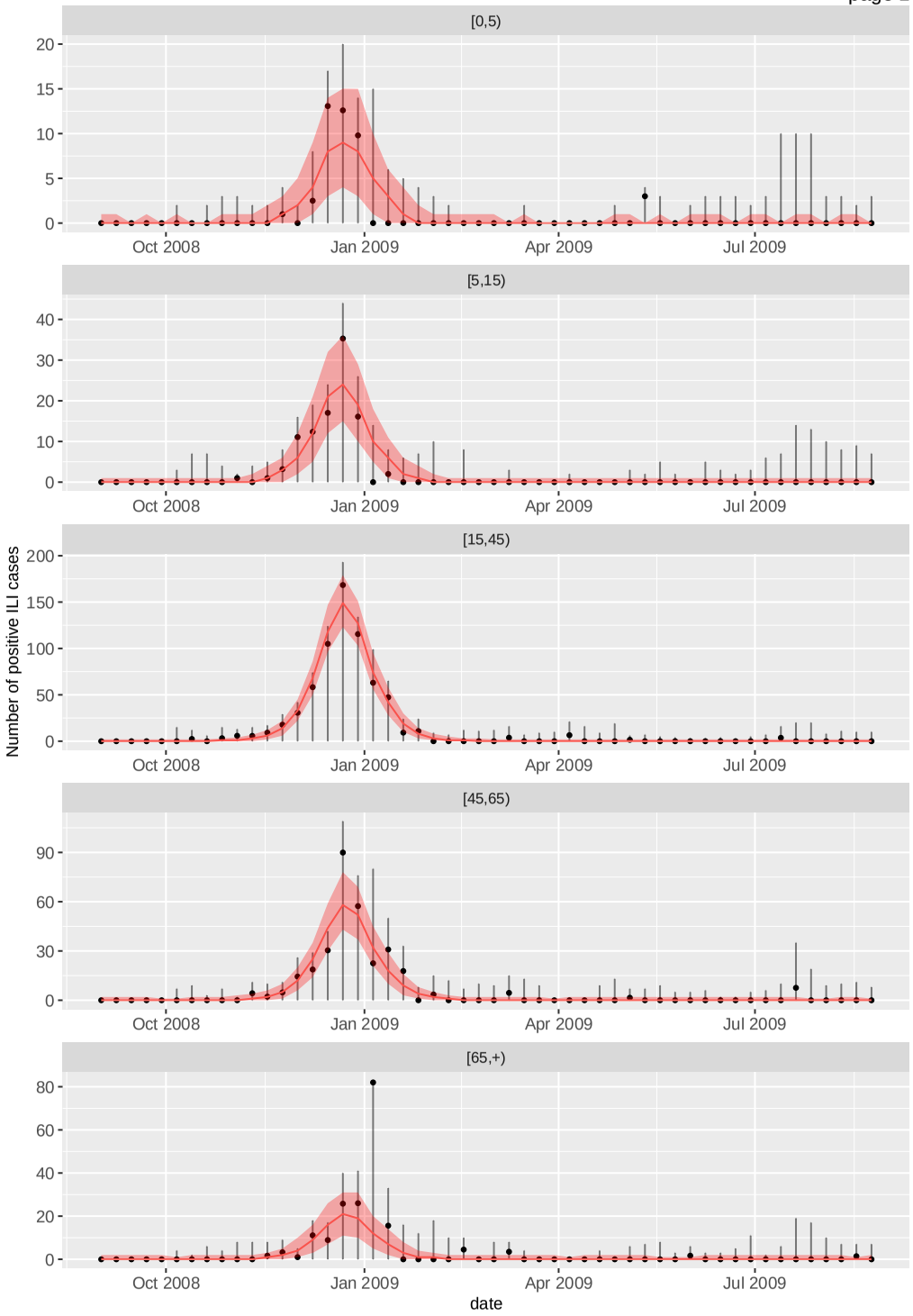
[0,5)
[5,15)
[15,45)
[45,65)
[65,+)
Number of positive ILI cases
Oct 2008
Jan 2009
Apr 2009
Jul 2009
date

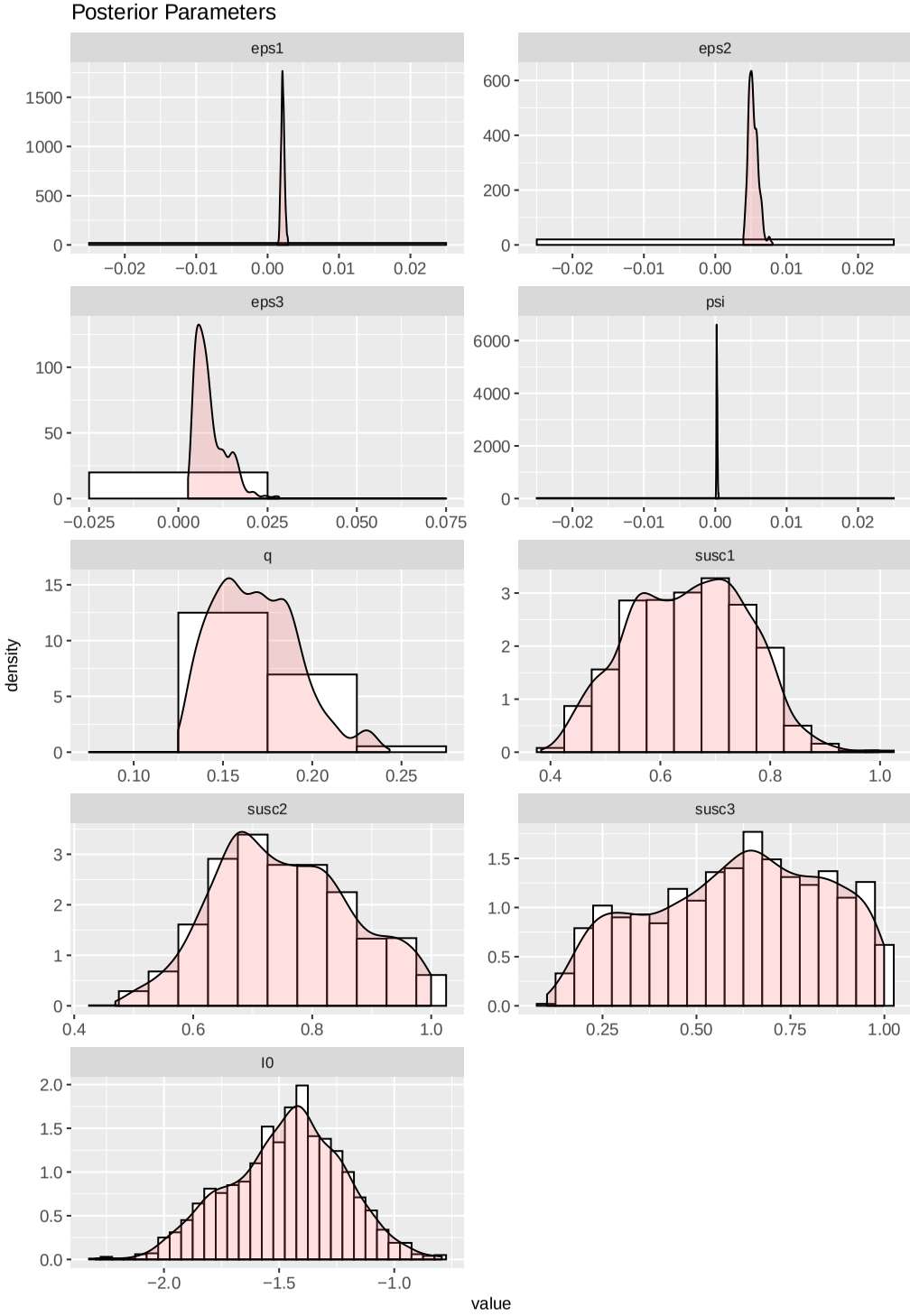
Posterior Parameters
eps1
eps2
eps3
psi
q
susc1
susc2
susc3
I0
density
value

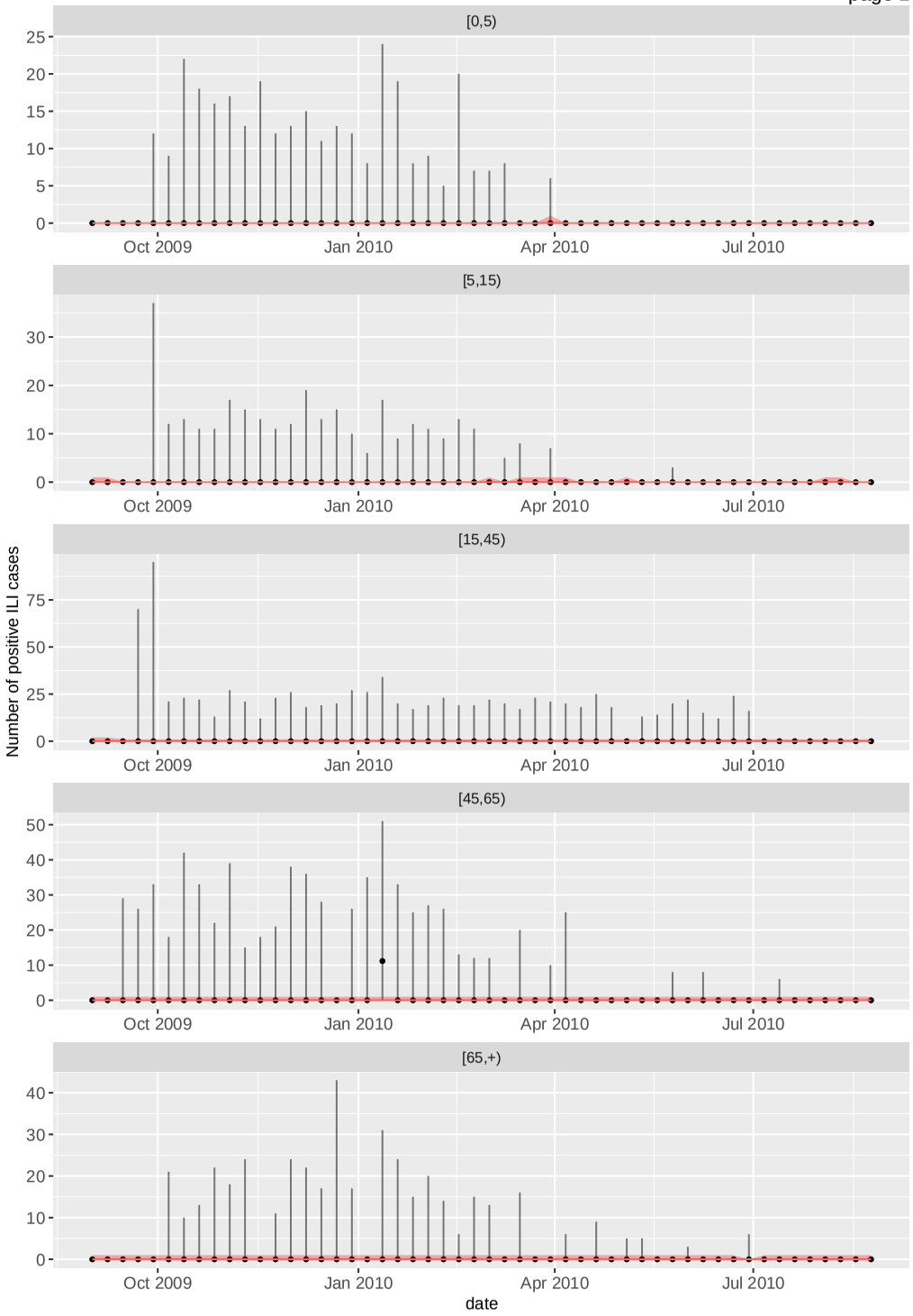
[0,5)
[5,15)
[15,45)
[45,65)
[65,+)
Number of positive ILI cases
Oct 2009
Jan 2010
Apr 2010
Jul 2010
date

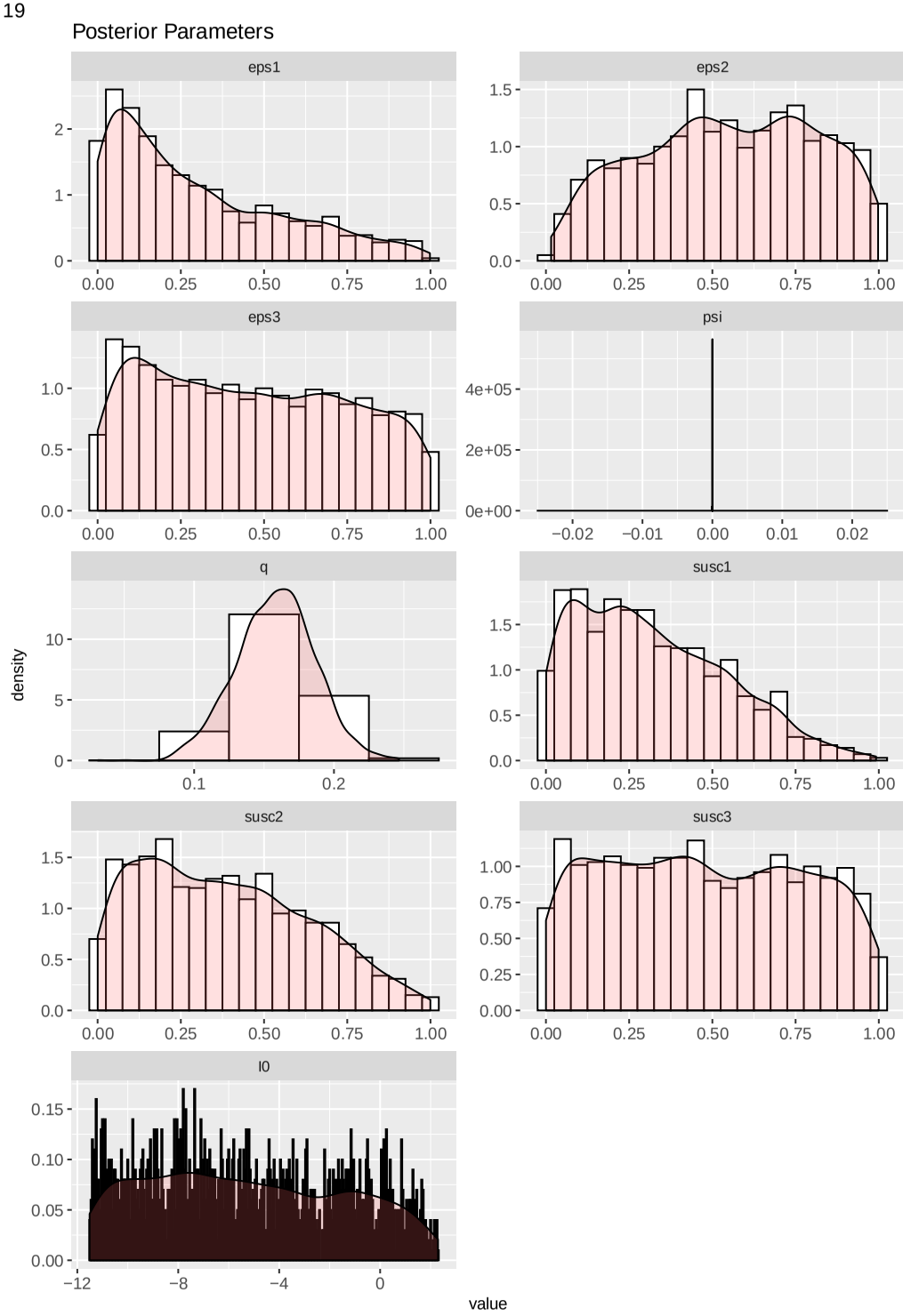
Posterior Parameters
eps1
eps2
eps3
psi
q
susc1
susc2
susc3
I0
density
value

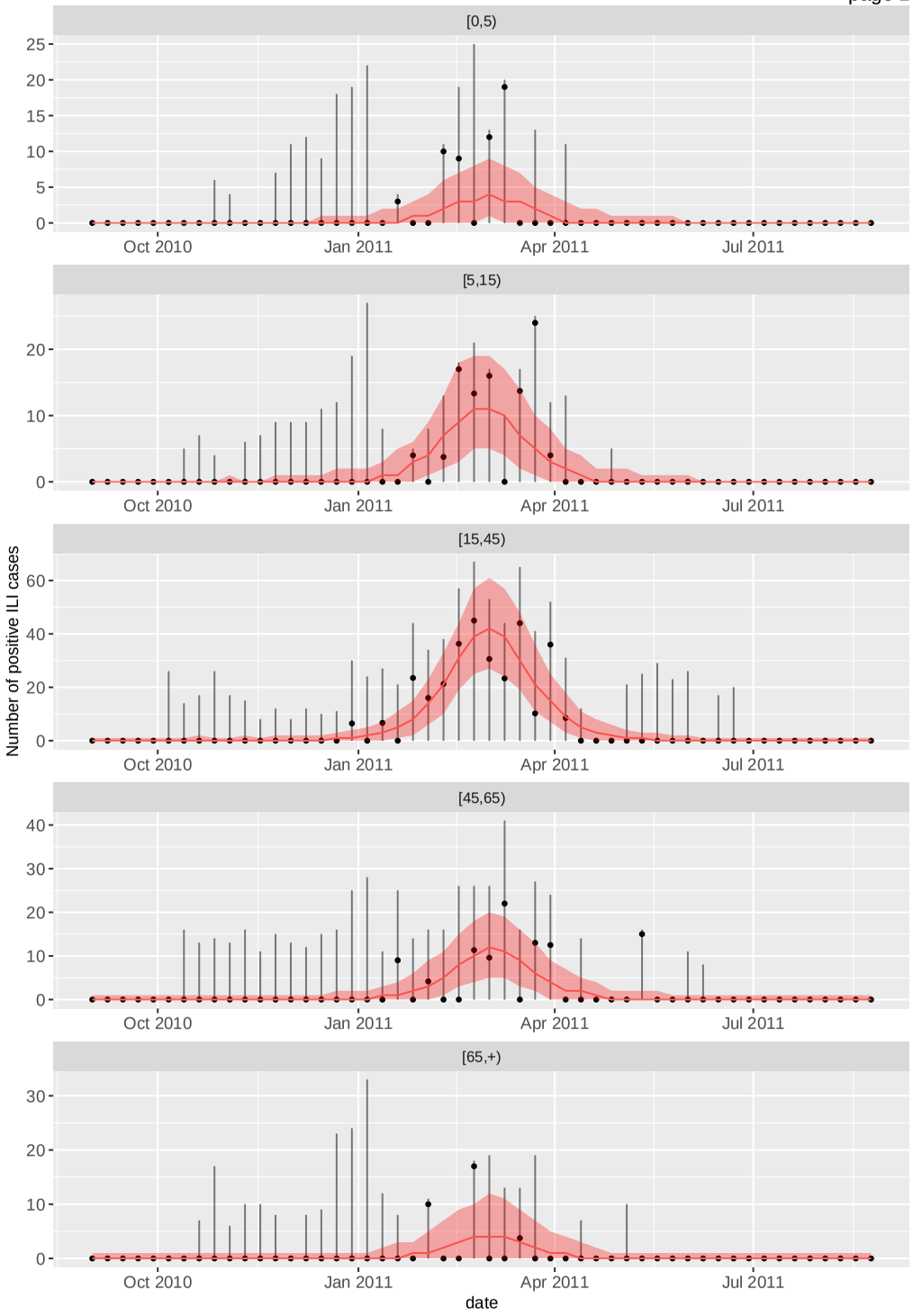

Posterior Parameters

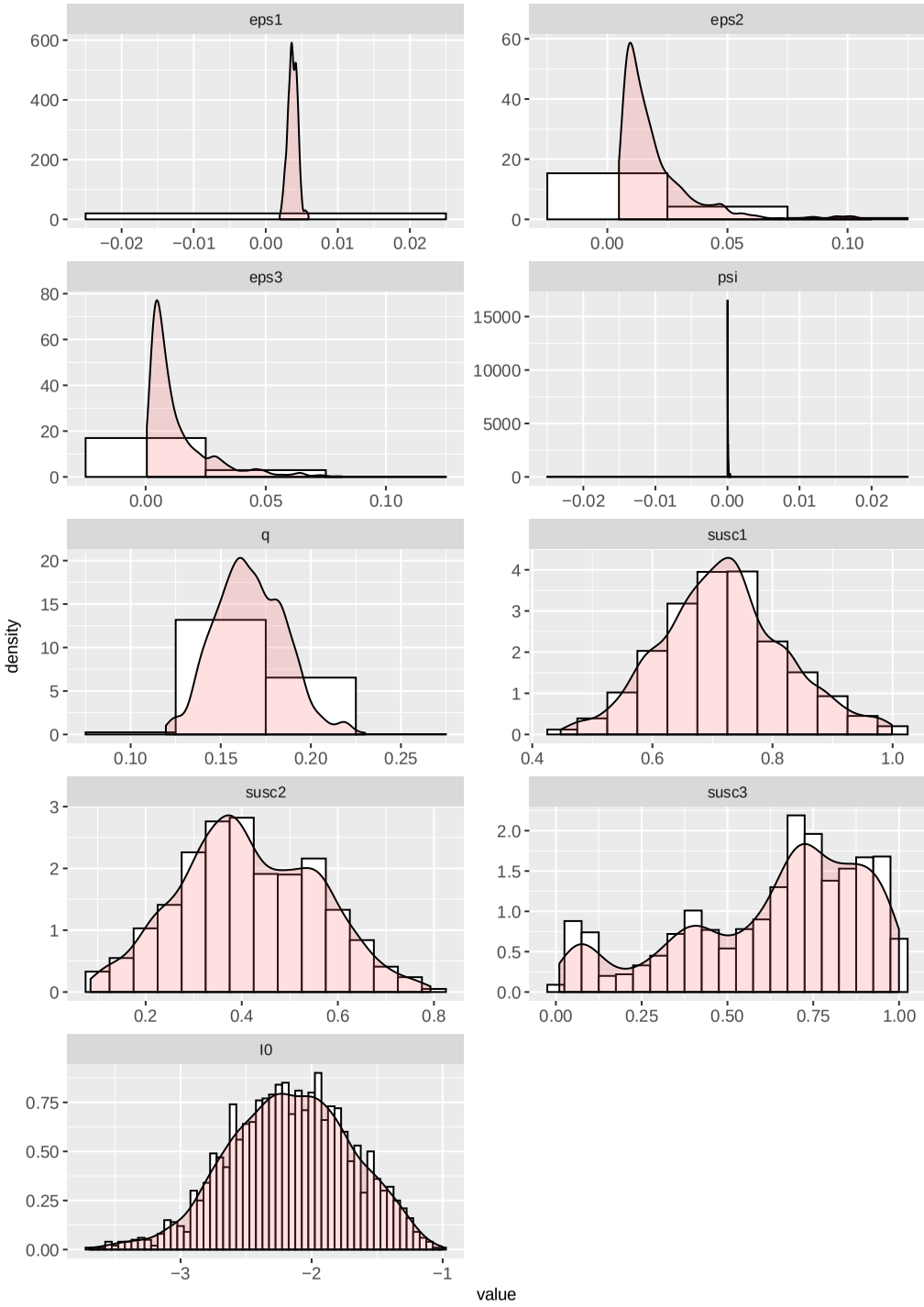

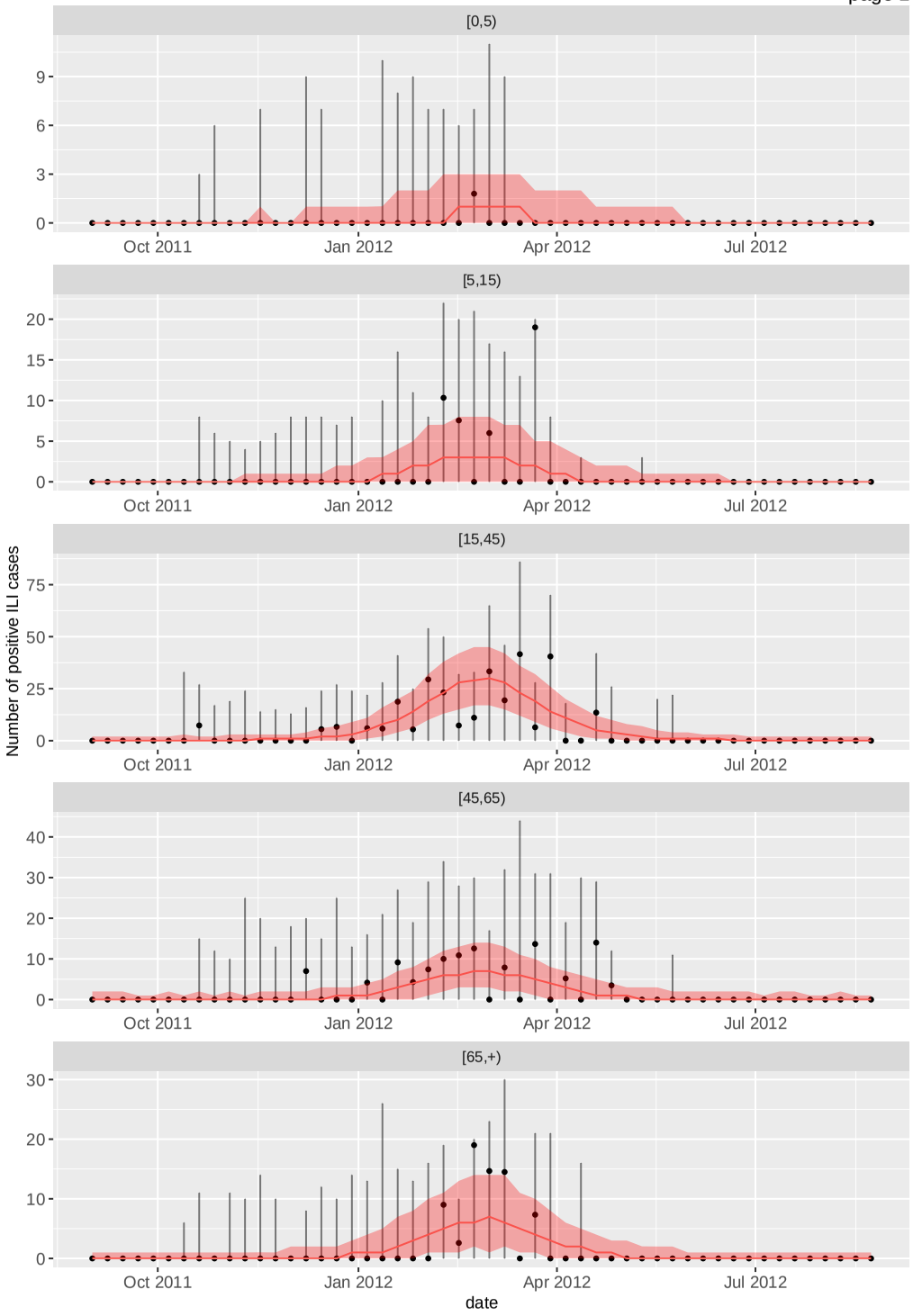
[0,5)
[5,15)
[15,45)
[45,65)
[65,+)
Oct 2011
Jan 2012
Apr 2012
Jul 2012
Number of positive ILI cases
date

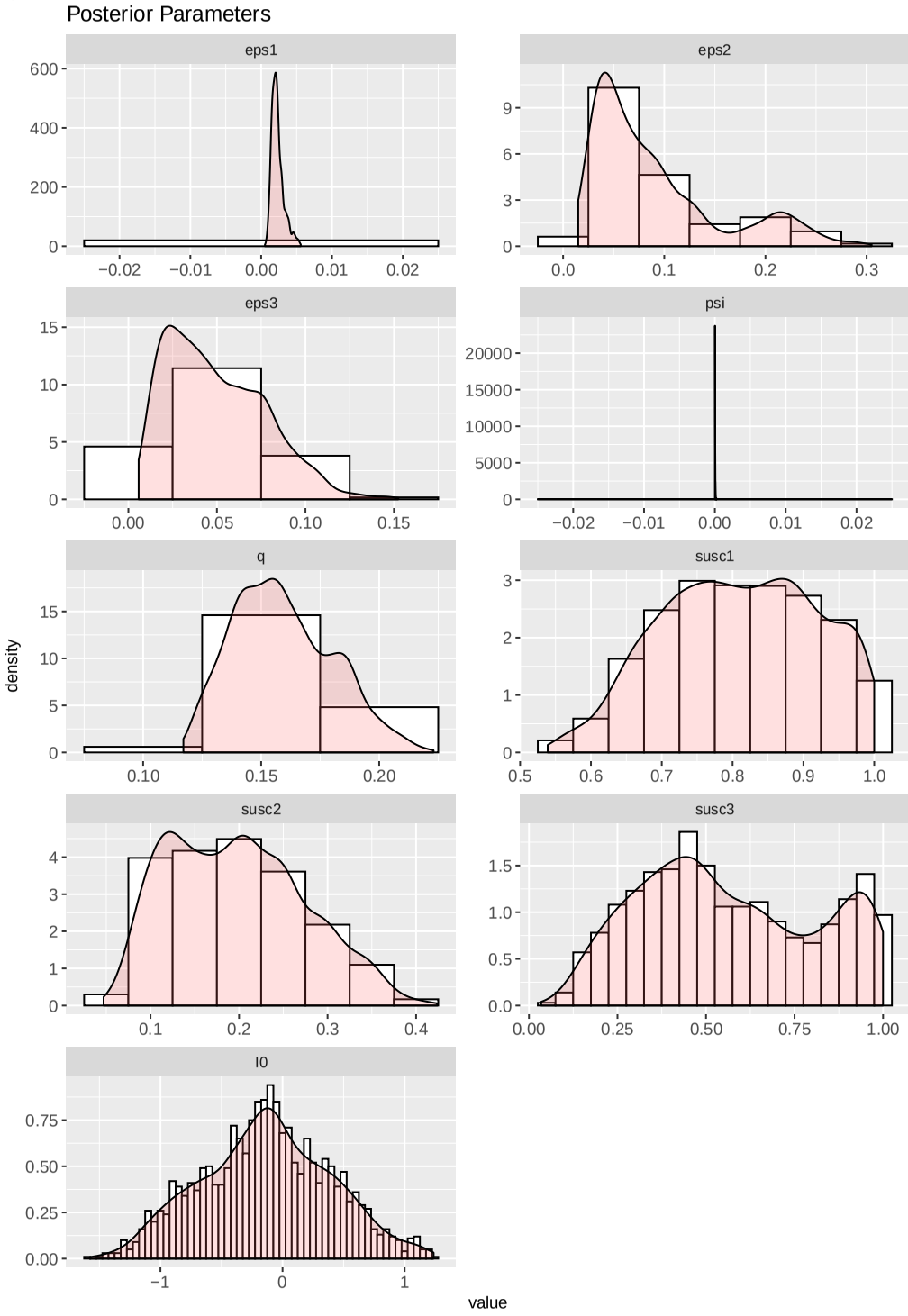
Posterior Parameters
eps1
eps2
eps3
psi
q
susc1
susc2
susc3
I0
density
value

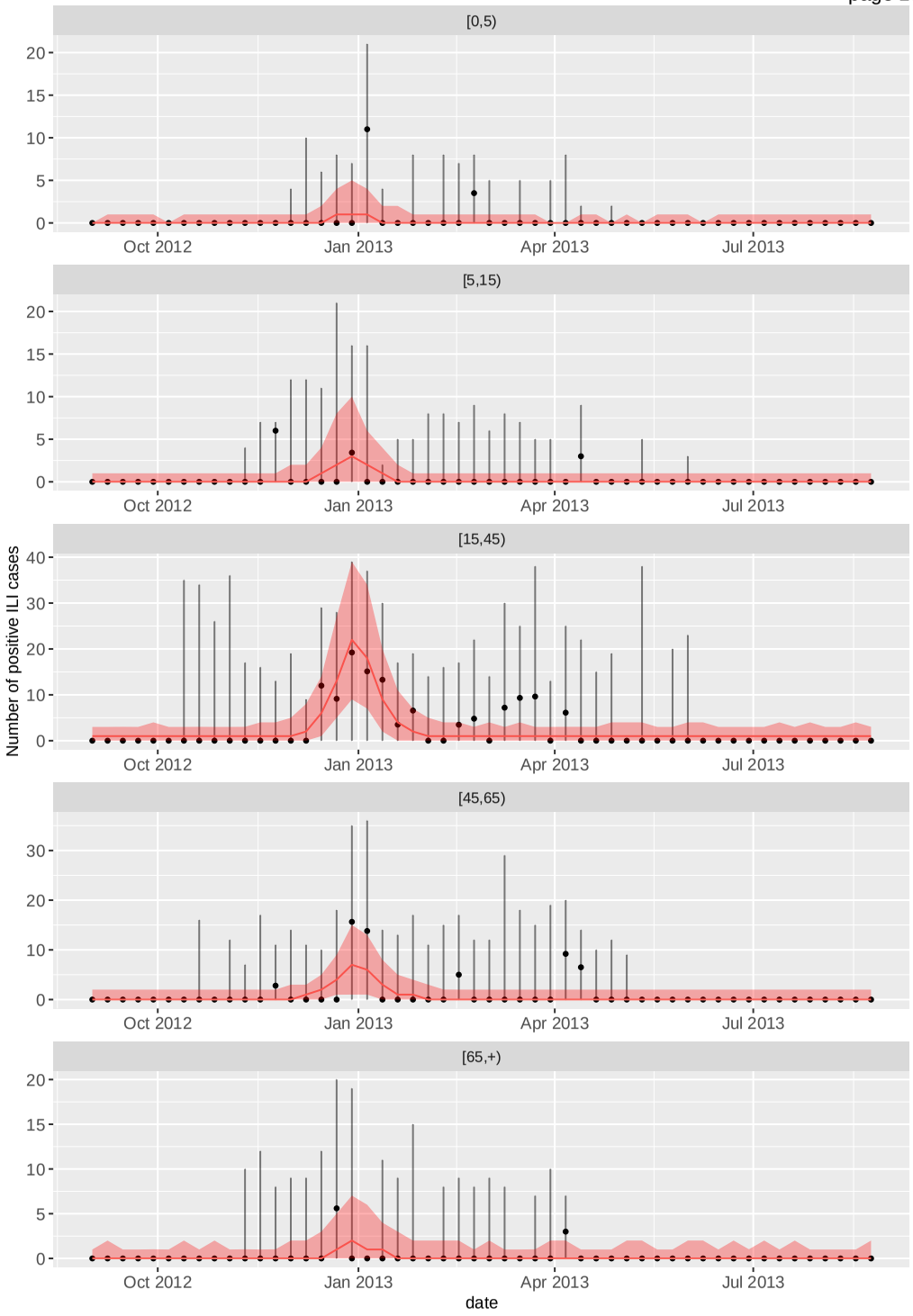

Posterior Parameters

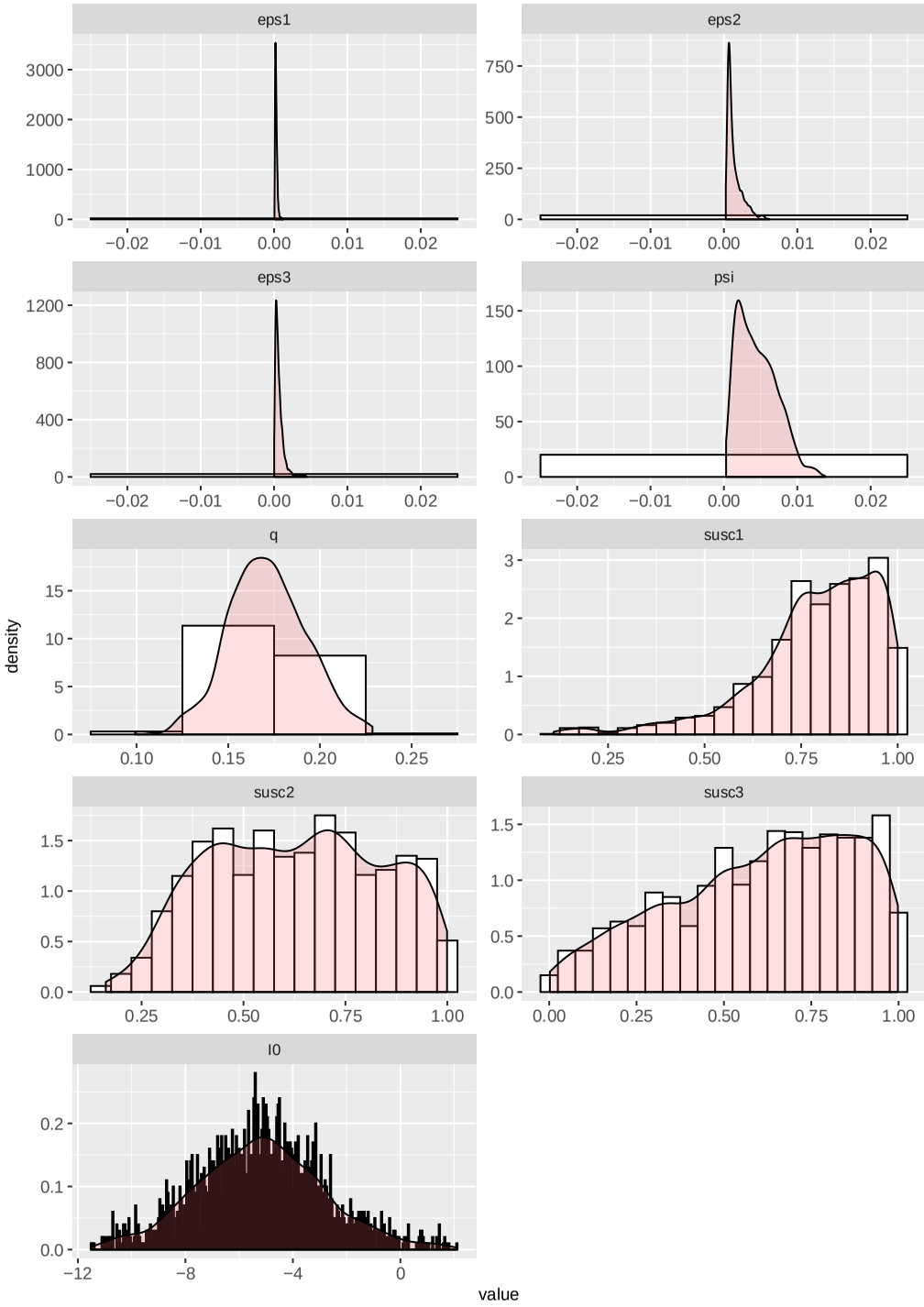

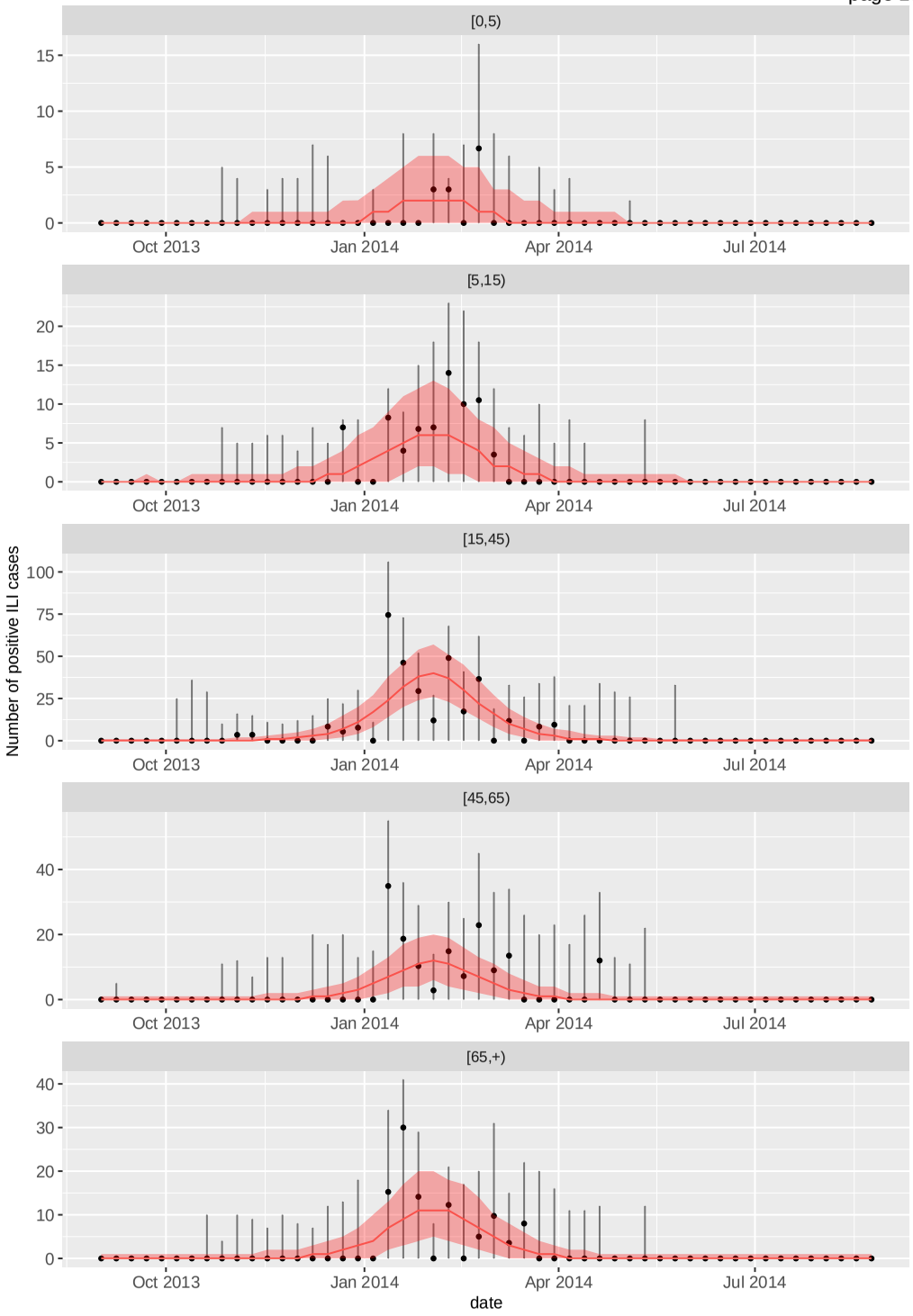
[0,5)
[5,15)
[15,45)
[45,65)
[65,+)
Number of positive ILI cases
Oct 2013
Jan 2014
Apr 2014
Jul 2014
date

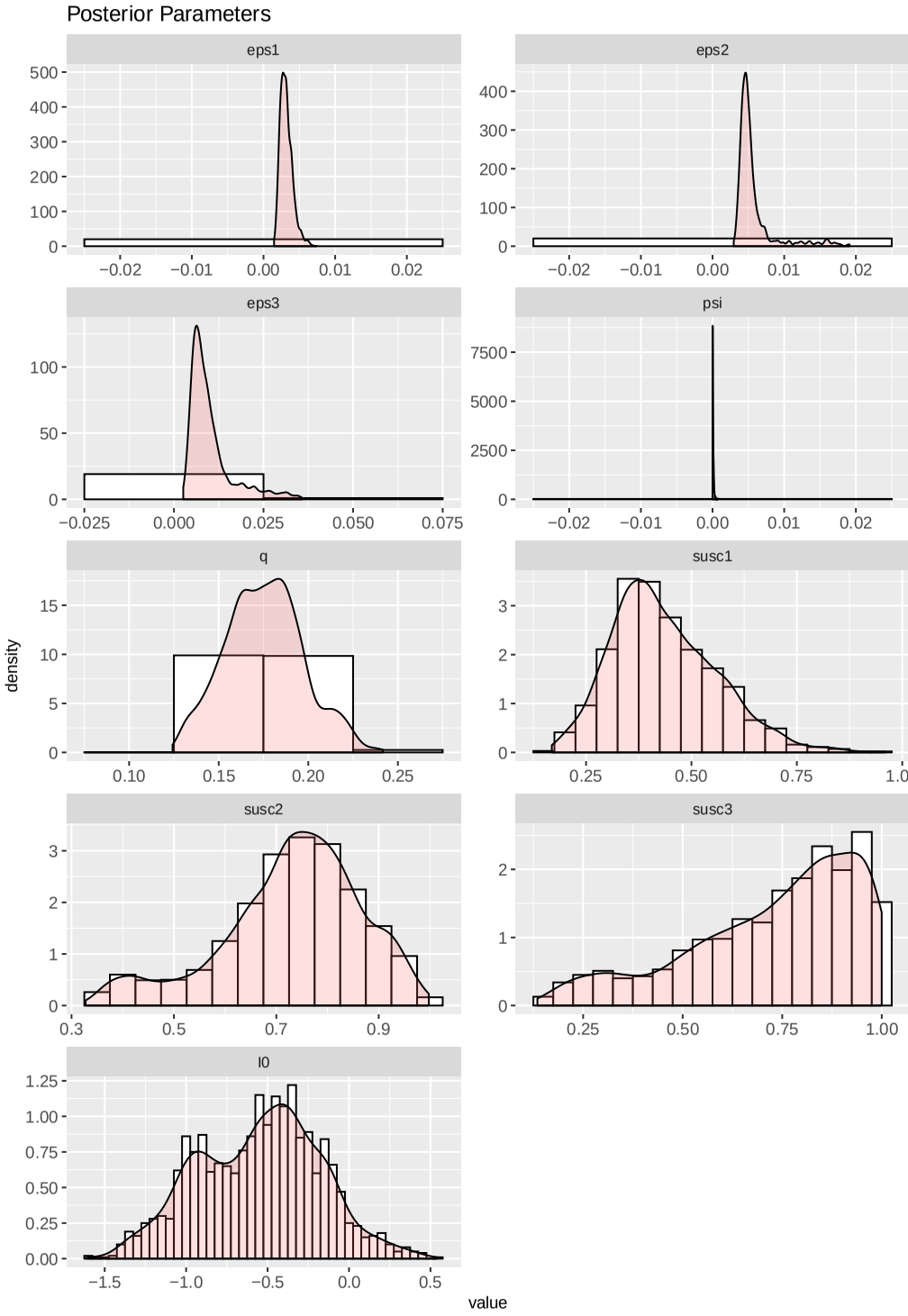
Posterior Parameters
eps1
eps2
eps3
psi
q
susc1
susc2
susc3
I0
density
value

A1.3 Model Fits for Influenza Strain B

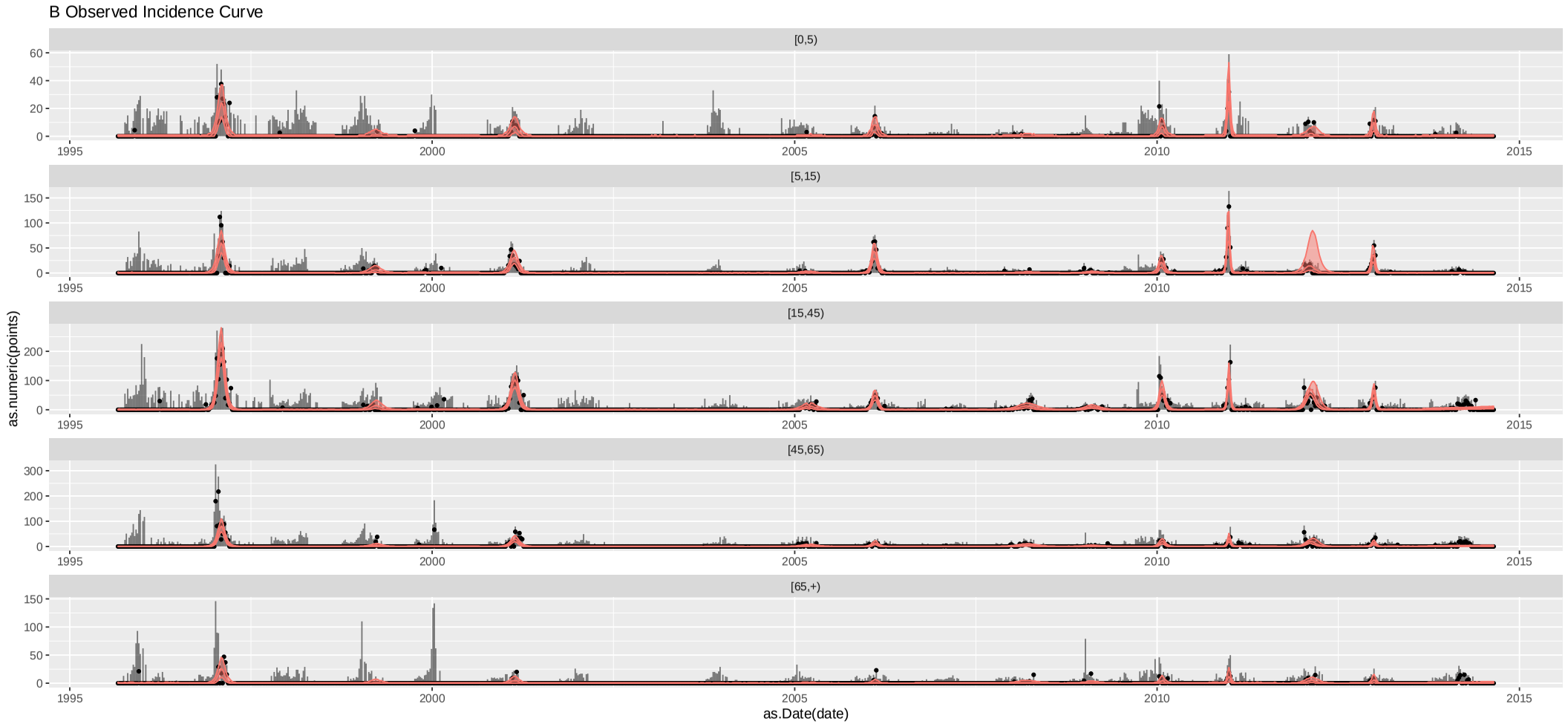
B Observed Incidence Curve
[0,5)
[5,15)
[15,45)
[45,65)
[65,+)
as.numeric(points)
as.Date(date)
1995
2000
2005
2010
2015

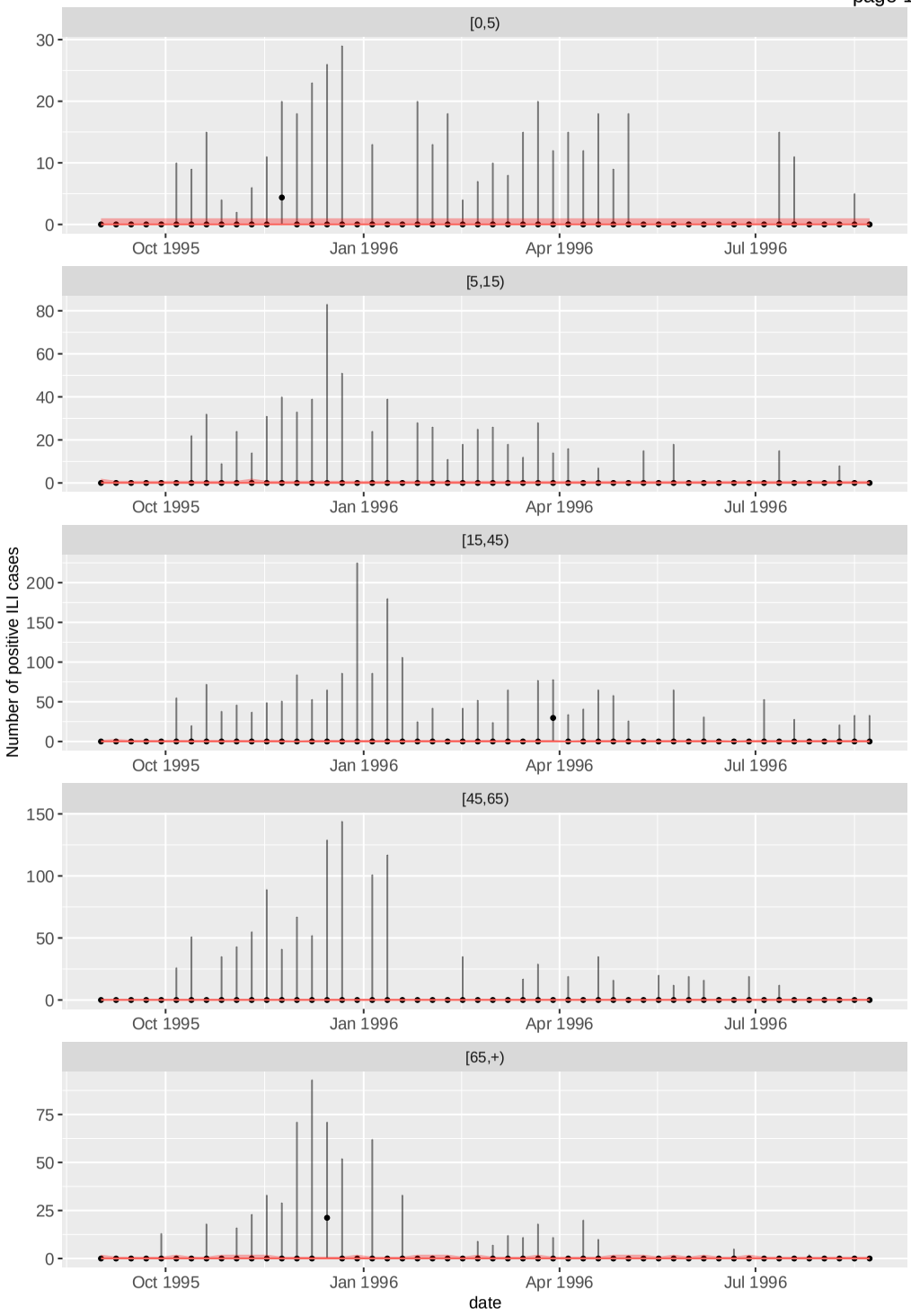
[0,5)
[5,15)
[15,45)
[45,65)
[65,+)
Number of positive ILI cases
Oct 1995
Jan 1996
Apr 1996
Jul 1996
date

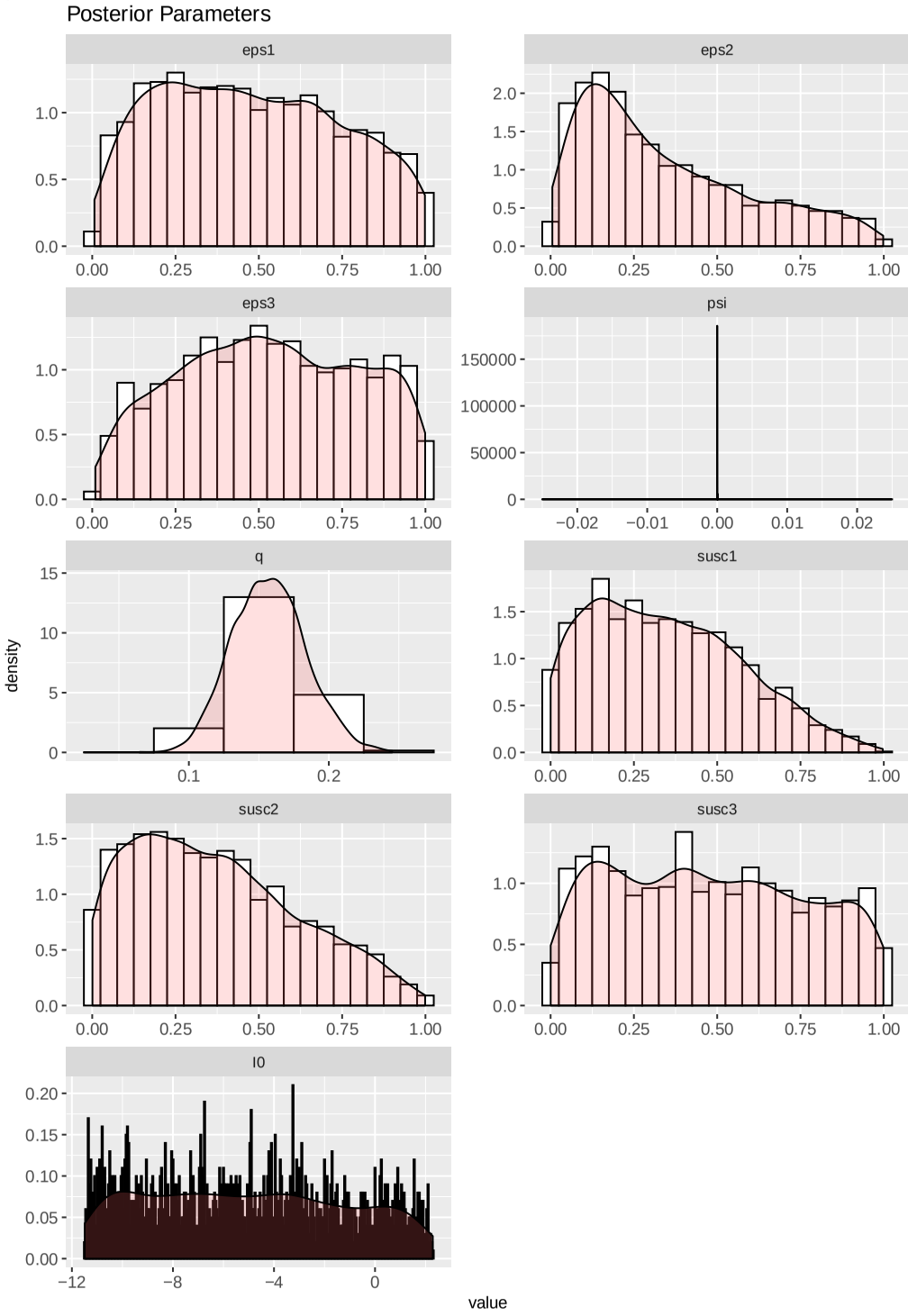
Posterior Parameters
eps1
eps2
eps3
psi
q
susc1
susc2
susc3
I0
density
value

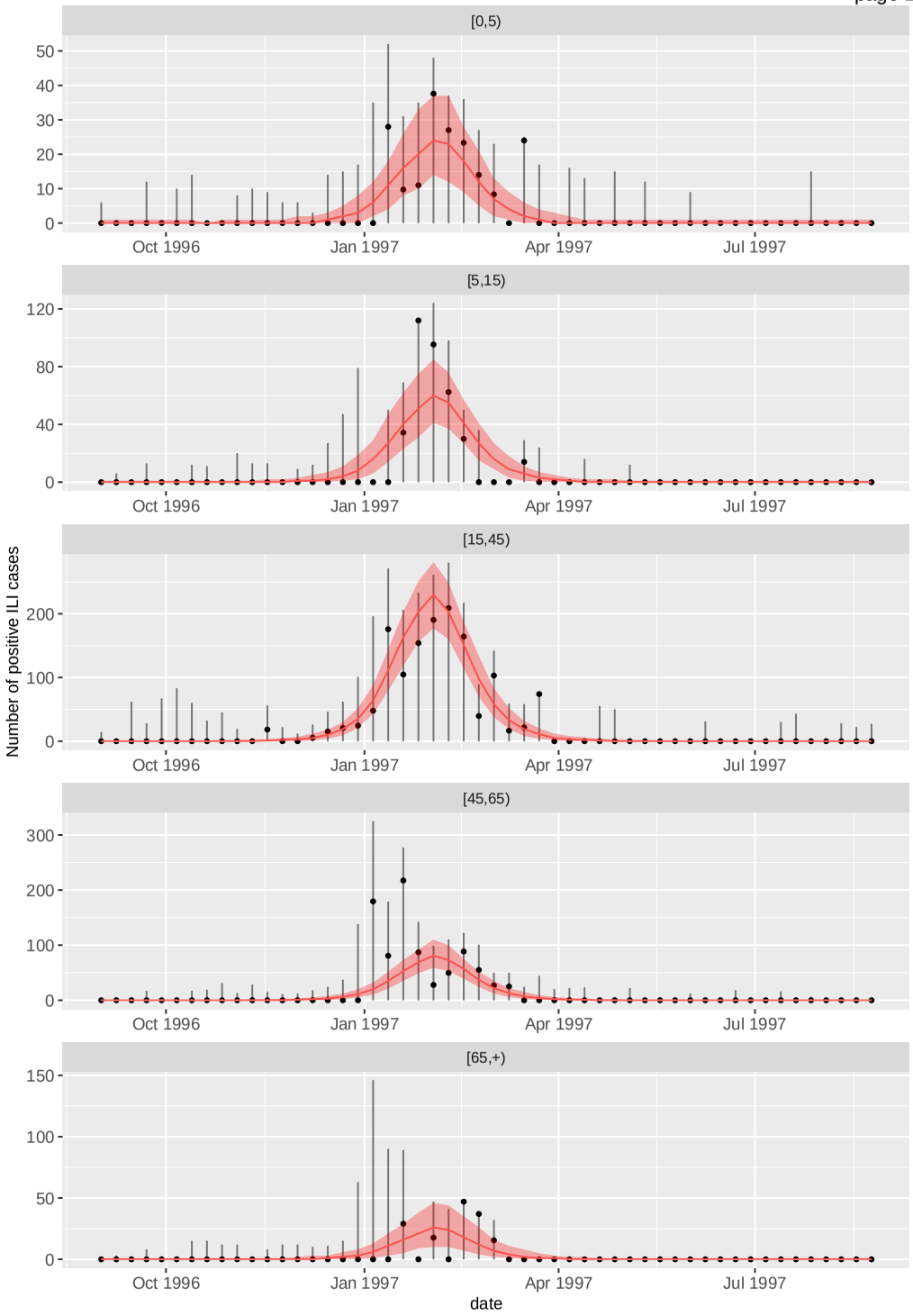
[0,5)
[5,15)
[15,45)
[45,65)
[65,+)
Oct 1996
Jan 1997
Apr 1997
Jul 1997
Number of positive ILI cases
date

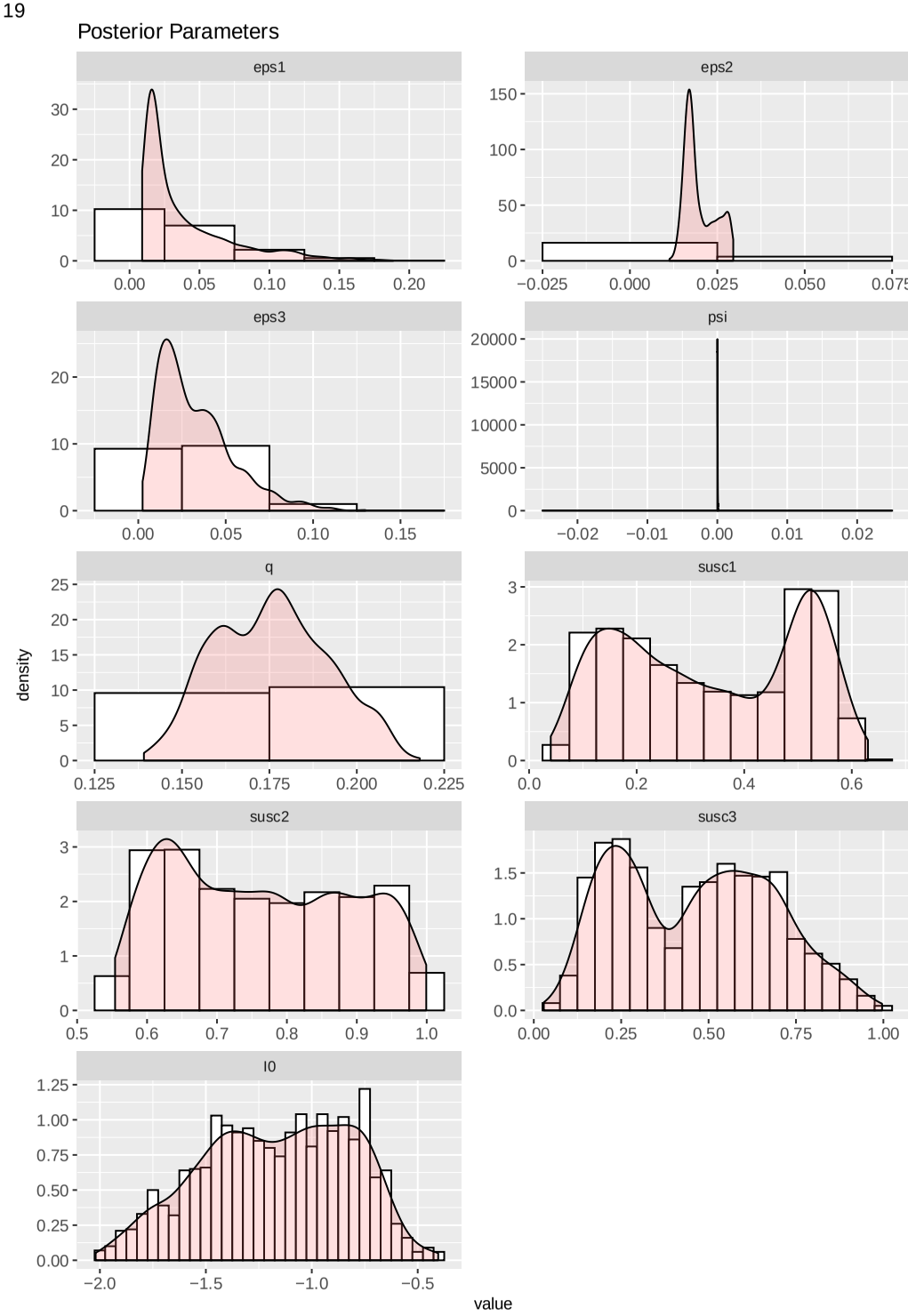
Posterior Parameters
eps1
eps2
eps3
psi
q
susc1
susc2
susc3
I0
density
value

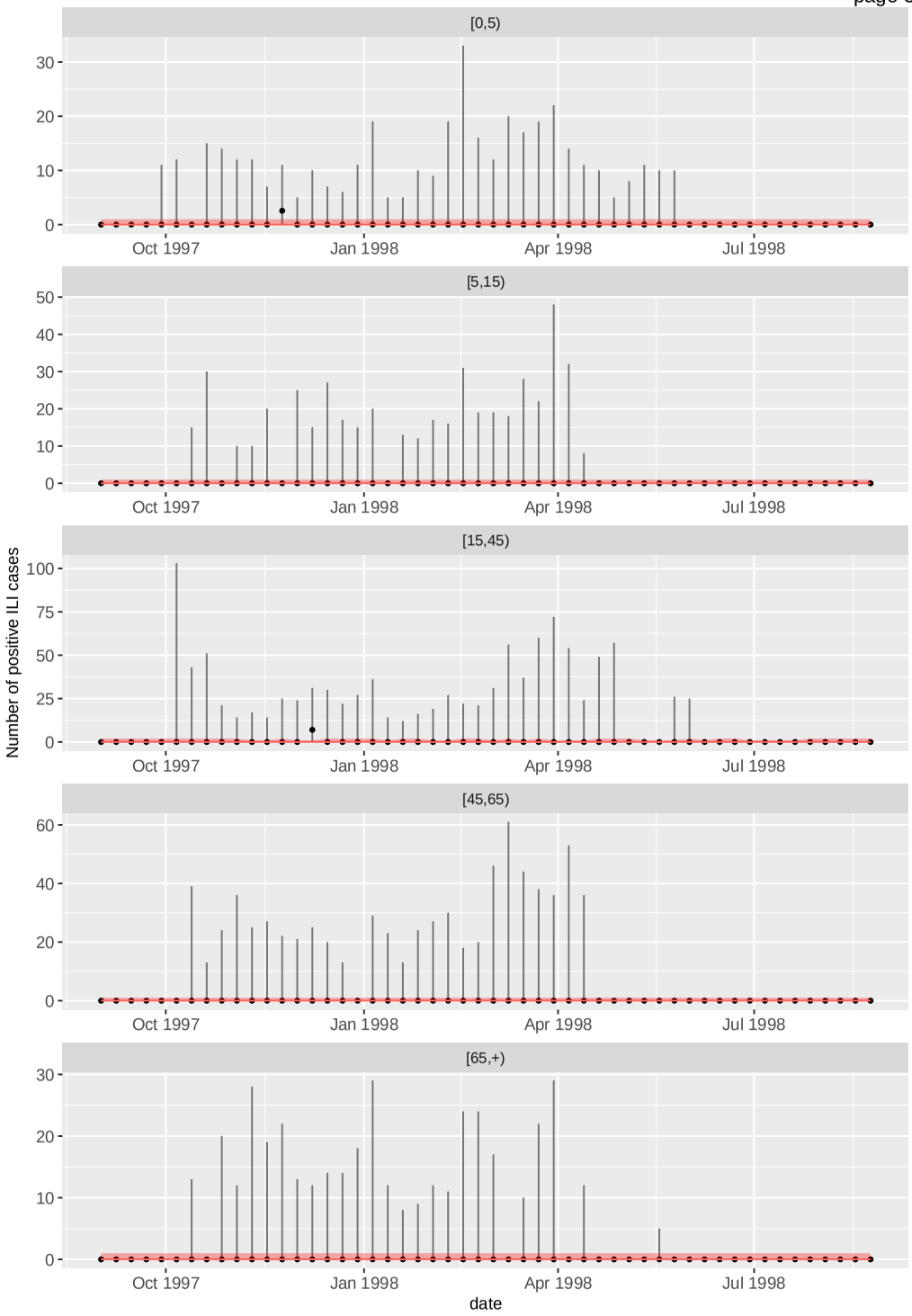
[0,5)
[5,15)
[15,45)
[45,65)
[65,+)
Oct 1997
Jan 1998
Apr 1998
Jul 1998
Number of positive ILI cases
date

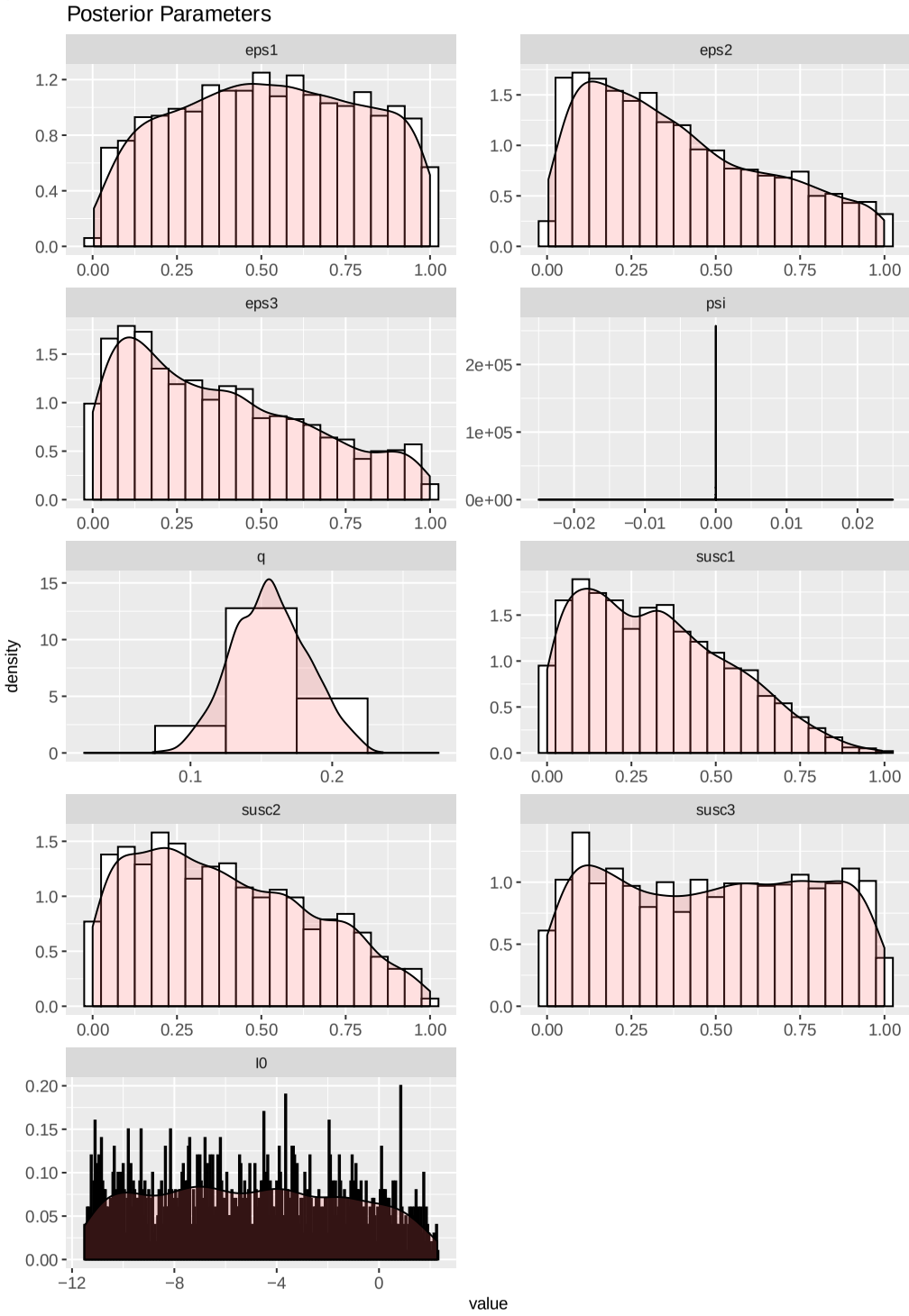
Posterior Parameters
eps1
eps2
eps3
psi
q
susc1
susc2
susc3
I0
density
value

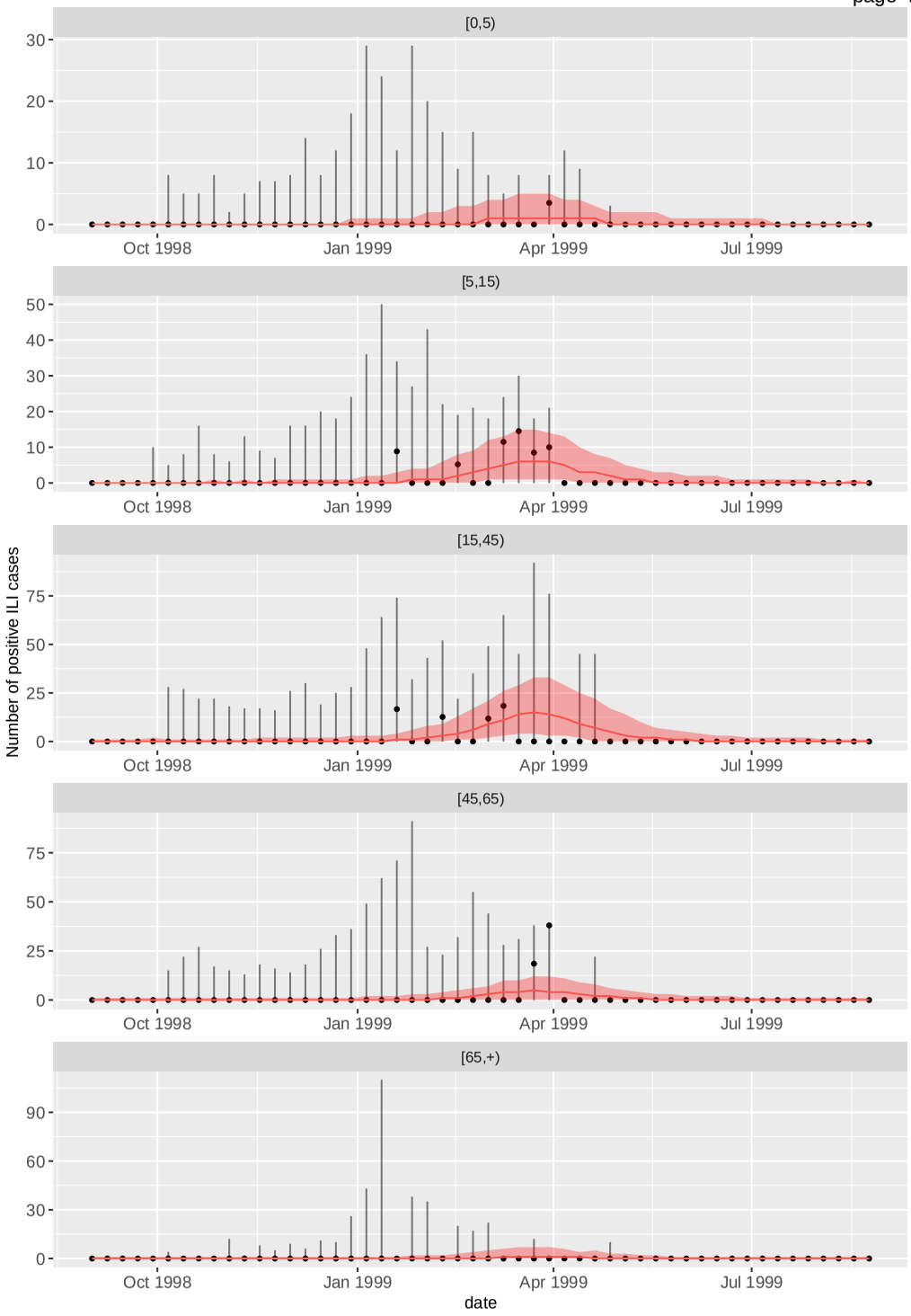
[0,5)
[5,15)
[15,45)
[45,65)
[65,+)
Oct 1998
Jan 1999
Apr 1999
Jul 1999
Number of positive ILI cases
date

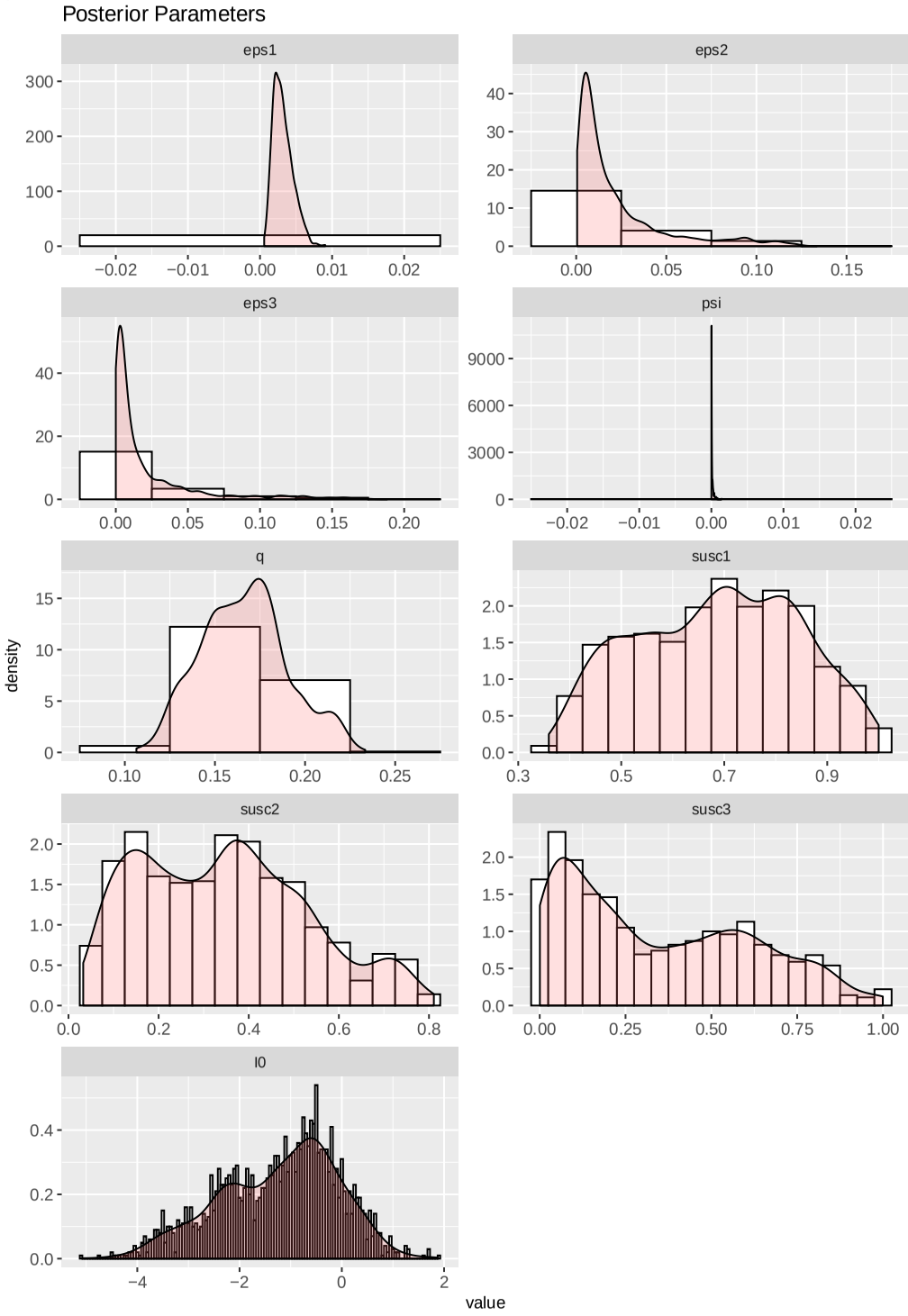
Posterior Parameters
eps1
eps2
eps3
psi
q
susc1
susc2
susc3
I0
density
value

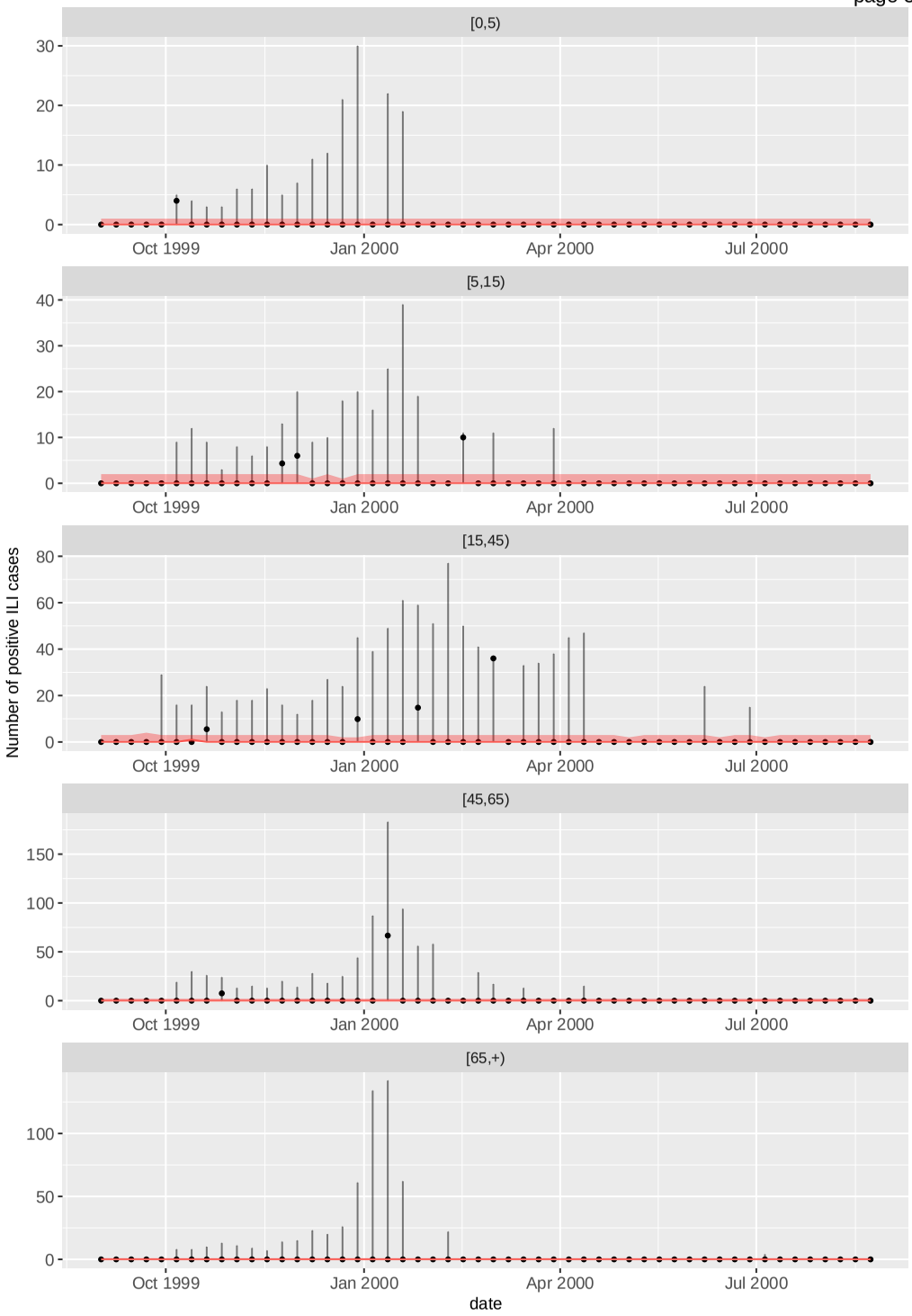
[0,5)
[5,15)
[15,45)
[45,65)
[65,+)
Number of positive ILI cases
Oct 1999
Jan 2000
Apr 2000
Jul 2000
date

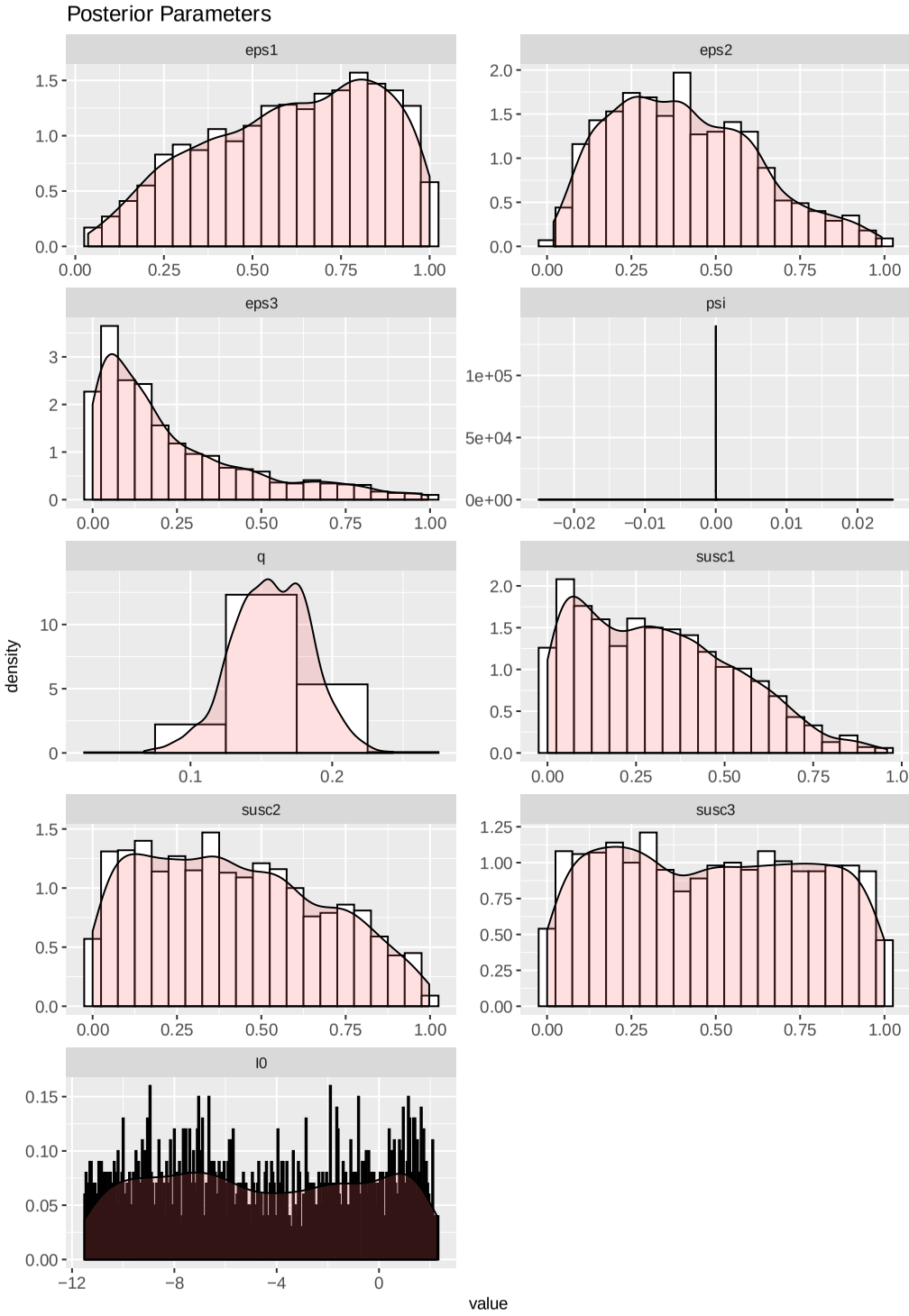
Posterior Parameters
eps1
eps2
eps3
psi
q
susc1
susc2
susc3
I0
density
value

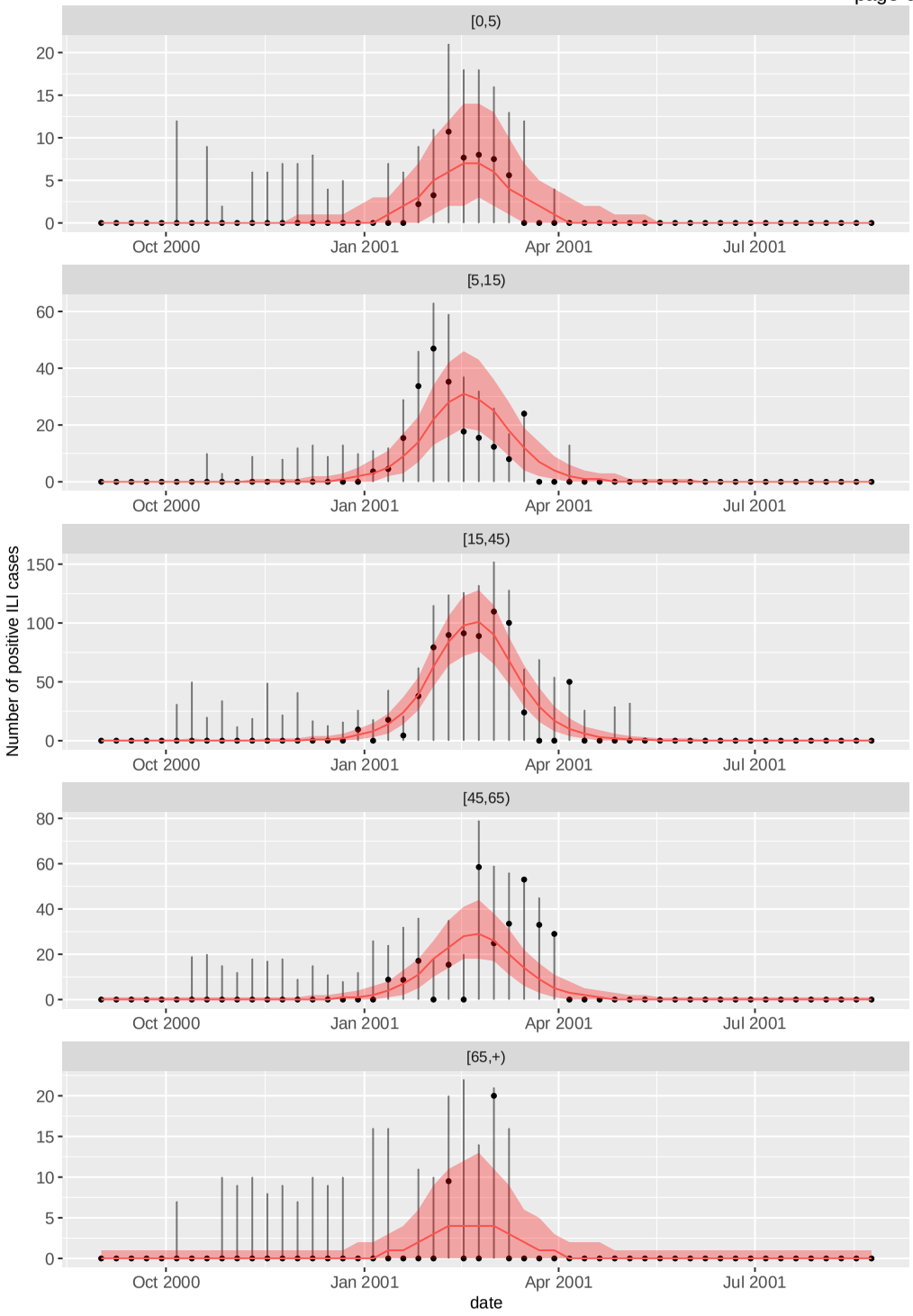
[0,5)
[5,15)
[15,45)
[45,65)
[65,+)
Oct 2000
Jan 2001
Apr 2001
Jul 2001
Number of positive ILI cases
date

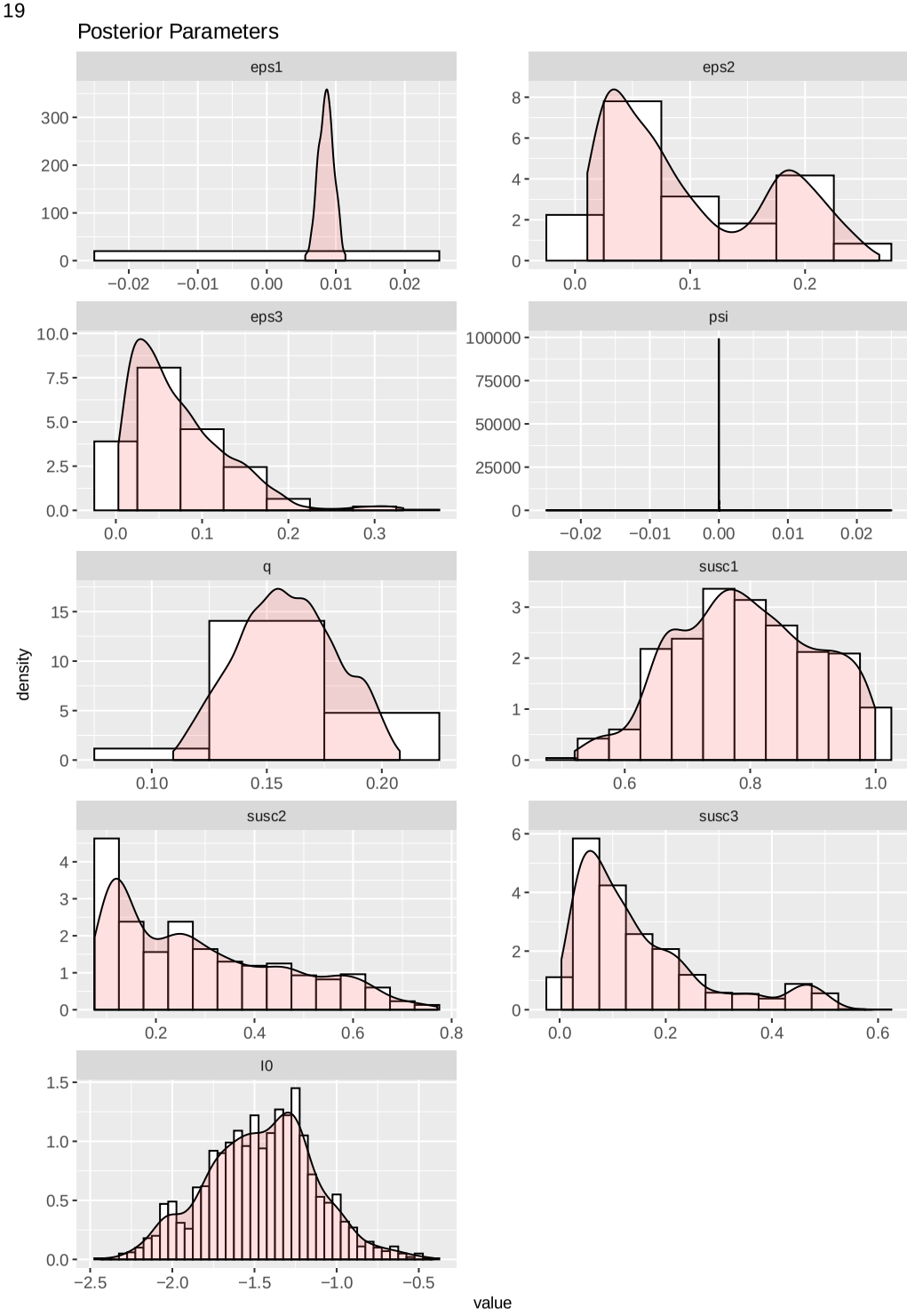
Posterior Parameters
eps1
eps2
eps3
psi
q
susc1
susc2
susc3
I0
density
value

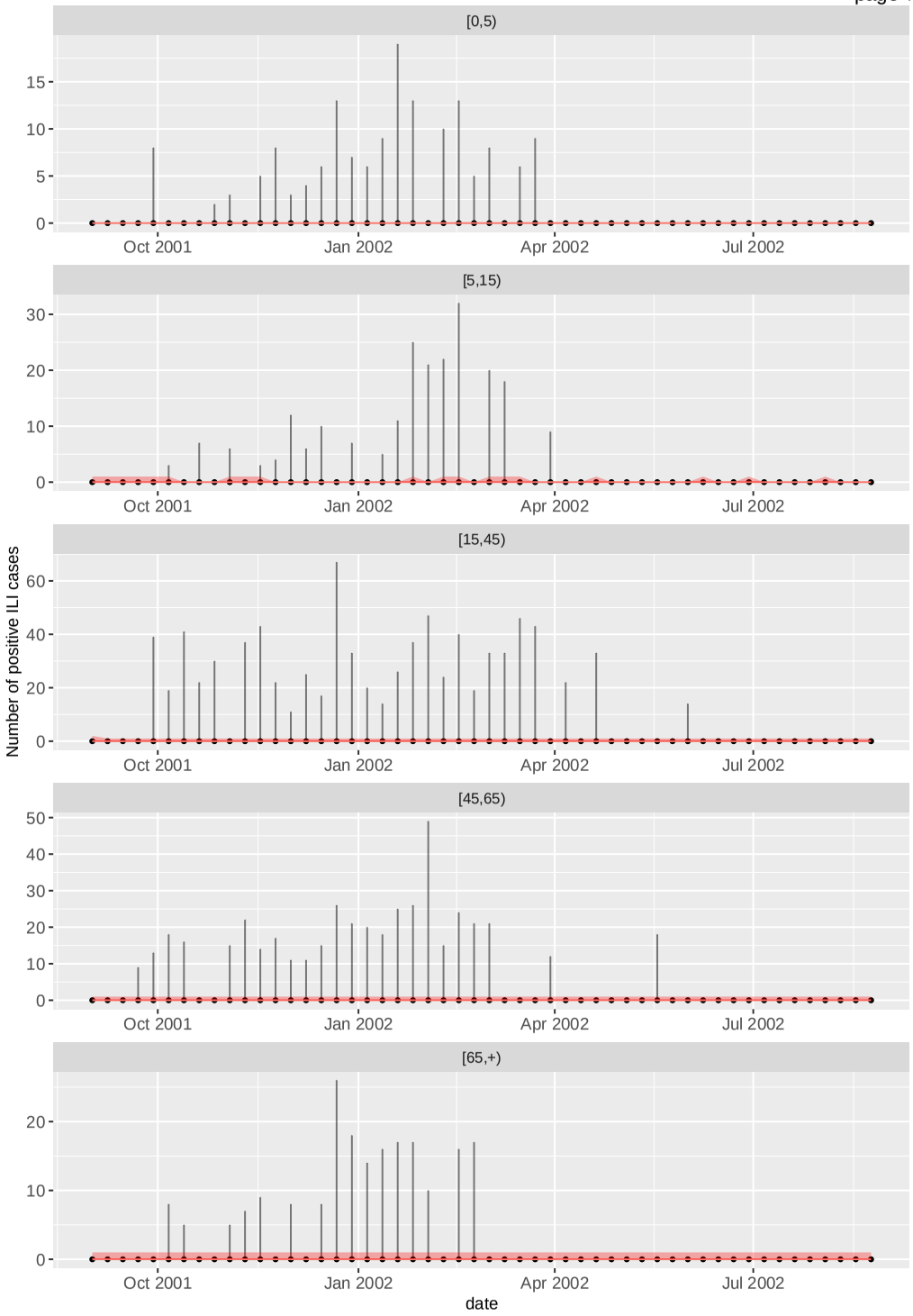
[0,5)
[5,15)
[15,45)
[45,65)
[65,+)
Oct 2001
Jan 2002
Apr 2002
Jul 2002
Number of positive ILI cases
date

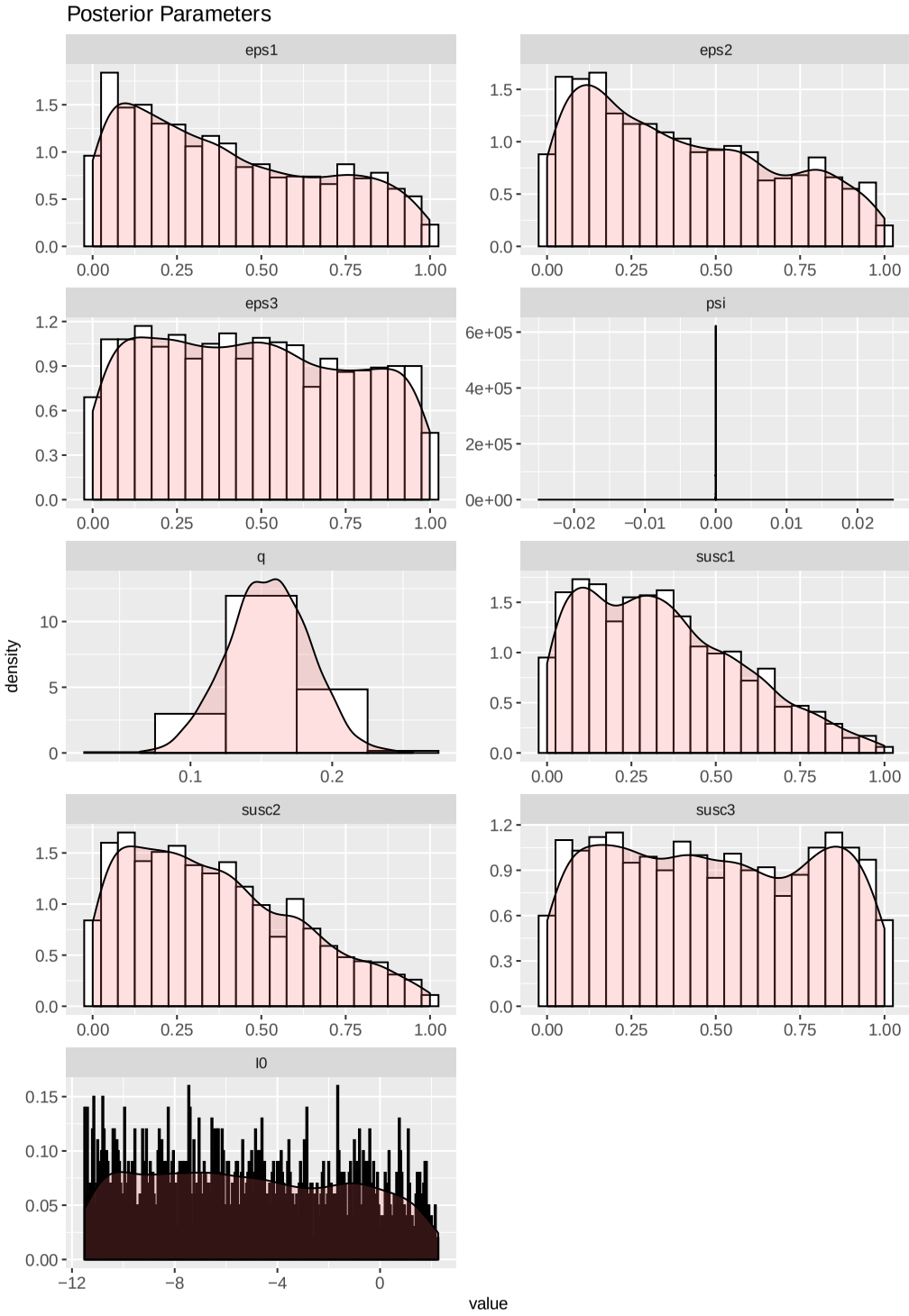
Posterior Parameters
eps1
eps2
eps3
psi
q
susc1
susc2
susc3
I0
density
value

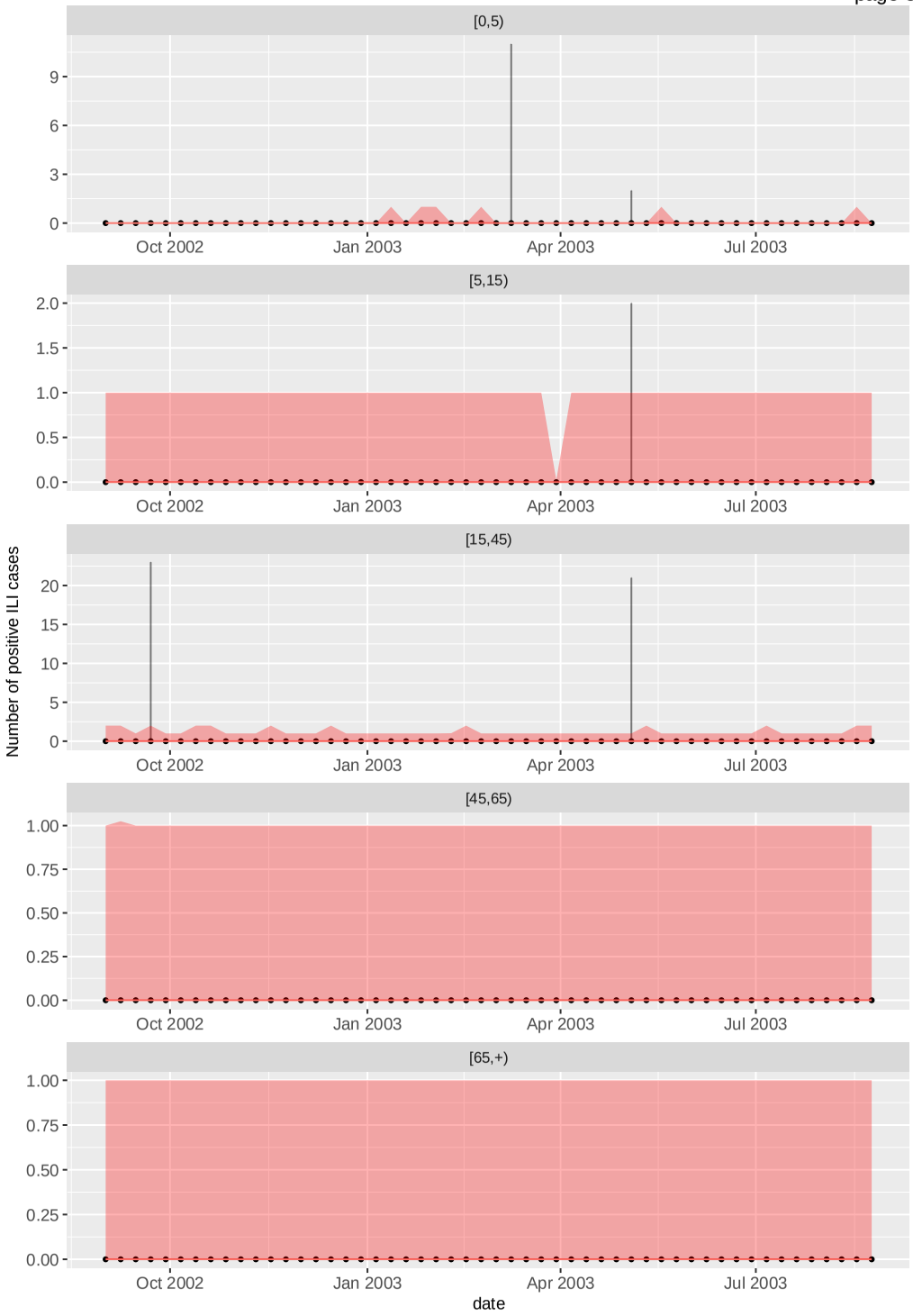
[0,5)
[5,15)
[15,45)
[45,65)
[65,+)
Number of positive ILI cases
Oct 2002
Jan 2003
Apr 2003
Jul 2003
date

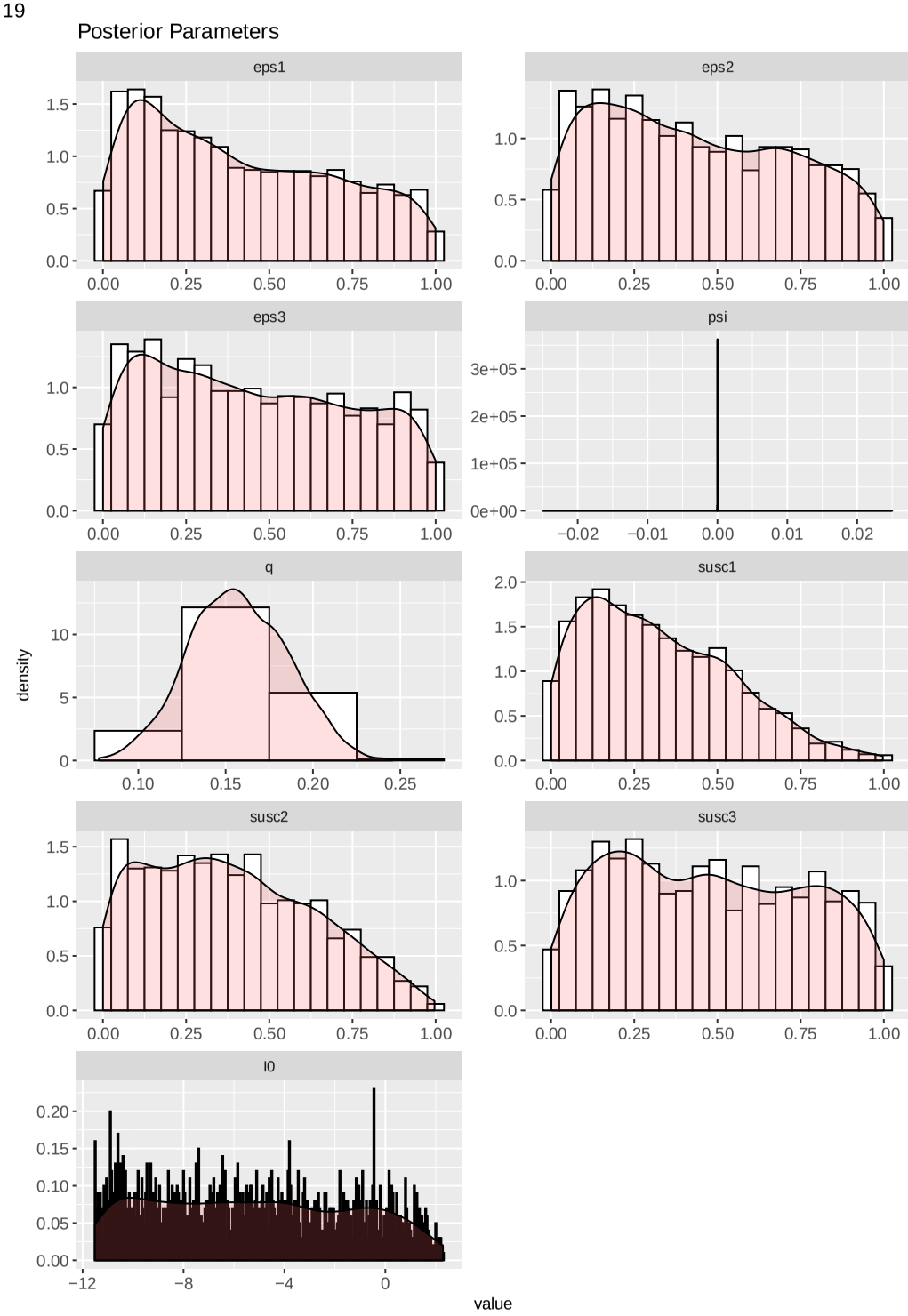
Posterior Parameters
eps1
eps2
eps3
psi
q
susc1
susc2
susc3
I0
density
value

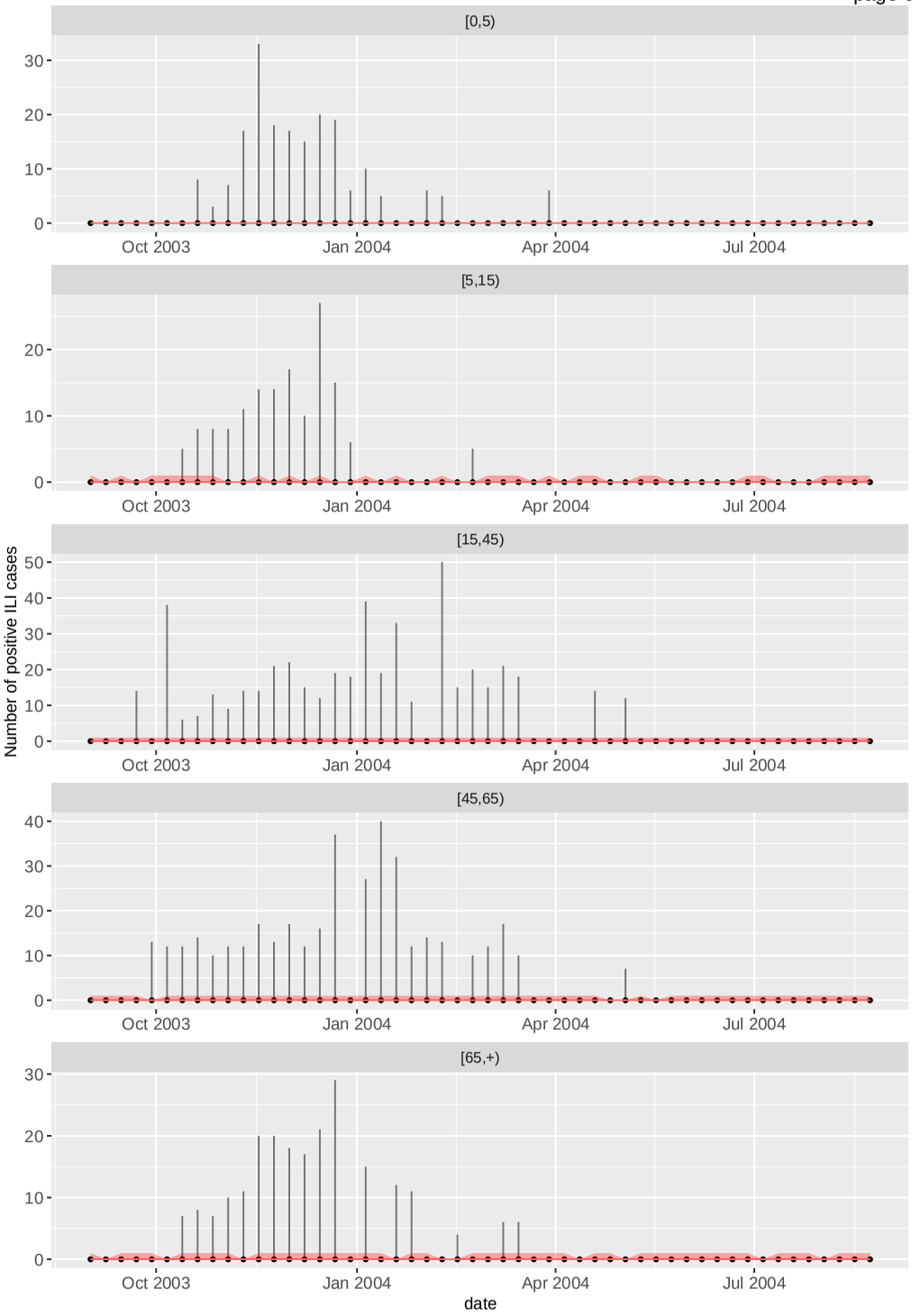
[0,5)
[5,15)
[15,45)
[45,65)
[65,+)
Number of positive ILI cases
Oct 2003
Jan 2004
Apr 2004
Jul 2004
date

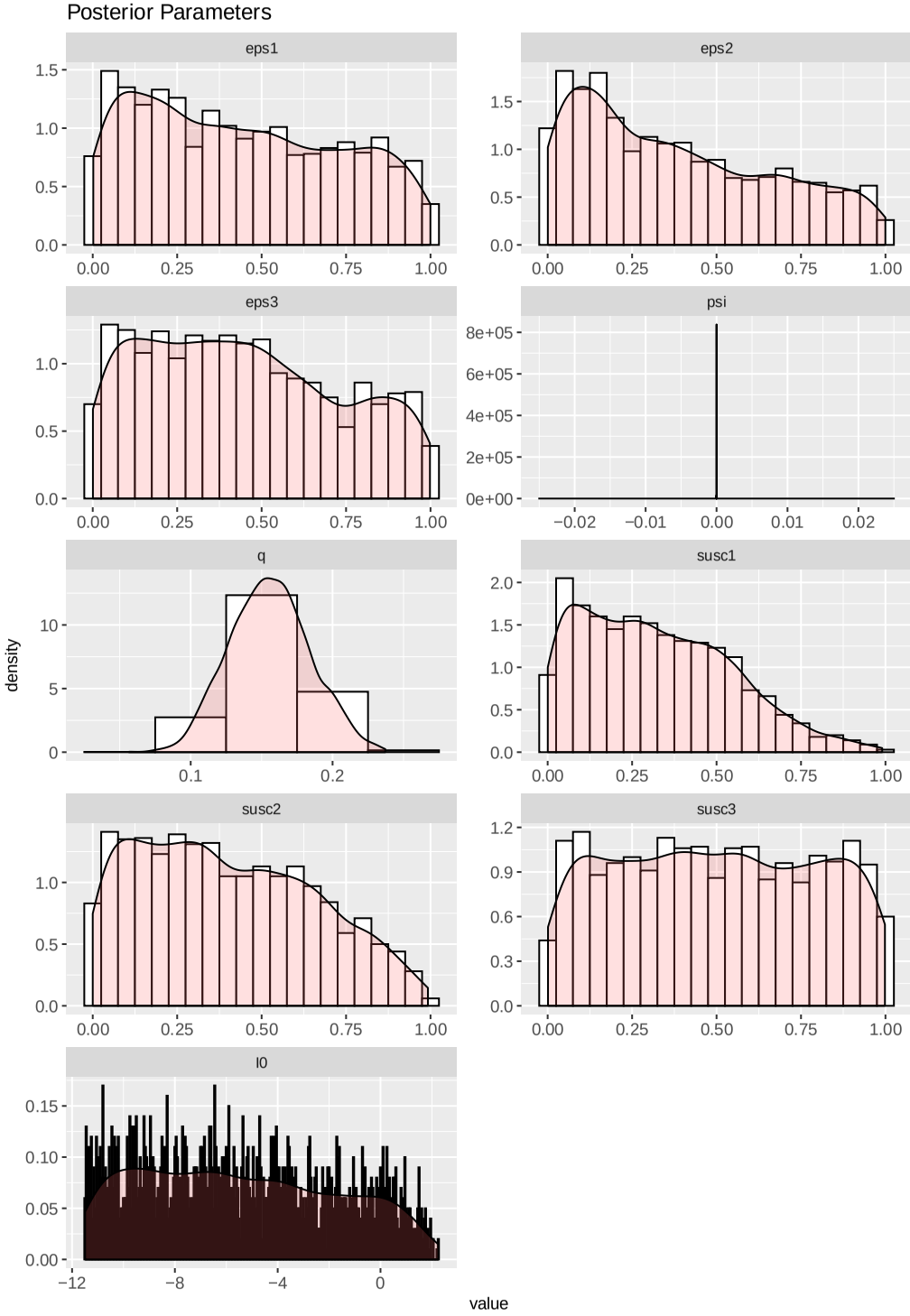
Posterior Parameters
eps1
eps2
eps3
psi
q
susc1
susc2
susc3
I0
density
value

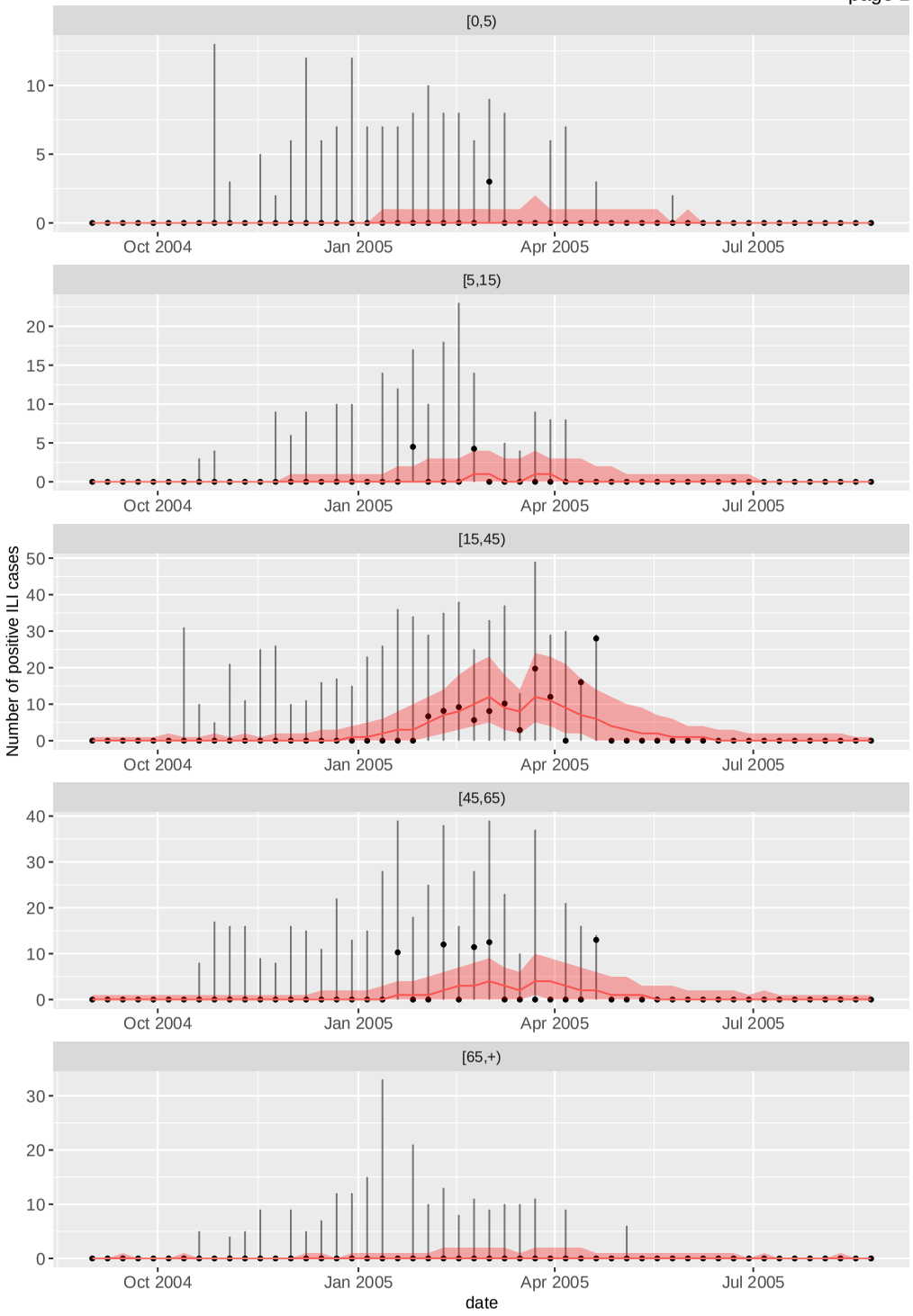
[0,5)
[5,15)
[15,45)
[45,65)
[65,+)
Number of positive ILI cases
Oct 2004
Jan 2005
Apr 2005
Jul 2005
date

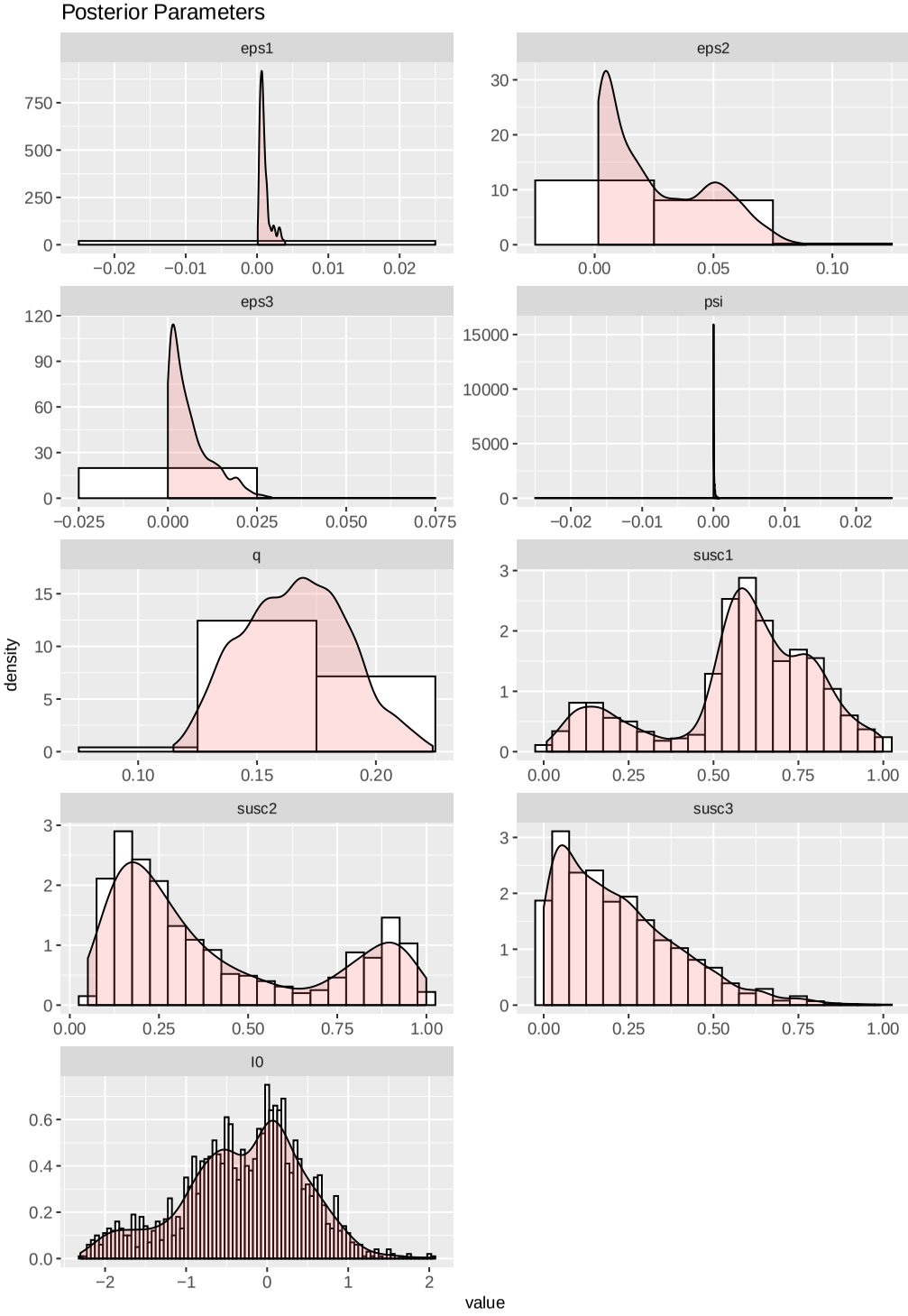
Posterior Parameters
eps1
eps2
eps3
psi
q
susc1
susc2
susc3
I0
density
value

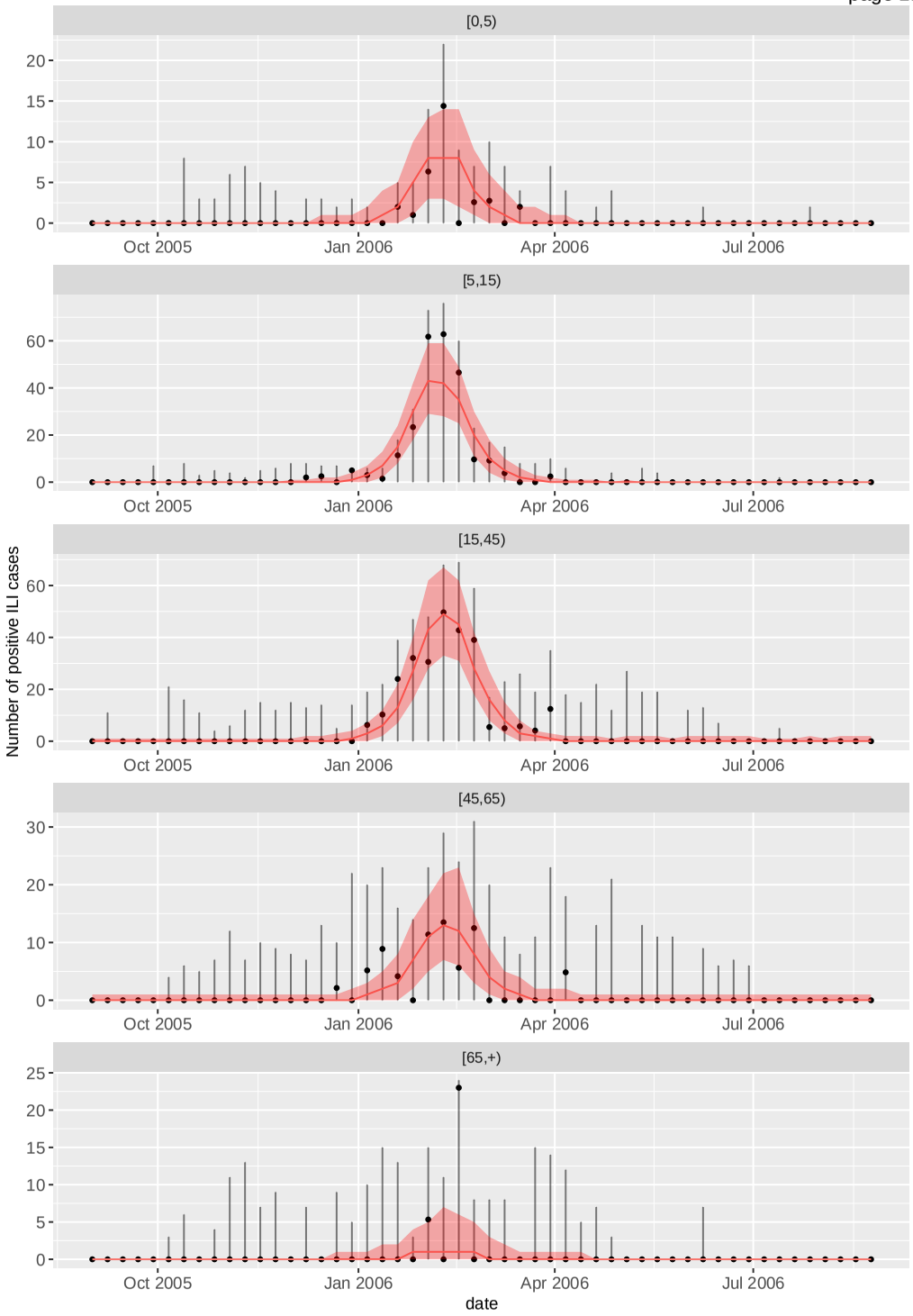
[0,5)
[5,15)
[15,45)
[45,65)
[65,+)
Number of positive ILI cases
Oct 2005
Jan 2006
Apr 2006
Jul 2006
date

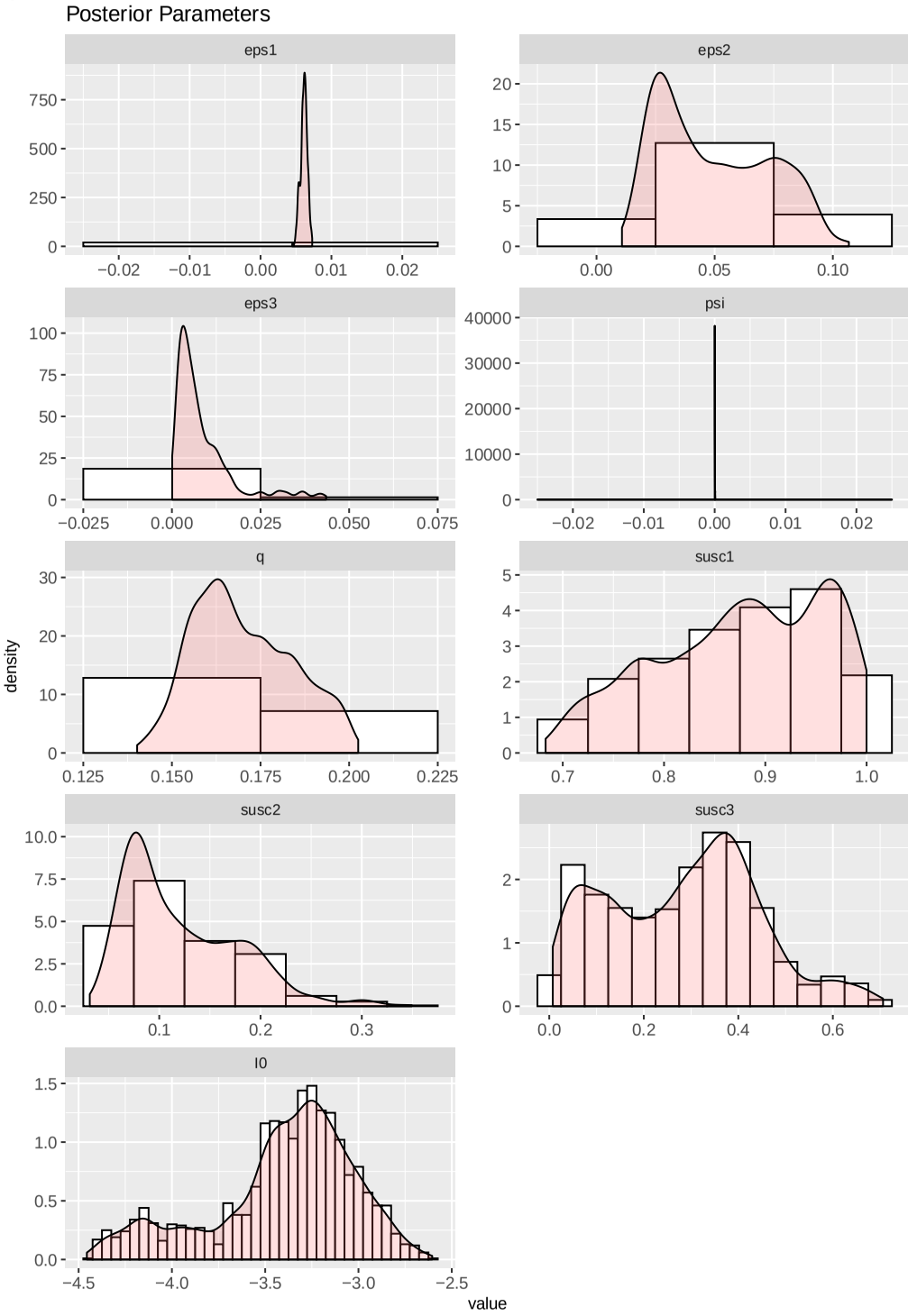
Posterior Parameters
eps1
eps2
eps3
psi
q
susc1
susc2
susc3
I0
density
value

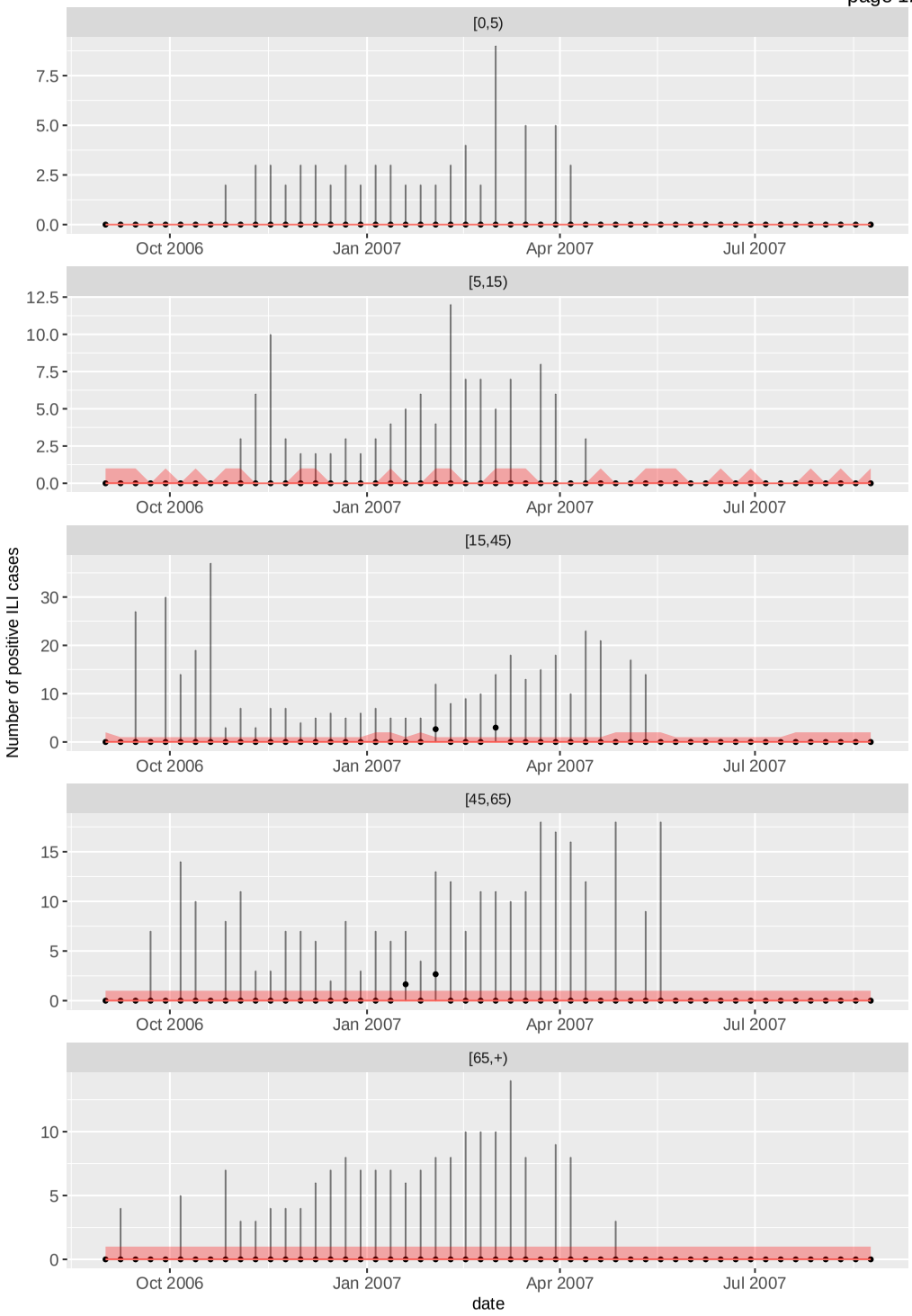
[0,5)
[5,15)
[15,45)
[45,65)
[65,+)
Oct 2006
Jan 2007
Apr 2007
Jul 2007
Number of positive ILI cases
date

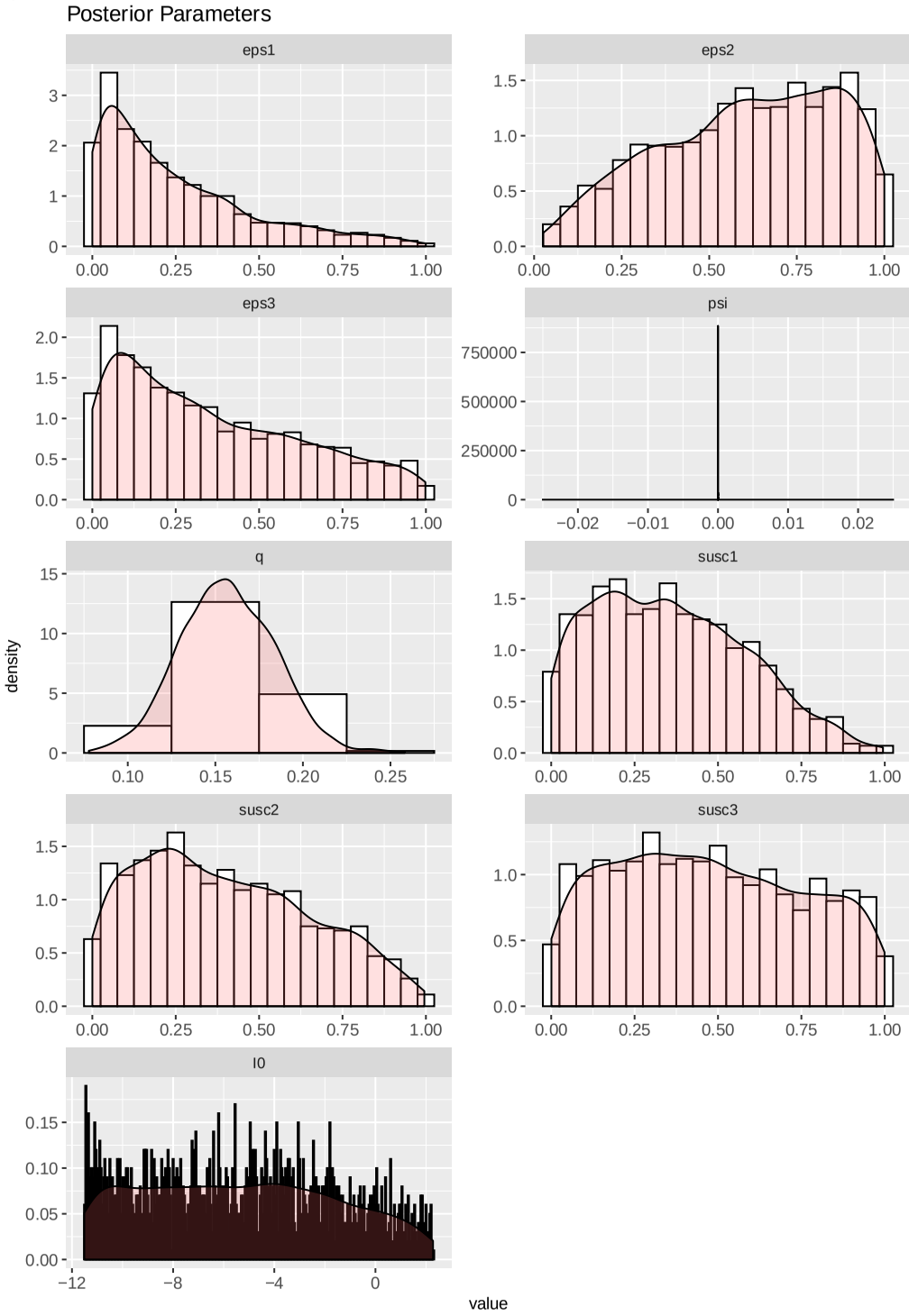
Posterior Parameters
eps1
eps2
eps3
psi
q
susc1
susc2
susc3
I0
density
value

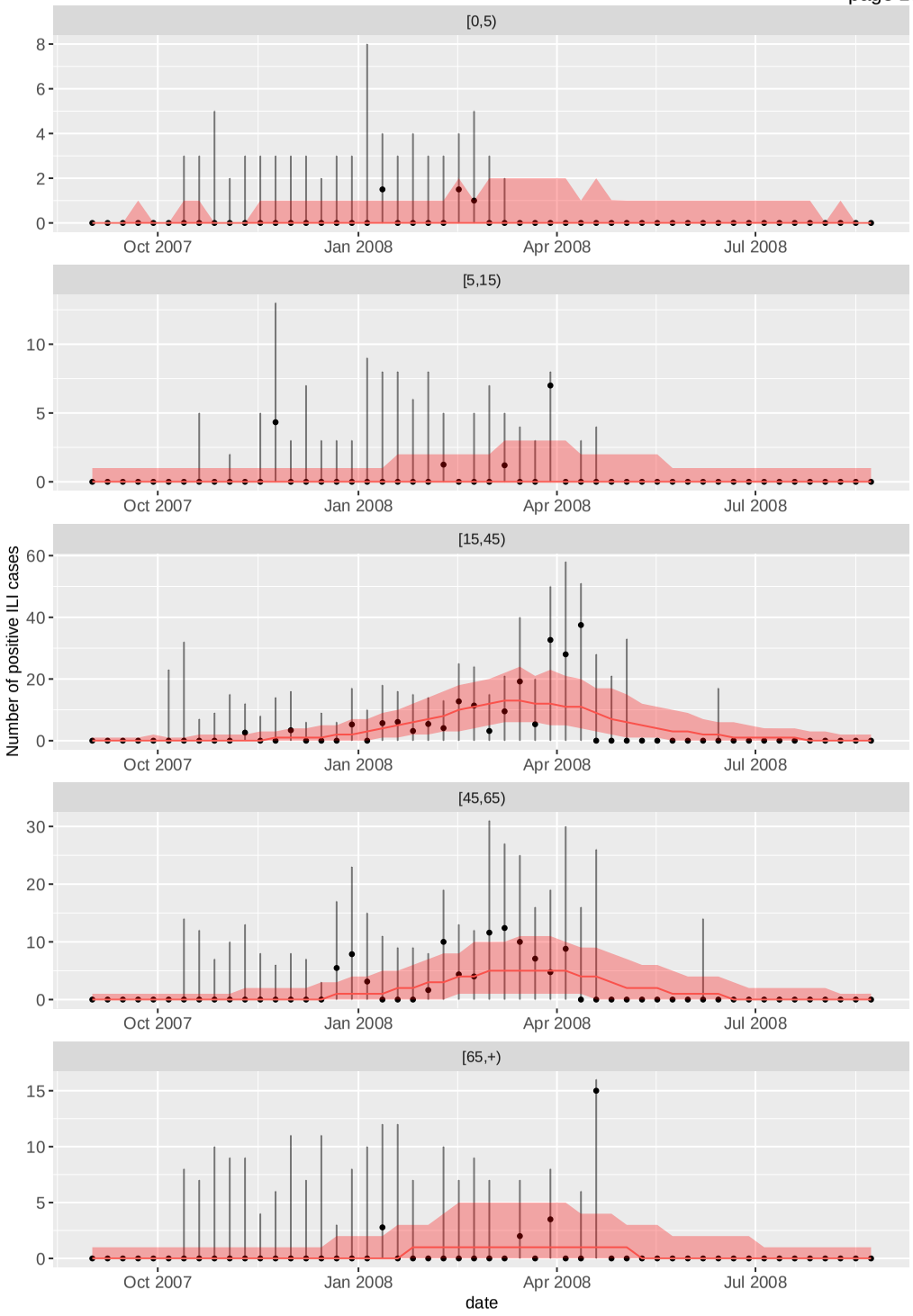
[0,5)
[5,15)
[15,45)
[45,65)
[65,+)
Number of positive ILI cases
Oct 2007
Jan 2008
Apr 2008
Jul 2008
date

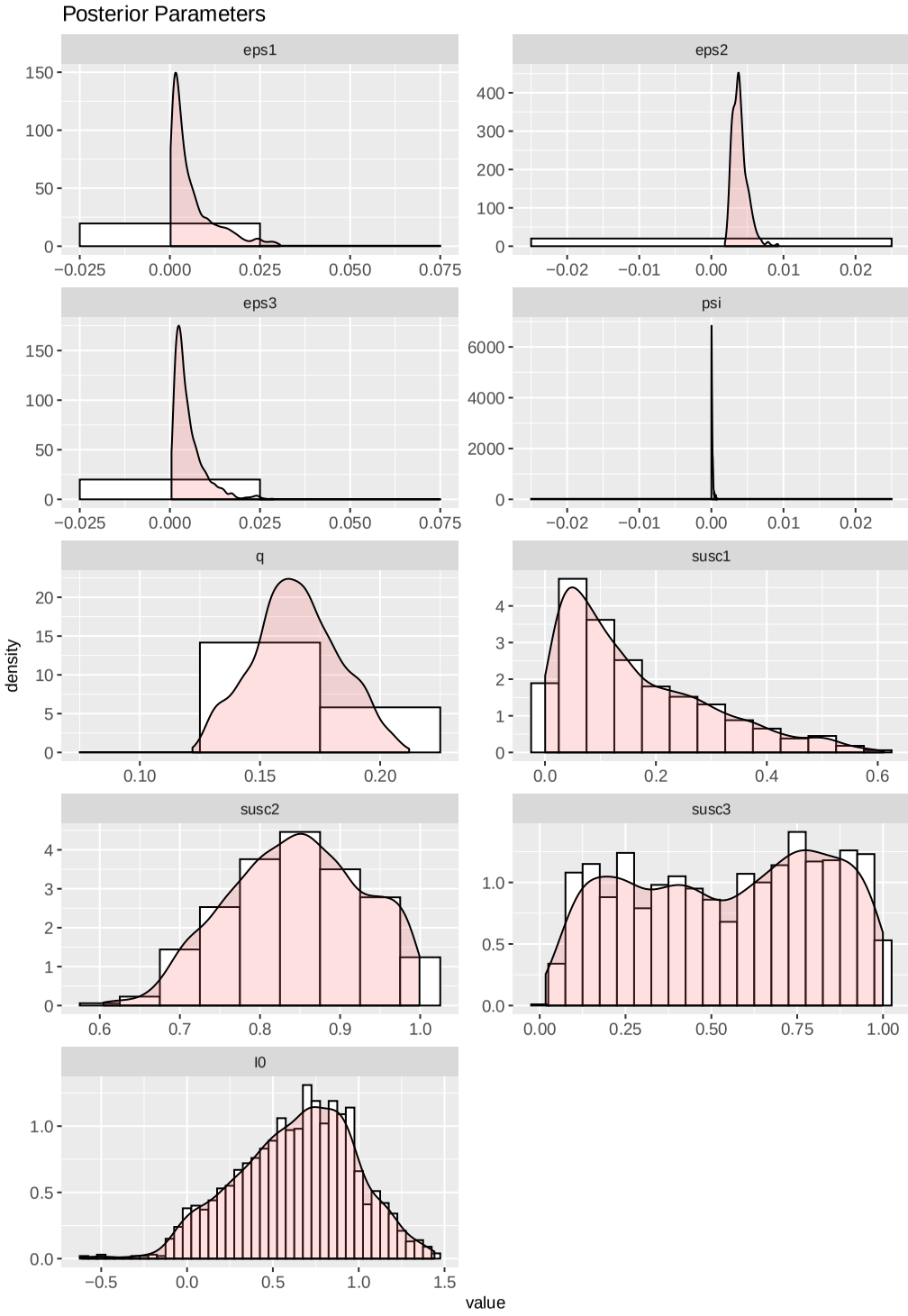
Posterior Parameters
eps1
eps2
eps3
psi
q
susc1
susc2
susc3
I0
density
value

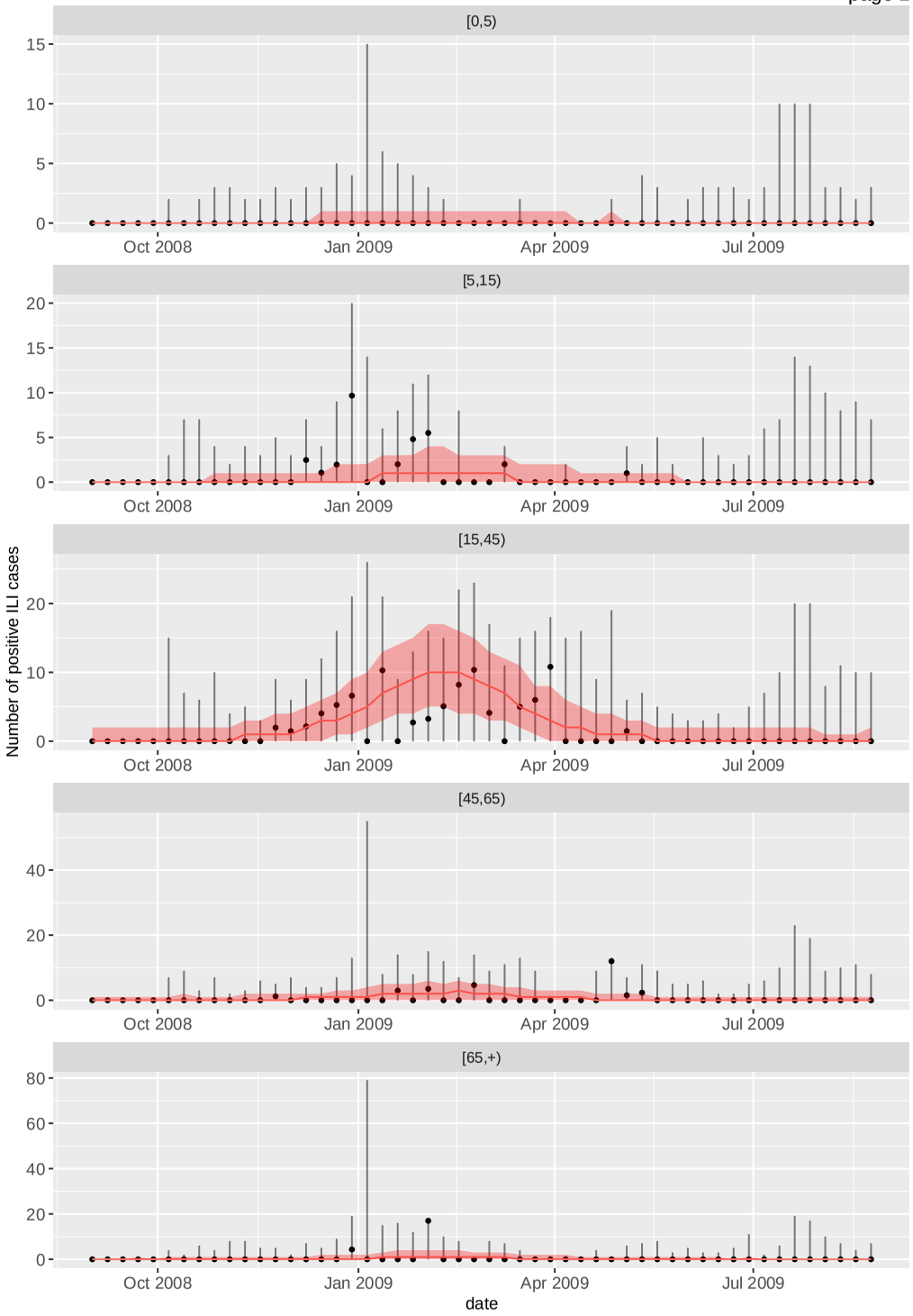
[0,5)
[5,15)
[15,45)
[45,65)
[65,+)
Number of positive ILI cases
Oct 2008
Jan 2009
Apr 2009
Jul 2009
date

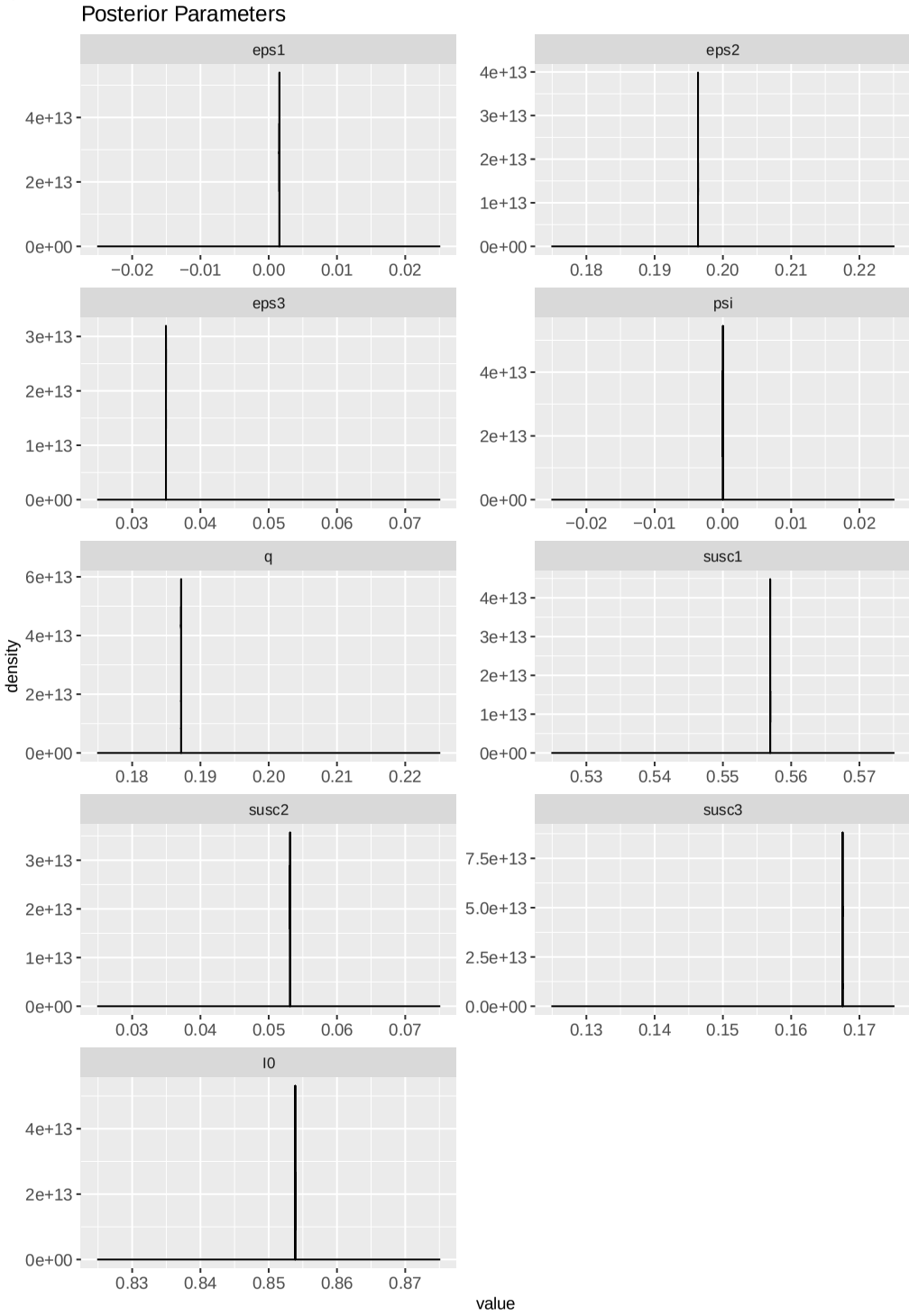
Posterior Parameters
eps1
eps2
eps3
psi
q
susc1
susc2
susc3
I0
density
value

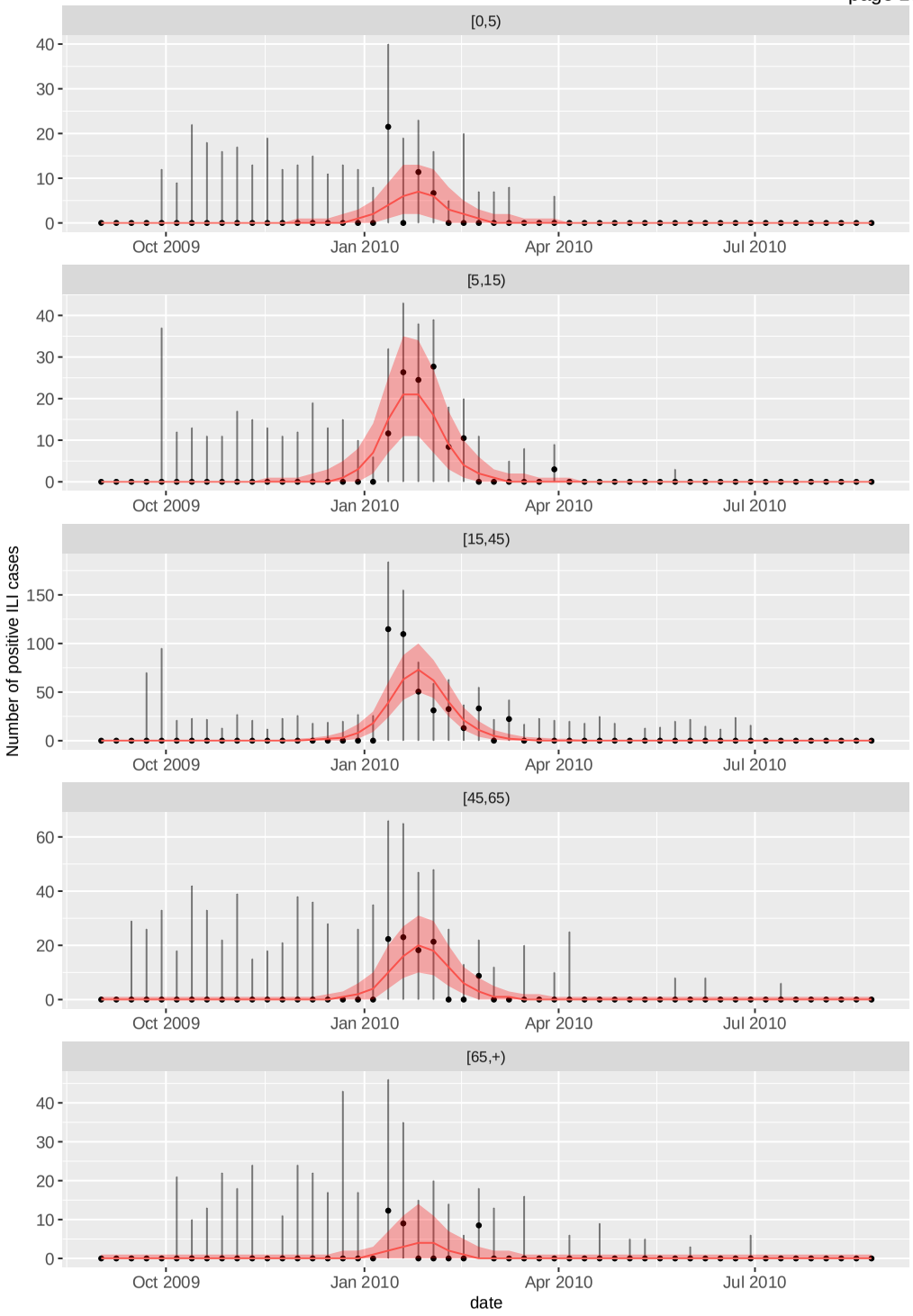
[0,5)
[5,15)
[15,45)
[45,65)
[65,+)
Number of positive ILI cases
Oct 2009
Jan 2010
Apr 2010
Jul 2010
date

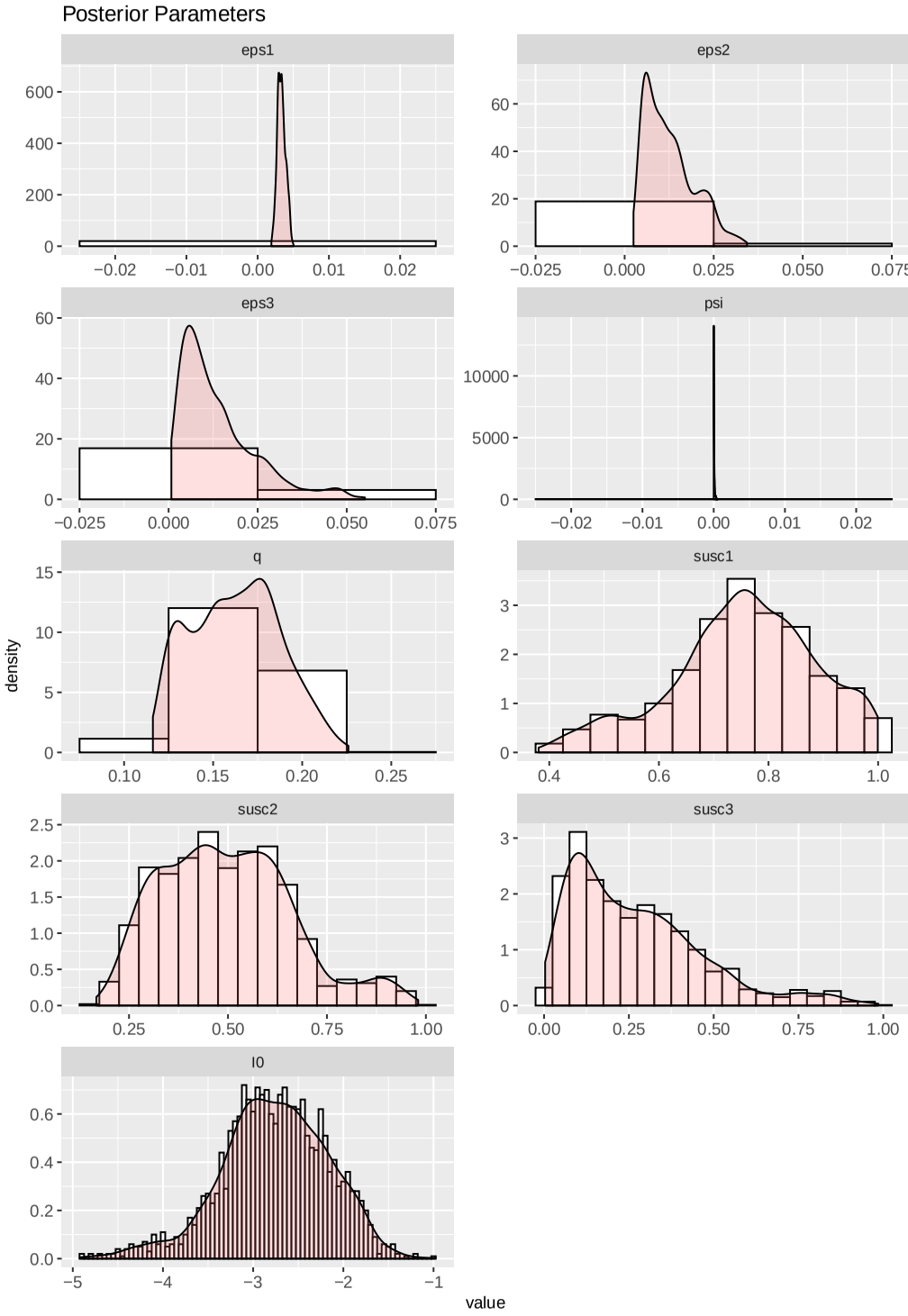
Posterior Parameters
eps1
eps2
eps3
psi
q
susc1
susc2
susc3
I0
density
value

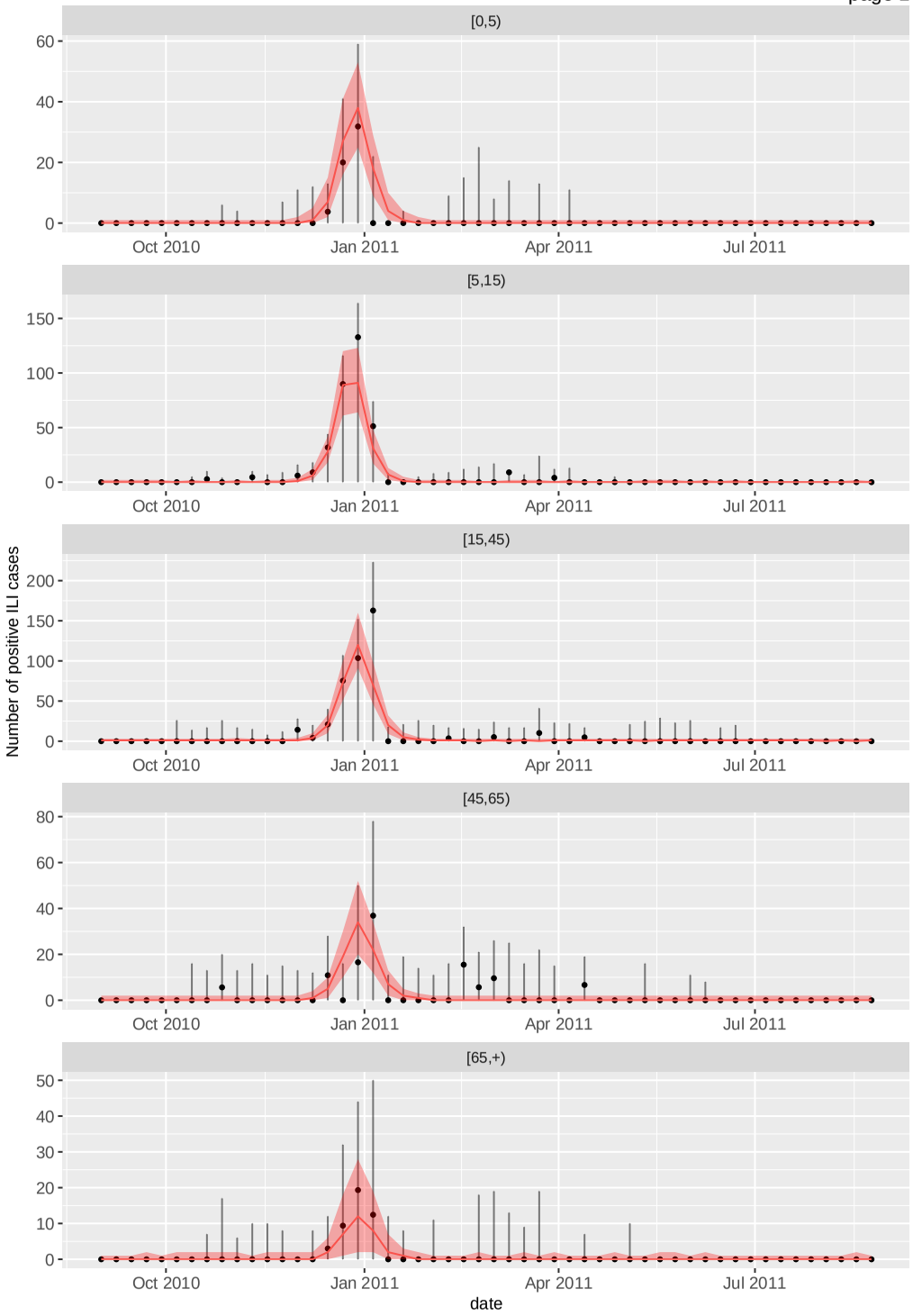

Posterior Parameters

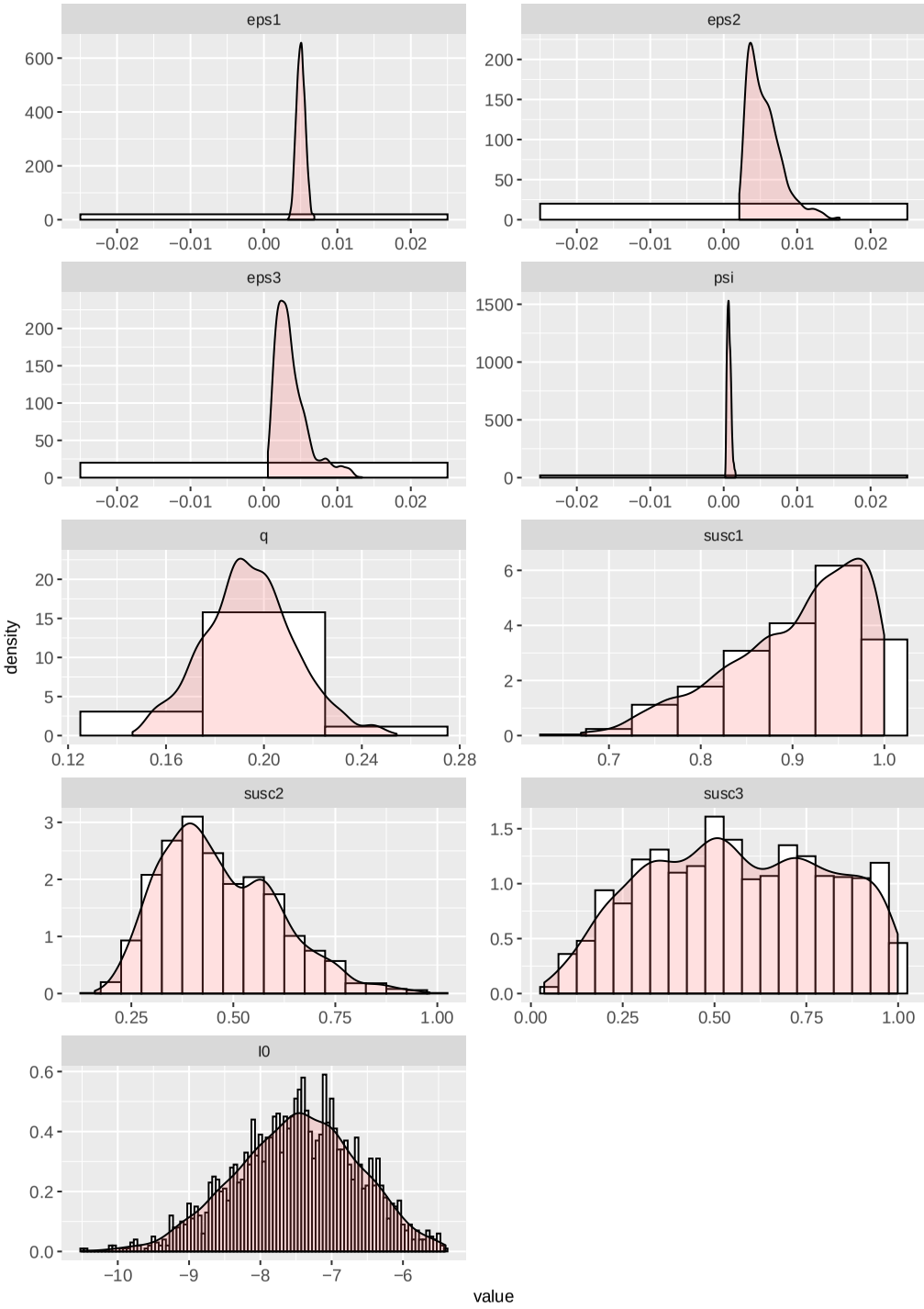

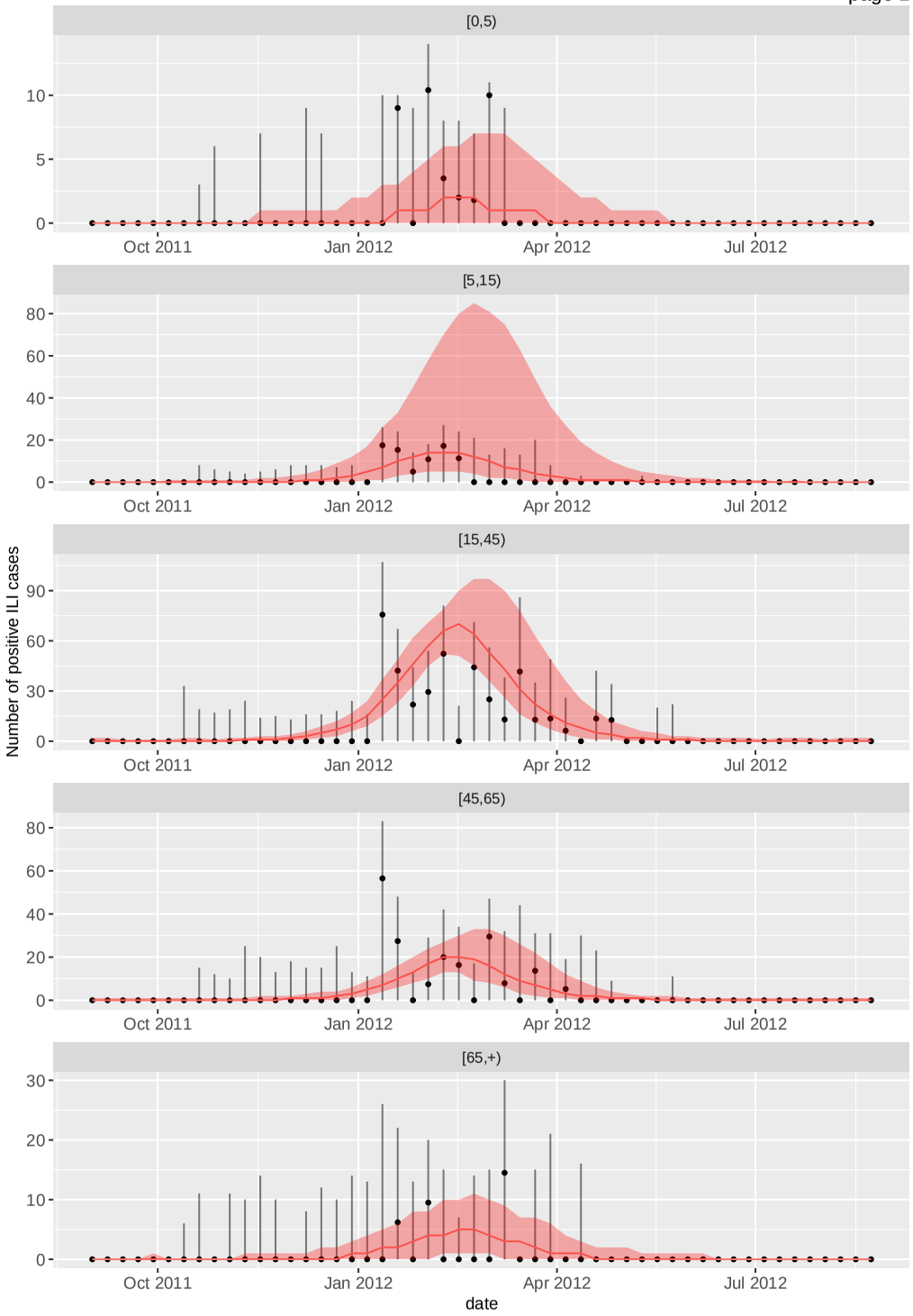
[0,5)
[5,15)
[15,45)
[45,65)
[65,+)
Oct 2011
Jan 2012
Apr 2012
Jul 2012
Number of positive ILI cases
date

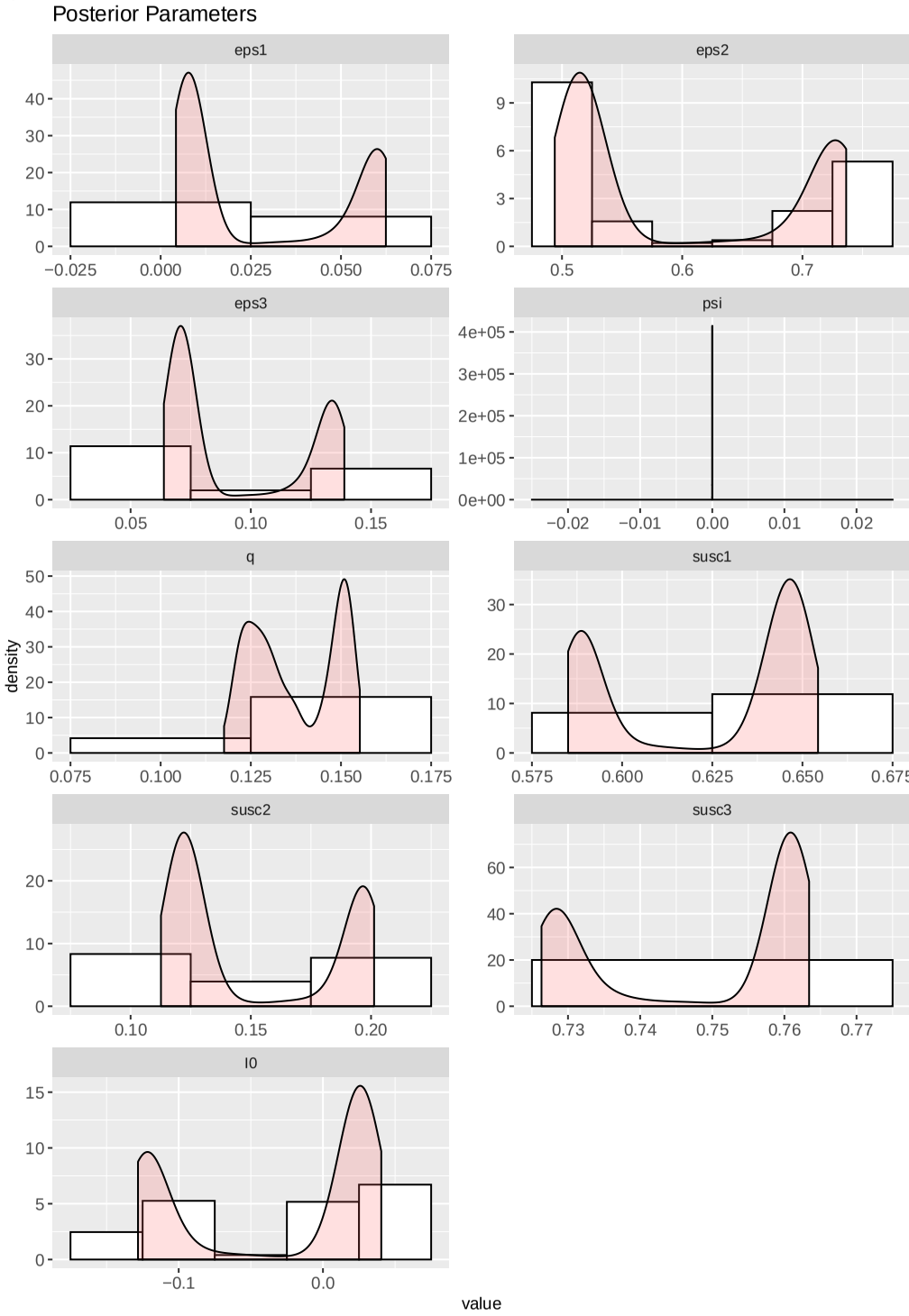
Posterior Parameters
eps1
eps2
eps3
psi
q
susc1
susc2
susc3
I0
density
value

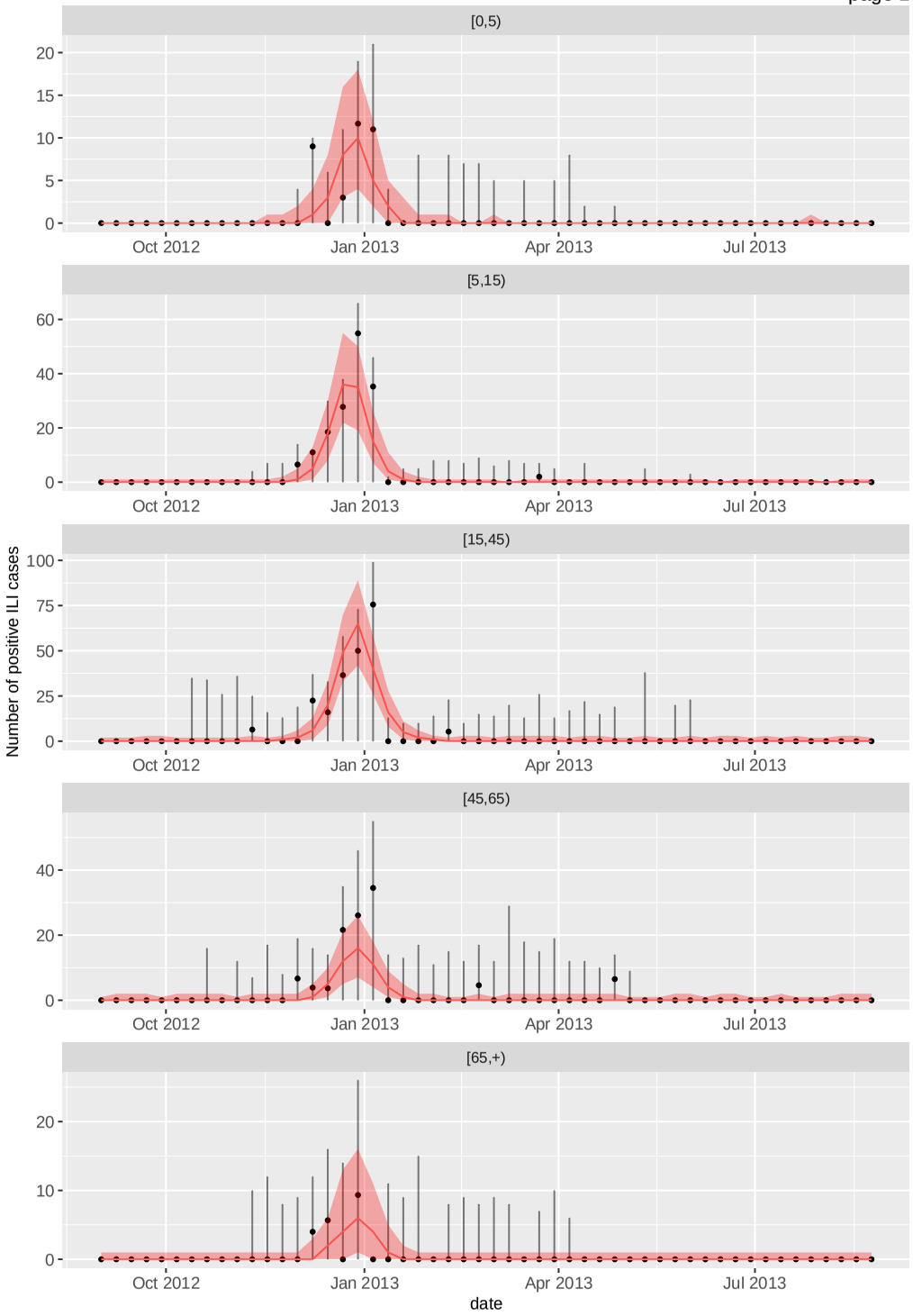
[0,5)
[5,15)
[15,45)
[45,65)
[65,+)
Number of positive ILI cases
Oct 2012
Jan 2013
Apr 2013
Jul 2013
date

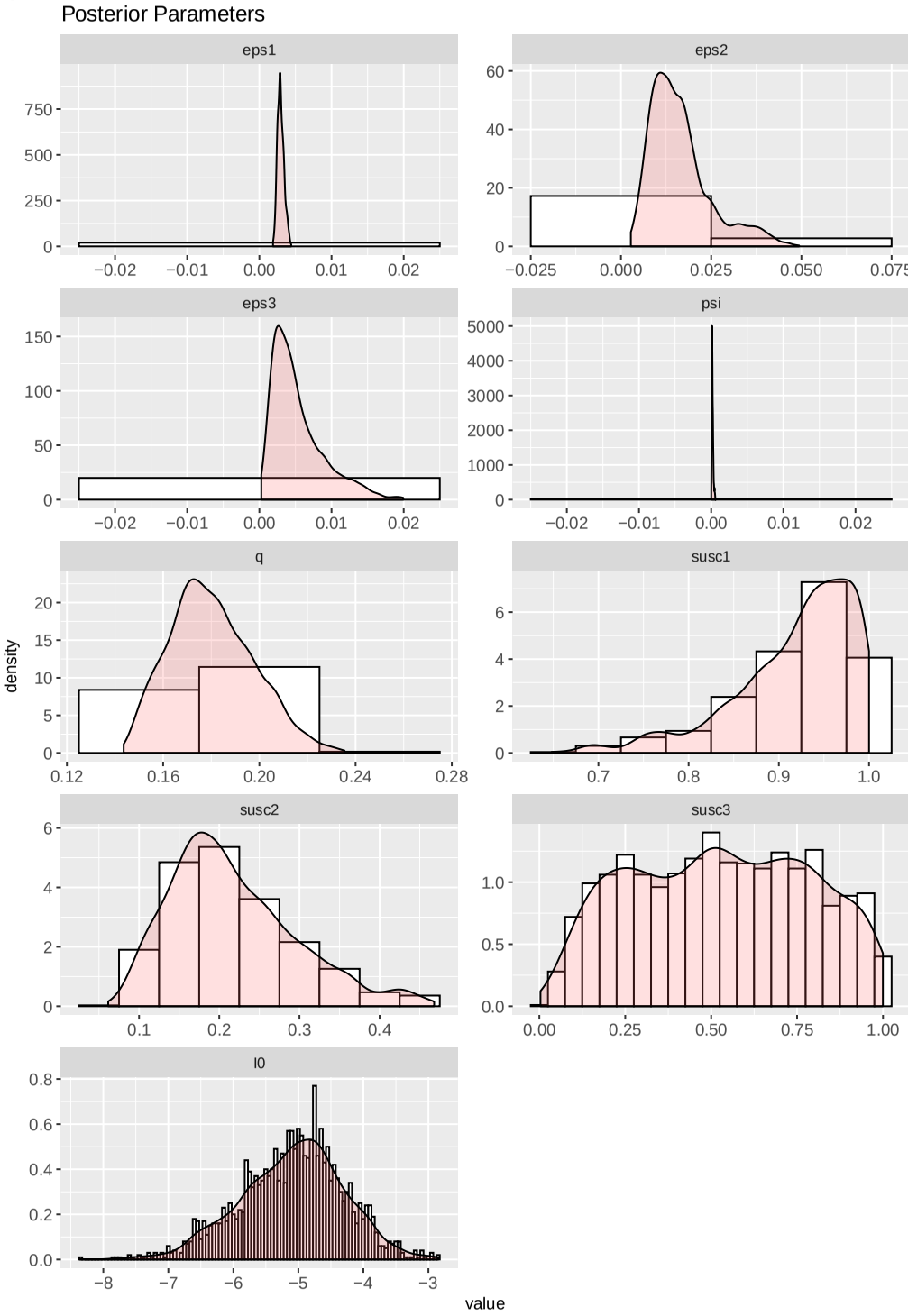
Posterior Parameters
eps1
eps2
eps3
psi
q
susc1
susc2
susc3
l0
density
value

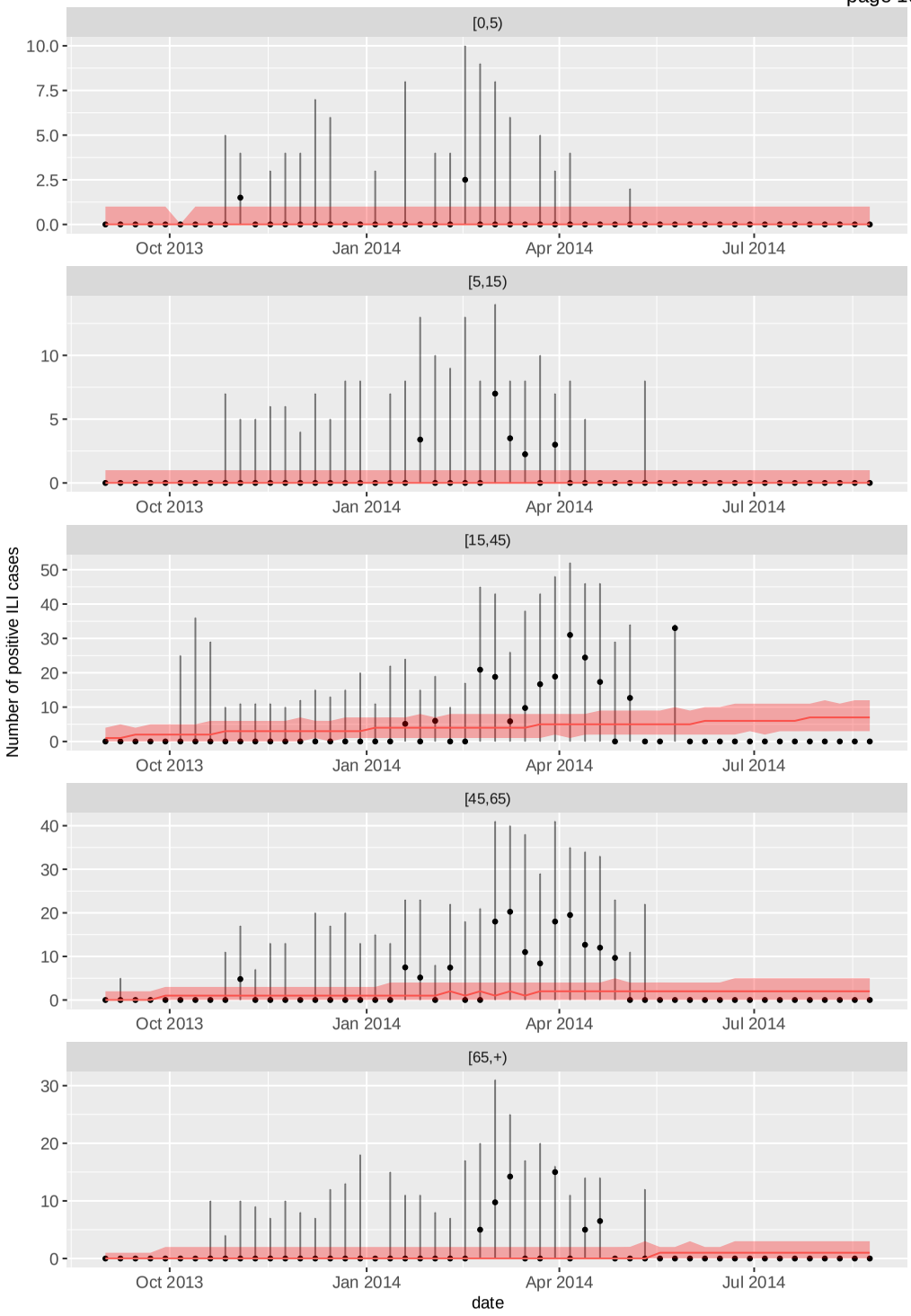
[0,5)
[5,15)
[15,45)
[45,65)
[65,+)
Oct 2013
Jan 2014
Apr 2014
Jul 2014
Number of positive ILI cases
date

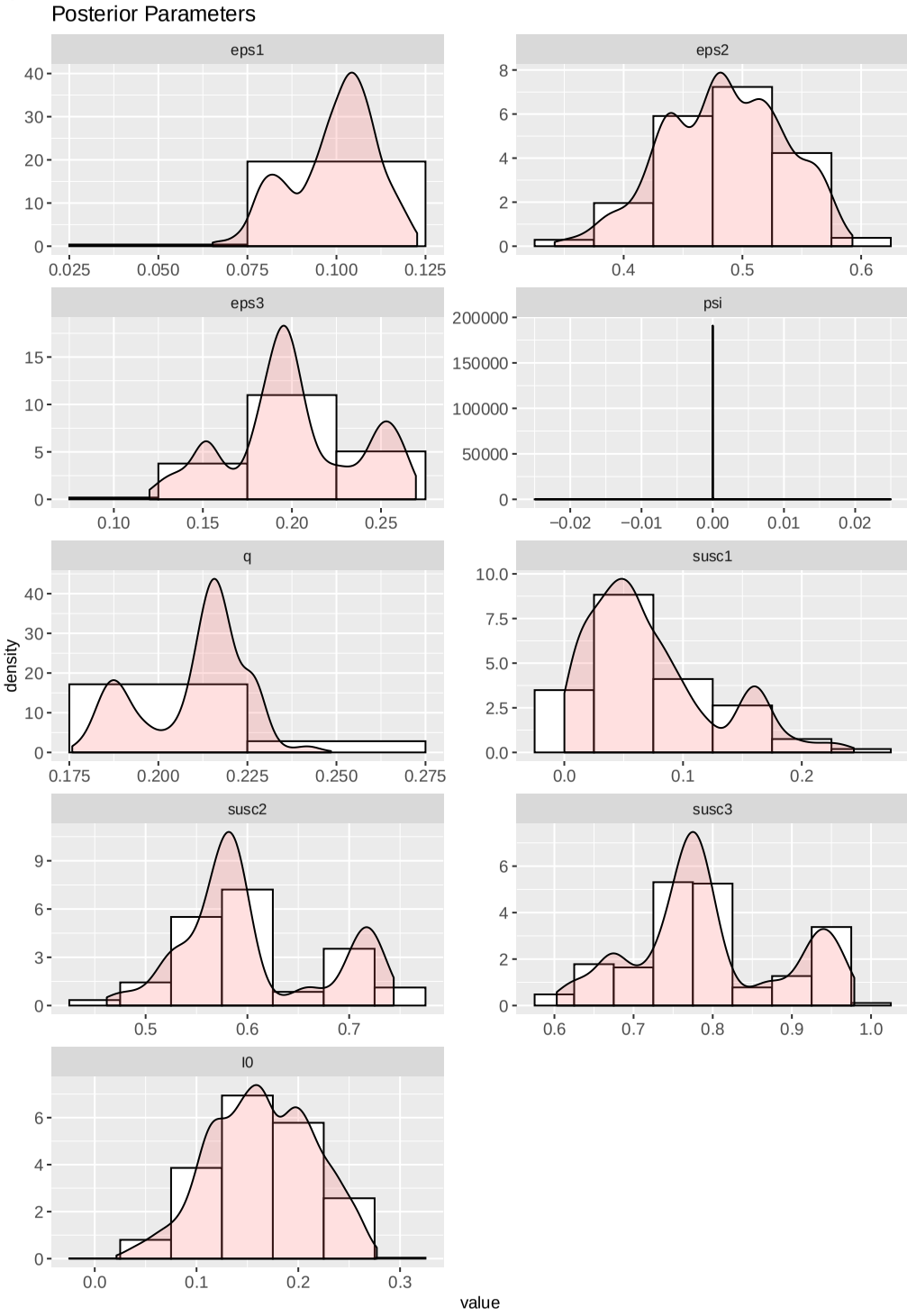
Posterior Parameters
eps1
eps2
eps3
psi
q
susc1
susc2
susc3
I0
density
value

A2 Variance in posterior contact matrices for Chapter 2

A2.1 Mean Number of Contacts and Standard Deviation

The following pages display the posterior contact matrices in a single color heat-map format. The left hand column displays the average number of contacts per day per age group interaction listed in the cell, while the right hand column displays the associated standard deviation around the mean. These graphs have not been adjusted for symmetry.

Average Number
of Contacts per day BE

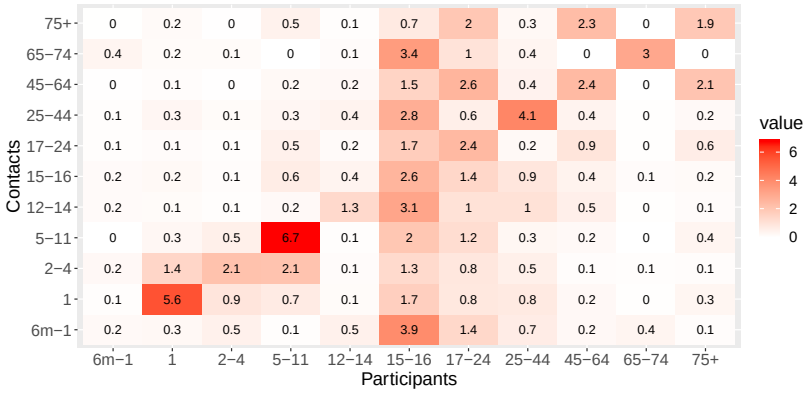

Standard Deviation
Among Number of Contacts per day BE

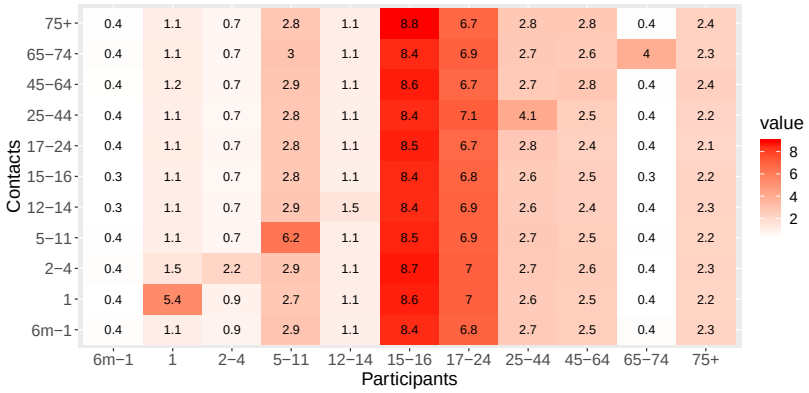

Average Number
of Contacts per day DE

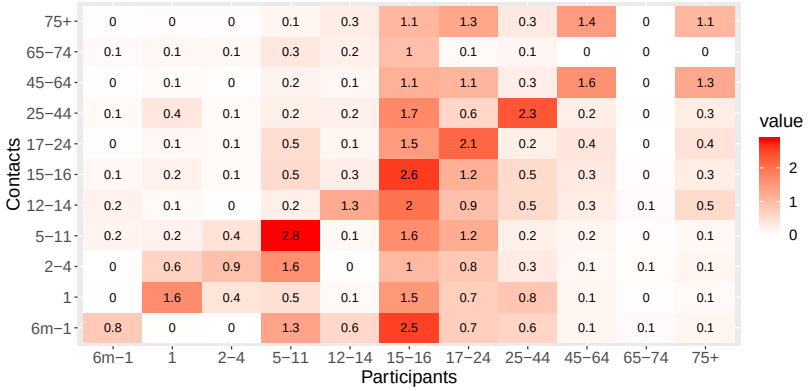

Standard Deviation
Among Number of Contacts per day DE

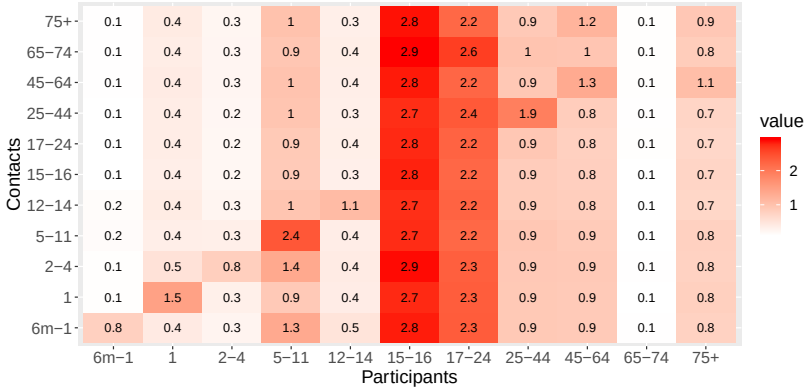

Average Number
of Contacts per day FI

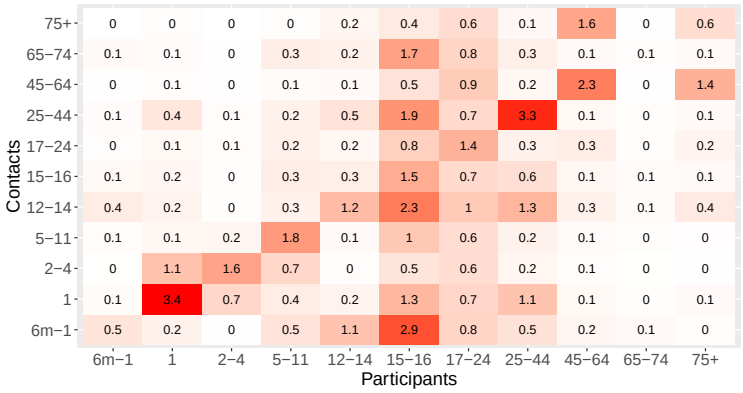

Standard Deviation
Among Number of Contacts per day FI

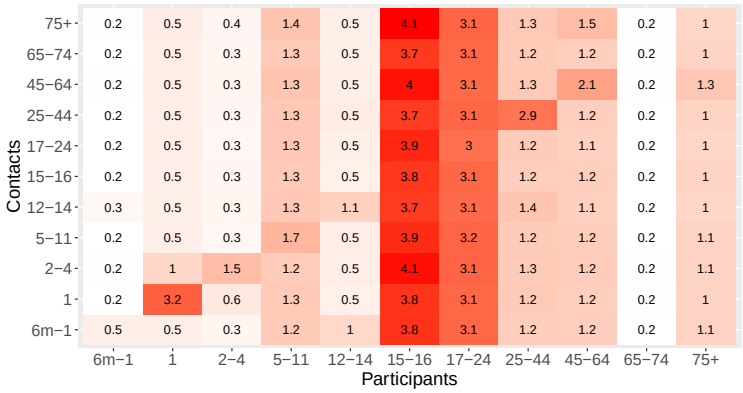

Average Number
of Contacts per day GB

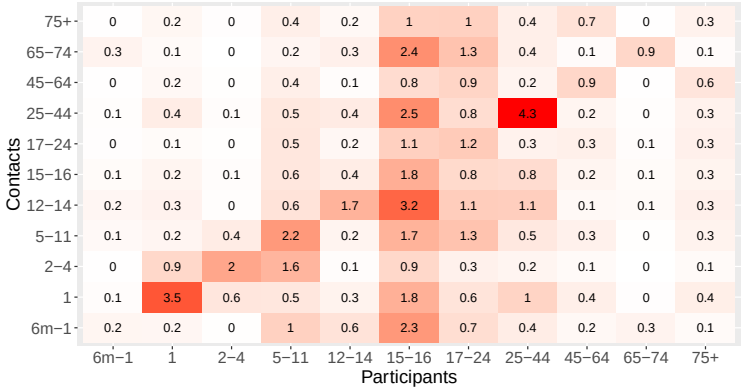

Standard Deviation
Among Number of Contacts per day GB

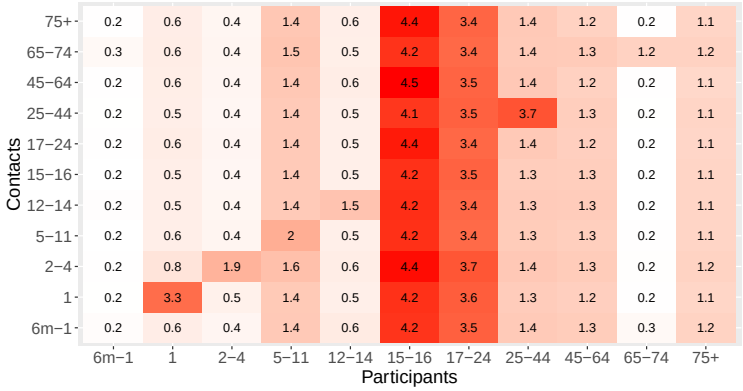

Average Number of Contacts per day IT

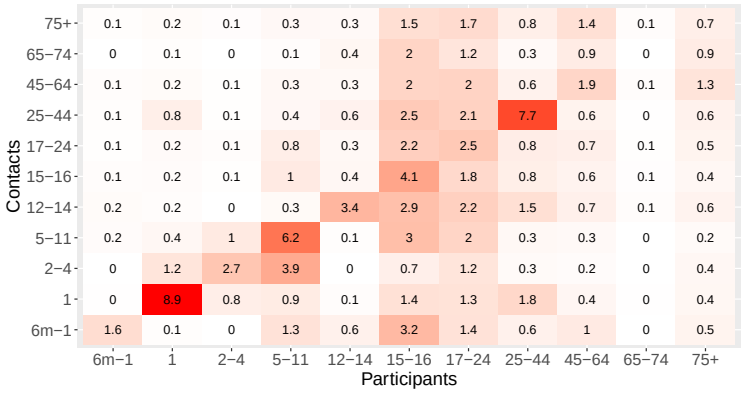

Standard Deviation Among Number of Contacts per day IT

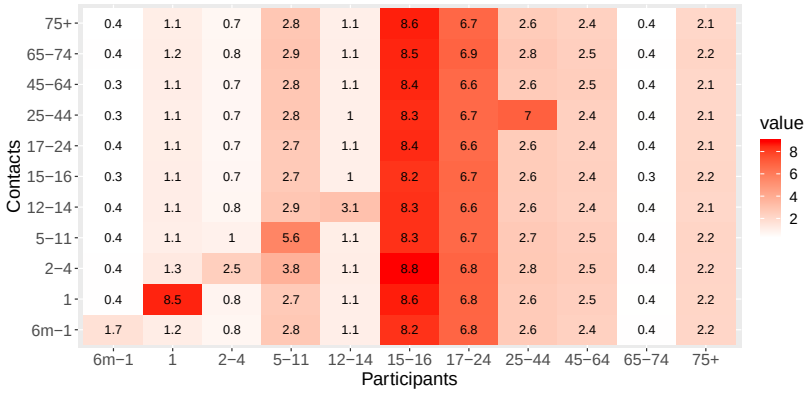

Average Number of Contacts per day LU

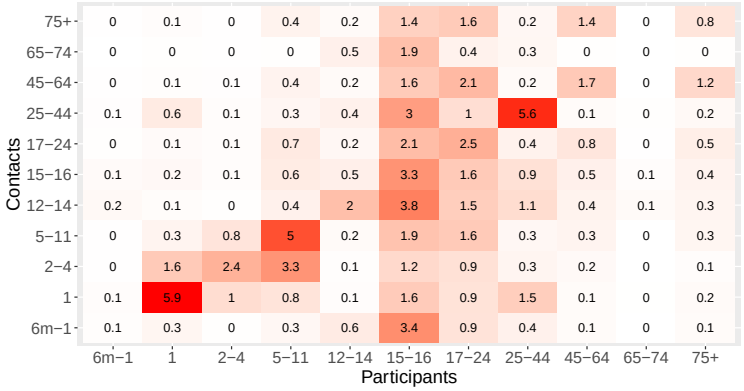

Standard Deviation Among Number of Contacts per day LU

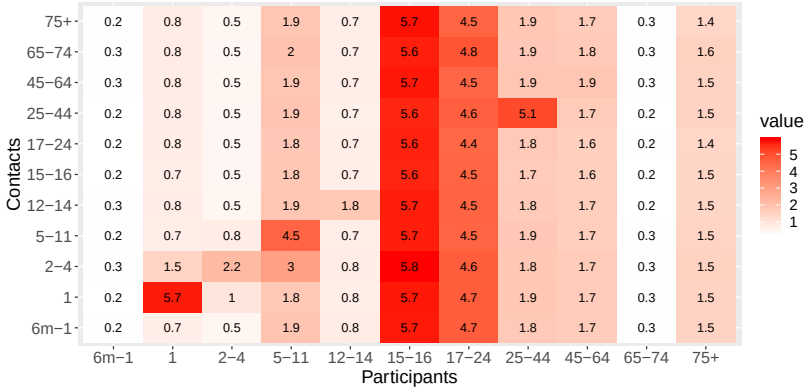

Average Number
of Contacts per day NL

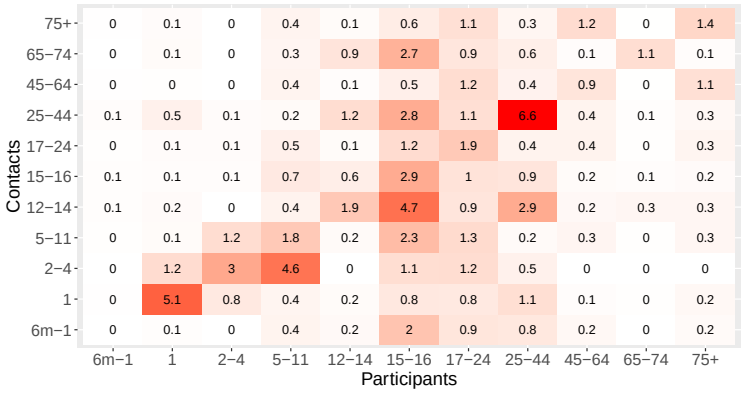

Standard Deviation
Among Number of Contacts per day NL

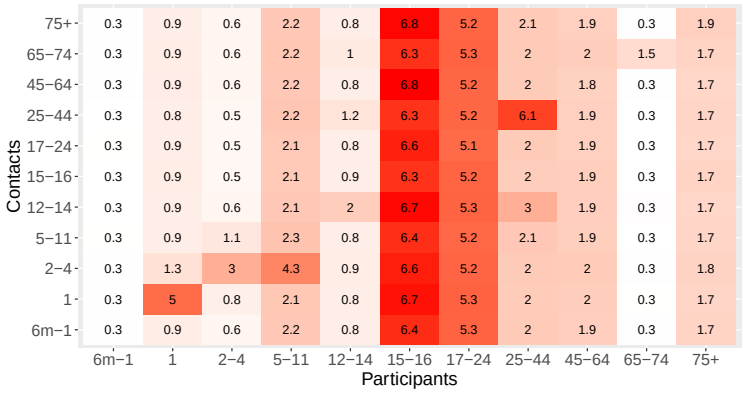

Average Number
of Contacts per day PL

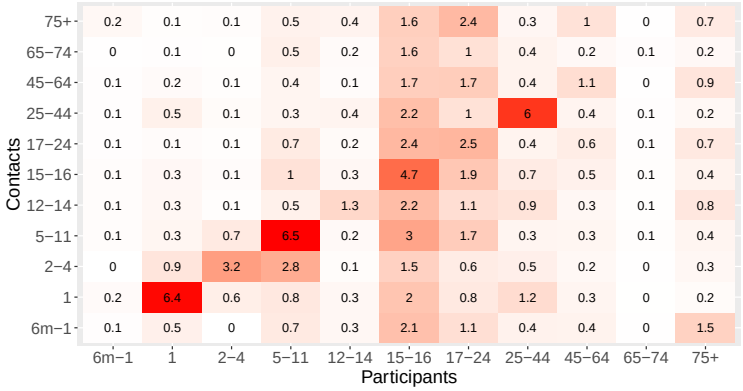

Standard Deviation
Among Number of Contacts per day PL

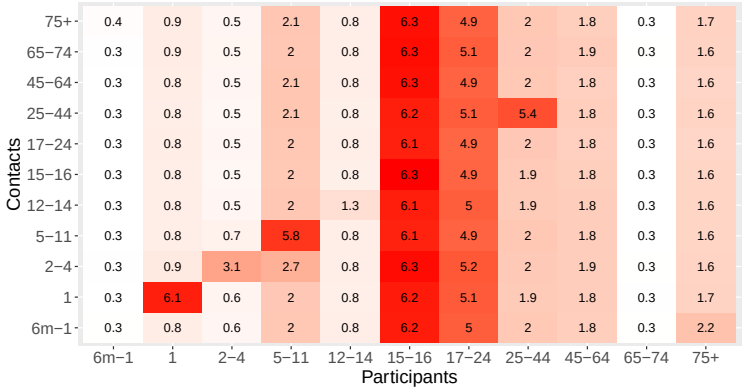

Average Number of Contacts per day PE

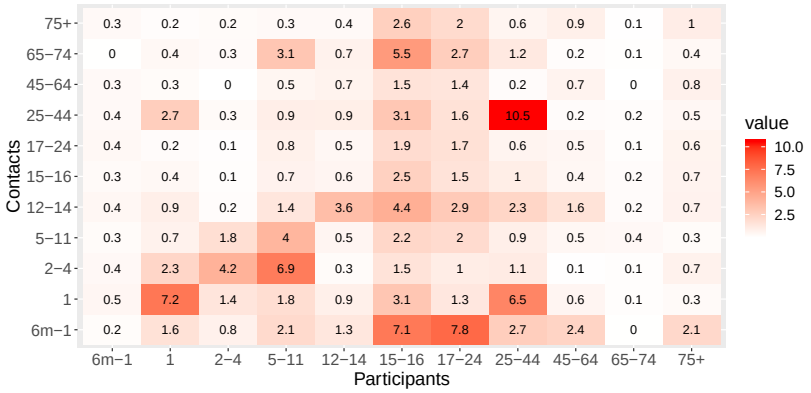

Standard Deviation Among Number of Contacts per day PE

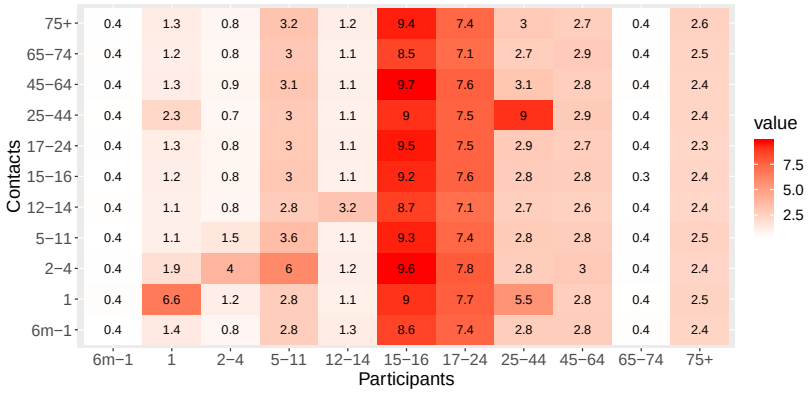

Average Number of Contacts per day FR

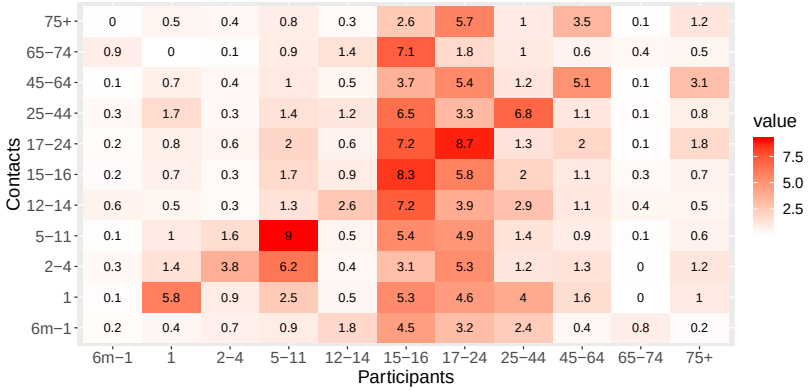

Standard Deviation Among Number of Contacts per day FR

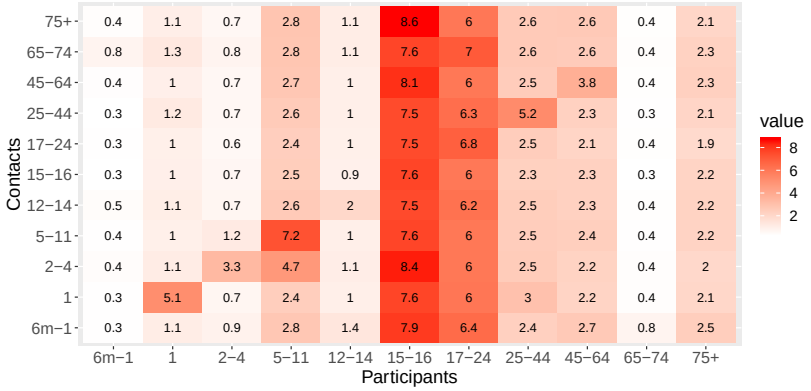

A2.2 Mean Relative Number of Contacts and Standard Deviation

The following pages display the posterior contact matrices in a single color heat-map format. The left hand column displays the relative number of contacts per day per age group interaction listed in the cell. The relative number of contacts is the proportion of an individual's total contacts are comprised of individuals in that age group. Using the Belgium (BE) contact matrix as an example, among 5-11 year old contact survey participants other 5-11 year olds comprise 40% of the average daily contacts. The right hand column displays the associated standard deviation around the relative mean. These graphs have not been adjusted for symmetry.

Proportion of Contacts per Age group BE

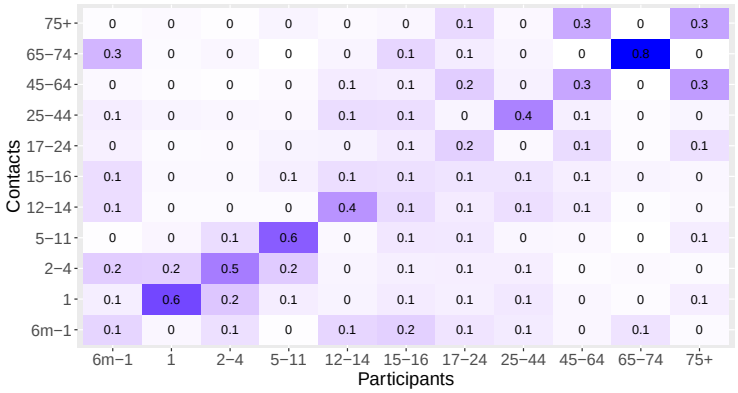

Standard Deviation Among Proportion of Contact per Age Group BE

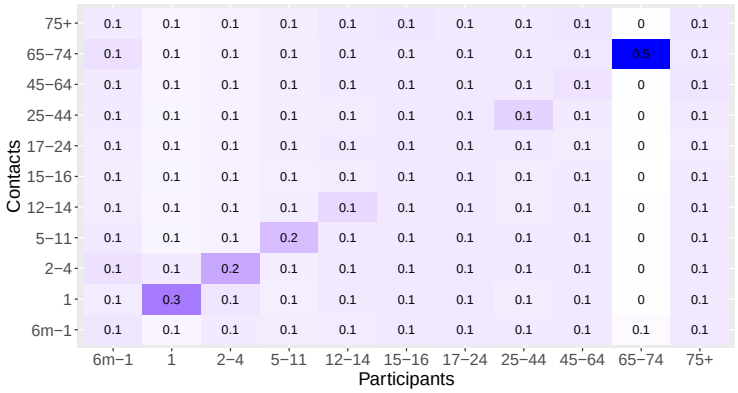

Proportion of Contacts per Age group DE

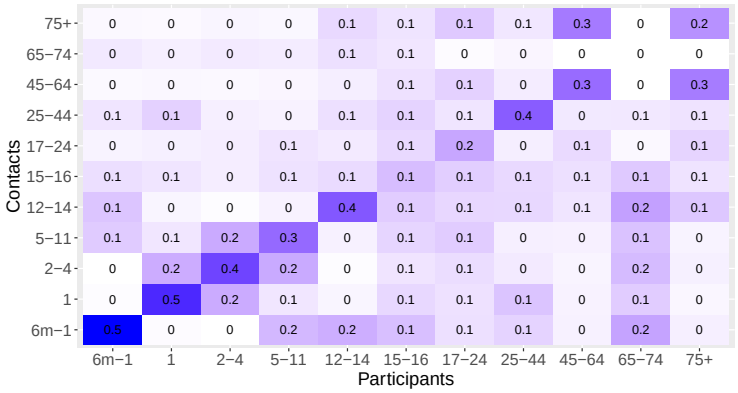

Standard Deviation Among Proportion of Contact per Age Group DE

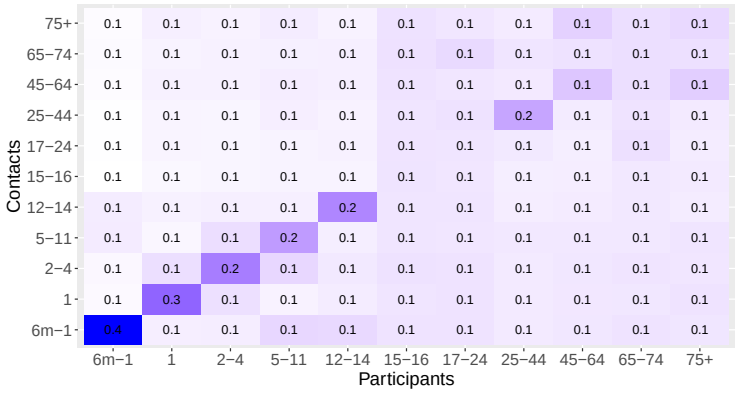

Proportion of Contacts per Age group FI

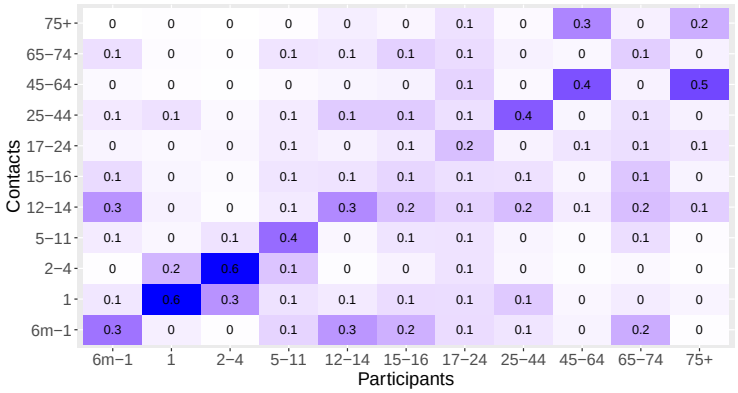

Standard Deviation Among Proportion of Contact per Age Group FI

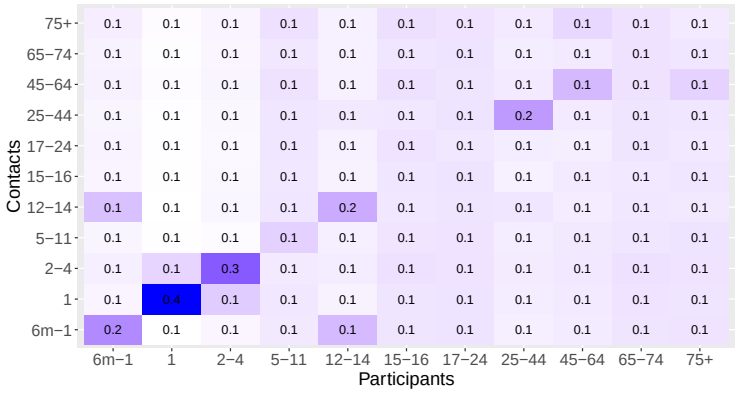

Proportion of Contacts per Age group GB

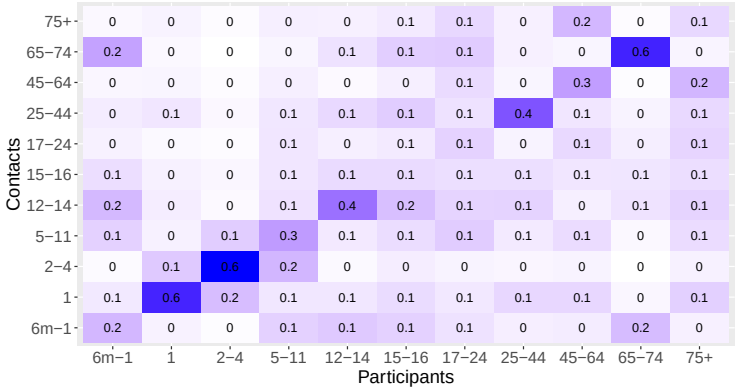

Standard Deviation Among Proportion of Contact per Age Group GB

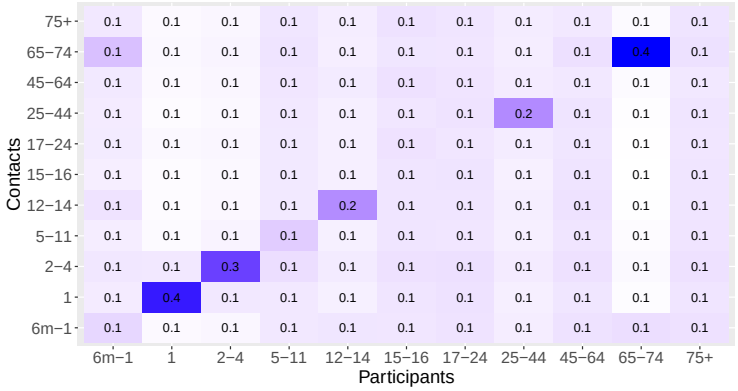

Proportion of Contacts per Age group IT

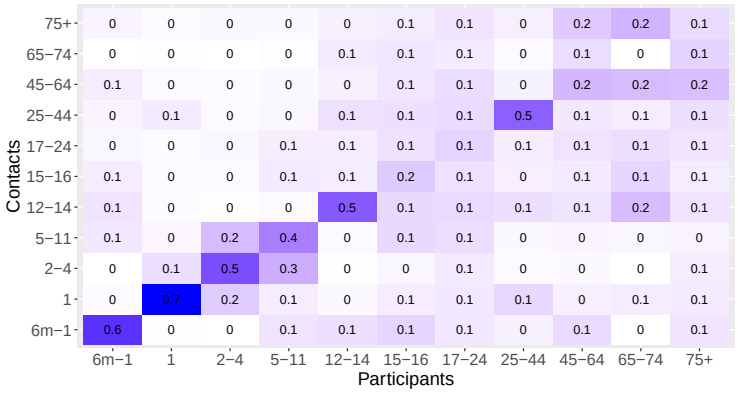

Standard Deviation Among Proportion of Contact per Age Group IT

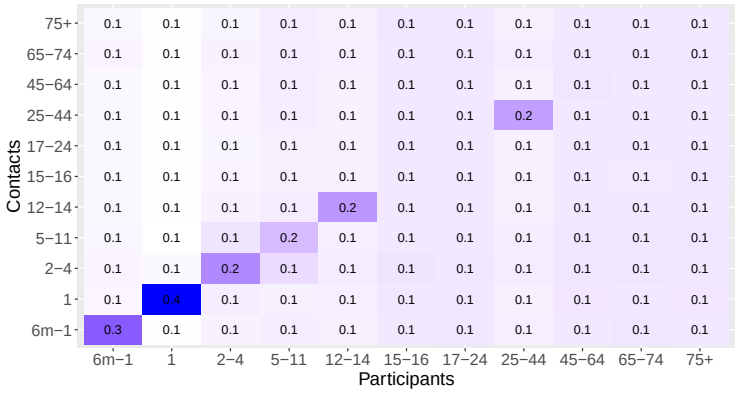

Proportion of Contacts per Age group LU

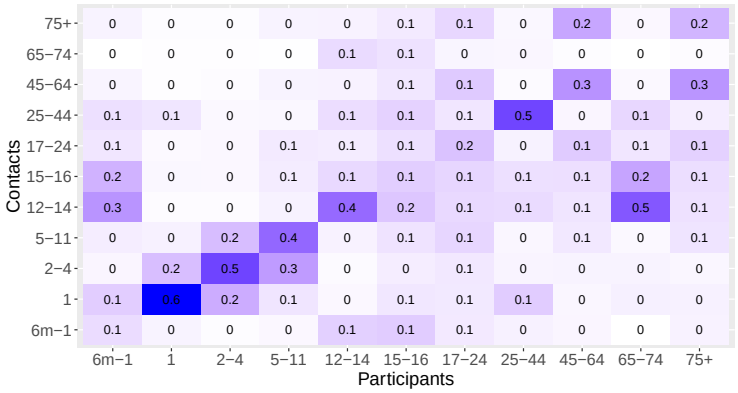

Standard Deviation Among Proportion of Contact per Age Group LU

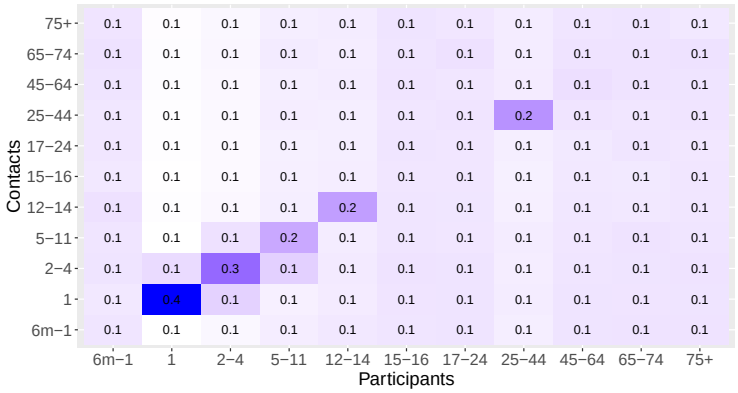

Proportion of Contacts per Age group NL

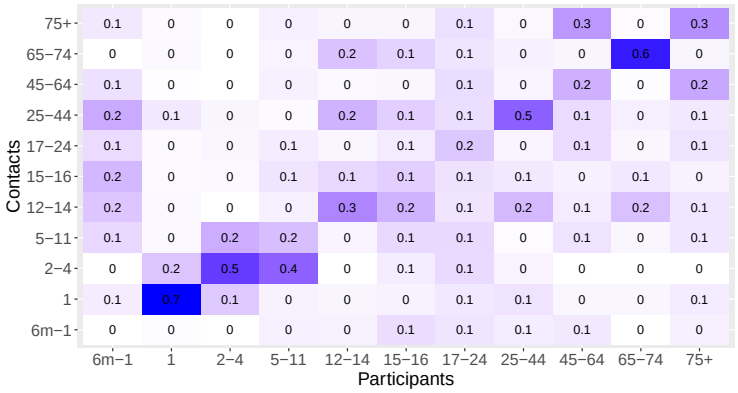

Standard Deviation Among Proportion of Contact per Age Group NL

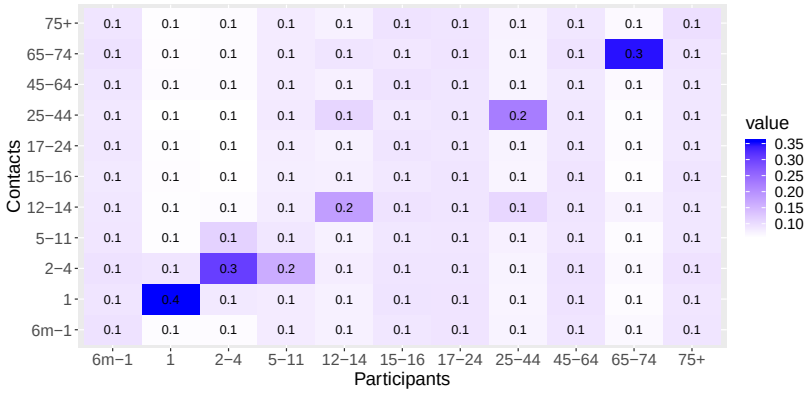

Proportion of Contacts per Age group PL

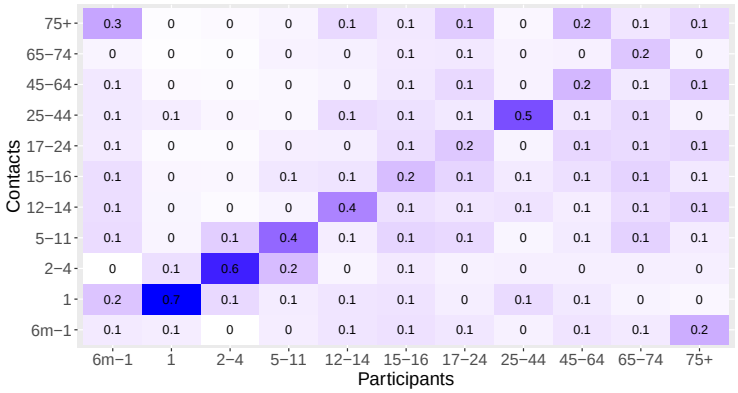

Standard Deviation Among Proportion of Contact per Age Group PL

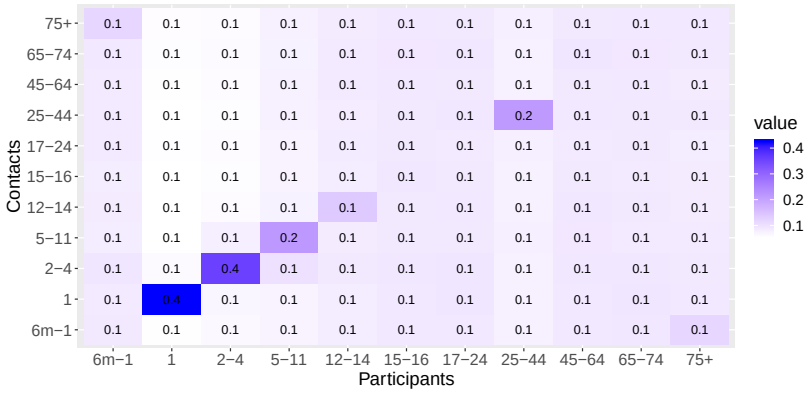

Proportion of Contacts per Age group PE

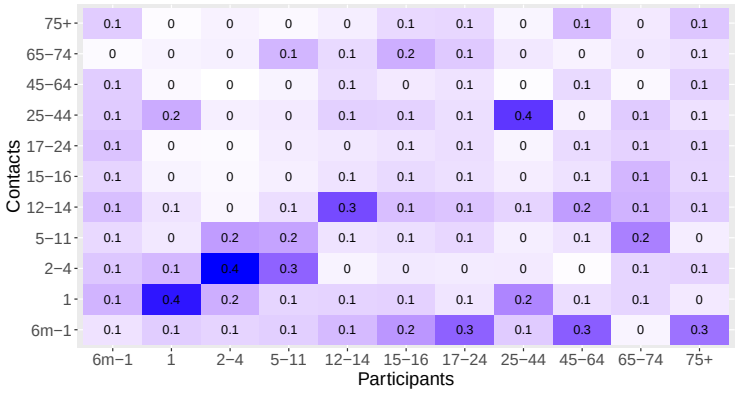

Standard Deviation Among Proportion of Contact per Age Group PE

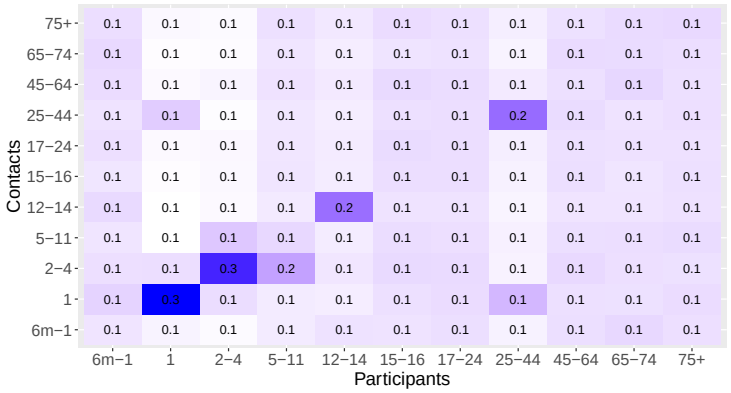

Proportion of Contacts per Age group FR

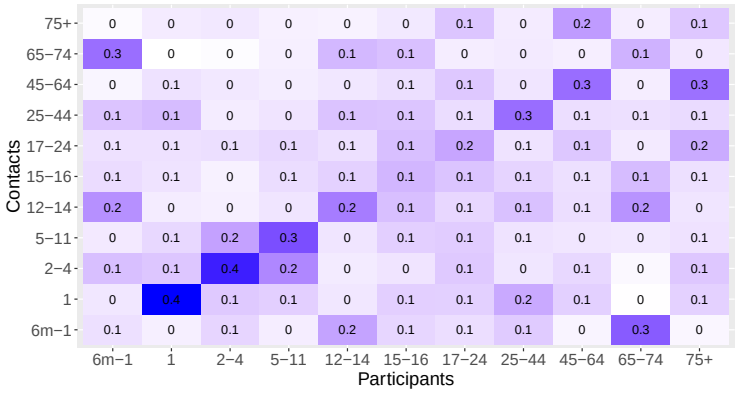

Standard Deviation Among Proportion of Contact per Age Group FR

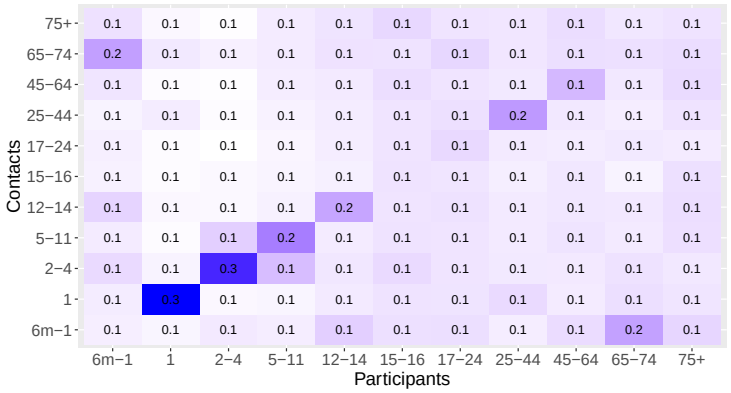

Acknowledgements

First, I would like to express my extreme gratitude to my advisor and committee chair Professor M. Elizabeth Halloran for her continuous support of my PhD study and related research. Your support, patience, good humor, immense knowledge, and research vigor were crucial to the completion of this dissertation and my degree. This research was funded by two of Professor Halloran's National Institute of Health grants, R37 AI032042 and U54 GM 111274

I would also like to express my gratitude to Professor Katherine Atkins who provided me with opportunity to work with Public Health England. Without our weekly meetings, her excellent tutelage, her continued support much of chapter 2 and 3 would not exist.

My sincere thanks to the rest of my doctoral reading committee: Professor Amanda Phipps and Professor Ruanne Barnabas for their perspective and encouragement.

I would like to thank Dr. Marcia Weaver and Professor Beth Devine for their insight into the field of cost-effectiveness analysis. In addition I would like to express my gratitude to Professor Marc Baguelin and Dr. Edwin van Leeuwan for their helpful feedback, their enthusiasm in my participation in their research, and for allowing me to tamper with their excellent model.

I thank my fellow students in the 2015/2016 Epidemiology cohort for the stimulating discussions and ceaseless passion for public health. A very special gratitude goes out to the following staff at the Center for Infectious Disease Inference and Dynamics (CIDID): Rebecca Allen, Stephanie Shadbolt, and Linda Lew for their unfailing support and assistance in conferences, finances, booking and scheduling.

Also I would thank my friends and colleagues at the Yale University Center for Infectious Disease Modeling and Analysis. In particular, I appreciate the many opportunities Professor Alison Galvani gave me at the beginning of my research career.

Last but not the least, I would like to thank my parents and grandparents for their continued support and encouragement throughout the dissertation and PhD process.

Bibliography

[1] W. G. Nichols, D. D. Erdman, A. Han, C. Zukerman, L. Corey, and M. Boeckh, "Prolonged outbreak of human parainfluenza virus 3 infection in a stem cell transplant outpatient department: insights from molecular epidemiologic analysis," *Biol. Blood Marrow Transplant.*, vol. 10, pp. 58–64, Jan. 2004.

[2] W. G. Nichols, A. J. Peck Campbell, and M. Boeckh, "Respiratory viruses other than influenza virus: impact and therapeutic advances," *Clin. Microbiol. Rev.*, vol. 21, pp. 274–90, table of contents, Apr. 2008.

[3] S. Pergram. personal communication, June 2018.

[4] National Center for Immunization and Respiratory Diseases Division of Viral Diseases, "Human parainfluenza viruses | clinical overview of HPIVs | CDC." url-https://www.cdc.gov/parainfluenza/hcp/clinical.html, Jan. 2019. Accessed: 2019-6-28.

[5] M. A. Elazhary and J. B. Derbyshire, "Aerosol stability of bovine parainfluenza type 3 virus," *Can. J. Comp. Med.*, vol. 43, pp. 295–304, July 1979.

[6] W. G. Nichols, L. Corey, T. Gooley, C. Davis, and M. Boeckh, "Parainfluenza virus infections after hematopoietic stem cell transplantation: risk factors, response to antiviral therapy, and effect on transplant outcome," *Blood*, vol. 98, pp. 573–578, Aug. 2001.

[7] D. A. Tyrrell, M. L. Bynoe, K. B. Petersen, R. N. Sutton, and M. S. Pereira, "Inoculation of human volunteers with parainfluenza viruses types 1 and 3 (HA 2 and HA 1)," *Br. Med. J.*, vol. 2, pp. 909–911, Nov. 1959.

[8] R. C. Team, *R: A Language and Environment for Statistical Computing*. R Foundation for Statistical Computing, Vienna, Austria, 2018.

[9] S. Greenland, J. Pearl, and J. M. Robins, "Causal diagrams for epidemiologic research," *Epidemiology*, vol. 10, pp. 37–48, Jan. 1999.

[10] H. Zhao, R. J. Harris, J. Ellis, M. Donati, and R. G. Pebody, "Epidemiology of parainfluenza infection in England and Wales, 1998-2013: any evidence of change?," *Epidemiol. Infect.*, vol. 145, pp. 1210–1220, Apr. 2017.

[11] B. D. Baxter, R. B. Couch, S. B. Greenberg, and J. A. Kasel, "Maintenance of viability and comparison of identification methods for influenza and other respiratory viruses of humans," *J. Clin. Microbiol.*, vol. 6, pp. 19–22, July 1977.

[12] K. J. Henrickson, "Parainfluenza viruses," *Clin. Microbiol. Rev.*, vol. 16, pp. 242–264, Apr. 2003.

[13] P. A. Gross, R. H. Green, and M. G. Curnen, "Persistent infection with parainfluenza type 3 virus in man," *Am. Rev. Respir. Dis.*, vol. 108, pp. 894–898, Oct. 1973.

[14] E. R. M. Sydnor, A. Greer, A. P. Budd, M. Pehar, S. Munshaw, D. Neofytos, T. M. Perl, and A. Valsamakis, "An outbreak of human parainfluenza virus 3 infection in an outpatient hematopoietic stem cell transplantation clinic," *Am. J. Infect. Control*, vol. 40, pp. 601–605, Sept. 2012.

[15] R. T. Maziarz, P. Sridharan, S. Slater, G. Meyers, M. Post, D. D. Erdman, T. C.-T. Peret, and R. A. Taplitz, "Control of an outbreak of human parainfluenza virus 3 in hematopoietic stem cell transplant recipients," *Biol. Blood Marrow Transplant.*, vol. 16, pp. 192–198, Feb. 2010.

[16] "Extension of the influenza immunisation programme to children in England," Tech. Rep. PHE publications gateway number: 2016182, Public Health England, Aug. 2016.

[17] "Influenza greenbook chapter 19," in *Immunisation against infectious disease* (M. Ramsay, ed.), Public Health England, Aug. 2018.

[18] M. Baguelin, S. Flasche, A. Camacho, N. Demiris, E. Miller, and W. J. Edmunds, "Assessing optimal target populations for influenza vaccination programmes: an evidence synthesis and modelling study," *PLoS Med*, vol. 10, p. e1001527, Oct. 2013.

[19] M. Baguelin, A. Camacho, S. Flasche, and W. J. Edmunds, "Extending the elderly- and risk-group programme of vaccination against seasonal influenza in England and Wales: a cost-effectiveness study," *BMC Med.*, vol. 13, p. 236, Oct. 2015.

[20] E. van Leeuwen, P. Klepac, D. Thorrington, R. Pebody, and M. Baguelin, "fluEvidenceSynthesis: An R package for evidence synthesis based analysis of epidemiological outbreaks," *PLoS Comput. Biol.*, vol. 13, p. e1005838, Nov. 2017.

[21] M. Baguelin and E. van Leeuwen, *fluEvidenceSynthesis: Flu Evidence Synthesis: Analysing Effectiveness of Vaccine Strategies*, 2017. R package version 1.0.0.

[22] A. Correa, W. Hinton, A. McGovern, J. van Vlymen, I. Yonova, S. Jones, and S. de Lusignan, "Royal college of general practitioners research and surveillance centre (RCGP RSC) sentinel network: a cohort profile," *BMJ Open*, vol. 6, p. e011092, Apr. 2016.

[23] J. Mossong, N. Hens, M. Jit, P. Beutels, R. Auranen Kari ands Mikolajczyk, M. Massari, S. Salmaso, G. S. Tomba, J. Wallinga, J. Heijne, M. Sadkowska-Todys, M. Rosinska, and W. J. Edmunds, "Social contacts and mixing patterns relevant to the spread of infectious diseases," *PLoS Med*, vol. 5, no. e74, pp. 381–391, 2008.

[24] M. Baguelin, M. Jit, E. Miller, and W. J. Edmunds, "Health and economic impact of the seasonal influenza vaccination programme in England," *Vaccine*, vol. 30, pp. 3459–3462, May 2012.

[25] C. Joseph, N. Goddard, and D. Gelb, "Influenza vaccine uptake and distribution in England and Wales using data from the general practice research database, 1989/90-2003/04," *J. Public Health*, vol. 27, pp. 371–377, Dec. 2005.

[26] Health Protection Agency, "Quarterly vaccine coverage data tables," May 2008.

[27] R. G. Pebody, H. K. Green, N. Andrews, H. Zhao, N. Boddington, Z. Bawa, H. Durnall, N. Singh, A. Sunderland, L. Letley, J. Ellis, A. J. Elliot, M. Donati, G. E. Smith, S. de Lusignan, and M. Zambon, "Uptake and impact of a new live attenuated influenza vaccine programme in England: early results of a pilot in primary school-age children, 2013/14 influenza season," *Euro Surveill.*, vol. 19, June 2014.

[28] R. G. Pebody, H. K. Green, N. Andrews, N. L. Boddington, H. Zhao, I. Yonova, J. Ellis, S. Steinberger, M. Donati, A. J. Elliot, H. E. Hughes, S. Pathirannehelage, D. Mullett, G. E. Smith, S. de Lusignan, and M. Zambon, "Uptake and impact of vaccinating school age children against influenza during a season with circulation of drifted influenza a and B strains, England, 2014/15," *Euro Surveill*, vol. 20, no. 39, 2015.

[29] R. Pebody, F. Warburton, J. Ellis, N. Andrews, A. Potts, S. Cottrell, A. Reynolds, R. Gunson, C. Thompson, M. Galiano, C. Robertson, N. Gallagher, M. Sinnathamby, I. Yonova, A. Correa, C. Moore, M. Sartaj, S. de Lusignan, J. McMenamin, and M. Zambon, "End-of-season influenza vaccine effectiveness in adults and children, United Kingdom, 2016/17," *Euro Surveill.*, vol. 22, Nov. 2017.

[30] NHS England/PH Commissioning, *FLU VACCINATION PROGRAMME DELIVERY 2018-19*. National Institute of Health, Aug. 2018.

[31] V. Demicheli, T. Jefferson, E. Ferroni, A. Rivetti, and C. Di Pietrantonj, "Vaccines for preventing influenza in healthy adults," *Cochrane Database Syst. Rev.*, no. 2, 2018.

[32] "Incorporating economic evaluation," in *Developing NICE guidelines: the manual*, vol. PMG20, pp. 121–156, National Institute for Health and Care Excellence, Oct. 2014.

[33] D. Cromer, A. J. van Hoek, M. Jit, W. J. Edmunds, D. Fleming, and E. Miller, "The burden of influenza in England by age and clinical risk group: a statistical analysis to inform vaccine policy," *J. Infect.*, vol. 68, pp. 363–371, Apr. 2014.

[34] P. Kind, P. Dolan, C. Gudex, and A. Williams, "Variations in population health status: results from a United Kingdom national questionnaire survey," *BMJ*, vol. 316, pp. 736–741, Mar. 1998.

[35] A. King, "CPIH annual rate:all items 2015 for national statistics." https://www.ons.gov.uk/economy/inflationandpriceindices/timeseries/l55o/mm23, Feb. 2019. Accessed: 2019-2-21.

[36] A. H. Briggs, K. Claxton, and M. J. Sculpher, *Decision Modelling for Health Economic Evaluation*. Oxford University Press, 2006.

[37] N. E. Basta, D. L. Chao, M. E. Halloran, L. Matrajt, and I. M. Longini, Jr, "Strategies for pandemic and seasonal influenza vaccination of schoolchildren in the United States," *Am. J. Epidemiol.*, vol. 170, pp. 679–686, Sept. 2009.

[38] I. M. Longini, Jr and M. E. Halloran, "Strategy for distribution of influenza vaccine to high-risk groups and children," *Am. J. Epidemiol.*, vol. 161, pp. 303–306, Feb. 2005.

[39] T. A. Reichert, N. Sugaya, D. S. Fedson, W. P. Glezen, L. Simonsen, and M. Tashiro, "The Japanese experience with vaccinating schoolchildren against influenza," *N. Engl. J. Med.*, vol. 344, pp. 889–896, Mar. 2001.

[40] R. J. Pitman, L. D. Nagy, and M. J. Sculpher, "Cost-effectiveness of childhood influenza vaccination in England and Wales: Results from a dynamic transmission model," *Vaccine*, vol. 31, pp. 927–942, Jan. 2013.

[41] S. Rajaram, W. Wiecek, R. Lawson, B. T. Blak, Y. Zhao, J. Hackett, R. Brody, V. Patel, and B. Amzal, "Impact of increased influenza vaccination in 2-3-year-old children on disease burden within the general population: A bayesian model-based approach," *PLoS One*, vol. 12, p. e0186739, Dec. 2017.

[42] E. W. Thommes, A. Ismaila, A. Chit, G. Meier, and C. T. Bauch, "Cost-effectiveness evaluation of quadrivalent influenza vaccines for seasonal influenza prevention: a dynamic modeling study of canada and the United Kingdom," *BMC Infect. Dis.*, vol. 15, p. 465, Oct. 2015.

[43] D. Hodgson, M. Baguelin, E. van Leeuwen, J. Panovska-Griffiths, M. Ramsay, R. Pebody, and K. E. Atkins, "Effect of mass paediatric influenza vaccination on existing influenza vaccination programmes in England and Wales: a modelling and cost-effectiveness analysis," *Lancet Public Health*, vol. 2, pp. e74–e81, Feb. 2017.

[44] R. Pebody, J. McMenamin, and H. Nohynek, "Live attenuated influenza vaccine (LAIV): recent effectiveness results from the USA and implications for LAIV programmes elsewhere," *Arch. Dis. Child.*, vol. 103, pp. 101–105, Jan. 2018.

[45] L. Curtis, "Unit costs of health and social care 2018," tech. rep., Personal Social Services Research Unit, Jan. 2019.

[46] "Agenda for change - pay rates." https://www.healthcareers.nhs.uk/working-health/working-nhs/nhs-pay-and-benefits/agenda-change-pay-rates, Apr. 2015. Accessed: 2019-2-19.

[47] R. FitzJohn, *odin: ODE Generation and Integration*, 2019. R package version 1.0.1.

[48] B. F. Johnson, L. E. Wilson, J. Ellis, A. J. Elliot, W. S. Barclay, R. G. Pebody, J. McMenamin, D. M. Fleming, and M. C. Zambon, "Fatal cases of influenza a in childhood," *PLoS One*, vol. 4, p. e7671, Oct. 2009.

[49] N. M. Ferguson, D. A. T. Cummings, S. Cauchemez, C. Fraser, S. Riley, A. Meeyai, S. Iamsirithaworn, and D. S. Burke, "Strategies for containing an emerging influenza pandemic in southeast Asia," *Nature*, vol. 437, pp. 209–214, Sept. 2005.

[50] M. Baguelin, A. J. V. Hoek, M. Jit, S. Flasche, P. J. White, and W. J. Edmunds, "Vaccination against pandemic influenza A/H1N1v in England: a real-time economic evaluation," *Vaccine*, vol. 28, pp. 2370–2384, Mar. 2010.

[51] F. Carrat, E. Vergu, N. M. Ferguson, M. Lemaitre, S. Cauchemez, S. Leach, and A.-J. Valleron, "Time lines of infection and disease in human influenza: a review of volunteer challenge studies," *Am. J. Epidemiol.*, vol. 167, pp. 775–785, Apr. 2008.

[52] A. J. van Hoek, A. Underwood, M. Jit, E. Miller, and W. J. Edmunds, "The impact of pandemic influenza H1N1 on health-related quality of life: a prospective population-based study," *PLoS One*, vol. 6, p. e17030, Mar. 2011.

[53] M. R. Siddiqui and W. J. Edmunds, "Cost-effectiveness of antiviral stockpiling and near-patient testing for potential influenza pandemic," *Emerg. Infect. Dis.*, vol. 14, pp. 267–274, Feb. 2008.

[54] A. Melegaro and W. J. Edmunds, "The 23-valent pneumococcal polysaccharide vaccine. part II. a cost-effectiveness analysis for invasive disease in the elderly in England and Wales," *Eur. J. Epidemiol.*, vol. 19, no. 4, pp. 365–375, 2004.

[55] N. Balov, "The Stata blog: Gelman–Rubin convergence diagnostic using multiple chains." http://blog.stata.com/2016/05/26/gelman-rubin-convergence-diagnostic-using-multiple-chains/. Accessed: 2019-3-10.

[56] National Health Service England, *Directed Enhanced Service Specification Seasonal influenza and pneumococcal polysaccharide vaccination programme 2018/19*, June 2018.

[57] K. Atkins, A. J. van Hoek, C. Watson, M. Baguelin, L. Choga, A. Patel, T. Raj, M. Jit, and U. Griffiths, "Seasonal influenza vaccination delivery through community pharmacists in England: evaluation of the London pilot," *BMJ Open*, vol. 6, p. e009739, Feb. 2016.

[58] L. Jackson, "Schools and class sizes in England & the UK: Social indicators page," Tech. Rep. Commons Briefing papers SN02625, HOUSE OF COMMONS LIBRARY, Nov. 2017.

[59] Department of Health Care, "Management and disposal of healthcare waste (HTM 07-01)." https://www.gov.uk/government/publications/guidance-on-the-safe-management-of-healthcare-waste, Mar. 2013. Accessed: 2018-12-31.

[60] M. Keeling and P. Rohani, "Modeling infectious diseases in Humans and Animals." urlhttp://www.modelinginfectiousdiseases.org/. Accessed: 2017-12-7.

[61] V. Isham and G. Medley, *Models for Infectious Human Diseases: Their Structure and Relation to Data*. Cambridge University Press, Mar. 1996.

[62] J. Mossong, N. Hens, M. Jit, P. Beutels, R. Auranen Kari ands Mikolajczyk, M. Massari, S. Salmaso, G. S. Tomba, J. Wallinga, J. Heijne, M. Sadkowska-Todys, M. Rosinska, and W. J. Edmunds, "Social contacts and mixing patterns relevant to the spread of infectious diseases," *PLoS Med*, vol. 5, no. e74, pp. 381–391, 2008.

[63] K. Prem, A. R. Cook, and M. Jit, "Projecting social contact matrices in 152 countries using contact surveys and demographic data," *PLoS Comput. Biol.*, vol. 13, p. e1005697, Sept. 2017.

[64] P. Rohani, X. Zhong, and A. a. King, "Contact network structure explains the changing epidemiology of pertussis.," *Science*, vol. 330, pp. 982–985, Nov. 2010.

[65] C. G. Grijalva, N. Goeyvaerts, H. Verastegui, K. M. Edwards, A. I. Gil, C. F. Lanata, N. Hens, and RESPIRA Peru project, "A household-based study of contact networks relevant for the spread of infectious diseases in the highlands of Peru," *PLoS One*, vol. 10, p. e0118457, Mar. 2015.

[66] G. Béraud, S. Kazmercziak, P. Beutels, D. Levy-Bruhl, X. Lenne, N. Mielcarek, Y. Yazdanpanah, P.-Y. Boëlle, N. Hens, and B. Dervaux, "The French connection: The first large Population-Based contact survey in France relevant for the spread of infectious diseases," *PLoS One*, vol. 10, p. e0133203, July 2015.

[67] A. Melegaro and W. J. Edmunds, "The 23-valent pneumococcal polysaccharide vaccine. part II. a cost-effectiveness analysis for invasive disease in the elderly in England and Wales," *Eur. J. Epidemiol.*, vol. 19, no. 4, pp. 365–375, 2004.

[68] M. Baguelin, A. J. V. Hoek, M. Jit, S. Flasche, P. J. White, and W. J. Edmunds, "Vaccination against pandemic influenza A/H1N1v in England: a real-time economic evaluation," *Vaccine*, vol. 28, pp. 2370–2384, Mar. 2010.

[69] M. Baguelin, S. Flasche, A. Camacho, N. Demiris, E. Miller, and W. J. Edmunds, "Assessing optimal target populations for influenza vaccination programmes: an evidence synthesis and modelling study," *PLoS Med*, vol. 10, p. e1001527, Oct. 2013.

[70] A. Gelman, J. B. Carlin, H. S. Stern, D. B. Dunson, A. Vehtari, and D. B. Rubin, *Bayesian data analysis*, vol. 2. CRC press Boca Raton, FL, 2014.

[71] M. Herdman, C. Gudex, A. Lloyd, M. Janssen, P. Kind, D. Parkin, G. Bonsel, and X. Badia, "Development and preliminary testing of the new five-level version of EQ-5D (EQ-5D-5L)," *Qual. Life Res.*, vol. 20, pp. 1727–1736, Dec. 2011.

[72] National Institute of Standards and Technology, U.S. Department of Commerce, "1.3.5.16. Kolmogorov-Smirnov Goodness-of-Fit test." url-https://www.itl.nist.gov/div898/handbook/eda/section3/eda35g.htm. Accessed: 2019-6-19.

[73] V. C. Barclay, T. Smieszek, J. He, G. Cao, J. J. Rainey, H. Gao, A. Uzicanin, and M. Salathé, "Positive network assortativity of influenza vaccination at a high school: implications for outbreak risk and herd immunity," *PLoS One*, vol. 9, p. e87042, Feb. 2014.

[74] M. E. J. Newman, "Mixing patterns in networks," *Phys. Rev. E Stat. Nonlin. Soft Matter Phys.*, vol. 67, p. 026126, Feb. 2003.

[75] E. Fenwick, K. Claxton, and M. Sculpher, "Representing uncertainty: the role of cost-effectiveness acceptability curves," *Health Econ.*, vol. 10, pp. 779–787, Dec. 2001.

[76] G. Béraud, S. Kazmercziak, P. Beutels, D. Levy-Bruhl, X. Lenne, N. Mielcarek, Y. Yazdanpanah, P.-Y. Boëlle, N. Hens, and B. Dervaux, "The French connection: The first large Population-Based contact survey in France relevant for the spread of infectious diseases," *PLoS One*, vol. 10, p. e0133203, July 2015.

[77] C. G. Grijalva, N. Goeyvaerts, H. Verastegui, K. M. Edwards, A. I. Gil, C. F. Lanata, N. Hens, and RESPIRA Peru project, "A household-based study of contact networks relevant for the spread of infectious diseases in the highlands of Peru," *PLoS One*, vol. 10, p. e0118457, Mar. 2015.

[78] A. Saltelli, *Sensitivity analysis of scientific models*. Hoboken, N.J.: Wiley, [online-ausg.]. ed., 2007.

[79] S. Marino, I. B. Hogue, C. J. Ray, and D. E. Kirschner, "A methodology for performing global uncertainty and sensitivity analysis in systems biology," *J. Theor. Biol.*, vol. 254, pp. 178–196, Sept. 2008.

[80] K. Prem, A. R. Cook, and M. Jit, "Projecting social contact matrices in 152 countries using contact surveys and demographic data," *PLoS Comput. Biol.*, vol. 13, p. e1005697, Sept. 2017.

[81] F. Iozzi, F. Trusiano, M. Chinazzi, F. C. Billari, E. Zagheni, S. Merler, M. Ajelli, E. Del Fava, and P. Manfredi, "Little Italy: an agent-based approach to the estimation of contact patterns- fitting predicted matrices to serological data," *PLoS Comput. Biol.*, vol. 6, p. e1001021, Dec. 2010.

[82] R. C. Team, *R: A Language and Environment for Statistical Computing*. R Foundation for Statistical Computing, Vienna, Austria, 2018.

[83] O. Diekmann, J. A. P. Heesterbeek, and M. G. Roberts, "The construction of next-generation matrices for compartmental epidemic models," *J. R. Soc. Interface*, vol. 7, pp. 873–885, June 2010.

Index

NATASHA WENZEL, MPH
natasha.wenzel@gmail.com

EDUCATION

University of Washington School of Public Health, *Seattle, WA*
PhD in Epidemiology Fall 2015-Dec 2019

Yale University, Yale School of Public Health, *New Haven, CT*
MPH in Epidemiology, Epidemiology of Microbial Diseases 2012- 2014

University of California, Berkeley *Berkeley, CA*
B.S. in Environmental Science: Society & Environment 2006- 2010
B.A. in English

RESEARCH EXPERIENCE

Center for Inference & Dynamics of Infectious Disease, Fred Hutchinson Cancer Research Center,
Prof. Elizabeth Halloran *Seattle, WA*
Research Assistant August 2015-*Dec 2019*

- Designed and conducted statistical analysis of a viral outbreak in a local Seattle hospital using electronic medical record data.
- Collaborated with multiple research groups at Fred Hutchinson Cancer Research Center, Seattle Cancer Care Alliance, and Public Health England.
- Created a new approach for structural uncertainty analysis on public health model assumptions about infectious contacts and mixing patterns.
- Designed and conducted multiple quantitative analyses; prepared manuscripts in LaTeX for publication of research findings.

Immunisation department, Public Health England, NHS
Prof. Katherine Atkins, Dr. Marc Baguelin, *London, UK*
Research Consultant June 2016 –Oct 2016

- Designed and conducted cost-effectiveness analysis of seasonal influenza vaccination strategies for the National Health Service (NHS) using multiple UK data sources and databases in an evidence synthesis approach.
- Updated and enhanced a previous analysis by improving model fits using Bayesian techniques on 19 years of influenza datasets.

Yale Center for Infectious Disease Modeling and Analysis,
Prof. Alison Galvani *New Haven, CT*
Research Associate May 2014-Dec 2015

- Responsible for daily operation of specialized modeling analysis projects within the Center for Infectious Disease and Analysis (CIDMA).
- Designed and performed mathematical model simulations, interpreted model results, developed graphics to convey results, and investigated, analyzed, and reached scientific conclusions related to model results under the direction of the senior researcher.
- Participated in grant writing, and manuscript writing, revisions, and submissions.
- Supervised MPH graduate students.

Yale Center for Infectious Disease Modeling and Analysis,
Prof. Alison Galvani *New Haven, CT*
Research Assistant Jan 2013—May 2014

- Developing deterministic and stochastic mathematical models of seasonal Nipah virus disease outbreaks in Bangladesh using Markov Chain Monte Carlo algorithms.
- Examined statistical correlations between sexually transmitted infections and urban-living related metrics (e.g. city size, city area) within Metropolitan Statistical Areas (MSA) in the US using multiple regression techniques.

Turner Lab, Yale Ecology & Evolutionary Biology,
Prof. Paul Turner *New Haven, CT*
Research Assistant Oct 2013—Jan 2014

- Examining viral diversity, growth, and emergence as a result of population immune status.
- Responsible for preparation and maintenance of cell lines and viral growth assays.

Integrated Refugee and Immigrant Services,
Yale School of Public Health *New Haven, CT*
Graduate Researcher Sept—June 2013

- Interviewed refugee adolescents in the New Haven community to evaluate utilization of mental health treatment and seeking behaviors.
- Analyzed qualitative interview results using content analysis to determine frequency and distribution of major health-related themes and barriers to care.
- Final research presented at North American Refugee Health Conference 2013.

Sutter Medical Foundation of Northern California,
Dr. Gnanagurudasan Prakasam *Roseville, CA*
Research Associate 2011—2012

- Designed and conducted analysis on patient social networking through a content analysis of messages posted on a Type 1 diabetes mailing-list as related to coping mechanisms, provider's scope, and internet connectivity from 2003 to 2011.
- Synthesized and presented final research at the American Diabetes Association 72nd annual conference (2012).

Sacramento County Office of Disease Control,
Dr. Cassius Locket *Sacramento, CA*
Medical Records Assistant 2011 – 2012

- Functioned as database clerk recording Confidential Morbidity Reports (CMR) from local health providers into the California Reportable Disease Information Exchange (CalRedie) System and checking data consistency.
- Conducted telephone interviews during foodborne outbreaks in Sacramento Country.

UC Davis Center for Health Disparities,
Dr. Sergio Aguilar-Gaxiola *Sacramento, CA*
Research Assistant 2010

- Performed systematic review of disparities in access to and quality of mental health care as related to changes in government policy and funding.
- Contributed to manuscript preparation, editing, writing, and coordinating varied author and literature contributions into continuous documents.

HONORS, AWARDS AND FELLOWSHIPS

Second Place Award, Thesis Presentation Day 2014, Yale School of Public Health	2014
Ruth and Milton Steinbach Scholarship, Yale School of Public Health	2013
Stolwijk Fellowship Recipient, Yale School of Public Health	2013
Susan Bliss Scholarship, Yale School of Public Health	2012 – 2013
UC Berkeley American Cultures Student Research Prize Nominee, UC Berkeley	2008 – 2009

SKILLS

- Extensive experience (6+ years) and expertise with statistical analysis software, such as R, Matlab, Mathematica, SAS (R preferred).
- Experience using UNIX shell (bash) languages for multiple computing clusters for high dimensional statistical procedures.

GRANTS

Galvani A.P. (PI), Ndeffo-Mbah, M. (Co-PI), Townsend, J. P. (Co-PI), Yamin, D. (consultant), **Wenzel, N.S. (consultant**), Boyko, R. (student), Skrip, L. (student), Lewnard, J. (student) – "Optimal allocation of both non-pharmaceutical and pharmaceutical interventions toward controlling Ebola transmission in West Africa". National Science Foundation, RAPID, $200,000 (2014).

PUBLICATIONS

Fitzpatrick, M. **Wenzel, N.S.,** Scarpino, S.V., Althouse, B.M., Atkins, K.E., Galvani, A.P., Townsend, J.P., Cost-effectiveness of next-generation vaccines: The case of pertussis. Vaccine (2016). doi:10.1016/j.vaccine.2016.04.010

Atkins, K.E., Pandey, A., **Wenzel, N.S.**, Skrip, L., Yamin, D., Nyenswah, T.G., et al., Retrospective Analysis of the 2014–2015 Ebola Epidemic in Liberia. Am. J. Trop. Med. Hyg. (2016). doi:10.4269/ajtmh.15-0328

Parpia, A., Ndeffo-Mbah, M., **Wenzel, N. S.,** Galvani, A. P. Effects of Response to 2014-2015 Ebola Outbreak on Deaths from Malaria, HIV/AIDS, and Tuberculosis, West Africa. Emerg. Infect. Dis. 22, 433–441 (2016).

Nsoesie, E. O., Ricketts, R. P., Brown, H. E., Fish, D., Durham, D. P., Ndeffo Mbah, M. L., Christian, T., Ahmed, S., Marcellin, C., Shelly, E., Owers, K., **Wenzel, N.**, Galvani, A. P. & Brownstein, J. S. Spatial and Temporal Clustering of Chikungunya Virus Transmission in Dominica. PLoS Negl. Trop. Dis. 9, e0003977 (2015).

Wells, C., Yamin, D., Ndeffo-Mbah, M. L., **Wenzel, N.**, Gaffney, S. G., Townsend, J. P., Meyers, L. A., Fallah, M., Nyenswah, T. G., Altice, F. L., Atkins, K. E. & Galvani, A. P. Harnessing case isolation and ring vaccination to control Ebola. PLoS Negl. Trop. Dis. 9, e0003794 (2015).

Atkins, K. E., **Wenzel, N. S.,** Ndeffo-Mbah, M., Altice, F. L., Townsend, J. P. & Galvani, A. P. Under-reporting and case fatality estimates for emerging epidemics. BMJ 350, h1115 (2015).

Scarpino, S. V., Iamarino, A., Wells, C., Yamin, D., Ndeffo-Mbah, M., **Wenzel, N. S.**, Fox, S. J., Nyenswah, T., Altice, F. L., Galvani, A. P., Meyers, L. A. & Townsend, J. P. Epidemiological and viral genomic sequence analysis of the 2014 Ebola outbreak reveals clustered transmission. Clin. Infect. Dis. (2014). doi:10.1093/cid/ciu1131

Pandey, A., Atkins, K. E., Medlock, J., **Wenzel, N.**, Townsend, J. P., Childs, J. E., … Galvani, A. P. (2014). Strategies for containing Ebola in West Africa. *Science*, science.1260612–. doi:10.1126/science.1260612

Galvani, A. P., Ndeffo-Mbah, M. L., **Wenzel, N.**, & Childs, J. E. (2014). Ebola Vaccination: If Not Now, When? *Annals of Internal Medicine*. doi:10.7326/M14-1904

Aguilar-Gaxiola, S., Sribney, W. S., Raingruber, B., **Wenzel, N.**, & Fields-Johnson, D. (2011). Chapter 5: Disparities in Mental Health, Mental Illness, and Care. In N. Cohen & S. Galea (Eds.), *Mental Health: Evidence, Policy and Public Health Practice* (pp. 69-91). New York, NY; Routledge.

WORKING PAPERS

Wenzel, N.S., Baguelin, M., van Leeuwen, E., Halloran, M.E., Atkins, K.E., (2019) Cost-Effectiveness of Influenza Vaccination Among School-Age Cohorts. *In prep.*

Wenzel, N.S., Baguelin, M., van Leeuwen, E., Halloran, M.E., Atkins, K.E., (2019) Characterizing Structural Uncertainty of Social Contacts in Cost-Effectiveness models. *In prep.*

Wenzel, N.S., Townsend, J., Childs, J., Galvani, A., Pitzer, V., Durham, D. (2014) An Analysis of the Emergence and Transmission of Nipah Virus from Flying Foxes using Simple Models. *In prep.*

PRESENTATIONS

Wenzel, N.S., Halloran, M.E., (2017) *Sensitivity of Seasonal Influenza to Population Contact Dynamics.* Poster presented at the Models of Infectious Disease Agent Study (MIDAS) Network Meeting 2017, May 22, 2017.

Wenzel, N.S., Townsend, J.P., Childs, J., Galvani, A. P., Pitzer, V. Durham, D. (2013) *Modeling the Zoonotic Transmission Dynamics of Nipah Virus: Implications for Outbreak Control and Model-Guided Fieldwork.* Poster presented at the Yale School of Public Health Thesis Presentation Day, April 30, 2014.

Wenzel, N.S, Townsend, J., Childs, J., Galvani, A., Durham, D. (2013) *Estimating Nipah Virus Transmission Dynamics using Markov Chain Monte Carlo Analysis.* Poster presented at the Clinic on Infectious Disease Dynamics and Data hosted by the Emerging Pathogens Institute, University of Florida from December 16-21, 2013.

Gibson, B., Gianfrancesco, M., Greene, C., Mergenthaler, C., Gupta, A., Reese-Masterson, A., **Wenzel, N.** (2013) *A Qualitative Study on Stress, Coping, and Mental Health Support in Adolescent Refugees.* Research poster presented at the 2013 North American Refugee Health Conference June 6-8, 2013.

Wenzel, N., Gnanagurudasan, P., Parise, C. (2012) *"Evolution of Social Networking Influence on Information Exchanges: Content Analysis of Type 1 Diabetes Discussions Among Impacted Families".* Poster presented at the 72nd Annual American Diabetes Association Conference June 8-12, 2012.

Wenzel, N. (2010). *GOOD FOR ME: An Examination of Agricultural Pesticide Use in Sacramento County as Related to Autism Spectrum Disorder (ASD) Prevalence in the Area.* Project presented to faculty panel at the College of Natural Resources, Berkeley, CA., December 2010.

CONFERENCES

- Models of Infectious Disease Agent Study (MIDAS) Network Meeting 2017, May 22-24, 2017
- Statistics and Modeling in Infectious Diseases (SISMED) 2017, July 12-26, 2017. Attended Sessions 2-5.
- Models of Infectious Disease Agent Study (MIDAS) Network Meeting 2016, May 23-24, 2016
- Clinic on Infectious Disease Dynamics and Data hosted by the Emerging Pathogens Institute, University of Florida from December 16-21, 2013.
- The 72nd Annual American Diabetes Association Conference June 8-12, 2012

AFFILIATIONS

The Union of Academic Student Employees at the University of Washington
Women in Science at Yale
Association of Public Health Laboratories
Yale School of Public Health Alumni Association
University of California, Berkeley Alumni Association